

**GEOLOGICAL INVESTIGATIONS  
OF THE CANADIAN BEAUFORT  
SEA COAST**

by

**Philip R. Hill, Arnaud Héquette, Marie-Hélène Ruz,  
and Kimberley A. Jenner**

**Hill Geoscience Research**



**GEOLOGICAL INVESTIGATIONS OF THE  
CANADIAN BEAUFORT SEA COAST**

by

**Philip R. Hill, Arnaud Héquette, Marie-Hélène Ruz,  
and Kimberley A. Jenner**

Hill Geoscience Research  
70 Neptune Crescent, Suite 220  
Dartmouth, N.S., B2Y 4M9

**GEOLOGICAL SURVEY OF CANADA  
OPEN FILE REPORT  
2387**

Hill Geoscience Research Project No: 88-1

Prepared for: Atlantic Geoscience Centre  
Geological Survey of Canada  
P.O. Box 1006, Dartmouth, N.S.  
B2Y 4A2

Scientific Authority: R.B. Taylor

Supply and Services File No. OSC88-00268-(009)

20 March 1990

**FUNDING SOURCES:**

NORTHERN OIL AND GAS ACTION PROGRAM (Project D.1)

MARINE ENVIRONMENTAL INITIATIVE OF THE GEOLOGICAL SURVEY OF CANADA

PANEL ON ENERGY RESEARCH AND DEVELOPMENT (Project 6.3)

FEBRUARY, 1991





## TABLE OF CONTENTS

	<b>PAGE</b>
<b>TABLE OF CONTENTS</b>	i
<b>LIST OF FIGURES</b>	vii
<b>LIST OF TABLES</b>	xvi
<b>1. INTRODUCTION</b>	1
1.1 History of Beaufort Sea Coastal Research	1
1.2 The NOGAP Program	3
1.3 Objectives of This Report	4
1.4 Organization of the Report	5
1.5 Credits and Acknowledgements	5
<b>2. BACKGROUND</b>	7
2.1 Geological Setting	7
2.2 Quaternary Geology	10
2.2.1 Coastal Plain	10
2.2.2 Offshore	13
2.3 Permafrost and Ground Ice	17
2.4 Climate	18
2.5 Mackenzie River Regime	18
2.6 Ice Regime	24
2.6.1 Winter	24
2.6.2 Break-Up	28
2.6.3 Summer	30
2.6.4 Freeze-Up	30
2.7 Oceanography	33
2.7.1 Water Column Structure	33
2.7.2 Currents	35
2.7.3 Waves	38
2.7.4 Storm Surge	43

<b>3. METHODS AND DATABASE</b>	45
3.1 Shoreline Surveys	45
3.2 Seismic Surveys	45
3.3 Lithostratigraphy	50
3.4 Geotechnical Properties	52
3.5 Sediment Transport	55
3.5.1 King Point Program, August 24 to September 16, 1985.	55
3.5.2 Tibjak Beach Study, August 27 to September 17, 1987.	57
3.5.3 Other Data Sets	58
<b>4. SEA LEVEL HISTORY</b>	60
4.1 Previous Sea Level Reconstructions	60
4.2 Samples	62
4.2.1 Eastern Shelf Non-Marine (Samples 11 -16)	62
4.2.2 Eastern Shelf Marine Samples (Samples 17 - 22)	65
4.2.3 Yukon Shelf Marine Sample	65
4.3 Holocene Relative Sea Level Curve	65
4.4 Discussion	67
4.5 Sampling of Coastal Marshes	67
4.5.1 Topkak Marsh	68
4.5.2 Atkinson Point Lagoon	72
4.5.3 Implications to the Holocene Sea Level Curve	72
<b>5. YUKON COAST: U.S BORDER TO SHALLOW BAY</b>	75
5.1 Quaternary Geology	75
5.2 Coastal Morphology	75
5.2.1 Sea Cliffs	75
5.2.2 Deltas	77
5.2.3 Spits and Barriers	83
5.2.4 Inner Shelf Morphology	90
5.3 Rates of Coastline Change	90
5.3.1 Coastal Retreat	90

5.3.2 Spit and Barrier Evolution	95
5.3.3 Delta Evolution	95
5.4 Seismic Stratigraphy	96
5.5 Lithostratigraphy and Sedimentology	98
5.5.1 King Point	100
5.5.2 Vibracores from nearshore zone between King Point and Sabine Point	106
5.6 Geotechnical Properties	106
5.6.1 Diamicton	106
5.6.2 Lacustrine	111
5.6.3 Marine Sediment	111
5.7 Sediment Erosion, Transport and Deposition	111
5.7.1 Wind regime	112
5.7.2 Currents and Plume Characteristics	112
5.7.3 Waves	115
5.7.4 Storm Surge	118
5.7.5 Ice-Related Coastal Processes	118
5.7.6 The King Point Sediment Transport Experiment	119
<b>6. MACKENZIE DELTA: SHALLOW BAY TO GARRY ISLAND</b>	<b>130</b>
6.1 Quaternary Geology	130
6.2 Coastal and Inner Shelf Morphology	132
6.3 Rates of Coastline Change	133
6.4 Seismic Stratigraphy	134
6.4.1 Pre-delta Stratigraphy	134
6.4.2 Late Wisconsinan Delta	137
6.4.3 Post-glacial Transgression	137
6.4.4 Holocene Delta	141
6.5 Lithostratigraphy and Sedimentology	141
6.5.1 Late Wisconsinan Delta	144
6.5.2 The Holocene Delta	144

6.6 Geotechnical Properties	158
6.7 Sediment Erosion, Transport and Deposition	162
6.7.1 Sediment Supply	162
6.7.2 Transport Processes at Distributary Mouths	164
6.7.3 Offshore Sedimentation Processes	167
<b>7. GARRY ISLAND TO SUMMER ISLAND</b>	<b>174</b>
7.1 Quaternary Geology	174
7.1.1 Ground Ice	176
7.2 Coastal and Inner Shelf Morphology	177
7.2.1 Sea Cliffs	177
7.2.2 Spits and Barriers	177
7.2.3 Deltaic Coast	181
7.2.4 Intertidal Flats and Mud Banks	181
7.2.5 Breached Lake Coastline of Eastern Richards Island	181
7.2.6 Inner Shelf	183
7.3 Coastal Change	183
7.3.1 Coastal Retreat	183
7.3.2 Spit and Barrier Evolution	187
7.4 Seismic Stratigraphy	187
7.4.1 Kringalik Bank	187
7.4.2 Ikit Trough	194
7.4.3 Akpak Bank	194
7.4.4 Interpretation of Seismic Data	203
7.5 Lithostratigraphy and Sedimentology	203
7.5.1 Kringalik Bank	205
7.5.2 Ikit Trough	215
7.5.3 Akpak Bank	220
7.6 Geotechnical Properties	222
7.7 Sediment Erosion, Transport and Deposition	222
7.7.1 Waves	226
7.7.2 Currents	226

7.7.3 Sediment Transport	229
<b>8. KUGMALLIT BAY</b>	<b>233</b>
8.1 Seismic Stratigraphy	233
8.2 Lithostratigraphy and Sedimentology	237
<b>9. TUKTOYAKTUK PENINSULA</b>	<b>246</b>
9.1 Quaternary Geology	246
9.2 Coastal Morphology	248
9.2.1 Headland and Peninsula Sea Cliffs	248
9.2.2. Drowned Tundra Coast	249
9.2.3 Spits and Barrier Islands	249
9.2.4. Inner Shelf Morphology	260
9.3 Rates of Coastline Change	260
9.3.1 Cliff Retreat	260
9.3.2. Spit and Barrier Evolution	260
9.4 Seismic Stratigraphy	273
9.5 Lithostratigraphy	278
9.6 Geotechnical Properties	278
9.7 Sediment Erosion, Transport and Deposition	278
9.7.1 Influence of Mackenzie Plume	278
9.7.2 Waves	279
9.7.3 Currents	279
9.7.4 Sediment Transport	284
9.7.5 The Tibjak Beach Study	284
<b>10. PRIORITIES FOR FUTURE COASTAL PROGRAMS</b>	<b>298</b>
10.1 Immediate Follow-Up	298
10.1.1. Publication of Selected Topics of Scientific Interest	298
10.1.2 New Research on Existing Data	300
10.2 Data and Information Gaps	301
10.3 AGC'S 'Clients' and Their Needs	304

10.3.1	Industry Plans and Perspectives	304
10.3.2	Inuvialuit Communities	306
10.3.3	Government Regulatory Requirements	306
10.4	Recommendations: Priority Issues	308
10.5	Recommended Programs	311
10.5.1	Regional Mapping Program: Beaufort Sea Nearshore and Inner Shelf	311
10.5.2	Dynamics of Muddy Shoreface and Inner Shelf Environments	312
10.5.3	Coastal Sedimentary Environments Program	313
10.5.4	Cliff, Beach and Barrier Monitoring Program	314
10.6	Coordination and Communication	315
10.6.1	Communication with Non-Technical Organizations	316
10.6.2	Communication with Other Technical Agencies and Industry	316
<b>APPENDIX:</b>	<b>Summaries of Contract Reports Completed under NOGAP D.1</b>	<b>329</b>



## LIST OF FIGURES

**Front Cover** Aerial view of ice-rich cliffs and barrier beach at King Point, Yukon Territory (photo by D.L. Forbes July 28, 1984).

**Figure 1.1** Beaufort Sea coastline between the Alaskan border and Cape Dalhousie.

**Figure 2.1** Tectonic regions of the Beaufort Sea - Mackenzie Delta region (after Young et al., 1976 and Yorath et al., 1980).

**Figure 2.2** Schematic structural - stratigraphic section through the Beaufort - Mackenzie Basin (from Dietrich et al., 1985).

**Figure 2.3** Surficial geology map of the Canadian Beaufort Sea coastal region (modified from Rampton 1982; 1988).

**Figure 2.4** Map of the Beaufort - Mackenzie region showing position of various Laurentide ice limits (based on Rampton, 1982; 1988; Hughes, 1988).

**Figure 2.5** Schematic cross-section of the Beaufort Shelf showing main stratigraphic units.

**Figure 2.6** Climatic zones of the Mackenzie Delta and surrounding regions (Burns, 1973).

**Figure 2.7** Temperature/precipitation graph for (a) Tuktoyaktuk and (b) Shingle Point (Burns, 1973).

**Figure 2.8** The distribution of winds (roses indicate the direction from which winds blow) at Shingle Point and Tuktoyaktuk (modified from Harper and Penland, 1987).

**Figure 2.9** The drainage basin of the Mackenzie River (Davies, 1975).

**Figure 2.10** Major distributary channels of the Mackenzie Delta.

**Figure 2.11** The annual discharge cycle of the Mackenzie River, showing mean and extreme years (from Lewis, 1988).

**Figure 2.12** The morphological zonation of Beaufort Sea ice (Dome et al. 1982).

**Figure 2.13** Beaufort Sea landfast ice morphology (Arctec, 1987).

**Figure 2.14** Flooded landfast ice during early stages of break-up in early May (Pilkington, 1988).

**Figure 2.15** The median position of the ice edge for late August in good, fair and poor years: 1961-1972 (Milne and Herlinveaux, 1977).

**Figure 2.16** Smoothed time series of monthly anomalies of the areal sea ice extent in the Chukchi - Beaufort Sea region (Mysak and Manuk, 1988).

**Figure 2.17** Temperature/salinity profiles measured northwest of North Head.

**Figure 2.18** Temperature/salinity transect across the Beaufort Shelf between June and September.

**Figure 2.19** Suspended sediment concentrations (mg/l) of the Mackenzie Delta plume (Harper and Penland, 1987).

**Figure 2.20** Directional frequency distribution of near-bottom currents from the eastern Beaufort Shelf (Harper and Penland, 1987).

**Figure 2.21** Directional frequency distribution of strong bottom currents (15-40 cm/s) from the eastern Beaufort Shelf (Harper and Penland, 1987).

**Figure 2.22** Directional distribution of currents from the inner Beaufort Shelf (Davidson et al., 1988).

**Figure 2.23** Offshore wave characteristics scatter plot for the North Head region (Pinchin and Nairn, 1987).

**Figure 2.24** Directional wave energy for the Beaufort Shelf as computed from the wave climate summaries of Baird and Hall (1980) and Harper and Penland (1987). The shaded area of the wave rose represents wave power components resulting in wave heights in excess of 2 m.

**Figure 3.1** Location map of cliff and beach survey measurements along the Beaufort Sea coast..

**Figure 3.2** Track plot of seismic data collected under NOGAP Project D.1 from 1985 to 1987.

**Figure 3.3** Map showing the locations of the North Head, 1984 and King Point, 1985 drilling programs.

**Figure 3.4** Map showing the locations of 1984 boreholes, Nahidik '86 gravity cores, and Nahidik '87 vibracores.

**Figure 3.5** Map showing the locations of King Point, 1985 and Tibjak Beach, 1987 sediment transport field measurements.

**Figure 4.1** Previous sea-level curves: (a) Forbes, 1980; (b) Hill et al. (1985).

**Figure 4.2** Map showing locations of samples used for constraining relative sea level.

**Figure 4.3** A revised Holocene relative sea level curve for the Canadian Beaufort Sea, based on the dates listed in Table 4.1.

**Figure 4.4** Map showing the location of three cores collected in 1987, in a tidal marsh behind Topkak Spit.

**Figure 4.5** Core C-88-1 from Topkak marsh.

**Figure 4.6** Core A2-87 collected at Atkinson Point on the backshore side of the spit extending into McKinley Bay.

**Figure 5.1** Surficial geology and location map of the Yukon coast.

**Figure 5.2** Distinct landforms resulting from erosional processes: (a) retrogressive thaw flow slide, (b) polygon block failure; (c) cliff face gully between King Point and Kay Point.

**Figure 5.3** (a) Clarence River Delta; (b) Malcom River alluvial fan delta system fronted by Nunaluk Spit; (c) Firth River alluvial fan delta complex fronted by Barriers 1 and 2 of the Nunaluk Spit system; (d) Spring River Delta; (e) Babbage River Delta fronted by Kay Point Spit (modified from Forbes, 1981); (f) Running River Delta; (g) Blow River Delta.

**Figure 5.4** (a) Advalek Spit; (b) Catton Point-Osborne Point Spit; (c) Stokes Point Barrier; (d) Kay Point Spit; (e) King Point Barrier; (f) Shingle Point and Escape Reef.

**Figure 5.5** The evolution of King Point from 1826 to 1970.

**Figure 5.6** Late Wisconsinan and 1986 paleogeography between Kay Point and Hershel Island (Forbes, 1981).

**Figure 5.7** Interpreted surficial seismostratigraphy of the Yukon Shelf (from Earth and Oceans Ltd., 1986).

**Figure 5.8** High resolution seismic record across the Yukon Shelf, southeast of Herschel Island, showing seismostratigraphic units described in the text. The arrow on the index map refers to both the seismic line location and the location of nearshore vibracores between King Point and Sabine Point.

**Figure 5.9** Location map for King Point, showing boreholes and survey lines (Hill, 1990).

**Figure 5.10** Lithostratigraphic summary of King Point based on borehole information (Hill, 1990). Transect A-A' shown in Figure 5.10. Transects A, B and C shown in Figure 5.12.

**Figure 5.11** Pollen profile of the lacustrine sequence in borehole KM10 (J. Shaw, pers. comm.).

**Figure 5.12** Barrier profiles at King Point (Hill, 1990).

**Figure 5.13** Four shallow vibracores - 112, 113, 116 and 117 - from the nearshore zone between King Point and Sabine Point.

**Figure 5.14** Plasticity chart for sediments from the King Point borehole program (data from O'Connor, 1986).

**Figure 5.15** The grain size distribution of (a) pre-Holocene, (b) lacustrine and (c) barrier facies from King Point.

**Figure 5.16** Water content and shear strength profiles for King Point borehole data: (a) KF1, (b) KF2, (c) KF10, and (d) KF7. For borehole locations see Figure 5.9.

**Figure 5.17** Time series of wind speed and wind direction from King Point for August and September, 1985 (Fissel et al., 1987).

**Figure 5.18** Current speeds and directions recorded during August and September, 1985 in 2.7 m water depth off of King Point.

**Figure 5.19** King Point water temperature records for August and September, 1985 at 5 m and 10 m water depth.

**Figure 5.20** Three representative beach profiles from King Point (for locations see Fig. 5.9).

**Figure 5.21** Schematic location of grain size samples from four zones along the King Point beach: the berm, the beach face, the nearshore zone and at 20 m and 50 m offshore (McLaren, 1986).

**Figure 5.22** Grain size distributions from King Point: (a) berm spectra, (b) beach face, (c) nearshore zone at 20 m water depth, and (d) nearshore zone spectra at 50 m water depth.

**Figure 5.23** Alongshore changes in grain size of beach face sediments at King Point.

**Figure 5.24** Wave height and wave period data recorded from Seadata meter 635-12 at King Point for August and September, 1985.

**Figure 5.25** Results of the hindcast and field data comparison (a) using offshore winds measured at the Explorer III site; and (b) using winds measured at King Point.

**Figure 6.1** Location map of the modern Mackenzie Delta coast stretching between the Blow River Delta and Richards Island.

**Figure 6.2** The development of the Olivier Islands from pre-1943 to 1987 (Jenner, 1989).

**Figure 6.3** Schematic cross-section through the Mackenzie Trough (Blasco et al. 1989).

**Figure 6.4** Air gun profile of the late Wisconsin delta sequence, MT1, downlapping onto the regional reflector MT2.

**Figure 6.5** Boomer profile 87-06C, with east-west orientation, showing the channels at the top of the late Wisconsinan sequence. The channels display flat bases and are comprised of complex stratified fill.

**Figure 6.6** Air gun profile showing two distinct reflectors at the top of the MT1 delta sequence (from Moran et al., 1989). See Figure 6.9 for location.

**Figure 6.7** Boomer profile 87-06 showing discontinuous gas-charged reflector near the top of the Holocene delta sequence.

**Figure 6.8** Composite section of the Mackenzie Delta compiled from the work of C.P. Lewis (1988) and seismic data.

**Figure 6.9** (a) Composite diagram of piezocone profile showing cone bearing ( $Q_c$ ), pore pressure ( $u$ ) and friction ( $f_c$ ) with the corresponding air gun reflection seismic profile. (b) Interpreted lithofacies and depositional environments of site MTW01 (Moran et al., 1989).

**Figure 6.10** Detailed location map of the Olivier Islands (from Jenner, 1989).

**Figure 6.11** Summary of sediment facies in the distributary mouth region of the Olivier Islands (from Jenner, 1989).

**Figure 6.12** The distribution of sediment facies throughout Pitt Island (from Jenner, 1989).

**Figure 6.13** Location of Nahidik 1987 vibracores in the Mackenzie Delta region.

**Figure 6.14** Sedimentological logs of the Nahidik 1987 vibracores taken from a nearshore transect in front of the Mackenzie Delta (Fig. 6.13); (b) Sedimentological logs of the Nahidik 1987 vibracores taken from a second nearshore transect in front of the Mackenzie Delta (Fig. 6.13).

**Figure 6.15** Detailed sediment logs for vibracores 27 and 30.

**Figure 6.16** Photographs of sedimentary structures from 3 m water depth: (a) graded bed of planar cross-laminated sand with sharp base, grading into silt and clay, Core 87-027, 62-77 cm; (b) sand bed with wave ripple near base, mudclast gravel layer in centre and ripples at top, Core 87-027, 22-37 cm.

**Figure 6.17** Photographs of sedimentary structures from 3 m water depth: (a) trough cross-lamination with organic-rich laminae, Core 87-027, 11-23 cm; (b) possible megaripple bedding, Core 87-027, 96-111 cm.

**Figure 6.18** Photographs of sedimentary structures from 3 m water depth: (a) climbing ripple lamination with particulate organic material in ripple troughs, Core 87-027, 185-200 cm; (b) convolute lamination, Core 87-027, 34-49 cm.

**Figure 6.19** Photographs of sedimentary structures from 3 m water depth: (a) thin clay beds with subvertical cracks or burrows, Core 87-027, 133-148 cm; (b) U-shaped loaded laminae, Core 87-027, 120-135 cm.

**Figure 6.20** Photographs of sedimentary structures from 4 m water depth: (a) organic-rich, parallel laminated silt, Core 87-030, 26-41 cm; (b) organic-rich silt infilling silt ripple trough, Core 87-030, 92-108 cm.

**Figure 6.21** Photograph of sedimentary structures in 4 m to 7 m water depth: (a) very fine, parallel laminated and poorly bioturbated silt, Core 87-011, 15-25 cm.

**Figure 6.22** Mean monthly sediment supply to the Mackenzie Delta from the Mackenzie River above Arctic Red River, 1974-1983 (Lewis, 1988).

**Figure 6.23** Map of nearshore ice-melt lagoon during the break-up period in late May (Pilkington, 1988).

**Figure 6.24** (a) Wind record for Pelly Island and (b) water level record for Reindeer Channel from July to September, 1987, showing correlation of high water levels with strong northwesterly winds (from Jenner, 1989).

**Figure 6.25** Wind data from the Explorer III at the Adlartok drill site in the Mackenzie Trough, August and September, 1985.

**Figure 6.26** Near surface current data from the Adlartok drill site in the Mackenzie Trough, August and September, 1985.

**Figure 6.27** (a) Return period for resuspension events based on silt beds in cores; and (b) the same data plotted as the frequency of bottom disturbance with values of mean bottom stress derived from wave and current data from various sites in the Beaufort Sea (data from Davidson et al., 1988).

**Figure 7.1** Detailed surficial geology of Richards Island area (from Rampton, 1988).

**Figure 7.2** (a) Morphology of Garry Island; (b) Morphology of Pelly Island; (c) Morphology of Hooper Island; (d) Morphology of Pullen Island.

**Figure 7.3** Intertidal flats and subtidal mudbank bordering the western coast of North Point.

**Figure 7.4** Morphology of eastern Richards Island.

**Figure 7.5** Retreat rates around North Point (Dallimore et al., 1988).

**Figure 7.6** Pelly Island morphological change from 1950 to 1985 (after Ruz et al., in prep.).

**Figure 7.7** Seismic track chart - Garry Island to North Head.

**Figure 7.8** Seismic profile 87-06, showing the well stratified character of sequence 1 over most of Kringalik Bank.

**Figure 7.9** (a) Seismic profile 86-20 194-200, showing stratigraphic thinning of sequence 1 over the centre of Kringalik Bank (b) Seismic profile 86-19, showing progradational reflectors within a low relief bank of sequence 1.

**Figure 7.10** Stratified character of gas-free sediments on Kringalik Bank; seismic profile 86-21.

- Figure 7.11** Ikit Trough seismic stratigraphy from Hill et al. (in press).
- Figure 7.12** Seismic profile 86-15, showing erosional base of the Ikit Trough reflector.
- Figure 7.13** Line drawing of seismic profile 86-20, showing a strong reflector which may represent a deeper part of Ikit Trough. For location, see Figure 7.7.
- Figure 7.14** Seismic profile 86-16, showing gas enhanced 20 ms reflector.
- Figure 7.15** Seismic profile 87-2 showing irregular unconformity surface. Bottom profile is a continuation of the upper profile.
- Figure 7.16** Seismic profile 87-2 showing planed off highs and truncation of underlying reflectors. Bottom profile is a continuation of the upper profile.
- Figure 7.17** Line drawing of seismic profile from the east side of North Head, showing sub-bottom high piercing the unconformity surface (Lewis, 1989).
- Figure 7.18** Summary sketch seismic section for the Garry Island to Summer Island region.
- Figure 7.19** Site specific 7 kHz profiles at locations of Cores 87-36 to 87-63, showing reflection character.
- Figure 7.20** Lithologic logs of vibracore transect across buried bank feature within sequence 1 (Fig 7.9).
- Figure 7.21** Typical lithology on the flanks of the bank where the sequence is thickest. Thin graded silt beds in predominantly bioturbated silty clay sequence, Core 87-036, 30-70 cm.
- Figure 7.22** Bank sequence lithologies: (a) Thin bedded sand, silt and clay, with sand-filled burrows, Core 87-045, 231-246 cm.
- Figure 7.23** (a) Poorly sorted slurry bed, Core 87-045, 186-202 cm; (b) sub-vertical cracks, Core 87-048, 164-184 cm.
- Figure 7.24** Lenticular sand, Core 87-048, 112-128.
- Figure 7.25** (a) Complex graded bed with five units, Core 87-048, 83-98 cm; (b) graded bed with shell hash, Core 87-048, 7-22 cm.
- Figure 7.26** Multiple graded bed, Core 87-048, 75-90 cm.
- Figure 7.27** Transect of Cores 87-66-87-84, in the Ikit Trough region, showing generalized lithology. Note abundance of bioturbated silt beds.
- Figure 7.28** Pervasively bioturbated silt beds, Core 87-069, 110-140 cm.
- Figure 7.29** Stratigraphy and surficial facies distribution of the 1984 North Head boreholes (from Hill and Nadeau, 1989).
- Figure 7.30** Deeper sediment facies from the 1984 North Head boreholes (from Hill et al., 1986).
- Figure 7.31** Plasticity chart for 1984 North Head borehole sediments.
- Figure 7.32** Downhole shear strength plots for bioturbated silts and laminated silts and clays, North Head boreholes.

**Figure 7.33** Significant wave height time series for three sites on the Garry Island to Summer Island inner shelf.

**Figure 7.34** Current meter records from the inner shelf north of Richards Island (from Davidson et al., 1988).

**Figure 7.35** Time series of (a) bottom stress derived from wave and current measurements at the T1.2 site, and (b) suspended sediment concentrations (SSC) from an optical backscatter sensor, mounted 1 m above the seabed.

**Figure 7.36** Suspended sediment concentrations and bottom stress near the seabed east of North Point from the 1987 program (from Hodgins, 1988).

**Figure 8.1** NAH86 seismic track plot from Kugmallit Bay.

**Figure 8.2** Depth to unconformity map of Kugmallit Bay, based on NAH86 and NAH87 seismic records (after Jenner, 1987).

**Figure 8.3** Seismic profile NAH87-3 with interpreted line drawing, west of Toker Point. Note section orientation shows west to the right and east to the left.

**Figure 8.4** Seismic profile NAH87-3 with interpreted line drawing (continuation of profile in Figure 8.3) just south of James Shoal.

**Figure 8.5** Sketch of seismic profile NAH86-5.1. Original record is too noisy for reproduction.

**Figure 8.6** Seismic and sidescan sonar records NAH87-3, west of James Shoal, showing pockmarks on seabed and active gas venting.

**Figure 8.7** Location map for gravity cores collected in Kugmallit Bay on NAH86 cruise (from Jenner, 1987).

**Figure 8.8** North-south core transect in Kugmallit Bay showing distribution of sediment facies (from Jenner, 1987).

**Figure 8.9** East-west core transect in Kugmallit Bay showing distribution of sediment facies (from Jenner, 1987).

**Figure 9.1** Location map for the Tuktoyaktuk Peninsula, showing geology, ice margins and place names.

**Figure 9.2** Map of the Tuktoyaktuk Peninsula showing the location of the other figures referenced in the text. Numbers refer to locations in Table 9.1.

**Figure 9.3** Location map of the spits and barrier islands of the south and east coast of Kugmallit Bay. Numbers refer to locations in Table 9.1. Box shows the location of Figure 9.10.

**Figure 9.4** Warren Point barrier-spit system. Legend applies to remaining spit and barrier figures in Chapter 9 unless otherwise included.

**Figure 9.5** Interpretation of sedimentary environments in the area of the Southwest Atkinson barrier island along the Tuktoyaktuk Peninsula (from Ruz et al., in prep.).

**Figure 9.6** Atkinson Point spit and barrier island system.



**Figure 9.7** The spits of the eastern shore of McKinley Bay.

**Figure 9.8** Relationship between the rates of landward migration of the spits and barrier islands of the Tuktoyaktuk Peninsula and the rates of potential longshore sediment supply (after Héquette and Ruz, in press).

**Figure 9.9** Conceptual geomorphic model of spit and barrier island migration in the southeastern Canadian Beaufort Sea showing idealized plane view and cross-section with major sediment transport paths. 1: Spit; 2: Barrier island (from Héquette and Ruz, in press.).

**Figure 9.10** Evolution of the coastline between 1935 and 1973 at one site on the southern shore of Kugmallit Bay, west of Tuktoyaktuk (site 3 in Fig. 9.5.). Only the largest lakes are shown. (From Ruz et al., in prep.).

**Figure 9.11** Comparison of 1950 and 1985 aerial photographs showing the coastwise progradation and the retreat of Mingnuk spit and the erosion of the adjacent bluffs (from Héquette and Ruz, in press).

**Figure 9.12** Aerial photograph comparison showing the landward migration of Cape Dalhousie barrier island system between 1950 and 1985 (after Héquette and Ruz, in press).

**Figure 9.13** Schematic geomorphic model illustrating the stages of barrier island formation in the southeastern Canadian Beaufort Sea from an hypothetical bluff shoreline (1). The model shows two different types of evolution depending on the exposure of the coast to wave energy (A: sheltered coastal environment; B: wave-exposed coastal environment). In the more exposed areas, the highest rates of coastal erosion result in larger amount of sediment supplied to the littoral zone which make possible the construction of larger coastal accumulation features. (From Ruz et al., in prep.).

**Figure 9.14** Locations of seismic profiles and vibracores (from Hequette and Hill, 1989).

**Figure 9.15** Typical seismic profile from Tuktoyaktuk Peninsula inner shelf (from Hequette and Hill, 1989).

**Figure 9.16** Summary of seismic units from Tuktoyaktuk Peninsula inner shelf (from Hequette and Hill, 1989).

**Figure 9.17** Wind speed and direction from Tuktoyaktuk during the Tibjak Beach program, Aug 27 to Sept. 17, 1987 (from Fissel and Byrne, 1988).

**Figure 9.18** Significant wave height and wave period time series for Tibjak Beach, Aug 27 to Sept. 17, 1987 (from Fissel and Byrne, 1988).

**Figure 9.19** Currents at Tibjak Beach, August 27 to September 17, 1987 (from Fissel and Byrne, 1988).

**Figure 9.20** Shoreface profile changes due to ice scour (from Hequette and Barnes, 1990).

**Figure 9.21** Map showing the study site and location of current meters, video camera and beach transects.

**Figure 9.22** Distribution of wave direction (upper diagram) and of significant wave height at breaking (lower diagram).

**Figure 9.23** Comparison of visual estimates of wave breaker height using video records with computed breaker height after refraction of the waves recorded in 3.5 m water depth.

**Figure 9.24** Relationship between breaker height ( $H_b$ ) and the surf-scaling parameter ( $\epsilon$ ). Breaking wave types are visual estimations using video records. The limits between beach morphodynamic domains are values from Wright and Short (1984) and from Carter (1988).

**Figure 9.25** Variations in beach profile and sediment texture at Tibjak Beach (see Fig. 9.12 for beach profiles location).

**Figure 9.26** Time-series plot of mean current velocity, significant breaker height, significant wave period, mean water level, and wave direction obtained from Sea Data model 621 current meter data recorded in 3.5 m water depth offshore of Tibjak Beach (instrument water depth is 2.4 m). Note that the significant breaker height represents computed values from significant wave height as recorded in 3.5 m water depth after refraction using a computer simulation; water depth is variable as it depends on the breaker height. The shaded area represents a storm event during which no offshore-directed currents occurred.

**Figure 9.27** Sidescan sonar record showing bands of megaripples and flat shallow channel-like features perpendicular to the coast, 200 m southwest of the Sea Data 621 current meter, 6 September 1987. Shore side at bottom. Water depth along side-scan trackline is 4.0 m above chart datum.



## LIST OF TABLES

- Table 3.1** List of field programs conducted in the Beaufort Sea coastal zone under NOGAP D.1, 1984-1988.
- Table 3.2** List of major desk studies on the Beaufort Sea coastal zone.
- Table 3.3** Seismic equipment used for NOGAP D.1 coastal zone surveys, 1985-1988.
- Table 3.4** Wave and current data sets collected by other agencies from the Beaufort Sea coastal zone and used in NOGAP D.1 studies.
- Table 4.1** Samples used to construct the most recent Holocene RSL curve.
- Table 4.2** Radiocarbon dates obtained from the cores in Atkinson Point, McKinley Bay and Topkak marsh.
- Table 5.1** Yukon Coast - average retreat rates (m/a).
- Table 5.2** Predicted wave conditions along the Yukon Coast.
- Table 7.1** Cliff retreat measurements in the Garry Island to Summer Island region.
- Table 7.2** Physical properties of fine-grained sediments, North Head borehole transect (from Hill et al., 1986).
- Table 7.3** Grain size distributions for coarse-grained sediment, North Head borehole transect (from Hill et al., 1986).
- Table 7.4** Predicted deep water wave heights for various return periods for North Head, based on a 14 year wave hindcast (from Pinchin et al., 1985).
- Table 9.1** Dimensions and retreat rate of spits and barrier islands along the Tuktoyaktuk Peninsula.
- Table 9.2** Average retreat rates calculated by coastal type (data from Harper et al., 1985).
- Table 9.3** Ground survey measurements of coastal retreat along the Tuktoyaktuk Peninsula.
- Table 9.4** Predicted deep water wave heights for various return periods for Atkinson Point, based on a 14 -year hindcast of winds at Tuktoyaktuk.
- Table 10.1** List of potential publications resulting from NOGAP Project D.1.
- Table 10.2** Persons interviewed during the course of this study for the evaluation of AGC's client needs.



## 1. INTRODUCTION

The Beaufort Sea coastline between the Alaska border and Cape Dalhousie (Fig. 1.1) is a unique environment in Canada. The entire coastline consists of low cliffs of unconsolidated, ice-bearing and permafrost-affected Quaternary sediments, that are extremely susceptible to erosion. The coastal plain and waters of the Mackenzie River provide a vital habitat to a variety of mammals, birds and fish, that in turn provide subsistence to the native human population. Since the 1970's, hydrocarbon exploration has proven the presence of substantial reserves of both oil and gas beneath the Mackenzie Delta and the Beaufort Sea. The production of these resources will require the construction of artificial islands, pipelines and other installations in the coastal zone. In addition to being a sensitive coastal environment, the understanding of arctic coastal processes, involving ice as well as waves, currents and tides, is relatively poor compared to that of coastal processes in more temperate regions. The need for coastal studies in the Beaufort Sea is therefore great.

### 1.1 Beaufort Sea Coastal Research

The pioneer of coastal studies in the Beaufort sea region was J. R Mackay, who conducted reconnaissance surveys of various coastal sites (Mackay, 1959; 1960; 1963a) and conducted a major geographical study of the Mackenzie Delta and adjacent regions (Mackay, 1963b). In the 1970's, the discovery of potential oil and gas reserves in the Beaufort Sea led to an acceleration of work in the region. McDonald and Lewis (1973) carried out a reconnaissance survey of the rivers and coastline of the Yukon Coastal Plain under the "Environmental-Social Program, Northern Pipelines" of the Canadian Government Task Force on Northern Oil Development. Subsequently, the Beaufort Sea project was established to provide a better database for decision making on environmental and development issues in the region. Numerous reports from the Beaufort Sea Project were published and remain today as an important base for geological and oceanographic studies of the region. Reports relevant to the coast include Lewis and Forbes (1975), Henry (1975), Davies (1975), Markham (1975), MacNeill and Garrett (1975), Huggett et al. (1975), Herlingveaux and de Lange Boom (1975), Pelletier (1975) and Rampton (1988).

Exploration continued during the late 1970's and the federal government established the Office of Energy Research and Development (OERD; later the Panel on Energy Research and Development, PERD) to support R&D in the energy sector. OERD established a set of themes, one of which was related to oil and gas. Funding was provided to various projects within this

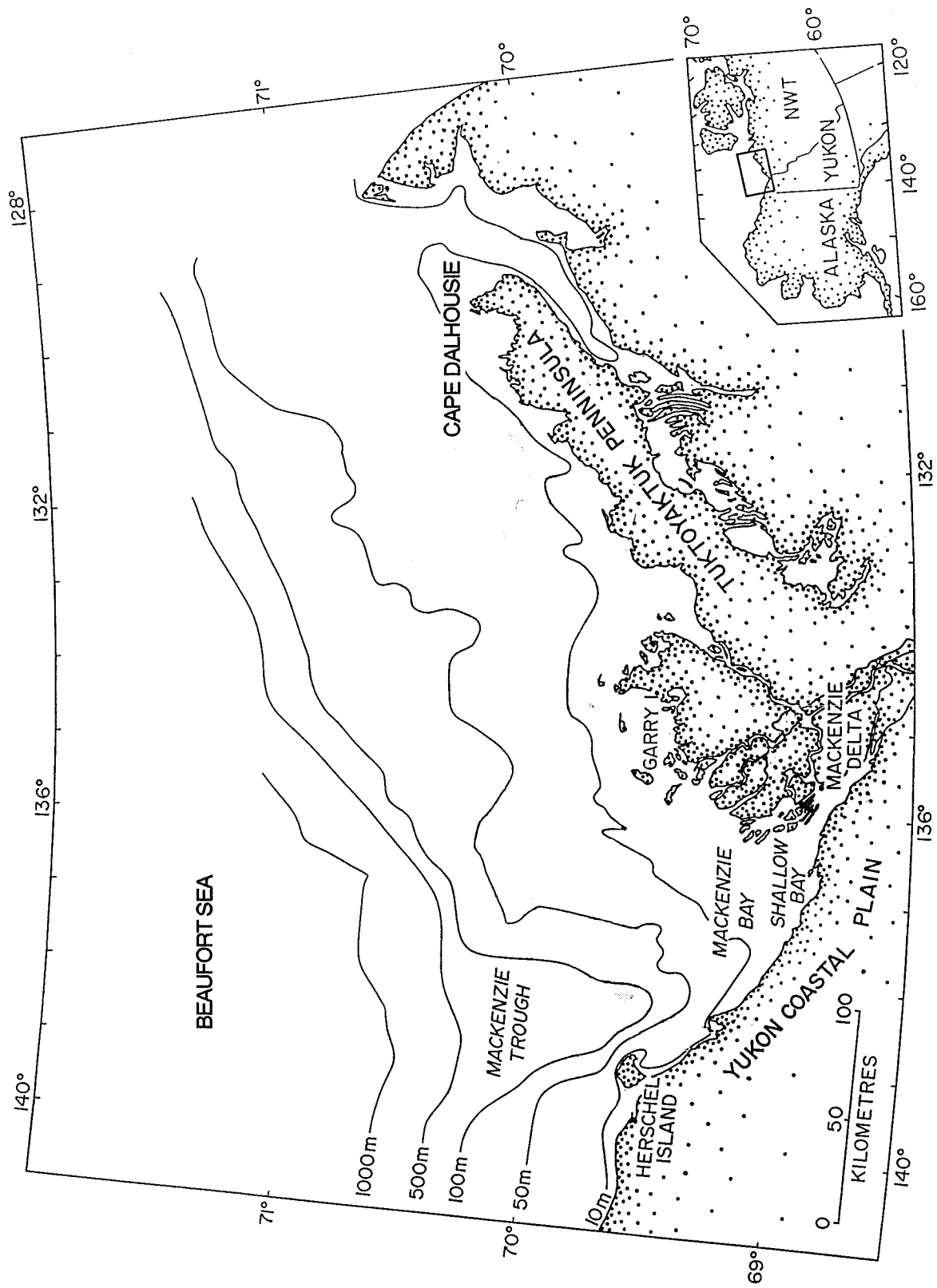


Figure 1.1 Beaufort Sea coastline between the Alaskan border and Cape Dalhousie.



theme, including two of direct relevance to exploration in the Beaufort. PERD projects 6.1 (Permafrost) and 6.3 (Beaufort Sea Geotechnics) supported geological, geophysical and geotechnical research in the Beaufort Sea through the 1980's (including parts of the offshore research reported on in this document), and are both still active today. PERD projects are administered by joint industry/government committees. The Geological Survey of Canada (GSC) was the government agency responsible for projects 6.1 and 6.3, with Terrain Sciences Division (TSD) taking the lead with project 6.1, and the Atlantic Geoscience Centre (AGC) taking the lead with project 6.3. The PERD program caters primarily to industry's needs for research and development, while keeping government agencies informed and up-to-date on important technical issues.

## **1.2 The NOGAP Program**

The principal operators in the Beaufort Sea submitted an Environmental Impact Statement (EIS), which was reviewed by an Environmental Assessment Review Board. The board made a variety of recommendations, which dealt with social and environmental issues resulting from the exploration and production of hydrocarbons in the Beaufort Sea. A principal recommendation was for the government to develop and conduct a wide-ranging research program on these issues. In response, Indian and Northern Affairs Canada developed the Northern Oil and Gas Action Program (NOGAP), involving proposals from various federal departments and territorial governments. Recognizing a need to obtain information on coastal stability, geotechnical conditions and sedimentation processes in the coastal zone of the Beaufort Sea, AGC proposed Project D.1, "Coastal Zone Geotechnics". The objectives of the NOGAP D.1 Project were stated as follows:

### ***General:***

Through geological, geophysical and geotechnical research on the processes taking place along the coasts of the Beaufort Sea and on the materials and permafrost features of the coast, to provide public information concerning the coastal zone as required by government for land use planning and regulation and as required by industry in the design of facilities and activities.

### ***Specific:***

1. To provide an understanding of rates and processes of coastline change to predict the impact of

proposed development.

2. To provide a knowledge base concerning the nearshore bottom materials which will be crossed or excavated or built on in the course of development.
3. To provide a knowledge base concerning the onshore geological materials adjacent to the coast and the associated permafrost conditions, that relate to the rate of coastal retreat and the recognition and assessment of geotechnical constraints encountered by onshore coastal engineering works.
4. To provide a knowledge of ice, wave, current and surge regimes in the coastal zone, as they affect coastal stability and interact with man-made facilities.
5. To demonstrate the effects of man-made features, such as pipelines, causeways, artificial islands and support bases on the coastal environment.

NOGAP and Project D.1 were approved in May 1984 and the G.S.C. was provided with two person-years to conduct the program, with an operating budget of \$300K to \$400K per year. One of these person-years was provided to A.G.C, and the second to TSD. Management of the project was undertaken by AGC. Scientific responsibilities were split between AGC and TSD in the following manner. AGC were to conduct aspects of the projects related to objectives 1, 2, 4 and 5, while TSD were responsible for projects related to objective 3. One modification to the objectives was subsequently made in consultation with GSC's Chief Geologist. It was recognized that there was overlap with PERD project 6.1 on the issue of permafrost. It was therefore decided that permafrost studies would be funded by PERD, whereas studies within NOGAP would concentrate on the mapping of materials, sedimentation processes and assessment of geotechnical constraints.

### **1.3 Objectives of This Report**

Although AGC had proposed a six-year program, funding for the program was approved by Treasury Board for a four-year period, 1984-1988. The entire NOGAP program was terminated in 1988, after the initial four years, with the loss of the assigned person-years and leaving a large amount of data unsynthesized. Funds to complete the project and this report were obtained from the Marine Environmental Initiative of the Geological Survey of Canada and from PERD 6.3. Hill Geoscience Research was contracted to undertake three main tasks: (i) to synthesise and make preliminary interpretations of the various data sets collected in the course of the AGC research program; (ii) to determine future priorities for coastal zone research in the

Beaufort Sea; and (iii) to recommend a new program of research to meet those priorities.

The intent of this report is to provide a comprehensive summary of our knowledge about the coastal zone. For purposes of this report, the coastal zone is defined as the region between the cliff line and the 10 m isobath, including depositional landforms such as deltas, spits and barrier islands. The report only includes analyses of field data collected by AGC or its contractors. Additional published information describing the adjoining offshore and land geology are included as background. For more detailed accounts of the terrestrial geology, permafrost and ground ice, the reader should contact the Terrain Sciences Division of the Geological Survey of Canada.

#### **1.4 Organization of the Report**

The hope in writing this report was that it would be a useful source of information for government, industry and community groups interested in the Beaufort Sea coastal zone. For this reason an extensive discussion of the geological and oceanographic background of the Beaufort Sea is presented in Chapter 2. Methods and data used in NOGAP D.1 studies are then outlined in Chapter 3. As relative sea level change is an important constraint on coastal evolution, Chapter 4 is devoted to new radiocarbon dates which can be used to determine Holocene relative sea level change in the Beaufort region. In chapters 5 through 9, the coastal geology of different sections of the coast are discussed in detail. Chapter 10 consists of a discussion of future research directions, through an identification of areas of needed research and an assessment of the objectives in the light of community, industry and government needs.

#### **1.5 Credits and Acknowledgements**

The information presented in chapters 4 through 9 has been produced during the NOGAP D.1 project. The project was directed in 1984 by D.L. Forbes and subsequently, from 1985 through 1988, by P.R. Hill. The NOGAP project funded most of the research reported on in this document, including numerous contract studies (see Appendix 1) and an MSc. thesis by K.A. Jenner. Some of the offshore research discussed in this report was financed under the PERD program, particularly PERD 6.3. Funding for the completion of the final report was provided by the Marine Environmental Initiative of the Geological Survey of Canada with supplemental funding from PERD 6.3.

The sediment transport field program at King Point was organized and supervised by P. Morgan in 1985, while employed at AGC on a term position. From May 1987 to October 1989,

post-doctoral fellow A. Héquette contributed substantially to the project, working particularly on aspects of the Tuktoyaktuk Peninsula coast. Héquette continued to work on the project until December 1989, with funding from an NSERC operating grant (to P.R. Hill). Marie-Hélène Ruz has also carried out studies in the Tuktoyaktuk Peninsula coast, as a private individual.

In the course of the project, numerous individuals have contributed through technical assistance, discussions and encouragement. We would particularly like to thank S.M. Blasco, R.A. Harmes, K. Moran, D. Gillespie, D.J.W. Piper, K. Robertson, D.L. Forbes, R.B. Taylor, P.W. Barnes, E. Reimnitz, S.R. Dallimore, J.R. Harper, D.B. Fissel, F. Jodrey, M. Hughes, B. Murphy, B. Chapman, and R. Sparkes. Vital logistic support was provided by the Inuvik Research Laboratory and the Polar Continental Shelf Project. Shipboard work was greatly facilitated by the captain and crew of *CCGS Nahidik*.

This report has been written by P.R. Hill with contributions from Héquette, Ruz and Jenner. The report includes summaries of contractor studies conceived and supervised by Hill and Forbes. In some chapters, the previous work of J.R. Mackay, V. Rampton, B.C. McDonald, C.P. Lewis, and others, have been used for the sake of completeness. Results from all these studies are clearly identified and credited to the author or contractor as appropriate. Finally, we would like to thank Bob Taylor, Scientific Authority for this contract, for his support and assistance throughout this contract.

## 2. BACKGROUND

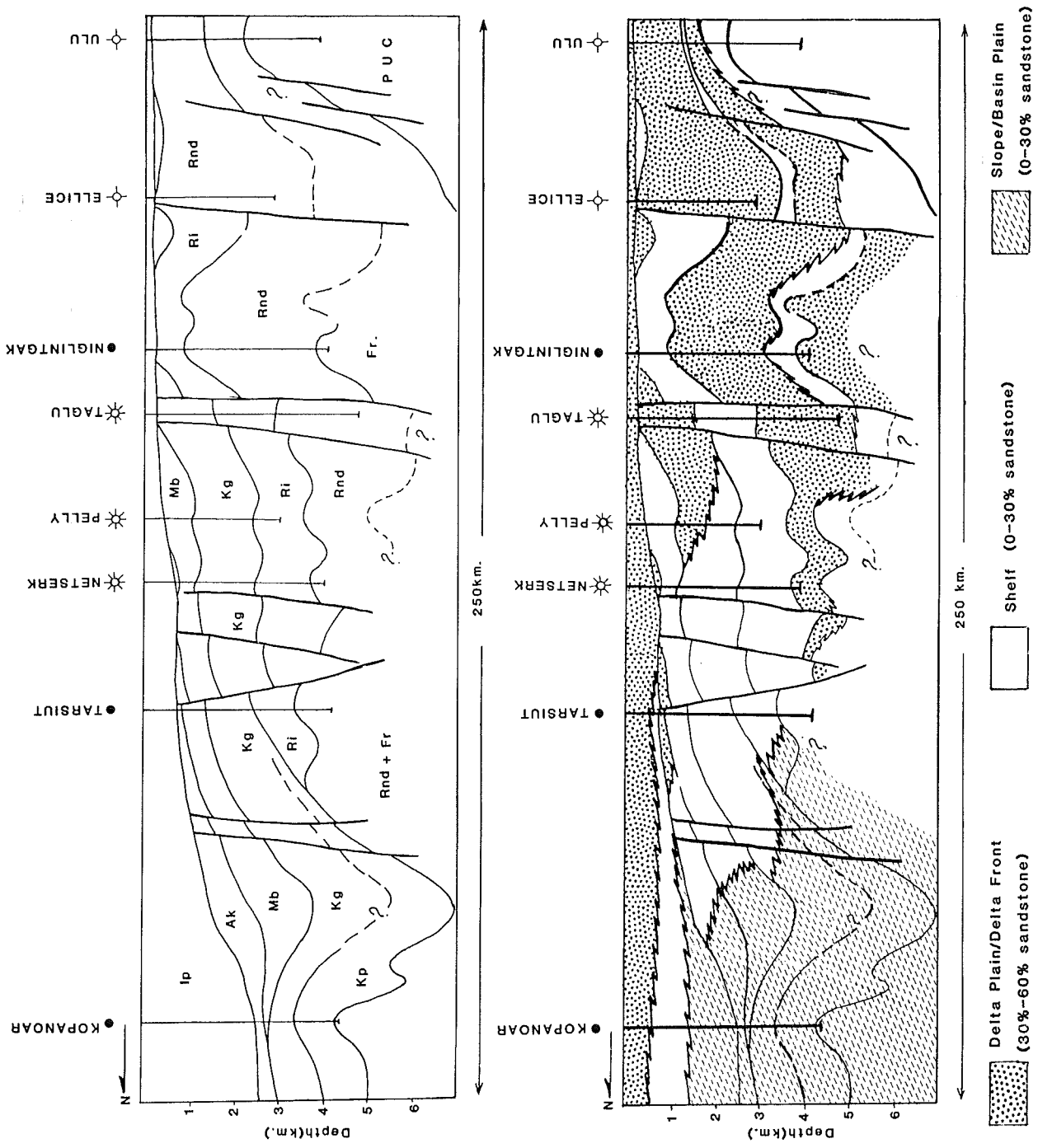
The coastal zone of the Beaufort Sea is influenced by a variety of factors including geology, climate, permafrost and ground-ice conditions, the Mackenzie River hydrological regime, the sea-ice regime, oceanographic parameters such as waves, currents and storm surges, and changing sea-level. In this chapter, an overview of these factors is presented to serve as background to the study. Sea-level change is treated exhaustively in Chapter 4, and is therefore not included here. With the exception of climate, permafrost and ground-ice, the other factors reviewed here will be discussed in more detail, by geographic region, in later chapters.

### 2.1 Geological Setting

The Canadian Beaufort Sea fills a broad embayment of the Arctic Ocean between the Alaskan Peninsula and the Queen Elizabeth Islands of northern Canada (Fig. 2.1). The embayment forms the southern part of the Canada Basin, which has been the site of major sediment deposition and basin downwarping since the mid-Cretaceous (Dietrich et al., 1985). The continental margin to the south of the basin consists of two principal tectonic zones: the Northern Interior Platform, consisting of largely undeformed Proterozoic and lower Paleozoic clastic and carbonate rocks overlain by Cretaceous clastic sediments; and the northern Canadian Cordillera, consisting mainly of folded and faulted Mesozoic rocks. The structure of the northern Cordillera is complex. Within an overall arch structure (the Aklavik Arch complex), numerous uplifted blocks are separated from intervening small basins by north-trending faults. The Rapid Fault Array, which intersects the coast between Shingle Point and Shallow Bay, is thought to have accommodated much of the major wrench-movements along the Kaltag Fault of central Alaska since the Early Cretaceous (Yorath and Norris, 1975).

The Beaufort - Mackenzie Basin is filled with over 6 km of Upper Cretaceous, Tertiary and Quaternary sediments. The basin margin is block faulted along the Eskimo Lakes fault system and numerous growth faults are present within the thick sequence of deltaic and marine sediments which fill the basin (Cote et al., 1975). Eleven major seismo-stratigraphic sequences have been recognised in the Beaufort - Mackenzie Basin (Fig. 2.2; Dietrich et al., 1985). The youngest two sequences, the Shallow Bay and Iperk (Ip on Fig. 2.2), overlie a regional unconformity that separates Miocene from Plio-Pleistocene sediments (S. Blasco, personal communication). Biostratigraphic control on the base of the Iperk sequence is limited but unpublished data suggests that the sequence represents at least 2.4 Ma of deposition (S. Blasco, personal communication). Within the Iperk, numerous depositional cycles representing delta and/or shelf progradation and





**Figure 2.2** Schematic structural - stratigraphic section through the Beaufort - Mackenzie Basin (from Dietrich et al., 1985).



transgression have been distinguished in multichannel seismic records (Fortin, 1990). Study of well logs suggests that each cycle is also associated with a layer of permafrost, so that the Iperk sequence consists of a multiple layers of frozen and unfrozen sediments (Fortin, 1990). This provides an important control on rates of compaction subsidence in the Beaufort - Mackenzie Basin.

## **2.2 Quaternary Geology**

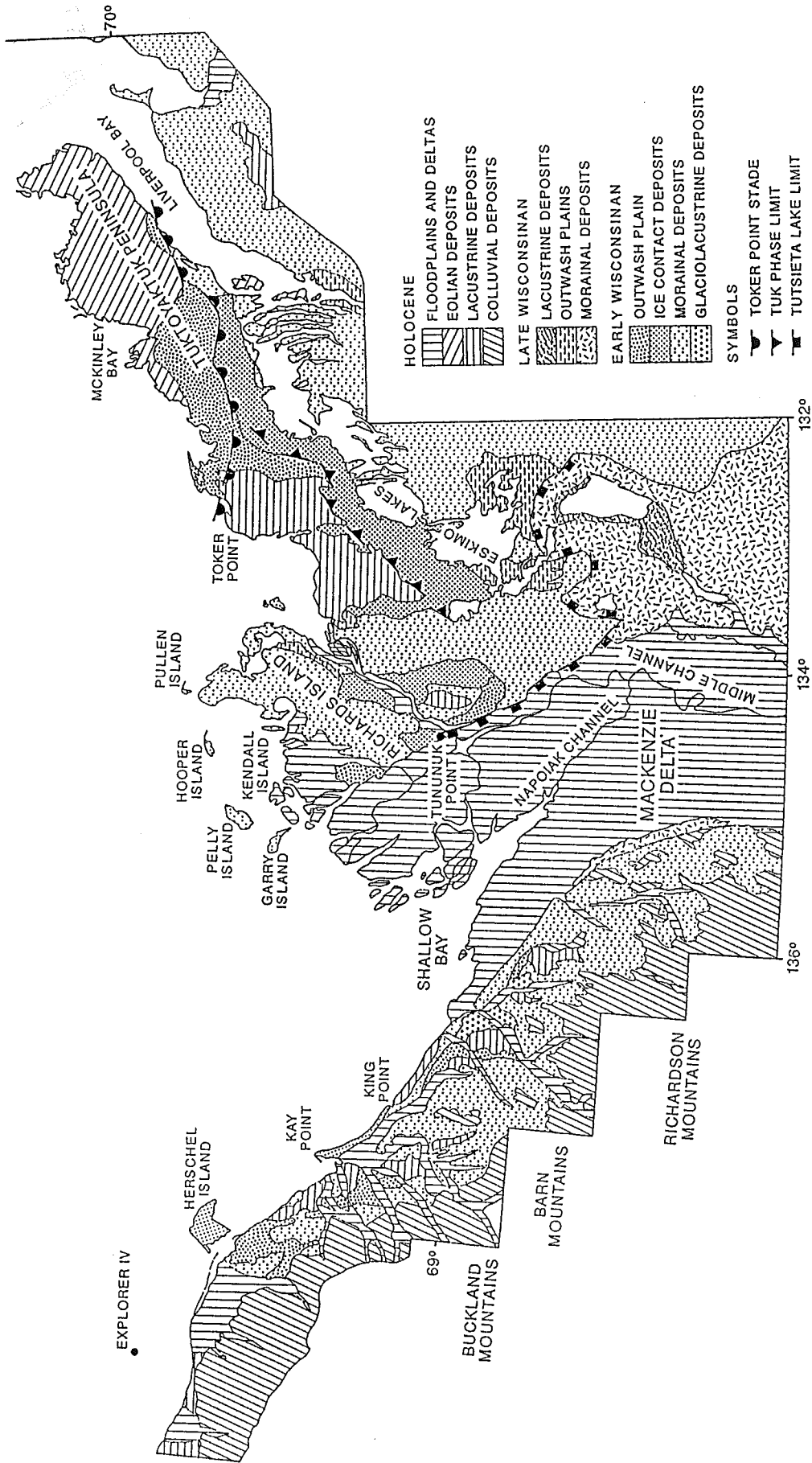
Whereas the Iperk sequence is approximately 5000 m thick at its depocentre near the modern shelf break, it thins to a few tens of metres at the basin margin (Dietrich et al., 1985). As the present coastline is relatively close to the basin margin, there is a significant difference in thickness of Quaternary sediments between the offshore and the adjacent coastal plain. This has led to problems in correlating across the coastal zone.

### **2.2.1 Coastal Plain**

A simplified surficial geology map of the coastal region is shown in Figure 2.3. Pleistocene deposits form the broad coastal plain of the Tuktoyaktuk Lowlands and the narrower coastal plain of the Yukon (Rampton, 1982; 1988). These two areas are separated by the extremely low-relief plain of the Mackenzie Delta, which occupies a broad trough extending from the Mackenzie Valley to the submarine feature known as the Mackenzie Trough.

The Yukon coastal plain between the Mackenzie Delta and the Malcolm River consists largely of glacial deposits which Rampton (1982) attributes to a single glacial advance and named the Buckland Glaciation. The Buckland glacial limit is marked by a series of morainic ridges which can be traced northwestwards along the foothills of the Richardson and Barn Mountains and the Buckland Hills, before swinging north to the coast just west of Herschel Island (Fig. 2.3). Several kame terraces and deltas are associated with this glacial limit. Within the limit, an extensive morainic terrain covers most of the Yukon coastal plain. At the coast, two areas of ice-thrust sediments (termed ice-thrust morainic ridges by Rampton) occur at Herschel Island and between Kay Point and King Point. The second of these features is interpreted by Rampton to represent a readvance or stillstand of the Buckland ice, named the Sabine phase. Several small outwash plains and valley trains cross the coastal plain, and outwash fans are associated with the Sabine phase limit.

The Buckland Glaciation represents the maximum all-time limit of Laurentide ice in the region (Hughes et al., 1981; Dyke and Prest, 1987) and is considered by Rampton to be of early Wisconsinan age. Some question nevertheless remains about the age of this event as the



**Figure 2.3** Surficial geology map of the Canadian Beaufort Sea coastal region (modified from Rampton 1982; 1988).

Laurentide maximum limit can be traced south to the Bonnet Plume Basin where it has been dated at less than 39,000 years (Hughes et al., 1981). On the other hand, there is clear evidence for a late Wisconsinan ice limit along the western margin of the Mackenzie Delta. This limit is correlated with the Tutsieta Lake Moraine to the southeast of the delta (Hughes, 1987).

Thermokarst processes have modified the Yukon coastal plain since the Buckland glaciation (Rampton, 1982). Many of the glacial deposits contain segregated ice and/or excess ice, which may melt when exposed by erosion (for example along coastal cliffs), resulting in retrogressive thaw flow slides. Rampton also documents the development of ice wedges, tundra polygons and thermokarst basins. The latter are generally associated with morainal deposits and are commonly filled by shallow thermokarst lakes. Lacustrine sediments consist of organic muds and peat and may completely infill the lakes.

To the east of the Mackenzie Delta, Rampton (1988) has identified an ice margin position which he correlates with the Buckland Glaciation and which, in the Tuktoyaktuk Peninsula area, is assigned to the Toker Point Stade. This glacial limit can be traced across the Tuktoyaktuk Peninsula from Liverpool Bay to Toker Point (Fig. 2.3), based primarily on the distribution of morainal deposits and other ice contact deposits (Rampton, 1988). These include subglacial meltwater channels, identified in the Eskimo Lakes area, and a prominent proglacial meltwater channel that crosses the Tuktoyaktuk Peninsula and can be traced to the head of McKinley Bay.

A second ice limit consisting of low sand and gravel hills converges eastward with the Toker Point limit but swings south below Hutchison Bay, before trending westward along the northern edge of the Eskimo Lakes (Fig. 2.3). This limit, named the Tuk phase limit, was originally proposed by Mackay et al. (1972) and Fyles et al. (1972), as a possible late Wisconsinan ice limit. Many valley trains and outwash plains on the Tuktoyaktuk Peninsula are associated with the Tuk phase limit, and although Rampton (1988) assigned it to the early Wisconsinan, Hequette and Hill (1989) have recently suggested that the later interpretation presents problems in explaining the large volumes of late Wisconsinan outwash sediment on the Beaufort Shelf.

Pleistocene deposits on Richards Island and the adjacent ring of islands (from Garry to Hendrickson Island) were deposited within the suggested Buckland - Toker Point limit (Rampton, 1988). The predominant surficial sediment in these areas consists of stony clayey diamicton and is most commonly present as a thin veneer less than 1 metre thick. This veneer overlies a complex sequence of older Pleistocene deposits including ice-thrust marine sediments, informally named "Kendall sediments" and "Hooper clay" (Rampton, 1988). Two sand units, the Kidluit Formation and the Kittigazuit Formation also form part of this older complex. The Kidluit Formation consists of grey, well-sorted medium- to fine-grained sand with common coal and wood detritus as well as

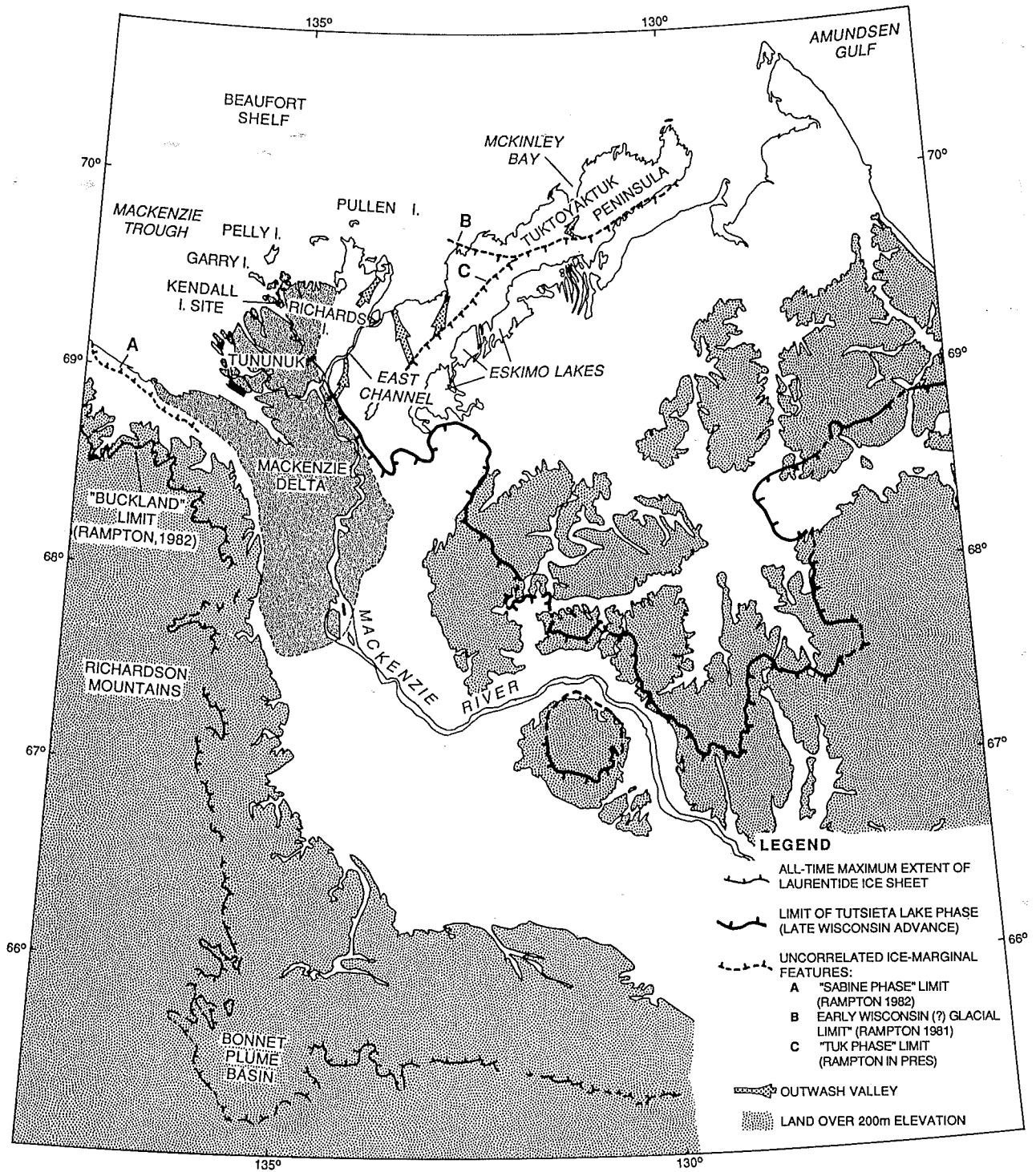
both freshwater and marine molluscs. The Kidluit Formation is interpreted by Rampton to be fluvial in origin with the marine shells being reworked from older sequences. The Kittigazuit Formation overlies the Kidluit Formation, usually with a sharp contact. It consists of light brown fine- to medium-grained sand and is characterised by large scale cross-bedding. Rampton (1988) interpreted the large dipping beds of the Kittigazuit Formation as delta foresets, but other workers have suggested that they may represent aeolian cross-beds (S. Dallimore, personal communication).

With the possible exception of the Tuk phase limit and its associated outwash deposits, there are no published observations of late Wisconsinan deposits on the coastal plains of either the Yukon Shelf or the Tuktoyaktuk Peninsula. At the northeastern end of the peninsula, beyond McKinley Bay, the outwash sand has been reworked into aeolian dunes but Rampton suggests that these are probably Holocene in age. Hughes (1987) has mapped an ice limit of late Wisconsinan age, the Tutsieta Lake Phase, lying well south of the Eskimo Lakes in the east. However, in the west, it runs northward along the eastern edge of the modern Mackenzie River as far as Tununuk. Radiocarbon dates indicate an age of 13,000 years or older for this ice limit (Hughes, 1987).

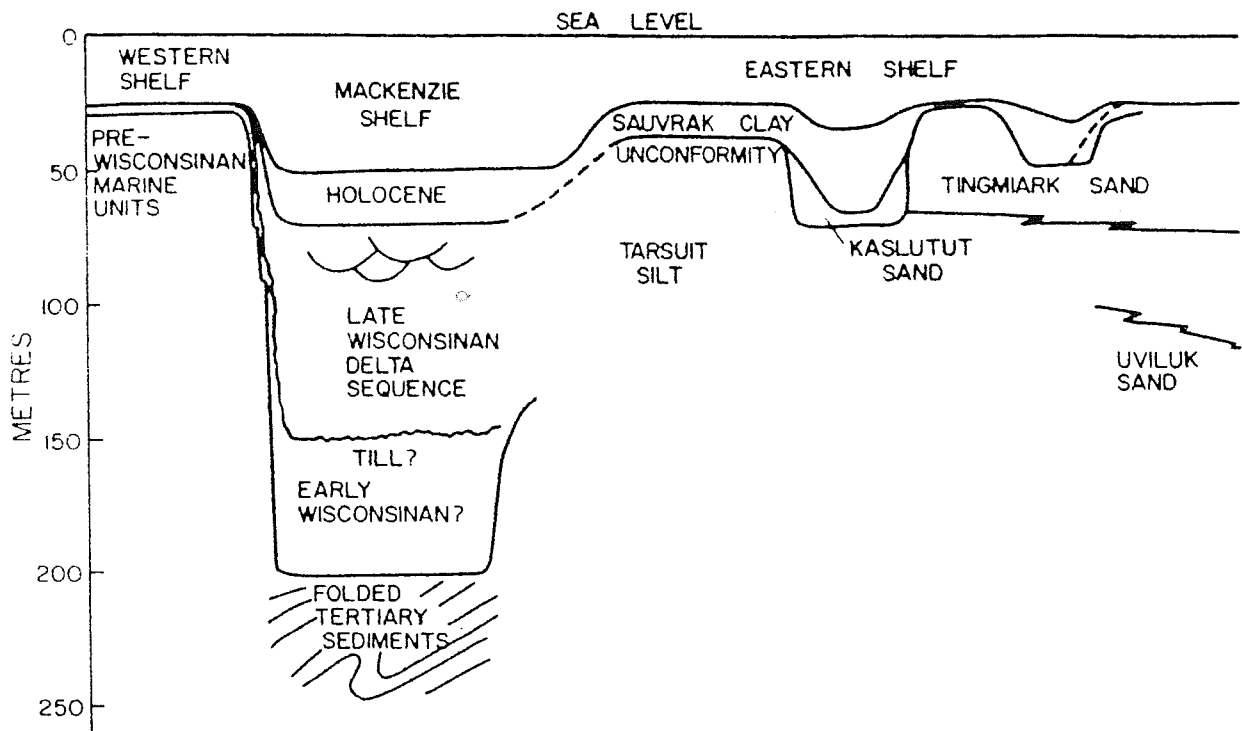
### **2.2.2 Offshore**

No glacial limits have been firmly identified on the Beaufort Shelf. However, the extent of the Buckland limit along the Yukon coast (Fig. 2.4) implies the presence of ice in Mackenzie Trough and on the Beaufort Shelf north of Richards Island, linking with the Toker Point limit of Rampton (1988). Diamicton has been recovered from boreholes just west of Pullen Island (Hill et al., 1986a) and the ring of islands from Garry to Pullen Island all show ice-thrust deformation (Mackay and Matthews, 1983). It therefore seems likely that the Buckland/Toker Point limit extends offshore at least to the vicinity of these islands. However, the relationships between potential ice-contact deposits in this area and the stratigraphy of the shelf seaward of the 20 m isobath, as described by Hill et al. (in press), have not been established.

Seaward of the 20 m isobath, there is no evidence for ice-contact deposits in the top 100 m of the shelf sequence. North of Richards Island and the Tuktoyaktuk Peninsula, a 40 m thick sand unit, named the Tingmiark Sand, is present over most of the shelf (Fig. 2.5; Hill et al, in press). Interpreted as an outwash deposit, the Tingmiark Sand has been dated at younger than 21 620 years (Hill et al., 1985). The sand is incised by broad infilled valleys which underlie the seabed morphological features of Ikit Trough and Kugmallit Trough, and extend across the shelf from the coastline. The valleys, which clearly post-date the Tingmiark Sand, were formed during a lowering of relative sea-level in the latter part of the late Wisconsinan, estimated between 15 000



**Figure 2.4** Map of the Beaufort - Mackenzie region showing position of various Laurentide ice limits (based on Rampton, 1982; 1988; Hughes, 1988).



**Figure 2.5** Schematic cross-section of the Beaufort Shelf showing main stratigraphic units.

and 10 000 years B.P. (Hill et al., 1985). From these constraints, the Tingmiark Sand appears to have been deposited in the early part of the late Wisconsinan, and may therefore be somewhat older than the Tutsieta Lake advance (Hughes, 1987).

Between the Mackenzie Trough and the Ikit Trough, the pre-Holocene sequence is assigned to the Tarsiut Silt Unit, which consists of interbedded silt and clay with relatively minor sand intervals (Hill et al., in press). Marine microfossils are present through much of the Tarsiut Silt, although parts of the sequence are barren and may represent marginal marine or deltaic environments. A peat bed, possibly representing the top of a deltaic cycle, occurs at 129 m below seabed within the Tarsiut Silt and has been dated at  $27\,340 \pm 470$  years B.P. (Hill et al., in press). The upper Tarsiut Silt and the Tingmiark Sand are therefore inferred to be laterally equivalent units of late Wisconsinan age.

Over most of the eastern shelf, Holocene marine mud (named the Sauvruk Clay; Hill et al., in press) overlies the subaerial Tingmiark Sand with a clear unconformity (Hill et al., in press). Over much of the shelf, the unconformity truncates small filled basins interpreted to be thermokarst depressions developed on the late Wisconsinan land surface prior to transgression. Where the Sauvruk Clay overlies the Tarsiut Silt, the unconformity is more variable in character. In some areas, the transition is marked by numerous disconformable surfaces rather than a single unconformity, whereas in other areas, the unconformity is clear and angular.

The Mackenzie Trough is a glacially excavated and partially-infilled valley which extends across the shelf to the shelf break at approximately 400 m depth (Shearer, 1971). The Trough probably extends a considerable distance southwards up the Mackenzie Valley in the area now occupied by the Mackenzie Delta. The thickness of Holocene sediment in Mackenzie Trough reaches more than 30 m and consists of silty clay (Moran et al., 1989). The clay overlies fine sand and silt deposited in a large Pleistocene delta which fills much of the southern part of the trough (Fehr, 1987; Moran et al., 1989). This is underlain by an acoustically complex sequence of sand and mud which may relate to the glacial event(s) which eroded the trough.

On the Yukon Shelf, the thickness of Holocene sediment decreases rapidly westwards from Mackenzie Trough. On the narrow section of shelf between the trough and Herschel Island, Holocene sediment has accumulated at water depths below approximately 10 m but the inner shelf is apparently swept clean of sediment (Hill, in press).

This section of shelf is interrupted by Herschel Basin, a small enclosed basin with water depths reaching 60 m. Mackay (1959) proposed that Herschel Basin was excavated by the same event that caused ice-thrusting of Herschel Island sediments. Subsequent investigations show that the basin is partly infilled by marine and lacustrine sediment that is partly frozen (Unpublished

GSC data). The age of the basin is uncertain.

The main part of the Yukon Shelf north and west of Herschel Island consists of a series of fifteen seaward-thickening and -younging seismo-stratigraphic units which progressively outcrop at the seabed (Brigham-Grette et al., in press). These units range from possibly early to mid-Pleistocene on the inner shelf to possibly late Wisconsinan at the shelf edge. The only age control results from a borehole located in the mid-shelf region where a combination of radiocarbon dates, thermoluminescence dates and amino acid ratios place the sequence in the early Wisconsinan. Holocene sediments are generally absent from the shelf with the exception of a surficial lag of gravelly mud which has been reworked extensively by ice-scouring.

### **2.3 Permafrost and Ground Ice**

The Beaufort Sea coastal zone lies within the zone of continuous permafrost. The thickness of permafrost varies significantly over the region, from over 700 m in the Richards Island area to less than 100 m in the outer Mackenzie Delta (Judge, 1986; Burgess et al., 1982). Deep taliks exist beneath the numerous lakes in the region (Mackay, 1979). Over most of the region, the thickness of the active layer ranges from 0.2 to 0.5 m (Mackay, 1975).

The unconsolidated Pleistocene sediments of the coastal lowlands contain significant volumes of ground ice, both as small inter-particle crystals that bond the sediment, and as polycrystalline ice bodies of variable form and size. Several broad types of ground ice have been identified. Vertical to sub-vertical ice wedges are associated with frost heave polygons and form by the alternate freezing and thawing of thermal contraction cracks that form the polygons (Mackay, 1974; 1980; Mackay and Matthews, 1983). The dimensions of ice wedges can reach up to 1 m wide and 5-8 m deep. Ice veins, lenses, and massive ice on various scales are common (Mackay, 1971; Mackay et al., 1972; Rampton and Mackay, 1971) and can have a variety of origins (Dallimore and Wolfe, 1988; Pollard and Dallimore, 1988). In situ segregation ice is formed where upward migrating water in porous sands encounters aggrading permafrost, commonly at a sand/clay interface (Mackay, 1971). Buried glacial ice has been identified on Richards Island (Dallimore and Wolfe, 1988) and buried snow ice on the Yukon coastal plain (Pollard and Dallimore, 1988). The presence of large bodies of ice on the coastal plain results in a variety of landforms, included under the general label of thermokarst topography.

Thick relict permafrost has also been observed offshore and may be as thick as permafrost on land. The offshore permafrost formed during periods of lowered sea-level, delta progradation and subaerial exposure of the shelf (Blasco et al., in press). The permafrost is distributed over much of the eastern shelf as a sequence of layers, equivalent to intervals of subaerial exposure.



The shallowest layer is discontinuous, whereas deeper layers appear to be more continuous. The coastal zone marks the transition between onshore permafrost and the relict offshore permafrost. Dallimore et al. (1988) document ice and geothermal conditions along two transects in the nearshore zone at North Head. Permafrost is preserved close to shore where sea-ice freezes to the bottom, allowing penetration of very low winter temperatures. Further offshore (beyond 2 m water depth), transgressed permafrost thaws rapidly and subsequent consolidation may result in sub-seabed thermokarst development beneath Holocene coastal and shelf deposits.

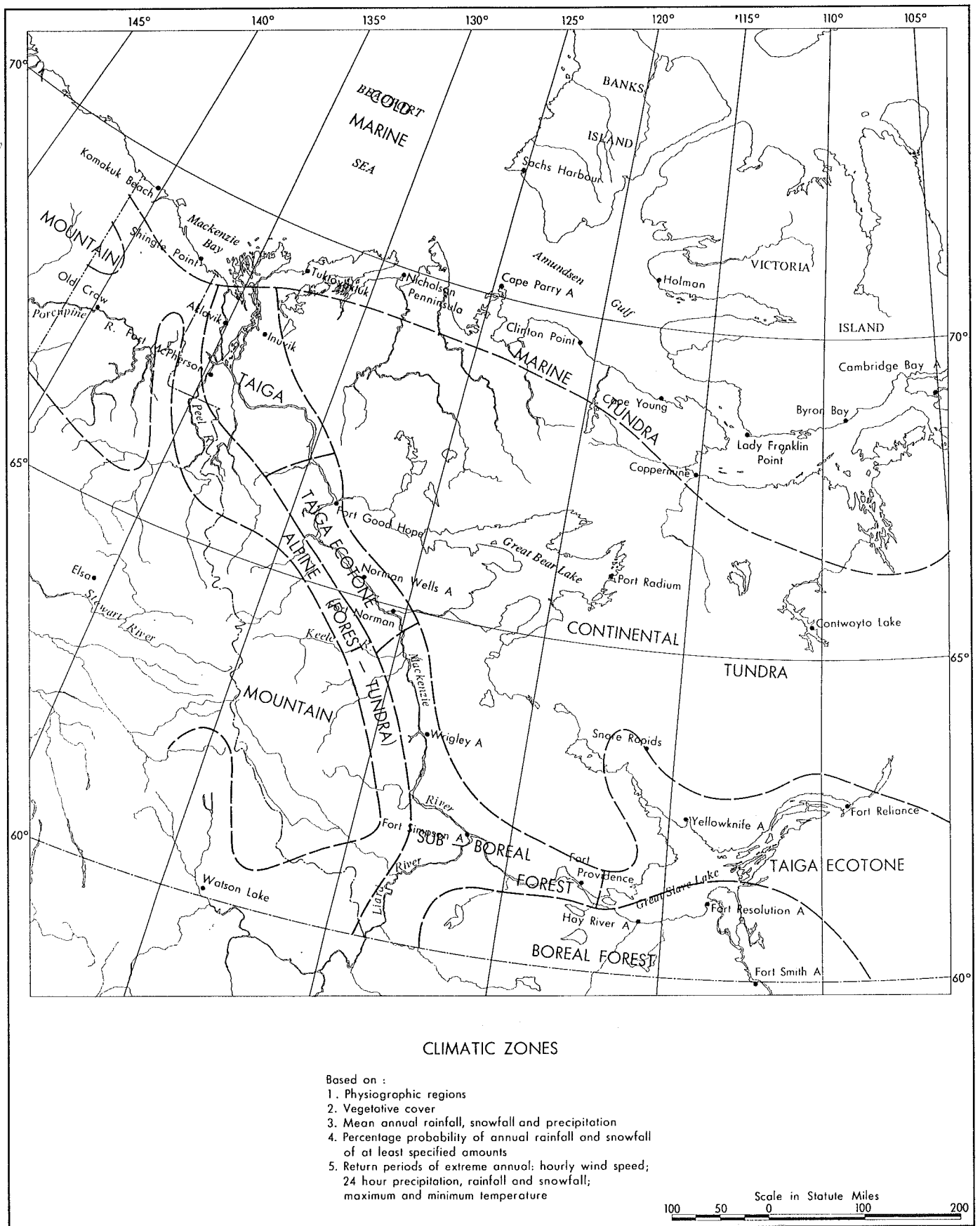
## **2.4 Climate**

The Beaufort coast lies within the "marine tundra" climatological zone of Burns (1973), characterized by long cool winters and short cool summers (Figs. 2.6 and 2.7). Cold arctic air dominates throughout the winter but maritime arctic air develops along the coast during summer. Precipitation is very low and more abundant during the summer when low pressure systems move along the Alaskan and Yukon coast. These systems also dominate wind patterns during the summer and fall, producing strong winds from the northwest quadrant (Fig. 2.8).

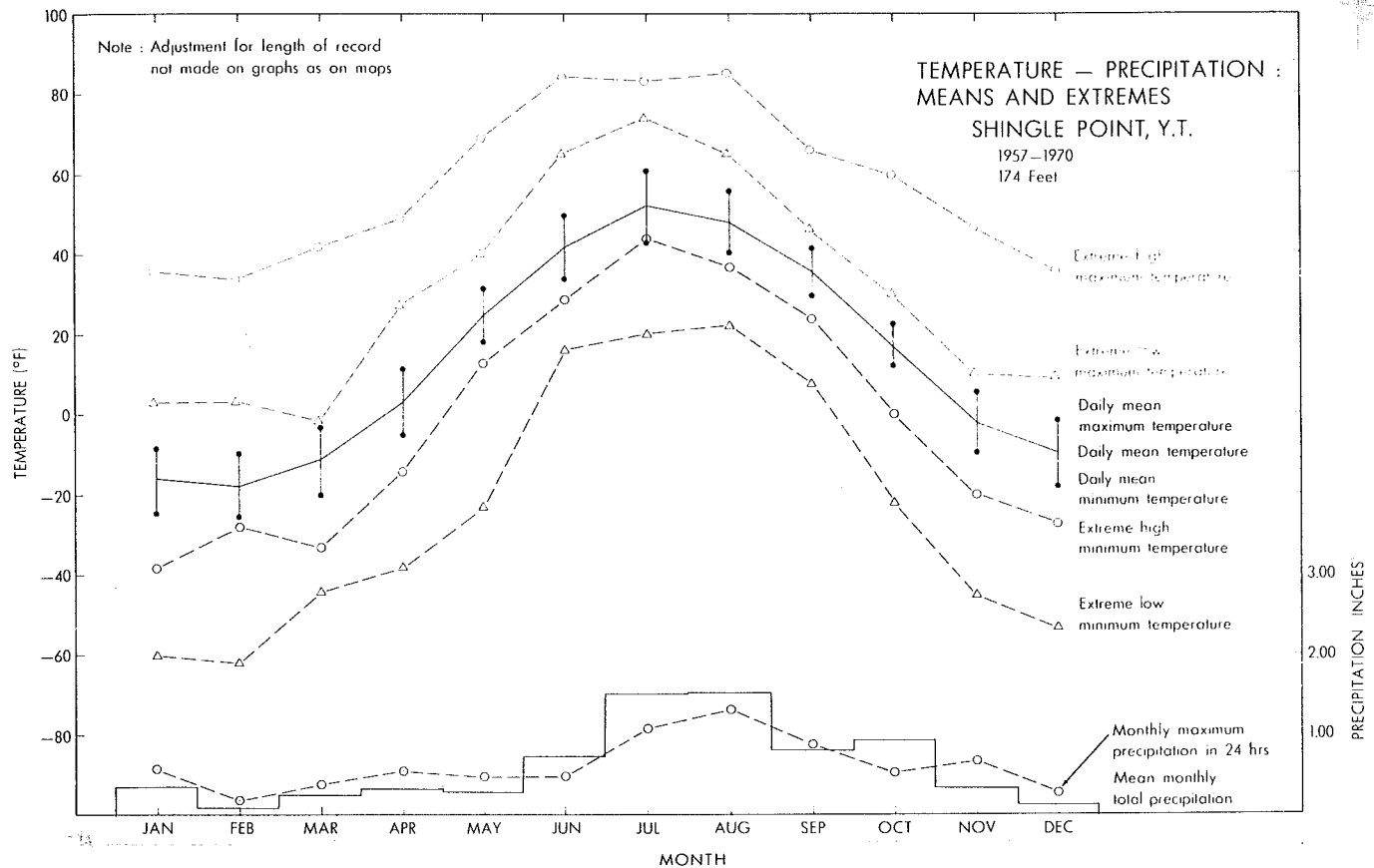
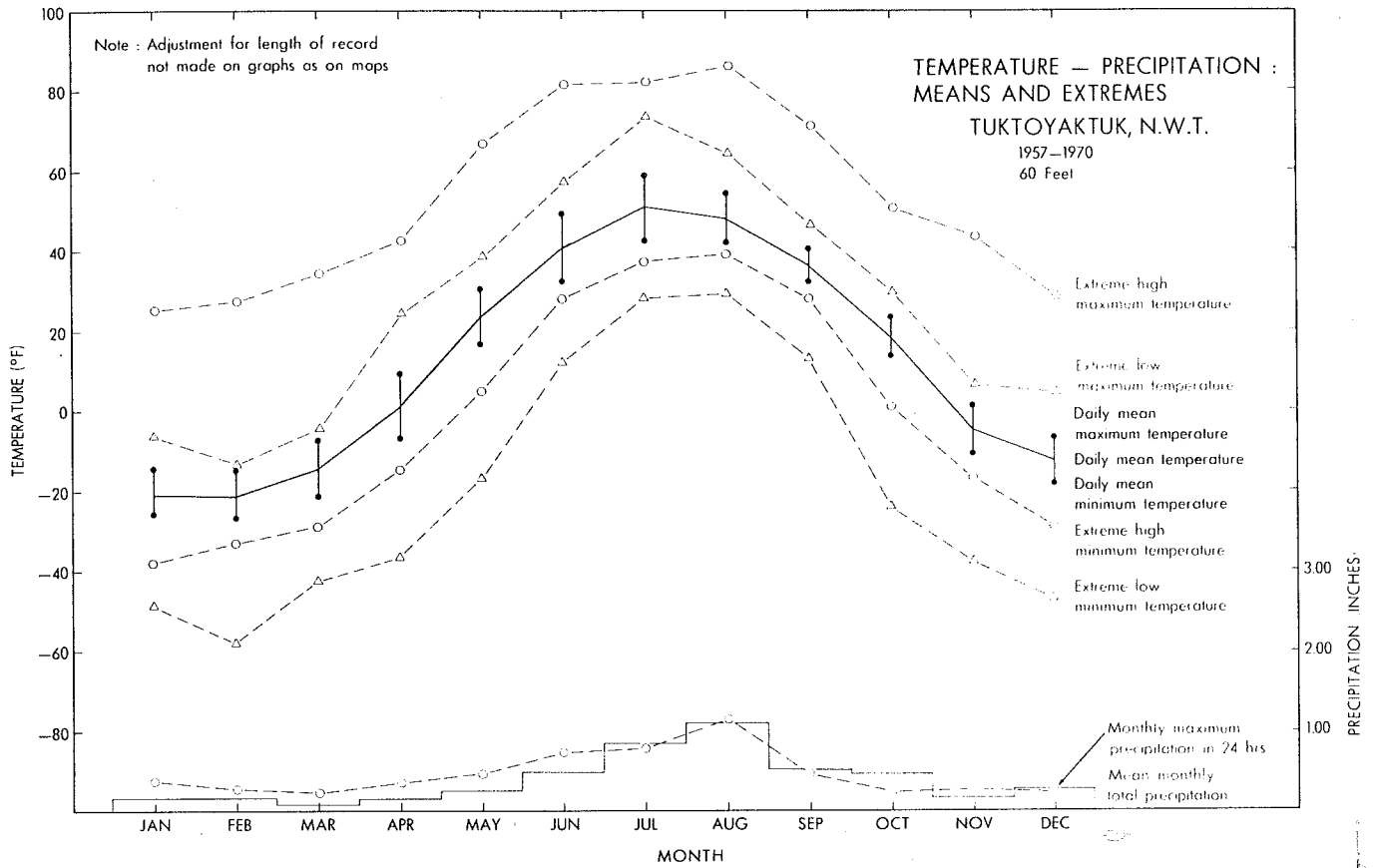
## **2.5 Mackenzie River Regime**

The Mackenzie River is the primary source of sediment to the Beaufort Shelf (Harper and Penland, 1982), contributing a yearly average of  $8.56 \times 10^7$  m<sup>3</sup> of suspended matter (Davies, 1975; C.P. Lewis, personal communication). The river has built one of the world's major river deltas at its entry to the Beaufort Sea. The Mackenzie discharge also plays a major role in controlling the timing of break-up, the extent of sea-ice during the summer and the temperature of surface water during the open water season.

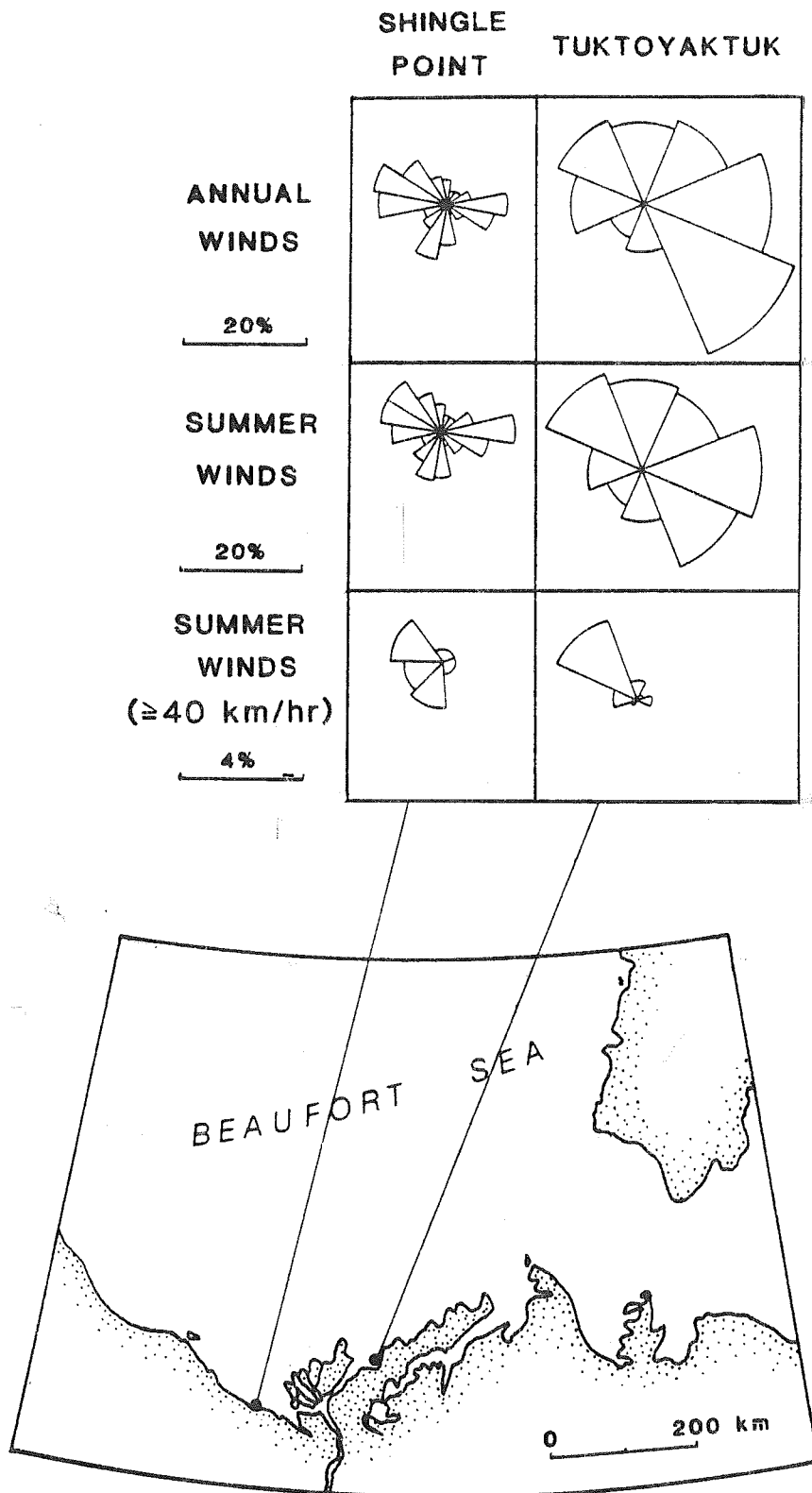
Originating at Great Slave Lake at an elevation of only 170 m, the Mackenzie River flows for more than 1600 km northward to the Beaufort Sea (Fig. 2.9). Several large rivers act as tributaries of the Mackenzie, the largest in terms of discharge being the Liard, which also collects water from the Nahanni River and joins the Mackenzie at Fort Simpson. From Great Slave Lake to Point Separation, the river flows in a single broad channel, but upon reaching the delta, the river splits into numerous distributary channels. Most of the flow (80-90%) is initially retained by Middle Channel, but the flow becomes further divided into three principal channels: East Channel, flowing into Kugmallit Bay (33%), Reindeer Channel flowing into Shallow Bay (37%), and Middle, Harry and Kumac Channels flowing into the Beaufort Sea west of Richards Island (Fig. 2.10; Davies, 1975). Minor amounts of Mackenzie water flow along the western margin of the delta through Aklavik and West Channels, and are supplemented by flow from the Rat and Big



**Figure 2.6** Climatic zones of the Mackenzie Delta and surrounding regions (Burns, 1973).



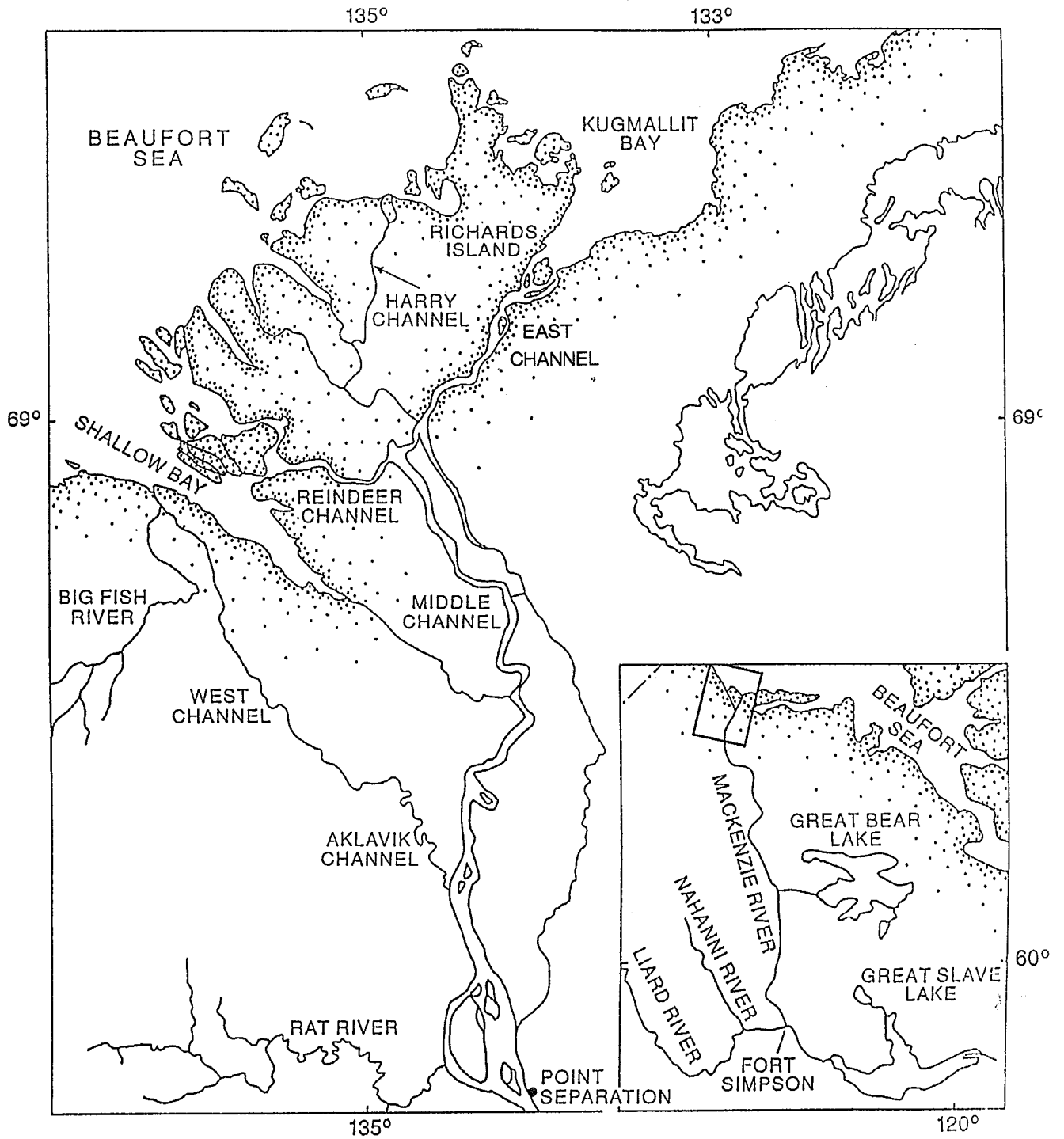
**Figure 2.7** Temperature/precipitation graph for (a) Tuktoyaktuk and (b) Shingle Point (Burns, 1973).



**Figure 2.8** The distribution of winds (roses indicate the direction from which winds blow) at Shingle Point and Tuktoyaktuk (modified from Harper and Penland, 1987).



**Figure 2.9** The drainage basin of the Mackenzie River (Davies, 1975).



**Figure 2.10** Major distributary channels of the Mackenzie Delta.

Fish Rivers.

The discharge of the Mackenzie River is highly variable over an annual cycle (Fig. 2.11) and also from year to year (Davies, 1975; Harper and Penland, 1982; Marko et al., 1983; Lewis, 1988). The winter months are characterised by low but continuous discharge through the main channels beneath an ice cover of 1 to 2 m. During May and early June, the discharge rapidly increases as snow melt occurs in the tributaries, resulting in the "spring freshet". Marko et al. (1983) note the importance of the Liard River flow at this time. The increasing discharge of relatively warm water causes initial overflow and then break-up of sea-ice in the vicinity of the distributary channel mouths. By June, the delta is generally free of ice and the river discharge gradually decreases over the open water season. Typically, several peaks in discharge, related to high rainfall events in the Liard and other tributary basins, occur over the summer and fall months.

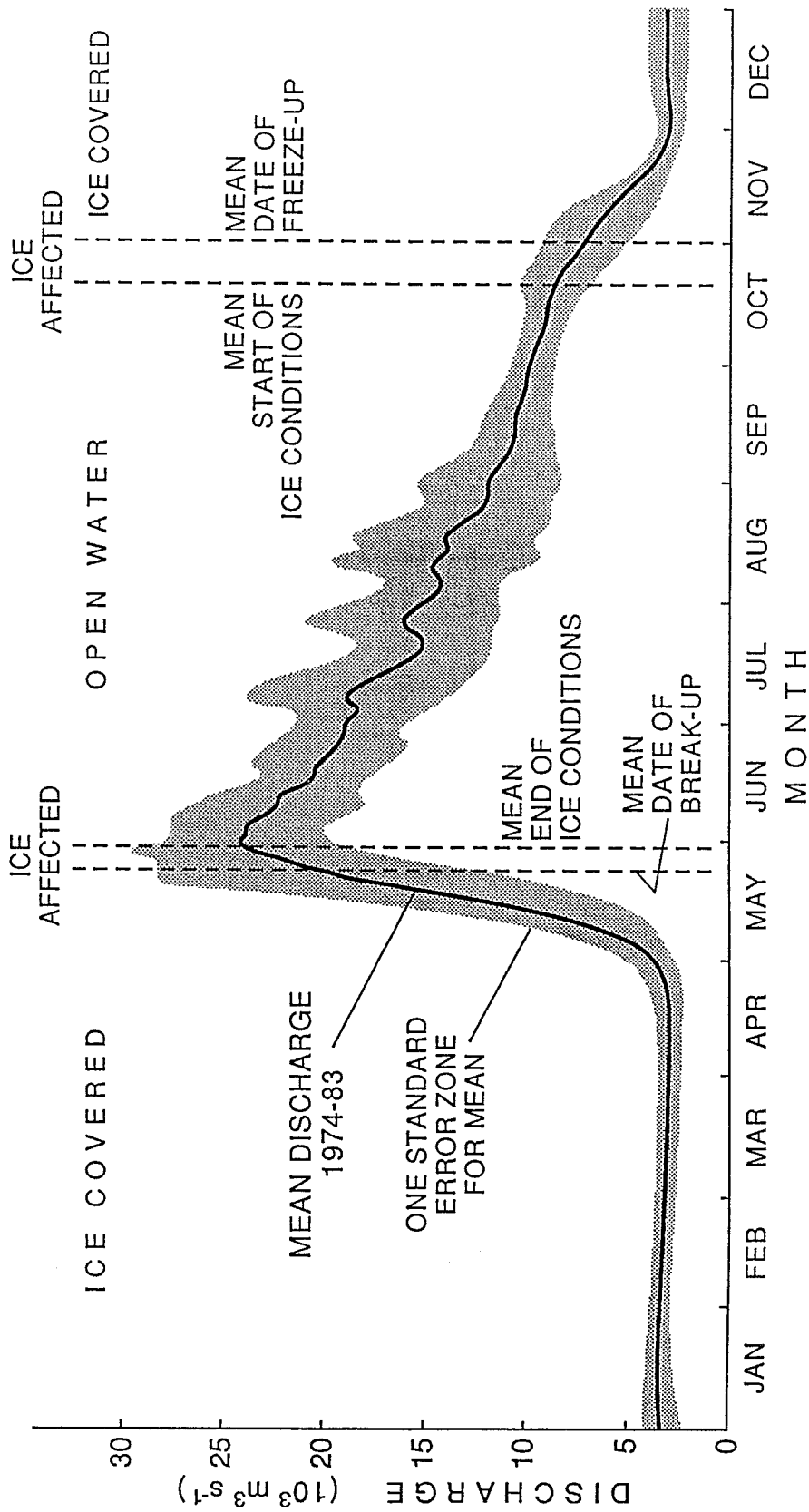
## 2.6 Ice Regime

### 2.6.1 Winter

During the winter months from October to June, the Beaufort Sea has a continuous surface layer of sea-ice. The ice cover consists of three main forms of ice: first year ice, multi-year ice and ice-island fragments (Arctec, 1987). First year ice generally reaches a maximum thickness of 2 metres, whereas multi-year ice can be thicker. Ice island fragments up to 50 m thick have occasionally been observed drifting across the Beaufort Shelf and smaller fragments have been known to become grounded close to shore along the Yukon coast (Kovacs and Mellor, 1971; Dome et al., 1982).

Four zones of ice, based on morphology have been recognised in the Beaufort Sea (Fig. 2.12; Dome et al., 1982). The *polar pack zone* consists of multi-year ice of the Arctic Ocean which drifts in a clockwise direction with the prevailing current (the Beaufort Gyre). The southern boundary of the polar pack usually lies at approximately 72°N, but occasionally moves further south (Dome et al., 1982). Coupled to the polar pack is *transition zone* ice which consists of multi-year pack ice and first year ice. Landward of the transition zone is the *active shear zone* where the mobile polar pack and transition zone ice move against the stationary *landfast ice*. The shear zone is characterised by mixed ice types, severe ridging and variable amounts of open water, depending on wind conditions (Arctec, 1987). Thick-keeled ridge ice developed in this zone is important as an anchor for landfast ice during winter, and as an agent of ice scour during the summer.

The landfast ice zone forms along the coast and can itself be divided into two zones (Fig. 2.13). Adjacent to the coast, where water depths are less than the maximum thickness of first year



**Figure 2.11** The annual discharge cycle of the Mackenzie River, showing mean and extreme years (from Lewis, 1988).



# BEAUFORT SEA ICE MORPHOLOGICAL ZONES

(Dome et al, 1982)

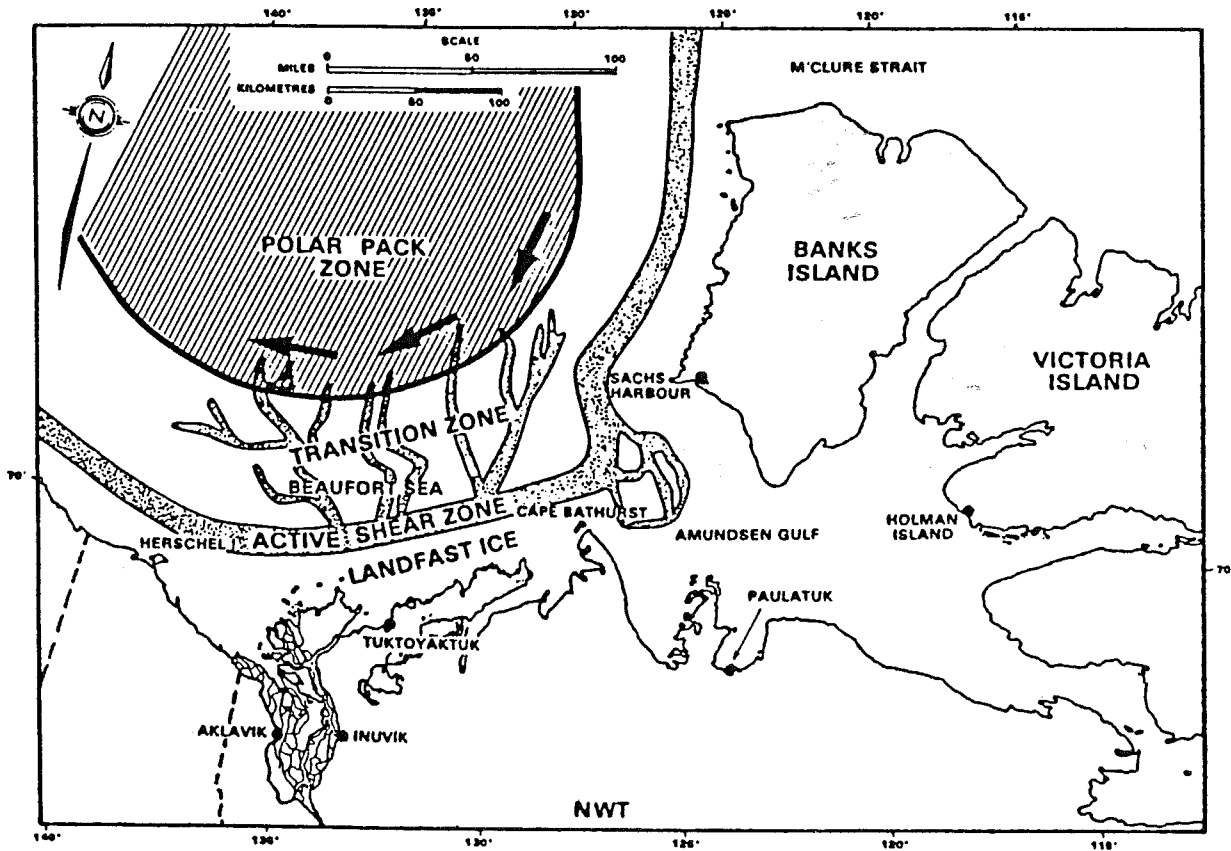


Figure 2.12 The morphological zonation of Beaufort Sea ice (Dome et al. 1982).

## LAND FAST ICE MORPHOLOGY

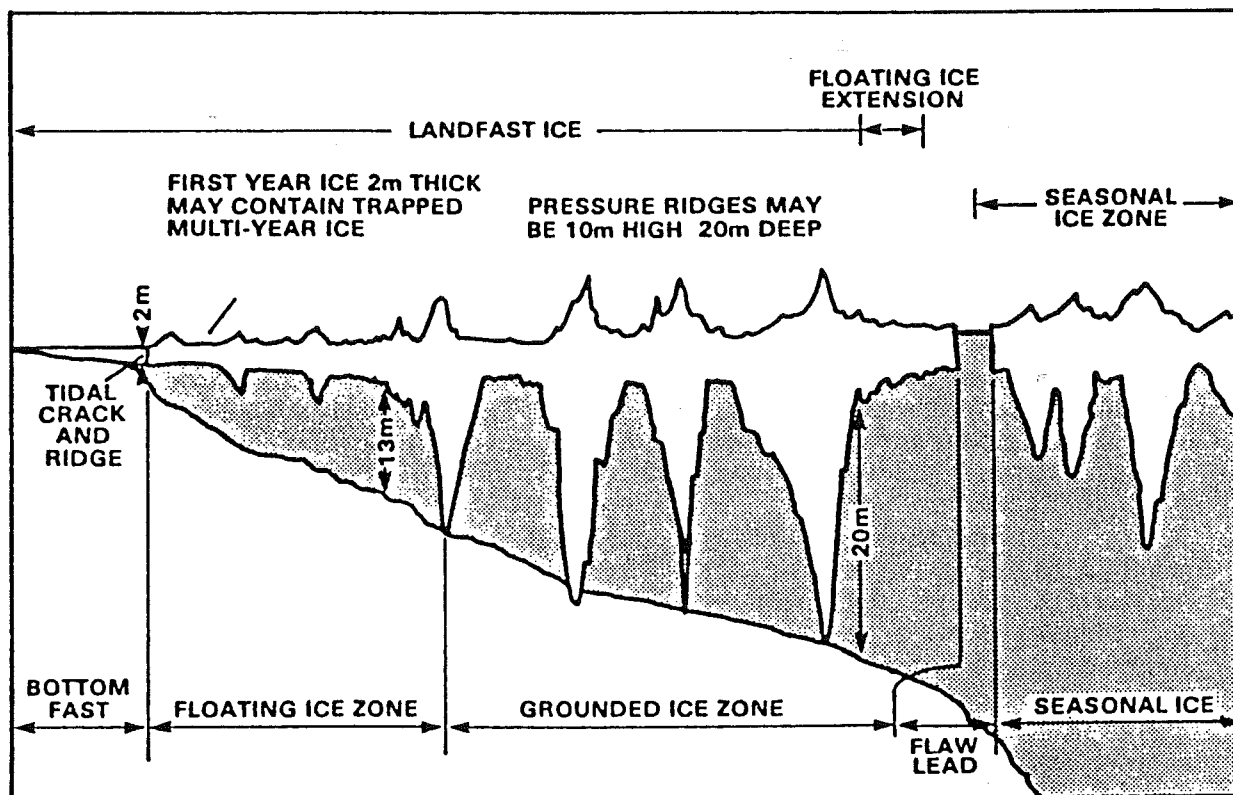


Figure 2.13 Beaufort Sea landfast ice morphology (Arctec, 1987).

ice (between 1.5 and 2 m), the ice is frozen to the seabed or *bottom-fast*. This ice is generally smooth and its extent offshore is controlled by the slope of the seabed. In the vicinity of the Mackenzie Delta, where the slope is very low, the bottomfast ice zone may be 10-20 km wide. Also, in this region, there must be channels through the ice or in the underlying seabed, to allow the drainage of the significant winter river flow from the Mackenzie. Elsewhere, the nearshore slope is much steeper and the bottomfast zone may be only a few metres wide.

At the seaward edge of the bottomfast zone, there is generally a tidal crack, where heave as a result of tidal motion repeatedly breaks the ice. A small ridge may also develop as a result of this process. Seaward of the tidal crack, the landfast ice is floating (*floating ice zone*), but consists primarily of first year ice. Small ridges may develop in this zone as a result of movements due to wind or thermal expansion during freeze-up. Relatively little motion occurs during the winter months as the grounded ice offshore tends to anchor the landfast ice. However, wind storms during the winter can cause small shifts in the ice, leading to the development of flaw leads and further ridging.

During the winter, sea-ice interacts with the coast in a number of ways, the most important of which are:

1. *Ice scour*: where deep draft ice-keels, associated with pressure ridges, plough into the seabed, forming linear scours.
2. *Ice push*: where a deep draft ice feature is driven broadside onto the beach.
3. *Ice override*: where movements within the landfast ice piles up and over the shoreline.

### **2.6.2 Break-Up**

Break-up processes along the Beaufort coast have been summarised by Thompson (1983), Pilkington (1988) who reviewed satellite and airborne radar imagery from the years 1974 to 1987, and Dickins (1987) who made a detailed aerial survey during break-up in 1987. The process of break-up begins in late April or early May each year when the Mackenzie River begins to rise and ice is lifted in the river channels. As flow beneath the bottomfast-ice is restricted, the river water commonly floods across the ice in the vicinity of the main distributary channels (Fig. 2.14). By late May, the warm river water melts out the bottomfast ice in these regions and open water lagoons form along the coast and the river water flows into the Beaufort Sea beneath the remaining landfast ice. The coastal lagoon widens until most of the coastline is free of ice. As the plume of river water extends offshore, melting of the shelf ice progresses slowly. By late June, the offshore ice pulls away from the landfast ice, leaving narrow ice barriers at the 5 to 6 m water depth in Mackenzie Bay and Kugmallit Bay. These barriers are generally breached between mid-June and



mid-July, leaving extensive open water conditions over the central Beaufort Sea. Break-up of the landfast ice along the Yukon and Tuktoyaktuk Peninsula sections of the coast is later than the central region, but is usually complete by mid-July.

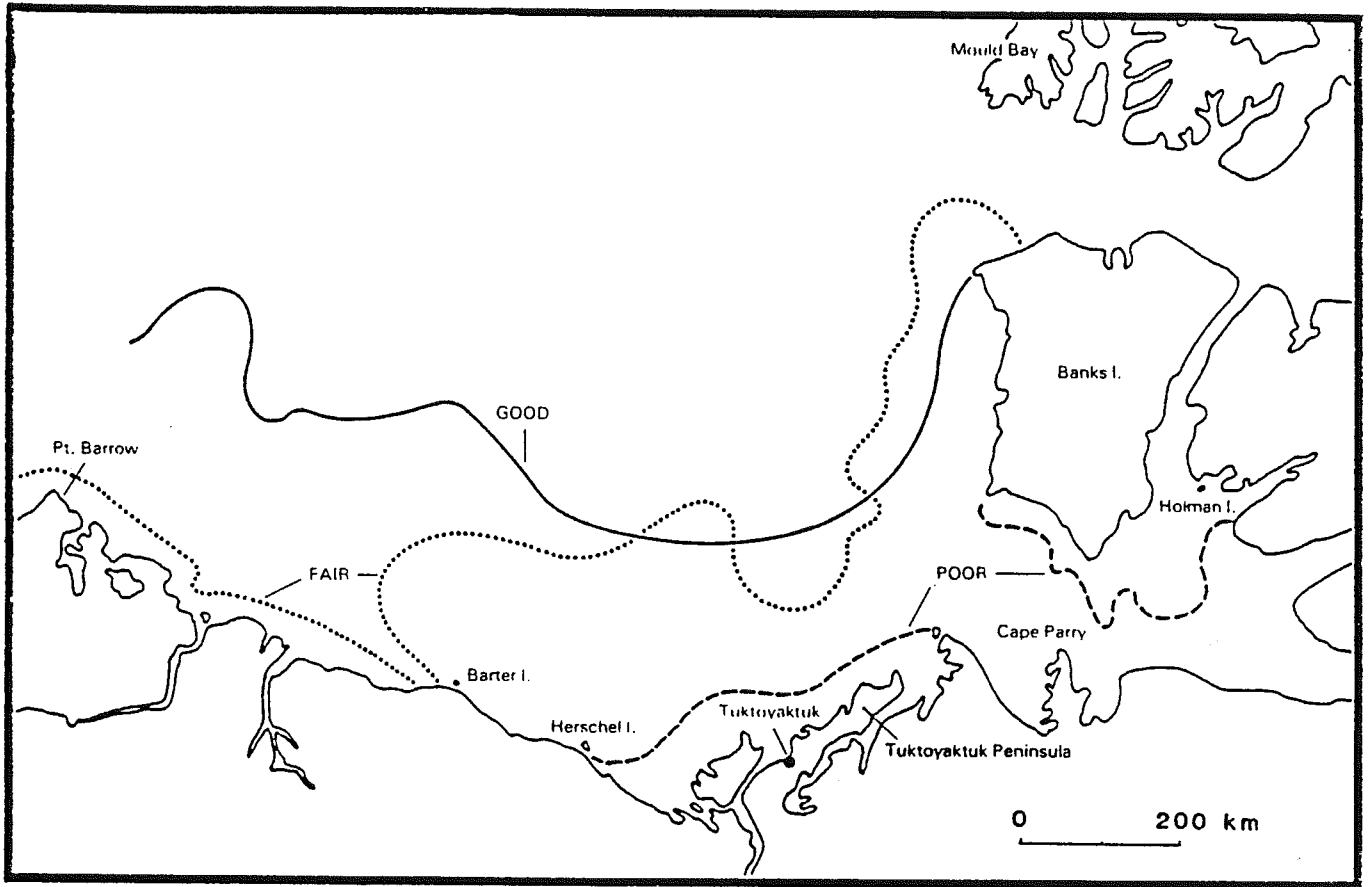
In the Alaskan Beaufort Sea, a unique process that occurs in the early stage of break-up has been documented by Reimnitz et al. (1974). *Strudel scour* occurs when river water overflows the landfast ice and plunges through small cracks in the ice. The jet of water flowing downwards can cause circular scours up to 10 m deep. The scour is rapidly filled in by sediment transported in the river water (Reimnitz and Kempema, 1982), but scours have been observed in sidescan sonar records on the Alaskan shelf. Strudel scours have been observed in Phillips Bay at the mouth of the Babbage River, Yukon Territory (Dickins, 1987), but never in the vicinity of the Mackenzie River, despite an extensive search of remote sensing data (Pilkington, 1988). This may be because of the wide area of bottomfast ice in the delta region, which would require flooding to extend tens of kilometres offshore.

### **2.6.3 Summer**

Whereas break-up of the ice cover in the Beaufort Sea is controlled largely by the discharge of the Mackenzie River, the distribution of ice during the summer months is controlled by more complex variables. From year to year, the distribution of ice is variable, with the edge of the polar pack ranging from a few kilometres to more than 300 km offshore (Fig. 2.15). The two most important variables controlling ice distribution are air temperature and wind patterns. Walsh and Johnson (1979) observed a negative correlation between long-term ice anomalies (deviations from average monthly ice concentrations) and 24 month running mean air temperature anomalies for the polar cap north of 60°. In other words, the Arctic pack is less extensive during warmer summers in the high arctic. Mysak and Manuk (1989), in a more detailed analysis of polar ice distribution, showed that the response varies from region to region within the arctic. In the Beaufort-Chukchi region, ice distribution fluctuates on a 4 to 6 year cycle (Fig. 2.16), which Mysak and Manuk proposed was related to the natural variability of atmospheric pressure patterns in the North Pacific and western arctic. On a more local scale, the edge of the polar pack ice is observed to respond to direct wind-forcing, so that a period of easterly winds will cause an expansion of open water, whereas a period of northwesterlies will cause the pack ice to encroach on the shelf.

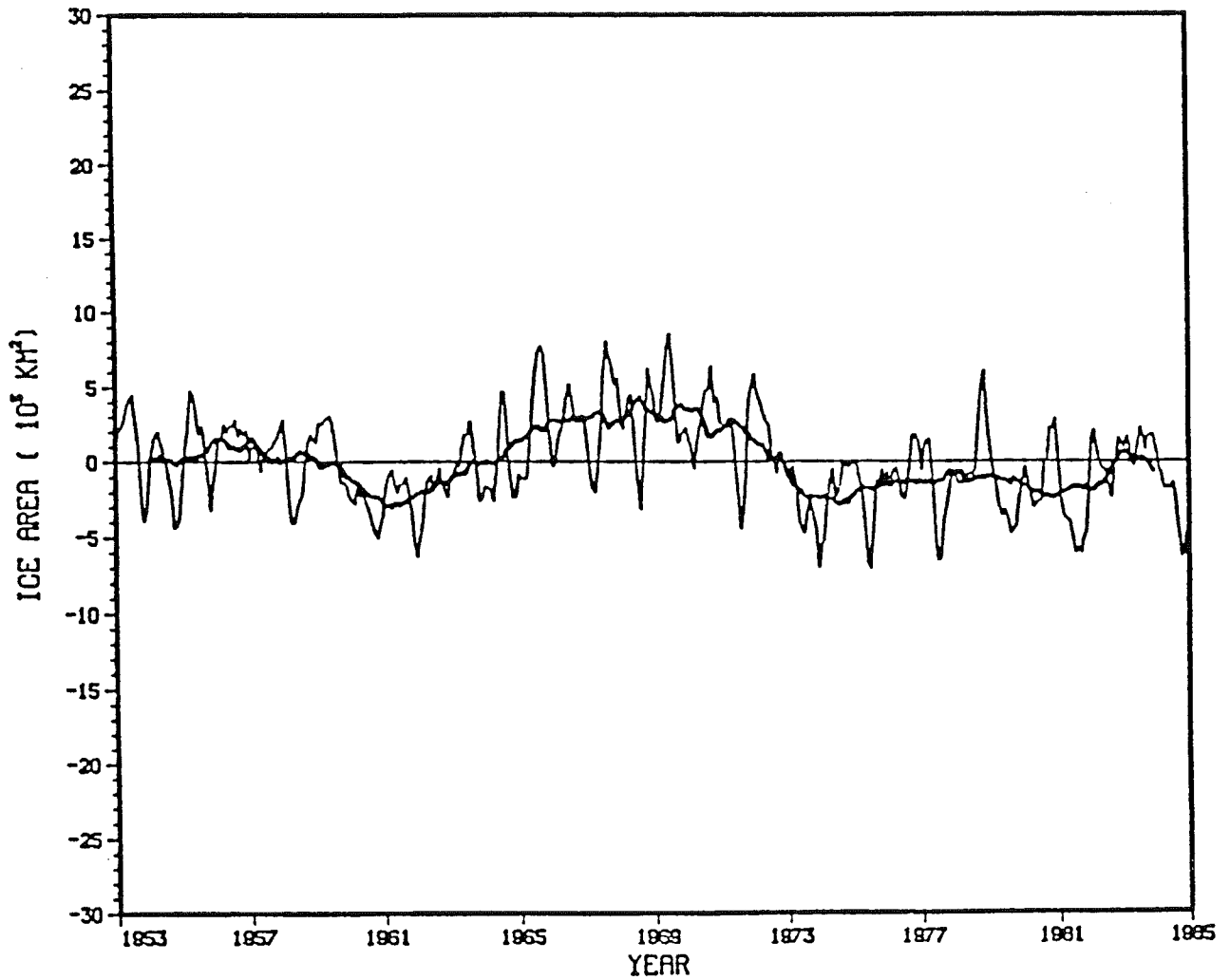
### **2.6.4 Freeze-Up**

Freeze-up generally begins in October, beginning with areas of freshwater around the Mackenzie Delta and in coastal lagoons and embayments along the Yukon and Tuktoyaktuk coasts.



**Figure 2.15** The median position of the ice edge for late August in good, fair and poor years: 1961-1972 (Milne and Herlinveaux, 1977).

# ANOMALIES



**Figure 2.16** Smoothed time series of monthly anomalies of the areal sea ice extent in the Chukchi - Beaufort Sea region (Mysak and Manuk, 1988).

According to Arctec (1987), the freeze-up then progresses uniformly across the open sea. There are few published reports of freeze-up processes in the Canadian Beaufort Sea, but Reimnitz and Kempema (1987) have described the process along the Alaskan Beaufort coast. Frazil ice (consisting of small ice crystals, 1-5 mm in diameter) first forms in freshwater lagoons and river estuaries along the coast, but as the temperature drops, frazil begins to form in sea-water, usually during wind storms when surface cooling is greatest. The wind may concentrate the frazil particles into slush ice (a descriptive term for a water-saturated internally mobile surface layer of granular ice; Reimnitz and Kempema, 1987), which accumulates in coastal embayments and lagoons. This process progresses with time, while at the same time, the polar pack moves landward until freeze-up is complete.

One important consequence of this freeze-up process at the coastline is the alteration of the dynamics of sediment transport at the shoreface. Reimnitz and Kempema (1987) observed that waves propagate through the slush ice, but do not break. Where slush ice was in contact with the seabed, large ripples developed and transport of cobbles was observed. Reimnitz and Kempema (1987) also suggest that this process may explain the presence of a broad flat shoreface which develops in some years in areas where slush ice accumulation has been observed.

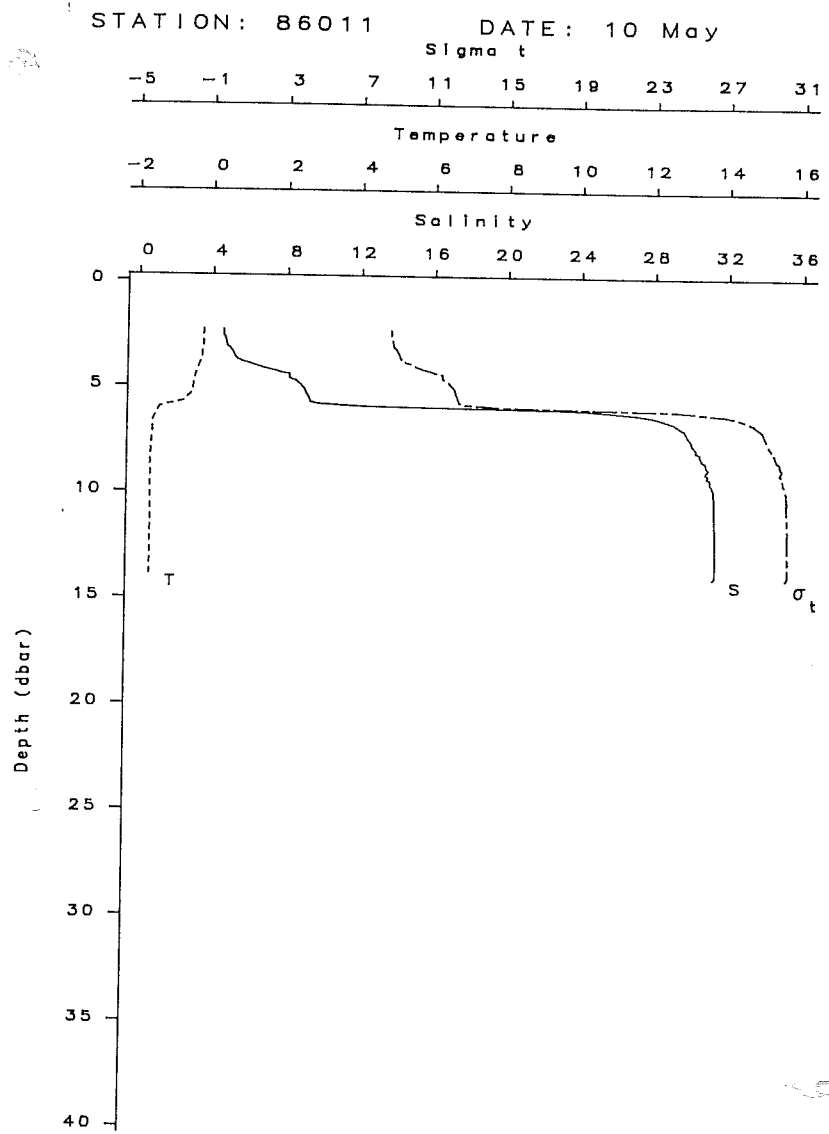
## **2.7 Oceanography**

There are several summaries of the oceanographic regime of the Beaufort Shelf, including Herlinveaux and de Lange Boom (1975), Huggett et al. (1975), Harper and Penland (1982), Fissel and Birch (1984), Davidson et al. (1988), and various consultants reports for the petroleum operators. Recently Arctic Sciences Ltd. have compiled data collected over the last 30 years to evaluate inter-annual variability in various oceanographic parameters.

### **2.7.1 *Water Column Structure***

During the winter months, there are relatively few oceanographic measurements beneath the ice canopy. An extensive set of winter salinity and temperature data (months of March and May, 1984 to 1988) has been collected by M.J. Lawrence and co-workers (Hopky et al., 1986, 1987, 1988a, 1988b) and a small amount of data from the inner shelf north of Richards Island was collected by the author in February 1989. Winter outflow from the Mackenzie River forms a fresh water layer up to 5 m thick at the ice-water interface by early May (Fig. 2.17). The pronounced stratification and very sharp halocline in these data attests to the low energy environment beneath the ice in winter. There are no measurements of oceanographic conditions during break-up (i.e. from mid-May to June) due to the extremely difficult operating conditions at this time of year.





**Figure 2.17** Temperature/salinity profiles measured northwest of North Head.

During the open water season, the Beaufort Shelf shows a predominantly stratified structure. Fresh water from the Mackenzie River mixes horizontally with shelf water, but a strong vertical stratification is maintained. The Mackenzie "Plume" forms a low-salinity layer, in the order of 5 m thick, over most of the eastern shelf between June and September (Fig. 2.18). The plume is also characterised by high suspended sediment concentrations (SSC) which generally decrease offshore. Satellite imagery, enhanced to show SSC distribution, reveals that the plume has a complex structure, consisting of numerous "packets" of water, with eddies apparent at packet boundaries (Fig. 2.19).

Hill and Nadeau (1989) have shown that the water column stratification breaks down in water depths less than 10 m during northwesterly storms, as a result of mixing under high energy conditions. Also following periods of northwesterly winds, the plume is often deflected to the east in a narrow band along the Tuktoyaktuk Peninsula (Harper and Penland, 1982). Less commonly, plume water is deflected westwards along the Yukon coast during periods of easterly winds.

Areas of cold water, low in SSC, have been observed to occur along the coast of the Yukon (Harper and Penland, 1982; Fissel et al., 1987; McDonald et al., 1987) and Tuktoyaktuk Peninsula (Fissel et al., in prep.). Coastal upwelling of deeper Beaufort Sea water may account for these phenomena, but it is not clear whether their origin relates to regional wind patterns, local katabatic winds, or topographic effects on current flow in these areas.

### **2.7.2 Currents**

Summaries of current circulation in the Beaufort Sea are given in Hugett et al. (1975), Harper and Penland (1982), Fissel and Birch (1984) and Davidson et al. (1988). There is little publicly-available information on currents beneath the ice in winter. It might be assumed that water motions are minimal and result from Arctic Ocean influences combined with tidal forcing. The tidal range of the Beaufort Sea is small, approximately 0.4 m at Tuktoyaktuk (Huggett et al., 1975). Melling and Lewis (1982) noted dense saline bottom flows moving off the shelf into the Arctic Basin as a result of salt fractionation during freezing. In coastal waters, the outflow of the Mackenzie River may produce significant currents local to the main discharge channels.

Under open water conditions, current circulation is primarily wind-driven (Fissel and Birch, 1984). Time series analysis of current records from the eastern shelf shows that the predominant periodicity is in the order of 2 to 20 days, corresponding to the periodicity of wind events. Significant current fluctuations also occur over a period-range corresponding either to semi-diurnal tides or to inertial oscillation (Fissel and Birch, 1984). Currents correlate strongly with winds in surface and coastal waters (Fissel and Birch, 1984; Davidson et al., 1988), but the

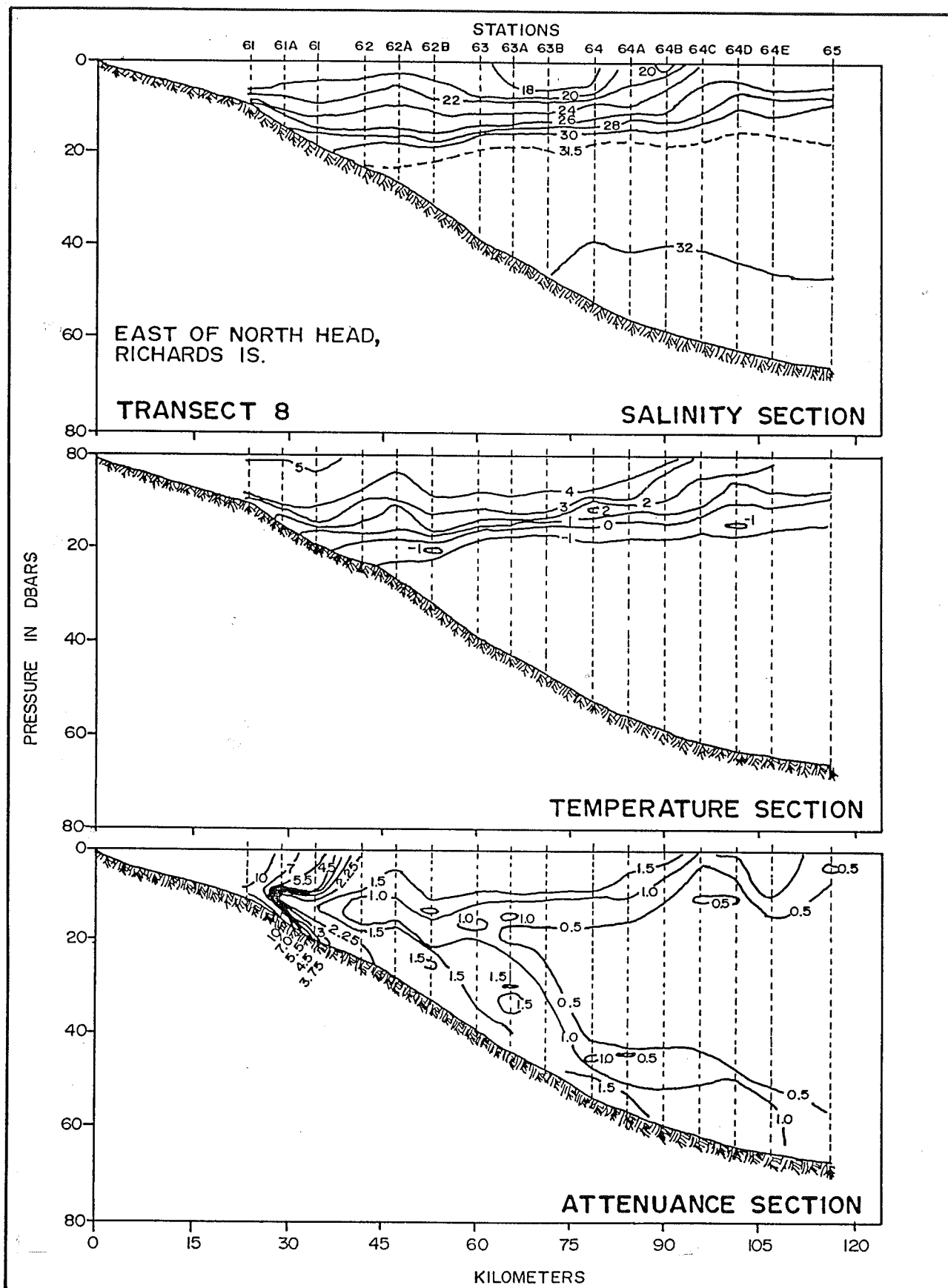


Figure 2.18 Temperature/salinity transect across the Beaufort Shelf between June and September.

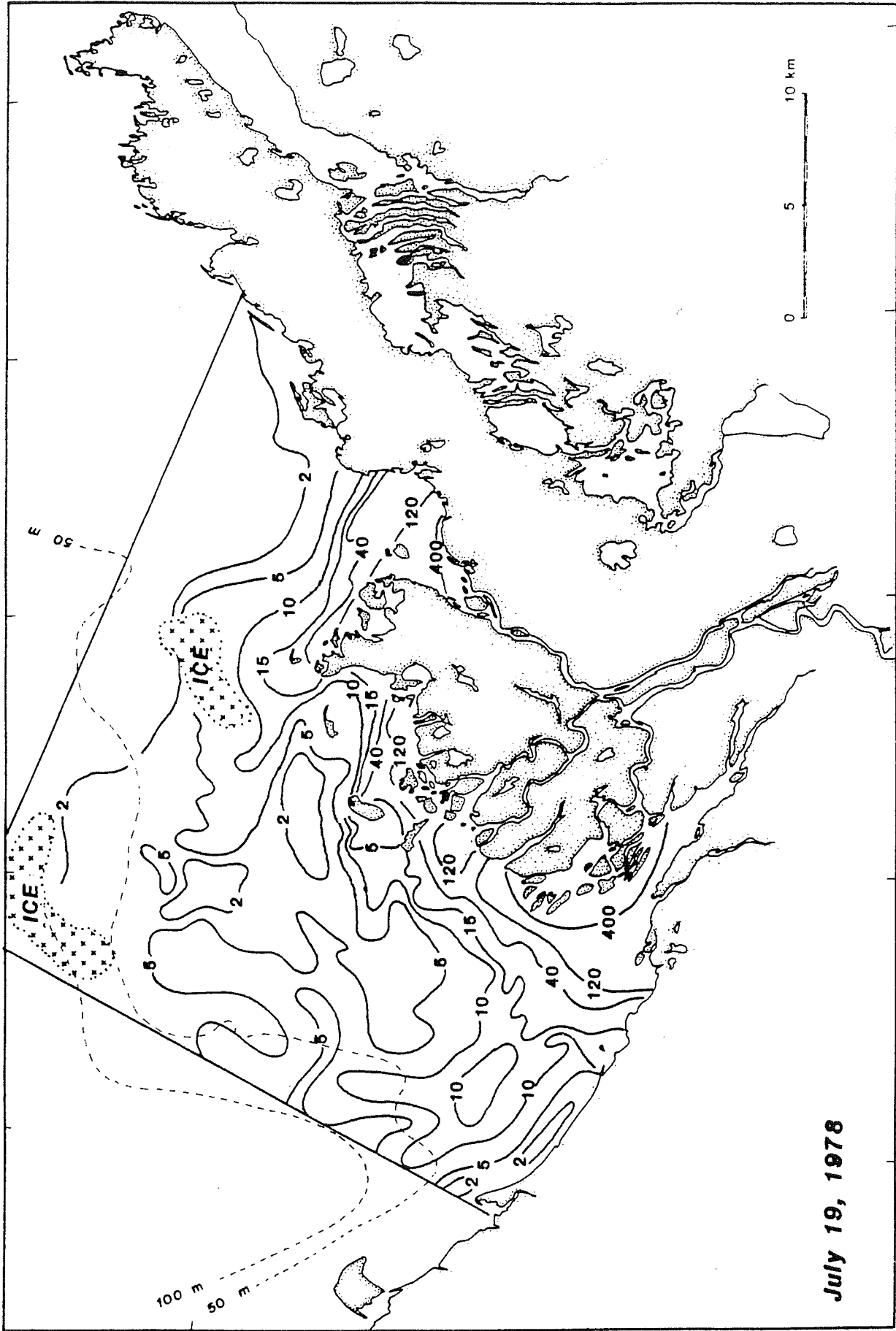


Figure 2.19 Suspended sediment concentrations (mg/l) of the Mackenzie Delta plume (Harper and Penland, 1987).

correlation becomes poorer for subsurface water due to decoupling of subsurface water from the wind-driven surface.

During periods of northwesterly winds, drogues and current meter records therefore indicate net easterly drift of surface water (MacNeil and Garrett, 1975; Fissel and Birch, 1984). This pattern is reversed during periods of easterly winds. However, the flow is complex and, particularly in coastal waters, influenced by topography. Figure 2.20 summarises bottom current direction data from a number of sites on the eastern shelf. Harper and Penland (1982) point out that strong current events (15-40 cm/s) show a more pronounced east- to northeastward drift (Fig. 2.21). On the inner shelf, directional variance becomes greater as local topographic effects and the influence of wave motions become more important (Davidson et al., 1988; Fig. 2.22). Correlation of winds and currents in this shallow water region indicates that current response to wind-forcing is greatest when the winds blow parallel to shore (or strictly to the local seabed contours).

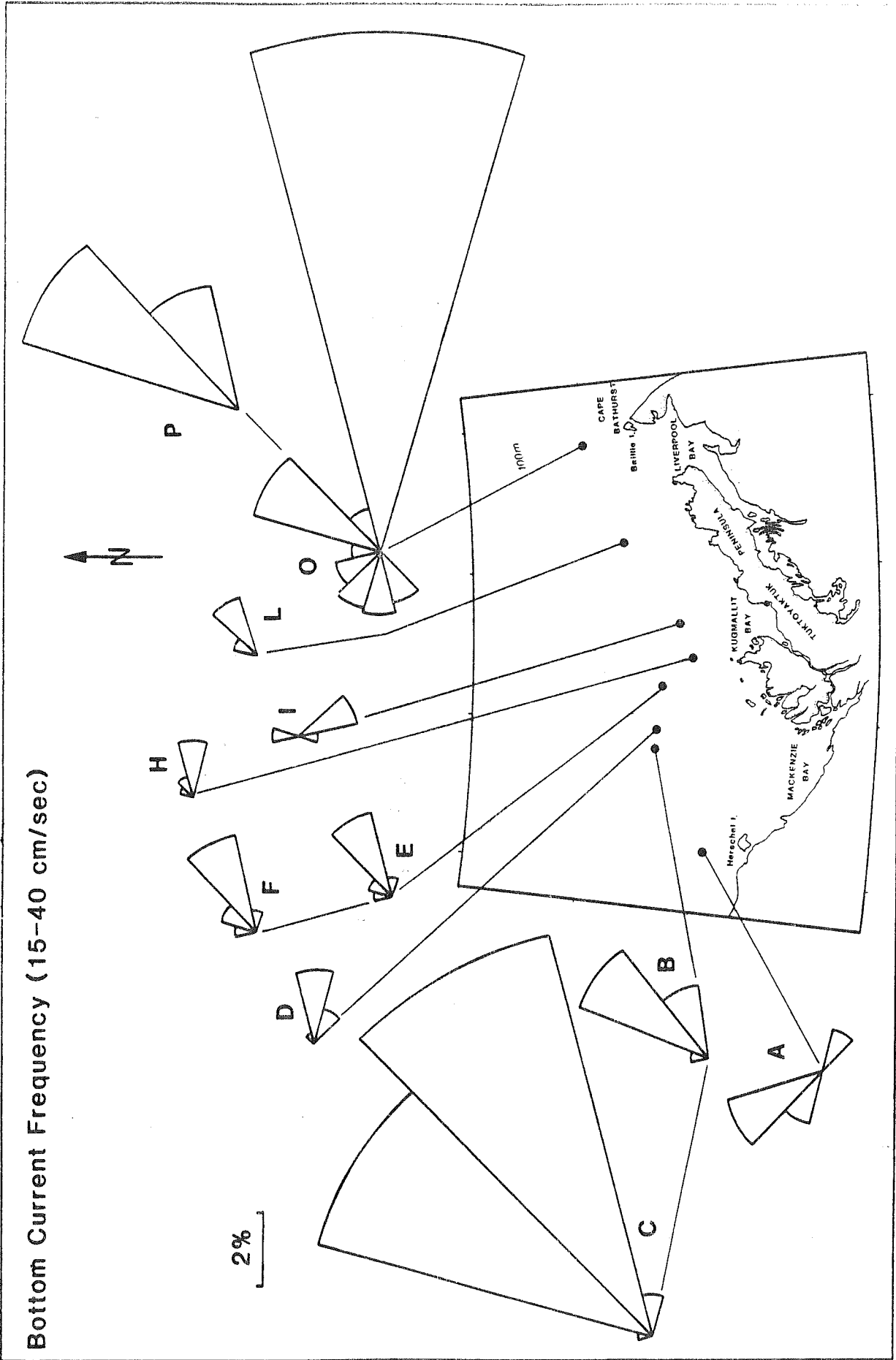
The above discussion has been restricted to the shelf west of Mackenzie Trough as there is very little current data from the trough or from the Yukon Shelf to the west. Strong currents are present in Mackenzie Trough (personal observations from the drillship M/V Broderick in September 1985) and in shallow water near King Point (Gillie, 1985).

### 2.7.3 *Waves*

Wave energy in the Beaufort Sea is largely controlled by the available fetch across open water and the wind direction. Winter ice cover means that waves are only important during the summer. Several hindcast model studies of the wave climate have been completed (Baird and Hall, 1980; Hodgins et al., 1981; Hodgins, 1983; Pinchin et al., 1985) using wind data from Tuktoyaktuk and varying fetch conditions. The Pinchin et al. (1985) hindcast model used 14 years of wind data, incorporated weekly ice charts to accurately determine fetch, and predicts shallow water wave conditions for seven sites along the Beaufort coast. Field measurements of wave characteristics including wave height, direction and orbital velocities have been collected over a number of years at offshore sites (Davidson et al., 1988; Fissel et al., in prep.) and in very shallow water (Gillie, 1986; Hodgins et al., 1986; Fissel and Byrne, 1988). However, none of these data sets are continuous across the entire open water season and few cover the stormy fall period prior to freeze-up. There are no multi-year data from any one site that could be used to verify the long term hindcasts.

The Beaufort Sea wave regime is characterised by wave heights and periods generally less than 4 m and 8 m respectively (Fig. 2.23). The strongest winds generally blow from the northwest, fetches are commonly longer to the northwest, and easterly winds are generally lighter,





**Figure 2.21** Directional frequency distribution of strong bottom currents (15-40 cm/s) from the eastern Beaufort Shelf (Harper and Penland, 1987).

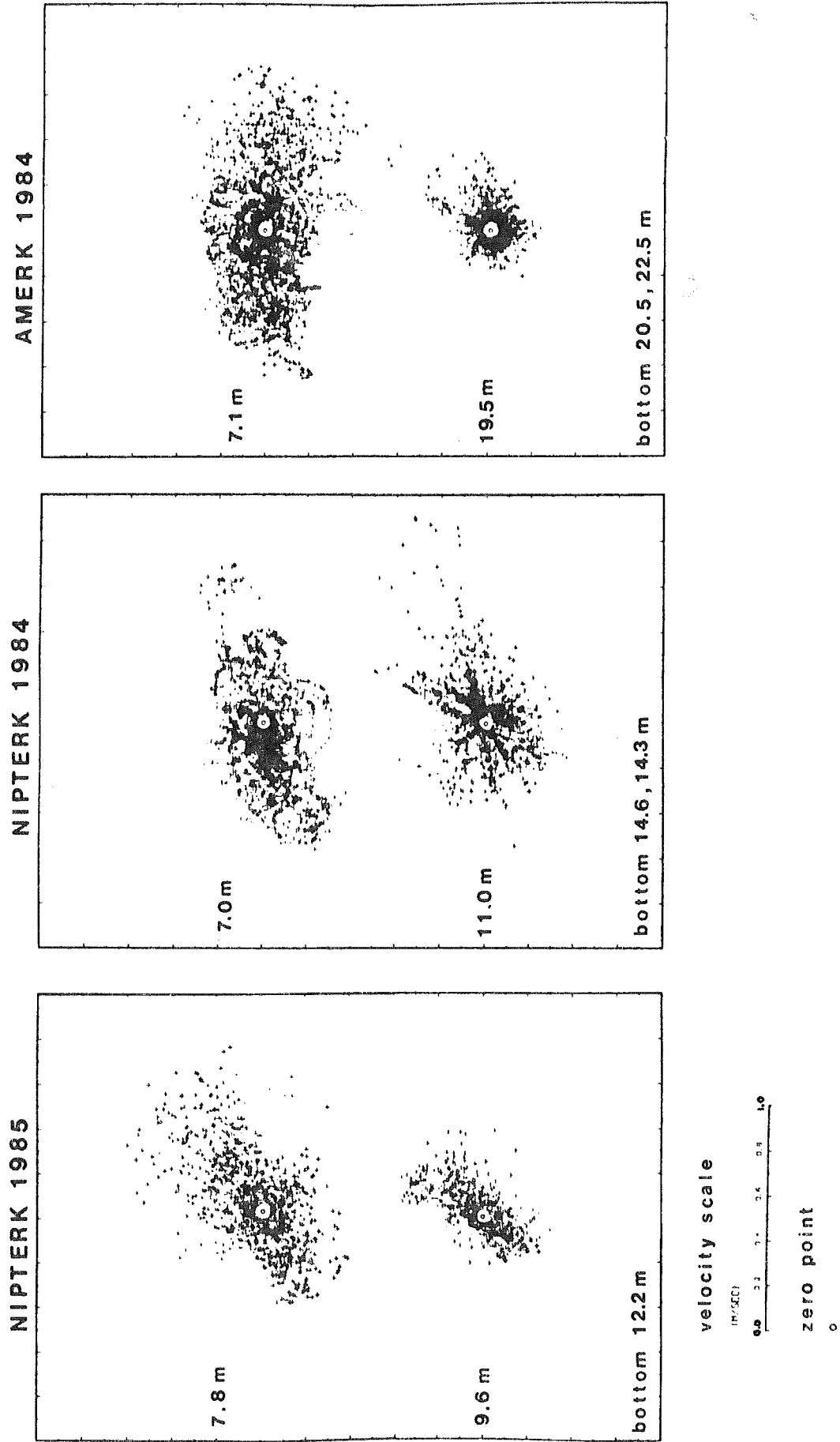
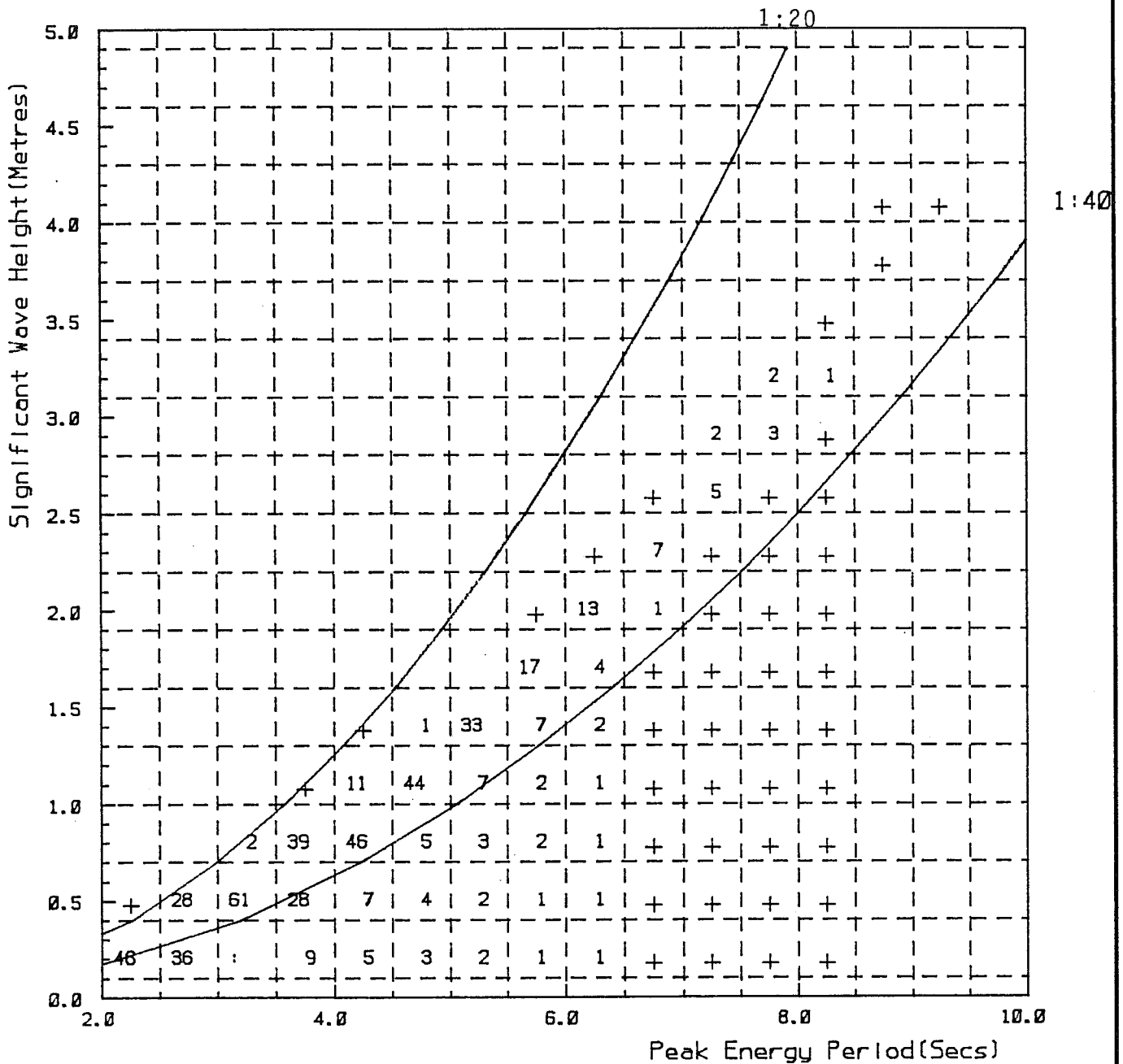


Figure 2.22 Directional distribution of currents from the inner Beaufort Shelf (Davidson et al., 1988).





Direction Limits: 0.0 TO 360.0

Values in parts per : 1000

Calms: 50.4 %

+ - Values less than 1 ppt

Dates: 17/6/70 to 28/9/83

Season: Summer, Fall

Total No. of Records: 32592

Waves Hindcast Using Wind Data from Tuktoyaktuk N.W.T.

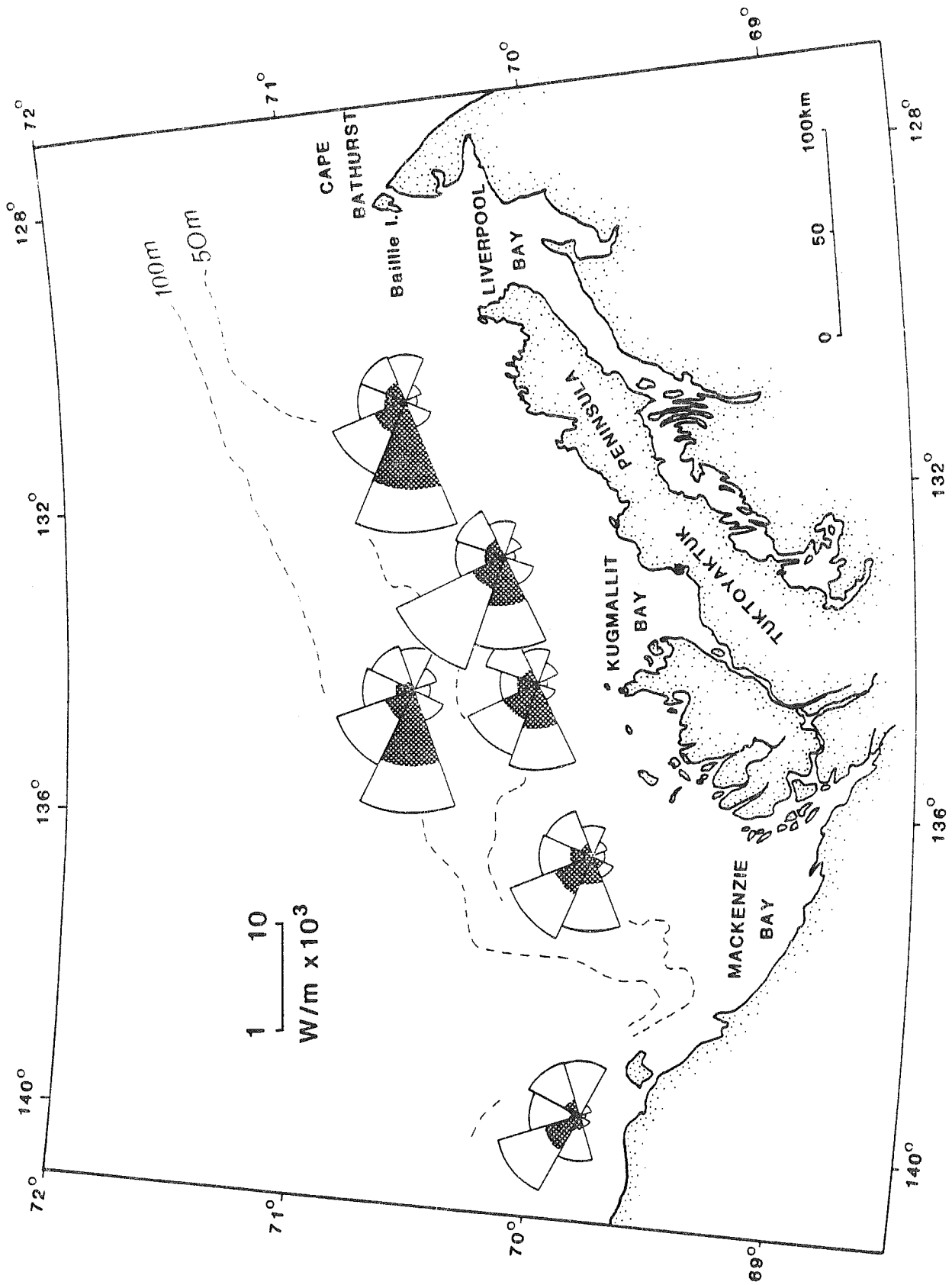
**Figure 2.23** Offshore wave characteristics scatter plot for the North Head region (Pinchin and Nairn, 1987).

with the result that the Tuktoyaktuk Peninsula and northwest facing coastlines experience the most severe wave attack (Fig. 2.24).

Predicting shallow water wave conditions is problematic in the Beaufort Sea, particularly in the vicinity of the Mackenzie Delta and Richards Island. The complex coastal configuration of Richards Island has to be taken into account as parts of the coastline are sheltered from deep water waves and locally-generated waves become more important (Pinchin et al., 1985). In addition, the very low slope and muddy seabed of the inner shelf in the delta and adjacent regions may lead to dissipation of wave energy through bottom friction (Hill and Nadeau, 1989).

#### **2.7.4 Storm Surge**

Water level elevations resulting from positive storm surges are extremely important for facilitating wave attack on the Beaufort coast and have been recognized as a potential hazard to coastal settlements and structures in both Canadian and Alaskan Beaufort Sea regions (Department of Public Works, 1971; Henry, 1975; Reimnitz and Maurer, 1979). Surge levels are poorly documented in the region, as a result of inopportune gaps in the tide gauge record from Tuktoyaktuk. Although caused by strong onshore-blowing winds, return periods cannot be predicted with confidence, as information on extreme winds is also limited. Surges have been studied using numerical models (Henry, 1975; 1984) and by field observations (Harper et al., 1988). Mapping of log-line deposits suggests a maximum storm surge level of 2.4 m above mean sea-level in the Kugmallit Bay region. Based on cultural material within the log debris, Harper et al. (1988) concluded that two known storm surges, in 1944 and 1970, were both of approximately this level. Maximum surge levels may occur along different sections of the coast at different times. Forbes (1989) points out that a major log-line redistribution occurred in the Babbage Delta area between the two storms of 1944 and 1970. Also, numerical model results suggest that the surge is amplified in large bays, such as Shallow Bay and Kugmallit Bay. Thus, estimation of the return frequencies of storm surges for any particular section of coast is difficult and has not been attempted to date.



**Figure 2.24** Directional wave energy for the Beaufort Shelf as computed from the wave climate summaries of Baird and Hall (1980) and Harper and Penland (1987). The shaded area of the wave rose represents wave power components resulting in wave heights in excess of 2 m.

### 3. METHODS AND DATABASE

This report is based on a variety of field and desk studies carried out over a period of four years (Tables 3.1 and 3.2). Most of the studies were carried out by contractors or with contract support under the supervision of Geological Survey of Canada staff. The following section summarises the methods used to accumulate the database used in the report.

#### 3.1 Shoreline Surveys

Two methods have been used to evaluate the rate and direction of coastline change: (a) aerial photographs collected in the 1950's, 1970's and 1980's were compared quantitatively (Harper et al., 1985); and (b) a long-term field monitoring program was established.

For the aerial photograph method, a magnifying optical comparator was used to measure perpendicular distances from the coastline to an inland point common to both photographs. For this analysis, operator error was less than 1% and range error due to distortion of the photographs was less than 10%. Long-term average rates of coastline change were estimated from this study.

Forbes and Frobels (1985) conducted surveys of cliff and beach profiles in 1984. The aim of the cliff surveys was to revisit sites previously surveyed and estimate retreat rates. The beach profiles were measured for use in the sediment transport study of Pinchin et al. (1985). The following year a detailed survey of the beach and nearshore zone was carried out at King Point (Gillie, 1986). Several of the Forbes and Frobels sites were remeasured in 1986 (Gillie, 1986) and new surveys were established at a number of other sites. Hequette (see Hill, 1988) revisited many of these sites in 1988. In addition, S. Dallimore (Terrain Sciences Division) has monitored coastal change in the vicinity of North Head for the last three years. The locations of these surveys are summarized in Figure 3.1.

All beach and cliff surveys were carried out to wading depth using a level, tape and survey rod. Semi-permanent markers in the form of wood or iron stakes were placed along the survey lines to establish the location and relative datum for repeat surveys. At King Point, previously established bench marks were used to locate the detailed survey. Where beach profiles were extended into the nearshore, precision echo sounders were used from a Zodiac and the R/V Karluk. Forbes and Frobels used range markers and theodolite angles to position the nearshore surveys, whereas Gillie used an electronic distance measurement (EDM) instrument.

#### 3.2 Seismic Surveys

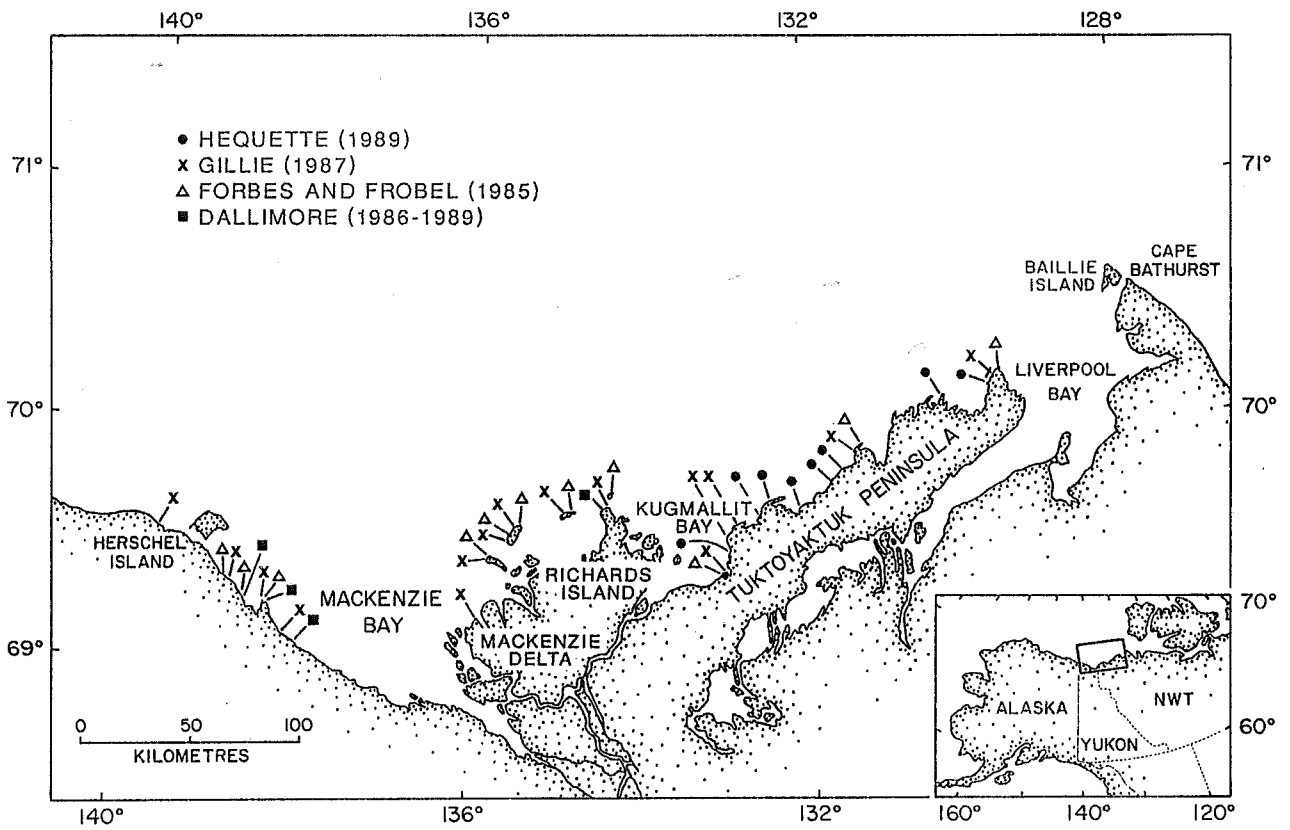
There were four cruises on which seismic data were collected (Table 3.1; Fig. 3.2). The different combination of seismic sources and receivers used on each cruise are summarised in Table 3.3. On all cruises except Karluk 85, on which only Satnav and radar were available,

**TABLE 3.1** Data Sources: List of field programs conducted in the Beaufort Sea coastal zone, under NOGAP Project D.1, 1984 to 1988.

- 1984**
1. Winter drilling program at North Head, February.  
Ref: Hill et al, 1986.
  2. Aerial video survey, U.S. border to Nicholson Peninsula, July-August.  
Ref: Forbes and Frobel, 1985; 1986.
  3. Cliff and beach survey, Komakuk Beach to Cape Dalhousie, July-August.  
Ref: Forbes and Frobel, 1985.
- 1985**
5. Winter drilling program, King Point, March. (INAC project, partially funded by NOGAP D.1)  
Refs: O'Connor, 1986; Hill et al., 1986; Hill, 1990.
  6. Sediment Transport Study, King Point, August-September.  
Refs: Morgan, 1986; Gillie, 1986.
  7. R/V Karluk Seismic cruise, U.S. Border to King Point, September.  
Ref: None.
- 1986**
8. CCGS Nahidik seismic and coring cruise, September.  
Ref: McGregor Geoscience Ltd., 1986.
  9. Cliff and beach surveys, Komakuk Beach to Cape Dalhousie, July-August.  
Ref: Gillie, 1987.
- 1987**
10. Video survey of break-up processes, U.S. Border to Cape Dalhousie, June.  
Ref: Dickins, 1987.
  11. Mackenzie Delta sedimentological study, July 12- August 20.  
Ref: Jenner (in Hill, 1988).
  12. Mackenzie Rver Delta suspended sediment sampling, August 12-20.  
Ref: Kranck and Milligan (in Hill, 1988).
  13. CCGS Nahidik seismic and vibracoring cruise, September 11-18.  
Ref: Hill, 1988.
  14. R/V Karluk seismic and sampling cruise, August 20 - September 16.  
Ref: Hequette (in Hill, 1988).
  15. Beach Dynamics Study, Tibjak Beach, August 22 - September 17.  
Refs: Hill, 1988; Fissel and Byrne, 1988.
- 1988**
16. Cliff and Beach surveys, coring of coastal marshes, August 5 - 19, 1988  
Ref: Hequette, 1989.

**TABLE 3.2** Data Sources: List of major desk studies on the Beaufort Sea coastal zone. See Appendix 1 for details.

1. Morphological zonation of the coast and estimates of coastal retreat rates from comparison of aerial photographs.  
Ref: Harper et al., 1985.
2. Numerical estimation of sediment transport and nearshore profile adjustment at coastal sites based on a 14-year wave hindcast.  
Ref: Pinchin et al., 1985.
3. Survey of suitable vessels and seismic techniques for shallow water.  
Ref: Harper, J.R., and Swift, S., 1985
4. Review of ice-related processes in the Canadian Beaufort Sea.  
Ref: Arctec, 1987.
5. Evaluation of inshore wave climate and coastal sediment transport prediction techniques at King Point (comparison of numerical hindcast to field data). (and) Numerical model of the effects of a structure at King Point.  
Ref: Pinchin and Nairn, 1987.
6. Detailed analysis of high resolution seismic reflection system requirements for shallow water surveys, including design and production of a prototype line-and-cone receiver.  
Ref: Simpkin, 1988.
7. Analysis of wave and current data from shallow water sites, including estimates of near-bed shear stresses.  
Ref: Davidson et al., 1988.



**Figure 3.1** Location map of cliff and beach survey measurements along the Beaufort Sea coast.

**TABLE 3.3** Seismic equipment used for NOGAP D.1 coastal zone surveys 1985-1988.

**KARLUK, 1985**

**NAHIDIK, 1986**

Huntec Sea Otter boomer source  
NSRF Ministreamer  
Raytheon PTR 3.5/7.0 kHz Profiler  
Huntec MS26B hydrophone

**NAHIDIK 1987**

EG&G Model 230 Boomer (Uniboom)  
Datasonics Model BPR-510 Bubble Pulser  
IKB Technologies Directional Hydrophone  
NSRF Ministreamer  
Datasonics BPH-540 Streamer  
Raytheon PTR 3.5 kHz Profiler

**KARLUK 1987**

ORE Boomer system  
Benthos Hydrophone streamer  
NSRFC Ministreamer  
Raytheon PTR 7 kHz and 200 kHz profiler



precise navigation ( $\pm 10\text{m}$  or better) was obtained using radio navigation systems. Some navigation problems were encountered on cruise Nahidik 1987 when the ship crossed the system baseline. In these locations, positioning was achieved by extrapolation using Satnav and dead reckoning.

The Karluk 85 cruise was a first attempt at collaboration between the USGS and GSC, centred on the Karluk. The 40-ft vessel was brought into the Canadian Beaufort Sea from Prudhoe Bay by Erk Reimnitz. The cruise track was limited to an excursion along the coast as far east as King Point. Bad weather and ice conditions forced the boat to return to Alaska early, so that relatively little work was accomplished in Canadian waters. A single seismic profile, in waters less than 20 m deep, was run along the Yukon coast (Fig. 3.2).

On the Nahidik 86 cruise, the high resolution boomer systems did not achieve good results with the horizontal streamer arrays in water depths less than 10 m. For much of the time, the single hydrophone system produced better quality records. Studies of the acoustic properties of sediments in the coastal zone indicated that the low signal to noise ratio achieved by this system was due to two main factors: (1) significant volume scattering by the sediments, particularly where thin silt and clay beds predominate; and (2) the horizontal streamers were averaging wide angle reflections and even refraction returns due to the very shallow water depth (Simpkin, 1988). A prototype line-and-cone receiver was designed to overcome these problems. The receiver consists of a large cone, approximately 1 m in diameter with a vertical array of three receivers. The cone captures signal from a low angle of incidence only and the signal to noise ratio is substantially improved. Field testing of the prototype (the IKB system) was carried out on the Nahidik 87 cruise and was remarkably successful. Good quality records were obtained in shallow water areas of the Mackenzie Delta, Kugmallit Bay and seaward of Richards Island.

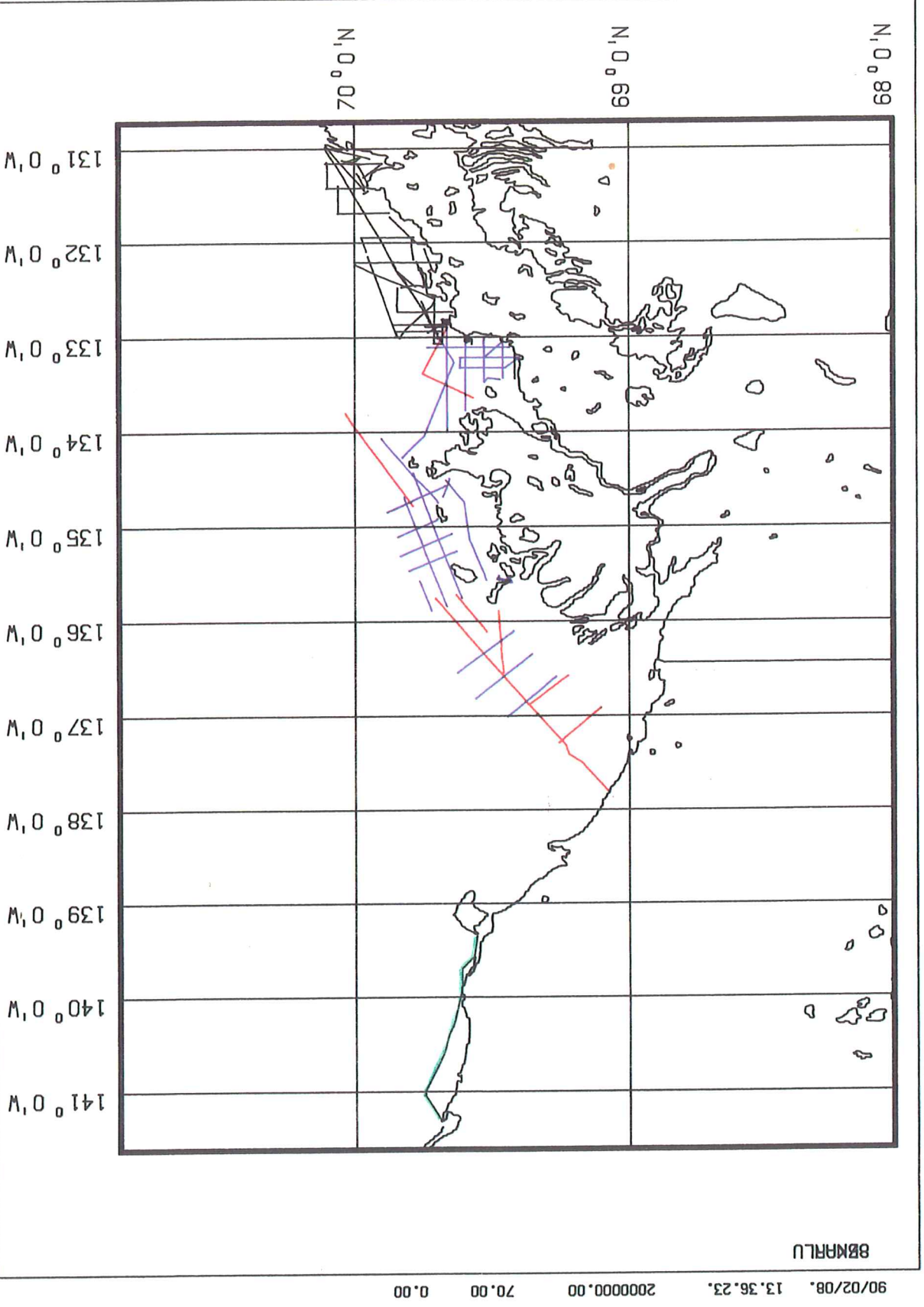
A second Karluk cruise took place in 1987, again in cooperation with E. Reimnitz and P. Barnes of the USGS. Effort on this cruise was concentrated on the coastal zone of the Tuktoyaktuk Peninsula. Although not equipped with the newly designed IKB system, good quality records were obtained with the high resolution boomer system. Volume scattering was not a problem in this region where sandy units occur within a few metres of the seabed.

During interpretation, selected lines were digitised into an Autocad-based data system called Supertech, by Earth and Oceans Research Ltd. This allowed the presentation of some long seismic sections in summary form. Reflectors were digitised directly from seismic profiles.

### **3.3 Lithostratigraphy**

Due to the common occurrence of harder sediments, especially silts and sands, in the coastal zone, conventional piston coring has proven to be largely unsuccessful. Most of the

BLACK=87KARLUK GREEN=85KARLUK RED=87NAHIDIK BLUE=86NAHIDIK  
 1:2,000,000 (MERCATOR, 70N)



ATLANTIC GEOSCIENCE CENTRE

Figure 3.2 Track plot of seismic data collected under NOGAP Project D.1 from 1985 to 1987.

lithostratigraphic data reported here comes from geotechnical boreholes or vibracores. Two drilling programs, at North Head in 1984 (largely PERD-funded) and at King Point in 1985 (joint INAC/NOGAP funding), were conducted in the coastal zone of the Beaufort Sea (Fig. 3.3). Both programs were conducted during the winter from the landfast ice. Data from both these programs were analysed under the NOGAP D.1 project.

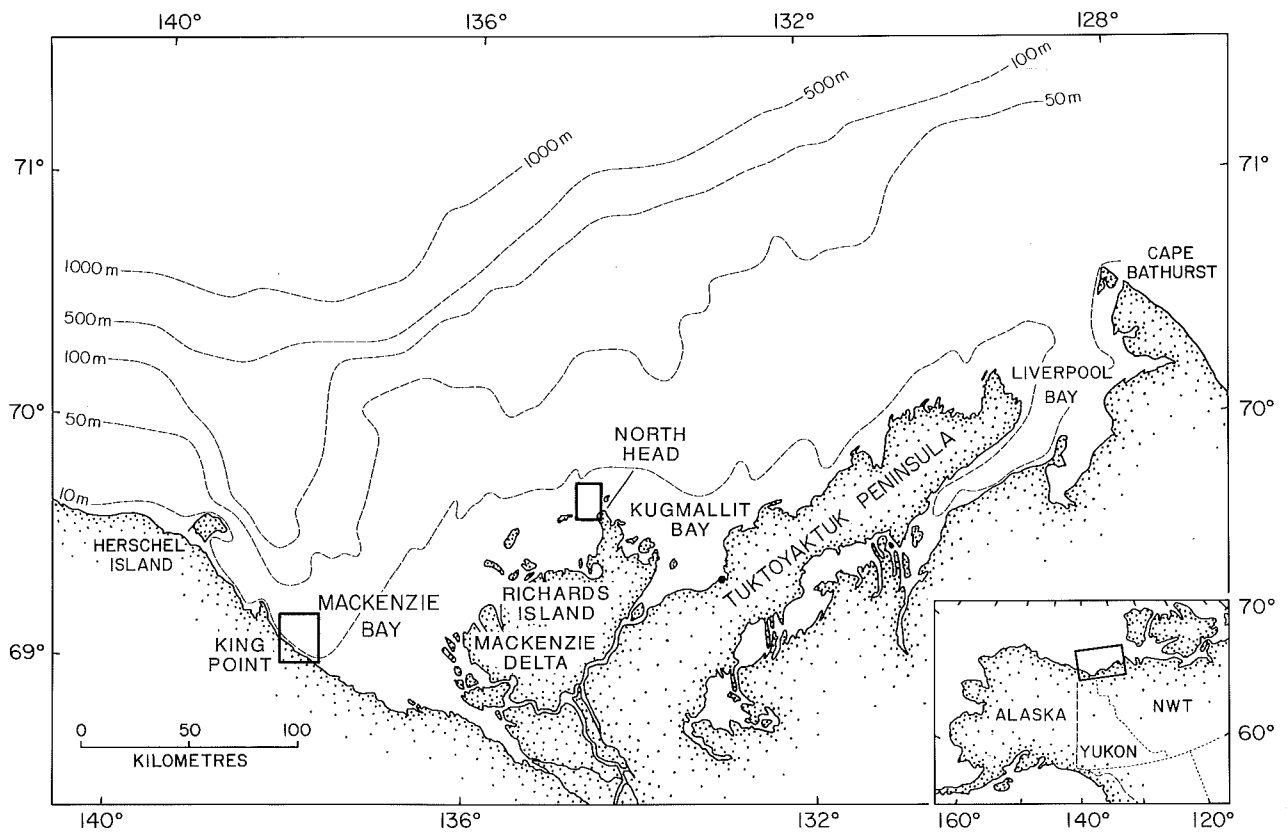
At North Head and for offshore samples at King Point, a rotary drilling method was used to penetrate unfrozen sediments. Sampling was carried out with steel Shelby tubes to obtain high quality cores for sedimentological and geotechnical analysis. The samples were extruded and carefully split at the site using a thin wire. A rotasonic drill rig was used to sample frozen sediments of the barrier and adjacent land area at King Point, but this method tended to heat the samples during penetration and core quality upon extrusion was lower than for the rotary drill method. Nevertheless, massive ice and frozen sediments were routinely sampled using the rotasonic rig. These samples were also extruded, split and described in the field camp. Additional core material was collected during the Nahidik '86 and '87 cruises using a conventional gravity corer and the BIO Vibracorer, fitted with a 3 m barrel (Fig. 3.4). These core samples were stored for approximately 1 year before being split. Acoustic piezocone penetrometer profiles were also obtained from the coastal zone off King Point (O'Connor, 1986) and North Head (Kurfurst, 1986; 1988). These profiles have been analysed by Dallimore et al. (1988).

### **3.4 Geotechnical Properties**

A variety of tests were carried out on borehole and vibracore samples to determine the physical properties of the coastal zone sediments. Testing was carried out in order to comply with ASTM standards.

Sub-samples were taken immediately after splitting for natural water content and bulk density. Water content was obtained by weighing three samples, drying them in a 40°C oven for 24 hours and obtaining the dry weight. Bulk density was obtained from the same samples using one of two methods. For both borehole programs, known volume samples were obtained using a specially-machined sampling syringe. For the Nahidik '87 samples, wet and dry volumes were obtained using the Penta Pycnometer which evacuates the samples, then replaces the air with a measured volume of helium.

Horizontal shear strength measurements were also made on the borehole samples immediately after splitting, using a computerised Wyckham-Farrance shear vane device. Shear strength was measured on the Nahidik '87 samples using a hand-held mini-vane. Liquid and plastic (Atterberg) limits were measured on samples from the two drilling programs in accordance with ASTM test method D424. Grain size analysis was carried out under contract using sieve and hydrometer methods for coarse and fine sediments respectively. Selected samples were analysed at



**Figure 3.3** Map showing the locations of the North Head, 1984 and King Point, 1985 drilling programs.

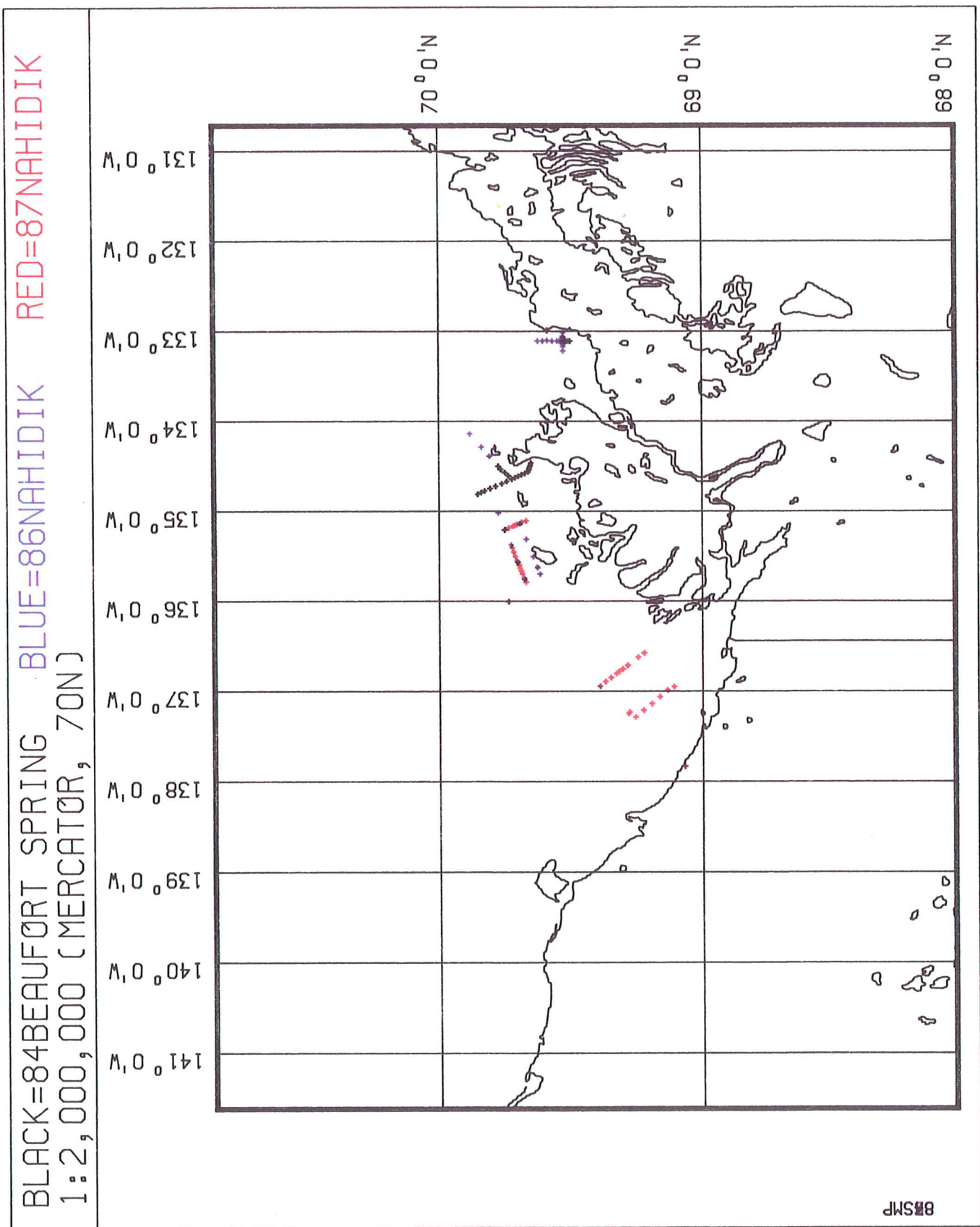


Figure 3.4 Map showing locations of 1984 boreholes, Nahidik '86 gravity cores, and Nahidik '87 vibracores.

the AGC Sediment Laboratory, using settling tube, Sedigraph and Coulter Counter methods.

### **3.5 Sediment Transport**

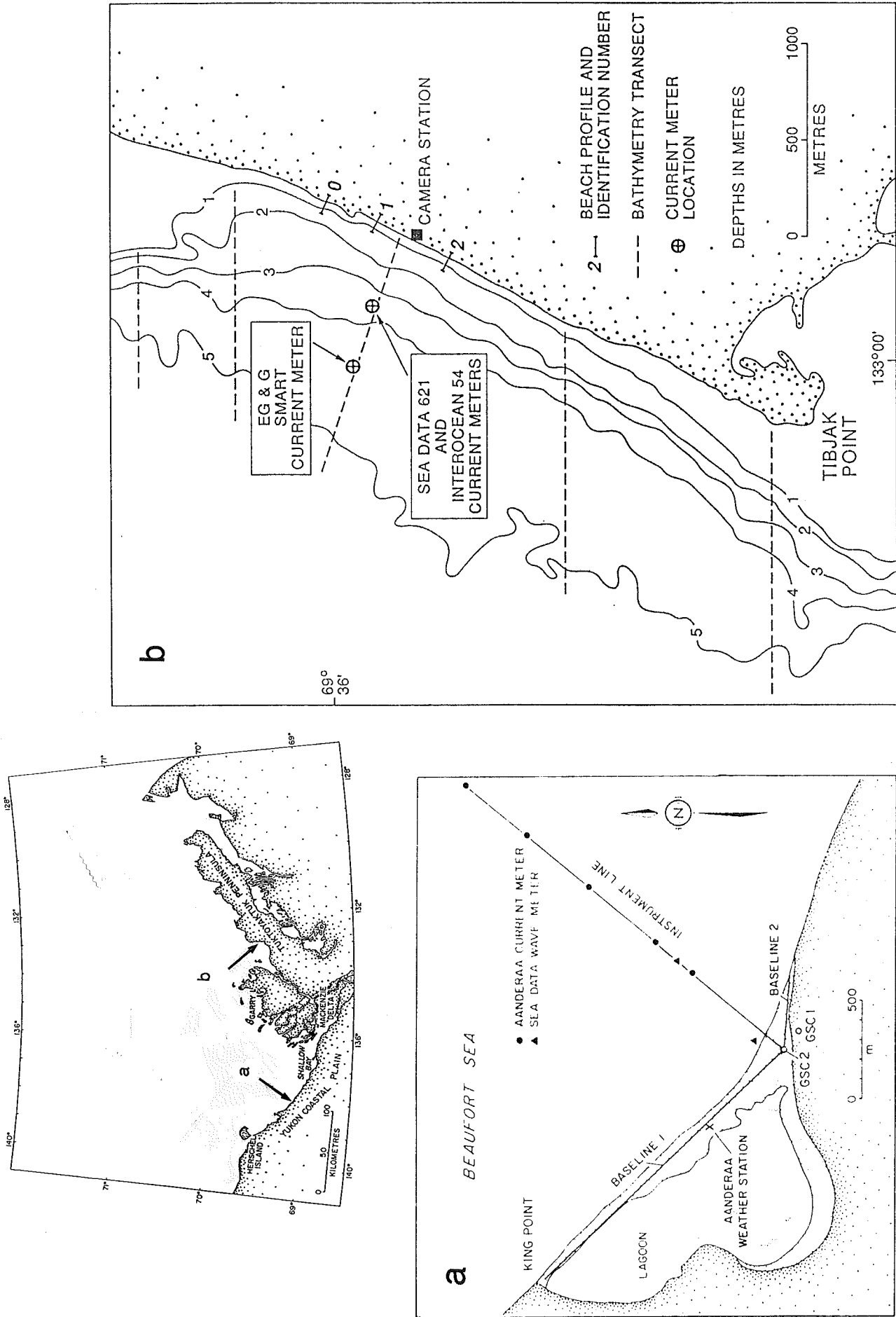
Numerical model estimates of coastal sediment transport rates were made by Pinchin et al. (1985) based on a 14-year hindcast of wave parameters. The numerical calculations used thirteen different published predictors of sediment transport, descriptions of which are available in Pinchin et al. (1985). Two attempts were made in the course of this study to obtain field measurements related to sediment transport: (i) at King Point in 1985; and (ii) at Tibjak Beach in 1987 (Fig. 3.5). As actual measurement of sediment transport is very difficult (Bowen et al., 1986), the field programs were aimed at measuring wave height and direction as well as currents in the nearshore zone, particularly where waves were breaking during storms. In addition to these data, winds and offshore wave conditions, measured, synchronously with observations of changes in beach profile and morphology.

#### **3.5.1 King Point Program, August 24 to September 16, 1985.**

The first program was carried out on the barrier beach south of King Point (Gillie, 1985). A detailed survey of the beach, lagoon and nearshore was carried out as described in section 3.1. An Aanderaa weather station was deployed at the beach to measure wind speed and direction. Five Aanderaa current meters, equipped with paddle rotors were deployed in a transect from shore in water depths ranging from 5 to 15 m. The current meters were attached to a weighted line supported by Vimy floats and positioned at 1.4 m above the seabed. To measure directional wave spectra and current velocities, two Seadata instruments were deployed on separate aluminium tripod frames, a model 621 in 2.7 m of water, 20 m from the shoreline and a model 635-12 in 5.6 m of water, 400 m from shore. Beach and seabed samples were collected and a suspended sediment sampler, consisting of a gas-powered pump and hose intake attached to the legs of the shallow water tripod, was used to take water sample. Observations, including visual estimates of wind speed and direction, wave height, form, breaking characteristics and angle of approach, and beach morphology were made on a daily basis.

The results of this program were disappointing. Numerous problems, mainly relating to the Aanderaa and Seadata equipment severely restricted the amount of useable data collected. The major problems were:

- (1) The mooring design of the Aanderaa current meters was inadequate for the high energy conditions they were deployed in. Two of the meters were lost, one became fouled in its mooring line and the remaining meters were coated with mud, indicating periods of contact with the seabed. Data from these meters are not considered reliable.



**Figure 3.5** Map showing the locations of King Point, 1985 and Tibjak Beach, 1987 sediment transport field measurements.

(2) The pressure sensor of the Seadata 621 meter was found to have malfunctioned, so no wave height measurements were available from the inshore site.

(3) The Seadata 635-12 meter, when recovered, was found to have tipped over during the deployment period. When reviewed, the data initially appeared stable until late in the deployment. Wave directions were estimated from the current meter burst data. However, subsequent analysis of the wave directions derived from this analysis indicates major discrepancies when compared with measured current data at the Seadata 621 instrument and littoral observations (Pinchin and Nairn, 1987).

(4) King Point is a complex site due to its northeasterly aspect (parallel to the dominant winds) and proximity to the mountains, resulting in the influence of local katabatic winds. Furthermore, the instruments were deployed at the apex of a major bend in the barrier, instead of along a straight section, which makes numerical modelling extremely difficult.

Consequently, the program at King Point did not achieve its main objective to produce directional wave data from the site that could be directly compared with numerical model results based on regional wind data.

### ***3.5.2 Tibjak Beach Study, August 27 to September 17, 1987.***

The second program was carried out on Tibjak Beach, approximately 12 km north of Tuktoyaktuk (Fissel and Byrne, 1988). This beach was selected because of its northwesterly aspect, the straightness of the beach and its proximity to Tuktoyaktuk. The instrumentation deployed consisted of two packages. The first, deployed in 3.5 m of water, consisted of a Seadata 621 directional wave and current meter, mounted on a three leg aluminium base, and an Interocean S4 current meter supported by Vimy floats. The second package, deployed in 5.0 m of water consisted of a Seadata 635-9 directional wave and current meter and an EG&G Smart acoustic current meter, moored in a similar fashion. All the meters deployed were true vector-averaging current meters, having no moving parts, and were therefore more suitable for measuring orbital wave velocities than the Aanderaa current meters used at King Point.

In addition to the offshore instrumentation, a pair of microprocessor controlled video cameras, mounted on a 4 m high aluminium platform, were used to monitor beach morphology changes. The cameras were set to operate for one minute every three hours during daylight hours. Notes on the beach morphology changes from the videotapes can be found in Hill (1988). Beach profiles were measured at this site three times during the instrument deployment period, including



both fair and storm conditions.

Preliminary results from this experiment are reported in Fissel and Byrne (1988). The Seadata 635-9 instrument leaked and failed to produce useable data from the deeper site, but the other instruments all provided full data sets.

### **3.5.3 *Other Data Sets***

In addition to the two field programs described above, data from various other wave and current measurement programs have been utilized in this study (Table 3.4). All the data sets in Table 3.4, except the 1987 data (items 7 and 8) were summarised in the NOGAP D.1 contract study by Davidson et al. (1988). The 1987 data are presented and analysed in the NOGAP B.6 study by Hodgins (1988).

**TABLE 3.4** Wave and current data sets collected by other agencies from the Beaufort Sea coastal zone and used in NOGAP D.1 studies.

	SITE	WATER DEPTH (m)	DATES	DATA DESCRIPTION
1.	Amerk	20.5	31/7/84 -26/9/84	Mean currents.
		22.5	24/7/84-27/9/84	Mean currents, near bottom.
		21.0	05/8/84-05/10/84	Wave height and period.
2.	Nipterk	14.6	05/8/84-26/9/84	Mean currents.
		14.3	24/7/84-26/9/84	Mean currents, near bottom.
3.	Arnak	7.6	28/8/85-3/10/85	Burst velocities, mean current, near bottom.
4.	Nipterk	12.2	26/8/85-14/10/85	Mean currents, near bottom.
5.	T1.1	10.5	18/8/86-24/9/86	Wave height, period and direction, burst velocities, mean currents, suspended sediment concentration.
6.	T1.2	5.9	18/8/86-24/9/86	Wave height, period, and direction, burst velocities, mean currents, suspended sediment concentration.
7.	SD1	c. 9	02/9/87-07/9/87	Wave height, period, and direction, burst velocities, mean currents, suspended sediment concentration.
8.	SD2	c. 7	02/9/87-07/9/87	Wave height, period, and direction, burst velocities, mean currents, suspended sediment concentration.

## 4. SEA LEVEL HISTORY

Knowledge of the rate of relative sea-level (RSL) change is critical to any discussion of coastal stability and development of coastal landforms. Relative changes in sea-level may occur in response to eustatic, isostatic, tectonic and consolidation effects. Eustatic change is related to the worldwide balance between water in the ocean basins and water tied up in the world's ice caps. Isostatic change results from the loading of the earth's crust by ice sheets during glaciations and by deposition of sediment. Generally, glacial isostatic effects are more important than sediment loading over shorter time scales. Tectonic activity can cause rapid changes in RSL through processes of regional uplift or subsidence. Reduction in void space during consolidation of buried sediment can also result in an RSL change.

In this section, new samples and dates pertaining to the RSL history of the Canadian Beaufort Sea region are described and tabulated. These dates allow us to present an improved reconstruction of the Holocene relative sea-level curve. Following this, new field data and radiocarbon dates from coastal marshes along the Tuktoyaktuk Peninsula will be described. These samples were collected in an attempt to better constrain the curve over the last 2000 years, but their interpretation is ambiguous with the present knowledge of palynological assemblages in Beaufort Sea coastal environments. The data were therefore not included on the RSL curve, but warrant treatment here as they have considerable potential for future reconstructions of RSL.

### 4.1 Previous Sea Level Reconstructions

Forbes (1980) compiled a large number of radiocarbon dates from the Alaskan and Canadian Beaufort Sea. Few of the dates could be directly related to sea-level, but in conjunction with the presence of drowned valleys along the Beaufort coast, they suggested that RSL has been rising over the last 15,000 years (Fig. 4.1a). Forbes concluded that the pattern was not compatible with solely eustatic sea level rise, but suggested that isostatic effects, as a result of late Wisconsinan glaciation, recent sediment loading, or both, were important.

Hill et al. (1985) reported a number of additional dates on freshwater peats from boreholes on the Beaufort Shelf. The majority of dates were from Holocene peats deposited in thermokarst lakes formed in the uppermost part of the Tingmiark Sand. A thin peat bed at the Tarsiut site was dated at 27,000 years B.P., suggesting that RSL was at least 140 m lower than present at this time (Fig. 4.1b). Hill et al. inferred that RSL rose between 27,000 years and approximately 15,000 years B.P., but was then lowered to a late Wisconsinan minimum of -70 m. This lowering was supported by seismic evidence for the incision of 30 - 50 m deep alluvial valleys across the Beaufort Shelf (Hill et al., 1985; in press). During the Holocene, Hill et al. suggested RSL rose steadily from -70 m to its present position. However, as all the dates were from lacustrine

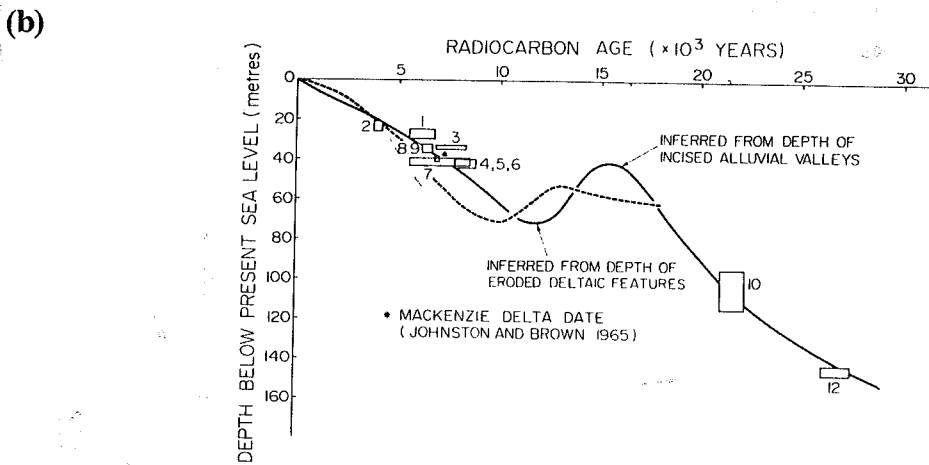
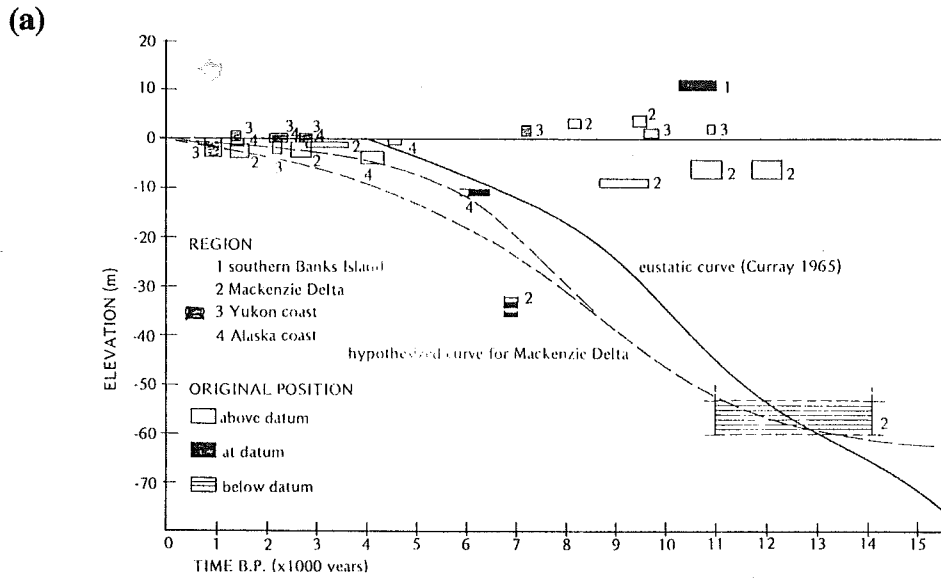


Figure 4.1 Previous sea-level curves: (a) Forbes, 1980; (b) Hill et al. (1985).

sediments, mostly deposited well above mean sea-level, the shape of the Holocene curve was not well constrained.

Hill et al. interpreted the RSL curve in a similar way to Forbes (1980), suggesting that glacial isostatic loading was the predominant cause of the sea-level fluctuations, even though this implied the presence of ice in the Beaufort-Mackenzie region during the middle Wisconsinan. Other workers had previously suggested that the area was ice-free during this period (Rampton, 1982; Mackay and Matthews, 1983). However, calculations of the potential effects of basin subsidence, movement on growth faults, sediment loading, and compaction subsidence (consolidation) suggest that, although significant, these mechanisms cannot account for the RSL changes observed.

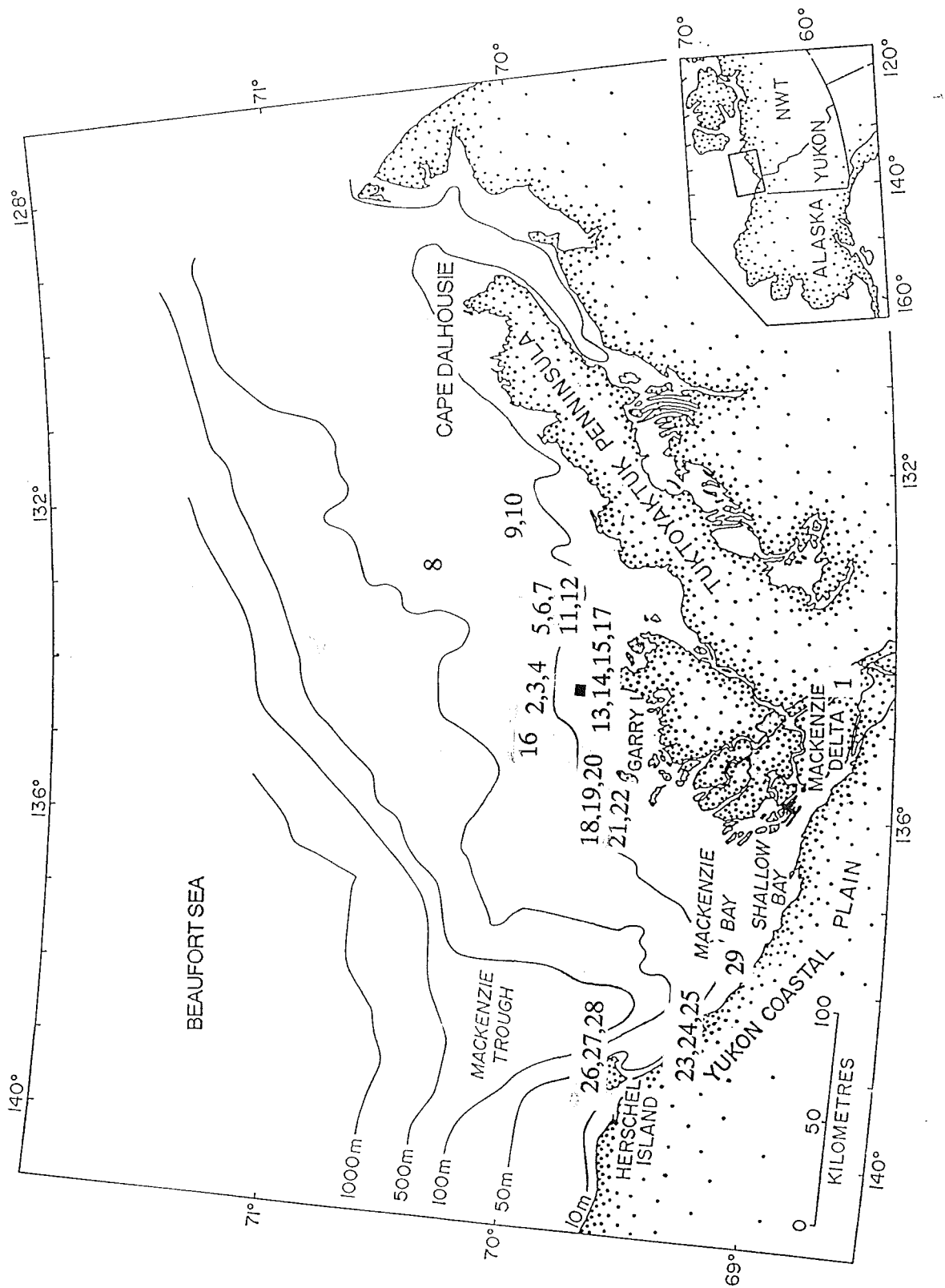
## 4.2 Samples

Since the publication of Hill et al.'s (1985) paper, thirteen new radiocarbon dates have been obtained from Holocene sediments in the Beaufort Sea region and can be used to better constrain the Holocene RSL curve. The locations of the samples are shown in Figure 4.2. Table 4.1 lists all samples used to construct the RSL curve. The table includes the most relevant samples used by Forbes (1980) and Hill et al. (1985). The new samples are of three types: (i) from the eastern shelf in non-marine sediments; (ii) from the eastern shelf in marine sediments; (iii) from the Yukon Shelf in marine sediments. Each group of samples is discussed below. Sample numbers refer to the left column in Table 4.1.

### 4.2.1 Eastern Shelf Non-Marine (Samples 11 -16)

Samples 11 and 12 were taken from boreholes at the East Amauligak drill site (Fig. 4.2). Sample 11 consisted of black fibrous peat consisting of abundant, well-preserved, herbaceous organic material. The sample contained low amounts of pollen, consisting of *Gramineae* (grass) and *Cyperaceae* (sedge), indicating a swampy grass-reed bog environment, similar to the modern Babbage River Delta (P. Mudie, personal communication). However such an environment could occur well above sea-level. Sample 12 consisted of peat, associated with layers of charophytes (calcareous algae) and freshwater ostracods. This sample contained abundant pollen with *Betula*, *Gramineae*, *Sphagnum* and *Salix* being the dominant forms. This assemblage and the absence of *Picea* (spruce) is compatible with an early Holocene age (P. Mudie, personal communication). Abundant freshwater desmids and *Pediastrum* in the sample suggests a freshwater bog environment. Both samples 11 and 12 contained low numbers of pre-Quaternary pollen, indicating that reworking is not a problem.

Samples 13, 14 and 15 were recovered from boreholes in shallow water close to North Head (Fig. 4.2). Sample 13 consists of fibrous peat, containing woody fragments. No



**Figure 4.2** Map showing locations of samples used for constraining relative sea level.

**Table 4.1** Samples used to construct the most recent Holocene RSL curve.

Sample No./Location	Location	Type of material	Elevation	Age ( yrs B.P.)	Error	Lab No.	Reference
1	MRC Borehole Mackenzie delta	Wood fragment	-38.00	6900	110	GSC-54	Johnston and Brown 1965
2	BH2	Freshwater peat	-24.80	6590	100	B-3033	Hill et al. 1985
3	BH6	Freshwater peat	-20.50	3740	70	B-3034	Hill et al. 1985
4	BH4	Freshwater peaty clay	-32.50	8300	90	B-3032	Hill et al. 1985
5	VC-07	Freshwater peat	-41.65	7740	90	B-4107	Hill et al. 1985
6	VC-07	Freshwater peat	-41.85	8820	100	B-4198	Hill et al. 1985
7	VC-07	Freshwater peat	-41.92	8740	70	B-5068	Hill et al. 1985
8	NT-82-S01	Freshwater peaty clay	-41.55	6000	70	B-6279	Hill et al. 1985
9	UB-82-S23	Freshwater peaty clay	-29.60	6640	80	B-6277	Hill et al. 1985
10	UB-82-S23	Freshwater clayey peat	-29.90	6310	100	B-6278	Hill et al. 1985
11	AE-84-S101, 15.45 m	Peat	-45.15	7840	130	B-12233	New
12	AD-84-S105, 15.6 m	Freshwater peat	-46.60	9910	150	B-12232	New
13	BH34+00, 18.45 m	Peat	-23.60	5580	80	B-9504	New
14	BH34+00, 18.62 m	Wood fragments in peaty silt	-23.75	6210	100	B-9507	New
15	BH38+00, 6.65 m	Plant debris in lacustrine silt	-12.55	9470	100	B-9508	New
16	KT-83-S02, 17.6 m	Peat in fluvial sand	-53.60	7730	160	B-9506	New
17	BH15+00, 13.37	Wood in marine sed.	-20.50	3530	80	B-9501	Hill and Nadeau, 1989
18	87NAH-39, 63-65	Marine bivalves	-7.30	1520	60	TO-1355	New
19	87NAH-48, 13-16	Marine bivalves	-8.40	1460	50	TO-1356	New
20	87NAH-60, 196-198	Marine bivalves	-10.80	2360	60	TO-1357	New
21	87NAH-75, 130-132	Marine bivalves	-8.60	1850	50	TO-1358	New
22	87NAH-81, 73-75	Marine bivalves	-8.60	1600	50	TO-1359	New
23	Babbage Delta	Peat	0.00	2260	130	S-1482	Forbes 1980
24	Babbage Delta	Plant material in delta seeds.	0.00	2110	90	GSC-2691	Forbes 1980
25	Babbage Delta	Peat	-1.30	2100	80	GSC-2323	Forbes 1980
26	Herschel Island	Charcoal in midden house	-0.70	990	95	S-1533	Forbes 1980
27	Herschel Island	Charcoal in midden house	-0.70	1570	60	S-1532	Forbes 1980
28	Herschel Island	Charred fat in midden house	-0.70	1510	90	S-1534	Forbes 1980
29	KF7, 9.4 m	Marine bivalve	-29.40	3970	120	RIDDL 429	New

palynological data are available from this sample, but the sedimentological characteristics of the adjacent sequence strongly suggests a terrestrial or lacustrine source. The sample is overlain by over 1 m of medium-grained, cross-bedded sand and black silty clay, and 11 m of organic-rich lacustrine clay and silt. It is underlain by 2 m of partly oxidized black peaty silt, from which sample 14 was taken and grey sandy silt with wood fragments. Sample 15 was taken from a black highly organic silt, containing numerous visible plant stems and fragments. The bed overlies a laminated silt and clay sequence, containing abundant rootlets. The sample contained numerous *Pediastrum* and desmids, indicating a freshwater origin (Burden, 1986). It also contained a *Betula* - *Picea* pollen assemblage, characteristic of an early Holocene age, with very low numbers of reworked pre-Quaternary pollen.

Sample 16 was collected from a borehole at the Kaslutut site in Ikit Trough (Fig. 4.2). The sample consists of sandy fibrous peat in a sequence of fluvial sands from sequence 2 of Hill et al. (in prep). The sample was barren of palynomorphs with the exception of rare fungal sclerotia (P. Mudie, 1986, written communication). The stratigraphic setting, presence of fungal remains and the absence of marine indicators all support a depositional environment above sea-level.

#### **4.2.2 Eastern Shelf Marine Samples (Samples 17 - 22)**

Sample 17 was taken from a large, log-sized piece of wood lying within a foraminifera-bearing sequence of marine silt and clay. The wood was well-preserved, showing growth rings and woody fabric. As the wood probably originated from the Mackenzie River and was transported into the Beaufort Sea, the age should be considered a maximum for marine conditions at this site.

A set of five accelerator dates was obtained on shell samples from marine sediments in vibracores from shallow water just north of Pelly Island. Sample 18 consisted of fragments of *Portlandia frigida*, sample 19 of fragments of *Portlandia arctica*, *P. frigida*, and *Cyrtodaria kurriana*, samples 20 and 21 of *C. kurriana* valves, and sample 22 of *C. kurriana* fragments, all marine bivalves.

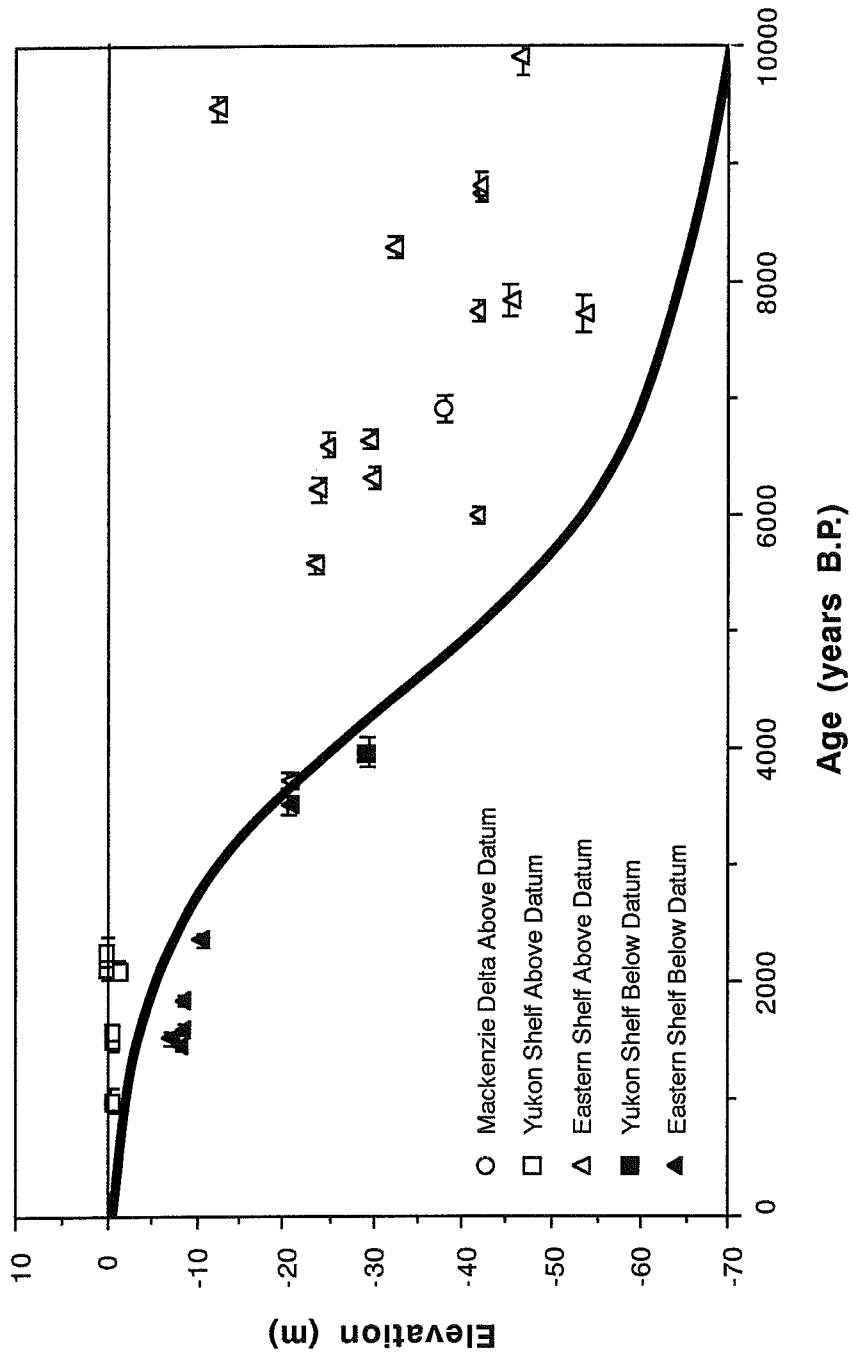
#### **4.2.3 Yukon Shelf Marine Sample**

Sample 29 was taken from a borehole located in 20 m of water off King Point (Fig. 4.2). The accelerator date was on an unidentified bivalve in foraminifera-bearing silty clay.

### **4.3 Holocene Relative Sea Level Curve**

The new Holocene RSL curve is shown in Figure 4.3. Solid symbols represent samples deposited below sea-level, while the open symbols represent samples deposited above sea-level, based on the paleoenvironmental interpretation from sedimentological, palynological and seismic





**Figure 4.3** A revised Holocene relative sea level curve for the Canadian Beaufort Sea, based on the dates listed in Table 4.1.

evidence. The curve is constrained to a narrow envelope for the last 4000 years, but is less constrained between 6000 and 10,000 years B.P. The bottom of the curve is drawn to show a maximum lowering of approximately 70 m, as inferred from morphological evidence by Forbes (1980) and Hill et al. (1985).

Analytical errors on the radiocarbon dates are small compared to the time scale being considered (Table 4.1). Dating errors related to contamination of older material are more difficult to quantify, but the samples have been carefully screened to eliminate samples with evidence for substantial contamination or evidence for reworking. No claim is made that any of the samples can be used as direct sea-level indicators. Most of the peat samples were deposited well above sea-level. The single peat sample, lying very close to the curve, was reported in Hill et al. (1985) to have been deposited possibly in a "coastal flood plain...similar to that found in the Babbage River delta".

#### **4.4 Discussion**

The constraints on the curve are sufficient to suggest that RSL rose relatively rapidly, averaging approximately 14 mm/a, during the middle part of the Wisconsinan, but levelled off to an average of 3 mm/a over the last 2000 to 3000 years. The mid Holocene RSL rise is significantly faster than suggested by either Forbes (1980) or Hill et al. (1985). This relatively rapid rise may be related to effects such as consolidation or basin subsidence, superimposed on post-glacial isostatic rebound and forebulge collapse. These effects are likely to be variable across the region, especially in terms of distance from the Mackenzie Delta where sedimentation over the late Wisconsinan and Holocene has been the greatest. There are still insufficient data to establish separate curves for the delta and the shelf areas to the east and west, as would be desirable to distinguish consolidation, subsidence and glacio-isostatic effects.

The flattening of the curve over the last 2000 years seems to indicate a slowing of RSL towards a global eustatic rate (Gornitz et al. 1982). It is this section of the curve which is most crucial to studies of coastal stability. Attempts by Forbes (in 1980 and 1989) to determine RSL change, from long term tide records at Tuktoyaktuk, have failed, due to uncertainties regarding the stability of the datum and the large variance in the data. An attempt has been made to obtain more exact RSL indicators for the last 2000 years, by sampling marsh sequences along the Tuktoyaktuk Peninsula. These efforts, while inconclusive at present, are described below.

#### **4.5 Sampling of Coastal Marshes**

Four shallow cores were collected in coastal marshes of the Tuktoyaktuk Peninsula: one core at Atkinson Point, on the western side of McKinley Bay, and three in a tidal-marsh located behind Topkak spit, on the eastern shore of Kugmallit Bay, approximately 7 km north of

Tuktoyaktuk (Fig. 4.4).

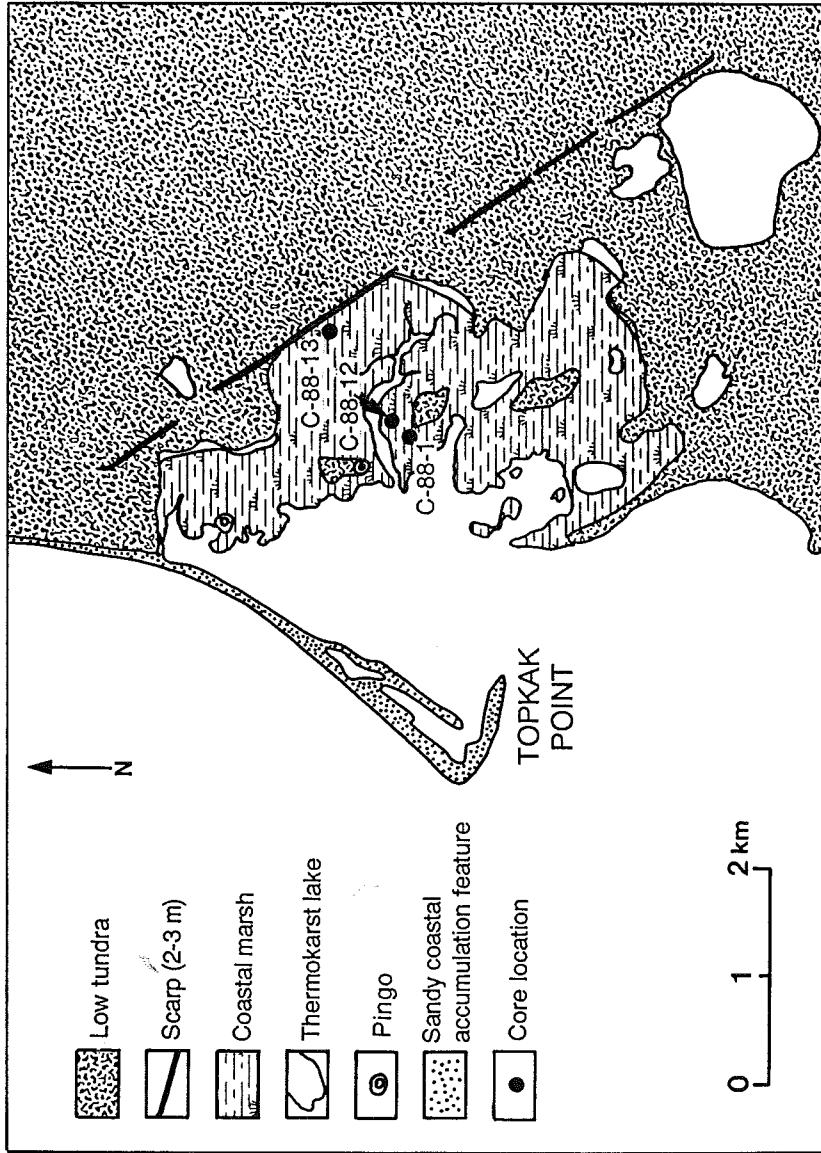
#### 4.5.1 Topkak Marsh

The cores in Topkak marsh typically consist of fine-grained sediment (clayey silt to silty clay) overlain by a variable thickness of peat (Fig. 4.5). The fine sediment forming the lower unit has a brown to grey colour and occasionally contains some gravel clasts. Coring at site C-88-12 revealed that this unit is at least 150 cm thick and mineralogical analyses suggest a composition very similar to diamict from the adjacent basin slope (P. Stoffyn, personal communication). This material progressively grades upwards into dark fibrous peat. In core C-88-1 (Fig. 4.5), two distinct peat beds are distinguished, separated by a 8-10 cm thick clayey unit that includes rare, fine gravel clasts. The lower peat bed is about 18 cm thick while the upper peat unit has a thickness of approximately 45 cm.

A distinct increase in marine influence in these cores is difficult to establish. Marine dinoflagellates are not abundant and every increase in their abundance is associated with an increase in freshwater dinoflagellates. However, a major change in aquatic flora is evident at some level in each core collected in this marsh. The change involves an increase in terrestrial palynomorphs, particularly *Alnus*, *Betula* and marsh elements of the *Cyperaceae* (Bujak Davies Group, 1988), together with a change in euryhaline dinoflagellate species, from *Naiadinium* sp. to *Peridinium limbatum*. *Pediastrum boryanum* is present above the same limit in cores C-88-12 and C-88-13, but its presence is not confirmed in the upper peat unit. The palynomorph changes also correspond to variations in lithology. In core C-88-1, the change occurs within a thin fine-grained unit containing a strong proportion of reworked palynomorphs between the two peat sequences (Fig. 4.5) and in core C-88-13 at the transition from silt to peat. In core C-88-12, the limit is outlined by a change from brown organic-rich silts to grey silty clays. Reworked palynomorphs are much more abundant below the palynomorph boundary, which occurs at about 25 cm below present mean sea level (MSL) in cores C-88-12 and C-88-13 and 10 cm below present sea level in core C-88-1.

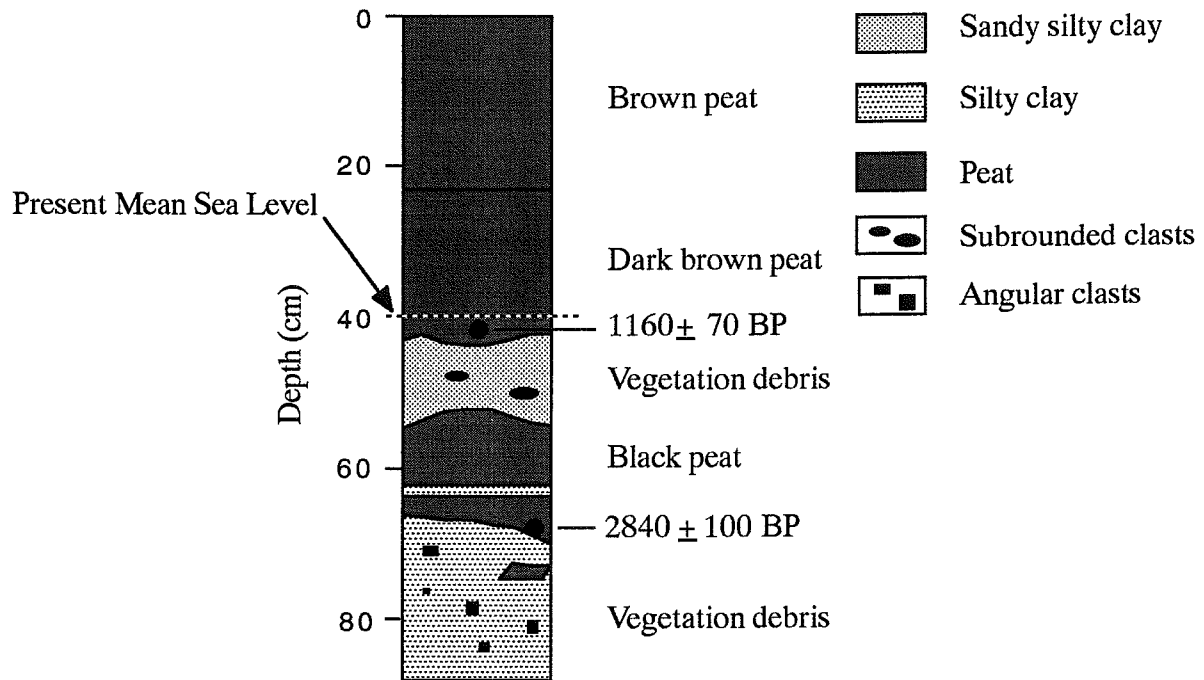
Several radiocarbon dates have been obtained in the various units described above and are listed in Table 4.2. As a preliminary interpretation, we suggest that the fine-grained unit underlying the peats represent lacustrine sediments deposited during the expansion of a thermokarst basin. As the basins were expanding during the Holocene, the resulting lakes were infilled through slumping and lake-margin erosion (Rampton, 1973). This could explain the similarity in texture and composition between the lacustrine sediment and the surrounding clayey glacial diamicton. Relatively old dates obtained for these fine-grained lacustrine sediments are consistent with an interpretation involving the reworking of older material.

The lower peats may represent a freshwater environment and probably developed in a



**Figure 4.4** Map showing the location of three cores collected in 1987, in a tidal marsh behind Topkak Spit.

### CORE C-88-1



**Figure 4.5** Core C-88-1 from Topkak marsh.

**Table 4.2** Radiocarbon dates obtained from the cores collected in Atkinson Point, McKinley Bay and Topkak marsh.

<u>Sample No</u>	<u>Location</u>	<u>Type of Material</u>	<u>Elevation (m)</u>	<u>Age (yrs. B.P.)</u>	<u>Error</u>	<u>Lab No</u>
30	Atkinson Point	Freshwater peat	-0.2	2950	70	B-28281
31	Atkinson Point	Organic-rich lagoonal (?) silty sand	-0.6	1280	70	B-28282
32	Atkinson Point	Freshwater (?) peat	-0.7	3830	90	B-28283
33	Topkak Marsh	Tidal-marsh (?) peat	-0.05	1160	70	B-34307
34	Topkak Marsh	Peat	-0.3	2840	100	B-34308
35	Topkak Marsh	Peat	-0.2	4920	220	B-34313
36	Topkak Marsh	Organic-rich silty clay	-0.4	2690	80	B-34310
37	Topkak Marsh	Organic-rich silty clay	-0.85	13590	280	B-34311
38	Topkak Marsh	Organic-rich silty clay	-1.15	14020	210	B-34312

shallow thermokarst lake. The major change in lithology and palynomorphs observed near the base of the uppermost peat is thought to represent a significant environmental change, possibly breaching of the lake by the transgressing sea. Because it is presently flooded by high tides, the upper peat must in part represent modern tidal-marsh conditions. The lack of marine indicators in this peat unit probably reflects the influence of freshwater discharge from the Mackenzie River in Kugmallit Bay and means that the transition from lacustrine to brackish marine conditions may be difficult to detect palynologically. Consequently, without a better knowledge of modern palynomorph distributions in Beaufort Sea coastal environments, precise elevations relative to former sea levels cannot be determined. However, the date of 1160 BP at the base of this peat sequence has potential to constrain recent sea-level rise if these problems can be resolved.

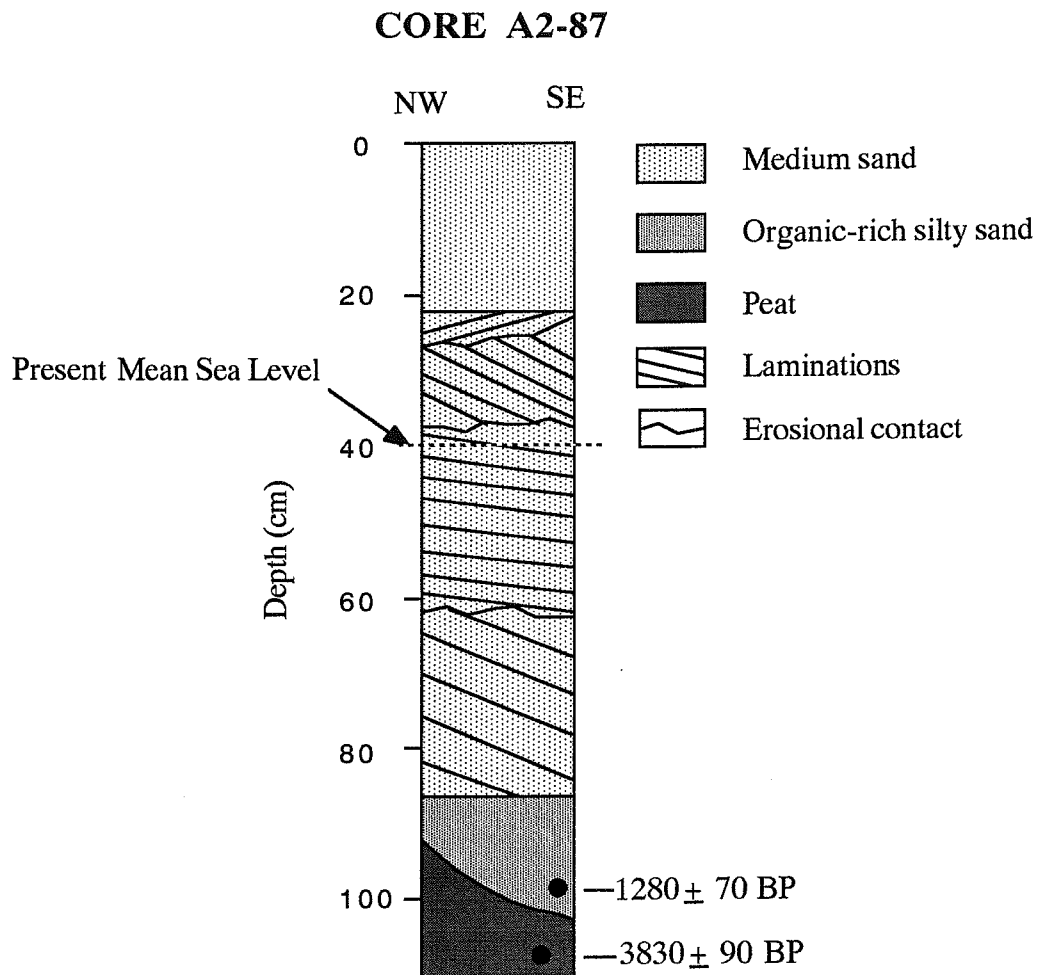
#### **4.5.2 Atkinson Point Lagoon**

At Atkinson Point, a 115 cm long core (A2-87) was collected on the backshore side of the spit extending into McKinley Bay. The bottom of the core, consists of fibrous peat with abundant herbaceous organic material containing sedge-type pollen (Fig. 4.6). This peat, which occurs approximately 60 cm below MSL, has been dated at  $3830 \pm 90$  BP (Beta-28283). This unit is overlain by a 10 to 18 cm thick organic-rich, silty sand deposit containing algae and brackish to freshwater dinoflagellates (*Naiadinium pallidum*, *Sigmopollis psilatus*, *Pediastrum boryanum* and *Ovoidites* sp). This unit is interpreted to have been deposited in a very shallow backbarrier lagoon. The freshwater species may be derived from the erosion of surrounding terrestrial material. The unit has been dated at  $1280 \pm 70$  BP (Beta-28282) and is covered by modern backbarrier sand. The base of the sand shows landward dipping laminae characteristics of washover sedimentation.

The lithostratigraphy and the location of the core relative to the spit suggest that the freshwater peat and the overlying silty sand unit have been buried by a landward migrating spit under rising sea level. A peat bed, similar to the one that occurs at the base of the core, outcrops on the foreshore of the spit, where it has been dated at  $2950 \pm 70$  BP (Beta-28281). When the spit was located farther seaward, rising sea level probably began to flood the peat about 1300 years BP, causing the sedimentation of silty sands over a shallow tidal flat. Subsequently, this unit was buried by barrier sands, with the retreat of the spit facilitated by storm-induced overwash processes.

#### **4.5.3 Implications to the Holocene Sea Level Curve**

The radiocarbon dates from Topkak marsh and the Atkinson lagoon could provide important control on the most recent part of the Holocene sea-level curve if better control of depositional environments can be achieved. If the preliminary interpretations outlined above are correct, the positions of the dates on the RSL curve would constrain the curve to flatten markedly



**Figure 4.6** Core A2-87 collected at Atkinson Point on the backshore side of the spit extending into McKinley Bay.



and imply relatively slow sea-level rise over the last 2000 years. This would mean that the relatively rapid rates of coastal retreat observed along much of the Beaufort Sea coast (see later chapters) is occurring despite a minimal rate of sea-level rise. The consequences of accelerated sea-level rise due to global warming to rates of coastal retreat may therefore be more dramatic than previously anticipated (Hill, 1988b).

Alternative explanations are possible, particularly as the core lengths were limited by the permafrost table and may not penetrate the total thickness of marsh accumulation. As a knowledge of the recent sea-level history is so important to the understanding of coastal retreat, further work should be carried out. This work should include (i) deeper coring of the marshes; (ii) detailed sampling of the modern freshwater and brackish water marshes along the Beaufort Sea to establish the horizontal palynological zonations in these environments, information that can then be applied to interpretations of marsh sequences in the cores; and (iii) further reconstructions of thermokarst lake breaching and barrier migration to aid in interpretation of the core sequences.

## 5. YUKON COAST: U.S BORDER TO SHALLOW BAY

This section of coastline is bounded by the U.S. border at 141°W in the northwest and modern delta deposits in the southeast. Holocene sediments of the Mackenzie Delta merge with deposits from the Blow River between Whitefish Station and Trent Bay (Fig. 5.1).

### 5.1 Quaternary Geology

The Quaternary geology of the Yukon coastal plain has been described by Rampton (1982) and the following is a brief summary based mainly on Rampton's work. Pre-Buckland deposits are exposed in the ice-thrust moraine ridges making up Herschel Island and the coast southeast of Kay Point, where folding of the sediments has exposed the older beds. Most of the pre-Buckland sediments are of uncertain age and consist of a wide range of lithologies from gravel to silt. Faunal and sedimentological analyses of these "mixed" sediments indicate that they were mostly deposited in a shallow marine or deltaic environment (Rampton, 1982). Immediately underlying the Buckland till, between Herschel Island and King Point, is a marine clay which locally grades into the Buckland till. Much of the Yukon coastal plain southeast of Herschel Island is covered by rolling and hummocky moraine consisting of a gravelly diamicton with a silty matrix. The morainic material contains ground ice in the form of ice wedges and segregated ice (Pollard and Dallimore, 1988). Consequently, the moraine surface was highly modified by post-depositional thermokarst processes. Holocene lakes formed on this irregular surface; and lacustrine deposits, as organic-rich beds and small filled depressions, are commonly exposed at the coastline.

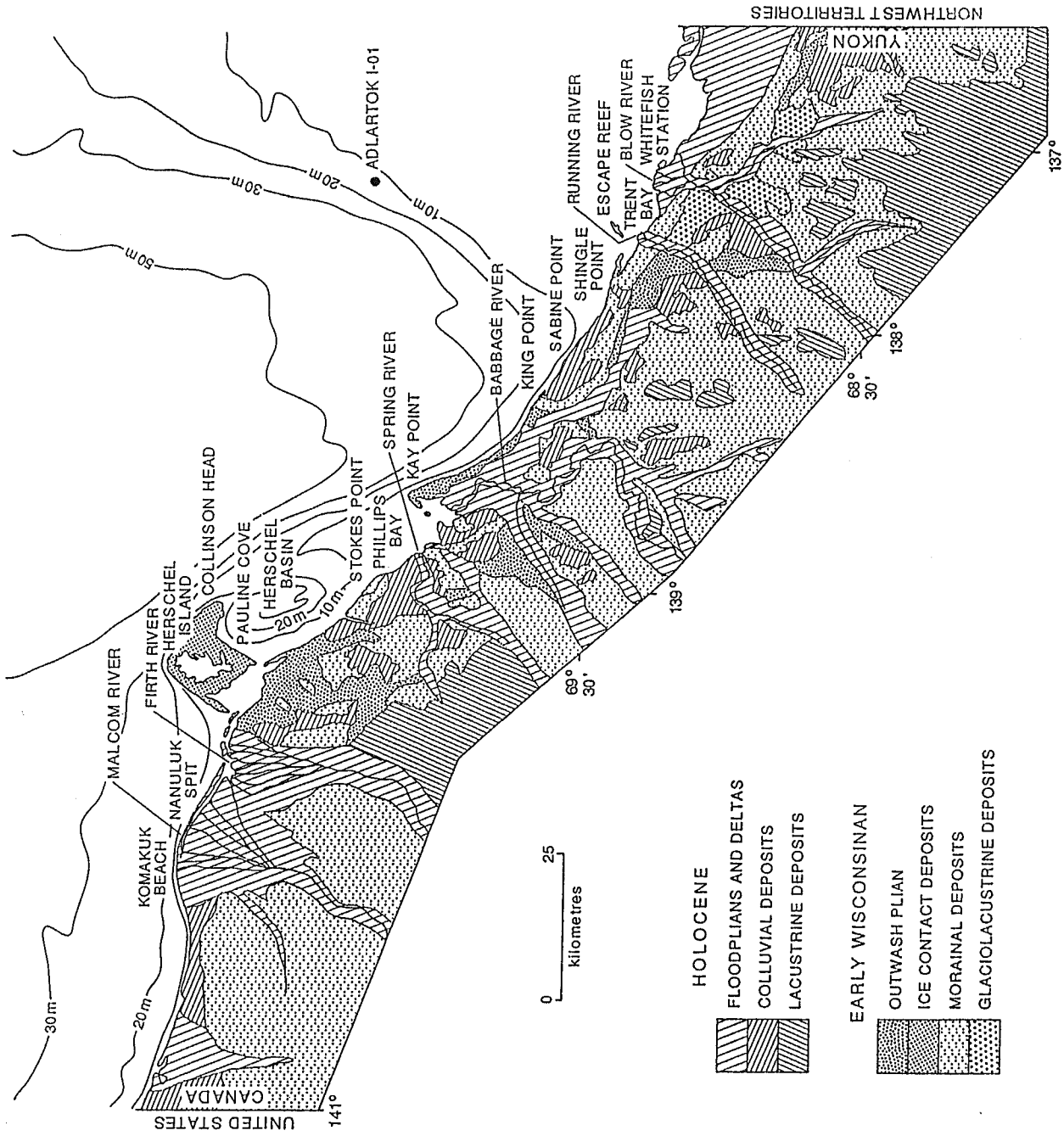
West of Herschel Island, the coastal plain is dominated by alluvial fan complexes associated with the Clarence, Malcolm and Firth Rivers. The fan complexes are made up of individual fans of various ages, dating from the early or middle Quaternary to present. The Holocene fans of the Malcolm and Firth rivers form fan deltas along the coastline from Herschel Island to Komakuk Beach. From Komakuk Beach to Clarence Lagoon, coastal deposits consist primarily of lacustrine deposits.

### 5.2 Coastal Morphology

The coastal morphology of the Yukon coast was first described by McDonald and Lewis (1973) and subsequently by Lewis and Forbes (1975). The following description is largely based on these studies and on aerial videotapes collected by Forbes and Frobel (1986). It is provided here as background to later sections.

#### 5.2.1 *Sea Cliffs*

Much of the Yukon coast consists of steep or near-vertical cliffs with narrow fringing



**Figure 5.1** Surficial geology and location map of the Yukon coast.

gravel and sand beaches. Along some sections of the coast, the beach may be very narrow or absent. The highest cliffs form along the ice-thrust sections of the coast, reaching more than 100 m, but other areas of undeformed moraine are typically less than 30 m high. Several erosional processes, resulting in distinct landforms, are common along this section of the coast:

(i) Where the ice content of the cliffs is high, retrogressive thaw flow slides are common (Mackay, 1966; Harry, 1985). These slides have a cirque-like morphology with a steep headwall and a gently sloping basin (Fig. 5.2a). They form as a result of the thawing of ground ice and ice-rich sediment in the cliff face. The thawed material flows down the face and is deposited at the bottom of the newly-formed scarp. Mud flow transport often continues across the beach and into the sea or onto the sea-ice. The slope may become stabilized unless removal of the redeposited material at the toe by wave action exposes fresh permafrost and retrogressive failure continues.

(ii) Erosion by wave action and undercutting of the cliff to form a wave-cut niche is also an active process. Niches as deep as 5 m have been observed along the Yukon coast (S.R. Dallimore, personal communication). This undermining of the cliff eventually results in the wholesale collapse of a thick section of the cliff face, commonly as block failures along ice-wedge polygon boundaries (Fig. 5.2b).

(iii) Gullying of the cliff face as a result of minor stream flow is a common process along steep sections of cliff, particularly between King Point and Kay Point (Fig. 5.2c). Headwall erosion of the gullies can penetrate deeply into the cliff.

Where wave-related erosional processes are active, the cliffs have a relatively steep profile. In other areas, cliff erosion is more cyclic. Along many sections of the coast, older thaw flow slides are vegetated, indicating stabilization of the upper part of the cliff. Cliffs may remain stable for many years until wave erosion and reactivation of melt-out processes causes erosion to resume.

### **5.2.2 Deltas**

Several major rivers with sources in the British, Barn and Richardson Mountains cross the Yukon coastal plain and form deltas at the coast. Smaller river valleys reaching the coast are generally drowned and are commonly fringed with spit or barrier systems forming shore-perpendicular lagoons. Six deltas are described below:

(a)



(b)



**Figure 5.2** Distinct landforms resulting from erosional processes: (a) retrogressive thaw flow slide, (b) polygon block failure.

### *Clarence River Delta*

Clarence River forms a small barrier-protected delta approximately 5 km southeast of the Yukon/Alaskan border (Fig. 5.3a). The delta is presently building into Clarence Lagoon, along with a second delta from an unnamed creek. Two principal distributary channels feed the delta, resulting in a fan-shaped complex of vegetated supratidal flats. The development of intertidal flats at the seaward margin of deposition is probably controlled by complex exchange of water between the tidal inlet at the northwestern edge of the barrier and the distributary channels.

### *Malcom River Fan Delta*

The Malcom River Delta comprises the northeastern tip of a prominent alluvial fan complex. The alluvial fan stretches from Komakuk Beach in the west and merges with the smaller Firth River alluvial fan to the east (Fig. 5.3b). The fan contains a complex interconnecting channel network which empties into a shore-parallel lagoon fringed by Nunaluk Spit. Near the distal end of Nunaluk Spit the Malcom River empties into the lagoon via three major distributaries forming an arcuate delta morphology dominated by vegetated supratidal flats. Unvegetated intertidal flats fringe the seaward margin of the delta plain and represent active sites of deposition.

### *Firth River Fan Delta*

The Firth River forms a broad fan delta centrally located within a larger alluvial fan complex immediately west of Herschel Island. Fine sand and silt is being deposited within a shore-parallel lagoon (McDonald and Lewis, 1973) protected from the Beaufort Sea by a linear barrier island chain which extends eastward from Nunaluk Spit (Fig. 5.3c). The delta is extensively bisected by anastomosing distributary channels forming a large complex of supratidal interchannel islands.

### *Spring River Delta*

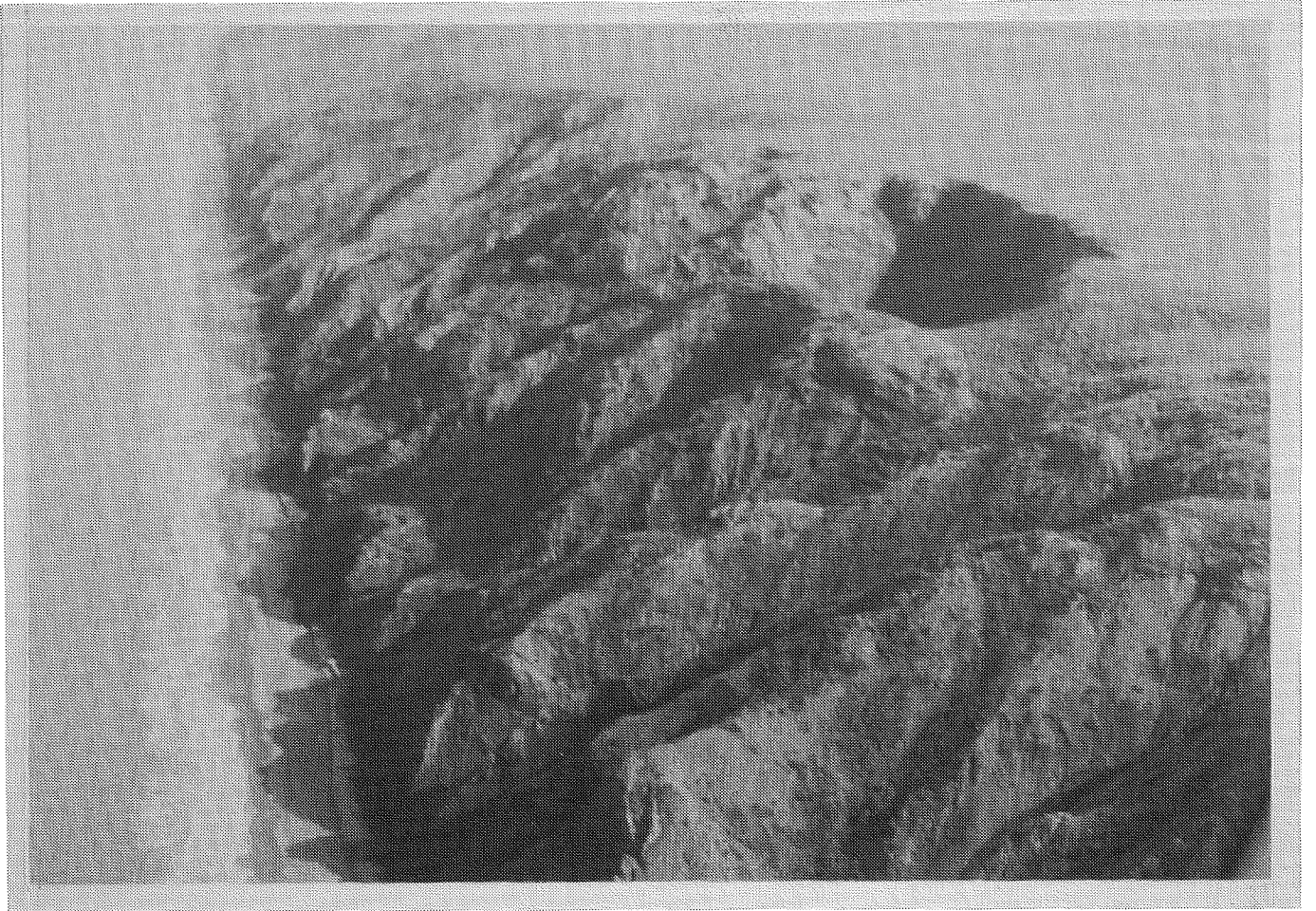
The Spring River reaches the coast between Stokes Point and Phillips Bay. A multiple recurved spit has formed at the river mouth, diverting the channel southeastwards and forming a shore-parallel estuary extending several kilometres (Fig. 5.3d). Most of the estuary is filled with supratidal flats which are largely vegetated, forming marsh. Several distributary channels meander across the supratidal flat and marsh, discharging through tidal inlets distributed along the length of the spit. At the proximal end of the fringing spit, several large washover lobes have been deposited on the delta supratidal flats.

### *Babbage River Delta*

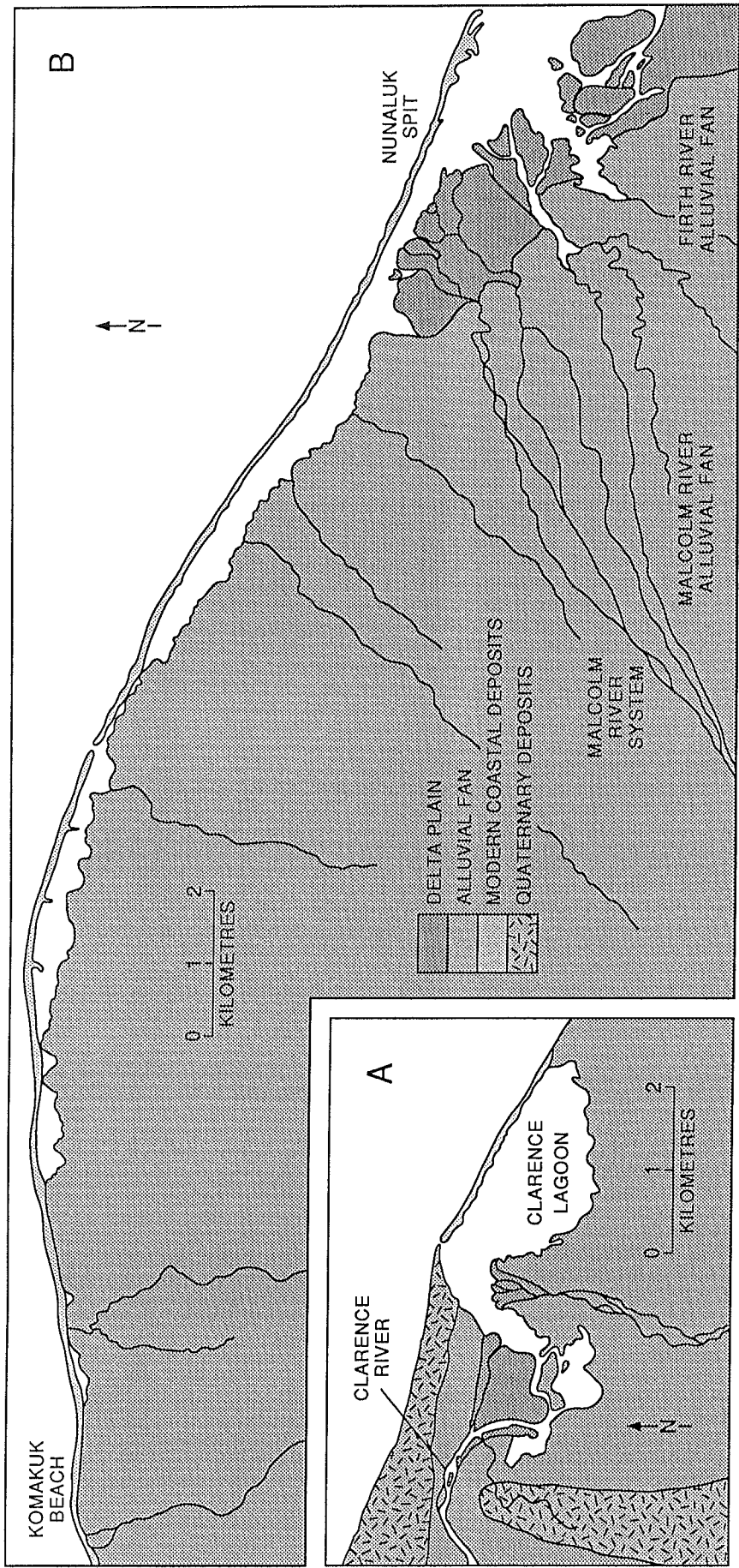
The lower course of the Babbage River is controlled by the coast-parallel ice-thrust ridge



(c)



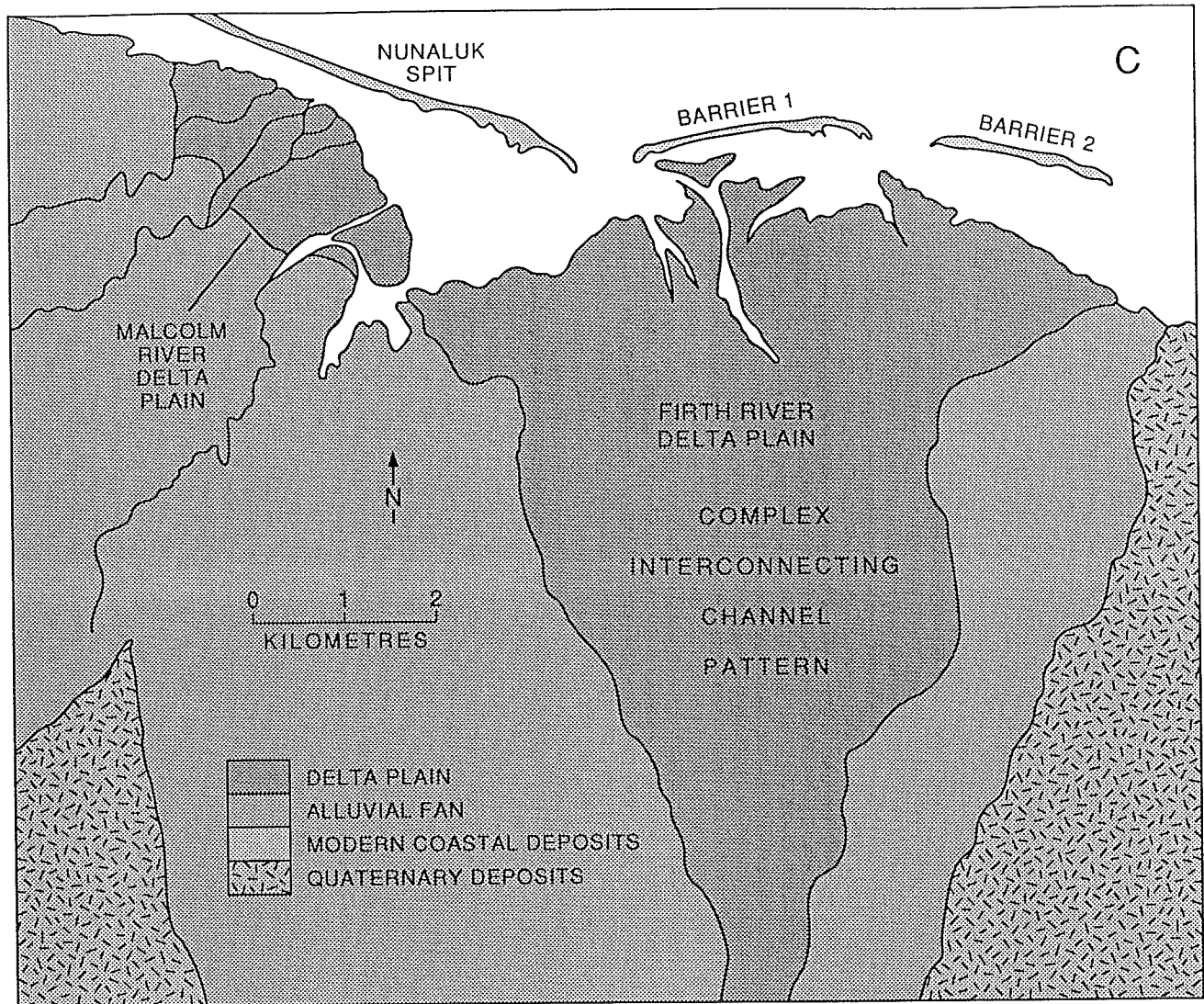
**Figure 5.2** (c) cliff face gullying between King Point and Kay Point.



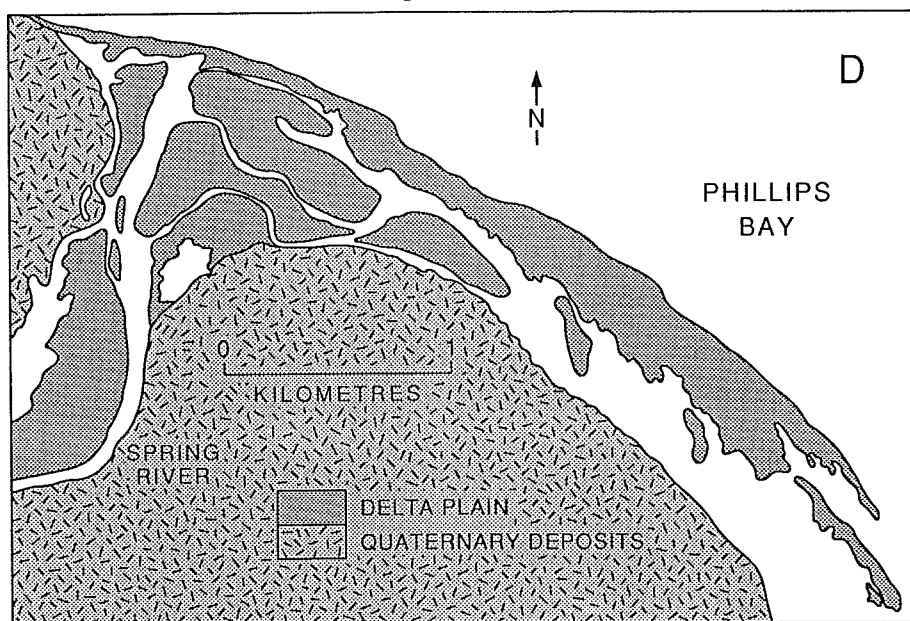
**Figure 5.3a** Clarence River Delta.

**Figure 5.3b** Malcom River alluvial fan delta system fronted by Nunavuk Spit.





**Figure 5.3c** Firth River alluvial fan delta complex fronted by Barriers 1 and 2 of the Nunaluk Spit system.



**Figure 5.3d** Spring River Delta.

which extends to Kay Point (Fig. 5.3e). The river therefore discharges into a large estuary south of Kay Point and behind the long spit formed at the end of the point. The delta forms an extensive area of supratidal and intertidal flats cut by four major distributary channels. The largest channel discharges near the southern end of the delta coastline. Most of the supratidal delta plain is vegetated and occupied by numerous lakes and ponds connected to the main distributary channels by narrow tidal channels. Supratidal flats are also present along the margins of the estuary, to the southwest and northeast. A more extensive and detailed description of the Babbage Delta can be found in Forbes (1981).

#### *Running River Delta*

The Running River forms a small delta approximately 4 km southeast of Shingle Point (Fig 5.3f). The delta is fringed by a spit, prograding from the coast to the northeast of the delta. The spit has a recurved distal portion, consisting of numerous ridge crests, and is breached by several inlets related to distributary channels of the delta. Behind the spit, the delta has formed a supratidal delta plain which is extensively vegetated.

#### *Blow River Delta*

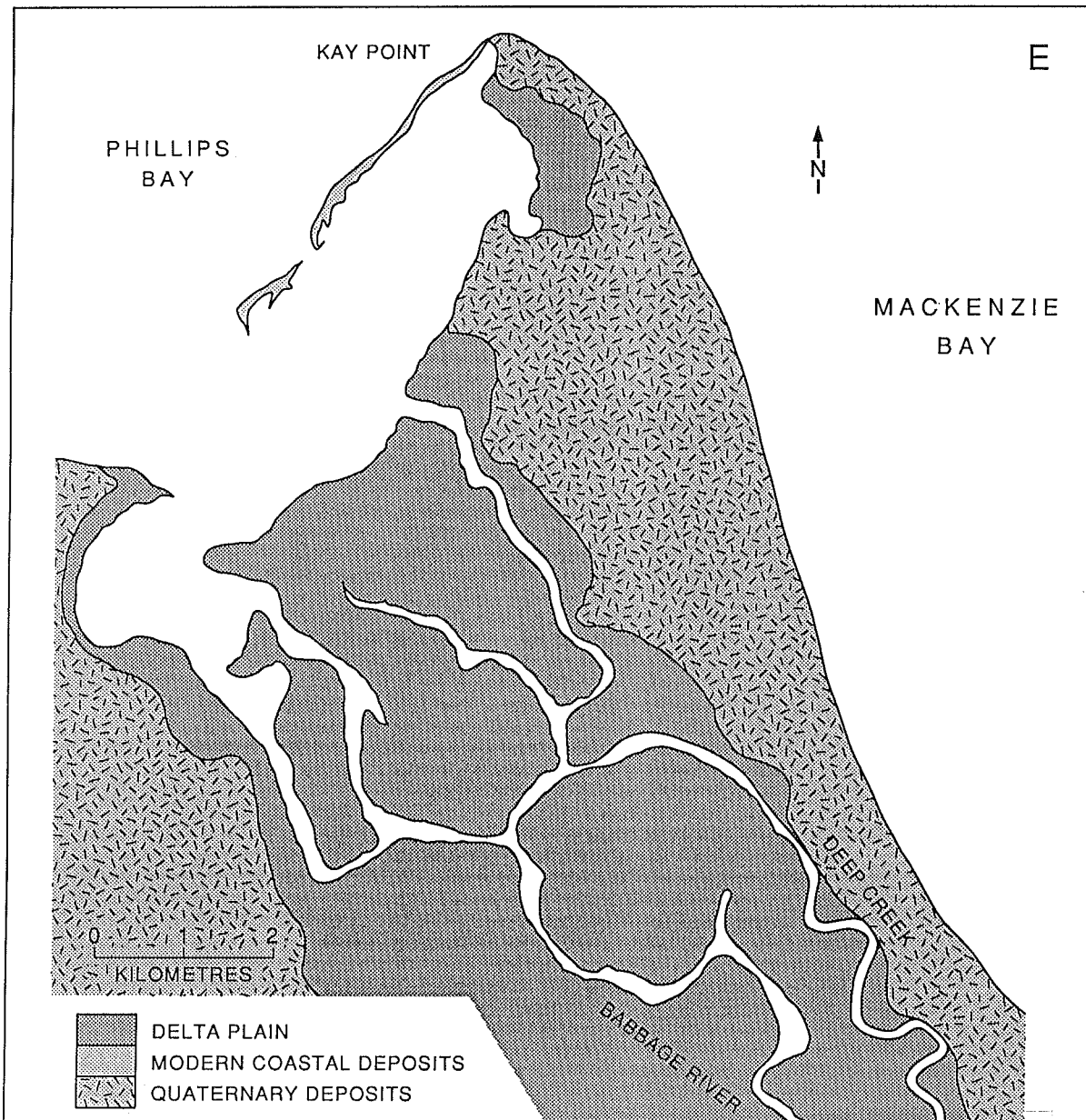
The Blow River enters the Beaufort Sea between Trent Bay and Shoalwater Bay forming a large, arcuate subaerial delta plain unprotected by spit or barrier island complexes (Fig. 5.3g). The delta plain is characterized by a pattern of anastomosing distributary channels across extensive, vegetated supratidal flats and unvegetated intertidal flats. Much of the delta plain is punctuated by thermokarst lakes. In the northwestern part of the delta, newly forming distributary mouth bars divide larger distributary channels and represent a minor accretional phase of the delta over the period of air photo coverage from 1952 to 1974. Older deltaic islands form organic-rich foreshore scarps less than 0.8 m in height (Lewis and Forbes, 1975).

### **5.2.3 Spits and Barriers**

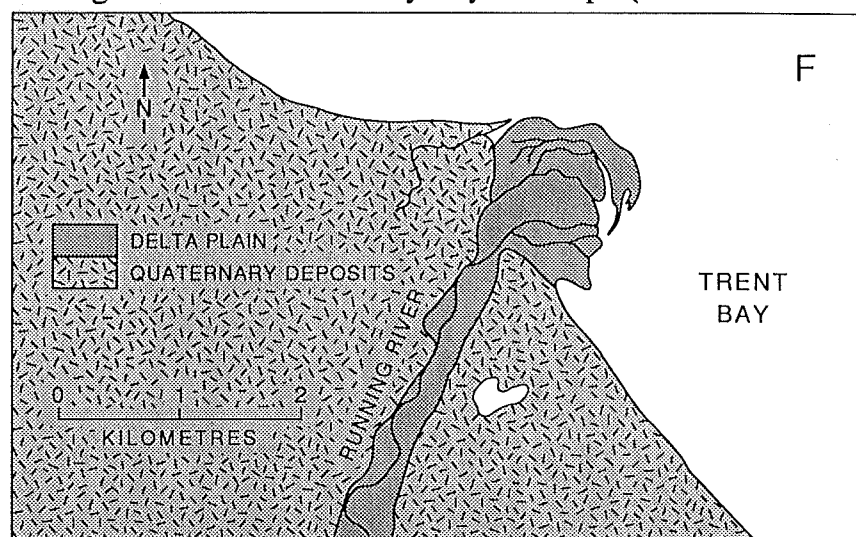
Several long spit and barrier systems have developed along the Yukon coast, enclosing river mouths and thermokarst lakes. The most prominent of these features are described briefly below. The descriptions here are based on aerial photographs, the aerial video survey of 1984 (Forbes and Frobels, 1986), and published ground survey observations (McDonald and Lewis, 1973; Lewis and Forbes, 1975; Gillie, 1986b; Forbes and Frobels, 1985).

#### *Nunaluk Barrier-Spit Complex*

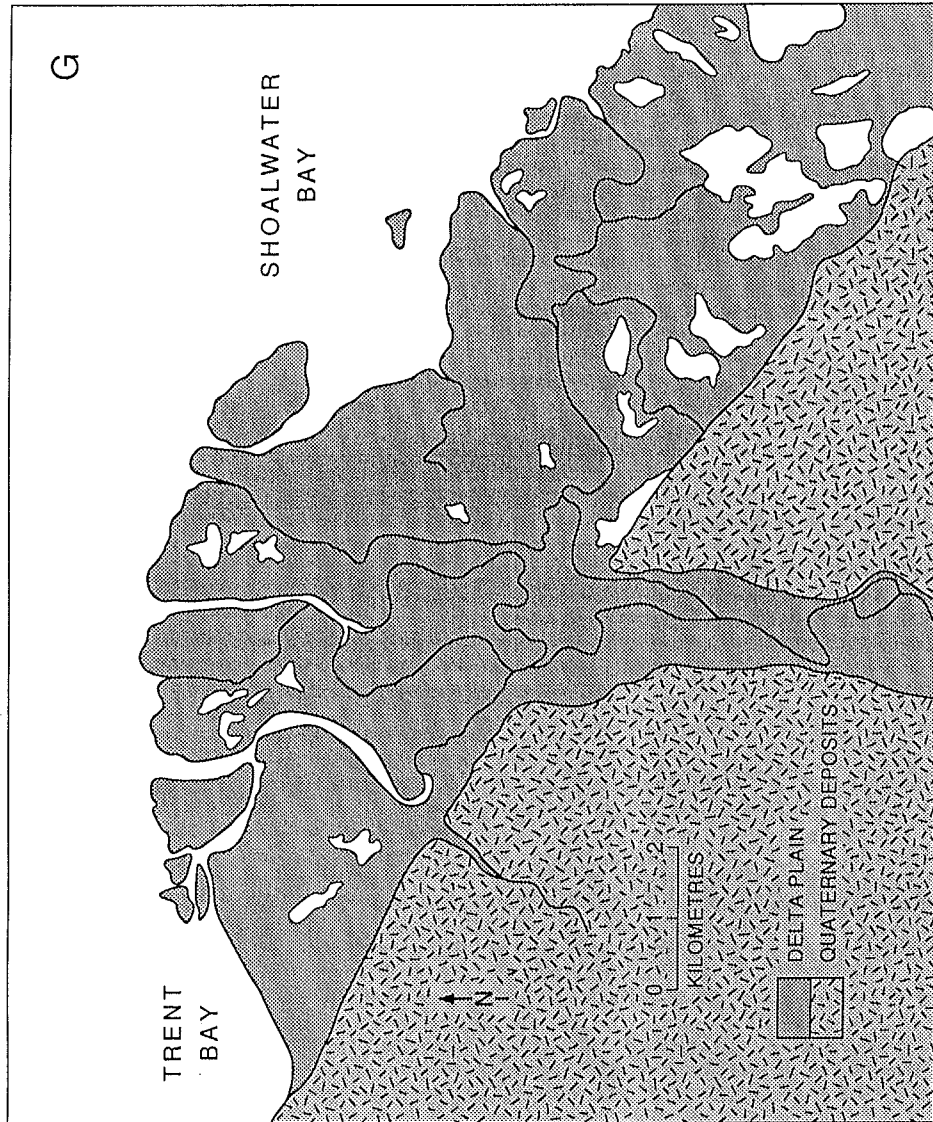
A long barrier-spit complex fronts the Malcom River and Firth River fan deltas (Fig. 5.3b, 5.3c, 5.4a). The western portion of the complex consists of a barrier beach, attached at several



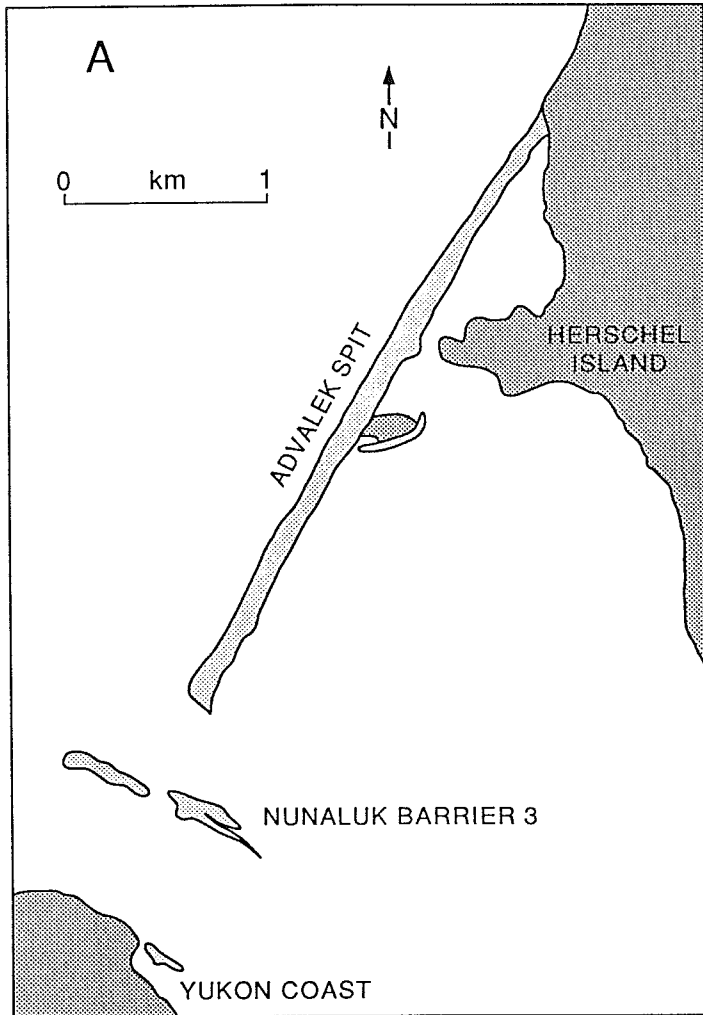
**Figure 5.3e** Babbage River Delta fronted by Kay Point Spit (modified from Forbes, 1981).



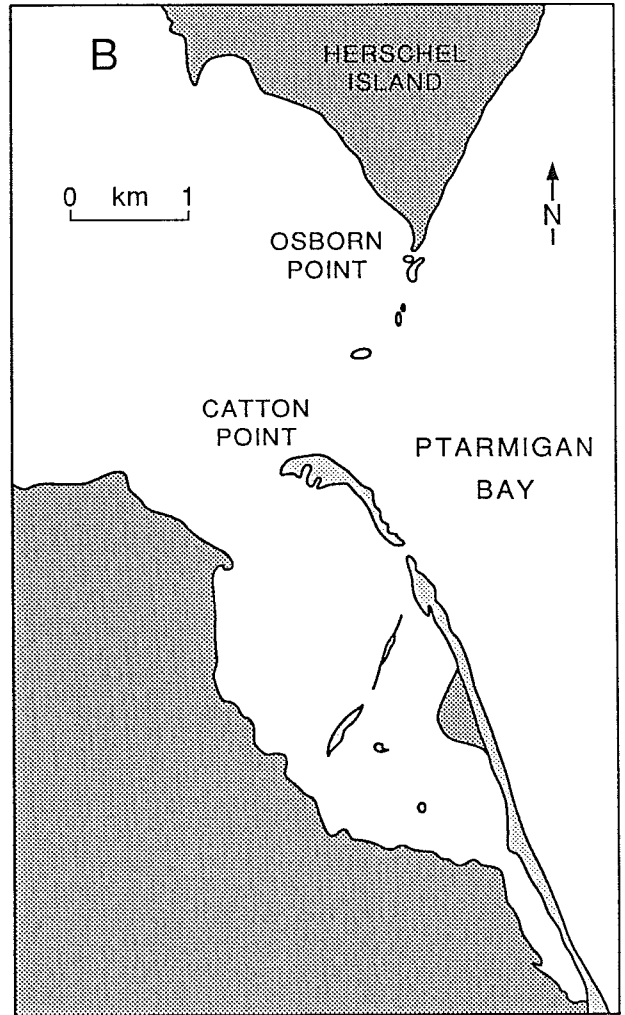
**Figure 5.3f** Running River Delta.



**Figure 5.3g** Blow River Delta.



**Figure 5.4a** Advalek Spit.



**Figure 5.4b** Catton Point-Osborne Point Spit.

locations to low-relief headlands of the Malcolm River fan delta. In front of the eastern part of the Malcolm River fan delta, a long narrow spit extends 11 km, to the mouth of the Firth River. The barrier complex extends further eastward across the Firth River fan delta in the form of three barrier islands. Nunaluk spit is comprised of fine to medium pebble gravel, with lesser amounts of sand concentrated on the two easternmost barriers (McDonald and Lewis, 1973). At its proximal end the spit is characterized by numerous spurs which project perpendicularly into the lagoon. The distal end of Nunaluk spit consists of multiple recurved beach ridges, with areas between the ridges being infilled with thin washover fan deposits and small beach-ridge parallel lakes. The three barrier islands east of Nunaluk spit are also comprised of numerous recurved beach ridges.

#### *Advalek Spit*

Advalek spit extends 3.7 km southward from the southwestern corner of Herschel Island and terminates just north of the most easterly barrier island of the Nunaluk barrier-spit complex (Fig. 5.4a). The spit is linear in shape and maintains a width of 95 m over its entire length. The distal end is comprised of several recurved beach ridges smoothed by thin washover sheet deposits (McDonald and Lewis, 1973).

#### *Catton Point - Osborne Point*

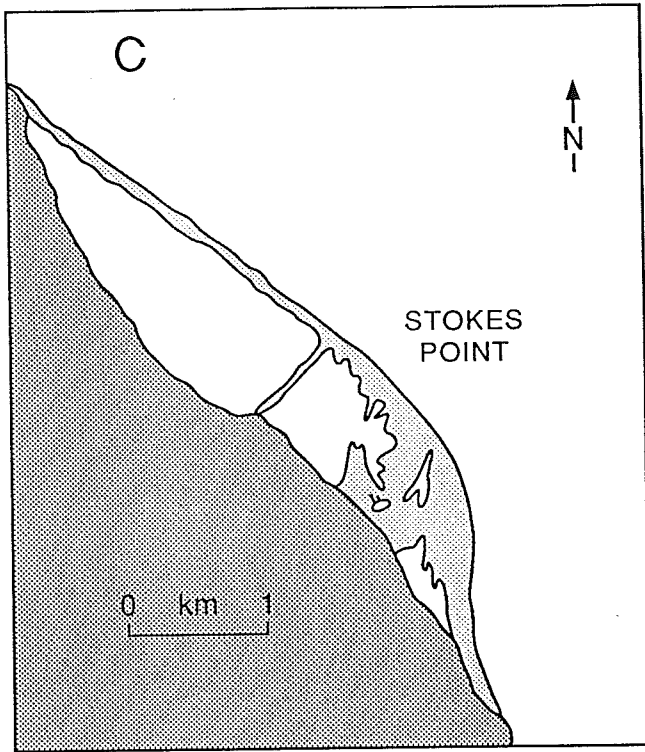
A 5 km long recurved spit, named Catton Point, extends outward from the coastline just south of Herschel Island, forming part of the western margin of Ptarmigan Bay (Fig. 5.4b). A major tidal inlet separates Osborne Point on Herschel Island from Catton Point. In 1952 the distal (N) portion of Catton Point spit consisted of several recurved accretional beach ridges and a spit extended from Osborne Point. By 1972 the Osborne Point spit was almost completely drowned, and a breach had developed toward the northern end of the Catton Point spit, producing a single recurved barrier island.

On the estuary side of the Catton Point spit, a thin, linear sand body perpendicular to the coastline, may represent a former spit which accreted landward from the large relict island now a part of the Catton Point spit complex.

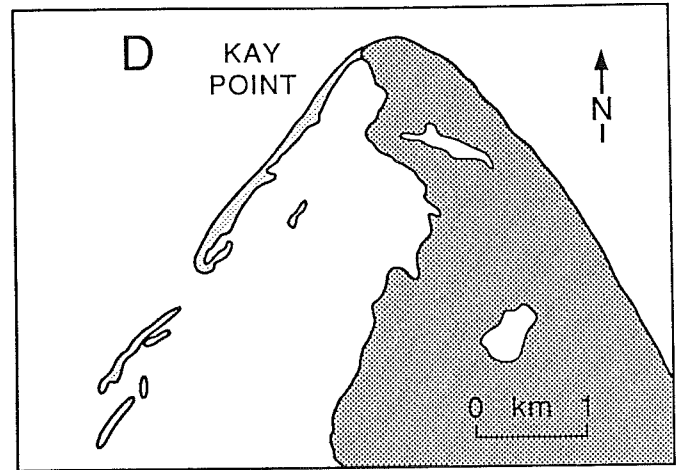
#### *Stokes Point*

At Stokes Point, a 1 km wide lagoon is enclosed by a sand and gravel barrier (Fig. 5.4c). The proximal (NW) end of the barrier is very narrow and relatively straight, with a few small washover fans, some of which are partly vegetated. At the proximal attachment point a small supratidal marsh has developed. The distal (SE) end of the barrier consists of numerous vegetated beach ridges showing accretional recurved morphologies. The recurved portion of the barrier actually forms the promontory of Stokes Point, where it is 700 m wide, with a crest elevation of

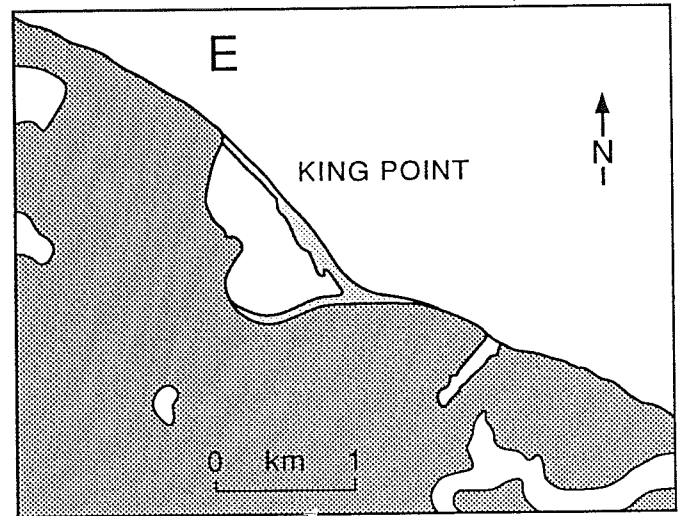




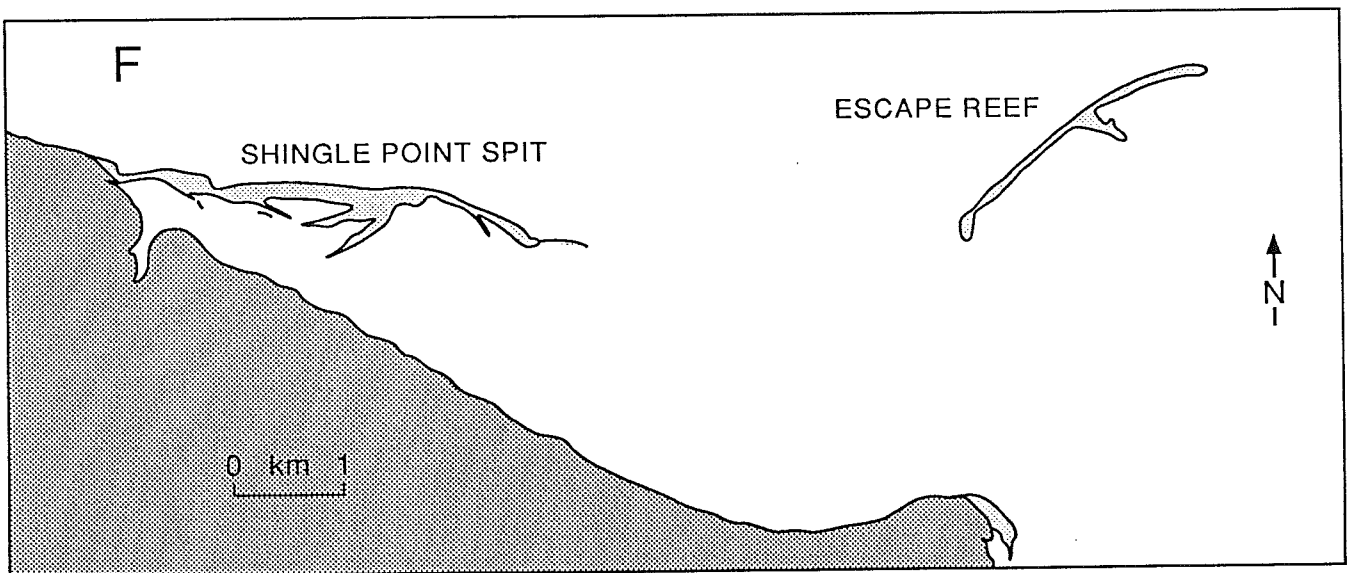
**Figure 5.4c** Stokes Point Barrier.



**Figure 5.4d** Kay Point Spit.



**Figure 5.4e** King Point Barrier.



**Figure 5.4f** Shingle Point and Escape Reef.

1.9 m (Forbes and Frobels, 1985). The most seaward ridges are overlain by washover fans. The morphology of the Stokes Point barrier suggests that it developed as an accretional spit whose distal end eventually merged with the shoreline to the southeast. The presence of washover fans and ephemeral inlets (D.L. Forbes, 1989, personal communication) suggest that the proximal end of the spit is transgressive.

#### *Kay Point*

A long recurved gravel spit extends from the northern tip of Kay Point, southwestwards into Phillips Bay and into the Babbage estuary (Fig. 5.4d). In 1984, the spit was no longer attached to Kay Point, due to the formation of an inlet at the proximal end of the spit (Forbes and Frobels, 1985). Two other breaches at the distal end of the spit were also observed during the 1984 video survey. Extensive washover flats were present in the proximal section of the spit, indicating the predominance of transgressive processes. The concave seaward profile of the narrow middle part of the spit is further evidence for transgression. Several spit-parallel shoals developed on the estuary side of the spit indicate the presence of a broad back-barrier platform (Forbes and Frobels, 1985).

#### *King Point*

A sand and gravel barrier has formed across an old thermokarst lake just southeast of King Point (Fig. 5.4e; Hill, 1990). At the northwestern end, the barrier is linear and approximately 50 m wide. Overwash processes dominate this part of the barrier. Gillie (1987) reports that several overwash channels, 2 to 5 m wide and approximately 0.5 m deep, formed at this narrow part of the barrier between September 1985 and July 1986. The barrier widens southeastwards to a maximum width of 215 m, the middle section of the barrier being characterized by a series of relict recurved ridges partially covered by a thin washover sheet. The southeastern end of the barrier has a concave-seaward plan and consists of a series of low beach ridges indicating progradation of this part of the barrier.

#### *Shingle Point and Escape Reef*

Shingle Point is a 3.5 km long spit formed at a minor change in coastline orientation, west of the Running River (Fig. 5.4f). The sand and gravel spit is comprised of numerous generations of progradational beach ridges which are partly vegetated in the backshore region. Several transverse ridges in the mid-section of the spit have prograded into the lagoon and the intervening areas have been filled by washover deposits. Small lakes have formed on the washover flats. The distal end of the Shingle Point spit consists of a narrow recurve.

Escape Reef is a detached barrier island, some three kilometres east of the Shingle Point



spit and northeast of the Running River delta (Fig. 5.4f). The reef is generally emergent at mean sea level, but is flooded during periods of high water. The island is convex-seaward in form, suggesting landward migration. The common orientation of local bottom contours in the vicinity of the Shingle Point Spit and Escape Reef suggests that the two features may previously have been related to each other.

#### **5.2.4 Inner Shelf Morphology**

There has been no systematic survey of inner shelf morphology along the Yukon coast under the NOGAP D.1 program. C.P. Lewis and D.L. Forbes (personal communication) collected some bathymetric data from the vicinities of Kay Point and Stokes Point in 1973 and 1984, to water depths no greater than 5 m. The seabed slope below the shoreface averaged  $0.4^\circ$  m both seaward of the Kay Point spit and off the Stokes Point spit. A detailed hydrographic survey of the shelf west of Herschel Island was carried out by Cansite Surveys Ltd. in 1984 (McGladrey, 1984), but the survey lines terminated in 10 m of water. Sounder profiles were collected during the sediment transport study at King Point, to water depths of 8 m. The slope below the shoreface at King Point ranged from  $0.4^\circ$  to  $0.9^\circ$ .

### **5.3 Rates of Coastline Change**

#### **5.3.1 Coastal Retreat**

Retreat rates along the Yukon coast vary, both from place to place and from year to year. Observations of coastline position have been carried out by Mackay (1963a), McDonald and Lewis (1973), Forbes and Frobel (1985), Harper et al. (1985) and Gillie (1987). Some of these authors and Hill (in press) have also used historical evidence to estimate retreat rates. The various estimates of retreat rates are summarised in Table 5.1 for individual sections of the coast. To synthesise these data, it was necessary to calculate mean values of coastal retreat for long sections of the coast. The mean values incorporate both spatial and temporal variation, as well as measurement errors.

The two most extensive sets of available data are based on photogrammetric studies (McDonald and Lewis, 1973; Harper et al., 1985). These two studies were based on essentially the same set of aerial photographs taken in the 1950's and 1970's, although the locations used for photogrammetric measurements were different. They provide retreat rates measured over a period of approximately 18 years. Comparison of the two sets of results provides a good indication of the natural variability. Nevertheless, taking this variability into account, the results are quite comparable and show that retreat along the Yukon coast is averaging between 0.3 and 2.7 metres per year. The highest retreat rates are seen at Kay Point, where erosion at the northern end of the

TABLE 5.1

YUKON COAST - AVERAGE RETREAT RATES (m/a)  $\pm$  s. d.

Area	Mackay (1963) Forbes (1981)	McDonald & Lewis (1973)	Harper et al. (1985)	Forbes & Frobel (1985)	Gillie (1988)
International Border to Komakuk Beach			1.09 $\pm$ 0.72 n=6		
Komakuk Beach to Herschel Island			0.56 $\pm$ 0.79 n=28		
Herschel Island (North Shore)	0.8*	1.03 $\pm$ 0.61	0.75 $\pm$ 0.35		
Herschel Island to Stokes Point		1.08 $\pm$ 0.33	0.46 $\pm$ 1.11		
Stokes Point to Spring River		0.34 $\pm$ 0.13 n=4	0.38 $\pm$ 0.52 n=8		
Kay Point Segment 1		2.67 $\pm$ 1.30 n=6	2.02 $\pm$ 0.95 n=5	1.52 $\pm$ 0.2 n=6	1.5
Kay Point Segment 2		1.40 $\pm$ 0.83 n=7	1.29 $\pm$ 0.39 n=6	1.10 $\pm$ 0.3 n=7	
Babbage Bight to King Point		1.47 $\pm$ 0.85 n=12	0.74 $\pm$ 0.58 n=18		
King Point to Sabine Point	several (>1 m)	0.77 $\pm$ 0.83 n=8	0.64 $\pm$ 0.76 n=21		
Sabine Point to Shingle Point		0.17 $\pm$ 0.37 n=5	0.46 $\pm$ 0.38 n=10		
Shingle Point to Blow River		0.16 $\pm$ 0.29 n=7	0.70 $\pm$ 1.09 n=8		
King Point	several m/a	Hill 1954-1985 Model 1 0.55	Hill 1954-1985 Model 2 Headland		

\*Based on profile in Fig. 2 of Mackay (1963) and the sea level curve presented in Chapter 4.

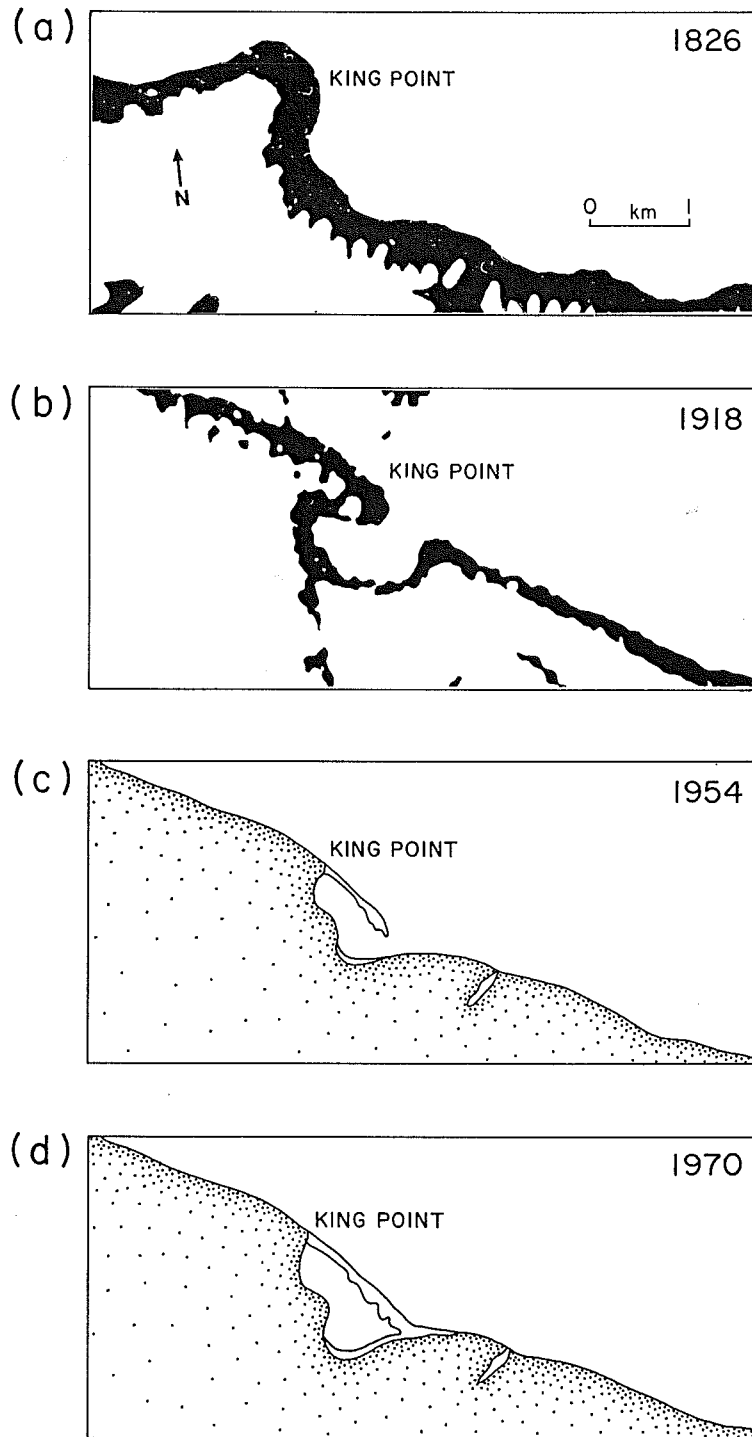
headland reaches as much as 5 m/a.

Repeated surveys to measure year-to-year variability have not been possible with the exception of two measurements at Kay Point where Gillie (1988) revisited localities one year after they were measured by Forbes and Frobel (1985). The one-year retreat at these sites (1.5 m and 1.1 m) were somewhat lower than the average rate.

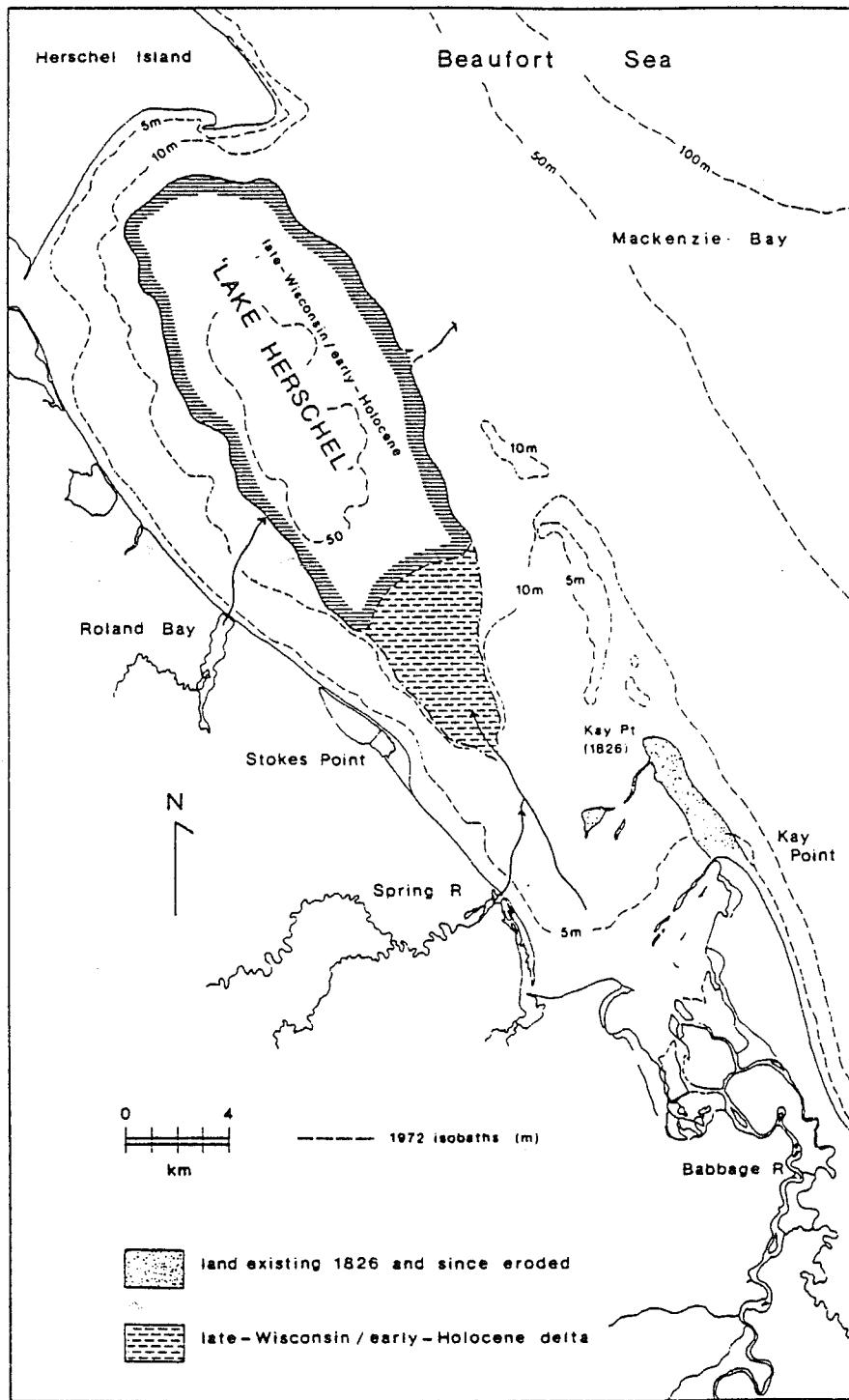
Longer-term estimates of retreat rates, based on historical documents are discussed by Mackay (1963a), McDonald and Lewis (1973), Forbes (1981) and Hill (1990). Several of these papers relate to the section of cliffs north of King Point (Fig. 5.5). Based on a comparison between maps from Franklin's 1826 expedition, Amundsen's 1905 expedition and the 1913-1918 Canadian Arctic Expedition, Mackay suggested that substantial straightening of the coastline between King Point and Sabine Point had occurred over the last 200 years. The destruction of the magnetic observatory hut left by Amundsen and the repeated movement of the Wiik grave marker provides a basis for estimating retreat rates of at least 1 m/a, but combined with the evidence for straightening of the coast, raises the possibility of retreat rates of several metres per year at King Point itself. Using the volume of sediment stored in the barrier beach southeast of King Point, and estimates of sediment transport potential from Pinchin et al. (1985), Hill (1990) suggested that the sediment was most likely supplied by the erosion of a prominent headland of morainic material in the vicinity of the modern point. This implies that retreat of the headland may have been quite rapid, perhaps in the region of 3 m/a or more.

Rapid rates of headland retreat are also suggested by Forbes (1981) for Kay Point. Based on the map and latitudinal observations of Franklin (1826), the headland at Kay Point may have retreated almost 6 km over 150 years, resulting in a retreat rate in the order of 40 m/a. This interpreted rate is an order of magnitude higher than the rate observed over the 18 year period measured by McDonald and Lewis (1973) and Harper et al. (1985). Comparison of distances measured from Franklin's map and modern hydrographic charts indicates that the Franklin map is inaccurate by as much as 60% of the measured distance. Reduction of the inferred retreat by this proportion still implies a retreat rate of 16 m/a. Furthermore, the geometry of Kay Point, as mapped by Franklin, is different from today's geometry (Fig. 5.6). A thin point extends from the broader peninsula formed by the ice-thrust ridge; the same point today is much shorter than depicted by Franklin.

It would not be unreasonable to believe that a narrow headland as depicted on Franklin's map would be susceptible to rapid coastal retreat. It is also possible that the point on the Franklin map may have been a spit or barrier island formed on the previously eroded headland surface and subsequently drowned. Several shoals along the same trend as Kay Point are present along the seaward margin of Herschel Basin (Fig. 5.6) and may have a similar origin. In fact, the Franklin map also shows a narrow island in the shoal region, oriented parallel to shore and having the



**Figure 5.5** The evolution of King Point from 1826 to 1970.



**Figure 5.6** Late Wisconsinan and 1986 paleogeography between Kay Point and Hershel Island (Forbes, 1981).

appearance of a barrier island. This feature is no longer present. Regardless of the exact nature of coastal change in the Kay Point region, it is clear that the change has been substantial in the 160 years since Franklin's visit.

Mackay (1963) presents a case for rapid coastal retreat at Herschel Island. By projecting the land profile offshore to the present submarine contour of -15 m, Mackay estimated an average retreat of 2.5 km. Using the sea-level curve in Chapter 4, relative sea-level was at -15 m approximately 3200 years B.P., giving an estimated retreat rate of 0.8 m/a. This value is consistent with the medium-term rates estimated from aerial photography (Table 5.1). However, it is not clear why the offshore profile should be continuous with the island profile as relative sea-level was previously much lower than -15 m. The offshore profile would therefore be influenced by erosion and deposition during transgression.

With the exception of Kay Point, there does not appear to be a major difference in medium-term retreat rates between cliffs of ice-thrust pre-Buckland sediments and the morainic sediments of the Yukon coast. Comparison of Herschel Island and Babbage Bight rates with rates from other sections of the coast shows no statistically significant difference in average retreat. The high values in the vicinity of Kay Point are most likely explained by focusing of waves from the predominant northwesterly direction at the headland, resulting in higher wave energy at this location, rather than by any higher susceptibility of the cliffs to erosion.

### ***5.3.2 Spit and Barrier Evolution***

The development of the King Point barrier is probably the most easily documented example of coastal evolution along the Yukon coast (Hill, in press; Fig. 5.5). No spit or barrier was apparently present in 1826 when the Franklin expedition passed by. The barrier initially developed as a spit extending from King Point into the breached thermokarst lake. By 1913, the spit had prograded approximately one-third of the distance across the embayment. Mackay (1960) was able to navigate into the bay in 1957, but aerial photographs indicate that the spit had grown to completely enclose the embayment by 1970. Through the 1970's and 1980's the main changes occurred at the southeastern end of the barrier, where seaward progradation of the barrier, in the form of progressive beach ridge development, took place.

### ***5.3.3 Delta Evolution***

Relatively little effort has been expended in this study to determine changes in deltaic coastal environments. The following brief discussion is based on the extensive study of the Babbage Delta by Forbes (1981).

Over the 18 year period of aerial photograph coverage, the Babbage Delta has not shown significant progradation, although changes in the distributary channel system can be noted.

However, development of the delta is complex due to major changes in configuration of the receiving estuary over the last few thousand years. Prior to transgression of the Herschel Basin sill (Fig. 5.1; possibly as recently as 3000 years B.P.; Forbes et al., 1987), the delta discharged into a large lake, now Herschel Basin (Fig. 5.6). The front of this late Wisconsinan or mid-Holocene delta can be tentatively placed north of Stokes Point, on the basis of bottom morphology and seismic profiles (Forbes et al., 1987). Since that time, the delta has retreated up the estuary to its present position. In addition, as discussed in sections 5.3.1 and 5.3.2, the headland of Kay Point has been eroded and the spit prograded across the Babbage estuary. Forbes (1981) points out that, within this framework, and due to the extreme annual and inter-annual variation in discharge and storm regimes, the interpretation of medium-term changes in delta morphology is almost impossible.

#### **5.4 Seismic Stratigraphy**

The seismic data base for the Yukon coastal zone is very limited. The following discussion is based on (i) a preliminary interpretation of seismic stratigraphy by Earth and Oceans Ltd. (1986) for the shelf west of Herschel Island; and (ii) a single seismic profiles collected during the NOGAP D.1 project from the Nahidik '87 cruise.

The Western Beaufort Shelf, north and west of Herschel Island is underlain by a series of seaward-dipping and -thickening seismic sequences that crop out at the seabed (Fig. 5.7). The oldest sequences are exposed at the seabed on the inner shelf and the sequences become progressively younger towards the shelf edge and Mackenzie Trough. Stratigraphic boundaries parallel the coastline and are truncated by the Mackenzie Trough southeast of Herschel Island. These units were therefore deposited before excavation of Mackenzie Trough. Based on dates from a mid-shelf borehole and correlations with the U.S shelf to the west, the mid to outer shelf sequences of the Western Beaufort Shelf are thought to be early Wisconsinan or older in age (Brigham-Grette et al., in prep.).

The inner shelf stratigraphy, west of Herschel Island, is poorly defined, due largely to the relatively low resolution of the air gun records and the deep draft of the survey vessel used in the survey (Banksland-1984 and Tully-1985 cruises; see McGladrey, 1984; Fehr, 1986). Earth and Oceans Ltd. (1986) indicate that the seabed is underlain by Unit L in water depths between 10 and 20 m (Fig. 5.7). Unit L is "unstratified, translucent or opaque to (3.5 kHz) profiler energy and highly scoured" (Earth and Oceans Ltd., 1986; our parentheses). A younger seismic unit (Unit Q) overlies and onlaps Unit L directly seaward of Clarence Lagoon and the alluvial fans of the Malcolm and Firth Rivers (Fig. 5.7). Earth and Oceans Ltd. describe Unit Q as ponded and transparent to stratified, and interpret the unit to be of lacustrine or lagoonal in origin. No data are available inside the 10 m isobath, although the above units are likely to continue inshore.





A similar situation pertains to the narrow shelf southeast of Herschel Island, with the additional constraint that there has been no systematic seismo-stratigraphic study of the deeper shelf. A high resolution seismic profile located between King Point and Kay Point is shown in Figure 5.8. The line extends inshore to a minimum water depth of 15 m. Although not strictly within the coastal zone as defined for this study, it is presented as the seismic stratigraphy may be extrapolated into shallower water. Three seismic sequences can be recognised in this profile:

**Sequence Y1** is transparent and unstratified, ranging in thickness from less than 5 m in approximately 15 m of water, to approximately 30 m in the centre of Mackenzie Trough. The seabed is highly irregular due to ice-scour disturbance. The same sequence is present near King Point, where it wedges out in water depths between 10 and 15 m, exposing older sequences at the seabed (Hill, 1990).

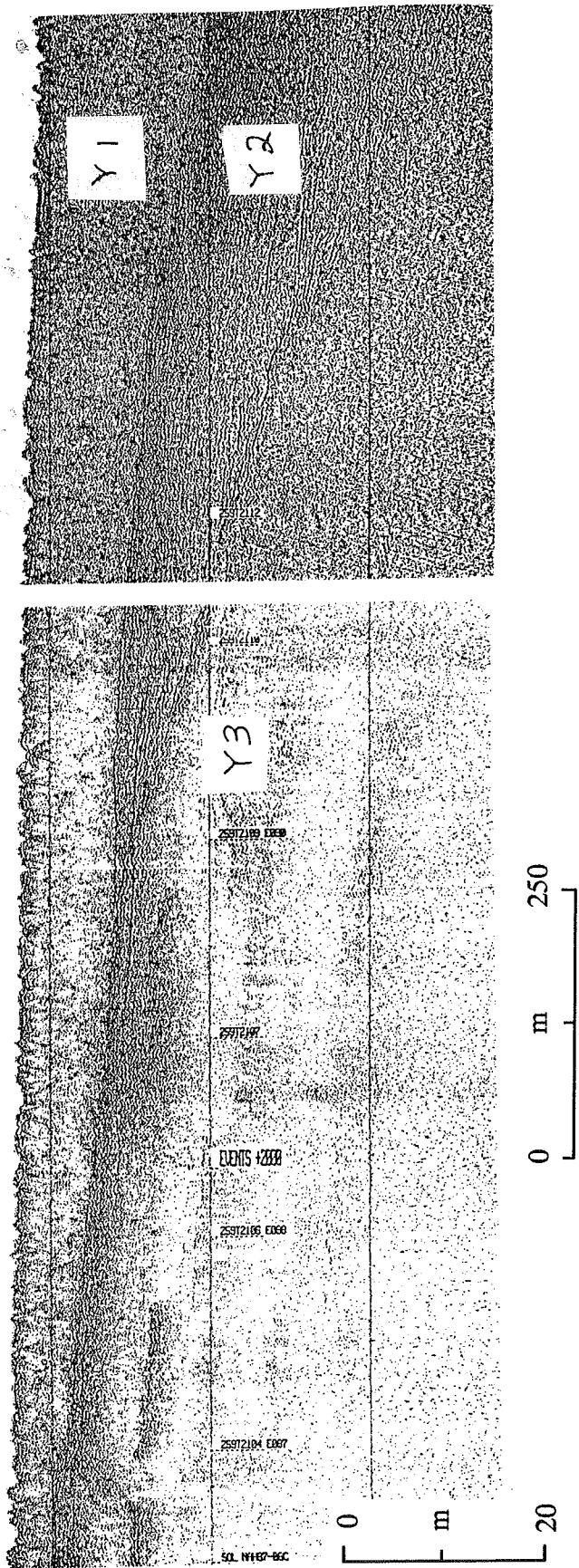
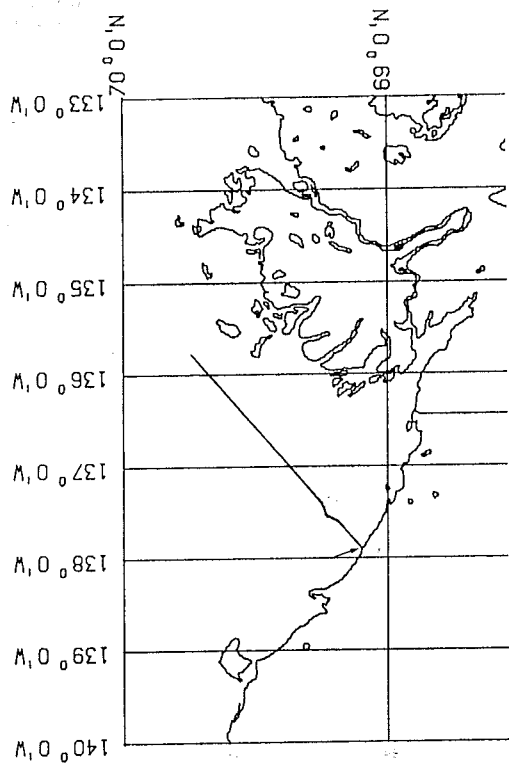
**Sequence Y2** forms a wedge-shaped unit at the erosional margin of Mackenzie Trough. It reaches a maximum thickness of approximately 25 m and is cut out at the unconformity that forms the base of sequence Y1. Sequence Y2 is well-stratified and the sub-horizontal reflectors clearly onlap the underlying unconformity. The unconformity reflector at the top of the sequence consists of a strong, sharp reflector along the inshore section, but becomes hummocky and more diffuse towards the margin of the trough.

**Sequence Y3**, which underlies Sequences Y1 and Y2, is bounded by a distinct but diffuse reflector. The sequence is largely opaque, with few internal reflectors, with the exception of a strong, discontinuous reflector, generally 15-20 m below the seabed, which may be acoustic permafrost (O'Connor, 1982a).

Sequence Y2 and Y3 are probably erosionally truncated at the margin of Mackenzie Trough. On Figure 5.8, the sequences appear to pass laterally into stratified reflectors of sequence MTW 01 (Fehr, 1987; see section 6.5). The interval between contains ill-defined reflectors and there is no evidence that sequences Y2 and Y3 are stratigraphically equivalent to MTW01. A similar interpretation has been made in seismic sections from further offshore (Earth and Oceans, 1986) where the erosional margin of the trough is more clearly seen. Folding within the adjacent MTW01 sequence suggests that the margin may be partly structural. Diapiric intrusions are also observed along this trough margin further to the north.

## 5.5 Lithostratigraphy and Sedimentology

Regional lithostratigraphic information in the offshore portion of the Yukon coastal zone is



**Figure 5.8** High resolution seismic record across the Yukon Shelf, southeast of Herschel Island, showing seismostratigraphic units described in the text. The arrow on the index map refers to both the seismic line location and the location of nearshore vibracores between King Point and Sabine Point.

very limited. However, during the NOGAP D.1 project, there was an opportunity to participate in a major drilling project, led by Indian and Northern Affairs, at King Point. The project was carried out to investigate the geotechnical conditions at King Point, in response to a commercial proposal to establish a deep water harbour that would service a potential granular borrow site further inland. The AGC component of this project was to investigate sedimentological and geotechnical conditions in the gravel barrier beach and immediate offshore. Shipboard coring along the Yukon coast was restricted to opportunist attempts aboard the Nahidik. Four vibracores from the nearshore zone midway between King Point and Sabine Point were collected from the Nahidik '87 cruise (Fig.5.8).

### ***5.5.1 King Point***

Details of the complete borehole program at King Point can be found in O'Connor (1986). Hill (1990) has summarised the stratigraphy of the coastal and offshore parts of the system (Figs. 5.9 and 5.10).

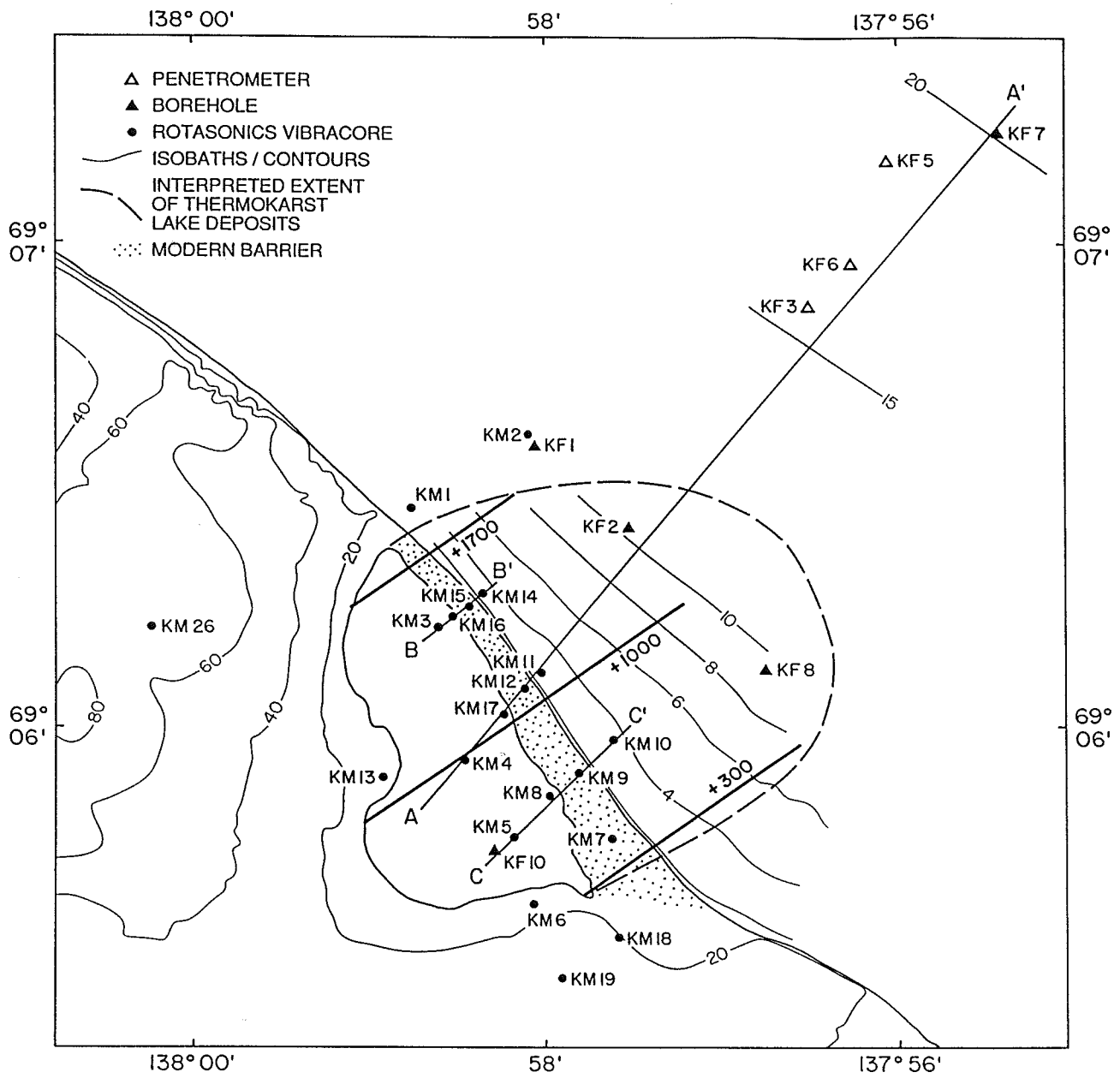
#### ***Diamict and Older Pleistocene Deposits***

Sediments drilled on land and in the lower sections of boreholes on either side of the barrier consist predominantly of very dark gray to black diamict. The diamict has a silty matrix containing up to 40% sand, commonly as inclined and microfaulted laminae. Angular gravel clasts up to 4 cm in size and rare wood fragments are scattered throughout the silty matrix. Visible ice as lenses and platelets was observed in this lithofacies when first split. The diamict is generally massive, but also contains deformed sandy laminations and brecciated beds. These deformations occur most commonly in the lower parts of the sequence and may be in autochthonous sediment underlying the diamict.

These older deposits outcrop on land, in the cliffs and morainic ridge surrounding the King Point lagoon. Offshore, they outcrop at the seabed or beneath a thin veneer of sand in boreholes KM1, KM2 and KF1 (Fig. 5.9). This lithology is also thought to outcrop at site KF3, where a cone penetrometer failed to penetrate the seabed.

#### ***Lacustrine Organic Muds***

The upper parts of cores from the lagoon and lower shoreface consist of laminated to bioturbated organic silt and clay which is very dark grey or black in colour when initially split, but oxidises to a lighter brown colour with time. The silt laminae contain up to 30% organic material, as brown (when oxidised) amorphogen and plant fragments. Individual silt laminae are generally parallel and conformable, although small scours, filled with coarser silt, and microfaults are present. In parts, the laminae are disrupted by bioturbation, although the primary structures are



**Figure 5.9** Location map for King Point, showing borehole and survey lines (Hill, 1990).

rarely obliterated entirely. In boreholes in or close to the barrier, sediments of this facies were frozen and contained veins of ice.

Based on the absence of foraminifera, the high detrital organic content of the sediment and the pollen yield, this lithofacies is interpreted to have been deposited in a thermokarst lake. The sequence is thickest in the modern lagoon where it reaches nearly 11 m (KF10, Fig. 5.10). Lacustrine sediments outcrop at the seabed, seaward of the barrier, in holes KF2 and KF8. The outline of the original lake is sketched onto Figure 5.10 based on these observations.

An accelerator radiocarbon date of  $11,850 \pm 150$  a (RIDDL # 768) was obtained on some spruce and willow twigs from the lacustrine mud near the bottom of hole KM17 (Fig. 5.9). The lacustrine sequence also yields a pollen profile typical of the region with an influx of alder pollen beginning at approximately 7 m in borehole KM10 (Fig 5.11; J. Shaw, personal communication). This influx is dated at 5.5 - 6.5 ka on the Mackenzie Delta (Ritchie and Hare, 1971; Hyvarinen and Ritchie, 1975), and 8.9 ka at a more upland site in the Yukon (Cwynar, 1982). The lake has infilled with at least 10 m of sediment over 12 ka, giving an average sedimentation rate of 0.8 mm/a. The ice content of the samples below the barrier indicates aggradation of permafrost beneath the barrier.

#### *Barrier Sand and Gravel*

The barrier sequence varies along the length of the barrier (Fig. 5.12). At the northwestern end, the barrier consists of 5.5 m of interbedded gravel and sand, directly overlying black lacustrine muds. On the seaward side of the barrier, the lower shoreface consists of sand overlying gravel while cores on the lagoonal side of the barrier penetrate directly into lagoonal mud. At the centre of the barrier, the sequence is similar except that the 6 m of interbedded fine gravel and sand overlies a 0.2 m thick sand at the boundary with the lagoonal mud. At the southeastern end of the barrier, a 1 to 2 m thick sand unit overlies lacustrine mud on the lagoonal side of the gravel barrier. This sand probably represents a distal portion of a previous recurved spit.

#### *Marine Sediments*

Marine sediments are found in borehole and penetrometer sites at locations greater than 2 km offshore. These sediments consist of homogeneous grey-brown silty clay, except for the bottom metre where the clay passes downward into laminated silt and clay and finally to thin sand beds. In x-radiographs, rare burrows and ice-rafted pebbles are observed in the clay, while bivalve shells as both fragments and paired valves are common. An accelerator radiocarbon date of  $3,970 \pm 120$  a (RIDDL #429) was obtained on shell material from 10 m below seabed in hole KF7. These fine-grained marine sediments are deposited under relatively gentle conditions below

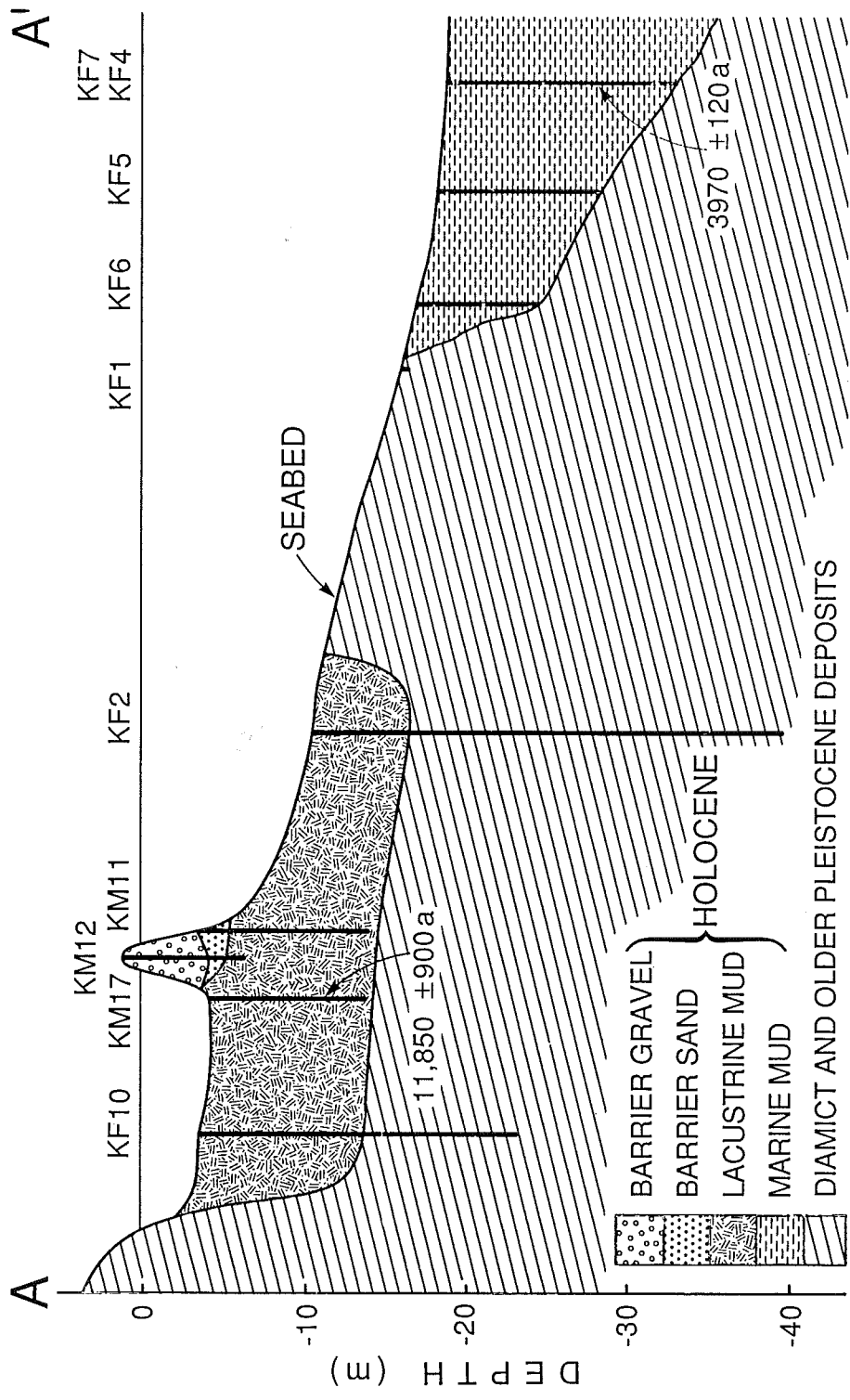


Figure 5.10 Lithostratigraphic summary of King Point based on borehole information (Hill, 1990).  
 Transect A-A' shown in Figure 5.10. Transects A, B and C shown in Figure 5.12.

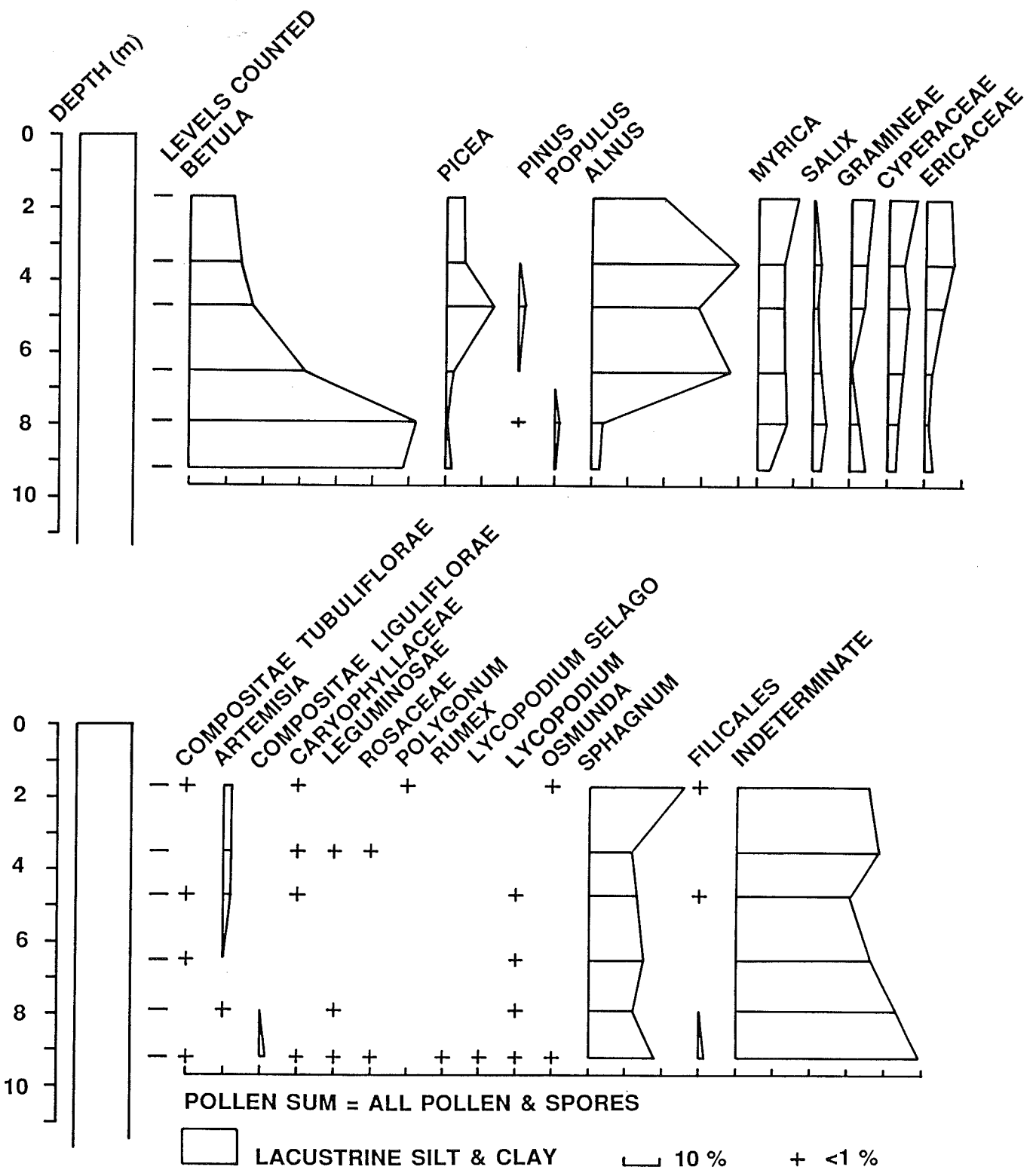
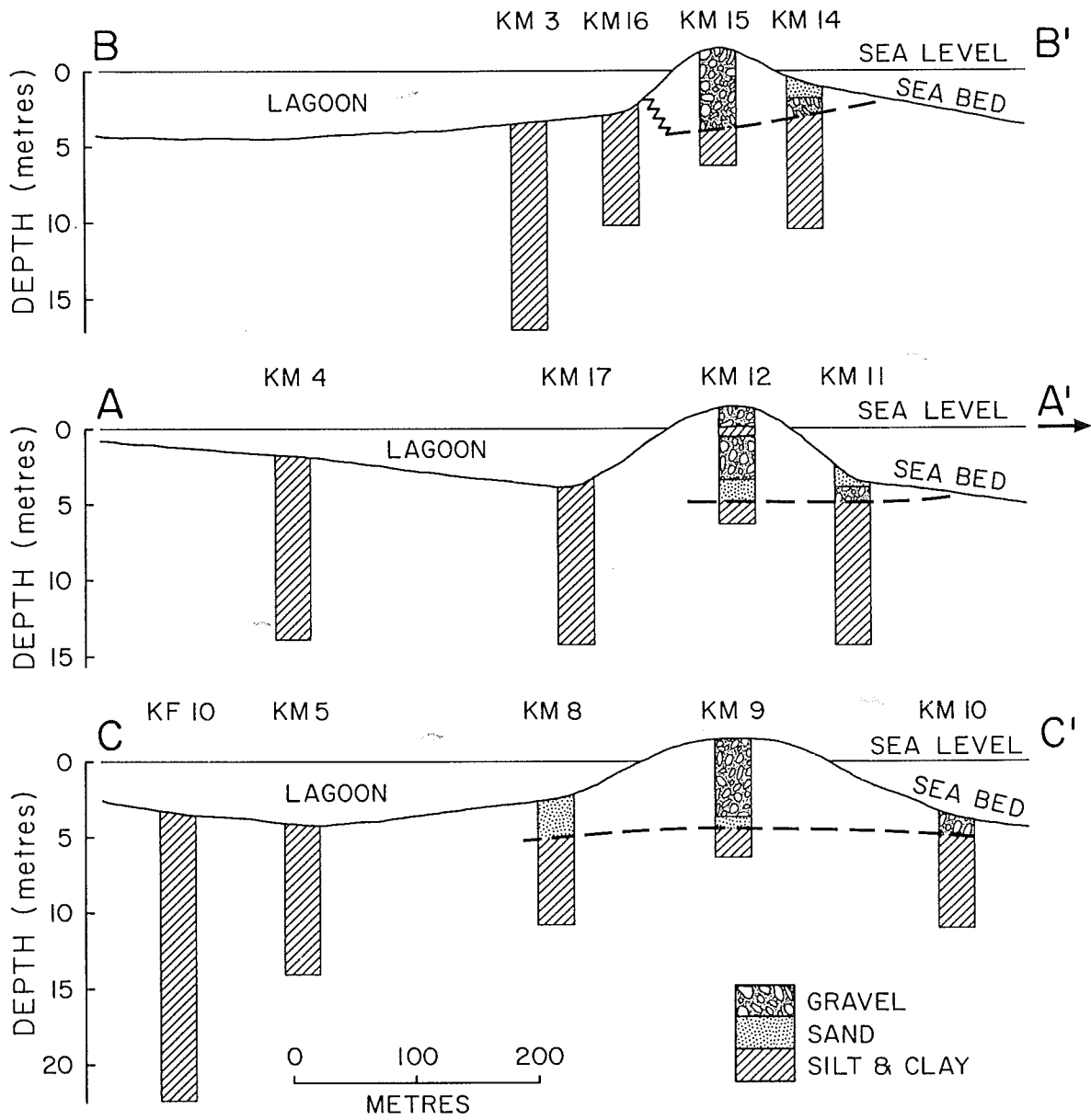


Figure 5.11 Pollen profile of the lacustrine sequence in borehole KM10 (J. Shaw, pers. comm.).



**Figure 5.12** Barrier profiles at King Point (Hill, 1990).



about 15 m water depth.

### ***5.5.2 Vibracores from nearshore zone between King Point and Sabine Point***

A series of four shallow vibracores (Fig. 5.13) were collected in the nearshore zone between King Point and Sabine Point (Fig. 3.4), in water depths ranging from 0.6 m to 4.5 m. The transect is located seaward of a narrow gravel and sand beach, fronting steep gullied cliffs. In the shallowest core, 55 cm of gravel was recovered and the presence of disturbed clay at the base of the core suggests that almost the whole thickness of gravel was recovered. The surficial gravel becomes finer offshore, thinning to 33 cm in the deepest core. In the three deeper cores, the sand-gravel bed overlies stiff clay with silt lenses, in places showing fold deformation. In view of the evidence for transgression in the area, these clays are interpreted to be older coastal plain deposits that lie below the erosional transgressive unconformity.

## **5.6 Geotechnical Properties**

Detailed measurements of the physical properties of sediments from the offshore portion of the Yukon coastal zone are restricted to the borehole program carried out at King Point and documented in O'Connor (1986). On this borehole program, both rotary drilling and sonic vibracore techniques were used to obtain samples, but due to the severe disturbance caused by the sonic vibracore method, data from the rotary drill holes has generally been used in this synthesis. The only exception is in the use of Atterberg limits data from the sonic cores.

The three facies with significant fines content have distinctly different properties. This is reflected in the plasticity chart (Fig. 5.14) where the three facies plot as separate fields along the A-line. Marine sediments exhibit the most plastic behaviour and diamicton the least plastic, with the lacustrine facies showing an intermediate behaviour and overlapping with both end-member fields. The characteristics of the three main facies are summarized below.

### ***5.6.1 Diamicton***

The diamicton facies was generally frozen, with visible ice in the form of lenses common. Some boreholes on land contained intervals of massive ice (O'Connor, 1986). The grain size distribution of this facies was generally poorly sorted (well-graded) with up to 20% gravel and a similar proportion of clay in a matrix of sandy silt (Fig. 5.15a). The clay content of the diamicton is generally less than 30 % and the sediment consequently falls between the low-plastic inorganic silt (ML) and clay (CL) fields on the plasticity chart (Fig. 5.14).

The water content of the frozen diamicton is highly variable (Figs. 5.16). In borehole KF1, located seaward of King Point itself, the water content ranges from 20% to 50%, with no systematic variation downhole (Fig. 5.16a). At several intervals, the water content is higher than

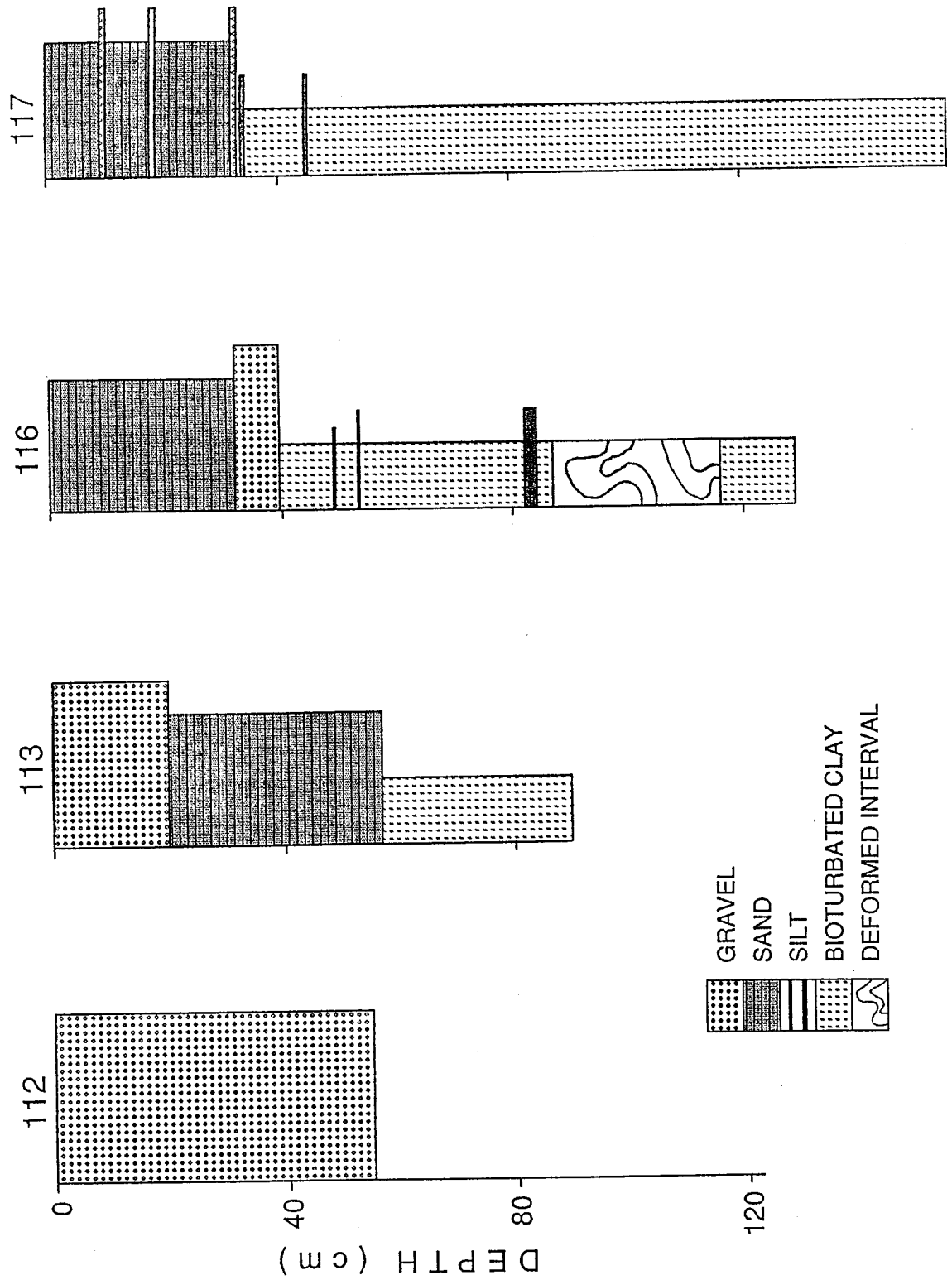


Figure 5.13 Four shallow vibracores - 112, 113, 116 and 117 - from the nearshore zone between King Point and Sabine Point.

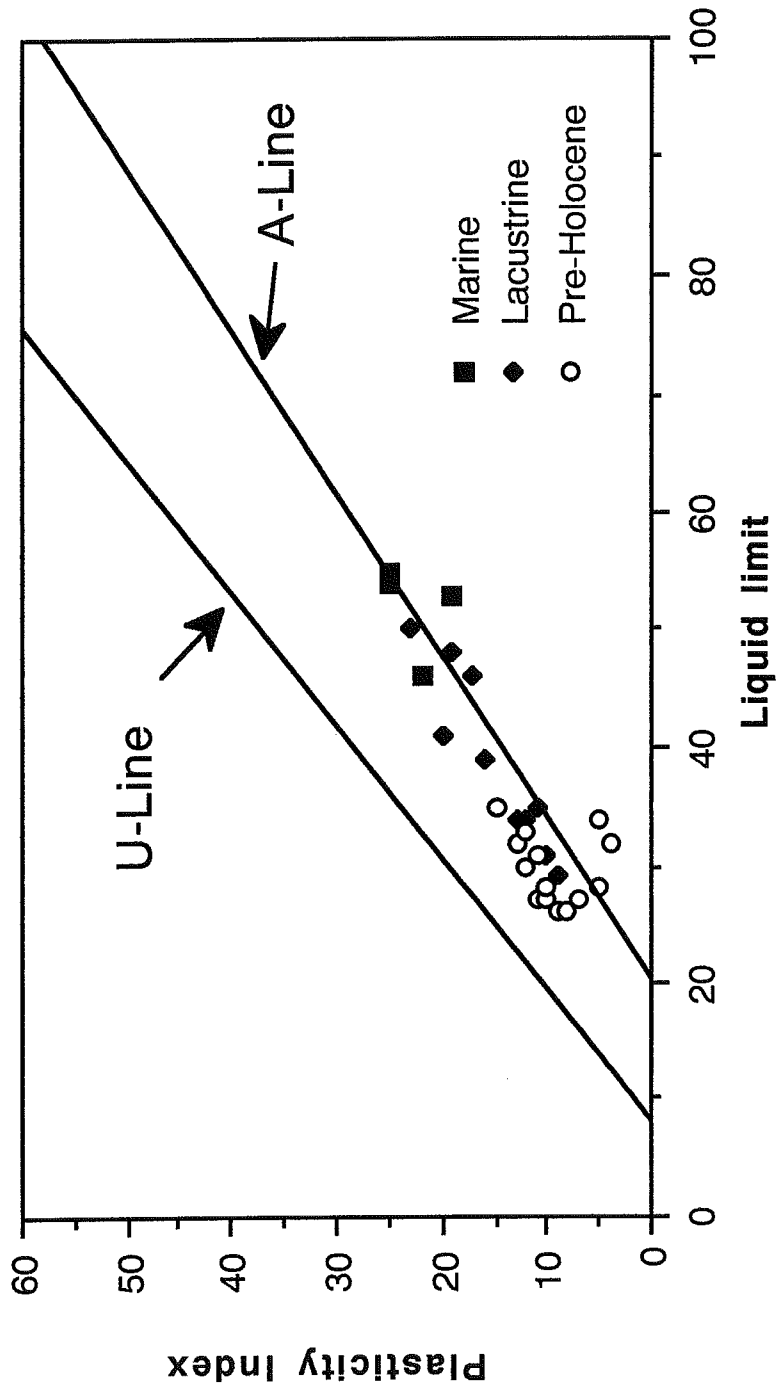
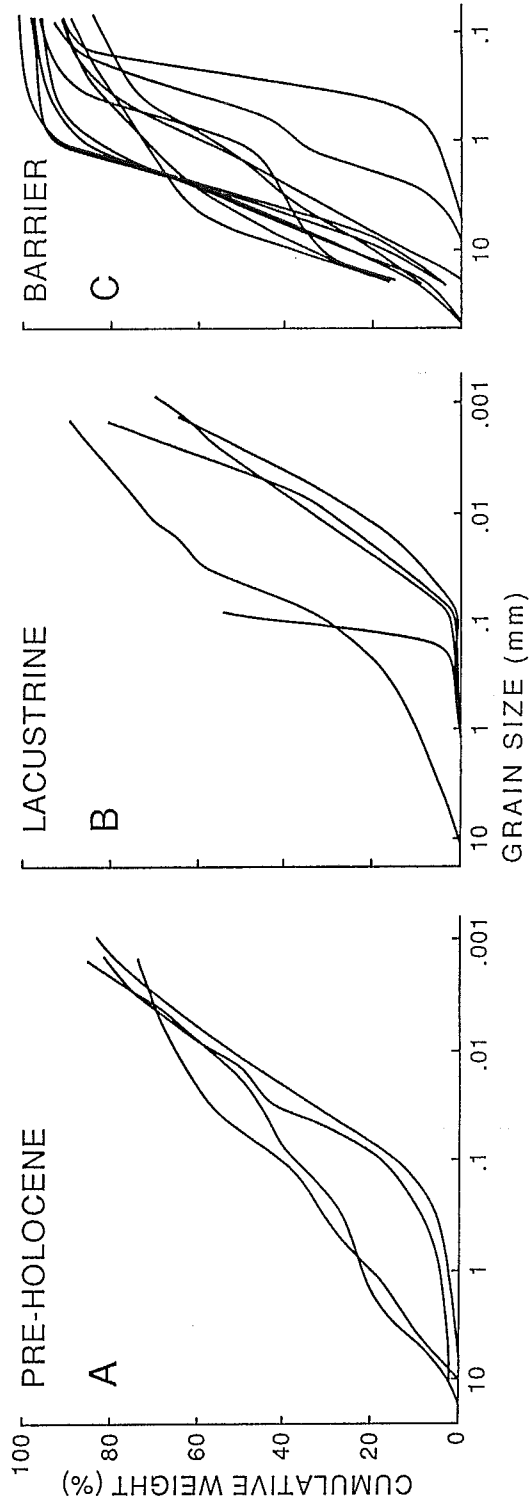
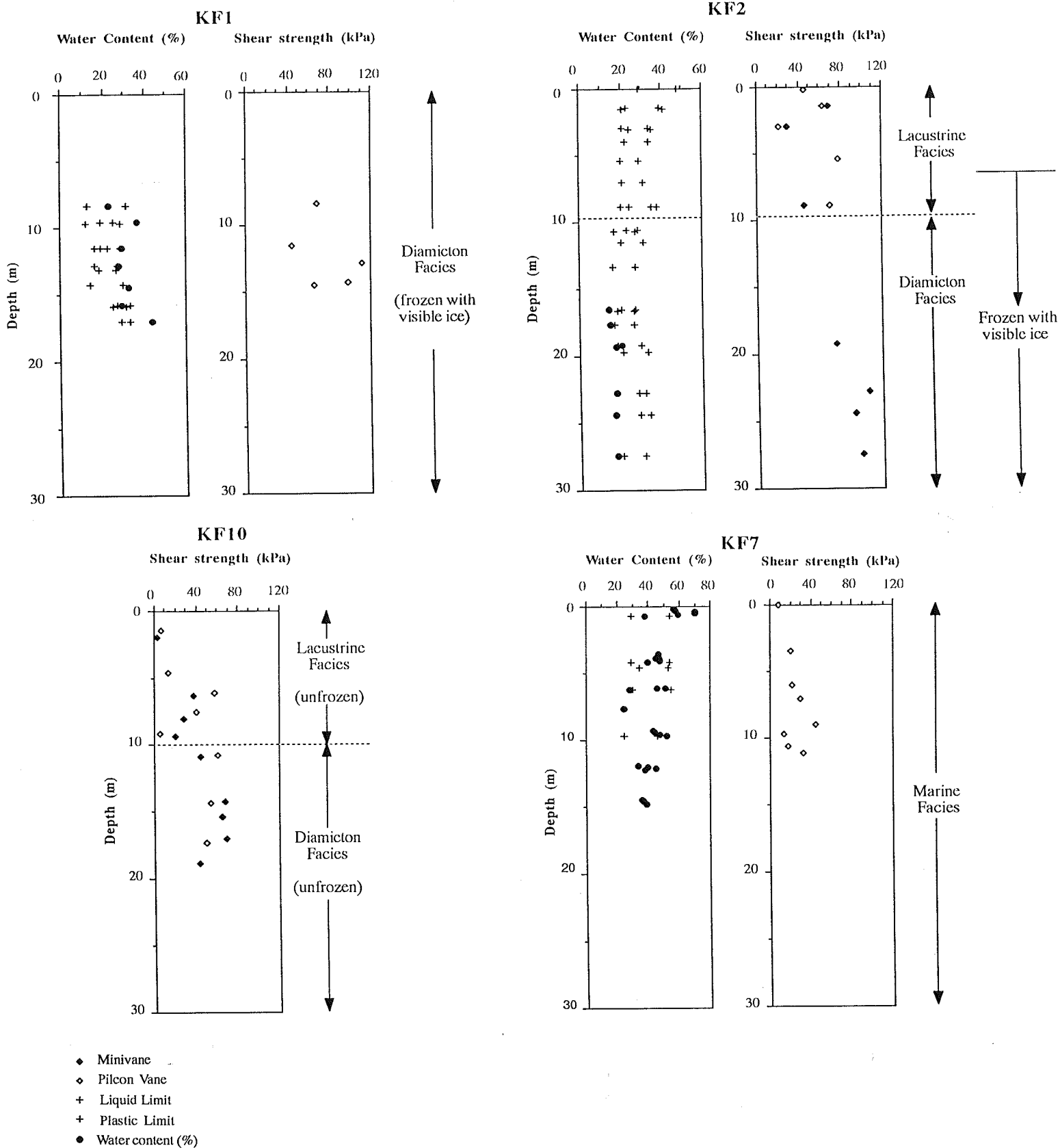


Figure 5.14 Plasticity chart for sediments from the King Point borehole program (data from O'Connor, 1986).



**Figure 5.15** The grain size distribution of (a) pre-Holocene, (b) lacustrine and (c) barrier facies from King Point.



**Figure 5.16** Water content and shear strength profiles for King Point borehole data: (a) KF1, (b) KF2, (c) KF10, and (d) KF7. For borehole locations see Figure 5.9.

the liquid limit (Liquidity Index,  $LI > 1$ ). Although sediment with this property will remain stable in the undisturbed state, thaw, followed by a sudden shock may transform the sediment into a liquid state (Das, 1983). By contrast, the diamicton in borehole KF2, located offshore of the barrier, shows much lower water content, generally less than 20% and below the plastic limit of the sediment (Fig. 5.16b).

Shear strength measurements were made on thawed samples from the two boreholes. In both cases the strength is highly variable, but generally increases with depth. Shear strength values are generally greater than 50 kPa, reaching greater than 140 kPa in KF1 (Fig. 5.16a,b).

### **5.6.2 Lacustrine**

The lacustrine sediments are generally unfrozen, except for immediately beneath the barrier where they are frozen and contain visible ice. These sediments have a better sorted size distribution than the diamicton and generally contain less than 10% sand (Fig. 5.15b). However, sandier intervals are present, particularly near the base of the thermokarst lake infill. Despite the observed organic content of these sediments, they place on the plasticity chart as low-organic clay and silt, ranging from low to high plasticity (Fig. 5.14). The lower plasticity is shown by laminated samples from deeper in the sequence where the silt content is higher. There is virtually no water content data for this facies. One value was obtained from borehole KF10, located in the lagoon: 43% at 7.5 m depth. The shear strength of the lacustrine sequence varies from less than 10 kPa to almost 80 kPa. The lower values are seen in KF10 (Fig. 5.16c), probably because the upper part of the sequence is preserved in the lagoon. In KF2 (Fig. 5.16b), seaward of the barrier, the upper part of the lacustrine sequence was probably eroded during transgression.

### **5.6.3 Marine Sediment**

The marine sediment consists of soft, inorganic silty clay which exhibits medium to high plasticity (Fig. 5.15). The water content is relatively high, ranging from 70% near the seabed to approximately 40% at 15 m depth (Fig. 5.16d). The water content exceeds the liquid limit in the top metre of the borehole and in a second interval at approximately 10 m depth. However generally, the water content falls within the plastic range. The shear strength of the marine sediment is low, being less than 10 kPa in the top metre and increasing steadily with depth to around 30 kPa at 12 m.

## **5.7 Sediment Erosion, Transport and Deposition**

In this section, knowledge of the environmental factors (wind, waves, currents) and processes (storm surge, ice-related) that control sediment erosion, transport and deposition will be discussed, followed by a summary of the littoral measurements made during a field investigation

at King Point and a discussion of the quality of sediment transport rate estimates based on field and numerical model results.

### *5.7.1 Wind regime*

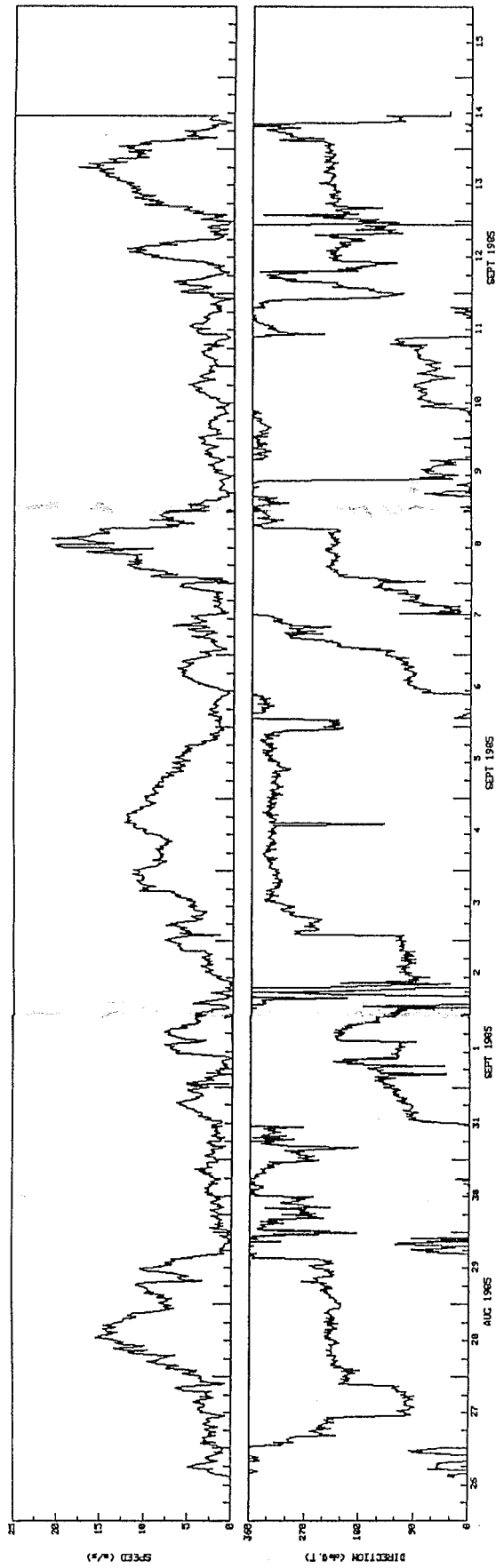
Summaries of the wind regime for the Canadian Beaufort Sea region have been compiled by Harper and Penland (1982) and Fissel and Birch (1984). For most of the region, wind directions are bimodal, with winds from the north west and the east being the most common (Fig. 2.8). Based on records from coastal locations, Harper and Penland (1982) suggest that the strongest winds blow from the northwest in the central region of the shelf. However, Fissel and Birch (1984) point out that the distribution of strong winds is highly variable from year to year. Hodgins et al. (1981) have suggested that two types of extreme storms exist in the Canadian Beaufort Sea: large scale low pressure systems travelling from west to east (Burns, 1973) and smaller scale but intense low pressure systems resulting from the onshore flow of cold air originating over the pack ice.

Along the Yukon coast, a third mechanism is important and results in strong southwesterly winds (i.e. blowing offshore), which are evident in the wind roses from Shingle Point (Fig. 2.8) and in time series from King Point (Fig. 5.17). These winds are caused by mountain barrier baroclinicity and orographic effects associated with downward flow of air over the Richardson and Barn Mountains (Fissel et al., 1987), as also observed in the Alaskan Beaufort Sea (Kozo and Robe, 1986). Wind speeds up to 20 m/s from the southwest are caused by this process.

### *5.7.2 Currents and Plume Characteristics*

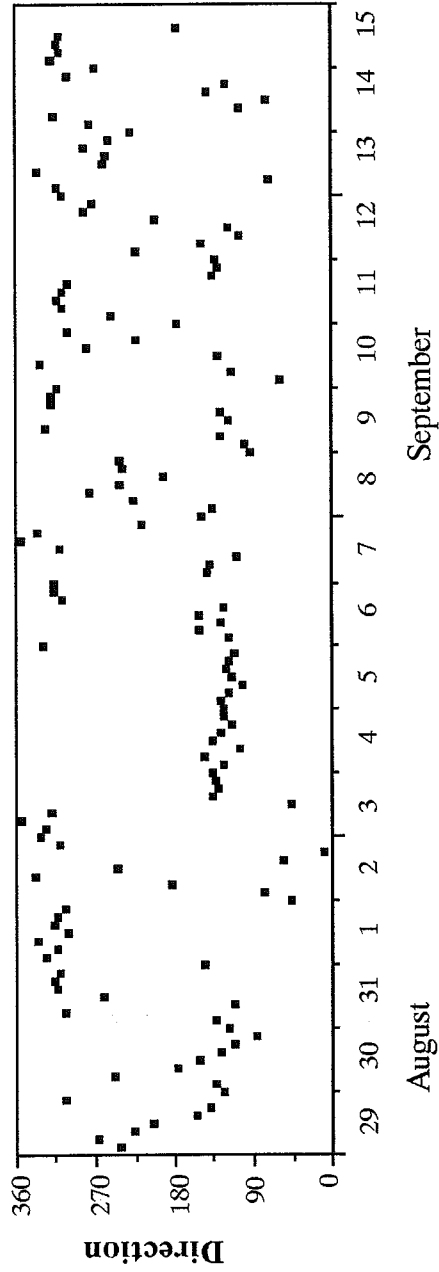
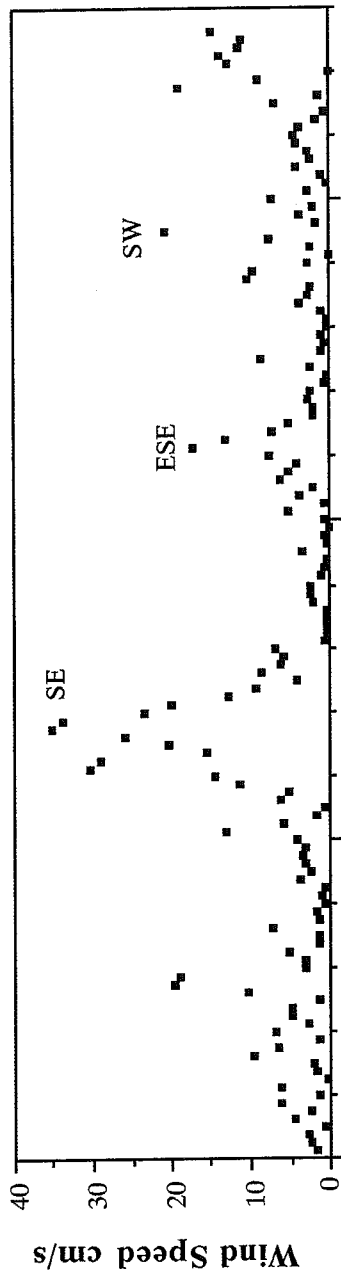
The Yukon coast southeast of Herschel Island is commonly influenced by warm, low salinity surface water originating from the Mackenzie River. Many satellite images show the presence of warmer, sediment laden surface water in a narrow band along the Yukon coast (Harper and Penland, 1982; Fissel et al., 1987). There are few current measurements along this section of the coast. The presence of Mackenzie plume water along the Yukon coast attests to a northwestward flux of surface water, probably as a result of southeasterly winds (Harper and Penland, 1982). Surface drifter observations in 1974 and 1975 led MacNeill and Garrett (1975) to suggest that even under northwesterly winds, when net drift over most of the Beaufort Sea is to the east, flow along the Yukon Shelf between Shallow Bay and Herschel Island is to the northwest. They show this flow as a clockwise eddy developed in Mackenzie Bay. There is little evidence to support this hypothesis.

In fact, current measurements in 2.7 m of water off King Point in 1985 indicate that a strong southeastward-directed coastal current occurs during periods of strong northwesterly winds (Fig. 5.18). One major event on September 3-4, when wind speeds at the King Point beach site



**Figure 5.17** Time series of wind speed and wind direction from King Point for August and September, 1985 (Fissel et al., 1987).





**Figure 5.18** Current speeds and directions recorded during August and September, 1985 in 2.7 m water depth off of King Point.

reached 40 km/hr from the northwest, produced mean currents of more than 35 cm/s. These were the strongest currents measured over the 17-day period of the deployment. Northwesterly currents with mean speeds of 15 cm/s were produced by moderate southeasterly winds (e.g. September 8-9), but the strong southwesterly baroclinic winds produced only weak and directionally variable currents (e.g. September 13-14).

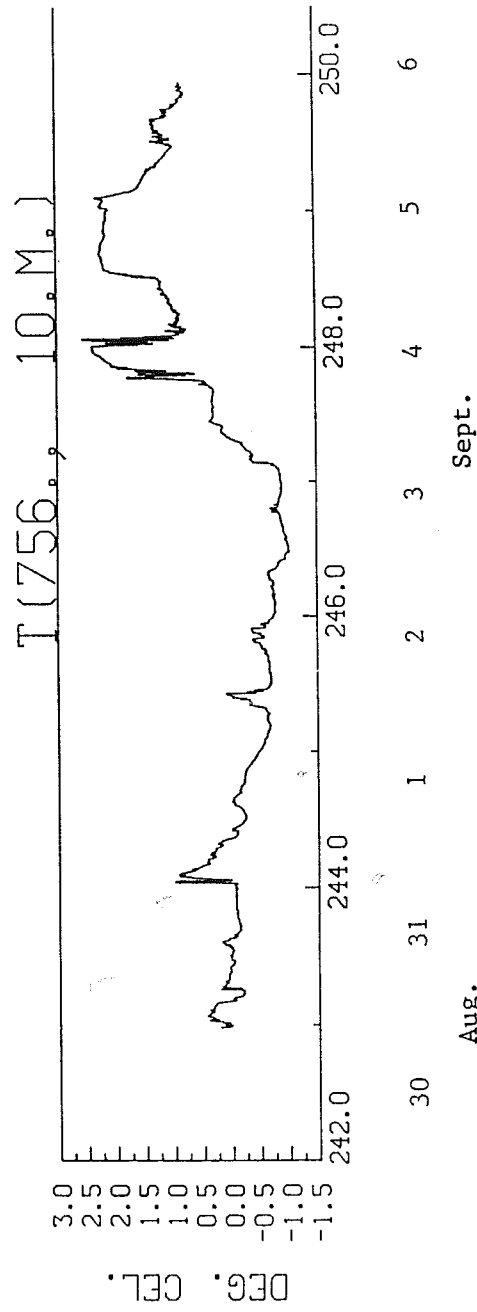
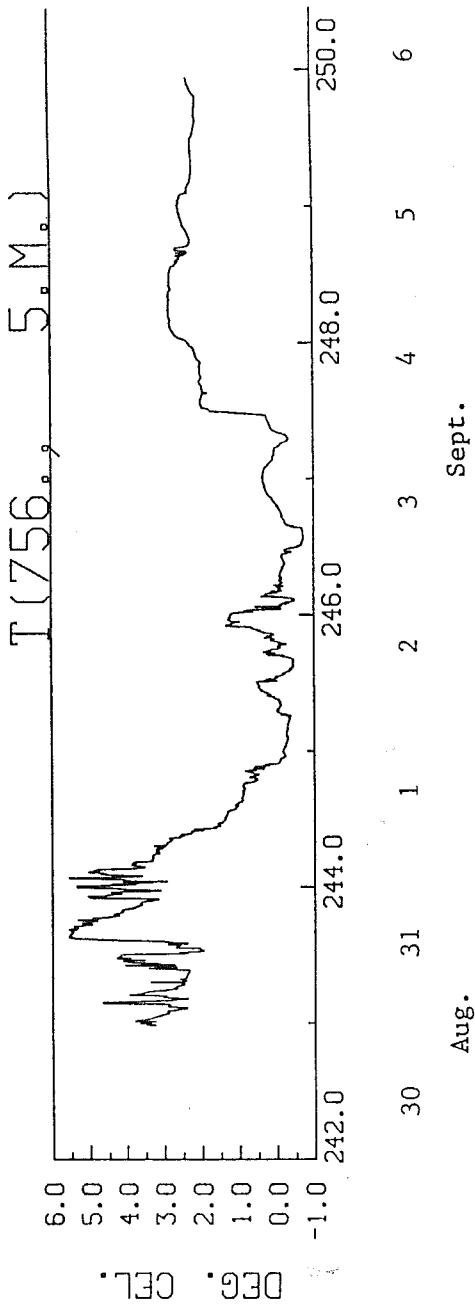
Two factors probably complicate current patterns along the Yukon coast. The intrusion of Mackenzie plume water probably results in frontal eddy motions. Water temperature records from the same King Point program show fluctuations of several degrees over time scales varying from hours to days (Fig. 5.19). It has also been suggested that upwelling of cold deeper water occurs along the Yukon coast (McDonald et al., 1987; Fissel et al., 1987). This has been explained either as a result of the interaction of the coastal circulation with topography (MacDonald et al., 1987) or due to the offshore transport of water during the southwesterly baroclinic winds (Fissel et al., 1987). Vertical motions resulting from upwelling will clearly have an effect on current circulation along the Yukon coast. Further work in terms of both current and water column measurements is needed to clarify the nature of these interactions and better define the coastal current regime.

### 5.7.3 *Waves*

There are no measurements of offshore waves between Herschel Island and Mackenzie Trough that can be used to analyse likely nearshore conditions. Wave data are available from sites to the east of Mackenzie Trough, but these stations are quite distant and well east of fetch paths for waves that may intersect the Yukon coast. Some data are available west of Herschel Island, but in this case are likely to be severely fetch-limited due to the restricted area of open water in this region during much of the summer. Wave measurements were carried out during the 1985 program at King Point, but these data are of short duration and in shallow water, making them very site specific (see later section). The use of numerical wave hindcast models are therefore the only method for assessing the range of wave conditions along the Yukon coast. As a result of the complex wind-field described above, the prediction of wave conditions along the Yukon coast is unfortunately quite difficult.

Pinchin et al. (1985) used 14 years of wind data at Tuktoyaktuk to generate wave conditions at King Point, Stokes Point, Kay Point and Pauline Cove (on the southeastern coast of Herschel Island). The results of this study in terms of predicted deep-water (generally taken as 30 m water depth) wave heights for different return periods are given in Table 5.2. With the exception of Pauline Cove, the sites show similar predicted wave regimes, with 100-year return period wave heights between 4.2 and 4.4 m. The predicted wave heights for Pauline Cove were somewhat lower, probably due to the southern aspect of the site.

However, Pinchin et al.'s results assume a uniform wind field over the entire Beaufort Sea



**Figure 5.19** King Point water temperature records for August and September, 1985 at 5 m and 10 m water depth.

**TABLE 5.2 PREDICTED WAVE CONDITIONS ALONG THE YUKON COAST\***

	Return Period (years)	Wave Height (HS)
<b>King Point</b>	1.0	3.1
	5.0	3.5
	10.0	3.7
	20.0	3.8
	50.0	4.0
	100.0	4.2
<b>Stokes Point</b>	1.0	3.3
	5.0	3.7
	10.0	3.8
	20.0	4.0
	50.0	4.2
	100.0	4.3
<b>Kay Point</b>	1.0	3.3
	5.0	3.7
	10.0	3.9
	20.0	4.1
	50.0	4.3
	100.0	4.4
<b>Pauline Cove</b>	1.0	2.1
	5.0	2.1
	10.0	2.1
	20.0	2.2
	50.0	2.2
	100.0	2.2

\*Based on 14 year hindcast of Tuktoyaktuk winds (from Pinchin et al., 1985).

region, in order that the wind record at Tuktoyaktuk can be used to predict waves along the Yukon coast. In a more recent study, Pinchin and Nairn (1987) determined that the winds at Tuktoyaktuk produce "acceptable but not good" results when hindcast waves were compared to measured waves at an offshore, deep water site west of Herschel Island. Local winds measured at the King Point site or at Shingle Point did not produce acceptable results when used as the basis for the hindcast. On the other hand, a hindcast based on winds measured at a drill site due north of King Point in Mackenzie Trough, produced by far the best results. Thus it appears that the local baroclinic winds along the Yukon coast do not have a significant effect on offshore wave conditions. Although the hindcast based on Tuktoyaktuk winds is less than perfect, there are no long-term data sets of offshore winds on which to base a superior wave hindcast study.

#### ***5.7.4 Storm Surge***

There has been little work to establish storm surge levels along the Yukon coast. From the general studies of storm surge levels in the Beaufort Sea (Henry, 1975; 1984; Henry and Heaps, 1976; Reimnitz and Maurer, 1978; 1979) surge levels are unlikely to exceed 3 m and the results of log-line surveys (Harper et al., 1988) suggest that maximum levels over the last 100 years have not exceeded 2.4 m. Positive storm surges in the Canadian Beaufort Sea are generally thought to result from northwesterly storms driving water southeastward onto the coast. The highest levels are therefore predicted for Kugmallit Bay and Shallow Bay (Henry, 1975). Under this scenario, the level of surge elevation decreases northwestwards along the Yukon coast. On the other hand, storm surges along the Alaskan Beaufort coast appear to reach similar levels (Reimnitz and Maurer, 1979) so that there would be no reason for ruling out 2 or 3 m storm surges even along the western part of the Yukon coast.

#### ***5.7.5 Ice-Related Coastal Processes***

In their study of ice-related coastal processes, Arctec (1987) reviewed the potential importance of these processes on the proposed King Point development. They concluded that the processes of ice push and ice override have a high likelihood of occurring due to the steep shoreface gradient. Similar gradients occur along much of the gravel beach shoreline of the Yukon coast and consequently Arctec's conclusion can be extrapolated to most of the coast. There have been no direct observations of ice override along the Yukon coast, but there is some evidence for the process of ice-push. Small ice islands, 10-15 m deep have been observed grounded offshore, 5 km north of King Point (Kovacs and Mellor, 1971). McDonald and Lewis (1973) observed ice-push ridges of gravel up to 2 m above mean sea-level on the Kay Point spit.

Although there have been relatively few observations of ice-push or override along the Yukon coast, or indeed in the Canadian Beaufort Sea, the process has been well-documented in the

Alaskan Beaufort Sea (Barnes, 1982; Kovacs, 1983; 1984) and elsewhere in the Arctic (Taylor, 1978; McLaren, 1982). However, Reimnitz et al. (1985) suggest that the overall contribution of ice "bulldozing" of sediment to the sediment transport budget is small.

Another ice-related process that has been well-documented along the Yukon coast is strudel scour. Forbes (1981) reported the appearance of several drainage holes off the Babbage River in Phillips Bay in May 1974. Dickins (1987) observed "dozens of strudel-like drainage patterns" within Phillips Bay, just seaward of the Kay Point spit during the spring break-up in June 1987. The strudel drainage holes occurred in ice located in 2.3 to 3.5 m of water and ranged from 1 to 6 m in diameter. Distinctive radial drainage channels were incised into the ice surface and active drainage was observed in some of the drainage holes. Beneath the drainage holes, strudel scour pits between 1 and 2 m deep were formed. It is not clear whether the scour pits were infilled at the time of the survey. One of the pits had a hard bottom, whereas the other was softer. However, the difference in apparent strength may have been related to permafrost conditions rather than to infill. The sediment load of the overflow river water was noted to have been low, and the pits remained at least partially open after the water had drained. Infill of the scours was therefore not contemporaneous with formation. Reimnitz and Kempema (1983) suggested that scour pits in relatively unprotected areas of the Alaskan Beaufort Sea, in front of the Kuparuk and Sagavanirktok Rivers, are infilled within 2 to 3 years by bedload processes. No information is available to determine the lifespan of the Babbage River strudel scour pits.

#### ***5.7.6 The King Point Sediment Transport Experiment***

In the summer of 1985 (24 August to 16 September), a field program was carried out with the objective of obtaining field data which could be used to constrain estimates of sediment transport rates at King Point. The site was chosen primarily because of the strong interest at the time in King Point as the site for a potential harbour development. The field program was the first such program attempted in the Canadian Beaufort Sea region and consequently experienced numerous logistic and equipment difficulties. An additional problem was that Dobrocky Seatech Ltd, the prime contractor for preliminary data analysis, went into receivership before a final report could be prepared. Nevertheless, a useful set of profile, wind, wave, current and sediment data was collected. The following summary is based partly on the unfinished contract report prepared by R.D. Gillie and on later analysis (Hill, 1990; this study). A location map (Fig. 5.9) and the morphology and stratigraphy of the King Point region have been discussed previously (Sections 5.2.2 and 5.5.2).

#### ***Beach and Nearshore Profiles***

A detailed survey of the entire barrier system was carried out for both the beach and

nearshore zones. Three representative profiles are shown in Figure 5.20. At the narrow northwestern end of the beach, the profile is steep and concave with the slope decreasing monotonically from  $0.09^\circ$  in less than 2 m water depth to  $0.01^\circ$  beyond 7 m. Towards the southeast, the profiles show a break in slope at approximately 3 m water depth, below which the slope decreases to less than  $0.01^\circ$ . This gentler slope occurs at the southeastern end of the barrier, which is characterised in the backshore by accretional beach ridges.

### ***Bottom Sediment Grain Size***

Samples for grain size analysis were collected from four zones along the King Point beach: on the berm, on the beach face and in the nearshore zone at 20 m and 50 m offshore, corresponding to water depths of approximately 2 m and 3 m respectively. The locations of these samples are shown schematically in Figure 5.21. Representative grain size distribution curves for locations at the northwest, central and southeast parts of the beach are presented in Figure 5.22.

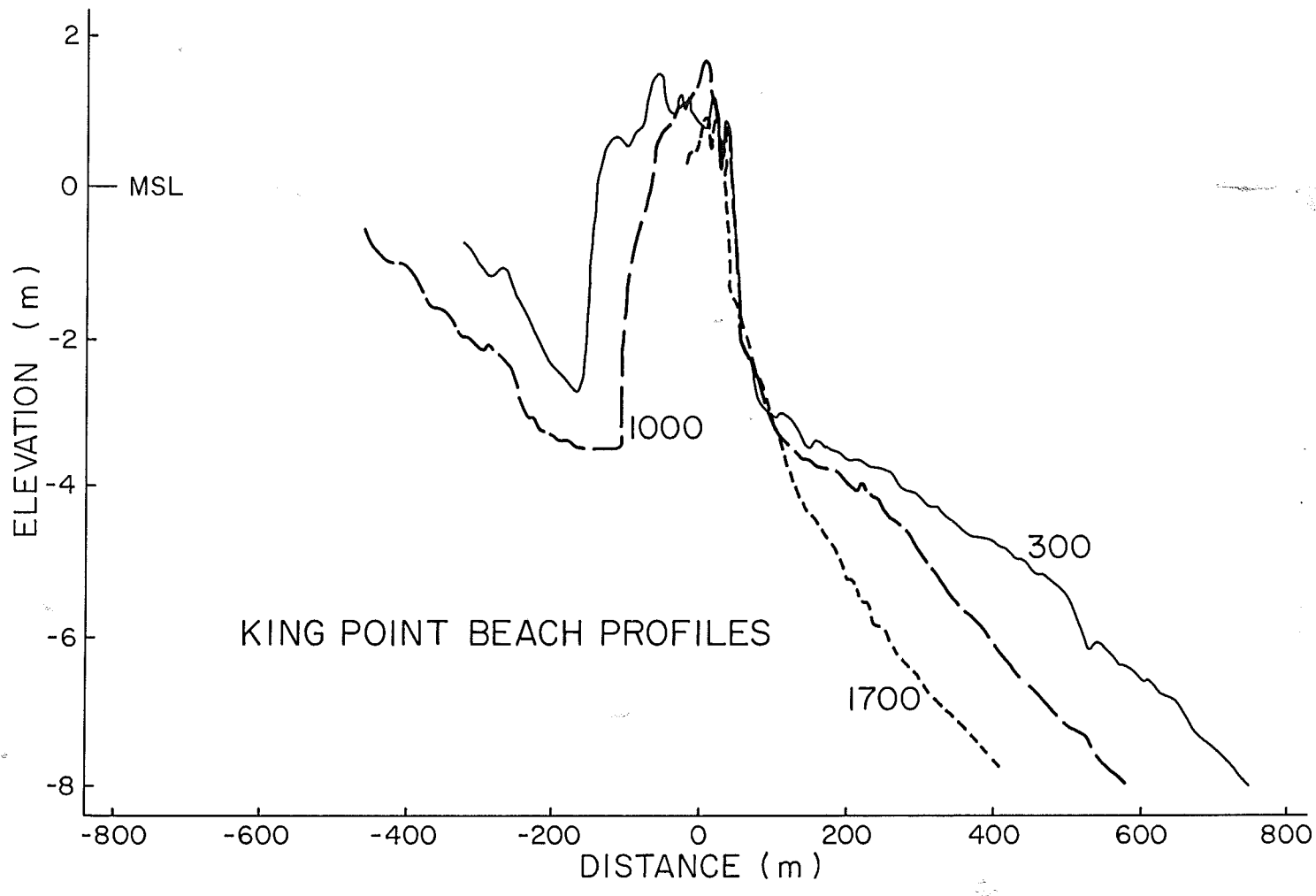
Two types of size distributions characterize berm sample (Fig. 5.22a), with no consistent trend along the beach. The most common type consists of gravel and coarse sand with a poorly sorted mode in the pebble size range (8-32 mm, Samples KP-33 and -43). The size of samples (generally 2-3 kg for gravel) was probably too small to adequately define the true mode of these sediments. The second type of size distribution found on the berm, more commonly towards the southeast, consisted of relatively well sorted granule-sized gravel (2-8 mm, e.g. Sample KP-23).

Beach face samples were quite variable in size distributions and generally show a bimodal, dominantly gravel size distribution, with modes in the pebble and coarse sand to granule ranges (Fig. 5.22b). Sandier samples show a weak third mode in the medium sand range. Although variable, some along-beach trends can be distinguished (Fig. 5.23). At the northwest end of the beach, the sand content increases gradually towards the southeast until the deflection point of the beach at the proximal end of the beach ridges. At this point, the sand fraction becomes almost negligible, before increasing again at the southeastern end of the beach.

In the nearshore zone, the proportion of gravel is significantly reduced, except for isolated samples consisting of almost 100% gravel which probably represent localised patches of gravel. Some samples also show a significant coarse tail (e.g. KP-84, Fig. 5.22d), probably indicating that the thickness of sand in the nearshore zone is minimal. The samples predominantly consist of well-sorted fine to medium sand with modes in the 0.1 to 0.3 mm range (Fig. 5.22c and d). The samples from 50 m offshore (approximately 3 m water depth) are consistently finer than the samples from 20 m offshore (2 m water depth).

### ***Wave Data***

Two Seadata wave and current meters were deployed in an effort to obtain directional wave



**Figure 5.20** Three representative beach profiles from King Point (for locations see Fig. 5.9).





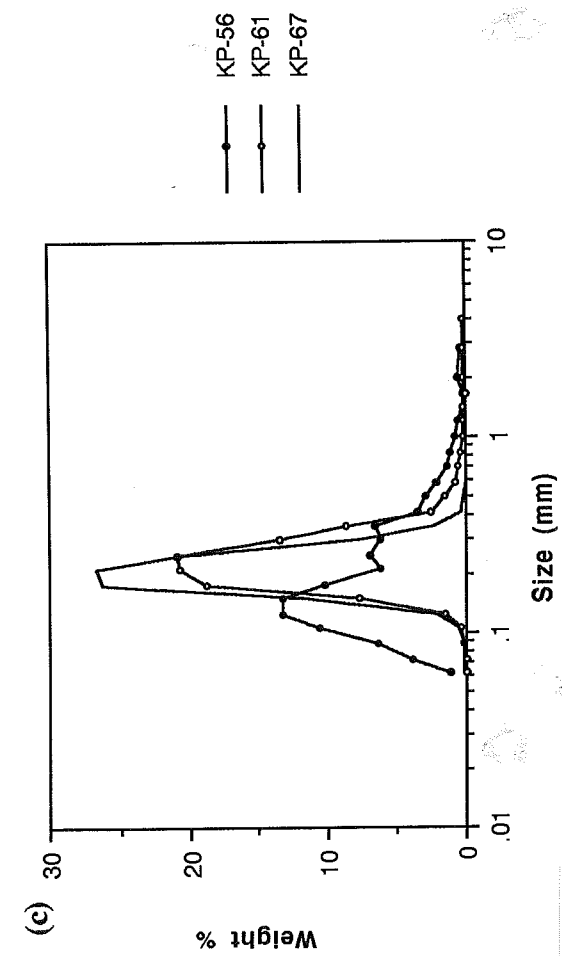
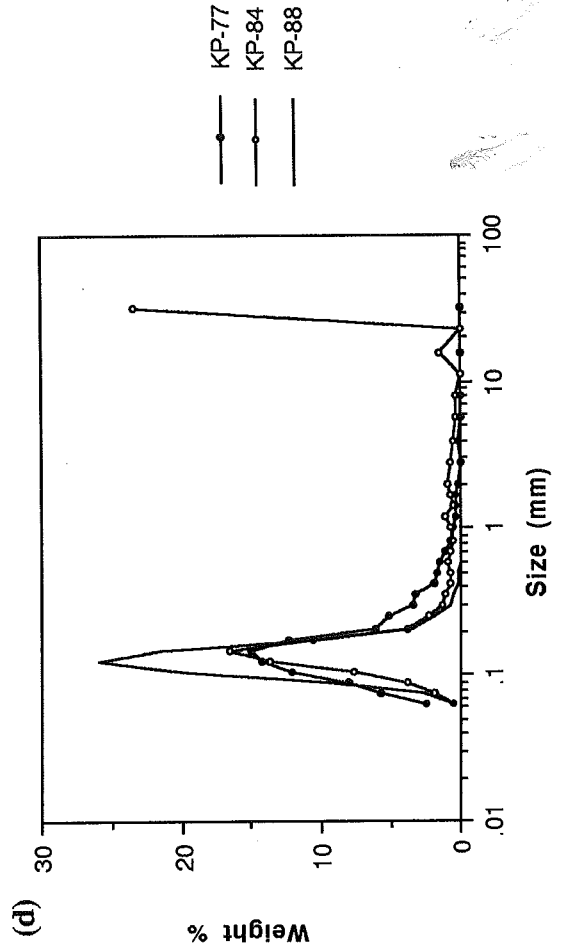
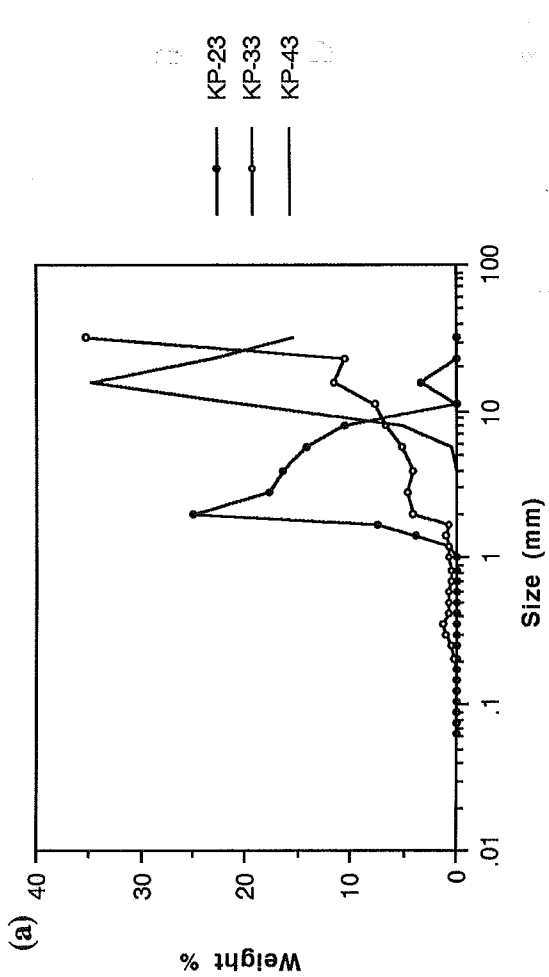
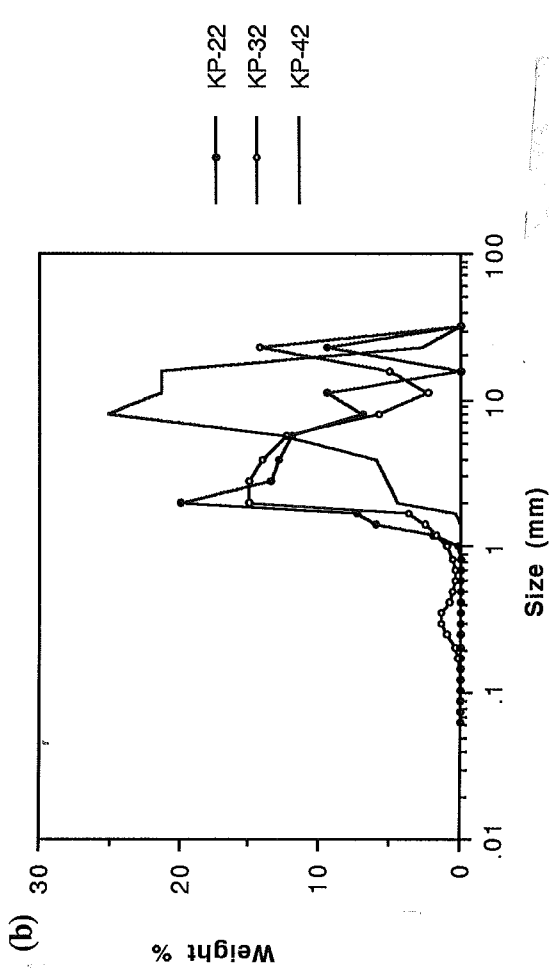
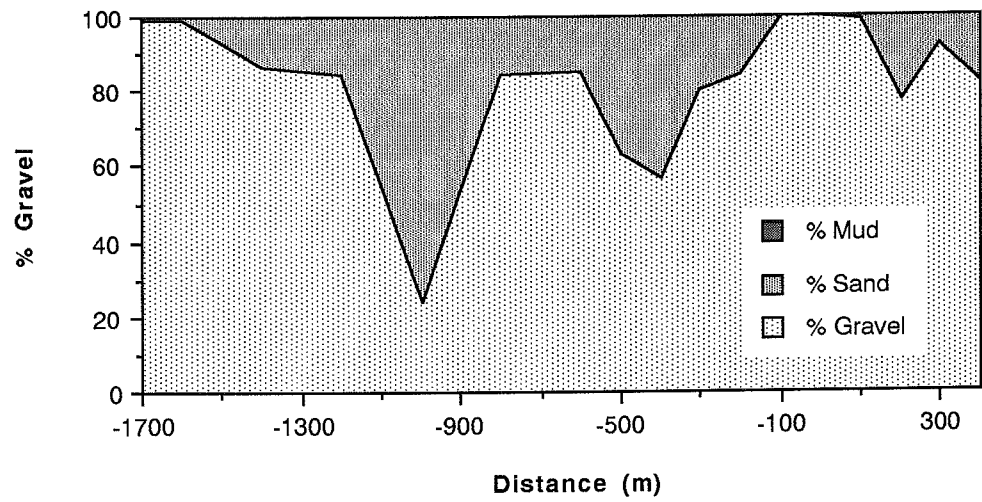


Figure 5.22 Grain size distributions from King Point: (a) berm spectra, (b) beach face, (c) nearshore zone at 20 m water depth, and (d) nearshore zone spectra at 50 m water depth.



**Figure 5.23** Alongshore changes in grain size of beach face sediments at King Point.

data. Problems were encountered with both meters so that directional data from both are suspect (for a detailed discussion of how this was determined, see Pinchin and Nairn, 1987). Reliable significant wave height data were obtained from the Seadata 635-12 meter and the time series record of these are shown in Figure 5.24. For the deployment period, the significant wave height did not exceed 0.8 m. Pinchin et al. (1985) predicted a 3.3 m significant wave height for a return period of 1 year from their hindcast model so that the measured waves do not appear to approach the extreme annual conditions at the King Point site. Nevertheless, several modest storm events are apparent from the wave data. The most important interval in terms of wave height occurred between August 2 and 4 when significant wave heights reaching almost 0.7 m were recorded. This interval has been studied in some detail by Pinchin and Nairn (1987) in an attempt to reconcile wave hindcast results with the actual field data.

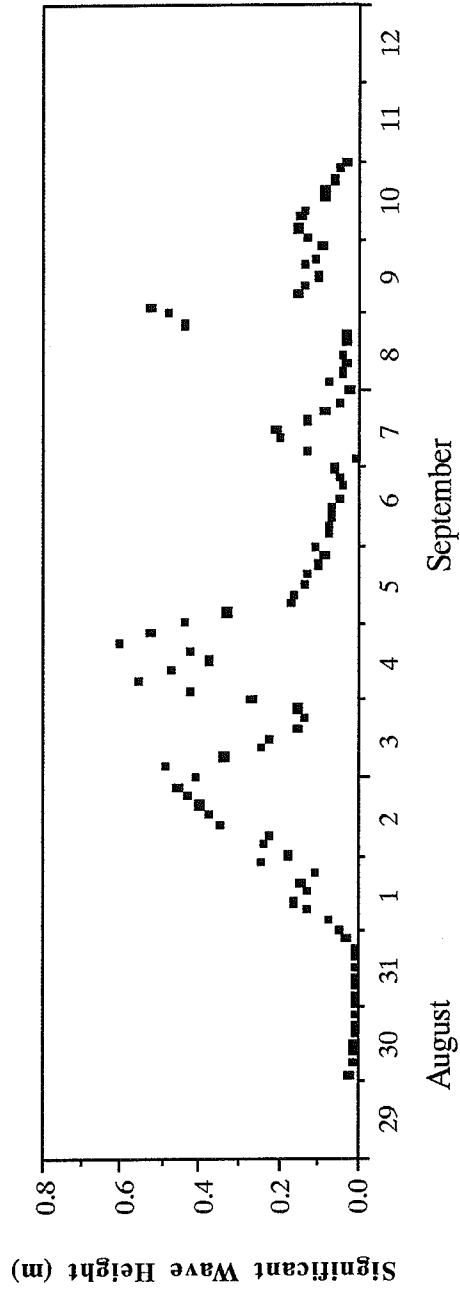
The wave data shows that waves at King Point built gradually during September 1 and 2 to a significant wave height of approximately 0.5 m, while winds at the site were moderate to weak. The wind direction fluctuated markedly over this time. Wave heights decreased again on September 3 before increasing rapidly to almost 0.7 m on September 4 under moderate (36 km/h) northwesterly winds. The wave heights decreased rapidly to less than 0.2 m by September 5.

Pinchin and Nairn discovered that despite the fact that offshore waves may be best predicted using winds from the offshore drill site, due north of King Point, a wave hindcast for the September 4 event based on these winds produced poor results when compared to the measured waves at King Point (Fig. 5.25a). The only acceptable results were obtained when the winds measured at King Point itself were used in the hindcast (Fig. 5.25b). The reason for this is that the center of the low pressure system from which the wind field developed passed directly along the coast generating east winds offshore, but southeast through southwest winds along the coastline. The winds generating the observed waves at King Point probably came from a direction between these, but closer to the wind direction measured at the beach.

The prediction of wave conditions at King Point is therefore a complex problem. Storm trajectories similar to the one discussed above are common (Burns 1973), although according to Hodgins and Harry (1982), the more extreme storms pass more commonly to the north of the coastline. The latter condition would provide a more uniform wind field for the area and a hindcast using offshore or regional winds would likely be more successful. Nevertheless, this field test of the wave hindcast approach served to highlight the complexities involved and to emphasize that care should be taken when using hindcast results, particularly in the further step of predicting sediment transport rates.

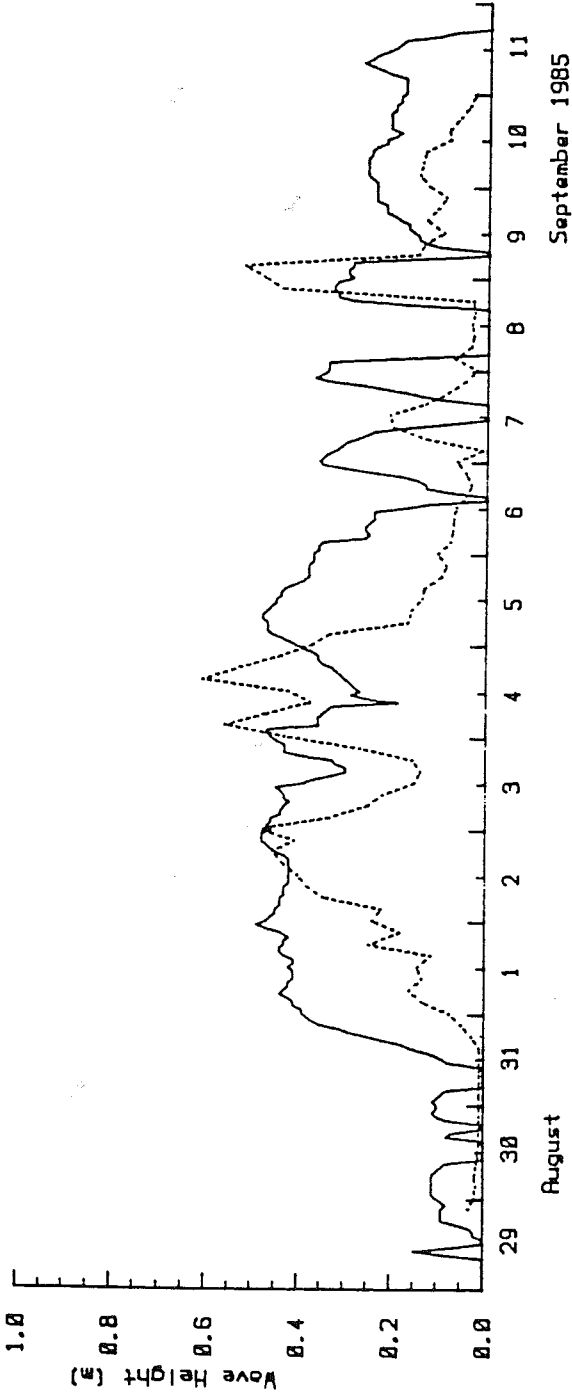
### *Currents*

The current records at King Point have already been discussed within the regional context



**Figure 5.24** Wave height and wave period data recorded from Seadata meter 635-12 at King Point for August and September, 1985.

Significant Wave Height



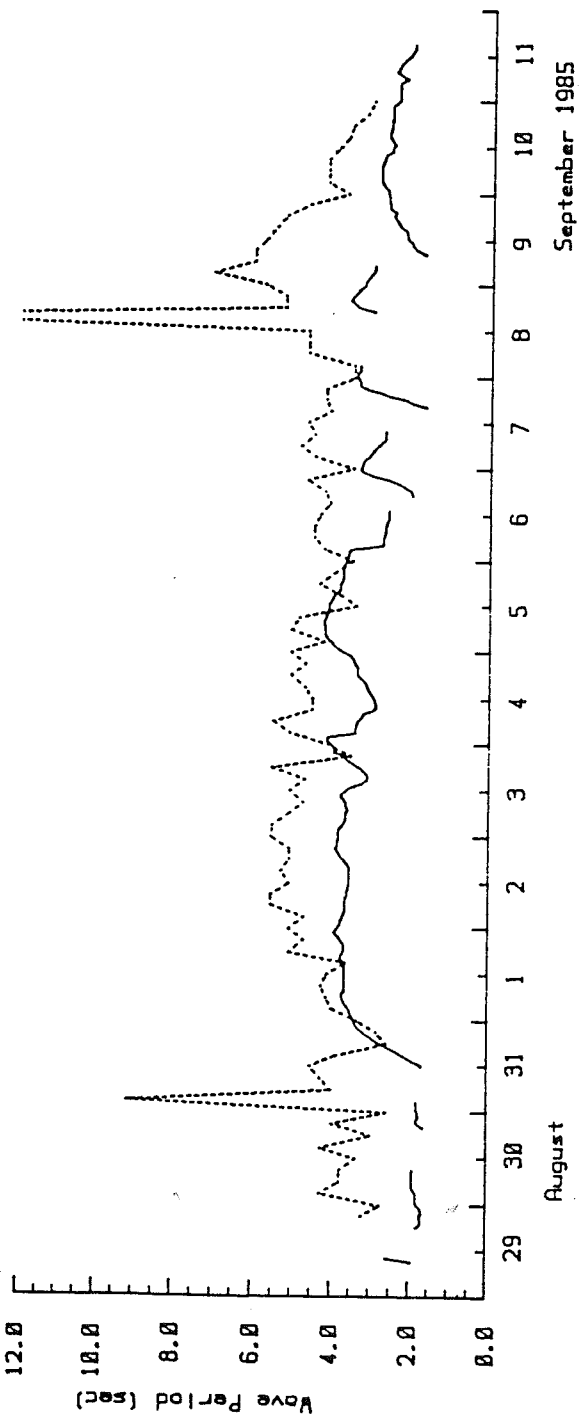
KEY

- (a) — Hindcast
- - - Measured
- (b) — Hindcast
- - - Measured

Hindcast KN-03

Explorer 3 winds  
height cor. x 0.8

Peak Wave Period

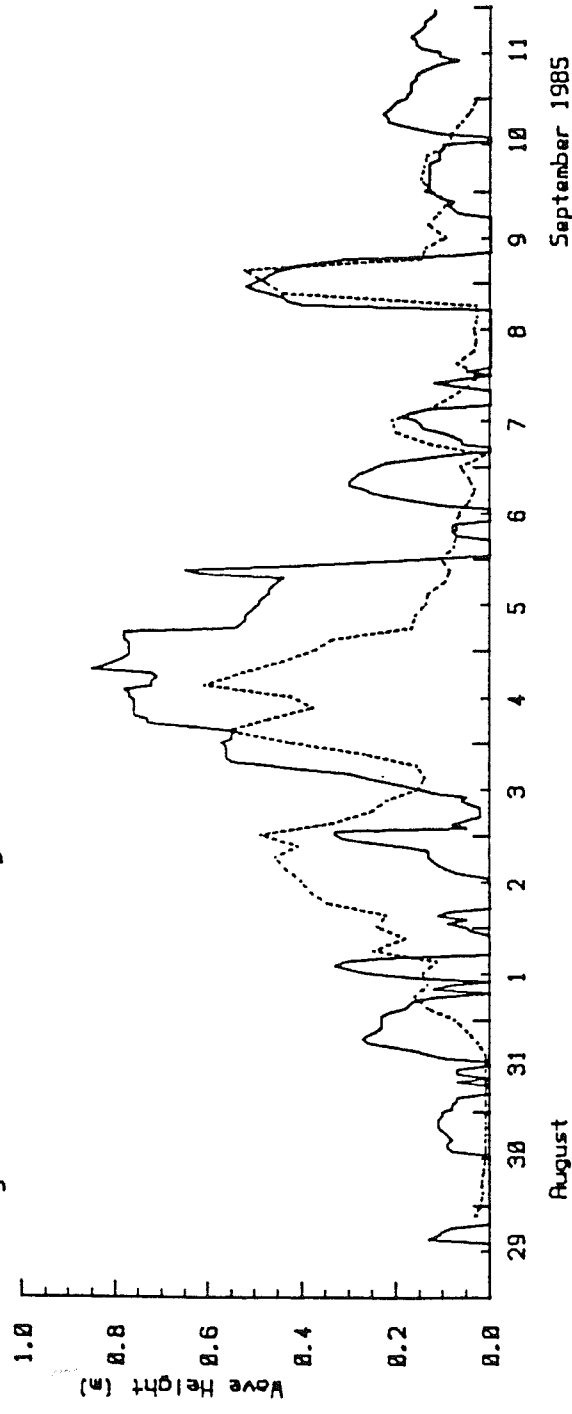


Donelan fetches

$T_p/T_s=1.15$

Figure 5.25 Results of the hindcast and field data comparison (a) using offshore winds measured at the Explorer III site; and (b) using winds measured at King Point.

Significant Wave Height



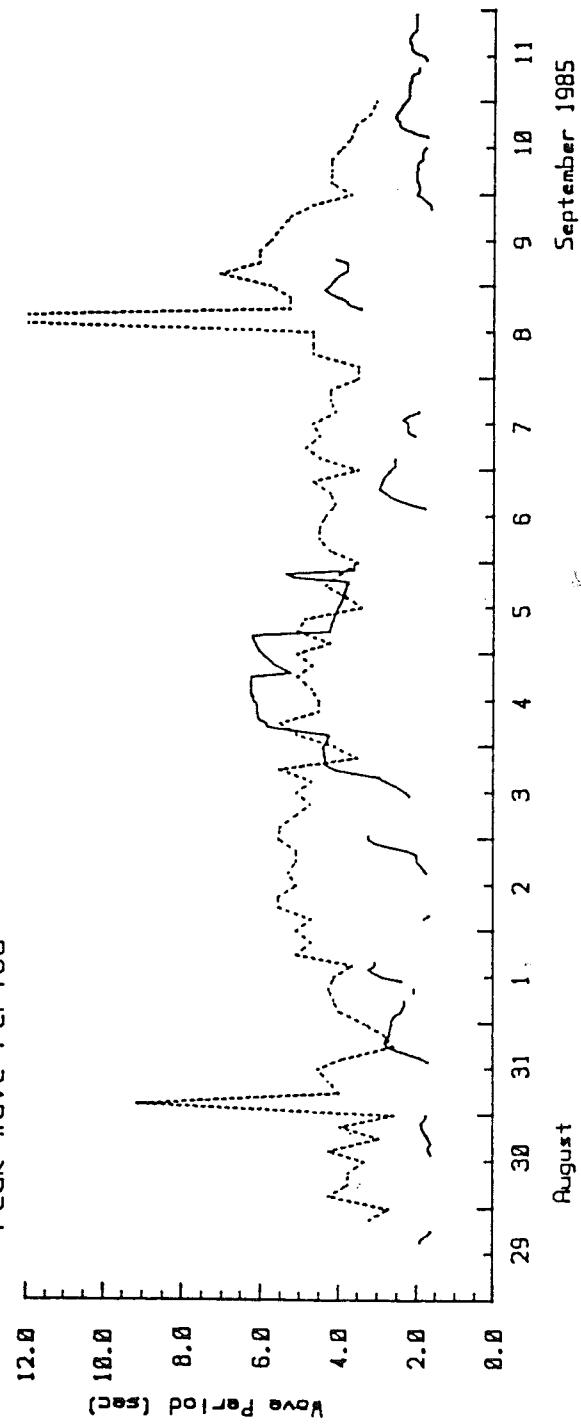
KEY

- (a) — Hindcast  
      ..... Measured
- (b) — Hindcast  
      ..... Measured

Hindcast KN-05

King Point winds

Peak Wave Period



straight fetches

$T_p/T_s=1.15$

(b)

of the Yukon Shelf (Section 5.7.2). The strong event of September 4 (Fig. 5.18) corresponds to the period of relatively high wave conditions. However, the low wave heights and mooring depth of the current meters are such that the current was measured well out of the surf zone and cannot be considered a wave-generated longshore current. Nevertheless, the peak current speed is high enough to produce significant sediment transport. In fact, the seabed between 5 and 15 m water depth appears to be swept bare of modern sediment (Fig. 5.12). As waves are very rarely large enough to cause significant oscillatory motions at this water depth, it seems likely that it is the presence of strong coastal currents in this region of the nearshore that prevents accumulation of suspended sediment from the Mackenzie plume.

### *Interpretation of Sediment Transport*

Various methods have been used to estimate the direction and rate of sediment transport in the King Point barrier system. McLaren (1986) used a statistical method based on bottom sample grain size trends to infer sediment transport directions on the beach and nearshore of the King Point barrier (the method is described in McLaren and Bowles, 1985). He determined that sediment transport was directed strongly southeastward in the beachface samples, but northwestwards for samples collected 20 and 50 m off the shoreline. Trends determined by McLaren at first seem unlikely as they indicate a strong reversal in transport direction within a short distance of the beach. However, due to the asymmetry of the beach, the samples used by McLaren for the two nearshore analyses may include a component of shore-normal transport. The trends might therefore be interpreted as transport towards shallower depths i.e. shoreward directed, which is compatible with the overall transgressive trend of the barrier system.

Based on the results of the 14-year hindcast of waves at King Point, Pinchin et al. (1985) estimated net potential sediment transport of  $10^4$  m<sup>3</sup>/a towards the southeast at the northwest end of the barrier and approximately  $3 \times 10^3$  m<sup>3</sup>/a towards the northwest at the southeastern end of the barrier. The limitations of the hindcast method previously discussed should be borne in mind when considering these values. Based on the volume of accreted beach sediment estimated from aerial photographs and the detailed survey of the barrier, approximately  $10^5$  m<sup>3</sup>/a of sediment was supplied to the barrier between 1954 and 1985. As the seabed is bare of modern sediment below 5 m water depth, it can be assumed that this sediment has not been supplied from offshore and must therefore have been provided by longshore transport. The Pinchin et al. (1985) estimates of longshore transport rates therefore appear to be an order of magnitude too low.



## 6. MACKENZIE DELTA: SHALLOW BAY TO GARRY ISLAND

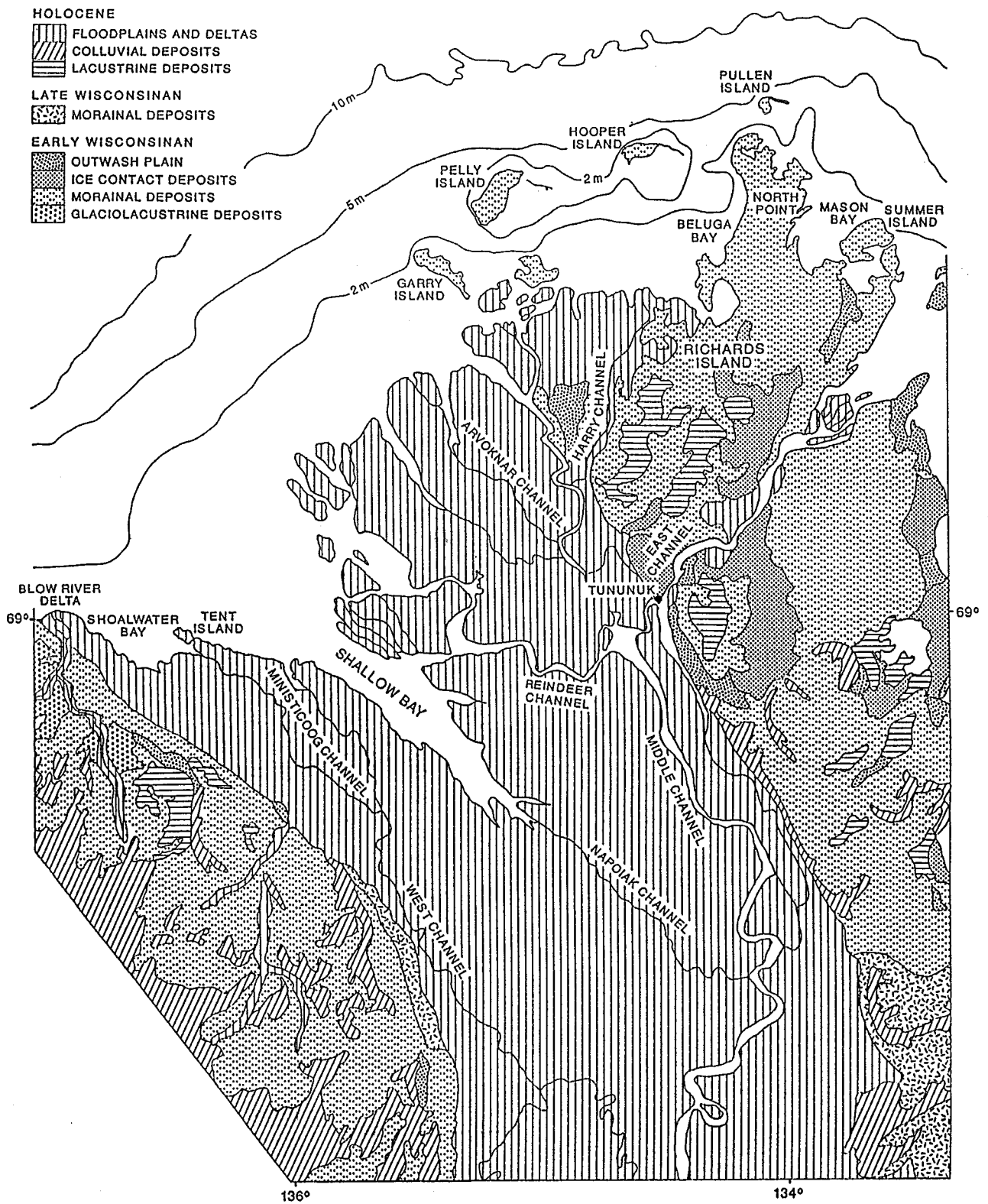
This section deals with the modern Mackenzie Delta coast, stretching between the Blow River Delta and Richards Island (Fig. 6.1). The western half of Richards Island is morphologically part of the Mackenzie Delta, being fed by a distributary channel known as Harry Channel. However, the offshore islands north of this section of the delta (Garry, Pelly and Hooper Islands) have higher elevations and stratigraphy more related to eastern Richards Island, and are therefore discussed in section 7. The coastal region discussed in this section includes Shoalwater Bay, Shallow Bay, the Olivier Islands and Ellice Island.

Two major reports prepared for the Water Resources Branch of the Inland Waters Directorate, Environment Canada contain a large amount of information on the Mackenzie Delta. Lewis (1988) summarises many years of study of the delta's sedimentary environments and processes, while Hirst et al. (1988) present an ecosystem evaluation which includes hydrologic and biological components. The latter report synthesises a large data set on the delta which was collected by B.C. Hydro during the evaluation of the impacts associated with a potential hydro dam development along the Liard River. An M.Sc. thesis completed by Jenner (1989) presents recent process and sedimentological interpretations in the distributary mouth area of the Olivier Islands. The work of Marsh and co-workers (Marsh and Bigras, 1988; Marsh and Hey, 1988; Marsh and Ferguson, 1988) on delta lake hydrology is also relevant to this study.

### 6.1 Quaternary Geology

The modern Mackenzie Delta has partially infilled a deep flat-bottomed trough, whose seaward expression is Mackenzie Trough and which links inland with the Mackenzie Valley. Shearer (1971) interpreted the valley as being glacial in origin. Seismic data in Mackenzie Trough clearly shows that the trough is erosional in nature (O'Connor, 1985; Fehr, 1987) and it therefore appears likely that glacial ice at some time extended across the shelf in the vicinity of the present-day trough, probably in the form of an ice tongue. The age of this erosional event is constrained by tentative correlation with the seismic stratigraphy on either side of the trough (Blasco et al., in press) to be early Wisconsinan or older. If early Wisconsinan in age, the erosion may have been related to the Buckland glaciation (Rampton, 1982).

Within the trough-fill sequence, a second unconformity may be evidence for a re-occupation of the trough by glacial ice. Blasco et al. (in press) suggest that this advance may have occurred in the middle Wisconsinan, based on the relative sea-level reconstruction of Hill et al. (1985) which required the presence of middle Wisconsinan ice. This interpretation is not supported by the earlier stratigraphic interpretations of Rampton (1982; 1988) in which there was no ice advance between the early Wisconsinan (Buckland) and the late Wisconsinan (Tutsieta Lake)



**Figure 6.1** Location map of the modern Mackenzie Delta coast stretching between the Blow River Delta and Richards Island.

glaciations. The Tutsieta Lake limit does not extend beyond Tununuk in the Mackenzie Delta region (Hughes, 1987). However, as discussed in Chapter 2, there is sufficient uncertainty concerning Wisconsinan events, that this discrepancy cannot be resolved at present.

The Holocene Mackenzie Delta has built out and infilled the trough from approximately the location of Point Separation (Fig. 2.4). The thickness of these Holocene deposits in the subaerial delta is not known, except at one location, 8 km southwest of Inuvik, where Holocene sediments are at least 30 m thick (based on a radiocarbon date of 6900 years B.P.; Johnston and Brown, 1965) and probably extend to a pebbly silty clay (possible late Wisconsinan till?) at 58 m below present sea-level (Lewis, 1988). Offshore, the Holocene delta overlies a flat-lying delta top of probable late Wisconsinan age at approximately 75 - 80 m below present sea-level (for discussion see section 6.4).

Knowledge of the nature and distribution of ground ice in the delta is very poor. The total thickness of permafrost is less than 200 m in the lower delta (Judge, 1986). In boreholes near Inuvik, ice lenses in sand units were reported to sub-bottom depths of 60 m (Johnston and Brown, 1965). Working in the Olivier Islands, Jenner (1989) documented an active layer thickness of 1.25 m in August 1987. Acoustic permafrost is not present in Holocene or late Wisconsinan deposits seaward of the modern delta (see section 6.4).

## **6.2 Coastal and Inner Shelf Morphology**

On the western side of Shallow Bay, Mackenzie Delta sediments merge with deposits of the Blow River Delta. The coastline around the Blow River is characterised by extensive intertidal flats. Elsewhere along this section of the coast, low coastal bluffs, less than 1 m high are present. A few small channels that drain thermokarst lakes reach the coast northwest of Shoalwater Bay, but no major Mackenzie distributary channels extend this far. Shoalwater Bay forms a broad embayment between Tent Island and Whitefish Station. The bay appears to be related to a shallow but prominent submarine valley (the 2 m isobath is deflected more than 10 km shoreward) located just offshore. Distributary channels, originating from West Channel, discharge into Shoalwater Bay, the largest being Ministicooog Channel.

Tent Island separates Shoalwater Bay from Shallow Bay, a deep funnel-shaped estuary which extends nearly 70 km inland and divides the Mackenzie Delta into eastern and western halves. Napoiak Channel discharges into the head of Shallow Bay, and a broad submarine channel, up to 8 m deep but apparently infilled in its upper reach, is present along the western margin of the bay. The coastline of Shallow Bay consists almost exclusively of intertidal flats with numerous distributary channels, including the major distributaries of West Channel and Reindeer Channel, discharging into the bay. Reindeer Channel splits into three major distributaries, two of which discharge into Shallow Bay and are separated by a number of unnamed islands. The more

southerly channel of these two extends 5 km into Shallow Bay as a submarine channel, possibly linking with the larger submarine channel of the bay. At the mouth of the more northerly channel, which is continuous with the main Reindeer Channel, two submarine channels extend up to 3 km offshore and several emergent distributary mouth bars have formed. The head of the bay is extremely shallow, consisting of a mosaic of intertidal bars separated by meandering tidal channels.

North of Shallow Bay, a group of islands known as the Olivier Islands (Oliver on some hydrographic charts) forms a discontinuous coastline between the major Reindeer Channel distributary and a third, now partially disconnected channel which runs along the western side of Ellice Island. The subaerial Olivier Islands are separated from each other by shallow channels with no obvious link to the larger distributaries and by intertidal flats which join several of the islands at low water stages. The islands are also separated from the mainland by a broad almost enclosed bay which is largely filled by a wide intertidal flat. The seaward coastlines of the higher elevation islands are characterised by low erosional bluffs.

East of the Olivier Islands, the delta coast is more continuous, with large "islands" such as Ellice Island separated by broad funnel-shaped channel mouths, including Arvoknar and Middle Channels. The islands are fronted by narrow intertidal flats. At the eastern side of this area, a submarine channel, originating from a distributary of Middle Channel, extends offshore just to the east of Garry Island.

Seaward of the delta, the inner shelf slopes very gently at approximately  $0.015^\circ$  to the 10 m isobath (Fig. 6.1). The 2 m isobath is found 15 km from the coast, and much of the area inside the 1 m isobath is uncharted and largely un-navigable. Profiles across the inner shelf show the bottom slope increasing gradually from 2 m to 10 m water depth, then more steeply below 10 m. The inner shelf forms a submarine delta platform

### **6.3 Rates of Coastline Change**

Compared to the Yukon coast, there has not been a history of coastal retreat measurements in the Mackenzie Delta. Historical accounts of Franklin and others do not provide reliable information on the coastal configuration of the delta. Aerial photograph comparison (Harper et al. (1985) therefore provides the most reliable information on coastline change. However, it should be pointed out that in an area of such low relief and extensive intertidal flats, large changes in coastal configuration can result from small changes in water level. There is no indication in the report of Harper et al. (1985) that this was taken into account in estimates of coastal retreat. A review of the tabulated data in the report indicates that most of the measurements were made to the water-line rather than to cliff top or base. Considerable error may therefore be associated with these measurements.

The measurements of Harper et al. (1985) suggest that the coastline of the Mackenzie Delta is retreating more rapidly than any other sections of the Beaufort Sea coast. Retreat of the Tent Island and Shoalwater Bay coast and the west coast of Shallow Bay is extreme, averaging 6.1 m/a. Individual values as high as 29 m/a are reported by Harper et al. (1985). High rates of erosion at Tent Island are confirmed by the necessary relocation of the Navigation Aid tower on the island in 1986, as the previous tower had fallen into the sea. Retreat rates east of Shallow Bay are less extreme, but still higher than other areas of the Beaufort Sea coast, averaging 2.1 m/a.

Locally, however, there is evidence for limited progradation of the delta, in the form of emergent distributary mouth bars and intertidal flats. Jenner (1989) has studied the area of the Olivier Islands in detail and has reconstructed the development of the area since 1948 (Fig. 6.2). Over this 40 year period, substantial growth of intertidal bars has occurred, both at the coastline and in the broad bay behind the coastal islands. Large areas of the bars have become emergent and vegetated since 1943. Nevertheless, the seaward coastlines of the more elevated islands in the region were observed by Jenner to have experienced erosion during storms.

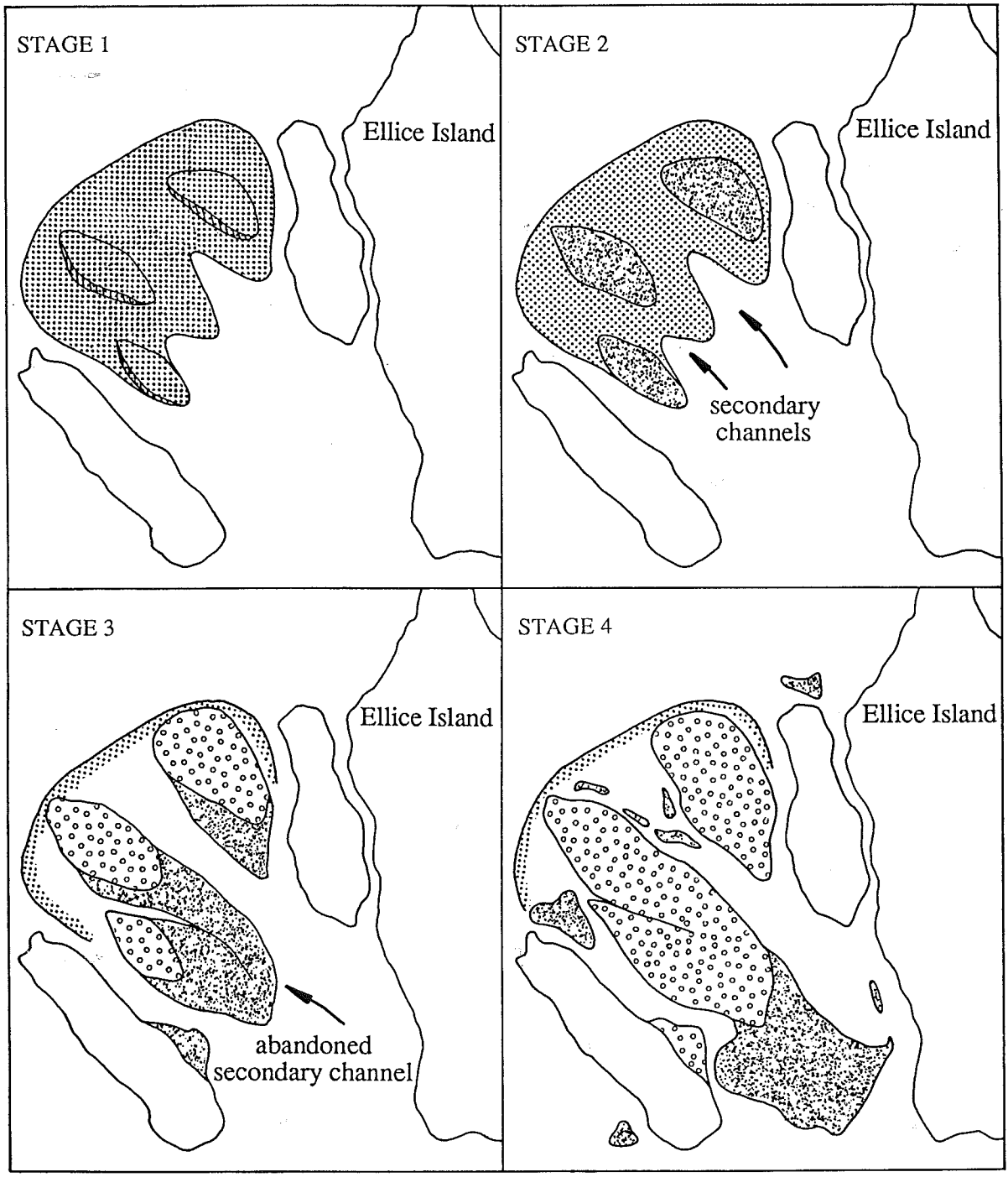
In summary, there is some question concerning the accuracy of coastal retreat measurements made in the delta using coastline positions from aerial photographs due to the effect of water level changes in such a low-lying area. These measurements indicate very high rates of retreat, yet locally delta progradation or accretion can be documented. The delta coast consists of both older, delta surfaces which form 1 - 1.5 m high bluffs at the coastline, and active very low-lying areas with extensive intertidal flats. The general trend appears to be retreat of the older delta surface together with shoreward reworking of active channel mouth areas (Jenner, 1989).

## **6.4 Seismic Stratigraphy**

In this section a discussion of the seismic stratigraphy of the delta seaward of the 2 m isobath is presented. This discussion deals with profiles extending some distance offshore, outside of the coastal zone. This is done to place the coastal stratigraphy into the broader context of the Mackenzie Trough stratigraphy of which it is a part.

### **6.4.1 Pre-delta Stratigraphy**

Regional seismic interpretation has revealed the presence of an infilled trough lying seaward of the modern Mackenzie Delta (Fig. 6.3) (Shearer, 1971, 1972; O'Connor, 1985; Lewis and Meagher, 1987; Blasco et al. 1989). The trough is approximately 75 km wide, more than 130 km long and on average 300 m deep. The basal part of the trough infill sequence is complex and consists of several seismic units capped by a hummocky regional reflector (top of unit MT2; Fig. 6.3). The present study deals primarily with the stratigraphy above this reflector, within unit MT1 of O'Connor, 1984).



LEGEND


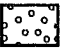

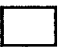
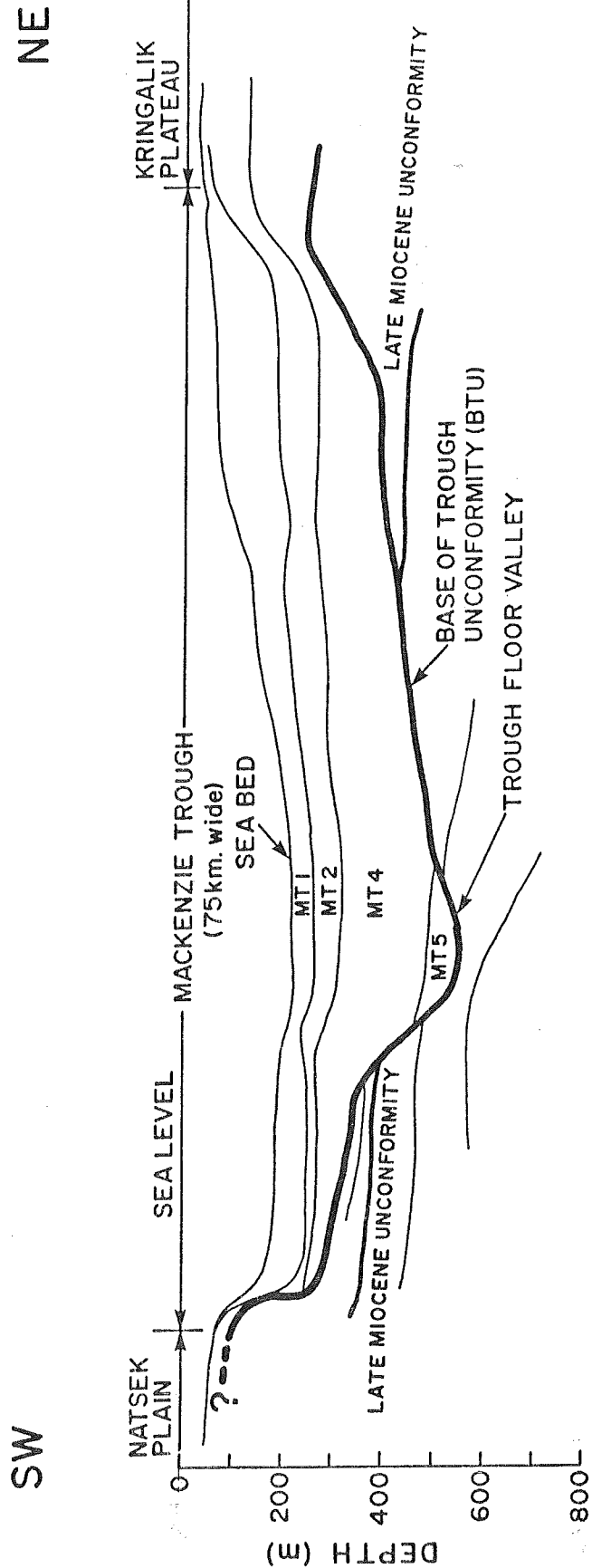
- |   |                   |   |                            |
|---|-------------------|---|----------------------------|
|  | subaqueous bar    |  | subaerial vegetated island |
|  | emergent sand bar |  | older island               |

Figure 6.2 The development of the Olivier Islands from pre-1943 to 1987 (Jenner, 1989).



SCHMATIC EAST-WEST (NE-SW) CROSS-SECTION OF MACKENZIE TROUGH  
AT APPROXIMATELY 70° NORTH

Figure 6.3 Schematic cross-section through the Mackenzie Trough (Blasco et al. 1989).

### **6.4.2 Late Wisconsinan Delta**

The late Wisconsinan delta is recognised as a thick depositional sequence (in the sense of Mitchum and others, 1977) which downlaps onto the regional reflector at the top of unit MT2 (Fig. 6.4). Long clinoform reflectors show progradation from south to north. The sequence is approximately 50 m thick in the south but thickens to a maximum of 100 m in mid trough, filling a depression in the surface of unit MT2.

At the top of the sequence, the clinoform reflectors are erosionally truncated by channels with dimensions of several hundred of kilometres width and up to 10 m depth. In the north-south oriented air gun profile of Figure 6.4, the channels are poorly resolved, but in the higher resolution boomer profiles with east-west orientations, the channels can be seen to have flat bases and a complex stratified fill (Fig. 6.5). Channel-fill reflectors commonly occur as sets of oblique prograding clinoforms, interrupted by younger channel-margin erosion surfaces. This pattern indicates lateral accretion and sedimentation in active channels.

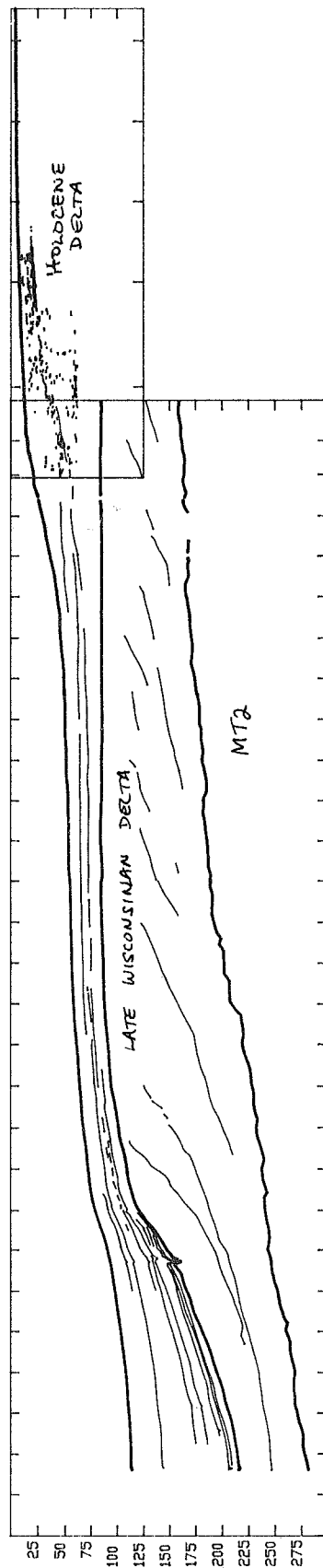
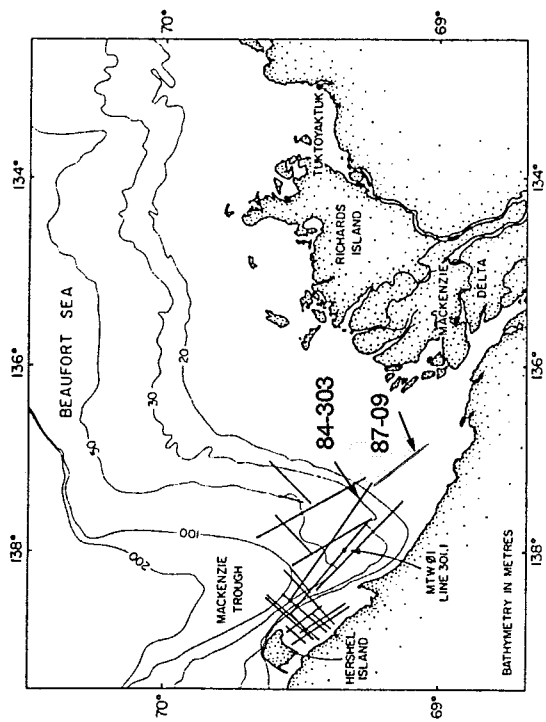
The delta top is seen in air-gun profiles as a strong, continuous reflector (Fig. 6.4). In the southern part of the trough, the surface is near-horizontal, with an elevation of approximately 60 - 70 m below present sea level, but to the north, it dips to approximately 90 m below sea-level. The most significant break in slope along the delta surface occurs at approximately 75 m below sea-level. Beyond this hinge-line, the delta surface reflector rapidly loses amplitude and ultimately becomes conformable with the basal clinoform reflectors. In the shallow-water, high-resolution boomer profiles, the delta surface reflector is more broken up but can be traced more or less continuously across the trough and clearly truncates underlying channel-fill reflectors (Fig. 6.5).

The position of the delta front has been mapped by Blasco et al. (1989). At its maximum, it extended into the trough approximately 90 km beyond the present delta front. A conservative estimate of the sediment mass represented by this portion of the delta is  $2.6 \times 10^{11}$  tonnes, which is 2000 times the estimated annual sediment load of the Mackenzie River. As sediment supply during deglaciation was likely comparable or higher than modern supply, it is likely that this delta built out very rapidly in the space of a few thousand years.

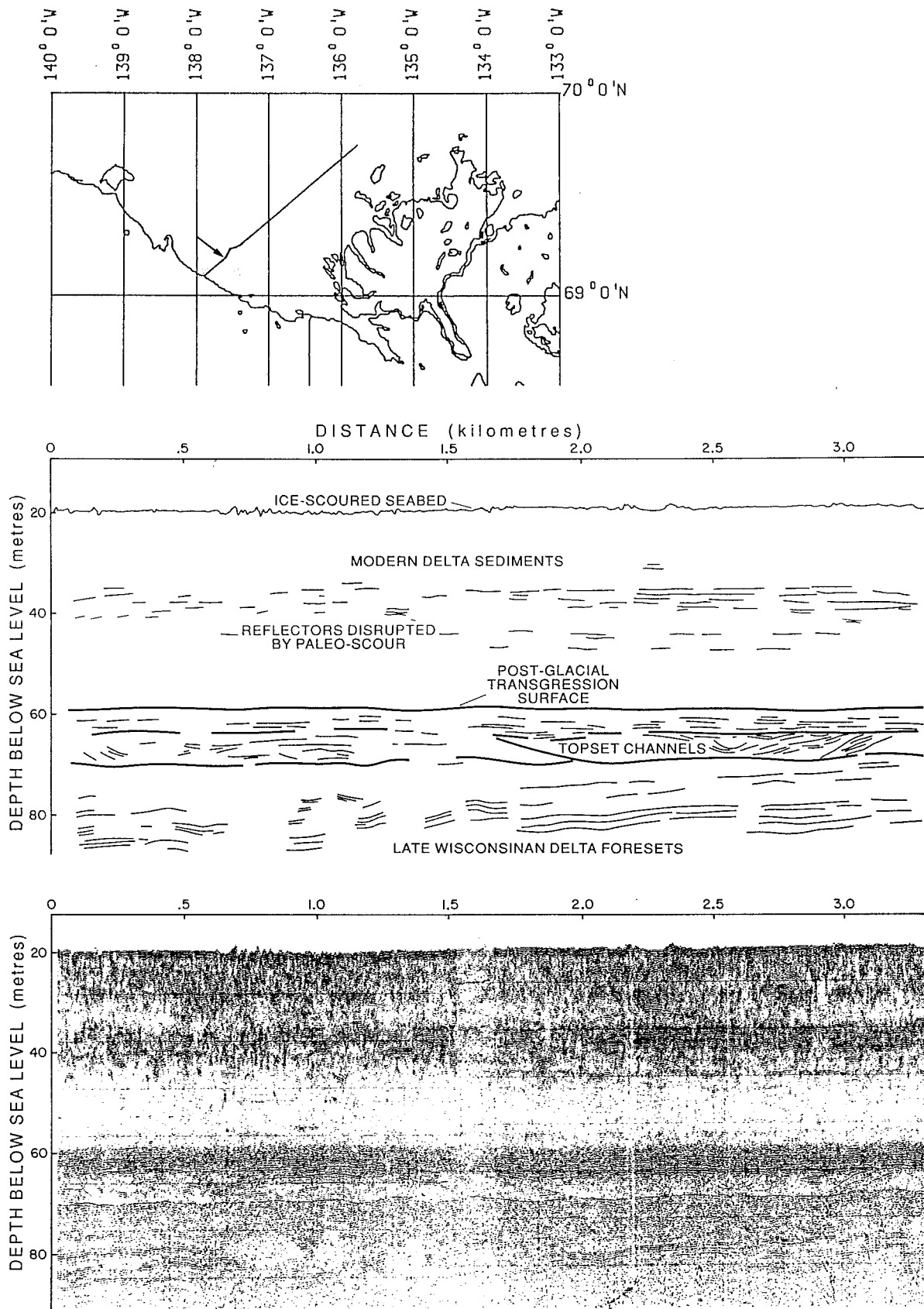
### **6.4.3 Post-glacial Transgression**

Several reflectors onlap against the steep clinoforms of the delta sequence in deep water (Fig. 6.4). Although it is impossible to identify onlap along the flat delta surface, the transgressive sequence probably extends into shallow water as a conformable stratified sequence. The basal transgressive surface cannot be identified as a single reflector over the entire area. Two distinct reflectors can be distinguished at the delta top in some seismic records (Fig. 6.6). The same reflectors can also be seen in the high resolution profiles as a set of semi-coherent reflectors lying immediately above the erosion surface (Fig. 6.5). It is not clear whether these reflectors represent

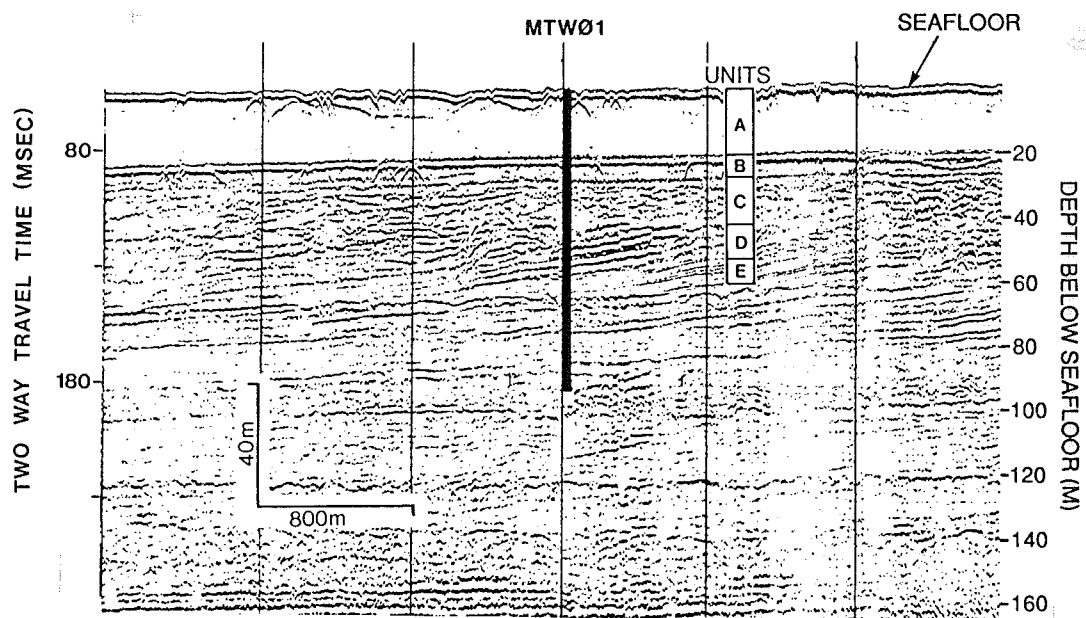




**Figure 6.4** Air gun profile of the late Wisconsin delta sequence, MT1, downlapping onto the regional reflector MT2.



**Figure 6.5** Boomer profile 87-06C, with east-west orientation, showing the channels at the top of the late Wisconsinan sequence. The channels display flat bases and are comprised of complex stratified fill.



**Figure 6.6** Air gun profile showing two distinct reflectors at the top of the MT1 delta sequence (from Moran et al., 1989). See Figure 6.9 for location.

the top of the delta sequence or part of the transgressive sequence overlying it. Moran and others (1989) recognised a distinct sedimentologic unit at this level in the MTW01 borehole. Some beds in this unit contain foraminifera indicating a marine environment of deposition. The interval is best interpreted as a marginal marine sequence (possibly reworked delta coast deposits) related to the early part of transgression. The strong reflector which in many parts of the area is used to define the top of the delta sequence may be more strictly interpreted as the top of reworked transgressive coastal deposits.

#### **6.4.4 Holocene Delta**

In the region between 5 and 10 m water depth, the seabed profile steepens significantly and it can be seen that a wedge-shaped depositional unit is present above the top of the late Wisconsinan delta. Stratification within this wedge is very discontinuous except for a strong hummocky reflector at 8 to 12 m below seabed in water depths between 5 and 6 m (Fig. 6.7). The surface of this reflector shows relief of up to 2 m and becomes more discontinuous in a seaward direction. It can be traced seaward as a zone of lower amplitude reflectors which have an overall clinoform profile (Fig. 6.4). Penetration below this reflector is very limited suggesting the presence of shallow gas at or just below the reflector. Inshore of the 5 m isobath, shallow gas is present just below the seabed and completely masks the lower section.

This sequence represents the modern Mackenzie Delta. It is possible that the strong reflector described above may represent a former subaerial delta plain, marking a maximum position of the subaerial delta. The hummocky surface may have resulted from frost-heaving and the development of shallow permafrost during subaerial exposure. This interpretation would be compatible with the presence of shallow gas which is commonly generated in shallow ponds and abandoned channels. Gas-bubbles have been observed in sediments in the modern subaerial delta (K. Jenner, personal communication, 1987). Apart from the presence of gas, the form of the reflector is similar to the delta top reflector in the late Wisconsinan delta (Fig. 6.4). However, as there have been no boreholes drilled through this part of the delta, it is not possible to rule out the alternative interpretation that the gas is simply enhancing a sedimentary layer with no particular significance.

### **6.5 Lithostratigraphy and Sedimentology**

A composite section of the Mackenzie Delta, compiled from the work of C.P. Lewis (based on numerous sources) and the seismic data described above, is shown in Figure 6.8. At this scale, the large volume of sediment tied up in the Holocene Mackenzie delta can be seen. The late Wisconsinan delta probably underlies the Holocene delta, at least as far as Inuvik. Older trough-fill deposits are seen only on seismic profiles offshore, but are likely to cover the base of the

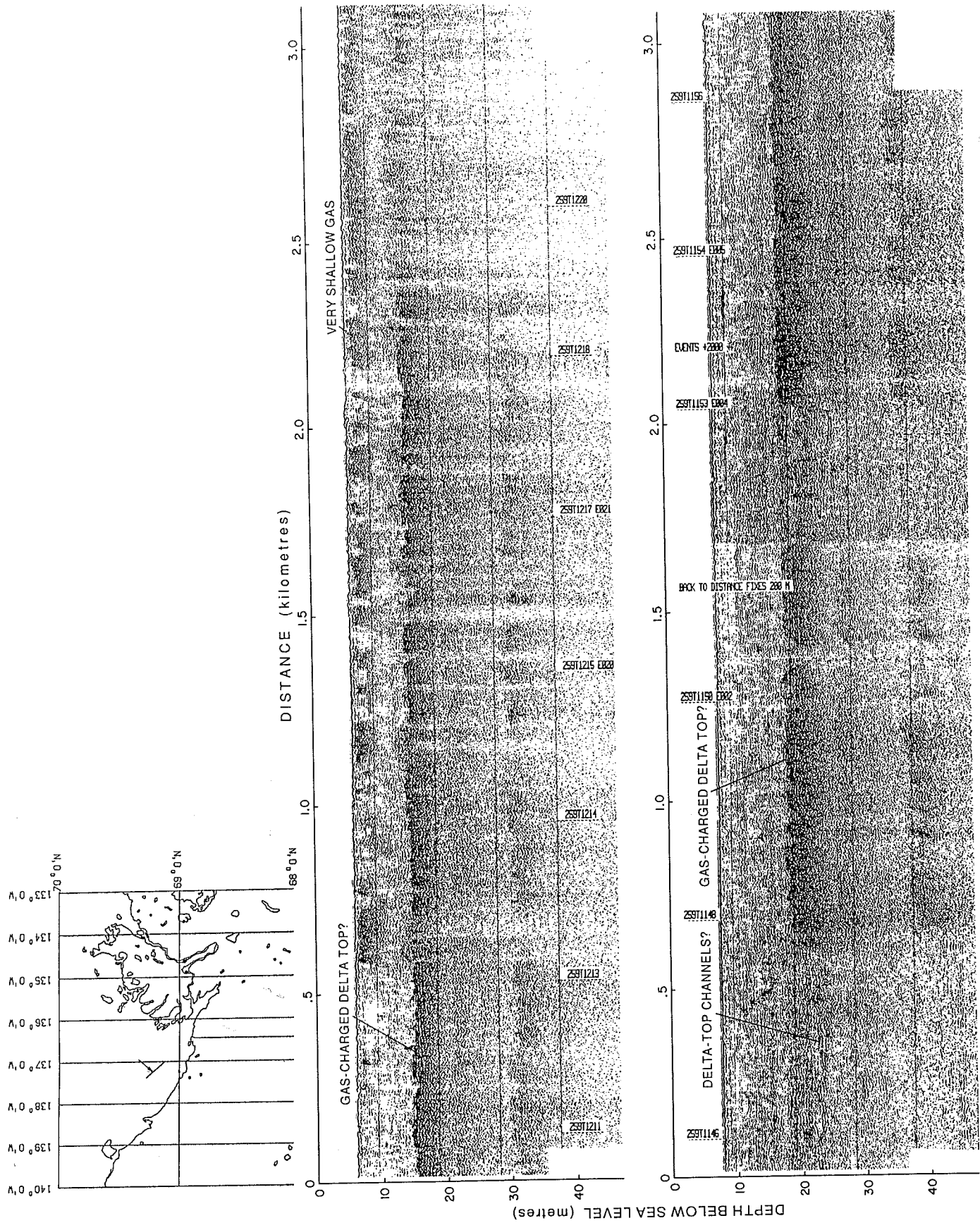
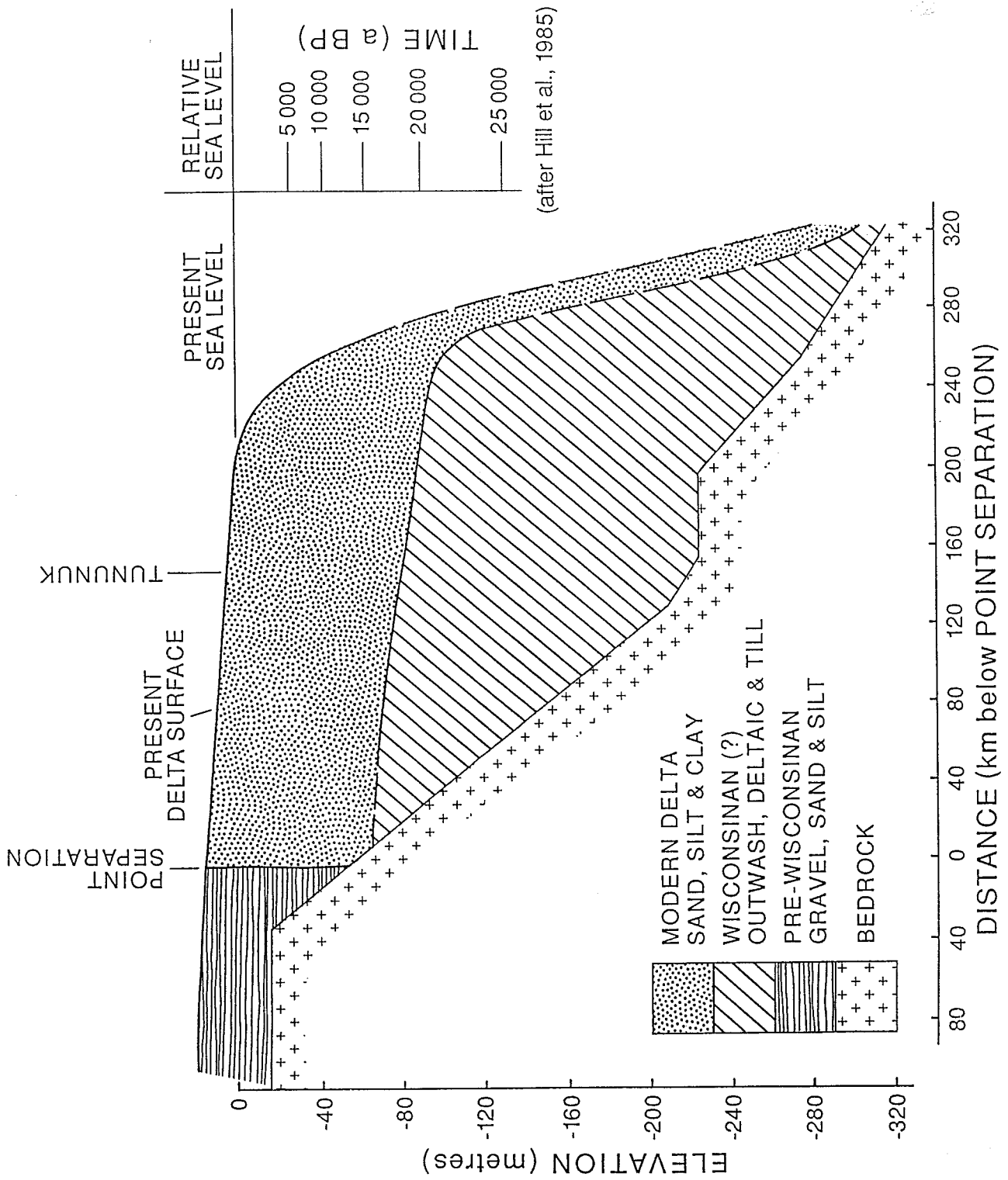


Figure 6.7 Boomer profile 87-09 showing discontinuous gas-charged reflector near the top of the Holocene delta sequence.



**Figure 6.8** Composite section of the Mackenzie Delta compiled from the work of C.P. Lewis (1988) and seismic data.

trough inland as well.

### ***6.5.1 Late Wisconsinan Delta***

Moran et al. (1989) have described the lithologic sequence through the late Wisconsinan delta complex, based on a borehole and cone penetrometer profile (Fig. 6.9) located in mid-trough. A coarsening upwards delta sequence can be distinguished from the piezocone profile. The basal clinoform foresets consist of sharp-based graded sand and silt beds with thick clay intervals. The sequence thickens and coarsens upwards into massive micaceous sandy silt and graded silt and sandy silt beds. Channels visible in the seismic profiles are filled with massive micaceous sandy silt with bed thicknesses of greater than 50 cm. The origin of the channels, whether fluvial or prodelta, is not clear.

Age control of the delta sequence is poor, but a late Wisconsinan age has been assigned (Moran et al., 1989) for several reasons. Radiocarbon dates on sediments from boreholes on the western margin of Mackenzie Trough (KF1, KF7; Fig. 5.9) and tentative seismic correlations suggest a minimum age of 40,000 years before present for unit MT2 below the delta and a Holocene age for the sequence above the delta (Fehr, 1987). The delta-top hinge-line depth of approximately 75 m is coincident with the minimum relative sea-level position for the late Wisconsinan (Forbes, 1982; Hill and others, 1985). A late Wisconsinan age for the delta therefore seems most reasonable. This thick wedge of sediment was probably supplied during deglaciation by a retreating ice tongue located in the Mackenzie Valley (Hughes, 1987; Rampton, 1988).

### ***6.5.2 The Holocene Delta***

A very small number of boreholes and jet-drill holes are available from the subaerial Mackenzie Delta despite the large amount of industry interest in the delta. The available data are from NRC Lake near Inuvik and a transect that runs west from Inuvik (Lewis, 1988). The holes show little consistency in stratigraphy but comprise 70 m of frozen silt and sand with common organic layers and occasional shell fragments. In the offshore, in the borehole sequence described by Moran et al. (1989), Holocene sediments, 20 m thick, consist of soft, bioturbated marine silty clay.

Two sets of lithologic data have been collected in the coastal zone during the NOGAP D.1 project. These data are summarised below.

### ***Distributary Mouth Sediments: The Olivier Islands***

Jenner (1989) carried out a sedimentological study of the Olivier Islands, using pit exposures and vibracores. The Olivier Islands are situated between two distributary channels, known as Reindeer and Nonsuch Channels (Fig. 6.10), and include an area where local

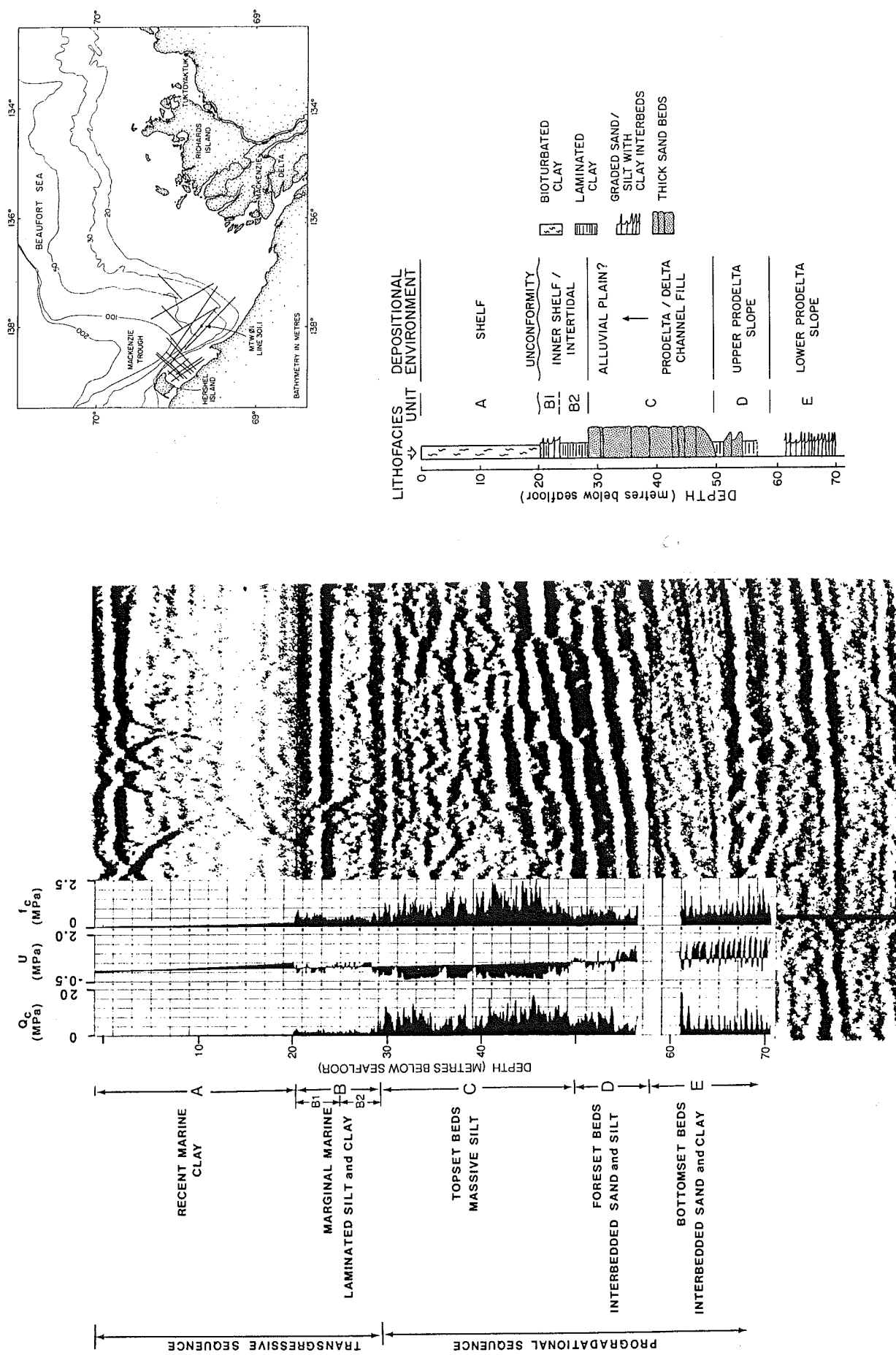
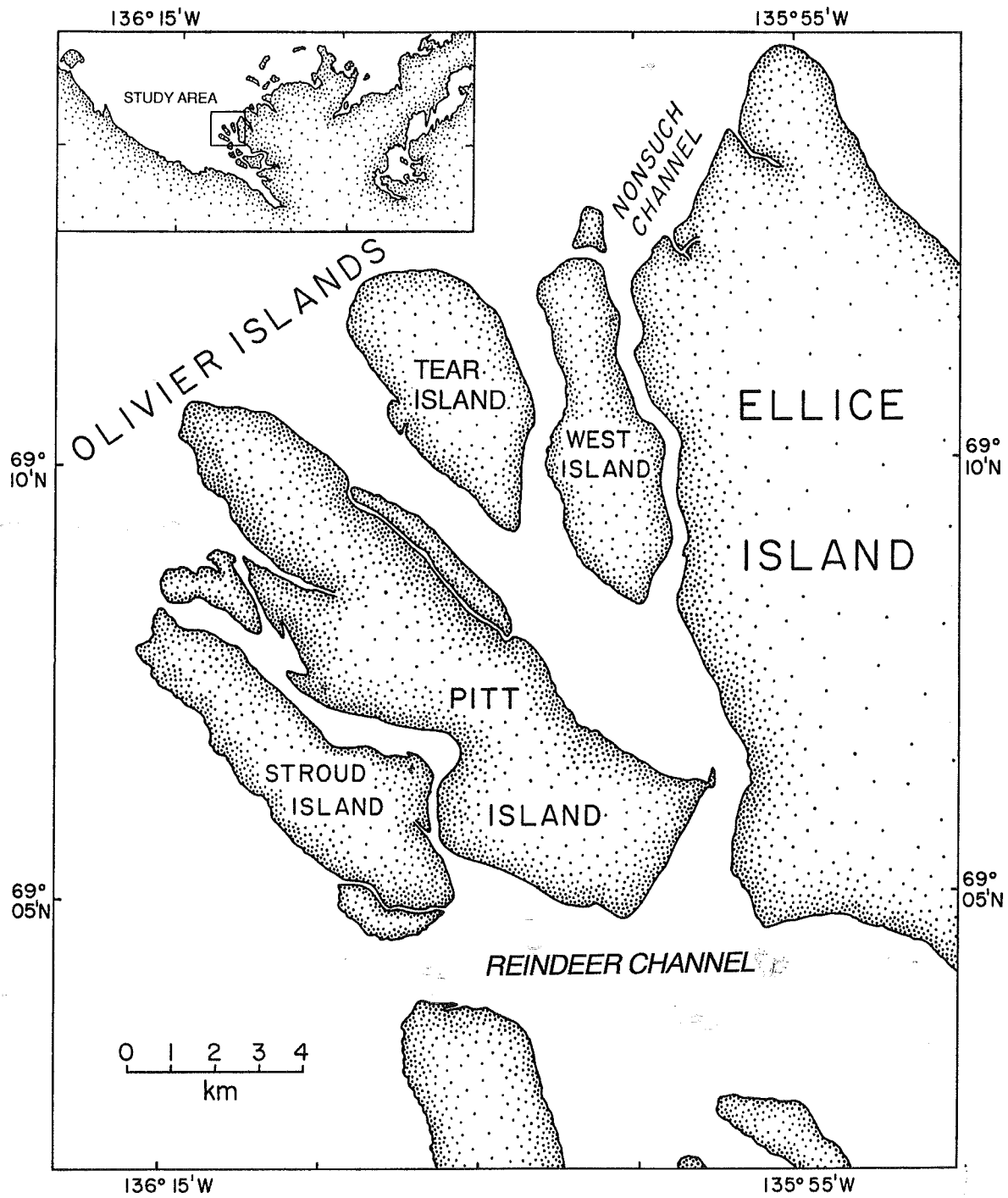


Figure 6.9 (a) Composite diagram of piezocone profile showing cone bearing ( $Q_c$ ), pore pressure ( $u$ ) and friction ( $f_c$ ) with the corresponding air gun reflection seismic profile. (b) Interpreted lithofacies and depositional environments of site MTW01 (Moran et al., 1989).





**Figure 6.10** Detailed location map of the Olivier Islands (from Jenner, 1989).

progradation and emergence has been documented over the last 40 years. The sequences described by Jenner therefore represent very recent sedimentation, but cover several different environments of deposition. Figure 6.11 illustrates the main facies recognised by Jenner and Figure 6.12 shows their distribution along two transects of vibracores.

The vibracores did not penetrate into permafrost and consequently most of the cores are less than 1.5 m long. A stiff clay (facies 1) was recovered from erosional channel margins and is thought to represent an older delta surface over which the very recent sequence has been deposited. Probably overlying this clay (although the contact was never observed), thin-bedded sand and silt with minor clay (facies 3 and 4) are extensive over much of the area. These deposits are interpreted to have been deposited in a subaqueous bar. Thick sequences of trough cross-laminated sand (facies 2) are locally present within the bar sequence and are thought to have been deposited during the abandonment of secondary channels. A thick graded and commonly convoluted sand deposit (facies 5) caps most of this sequence. This sand was probably deposited during elevated water levels related to a large storm, possibly the major storm of 1970. Over much of the area, the storm sand bed marks the transition from subaqueous to subaerial conditions. Sediments overlying it are rooted and consist of interbedded silt and sand or sand and clay (facies 6 and 7).

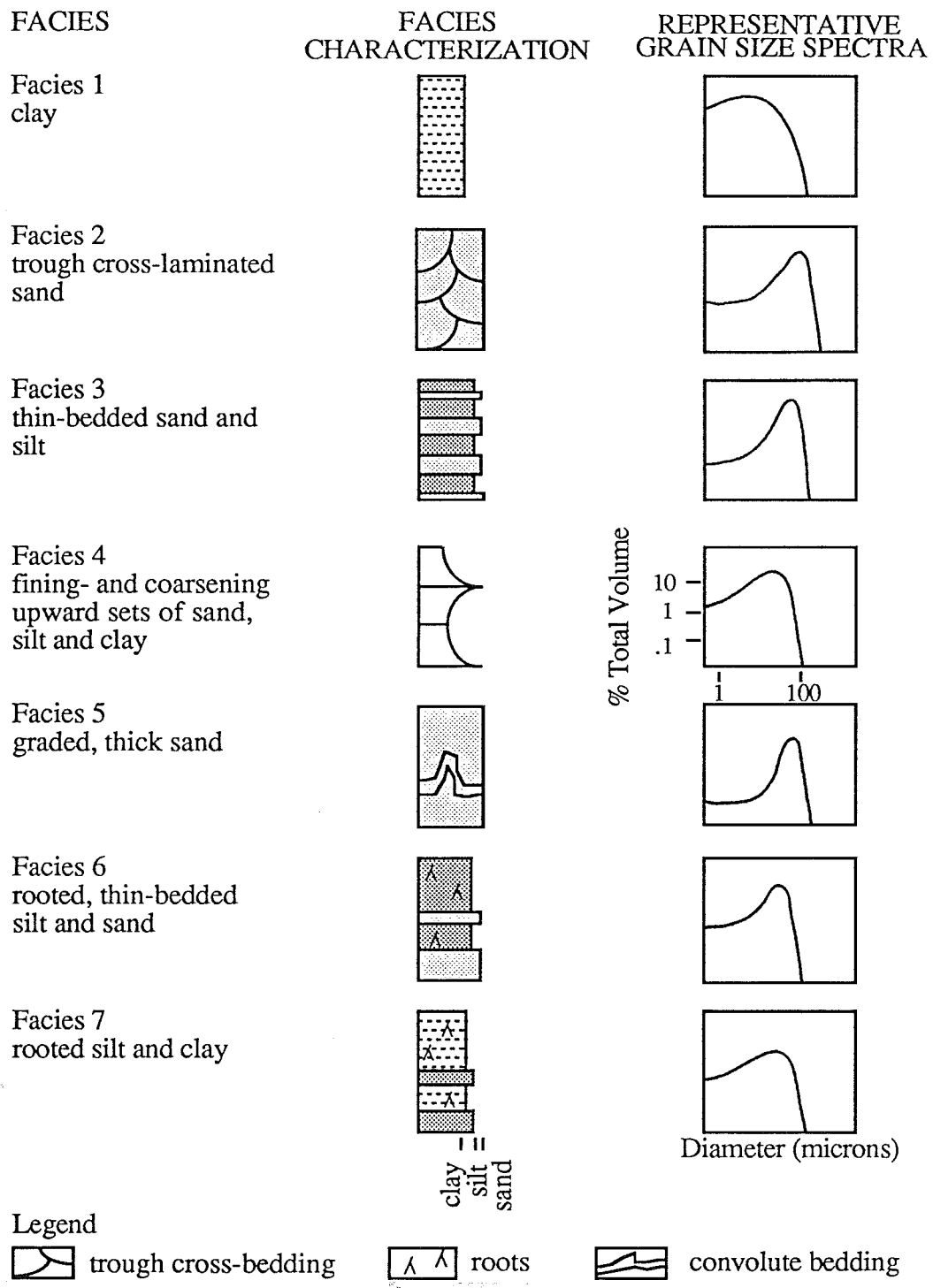
A detailed discussion of the sedimentological evolution of the Olivier Islands and a comparison with other deltaic areas is contained in Jenner (1989).

### ***Inner Shelf Sediments***

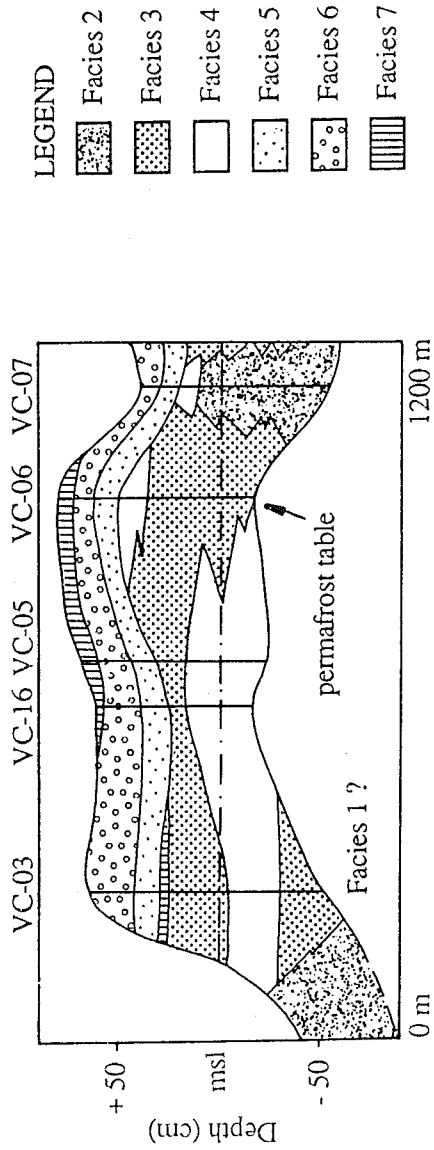
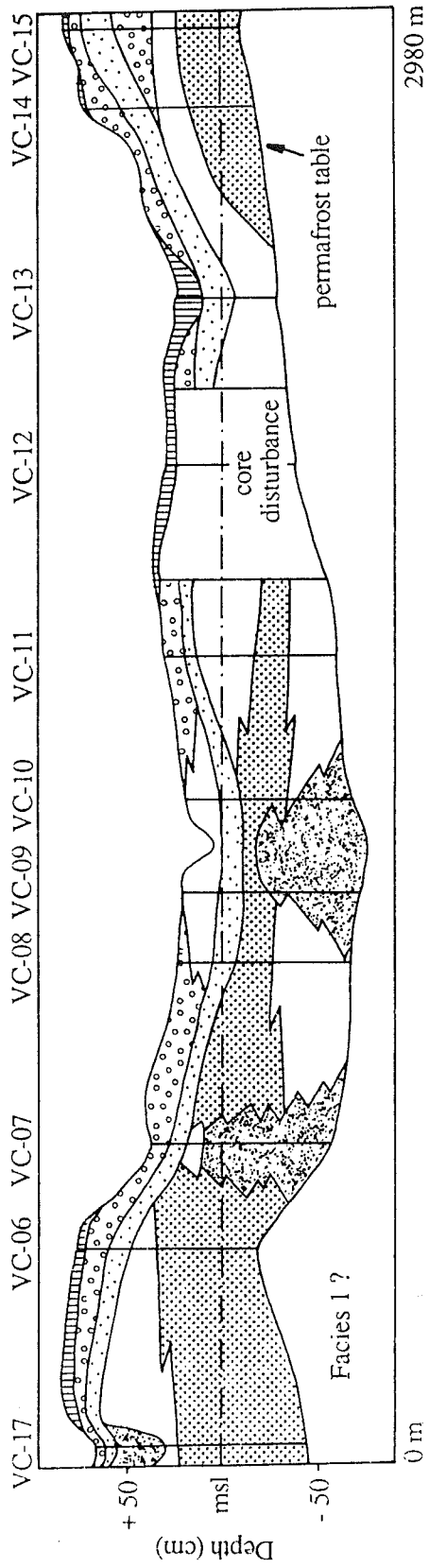
Vibracores were collected on the Nahidik'87 cruise, in water depths ranging from 3 to 11 m along two transects in front of the Mackenzie Delta (Fig. 6.13). Graphic logs from the two transects are presented in Figure 6.14. Both transects have similar characteristics. The inshore cores consist of thin- to medium-bedded well- to moderately-sorted sand and well-sorted silt with very minor intervals of clay. Moving offshore, bed thickness decreases and the sediments become finer. In about 6 m of water, sand is rare, the silt beds are rarely more than a few centimetres thick and are separated by thicker intervals of bioturbated clay. By 10 m water depth, the section is predominantly bioturbated clay, with rare very thin beds or laminae of silt.

The sand and silt beds of the shallow water cores show a variety of sedimentary structures. A detailed sedimentological log for core 27, collected in 3 m of water is shown in Figure 6.15 and brief descriptions of the main structures are given below:

(i) Most of the sand and silt beds have sharp bases and show crude to well-developed *grading* (in the geological sense of fining upwards rather than the engineering sense of size sorting; Fig. 6.16a). The average bed thickness is in the order of 5 to 10 cm. The predominant grain sizes



**Figure 6.11** Summary of sediment facies in the distributary mouth region of the Olivier Islands (from Jenner, 1989).



LEGEND

- Facies 2
- Facies 3
- Facies 4
- Facies 5
- Facies 6
- Facies 7

Figure 6.12 The distribution of sediment facies throughout Pitt Island (from Jenner, 1989).

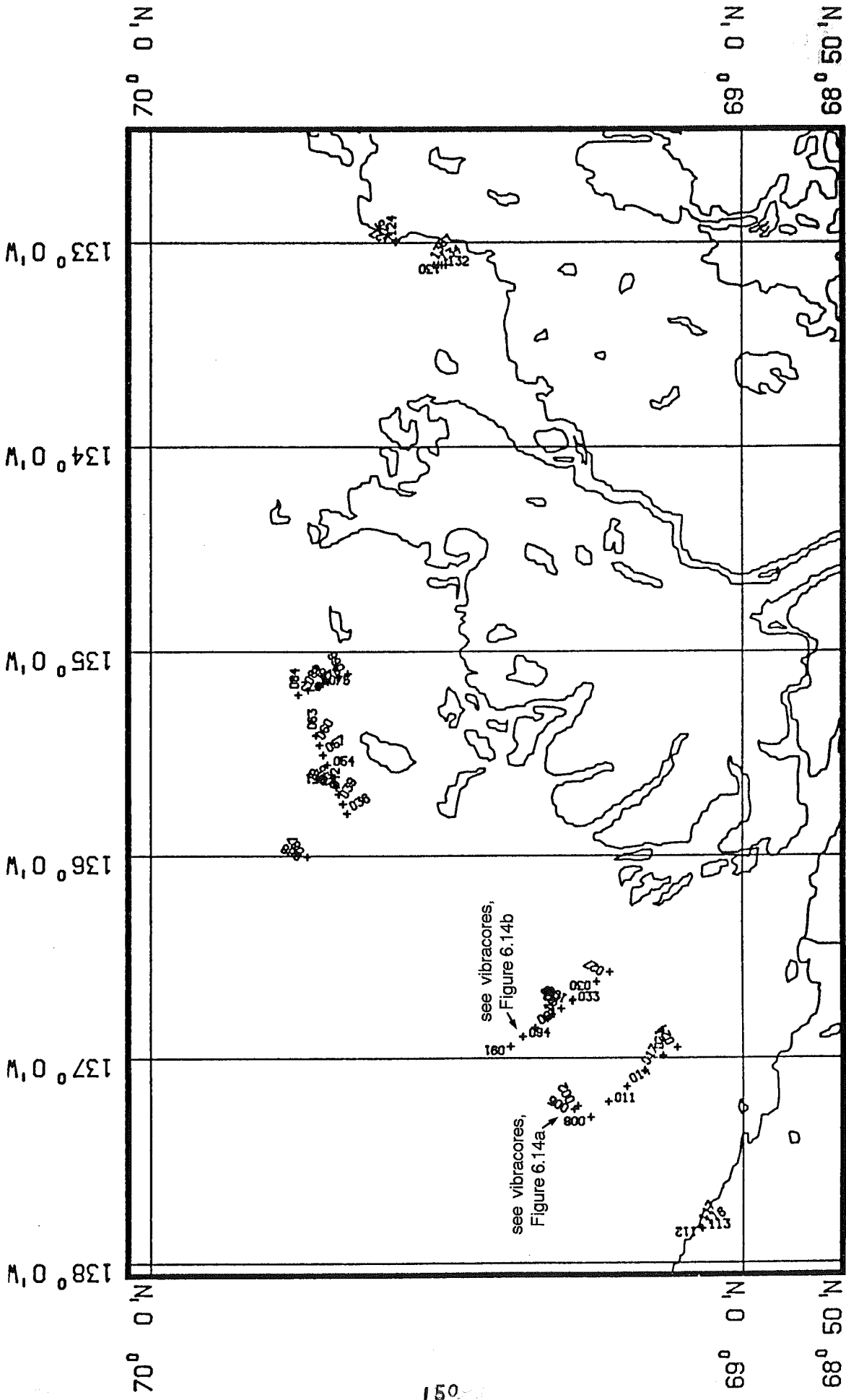
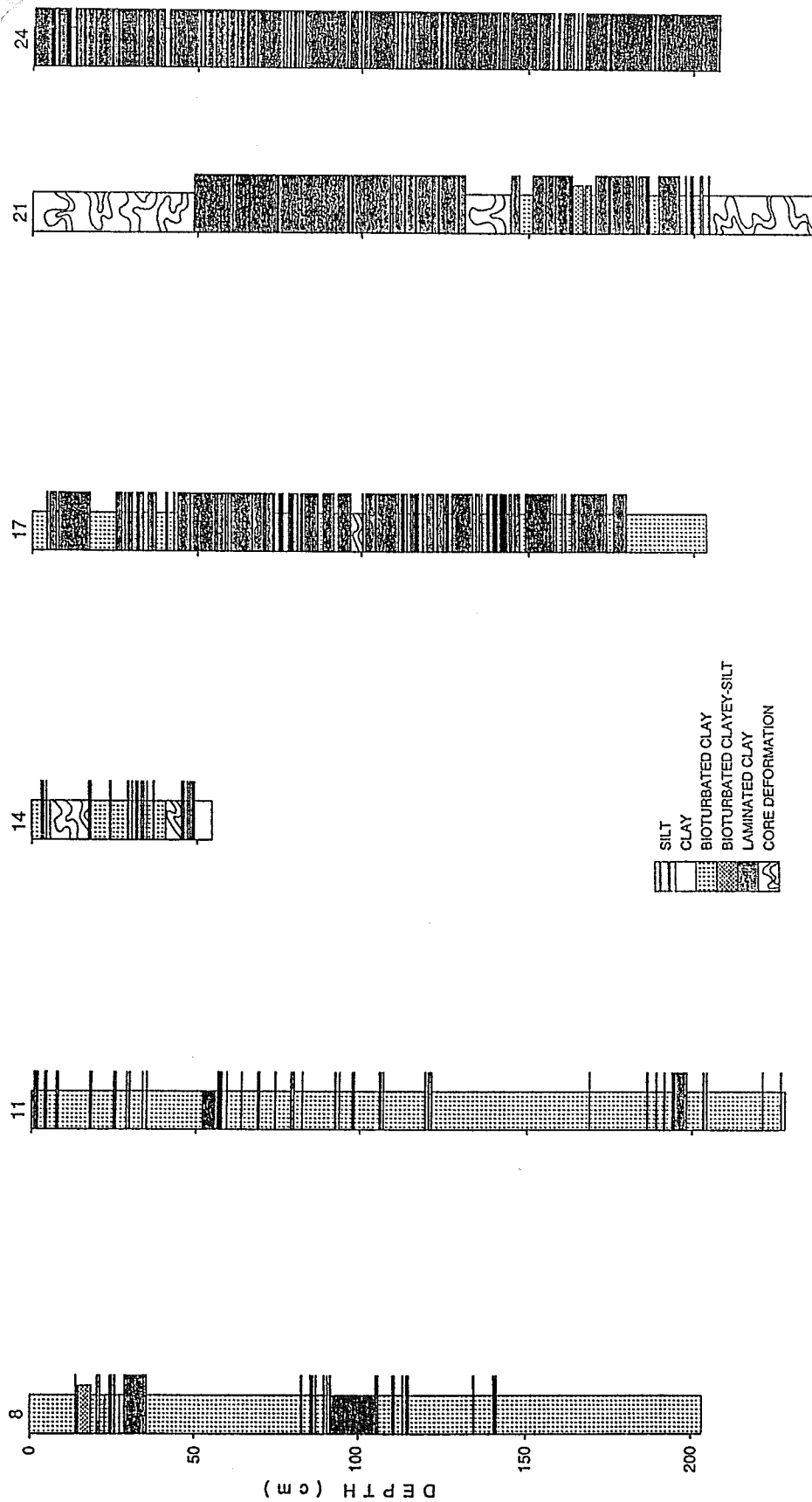
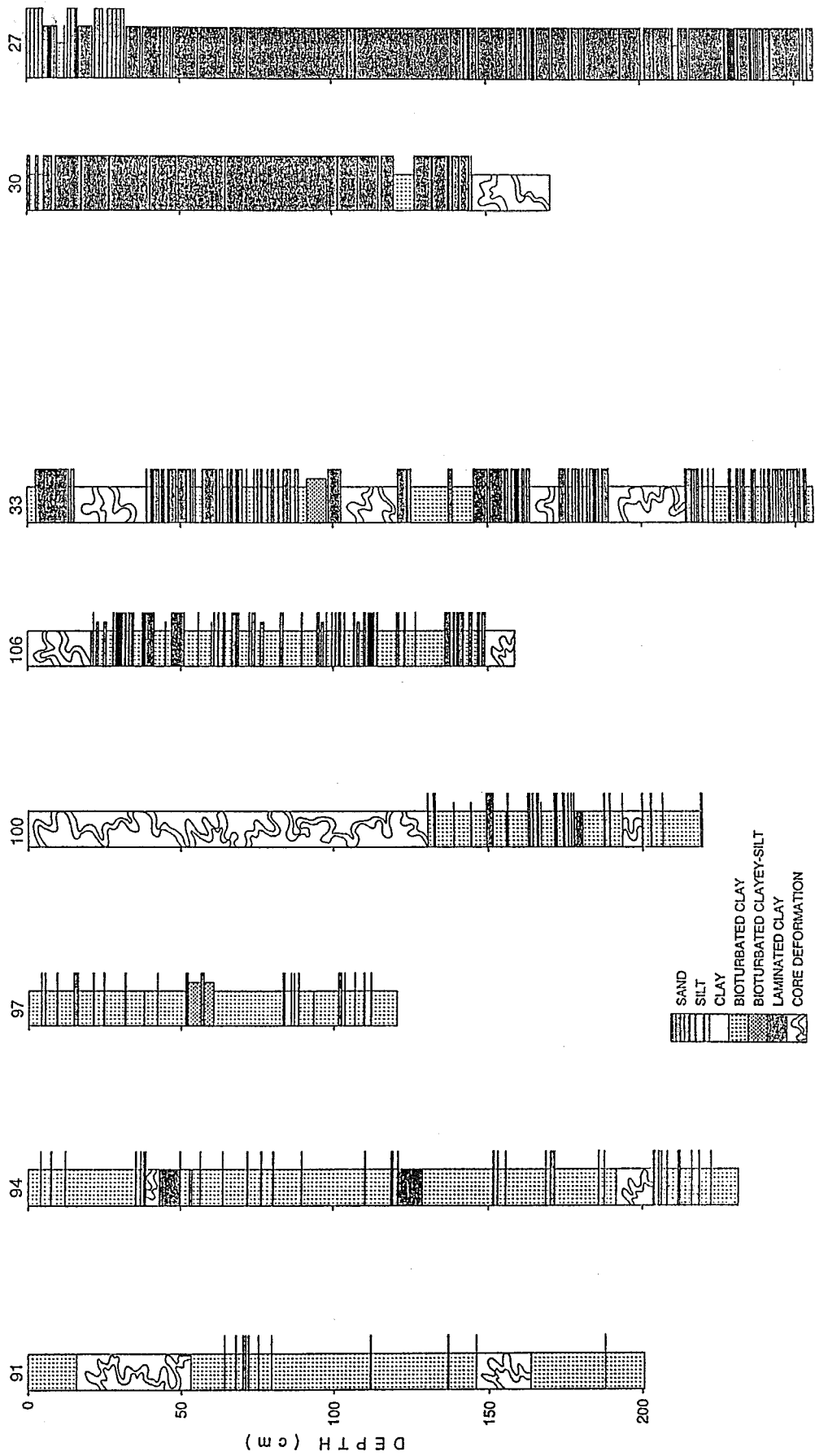


Figure 6.13 Location of Nahidik 1987 vibracores in the Mackenzie Delta region.

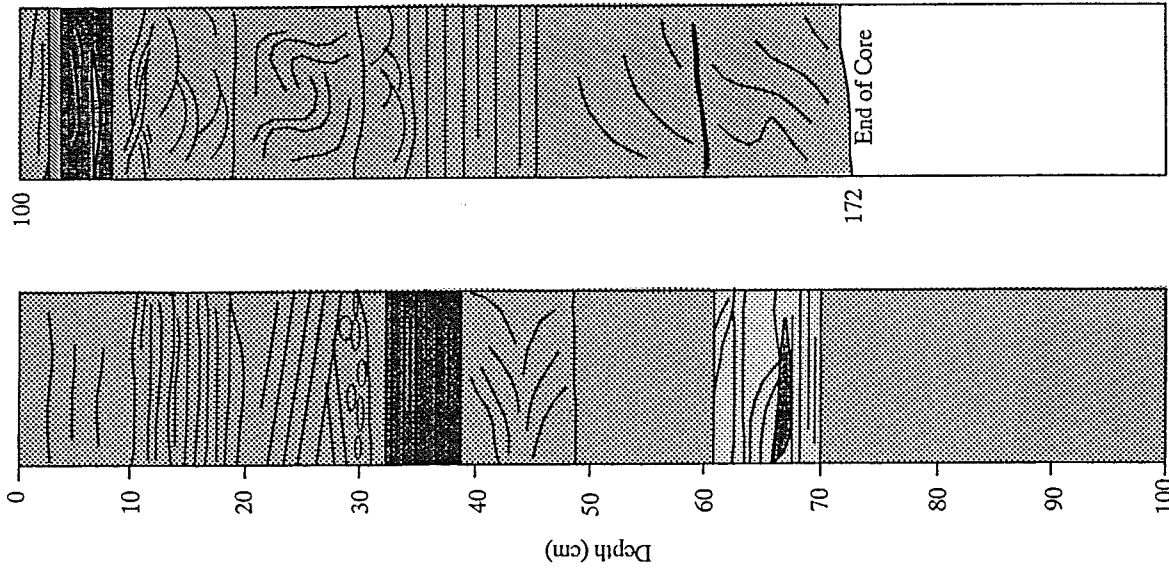


**Figure 6.14a** Sedimentological logs of the Nahidik 1987 vibracores taken from a nearshore transect in front of the Mackenzie Delta (Fig. 6.13).



**Figure 6.14b** Sedimentological logs of the Nahidik 1987 vibracores taken from a second nearshore transect in front of the Mackenzie Delta (Fig. 6.13).

NAH-87 030



NAH-87 027

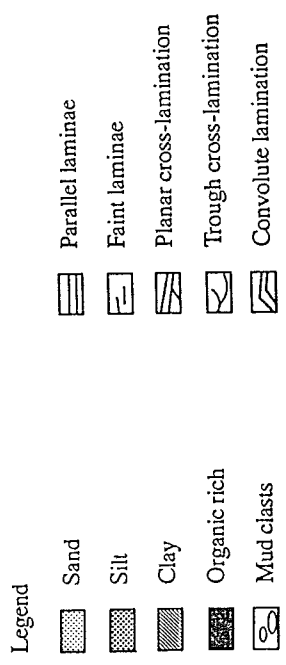
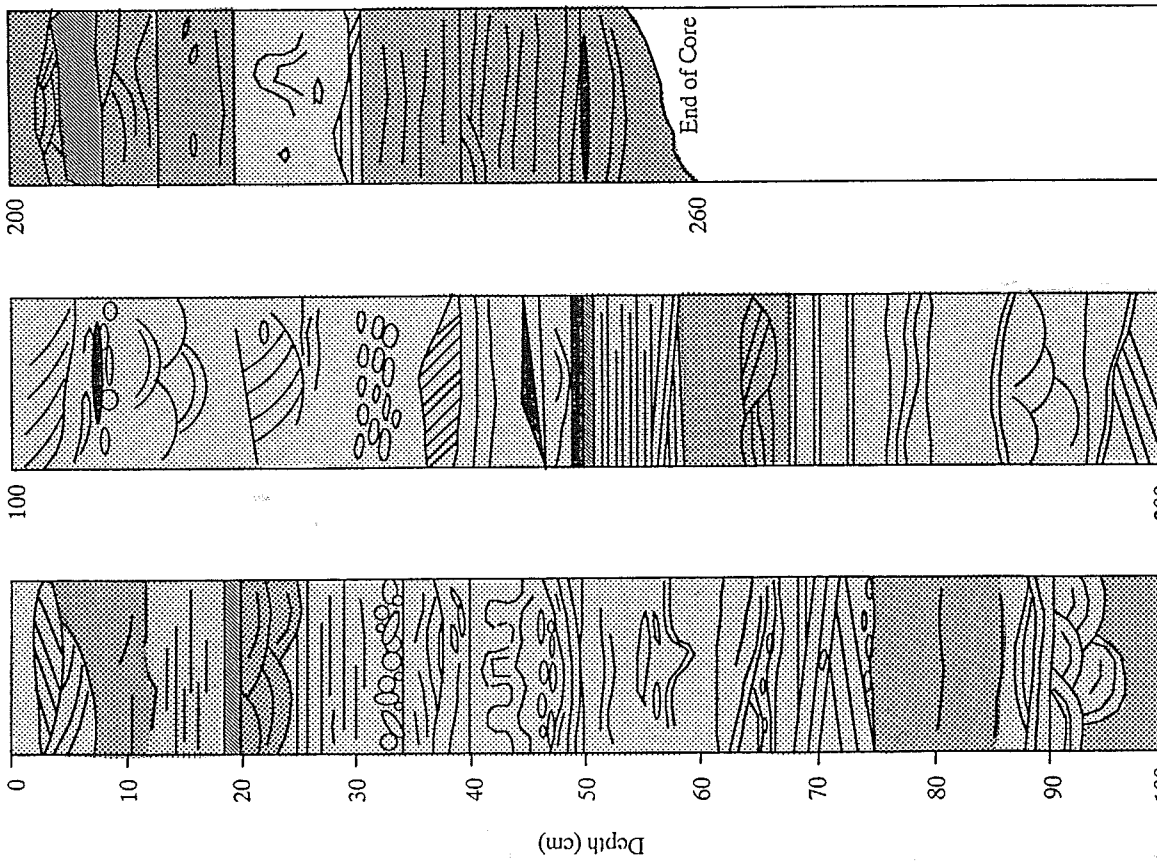
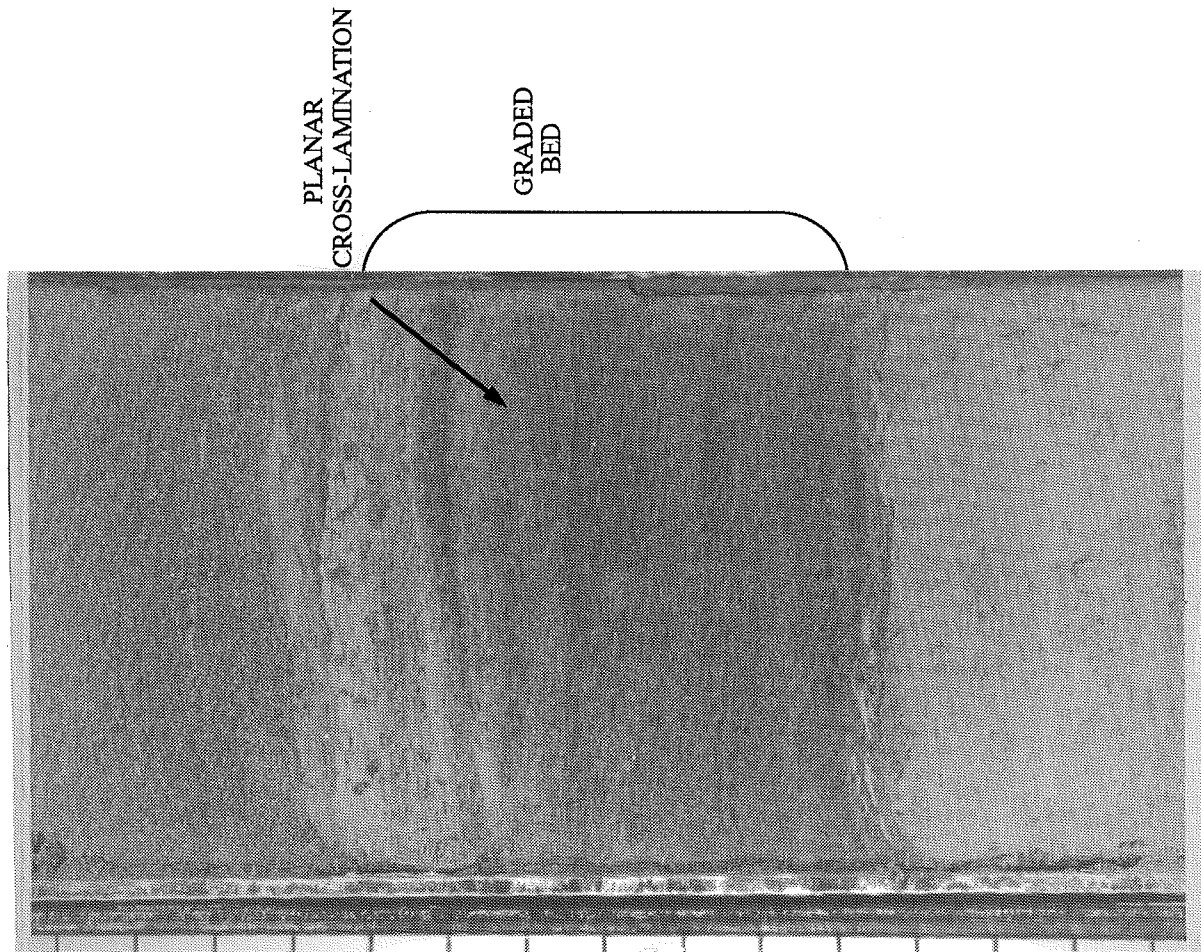
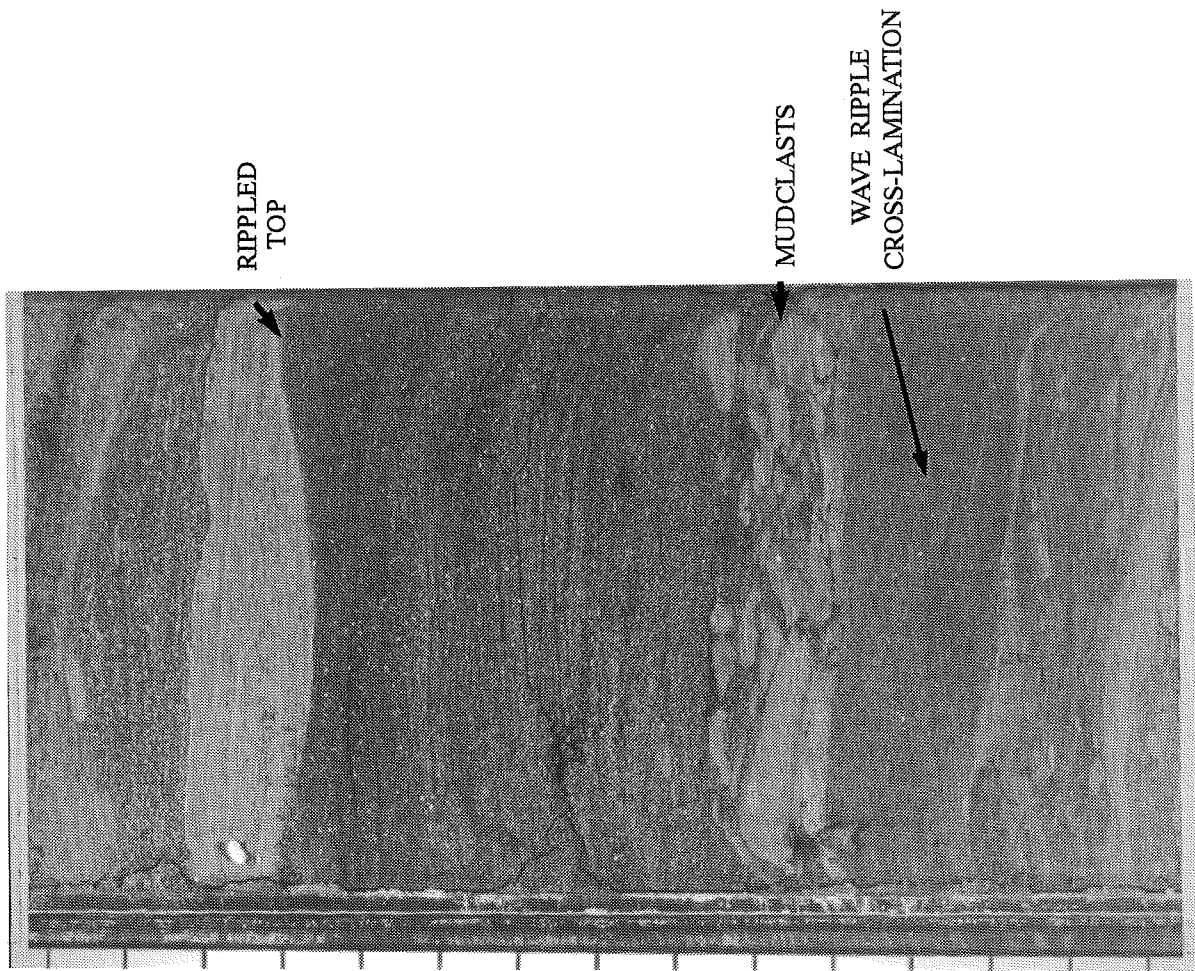


Figure 6.15 Detailed sediment logs for vibracores 27 and 30.





(a)



(b)

**Figure 6.16** Photographs of sedimentary structures from 3 m water depth: (a) graded bed of planar cross-laminated sand with sharp base, grading into silt and clay, Core 87-027, 62-77 cm; (b) sand bed with wave ripple near base, mudclast gravel layer in centre and ripples at top, Core 87-027, 22-37 cm.

are fine sand and coarse silt, but the beds are extremely variable, containing amounts of clay and particulate organic material. The tops of some beds are sharp and undulating, defining ripples with wavelength approximately 8 - 10 cm (Fig. 6.16 b).

(ii) *Parallel lamination* and low angle *planar cross-lamination* are also common in the sand beds (Fig. 6.16a). Laminae consist both of alternations of fine and medium sand or very fine sand and silt, and of particulate organics and cleaner sand.

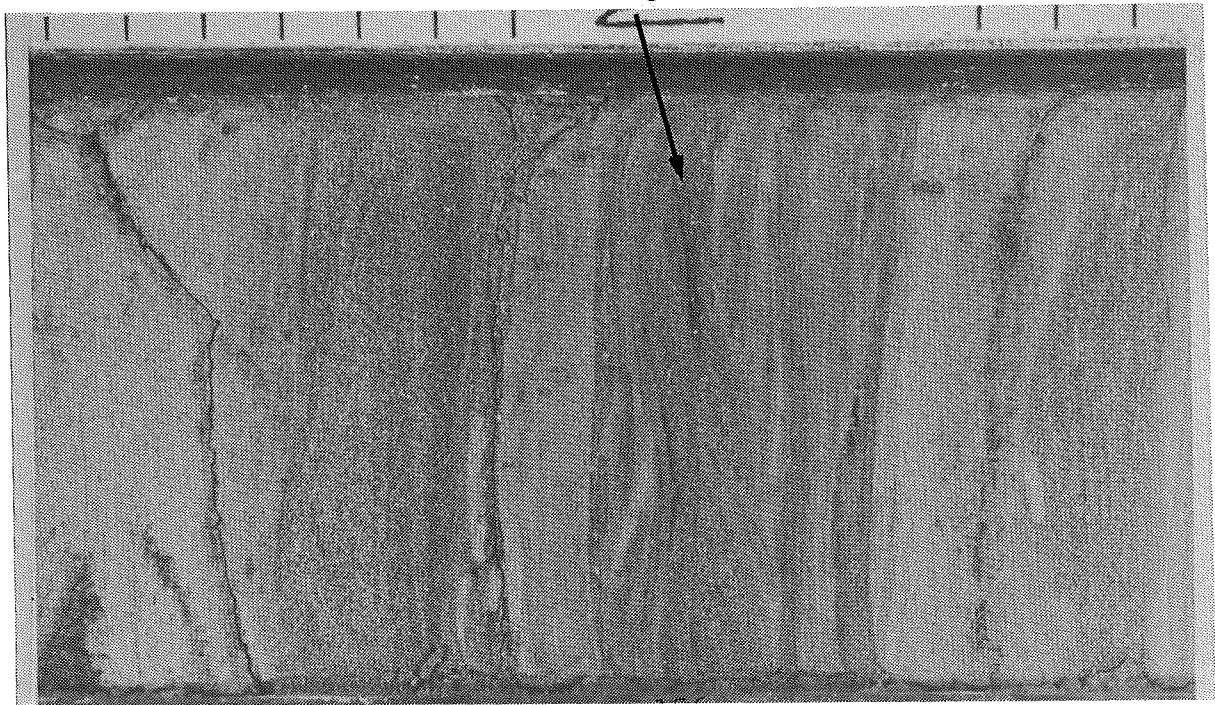
(iii) Laminae in some of the sand beds clearly define symmetrical *wave ripple cross-lamination* (Fig. 6.16b). The wave ripple in the example shown has a height of just over 1 cm and a wavelength of approximately 10 cm, although the core width precludes identification of an adjacent ripple.

(iv) The sandier intervals commonly show *trough cross-lamination* (Fig. 6.17a). Trough sets are generally in the order of 1 to 2 cm deep and up to 10 to 12 cm wide. The laminae forming the troughs generally consist of fine to very fine sand and silt, but laminae of particulate organic material are also common. These structures are produced by the migration of small linguoid ripples (Reineck and Singh, 1973).

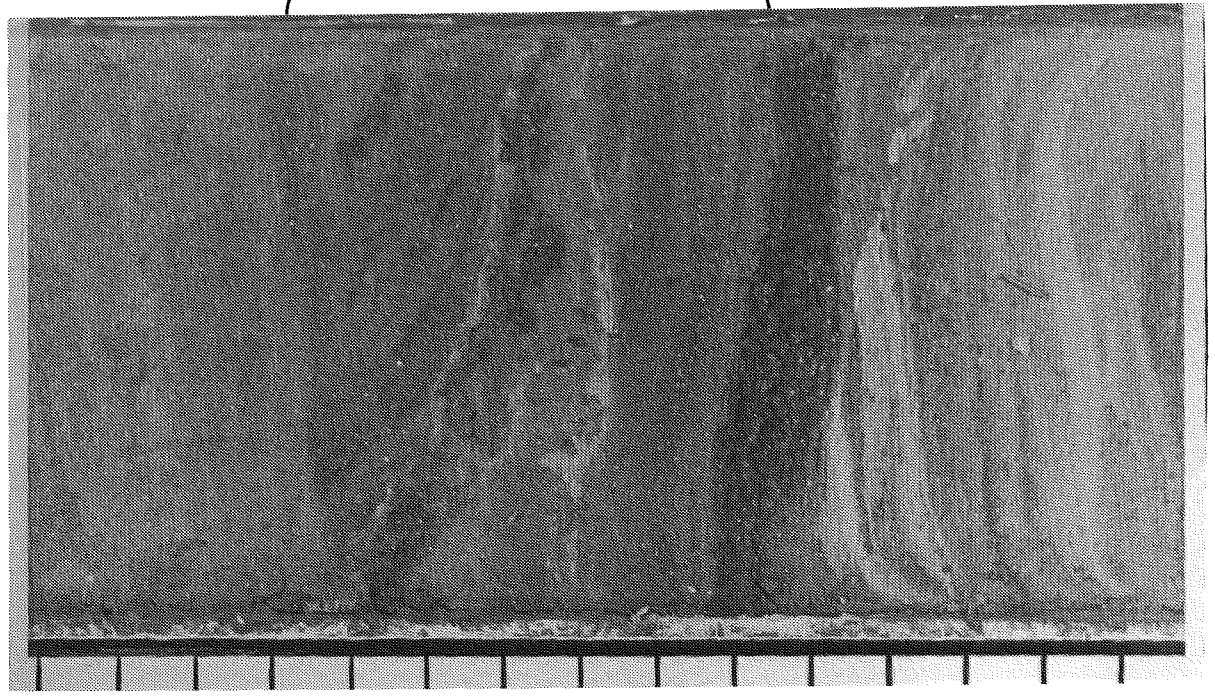
(v) Less commonly, steeply inclined sand clay and organic laminae in sets approximately 4 cm thick, with truncated upper surfaces are observed (Fig. 6.17b). The total width of the trough of which these inclined laminae form a part is much larger than the width of the core. Individual laminae are thicker and more poorly-defined than the smaller -scale trough cross-laminae. The larger scale cross-sets are tentatively interpreted as *mega-ripple bedding* (Reineck and Singh, 1973) being formed by the migration of megacurrent ripples.

(vi) Intervals of *climbing ripple lamination* are also present within the sand beds, generally as ripple drift bedding (Fig. 6.18a). The ripple set bounding surfaces are 1 to 1.5 cm apart and climb at an angle of 10° to 15°. The ripple troughs, which downlap onto the bounding surfaces, commonly contain high proportions of particulate organic material making the troughs appear as a irregular dark band (Fig. 6.18 a).

(vii) *Convolute laminations* are a common feature of sand beds in these shallow water cores (Fig. 6.18b), providing evidence for in situ liquefaction. The beds showing this characteristic all show sharp planar tops overlain by clay-rich silt or clay. The overlying beds probably have low permeability and therefore prevent fluid escape when the convoluted bed was



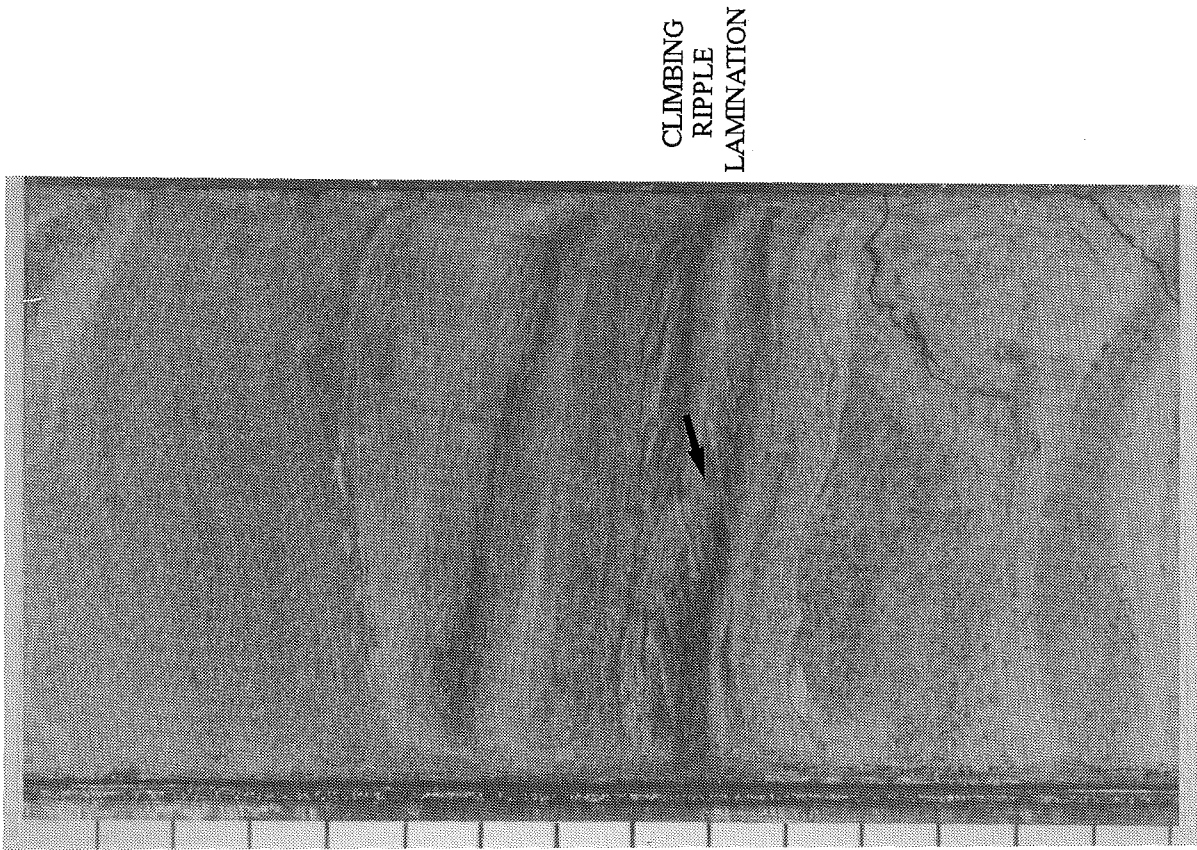
(a)



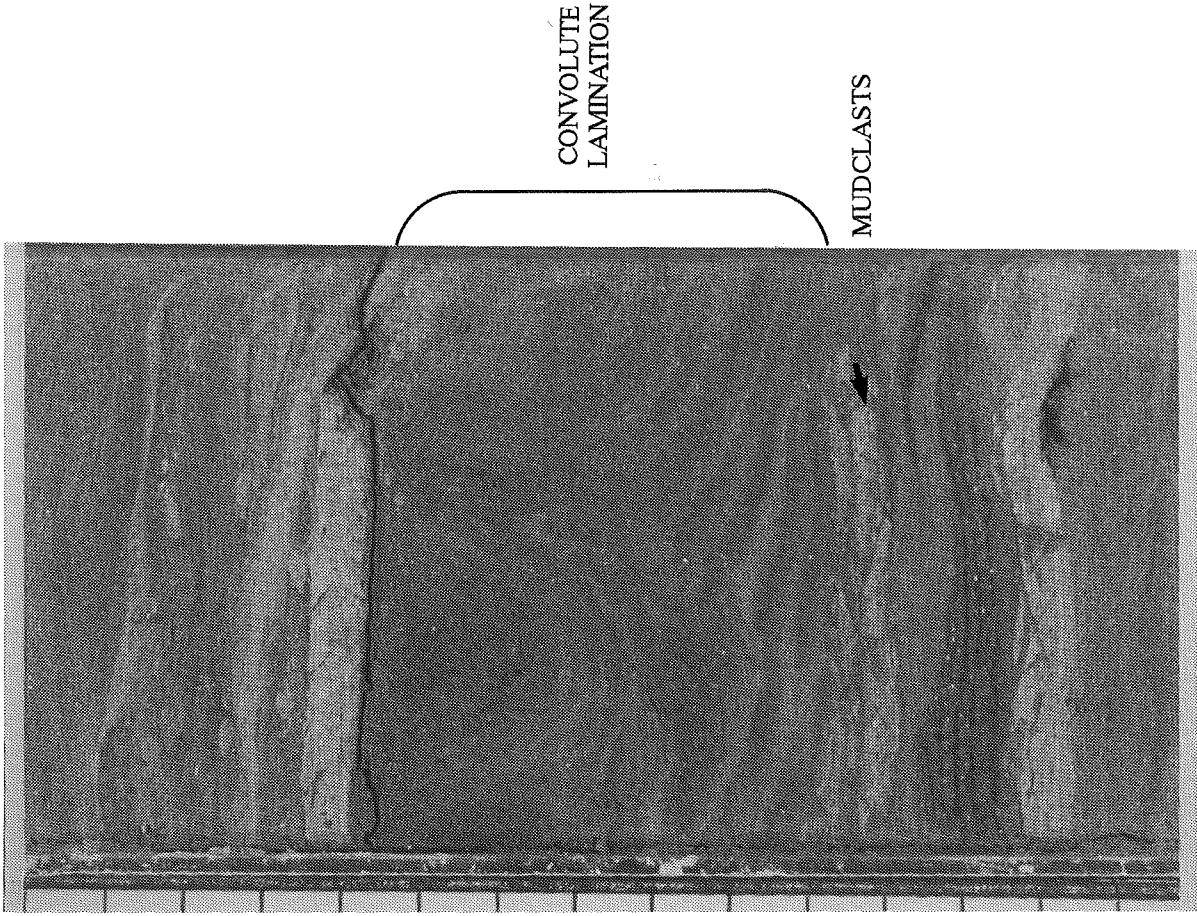
(b)

**Figure 6.17** Photographs of sedimentary structures from 3 m water depth: (a) trough cross-lamination with organic-rich laminae, Core 87-027, 11-23 cm; (b) possible megaripple bedding, Core 87-027, 96-111 cm.





(a)



(b)

**Figure 6.18** Photographs of sedimentary structures from 3 m water depth: (a) climbing ripple lamination with particulate organic material in ripple troughs, Core 87-027, 185-200 cm; (b) convolute lamination, Core 87-027, 34-49 cm.

loaded.

(viii) *Mudclasts* are very common in the sand beds, primarily as tabular but rounded *rip-up clasts* forming layers of gravel-sized material at the base of the bed (Figs. 6.16b, 6.18b). Individual rounded mudclasts are also found floating within sandy beds. The process by which these clasts are ripped up during erosion of the seabed may be assisted by the presence of thin subvertical cracks or burrows within thin clay beds elsewhere in the cores (Fig. 6.19a).

(ix) Clay laminae also become incorporated into sand beds through *loading*. Distinctive U-shaped clay laminae, a millimetre or two thick and 1 to 2 cm across, underlie small load structures at the base of sandy beds (Fig. 6.19b).

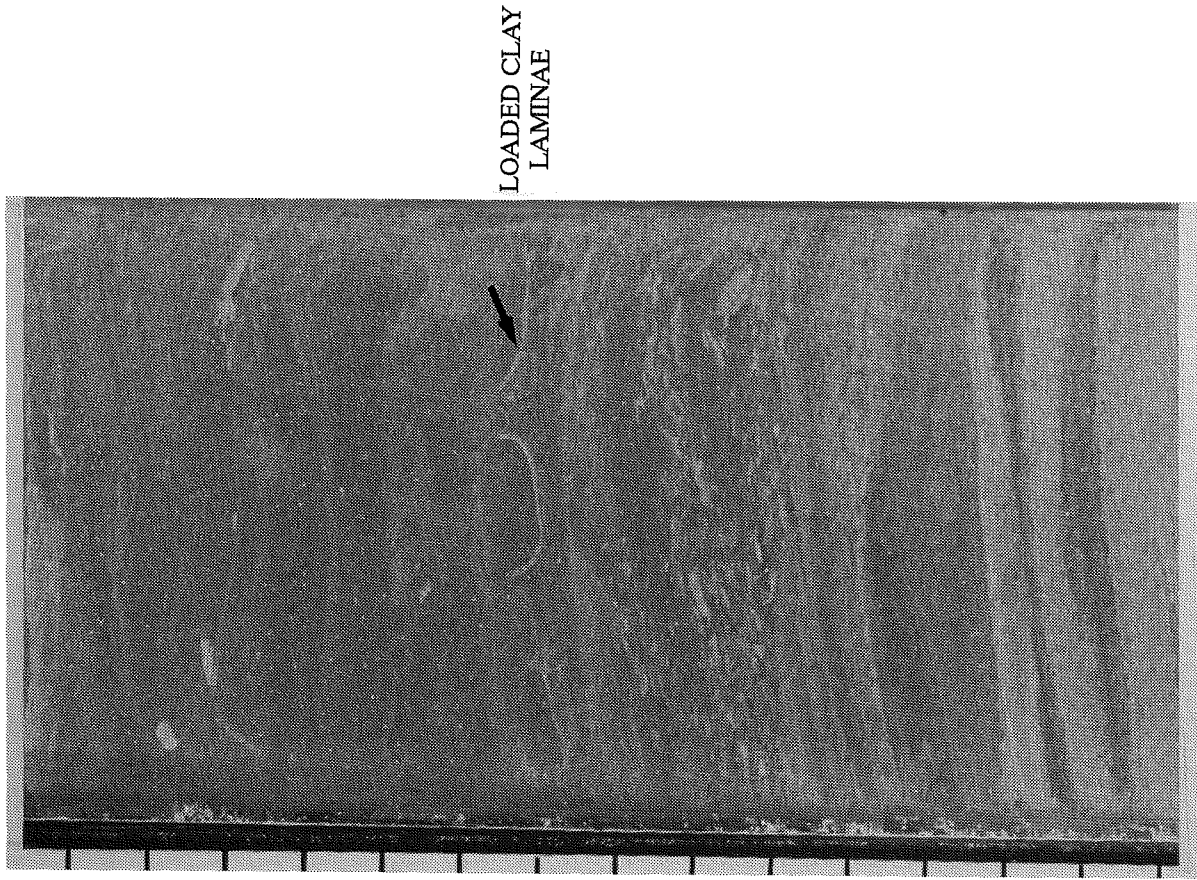
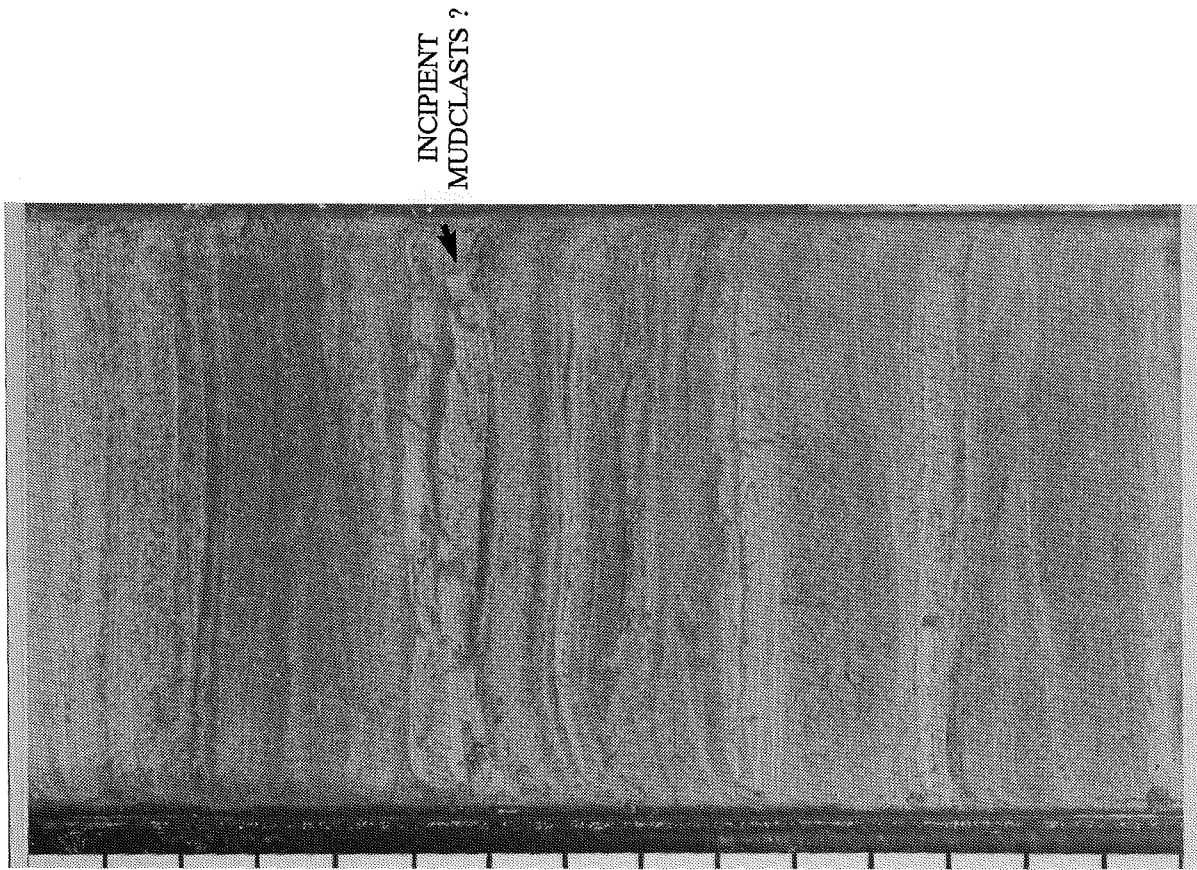
In only slightly deeper water (4 m: Core 30, Fig. 6.15), the beds are still relatively thick, but the proportion of sand is substantially reduced. Most beds consist of silt (with some very fine sand) and are commonly parallel laminated. Cross laminations are less common but both planar and trough cross lamination were observed. The silts at this water depth have a relatively high particulate organics content which are visible as dark laminae within parallel laminated beds (Fig. 6.20a) and as trough infills (Fig. 6.20b).

Progressing offshore, the silt beds become thinner and finer grained. In core 33 (Fig. 6.14), the thin silt beds show very fine parallel laminations but are more affected by bioturbation (Fig. 6.21). By 7 m water depth, the silt beds are most commonly less than 1 cm thick. They are generally irregular beds, as a result of pervasive bioturbation. Where beds are not reworked by bioturbation, the beds can be seen to be sharp-based and graded. By 10 m water depth, silt beds are very rare and the cores consist almost entirely of bioturbated silty clay with very few primary structures visible.

## 6.6 Geotechnical Properties

Bulk density and water content measurements were made on the cores shown in Figure 6.14. However, extreme and unreasonable values of bulk density, as well as large fluctuations of water content within short sections of core suggest that these data may be unreliable. As the samples were extracted and analysed more than 1.5 years after core recovery, there are additional grounds for regarding the data as suspect. The data are therefore not presented here.

This leaves very little information on the geotechnical properties of the delta sediments. Sediments from industry boreholes north of the delta, consisting of silts with traces of clay and fine sand, and organic laminae, have water contents in the range of 20% to 40% to subbottom depths of 20 m. Corresponding bulk densities are in the general order of 2 g/cm<sup>3</sup>, decreasing

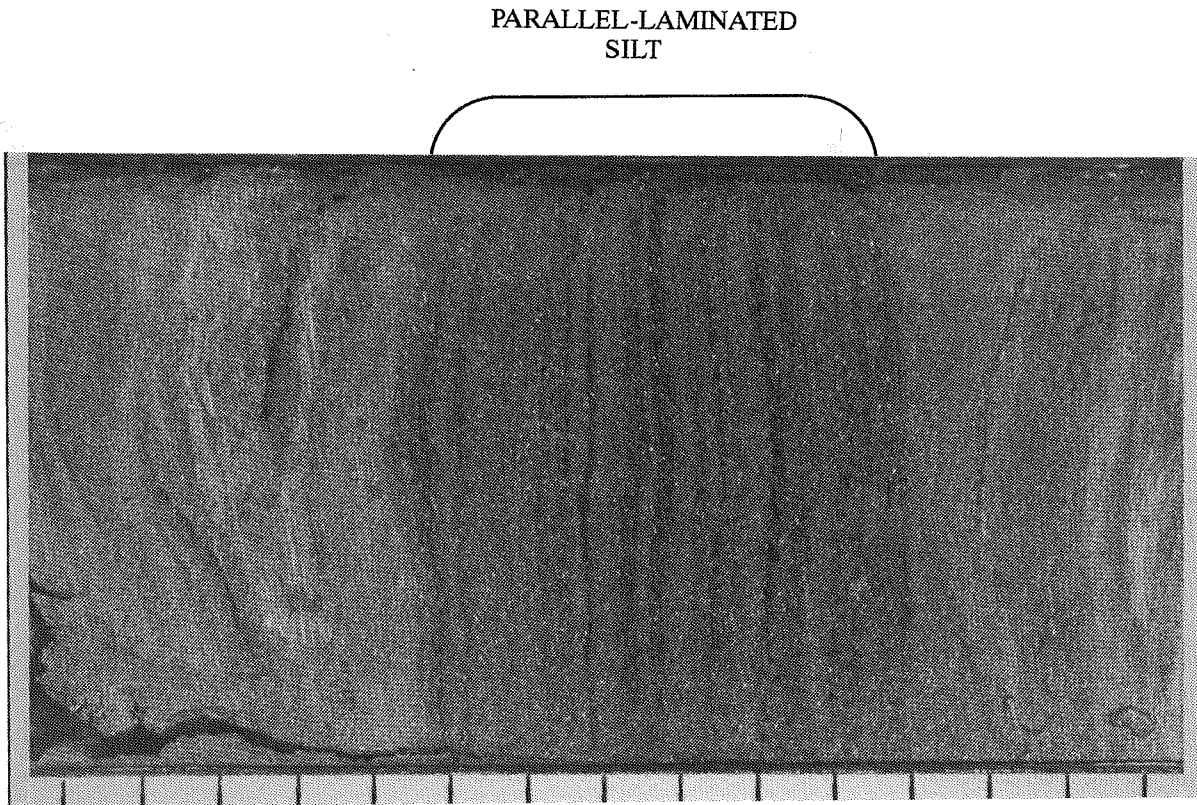


(a)

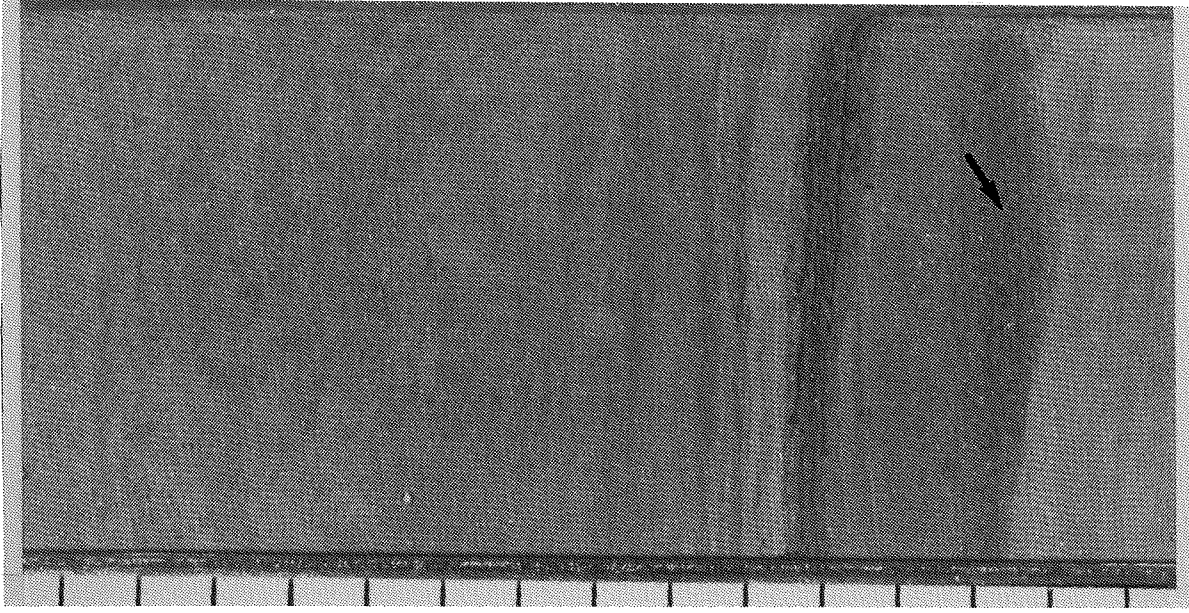
(b)

**Figure 6.19** Photographs of sedimentary structures from 3 m water depth: (a) thin clay beds with subvertical cracks or burrows, Core 87-027, 133-148 cm; (b) U-shaped loaded laminae, Core 87-027, 120-135 cm.



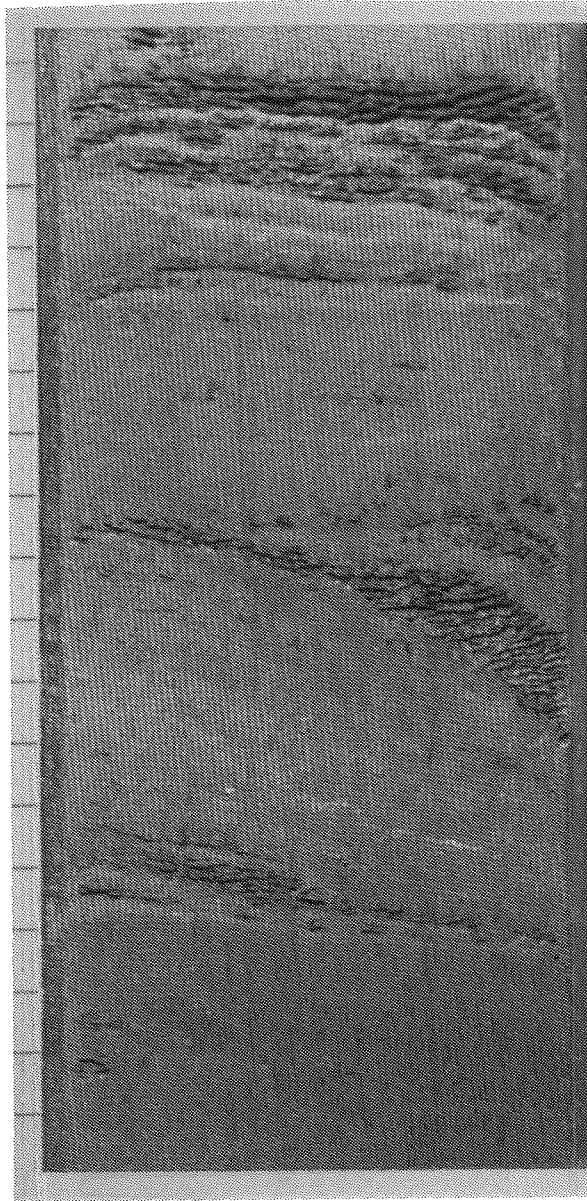


(a)



(b)

**Figure 6.20** Photographs of sedimentary structures from 4 m water depth: (a) organic-rich, parallel laminated silt, Core 87-030, 26-41 cm; (b) organic-rich silt infilling silt ripple trough, Core 87-030, 92-108 cm.



**Figure 6.21** Photograph of sedimentary structures in 9 m water depth: very fine, parallel laminated and weakly bioturbated silt Core 87-011, 15-25 cm.



markedly to 1.7 g/cm<sup>3</sup>, in zones where organic laminations were present.

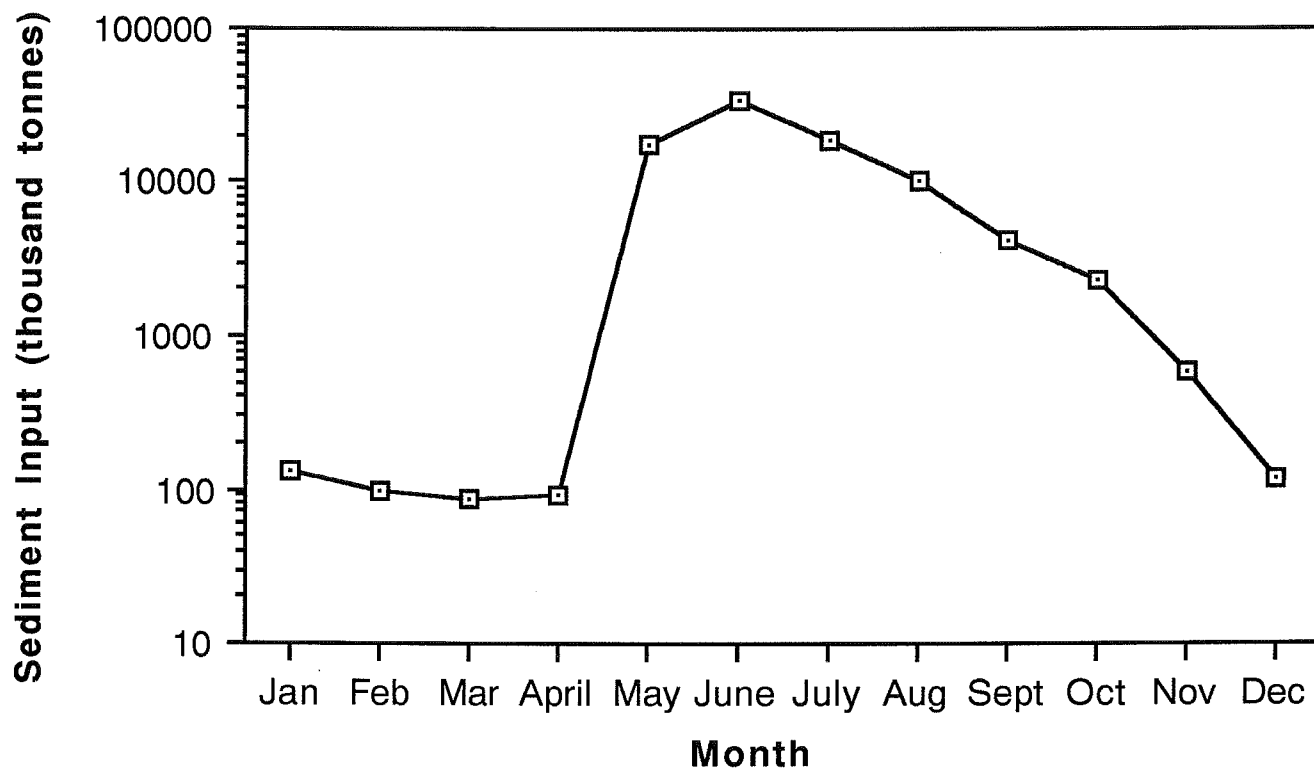
## **6.7 Sediment Erosion, Transport and Deposition**

Evidence from the distributary mouth study of Jenner (1989) and cores collected from the nearshore and inner shelf (Section 6.5) suggest that sedimentary processes in the Mackenzie Delta region involve a complex interaction between Mackenzie River discharge, storm waves, storm surges and currents. Unfortunately, there are no wave and current measurements between the coastline and the 40 m isobath. Attempts to recover data from the inner shelf in 1987 were frustrated by the loss of a Seadata wave and current meter. In this section therefore, data from adjacent coastal areas is extrapolated to the delta where it is reasonable to do so. Available data are also biased towards the summer open water months due to the logistic difficulties of fieldwork during winter and particularly during the critical spring break-up period.

### **6.7.1 Sediment Supply**

Sediment is supplied to the coastal region of the delta by the major distributaries of West and Middle Channels (Fig. 6.1). Calculations by Lewis (1988) suggest that the sediment load of the Mackenzie distributary channels consists of predominantly silt and clay, with less than 5% sand carried in bedload. Qualitative observations of core material and subaerial deposits in the Olivier Islands region suggest that a significant proportion of the sediment load consists of particulate organic material, mostly in the form of plant stems and wood fragments. Some of this material may originate from erosion of the older deltaic islands.

Sediment transport in the distributaries is variable on both annual and shorter time scales. Figure 6.22 shows the monthly sediment supply to the delta from the Mackenzie River above Arctic Red River, averaged over the period 1974 to 1983. It can be seen that the sediment supply peaks dramatically in late May and early June as a result of spring snowmelt in the tributary regions of the delta. The spring freshet precedes the break-up of sea-ice, so that outlets to the open sea are limited. Dickins (1987) and Pilkington (1988) document that overflow of the river water onto the ice occurs at the major distributaries in late May, but the areas flooded are relatively small so that most of the flow is channelled into the Beaufort Sea. Submarine extensions of the major distributary channels and possibly channels within the ice itself must be the only conduits for river discharge through the bottomfast ice zone during this peak flow. There have been no studies aimed at detecting these flow conduits during the freshet, so neither their form nor extent are known. However, if they exist, the potential for scour along such features is high. If they extend beyond the submarine distributary channels shown on the hydrographic charts, they may be ephemeral, becoming rapidly infilled by later sedimentation during break-up or later storm events. Alternatively, it is possible that the hydraulic head of the river water is sufficient to lift the



**Figure 6.22** Mean monthly sediment supply to the Mackenzie Delta from the Mackenzie River above Arctic Red River, 1974-1983 (Lewis, 1988).

bottomfast ice off the bottom and thereby allow the river water to spread out.

The above conditions last for only a few weeks, before ice along the coast becomes melted out. Typically, ice melt lagoons form in the vicinity of the main channels (Fig. 6.23). Jenner (1989) has suggested that during this period substantial sedimentation occurs in the ice-melt lagoons as the channelised flow becomes unconfined, spreads laterally and decreases in velocity. This "settling pond" mechanism is thought to contribute to the initial development of distributary mouth bars.

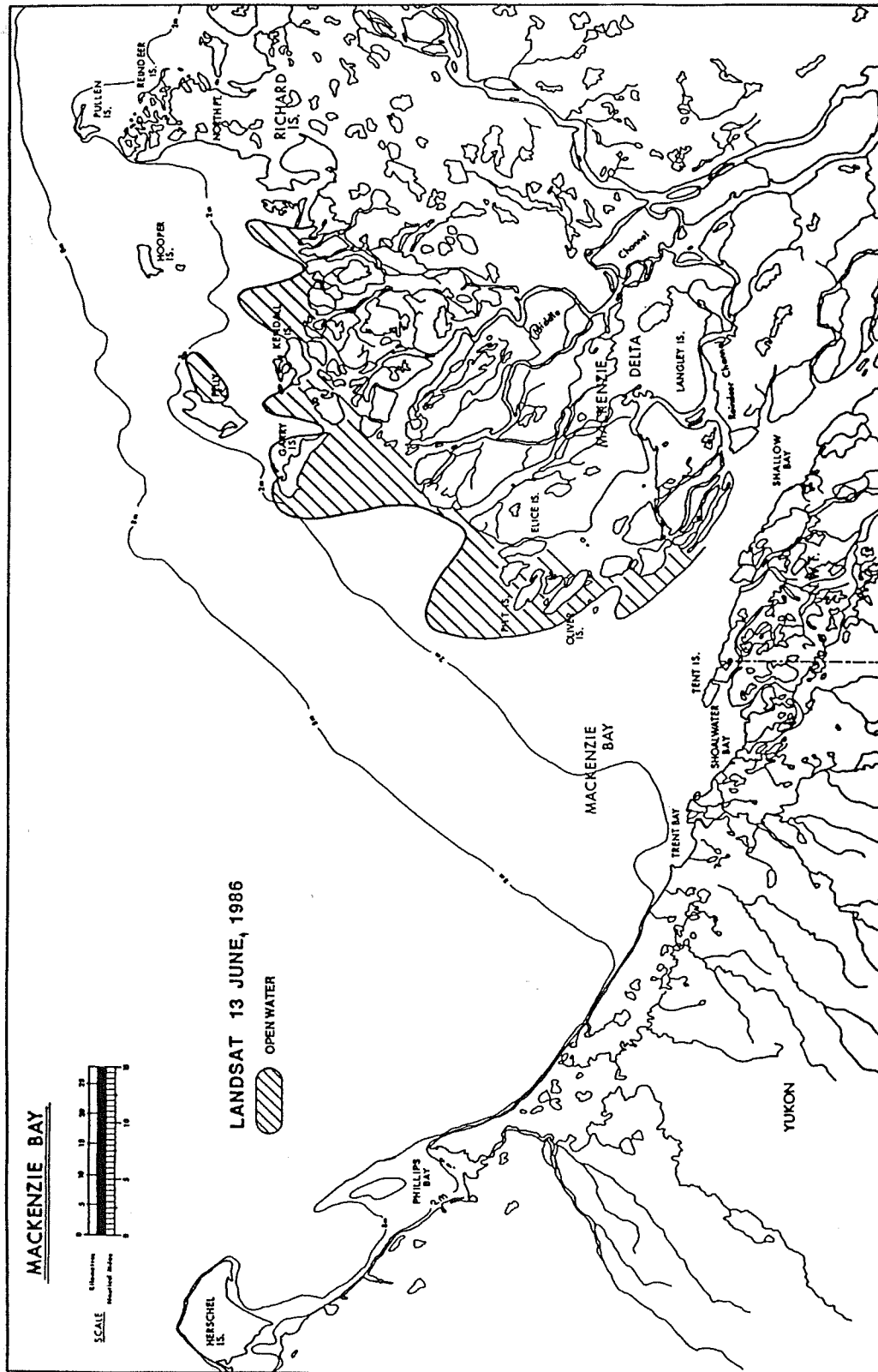
During the summer months when coastal ice has dispersed, the supply of sediment gradually decreases. On occasion, significant pulses of sediment originating from events in tributary drainage basins can be detected at the delta coast. One such event was documented by Jenner (1989) during August 1987. The sediment load of the river in the Olivier Islands region increased five fold for a period of 3 to 4 days. The same event was observed upstream by K. Kranck at the confluence of the Liard and Mackenzie Rivers. The increased sediment supply was the result of exceptionally heavy rainstorms in the Liard drainage basin.

### ***6.7.2 Transport Processes at Distributary Mouths***

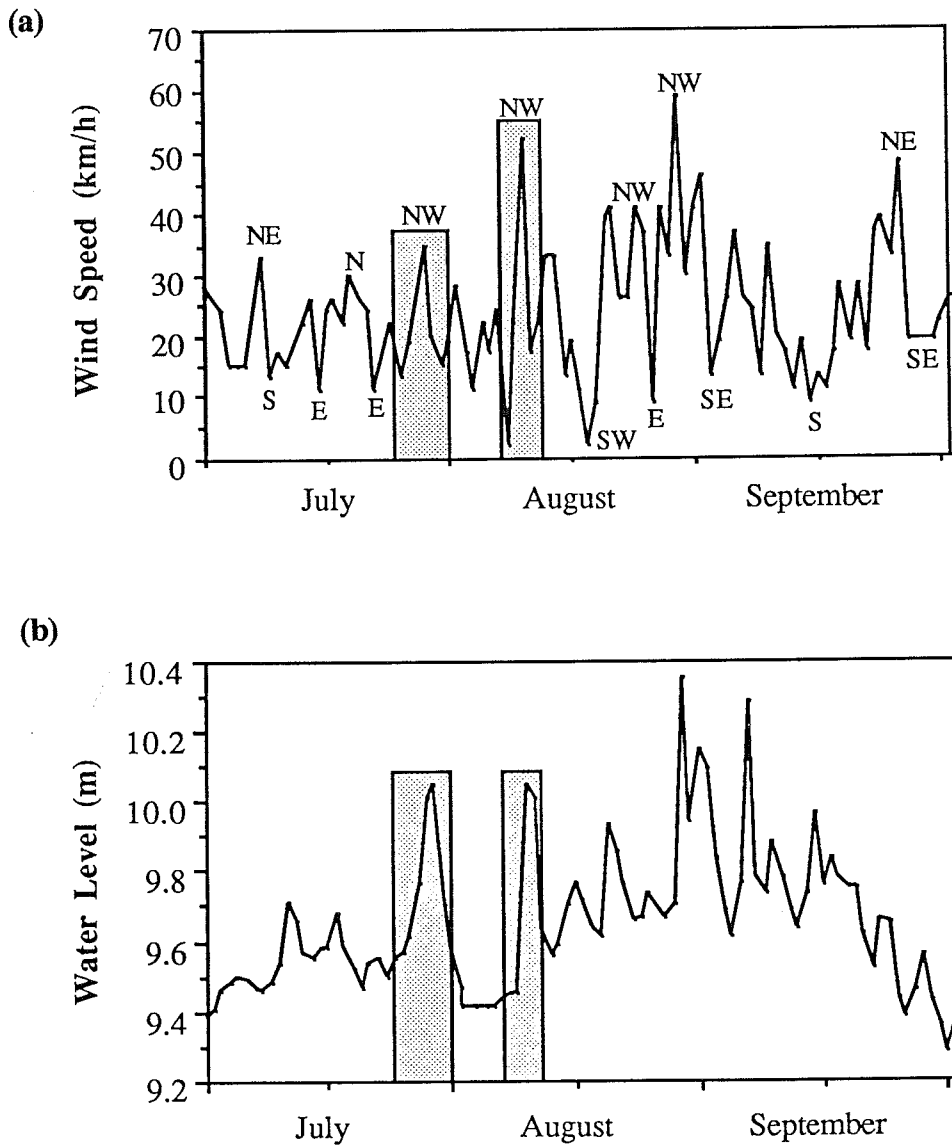
With the exception of the short period during which ice-melt lagoons are present in front of the channel mouths, a large proportion of the sediment supply bypasses the coastal region (Jenner, 1989). However, sufficient sediment supply is available to allow local accretion of distributary mouth bars. Sediment transport processes in the Olivier Islands distributary mouth region have been examined by Jenner (1989).

A primary control on sedimentation in the region is water level, which is controlled by river flow and storm surge. Figure 6.24 shows water level variations at the Olivier Islands and a wind record for nearby Pelly Island during July and August 1987. The two graphs clearly show the effects of moderate storm surges resulting from northwesterly winds in elevating water levels by almost 1 m from the mean. This is sufficient to submerge much of the unvegetated and some of the vegetated bars and flats in the region. River flood events such as the Liard event may also significantly elevate water levels. The other effect of a storm surge is to force water into the channels, thereby either retarding the outflow or causing a flow reversal in the channels. This reduction in flow velocity combined with flooding of the bars allows accretion of the intertidal bars and flats. This takes place as a vertical upbuilding of the bar or flat and a landward infilling of secondary channels.

There is some evidence that extreme storm events may contribute significantly to changes in bar configuration. Within the core sequences described by Jenner (Figs. 6.11 and 6.12), a storm bed of relatively coarse, either massive or convoluted, well-sorted sand covers much of the Olivier



**Figure 6.23** Map of nearshore ice-melt lagoon during the break-up period in late May (Pilkington, 1988).



**Figure 6.24** (a) Wind record for Pelly Island and (b) water level record for Reindeer Channel from July to September, 1987, showing correlation of high water levels with strong northwesterly winds (After Jenner, 1989).

Islands. This bed is interpreted as the product of an extreme storm surge event in 1970, which elevated water levels in the Tuktoyaktuk area by 1.9 m (Harper et al., 1988). Although the timing has not been confirmed through dating, facies changes above and below the storm deposit indicate that extensive areas of previously submerged bars became subaerially exposed and vegetated following the storm (Jenner, 1979).

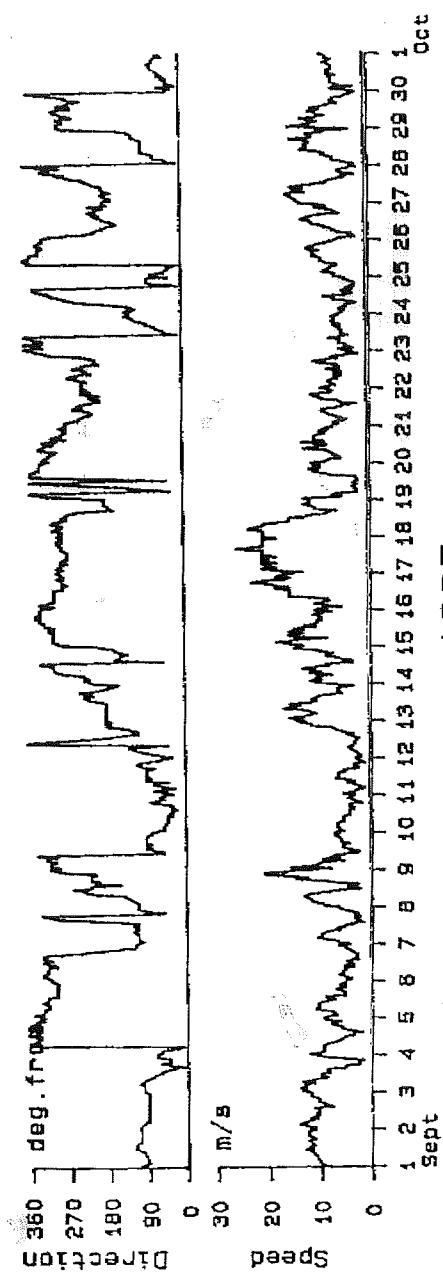
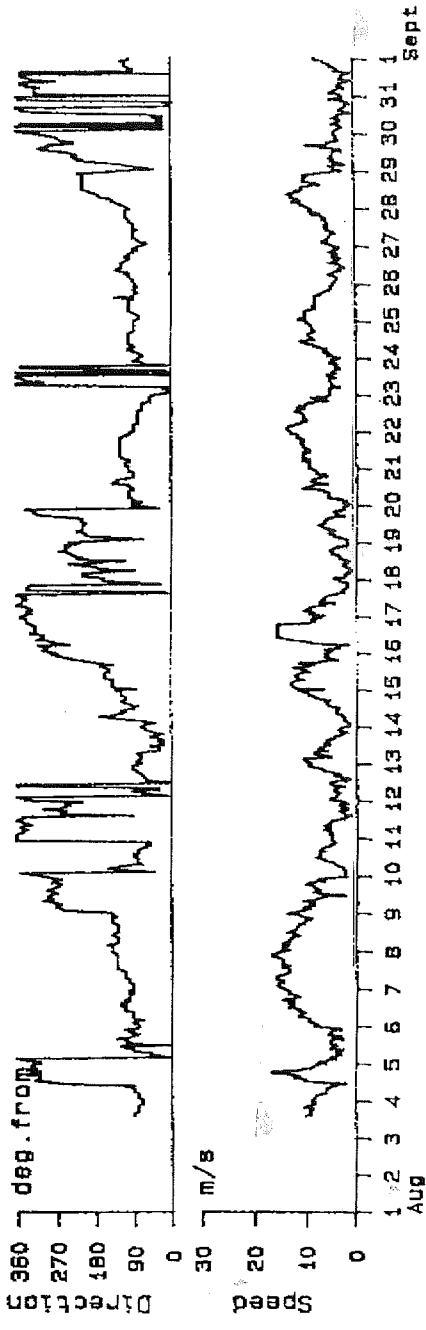
### **6.7.3 Offshore Sedimentation Processes**

Sediment that bypasses the coastal zone is transported seaward by the horizontal momentum of the river discharge, forming a surface layer of fresh water which mixes rapidly with saline Arctic Water in a horizontal direction. Most of the Beaufort Sea shows a well-developed stratification during the summer months. Fissel et al. (1987) distinguish "intense plume" water from "diffuse plume" water, based on salinity and temperature characteristics. The intense plume is generally restricted to the area immediately seaward of the delta and is separated from the diffuse plume by a pronounced horizontal gradient in both water properties and suspended sediment concentration (SSC). In visible wavelength satellite images, this front is also pronounced. Both the front and the distribution of SSC within the diffuse plume show eddy structures indicating complex flow patterns within the surface layer.

Vertical sections from areas adjacent to the delta suggest the presence of a near-bottom turbid layer extending offshore from the inner shelf (Fissel and Birch, 1984). The origin of this bottom layer is probably due to a combination of (i) settling of surface layer sediments to the more turbulent bottom boundary layer; (ii) advection of suspended sediment in the bottom layer itself; and (iii) resuspension of sediment from the seabed. Fissel and Birch (1984) established a weak relationship between bottom layer SSC and current speed or wind speed (which is positively correlated with current speed) at several offshore sites.

A study of waves, currents and SSC time series data from moorings to the east of the delta has shown that in shallow water, intense resuspension of bottom sediment occurs during storms in water depths of less than 10 m (Davidson et al. 1988; Hill and Nadeau, 1989). Calculations of bottom shear stresses due to oscillatory motions and steady flow indicate that the resuspension is primarily a result of wave energy. Net transport resulting from the steady flow component is highly variable but more pronounced in the alongshore direction. Details of these results will be discussed in section 7. The presence of graded sand and silt beds, sedimentary structures related to wave and current motions and evidence of scour and erosion (e.g. rip-up clasts) on the inner shelf off the Mackenzie Delta all indicate that similar processes occur in this region.

The most useful available wind data for the Mackenzie Delta was collected in August and September 1985 from the Explorer III at the Adlartok drill site in Mackenzie Trough. These data are shown in Figure 6.25 and show a pattern similar to other wind records in the Beaufort Sea



1985

Figure 6.25 Wind data from the Explorer III at the Adlartok drill site in the Mackenzie Trough, August and September, 1985.

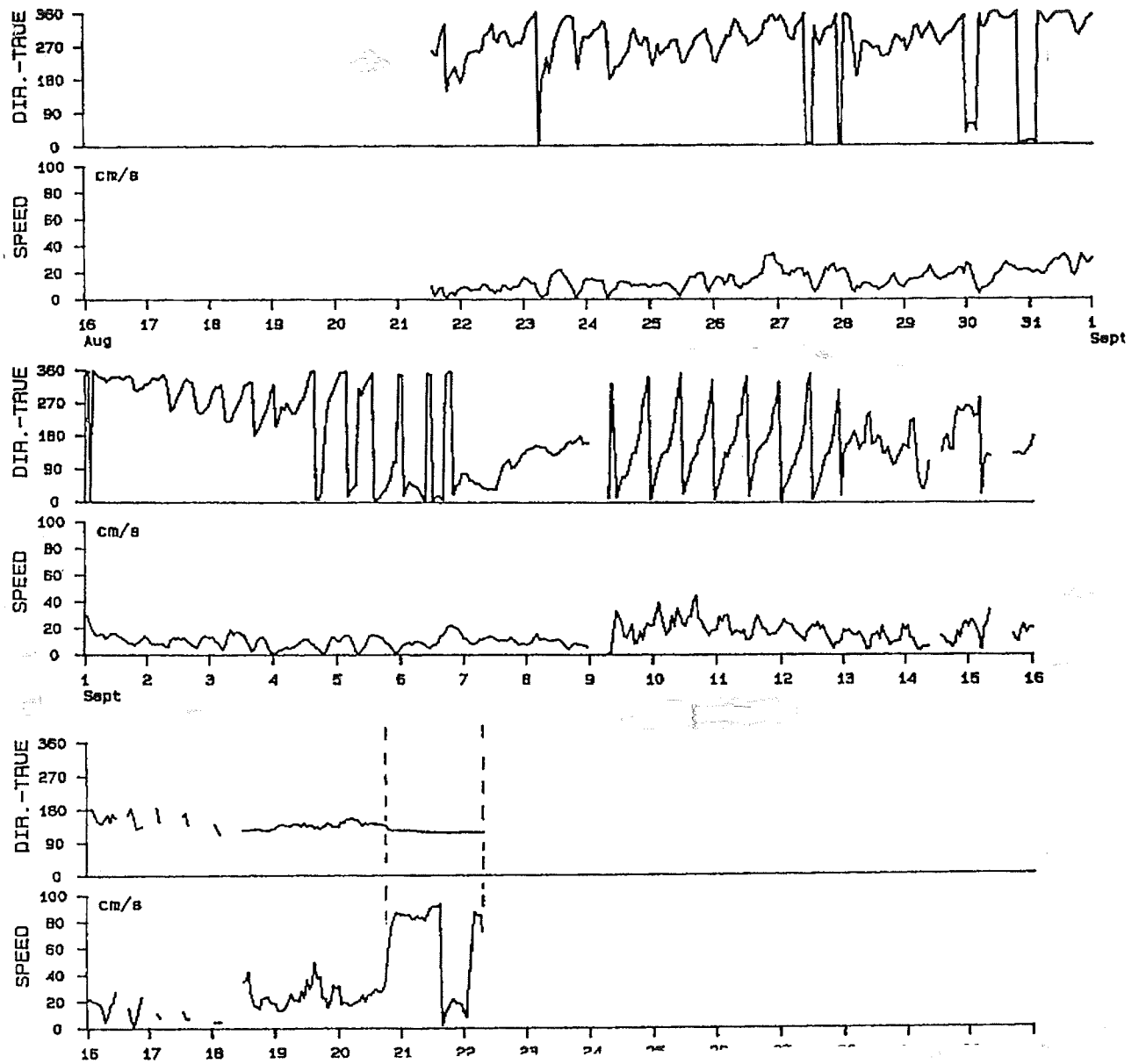
region, with periods of easterly winds interrupted by less directionally stable periods of the north to northwesterlies. A particularly long northwesterly event is recorded between May 15 and 21. No wave hindcasts have been carried out specifically for the delta, but Pinchin and Nairn (1987) completed hindcasts to the King Point site and to a deep water site west of Herschel Island (Explorer IV, Fig. 6.1). As discussed in Section 5.7, prediction of waves at King Point is problematic due to the complexities of local orographic winds and tracking of low pressure systems along the coast. A wave hindcast for the delta coast would be possible based on either Explorer III winds for the 1985 period or on Tuktoyaktuk winds for a longer period. However, to date there have been no successful measurements of waves in the trough or delta region to calibrate hindcast waves. A further complication would be the transformation of deep water waves across the very low slope of the inner shelf fronting the delta.

Current data from the inner shelf of this region is also lacking. Near surface current data is available from the Adlartok site (Fig. 6.26). Although these data are from a site located in over 66 metres of water, they contain an interesting event which may be relevant to the coastal zone. For the most part, currents remain less than 20 cm/s and fluctuate in direction according to wind direction. However, following the five days of strong northwesterly winds from May 15 to 20, a sudden increase in current velocity is present on the current meter record late on May 20 and May 21. This current reached over 90 cm/s and flowed constantly to the southeast. Such an event is unusual for the Beaufort Sea and the data was considered suspect by Birch (1988) following initial data reduction. However, my own independent observations at the Explorer III and on M/V Broderick, which was anchored at the same site during this event, suggest that it is in fact real. The current which was visibly estimated at 3 to 4 knots (>100 cm/s) caused severe manouevring problems for shipping and led in one instance to the breaking of a mooring line between the Explorer III and a tugboat. The current was also strong enough to deflect the steel drilling casing being used on the Broderick and prevent spudding of a drill hole.

The cause of this very strong current is not known but warrants investigation. It raises the possibility of there being extreme currents and processes at work in Mackenzie Trough, about which very little is known.

There is some direct evidence for resuspension of seabed sediments on the inner shelf of the Mackenzie Delta. During the Nahidik 87 cruise, strong northwesterly winds on September 13 caused the termination of seismic surveying and the ship to hove to in approximately 10 m of water to ride out the storm. During the ten hours of the peak of the storm, significant drift of the ship was noted despite the fact that it was anchored, and major discoloration of the water around the ship due to the high SSC was apparent. Half-litre water samples taken during this period contained enough sediment to settle out 0.5 cm of sediment. Measurements of SSC on these samples have not been made to date as they were taken for palynological analysis still to be





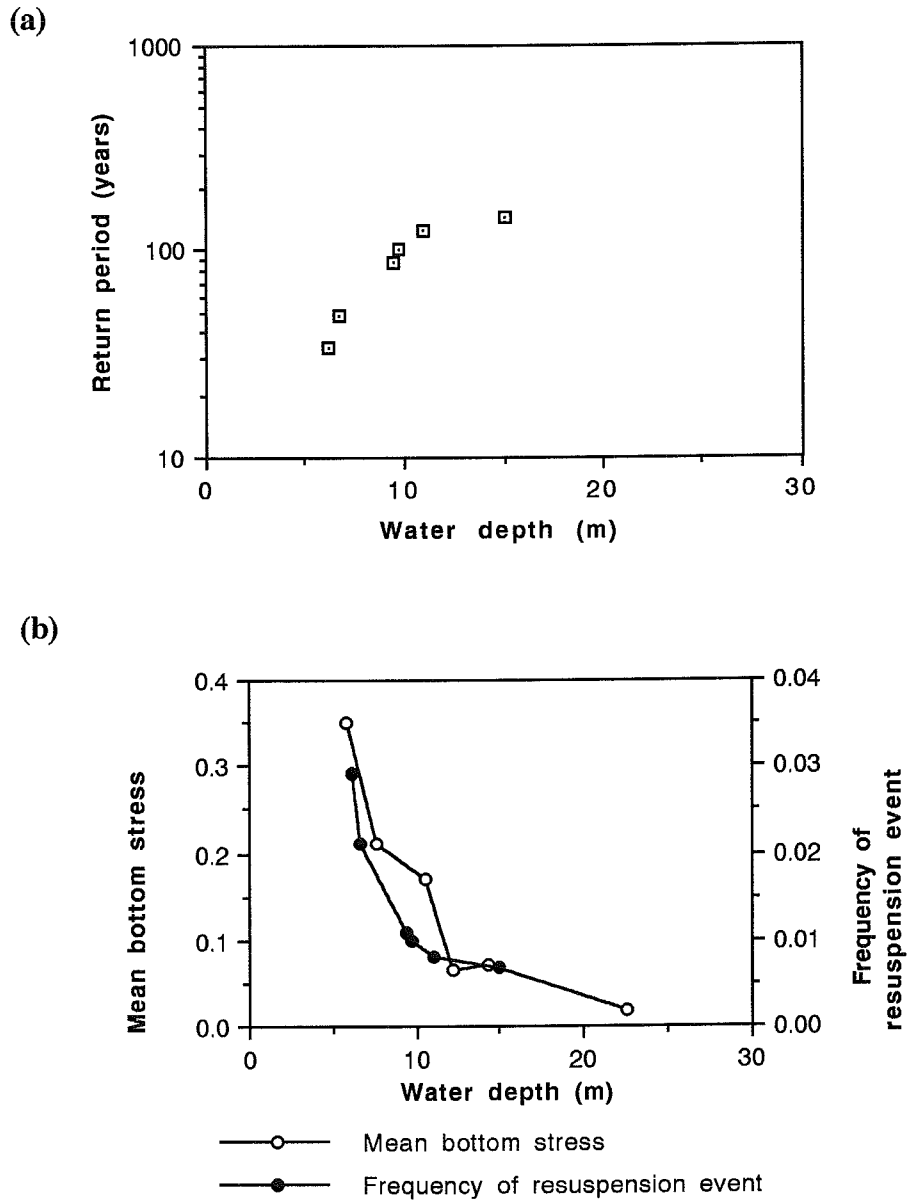
**Figure 6.26** Near surface current data from the Adlartok drill site in the Mackenzie Trough, August and September, 1985.

completed. However, rough calculations indicate that SSC values in the order of several grams per litre were present. Such values would be consistent with values obtained from optical backscatter sensors further east in 1986 (Hodgins et al., 1986). Assuming such concentrations were present throughout the water column, the resultant deposit from this suspension may have been in the order of 1 centimetre or more thick.

Sedimentological analysis of cores from the same region has revealed the presence of thick graded sand and silt beds, showing a range of high energy sedimentary structures (section 6.5). The relative frequency and intensity of bottom reworking can be determined from the proportion and thickness of silt and sand beds compared to clay beds in each core (Fig. 6.14). In water depths of 10 m or greater, silt beds are very thin and comprise a very minor part of the core sequence. The proportion and thickness of silt beds increases into shallower water, becoming predominant inshore of approximately 6 m water depth. Cores from 3 to 4 m water depth consist of almost entirely silt and fine sand with very thin clay interbeds occasionally preserved. It is these cores that show the wide variety of wave and current structures. The core data clearly indicates that storm waves and currents cause frequent resuspension in water depths less than 6 m, with the intensity increasing into shallow water. Silt beds in cores from deeper water (6 to 10 m) record relatively infrequent reworking which presumably relates to extreme wave conditions.

Extrapolating sedimentation rates from dated cores to the east, a quantitative estimate of the frequency of significant storm beds can be obtained. Figure 6.27 (a) shows the return period of silt beds in the cores from deeper than 5 m water depth shown in Figure 6.15. Cores from shallower water were not used because the silt beds are so thick that erosive events probably removed previous deposits. From Figure 6.27 (a), it can be seen that the silt beds in approximately 10 m water depth correspond to events with a 100 year return period and the return period decreases in shallower water. Extrapolation of this curve suggests that seabed less than 4 m water depth is reworked every year. Figure 6.27 (b) is a plot of the same data as the frequency of bottom resuspension, superimposed on a plot of mean bottom shear stress which was derived from wave and current measurements at various shallow water sites in the Beaufort Sea (Davidson et al., 1988). As would be expected, both bottom shear stress and frequency of resuspension show a similar hyperbolic decrease with water depth implying a close relationship between the two variables. This provides some confidence that the silt beds are related to storm events and the method may therefore be useful for evaluating the probability of scour in the Beaufort Sea.

One final issue related to sediment transport in the Mackenzie Delta area that should be mentioned is the potential for liquefaction. Cyclic loading tests by Konrad (1985) suggest that under the right loading cyclic conditions, Beaufort Sea silt would be susceptible to liquefaction. The seabed of the inner shelf region of the delta consists predominantly of silt and fine sand and is in a zone of significant wave action. Qualitatively therefore, the potential for wave-induced



**Figure 6.27** (a) Return period for resuspension events based on silt beds in cores; and (b) the same data plotted as the frequency of bottom disturbance with values of mean bottom stress derived from wave and current data from various sites in the Beaufort Sea (data from Davidson et al., 1988).

liquefaction might be considered quite high. Convolute bedding is a common feature of cores from 3 to 4 m water depth. However, convolutions may be caused both by dewatering during rapid deposition of the bed or by subsequent loading. To date, no indications of liquefaction have been observed in sidescan sonar records or seismic profiles. In other delta areas where liquefaction is known to occur, slide failures and collapse structures are visible on these types of record (Prior and Coleman, 1980; Prior et al., 1986). However, they are generally associated with a relatively steep seabed slope compared to that seaward of the Mackenzie Delta. Too little is presently known about seabed conditions in the Mackenzie Delta to exclude the possibility of liquefaction in offshore sediments.

## 7. GARRY ISLAND TO SUMMER ISLAND

This section deals with the coastline of Richards Island and the ring of islands immediately seaward of the island (Fig. 7.1). The western part of Richards Island is technically part of the Mackenzie Delta, being low-lying and dissected by distributary channels. Small outliers of higher ground occur within the delta plain of western Richards Island. Eastern Richards Island and the peninsula of North Point consist of more elevated land (< 50 m) dissected by numerous thermokarst lakes. Whereas the western coast of North Point is relatively continuous, the eastern coast is very irregular with numerous small islands lying close to the mainland. Beluga Bay is the broad, shallow bay between North Head and Kendall Island. Access to Beluga Bay is limited by the presence of several large islands: from the west, Garry, Pelly, Hooper and Pullen Islands. Pelly and Pullen Islands show relief similar to Richards Island, but both Garry and Hooper Islands have greater relief with elevations reaching to almost 70 m.

### 7.1 Quaternary Geology

The detailed surficial geology of the area is shown in Figure 7.1. This region lies within the maximum glacial limit as suggested by Rampton (1988; Fig. 2.3). Ice thrust deposits, related to this limit, and interpreted to be early Wisconsinan in age, are found on Garry and Hooper Islands. Ice contact deposits and meltwater channels, found on southern Richards Island, and a discontinuous line of outwash plain deposits, forming outliers within the Holocene delta deposits along the western margin of the island, are also associated with this glacial advance. Rampton (1988) assigned these deposits to the Toker Point (glacial) Stade and correlates the glacial advance to the Buckland glaciation of the Yukon coastal plain (Rampton, 1982).

With the exception of the low-lying delta plain of eastern Richards Island, surficial deposits over most of this region are mapped as morainal material, which forms a veneer less than 1 m thick (Rampton, 1988). The morainal sediment consists of a gravelly clayey diamicton and overlies a laterally variable sequence of older deposits, interpreted by Rampton (1988) to be significantly older. Several units, some given formation status by Rampton, are identified in this area:

#### *(i) Kendall sediments and Hooper clay*

These sediments are exposed in the sea-cliffs in areas of ice thrusting, particularly on Hooper, Pelly, Kendall and Summer Islands. The Kendall sediments consist of interbedded sand and clay with an abundance of marine fossils. They are overlain by the Hooper clay, which contains thin beds of silt and sand, as well as marine fossils. Both sequences are generally thin, rarely exceeding 20 m in total thickness. They are the oldest sediments exposed in cliffs along this section of the Beaufort coast, although their absolute age is uncertain. Rampton (1988) asserts that

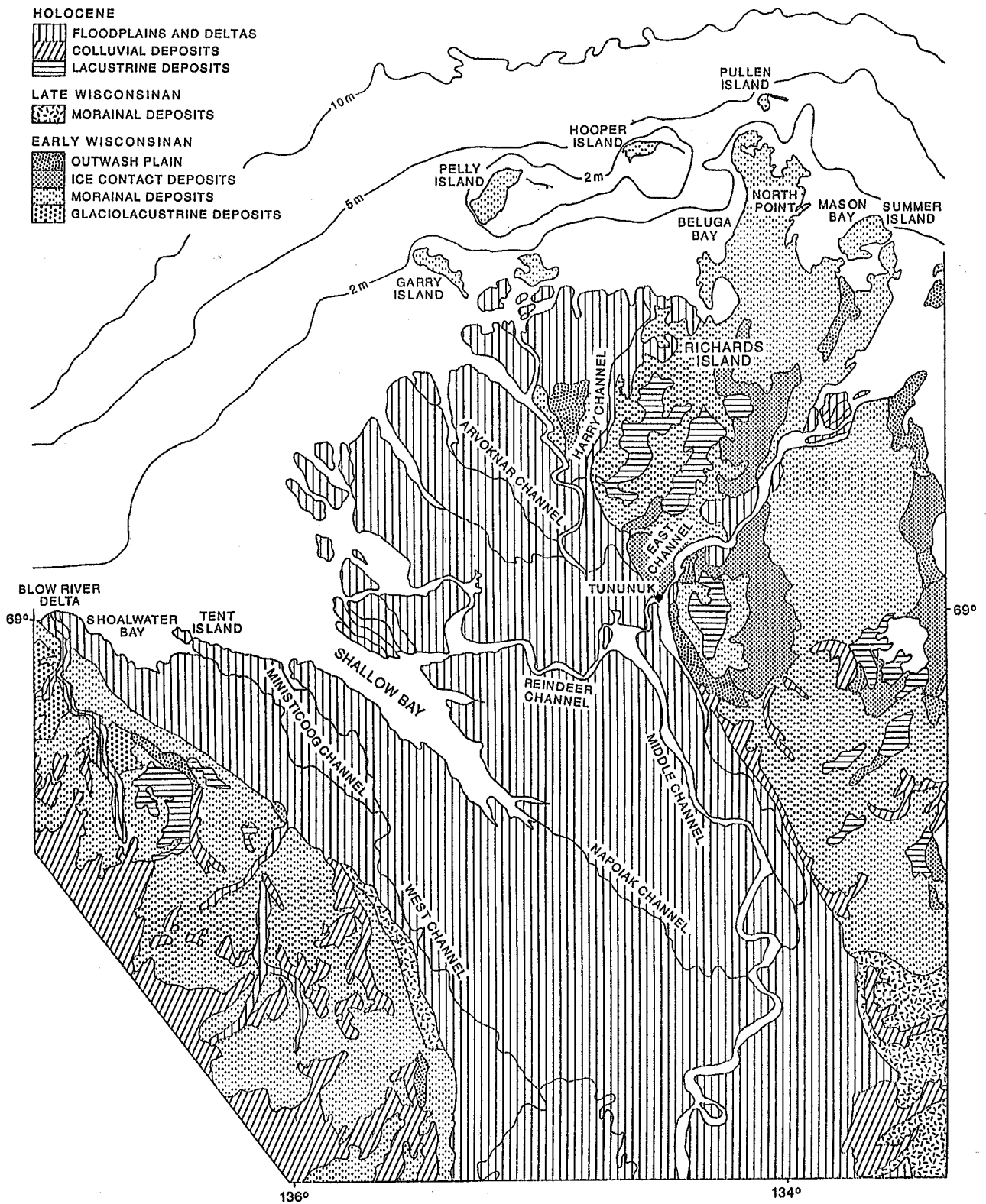


Figure 7.1 Detailed surficial geology of Richards Island area (from Rampton, 1988).

they are certainly older than Wisconsinan and tentatively places them as pre-Illinoian.

### **(ii) *Kidluit Formation***

The Kidluit Formation consists of grey, well-sorted, medium- to medium-fine grained sand in planar and, less commonly, cross-bedded units. The sands commonly contain wood detritus, coal fragments and gravel lenses. Both freshwater and marine shells have been recovered from the Kidluit Formation, but the marine shells were generally fragmented and thought to be reworked from the underlying marine sediments (Rampton, 1988). The thickness of the formation ranges from 2 m to 11 m and Rampton (1988) interpreted the depositional environment of the sands to be a braided alluvial plain. The formation is recognised over much of the Tuktoyaktuk coastlands from Liverpool Bay to Pelly Island. Its age is poorly constrained, with all radiocarbon dates giving infinite ages, but Rampton tentatively suggests it pre-dates the Wisconsinan glaciation.

### **(iii) *Kittigazuit Formation***

Overlying the Kidluit Formation are light brown, silty fine-grained to medium-grained sands of the Kittigazuit Formation. This sand is characterised by cross-bedding on a variety of scales. Rampton (1988) described the bedding as foreset bedding. However, my own observations of the Kittigazuit Formation exposed on Summer Island, suggests that the stratification is more complex. On Summer Island, trough cross-bedded sand, with single cross-sets generally 1 to 1.5 m thick, overlie larger scale cross-bedding, where single sets are in the order of 4 to 5 m thick. The Kittigazuit sand contains few macrofossils, with the exception of a few twigs and lenses of fine organic material, but the organic lenses contain fossil arthropods in some abundance, suggesting non-marine conditions of deposition. The age and origin of the Kittigazuit Sand are as uncertain as other stratigraphic units described above. The sand pre-dates the last glacial advance, which Rampton (1988) and Mackay and Matthews (1983) place in the early Wisconsinan. The possible environments of deposition for the Kittigazuit sands include deltaic (Rampton, 1988), aeolian (Hopkins, 1982) or fluvial.

#### **7.1.1 *Ground Ice***

Most of the sediments in the area contain ground ice, either as ice bonding or as visible ice (Rampton, 1988). The distribution of ice in relation to the various stratigraphic units is difficult to document due to the rapid melting of ground ice upon exposure at a cliff face. Where fresh exposures have been visited, several forms of ground ice have been observed. Massive ice, interbedded with silt and clay of the Kendall sediments have been described by Rampton (1988). Ice wedges at the top of the Kidluit Formation have been described by Mackay and Matthews (1983). Further inland, ground probing radar surveys and boreholes reveal massive ice layers up

to 6.7 m thick in ice-contact glacial-fluvial sediments of possible early Wisconsinan age. Some of this ice has been interpreted to be buried glacial ice (Dallimore and Wolfe, 1988). Mackay and Matthews (1983) give average ice content values of 300% (proportion of ice to sediment by weight) for sediments in the cliffs of Hooper Island.

## **7.2 Coastal and Inner Shelf Morphology**

### **7.2.1 Sea Cliffs**

A variety of cliff types are present in this region. Harper et al. (1985) defined three major cliff types in their regional study of the Beaufort coast. These were: (a) ice-poor cliffs, usually consisting of sands or gravelly sands and dominated by debris-flow or surface wash erosion; (b) ice-rich cliffs, typically showing retrogressive thaw failures; and (c) low tundra cliffs, generally less than 1 m high. All three types of cliff occur in the Garry Island to Summer Island region. Low tundra cliffs dominate in the delta area to the west, whereas ice-rich and ice-poor cliffs are interspersed throughout Richards Island and the outer islands. The Harper et al. (1985) study is very generalized and somewhat subjective, but a detailed study of cliff landforms has not been carried out at a local scale.

The seaward-facing cliffs of North Point, Pullen Island and Hooper Island show the most erosional cliff profiles. In these regions active retrogressive thaw failure and gullying from surface run-off are common and cliff faces are kept steep by constant erosion at the toe of the cliff by waves. Mud flows from active thaw failures commonly flow across the beach, depositing lobes of sediment which are rapidly removed by wave action. Many sections of the coast, particularly along coastal sections sheltered from the north and west, have relatively stabilized cliffs. In these regions, it is not always clear whether the cliff initially failed through thawing or some other process (illustrating a weakness of the Harper et al. classification). However, the cliff may be stabilized by vegetation growth or protection from wave attack through the local presence of a beach storm ridge or driftwood armour. In areas of fine sediment deposition, for example along the western coast of North Point, cliffs may be stabilized by the accretion of an extensive supratidal marsh and/or intertidal mud bank.

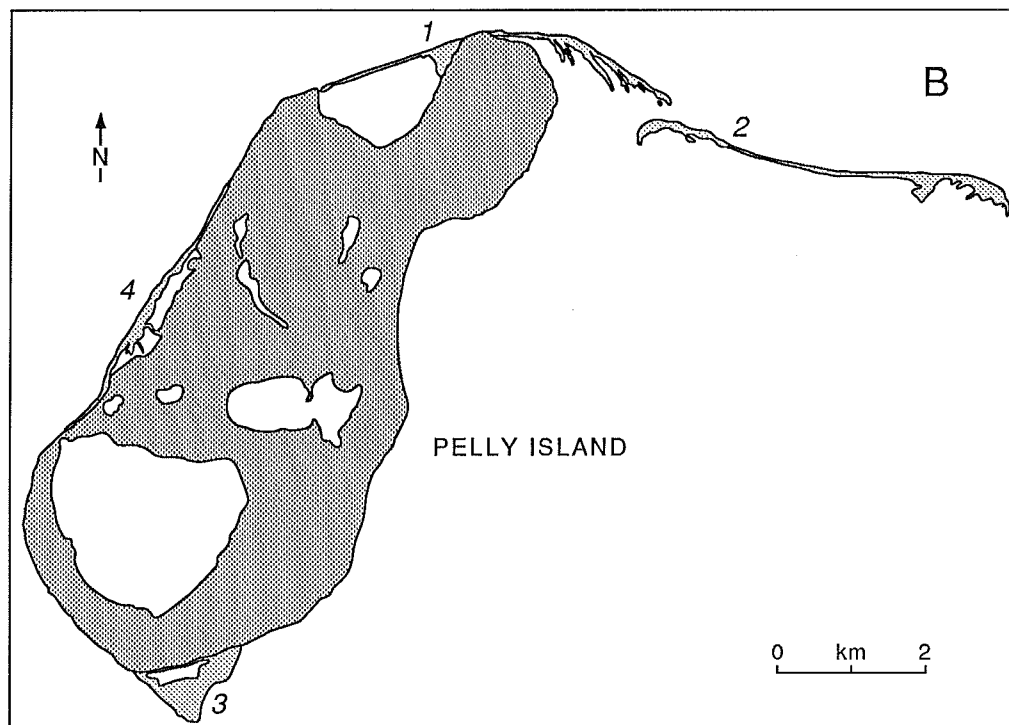
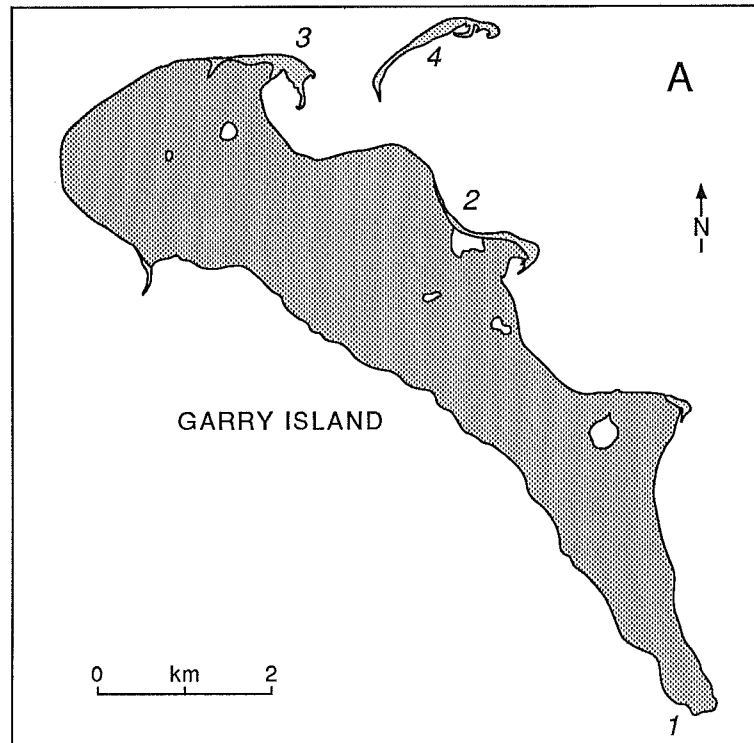
### **7.2.2 Spits and Barriers**

Spectacular spit, barrier and barrier island complexes have formed as a result of the erosion of Garry, Pelly, Hooper and Pullen Islands (Fig. 7.2). The descriptions here are based primarily on aerial photographs and the aerial video survey of Forbes and Frobel (1986).

#### *Garry Island*



**Figure 7.2a** Morphology of Garry Island.



**Figure 7.2b** Morphology of Pelly Island.

The southern tip of Garry Island is formed by an eastward prograding recurved spit, which encloses an extensive area of intertidal and vegetated supratidal flats (1, Fig. 7.2a). On the east coast, a broad embayment of the coast has been closed off by a narrow barrier to form a lagoon (2). Vegetated accretional beach ridges are present in the western end of the lagoon and behind a recurved spit complex that has formed off the eastern headland. At the northern end of the island, a small multiple recurved spit has prograded eastward (3) and is characterised by extensive washover flats and vegetated beach ridges. It is probably related to a disconnected barrier island (4), now separated by a broad inlet to the east. The barrier island has recurved ends and shows well-developed washover flats.

### *Pelly Island*

The northern end of Pelly Island is flanked on both sides by sandy spit and barrier systems (1, Fig. 7.2b). To the west of the headland, a narrow barrier spit has almost entirely enclosed a 2 km wide thermokarst lagoon. A narrow inlet separates the spit from the mainland to the southwest. To the east of the northern headland, a 2 km long multiple recurved spit has prograded eastward. It is separated from a 4 km long barrier island (2) by a wide inlet. The barrier island has a concave seaward plan, and complex southward-directed recurves at either end. Narrow washover flats are common along most the barrier island. The southern tip of Pelly Island is characterized by a series of accreted beach ridges which are largely vegetated (3). On the western side of the island, a broad embayment has been filled by a series of vegetated accretional beach ridges (4). The ridges have been substantially modified by thermokarst processes and are now fronted by a long narrow barrier and lagoon. At the northern end of the barrier, washover flats have prograded over the low-lying tundra surface.

### *Hooper Island*

Hooper Island is flanked on both east and west sides by prograded barrier systems (Fig. 7.2c). On the eastern side, a linear sandy spit extends 4 km from the island (1). Narrow washover flats characterize the distal end, but broader washover fans are more common on the proximal portion of the spit. In 1986, transverse bars were present on the backshore side of the spit and shore parallel bars were present in the foreshore. The western spit (2) curves southward and consists of broad washover flats behind irregular transverse beach ridges. The spit is breached at the distal end by numerous inlets.

### *Pullen Island*

Pullen Island consists of several tundra remnants linked by a complex of sandy barriers and washover flats (Fig. 7.2d). The southern part of the island consists of a multiple recurved spit (1)

Figure 7.2c Morphology of Hooper Island.

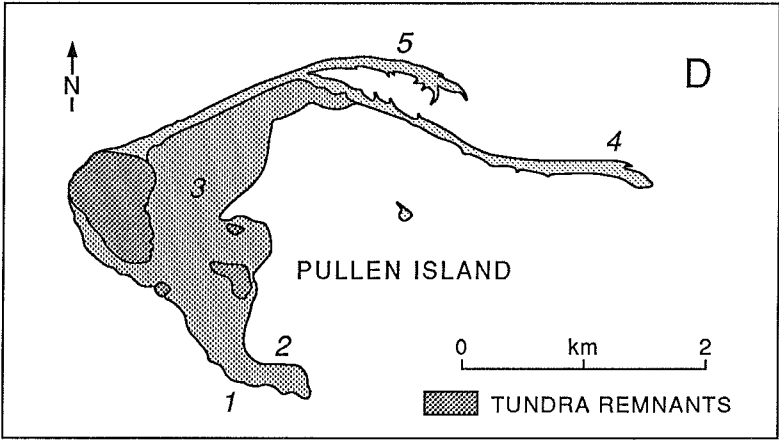
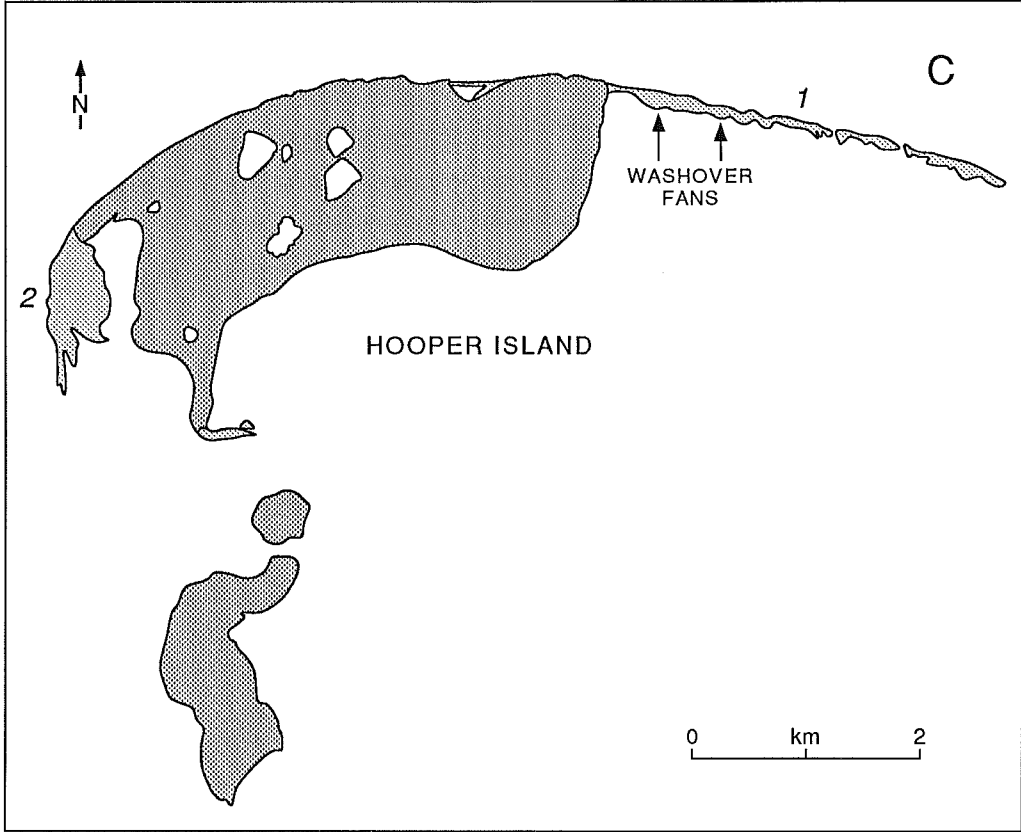


Figure 7.2d Morphology of Pullen Island.

extending towards the southeast. A second parallel spit (2) extends along the backshore of the recurved spit. Although not connected to the primary spit in the 1985 air photograph on which Figure 7.3d is based, the secondary spit was seen in the video survey of Forbes and Frobel (1986) to be longer and welded to a prominent recurve of the primary spit. The northern side of the island consists of a broad washover flat (3) fronted by a linear beach. At the eastern end of this beach, two spits extend to the east. An older spit (4) is deflected south from the line of the updrift beach and extends 3 to 4 km to the southeast. Broad washover flats are present at the distal end of the spit, while the proximal spit, now sheltered from the north by the younger spit, shows several transverse bars on its seaward side. The younger spit (5) has a recurved morphology and has prograded eastward to the north of the older spit.

### ***7.2.3 Deltaic Coast***

The low-lying delta plain coast forming the western part of Richards Island has two active distributary channels: Harry Channel, which flows to the east of Taglu Island and Middle Channel a branch of which forms a deep submarine channel extending offshore just south and east of Garry Island. Most of this coastal region consists of low-lying islands with bluffs less than 1 m high on their seaward sides. Intertidal flats are surprisingly uncommon except in the immediate vicinity of the two distributaries.

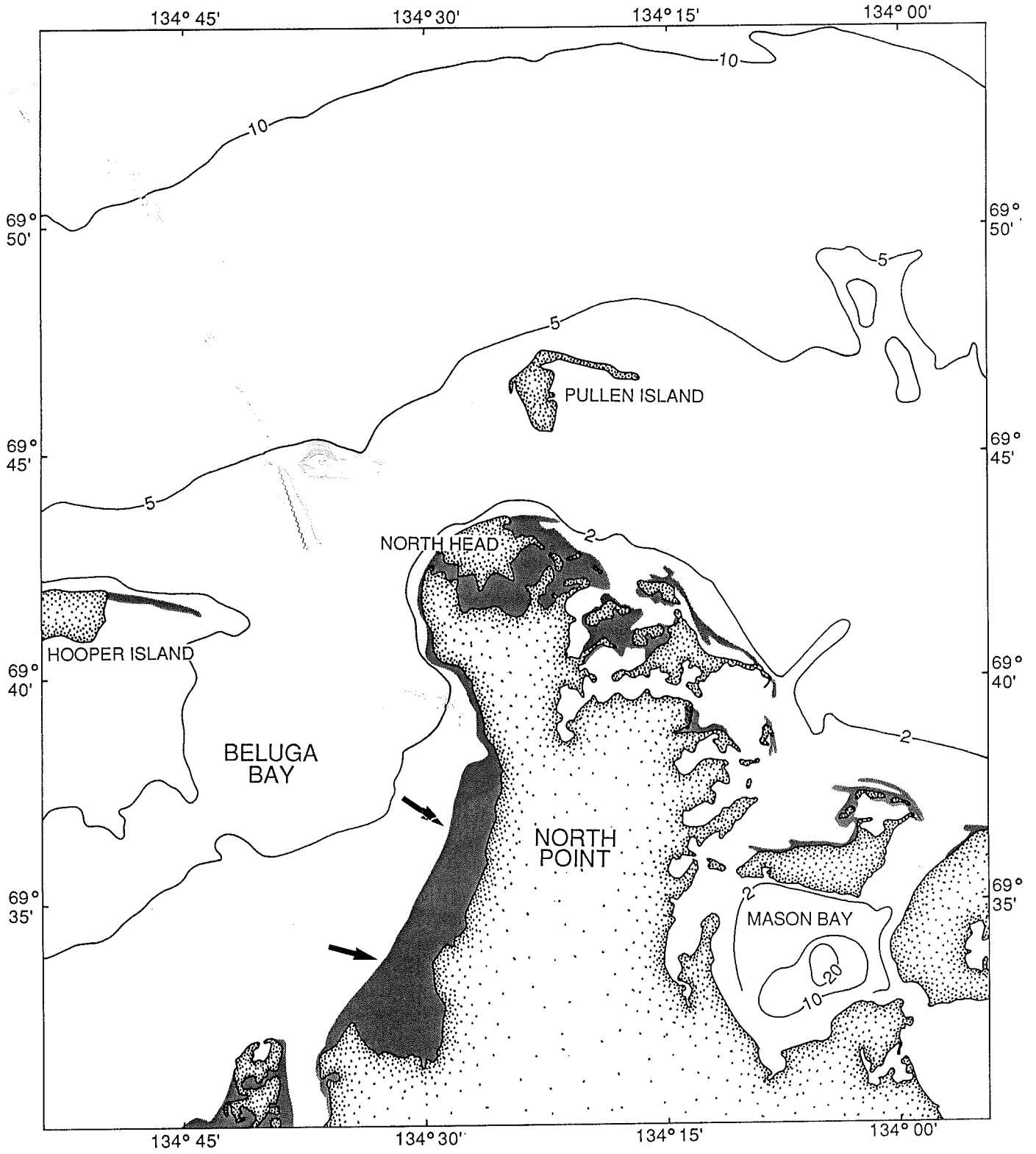
### ***7.2.4 Intertidal Flats and Mud Banks***

An extensive area of intertidal flats and a large, mainly subtidal mudbank border the western coast of North Point (Fig. 7.3). The mudbank infills a broad embayment and, although not seen on Figure 7.3, is separated from the coast by a narrow lagoon. Most of the bank is subtidal, but irregular, shore-parallel ridges are apparent on the surface of the subtidal bank from the air. The irregularity shown by these ridges increases in a shoreward direction and is probably caused by the wallowing of sea-ice blocks that get trapped on the bank during periods of high water. Parts of the bank were emergent during the 1986 video survey and had a smooth surface. No detailed studies of the mud bank have been carried out.

At the base of the coastal bluff along this section of the coast, supratidal marsh is developed as a fringing platform. A gravel or driftwood beach is also found at the base of the bluffs, but it is not known whether these are recent storm deposits or whether they are relict and the marsh has grown over them. The marshes also show some relief due to ice wallow, so that it is likely that the beaches are active during storm surges, when the water level is elevated.

### ***7.2.5 Breached Lake Coastline of Eastern Richards Island***

The eastern side of North Point has an extremely complex coastline, characterised by



**Figure 7.3** Intertidal flats and subtidal mudbank bordering the western coast of North Point.

numerous deep embayments separated by narrow peninsulas and islands (Fig. 7.4). This morphology results from the breaching and drowning of a dense pattern of thermokarst lakes. Extensive washover flats, intertidal flats, flanking spits and occasional barriers occur at the entrances to many of the embayments. Small pocket beaches and intertidal flats are present along the coastlines of the embayments themselves.

A long spit/barrier complex occurs in front of a small group of islands known as the Reindeer Islands (Fig. 7.4). Broad intertidal flats are developed behind the barrier and some dunes are present on the broad washover flats at its northern end. A second long spit system is developed off Summer Island.

### **7.2.6 Inner Shelf**

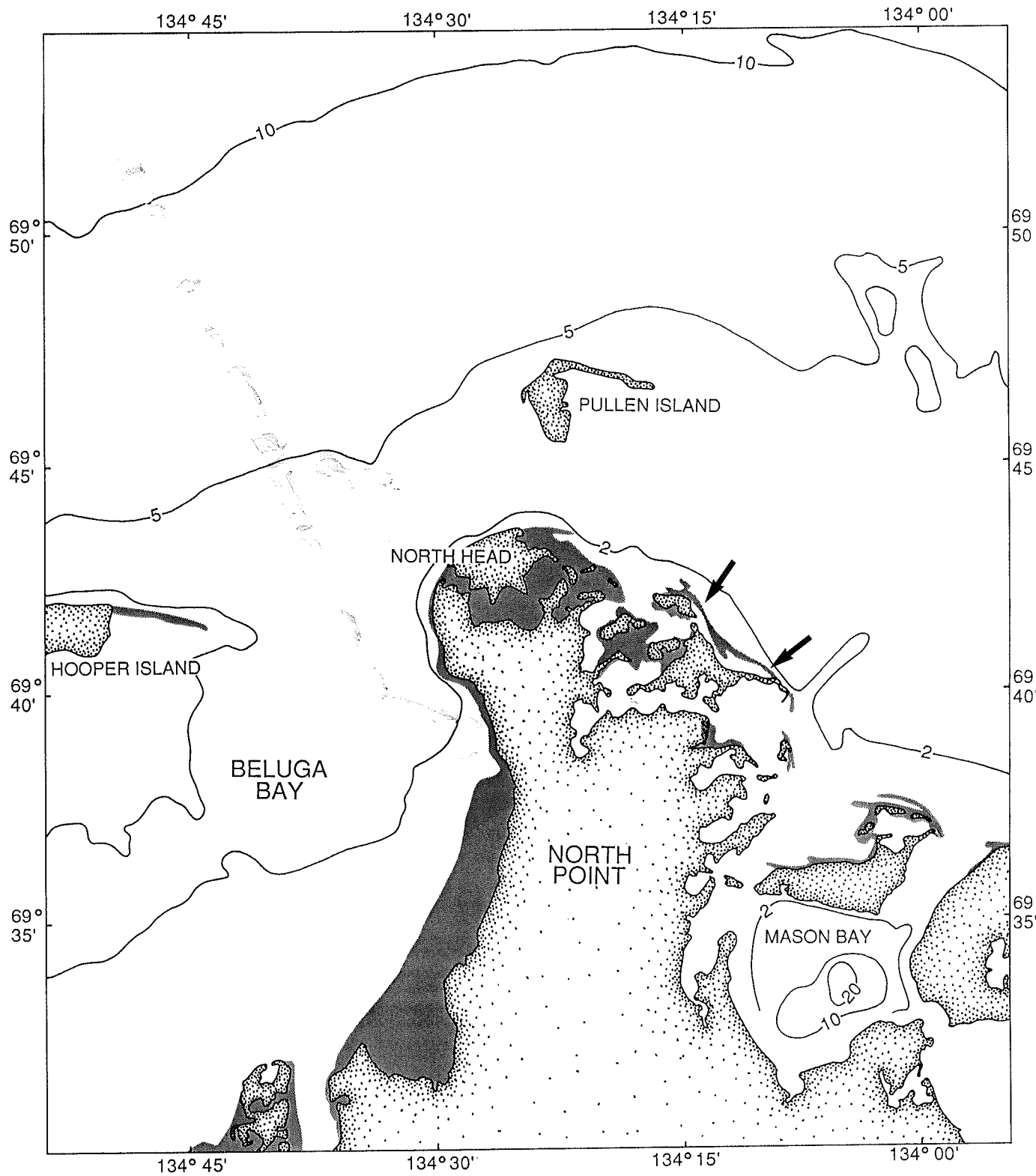
The inner shelf of this region, beyond the outer islands, slopes gently seaward to the 10 m isobath at approximately  $0.3^\circ$  (Fig. 7.1). The outer islands themselves are flanked by broad shoals, clearly delineated by the 2 m isobaths. Beluga Bay, behind the outer islands is extremely shallow, with no part of it less than 3 m deep. On the eastern side of Richards Island, an almost enclosed bay called Mason Bay is anomalously deep, with depths greater than 20 m in two small basins.

## **7.3 Coastal Change**

### **7.3.1 Coastal Retreat**

The islands off this section of coast have received considerable attention in terms of measuring coastal retreat over the last 30 years. As with the Yukon coast, measurements of coastal retreat from both aerial photographs and ground surveys are available and the two data sets show reasonable consistency (Table 7.1). Most of the data are from the outer islands, where retreat rates are high. The cliffs of Pelly Island and Pullen Island both retreated at rates over 5 m/a between 1971 and 1976, with a maximum rate at one site of 13.2 m/a. The single site on Pelly Island that was resurveyed in 1984 and 1986, shows a decrease in retreat rate during the 1980's. This change may be in part an artefact of the surveying method which relates to the cliff top, so that high variability is expected in regions where retrogressive thaw failure is an active process (Forbes and Frobel, 1985). Hooper Island shows retreat between 1.4 and 2.7 m/a with no consistent change over the various time periods measured. Garry Island shows the most modest rates of retreat at 0.7 to 1.8 m/a.

On the mainland, the highest rates of retreat are observed along the northwest-facing bluffs of North Head (the northern part of North Point) with rates between 0.6 and 3.2 m/a (Fig. 7.5). South of North Head, along the western coast of North Point, the coastal bluffs are stable, being fronted by broad intertidal flats. Elsewhere on the mainland, measurements from aerial

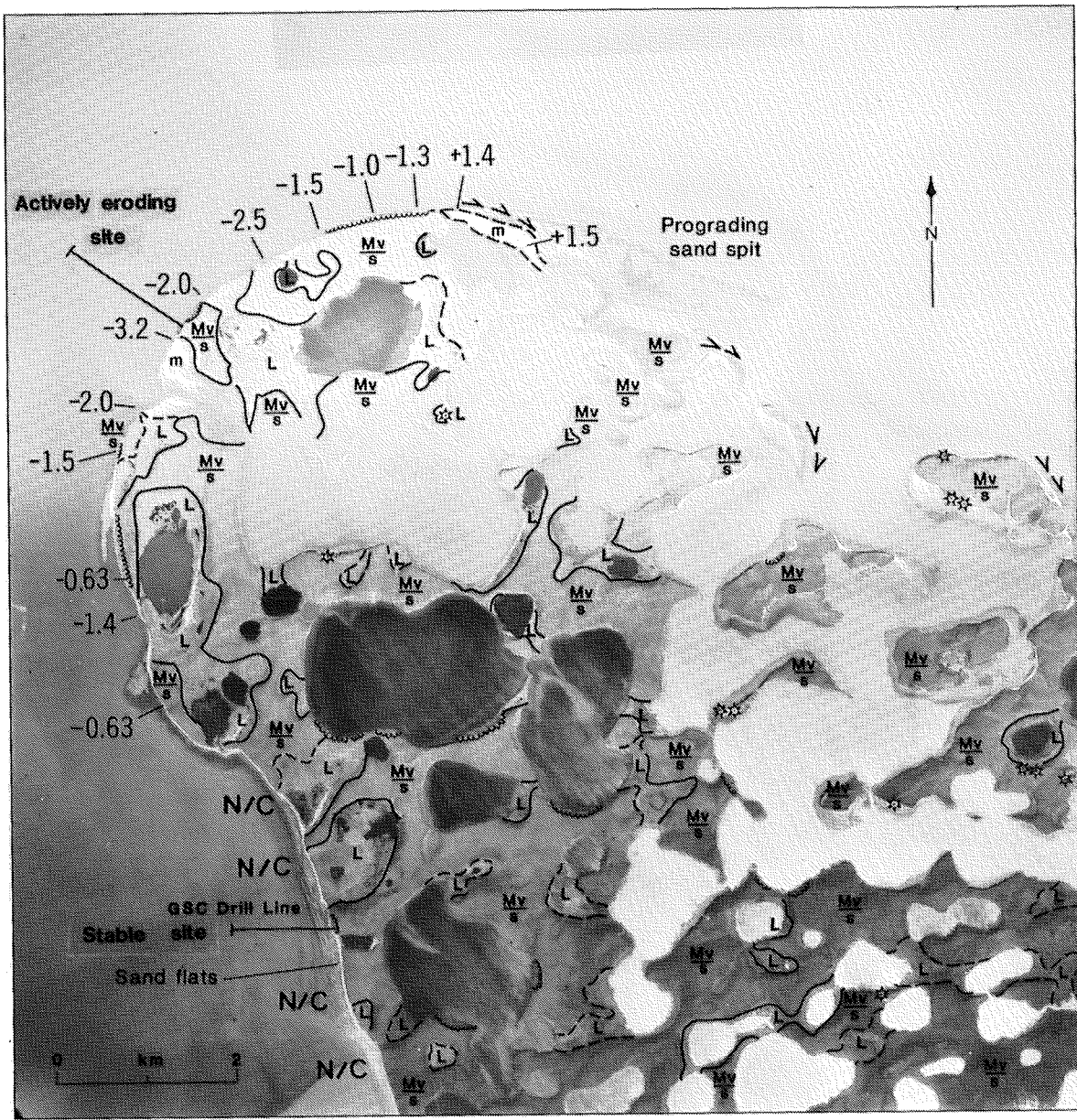


**Figure 7.4** Morphology of eastern Richards Island.

**Table 7.1** Cliff Retreat Rate Measurements in the Garry Island to Summer Island region.

Site	Harper et al. (1985) Aerial Photographs (1950-73/4)	Forbes and Frobel (1985) Ground Surveys (1964-71) (1971-76) (1976-84)	Gillie (1987) Ground Surveys (1984-86)
<b>Garry Island</b>			
1	(Average) 1.04	1.8 ( $\pm 0.3$ )	1.5 ( $\pm 0.5$ )
2		0.9 (0.1)	1.0 ( $\pm 0.2$ )
<b>Pelly Island</b>			
1			0.7 ( $\pm 0.1$ )
2a		5.5 ( $\pm 0.2$ )	1.2 ( $\pm 0.1$ )
2b	(Average) 5.81	13.2 ( $\pm 0.2$ )	
3a		7.0 ( $\pm 0.2$ )	
3b		7.9 ( $\pm 0.2$ )	3.5 ( $\pm 0.3$ )
4		7.7 ( $\pm 0.2$ )	2.1 ( $\pm 0.9$ )
<b>Hooper Island</b>			
1		9.7 ( $\pm 0.6$ )	
2		1.4 (0.1)	0.9 ( $\pm 0.0$ )
3		1.5 ( $\pm 0.1$ )	1.2 ( $\pm 0.1$ )
4		2.1 ( $\pm 0.1$ )	1.5 ( $\pm 0.1$ )
<b>Pullen Island</b>			
1	0.83	2.7 ( $\pm 0.4$ )	2.1 ( $\pm 0.4$ )
		<b>1972-76</b>	
		9.2 ( $\pm 0.2$ )	2.7 ( $\pm 2.3$ )





Sedimentation . . . . .  
 Stable coastline . . . . .N/C

Average coastal retreat (m/yr). . . . .-2.5

**Figure 7.5** Retreat rates around North Point (Dallimore et al., 1988)

photographs (Harper et al., 1985) show quite variable rates of retreat. The delta coastline of western Richards Island is retreating at approximately 1 to 2 m/a. On the complex coastline of eastern Richards Island, retreat rates are generally less than 1 m/a, especially where intertidal flats front the coastal bluffs. On the more exposed headlands such as Crumbling Point on Summer Island, higher rates of retreat are observed, with rates as high as 2.5 m/a.

### **7.3.2 Spit and Barrier Evolution**

Significant changes of spit and barrier morphology along this section of the coast are noticeable in aerial photographs from the 1950's, 1970's and 1980's. Detailed analysis of the morphological changes was not carried out under this contract, as this research was being carried out separately by M.H. Ruz and A. Hequette. However, the following description of morphological changes at Pelly Island, from Ruz et al. (in prep.) is provided as an example of the rapid coastline changes occurring in this region.

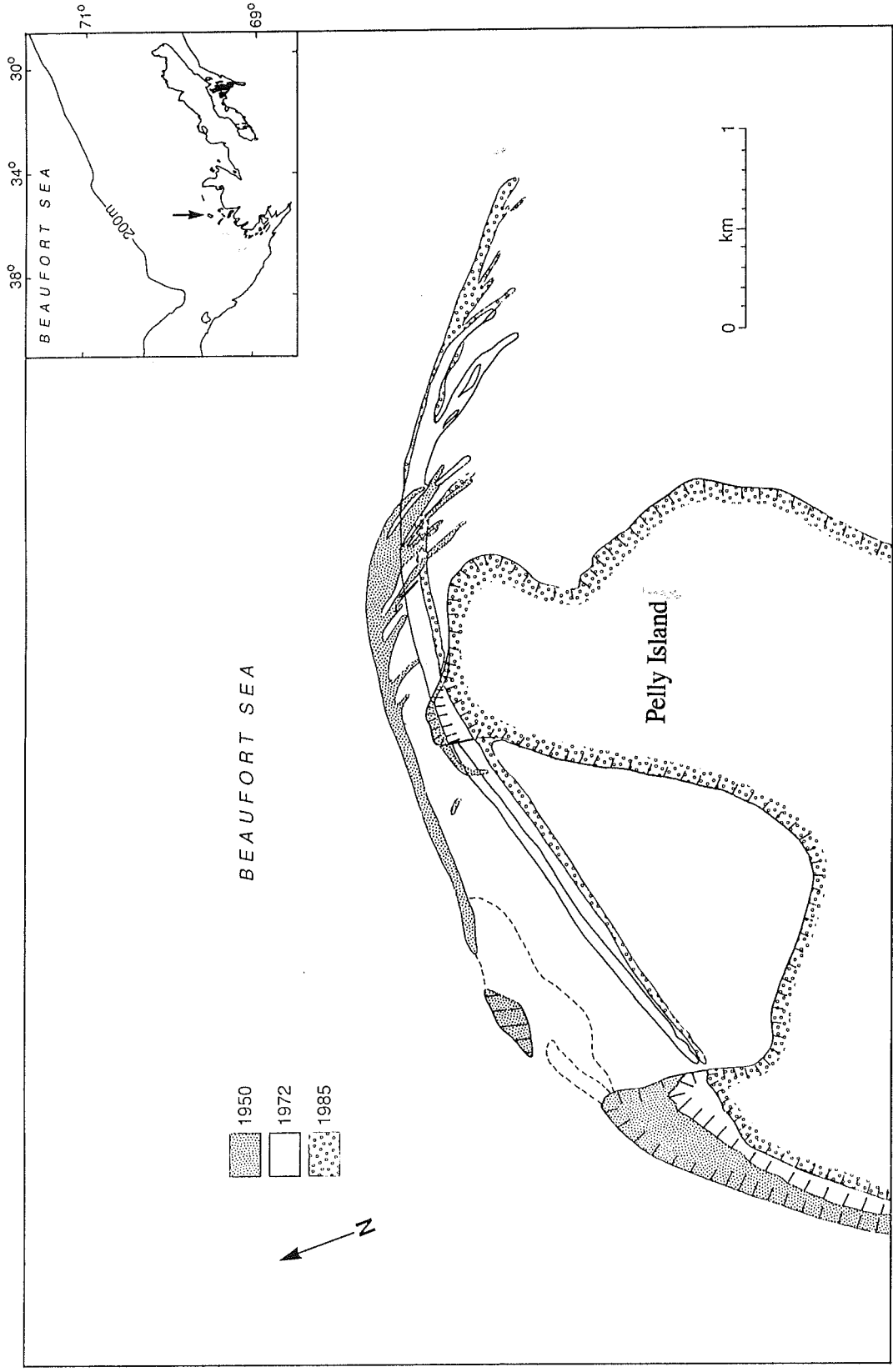
At the northern extremity of Pelly Island, a 2.5 km long barrier island lay eastward of a small island in 1950 (Fig. 7.6). Between 1950 and 1972, the small island was completely eroded and the barrier island migrated landward at an average rate of 12.3 m a<sup>-1</sup>. As the bluffs of the main island were retreating at a slower rate, the barrier became attached to the northern tip of Pelly Island by 1972, and was transformed into a double spit. Subsequently, the eastern spit lengthened and on both sides of the headland, the spits retreated at a much slower rate.

## **7.4 Seismic Stratigraphy**

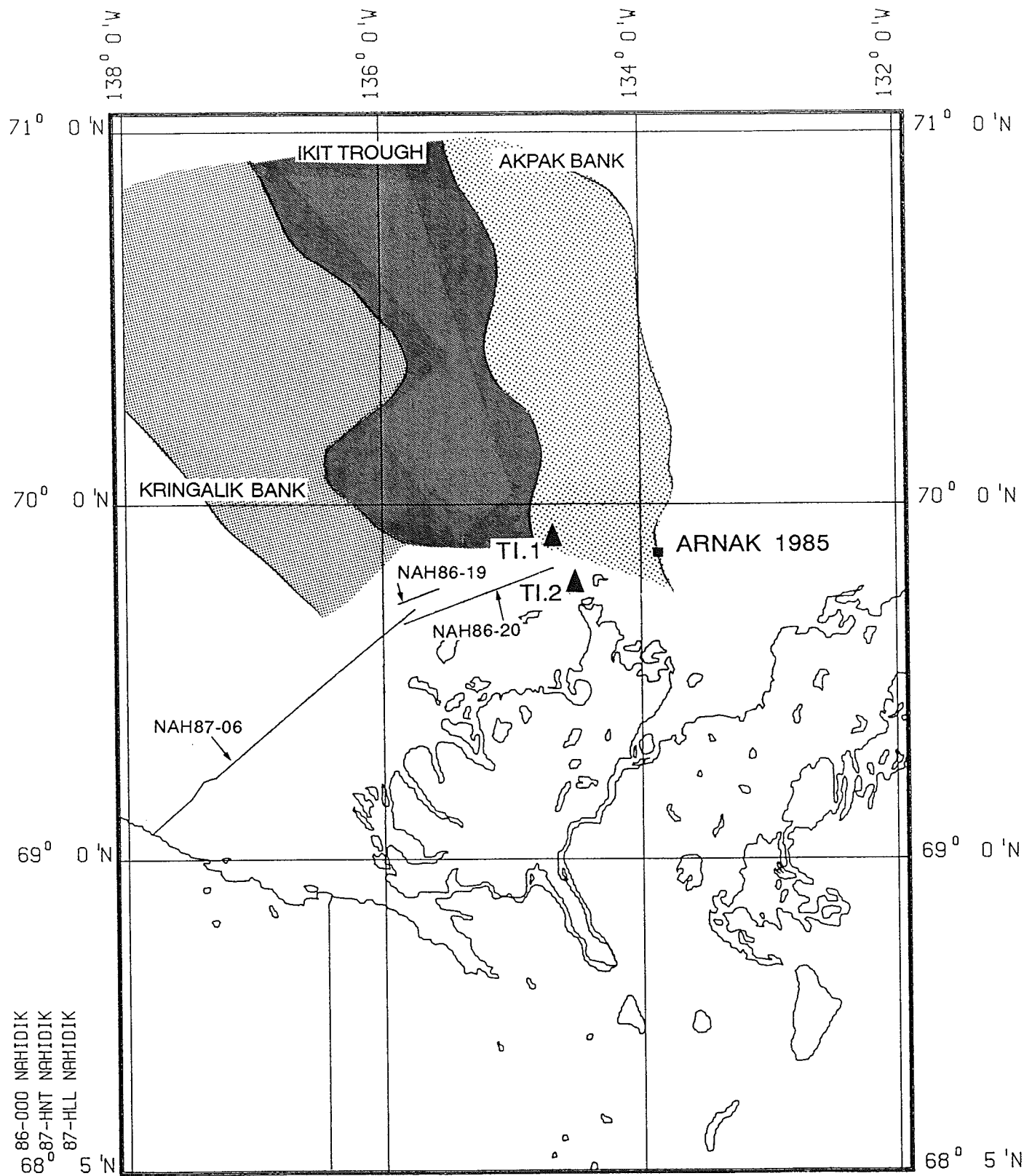
The Garry Island to Summer Island section of the coast corresponds to three zones defined by O'Connor (1982b) and used in PERD studies of offshore stratigraphy, permafrost and geotechnics. The three zones, namely Kringalik Bank, Ikit Trough and Akpak Bank (Fig. 7.7) have distinctive seismic, stratigraphic and geotechnical characteristics (O'Connor, 1982b; Hill et al., in prep.) and have been adopted by industry geotechnical engineers for discussion of seabed conditions. During seismo-stratigraphic analysis for this contract, it became apparent that the zones could be extended to the coastal zone and form a convenient basis of subdivision for the region between Garry and Summer Islands. In the following discussion of seismic stratigraphy, the same zonation is therefore used.

### **7.4.1 Kringalik Bank**

The seismo-stratigraphy of Kringalik Bank has proven difficult to interpret in detail. O'Connor (1982) recognised two "unconformities" on the middle shelf which could be traced as far as Ikit Trough. Hill et al. (in prep.) later suggested that only one of these unconformities was truly erosional and significant regionally, but noted the presence of laterally discontinuous and



**Figure 7.6** Pelly Island morphological change from 1950 to 1985 (after Ruz et al., in prep.).



**Figure 7.7** Seismic track chart - Garry Island to North Head.

local erosion surfaces on shallower parts of the bank. These were interpreted to indicate that significant sedimentation occurred during transgression, resulting in a complex sequence of fine-grained coastal sediments.

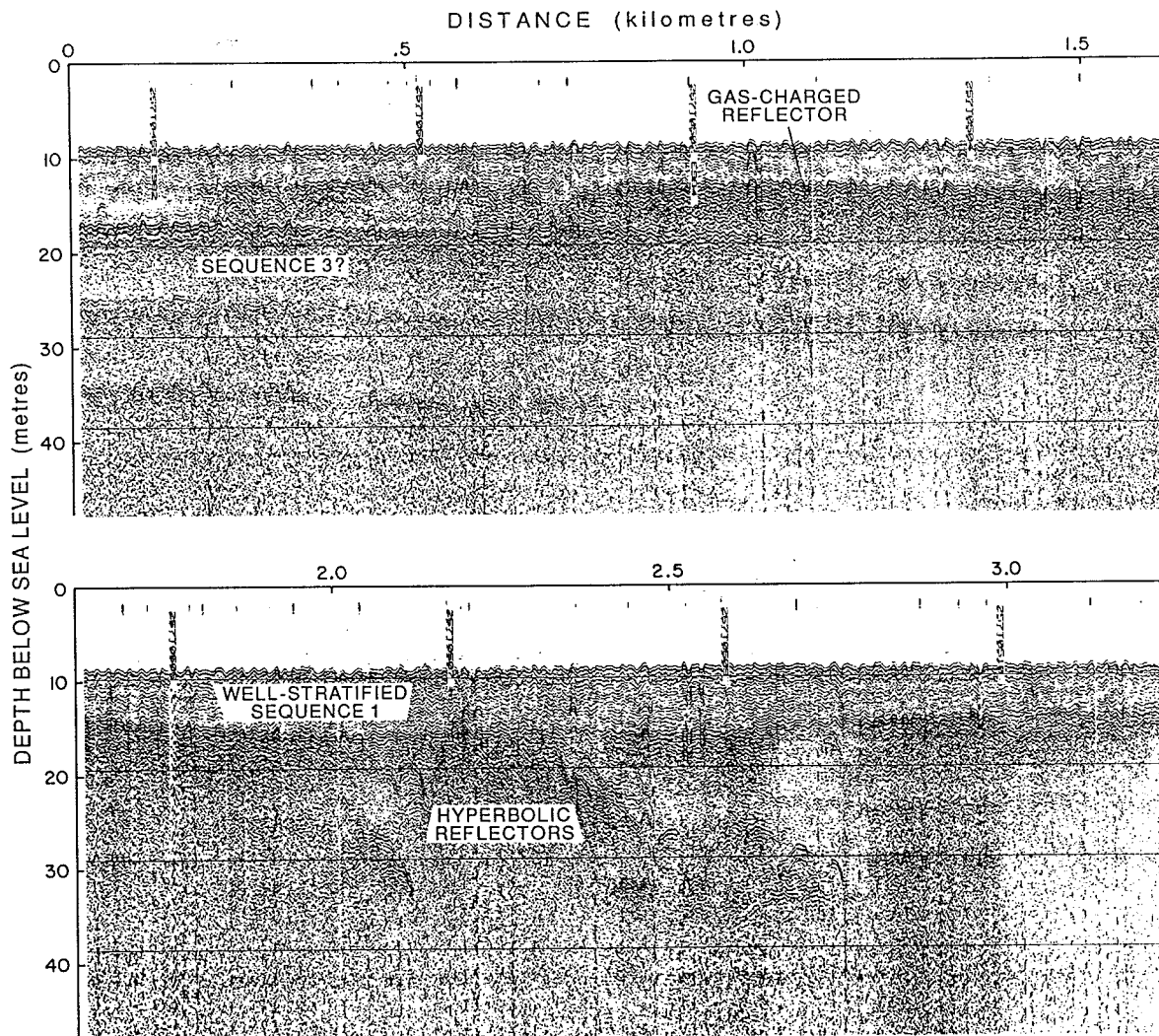
Relatively few good quality lines run across the inner shelf of Kringalik Bank. Three lines (NAH87-06, NAH86-19 and NAH86-20; Fig. 7.7) provide some information, but considerably more data are required to make more complete interpretation. Due to the presence of gas, the boundary between Mackenzie Trough and Kringalik Bank is not seen and interpretation is severely inhibited. Sequence boundaries are difficult to define as reflectors are rarely regionally continuous. Strong reflectors at several horizons can be traced for several kilometres and show discordant relationships, but these cannot be regarded as unconformities of regional significance and are therefore not used to define formal sequence boundaries.

In water depths greater than 5 m, a well-stratified to transparent unit is present at the surface over most of Kringalik Bank (Fig. 7.8). At the east and west sides, the near-surface stratified sediments are up to 9 m thick, but in the centre of the bank, the same unit appears to be thinner. This is partly as a result of true stratigraphic thinning (Fig. 7.9a) and partly because reflectors within the stratified sequence change character laterally, gaining amplitude and masking the underlying sediments (Fig. 7.8). The strong reflector at the base of stratified sediments in Figure 7.8 is the lowest stratigraphic horizon observed on Kringalik Bank in this study and may be equivalent to one of the regional unconformities noted by Hill et al. (in prep.) on the middle shelf.

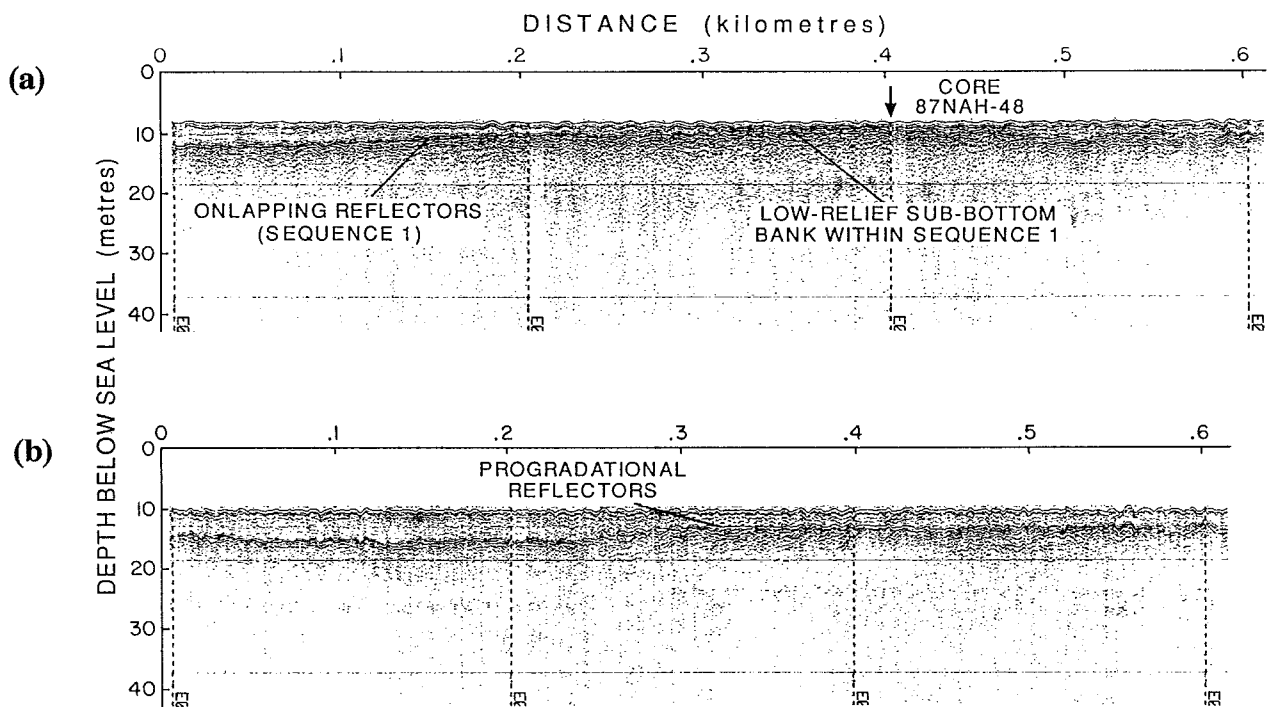
Some of the reflectors which originate within the stratified sediments can be traced into the central bank area as strong, possibly gas-charged reflectors (Fig. 7.8). They locally show gentle positive relief of one or two metres and in some locations possibly truncate underlying reflectors (Fig. 7.8). Rarely, these low-relief banks are underlain by dipping reflectors which suggest the relief is constructional (Fig. 7.9b). Overlying strata locally onlap these banks (Fig. 7.9a). At the centre of the Kringalik area, stratification is disrupted by gas, giving a hummocky reflector close to the seabed. Gas-disrupted areas are closely associated with the underlying strong reflectors within the stratified sediments.

In two locations, sections of numerous hyperbolic reflectors defining a high-relief sub-bottom surface are observed (Fig. 7.8). In both cases, stratified sediments dip inwards towards the hyperbolic reflectors, forming small basins. These features are similar in general appearance to pingo-like features (PLF's) observed elsewhere across the shelf (Poley, 1982). The basins have been completely infilled by stratified sediments leaving no relief at the seabed.

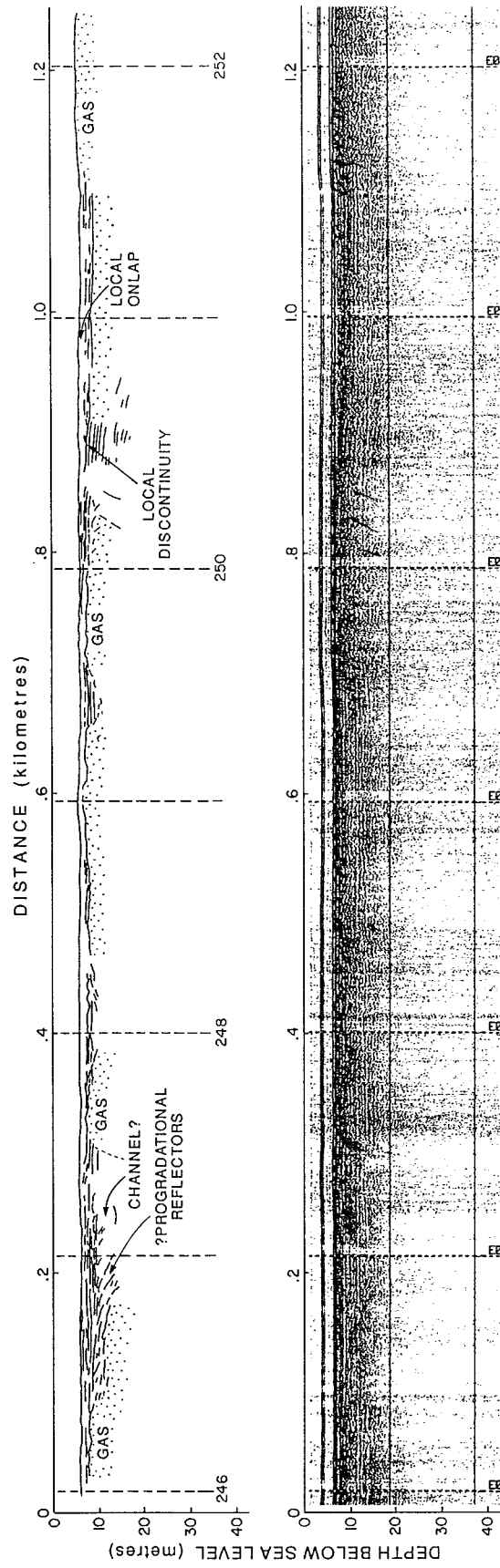
In water depths of around 5 m, as profiled on Line NAH86-21, sediments free of gas show a stratified character (Fig. 7.10). Subtle discontinuities can be distinguished within the stratified sediments, with local pinching out and onlap of reflectors over relief of 2 - 4 m. Windows through the gas reflectors give the impression of small channel or basin features. It cannot be determined



**Figure 7.8** Seismic profile 87-06, showing the well stratified character of sequence 1 over most of Kringalik Bank.



**Figure 7.9** (a) Seismic profile 86-20 194-200, showing stratigraphic thinning of sequence 1 over the centre of Kringalik Bank (b) Seismic profile 86-19, showing progradational reflectors within a low relief bank of sequence 1.



**Figure 7.10** Stratified character of gas-free sediments on Kringalik Bank; seismic profile 86-21.



whether these features are related to real sub-bottom morphology or merely an artefact of the gas distribution.

#### **7.4.2 *Ikit Trough***

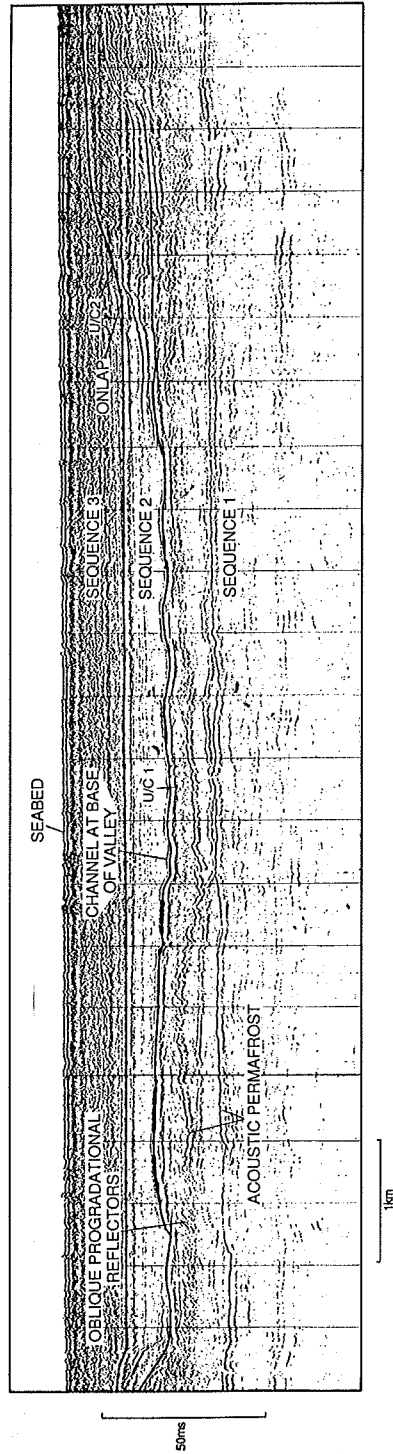
Detailed interpretation of the sequence in Ikit Trough is inhibited mainly by data quality as coverage is mostly with NAH86 lines (Fig. 7.7). Shallow gas is present inshore of the 5 m isobath, but does not extend so far offshore as on Kringalik Bank. The seismic stratigraphy of the inner shelf portion of Ikit Trough is similar to that described by O'Connor (1982b) and Hill et al. (in prep.) for the middle shelf (Fig. 7.11). These authors identified Ikit Trough as a linear valley feature, filled with two unconformity-bounded sequences, an older one restricted largely to the valley sides and a younger one showing onlap against the valley margins and almost filling the original topographic feature.

On the inner shelf, the base of the valley can be recognised at between 30 and 35 m below present sea-level in N-S lines NAH86-15 and -16 (Fig. 7.12). At one location, on Line 86-20, a reflector at approximately 52 m b.s.l. may represent a deeper part of the trough (Fig. 7.13). This reflector can be traced up to a flat-lying terrace at an elevation of 36 m and then rises again to merge with a strong reflector at 24 m b.s.l. Just below this surface, a sequence of faint cliniform reflectors, forming a wedge-shaped unit, can be recognised. This unit may be equivalent to Sequence 2 of Hill et al. (in press; Fig. 7.11). In E-W lines, the base of the trough cannot be followed continuously across the whole area. Better quality profiles in the eastern part of the trough show that the underlying sequence, equivalent to Sequence 3 of Hill et al. (in prep.; Fig. 7.11) shows complex stratification. The base of the trough clearly truncates cut-and-fill stratification and in one location, a PLF is present at the base of the trough.

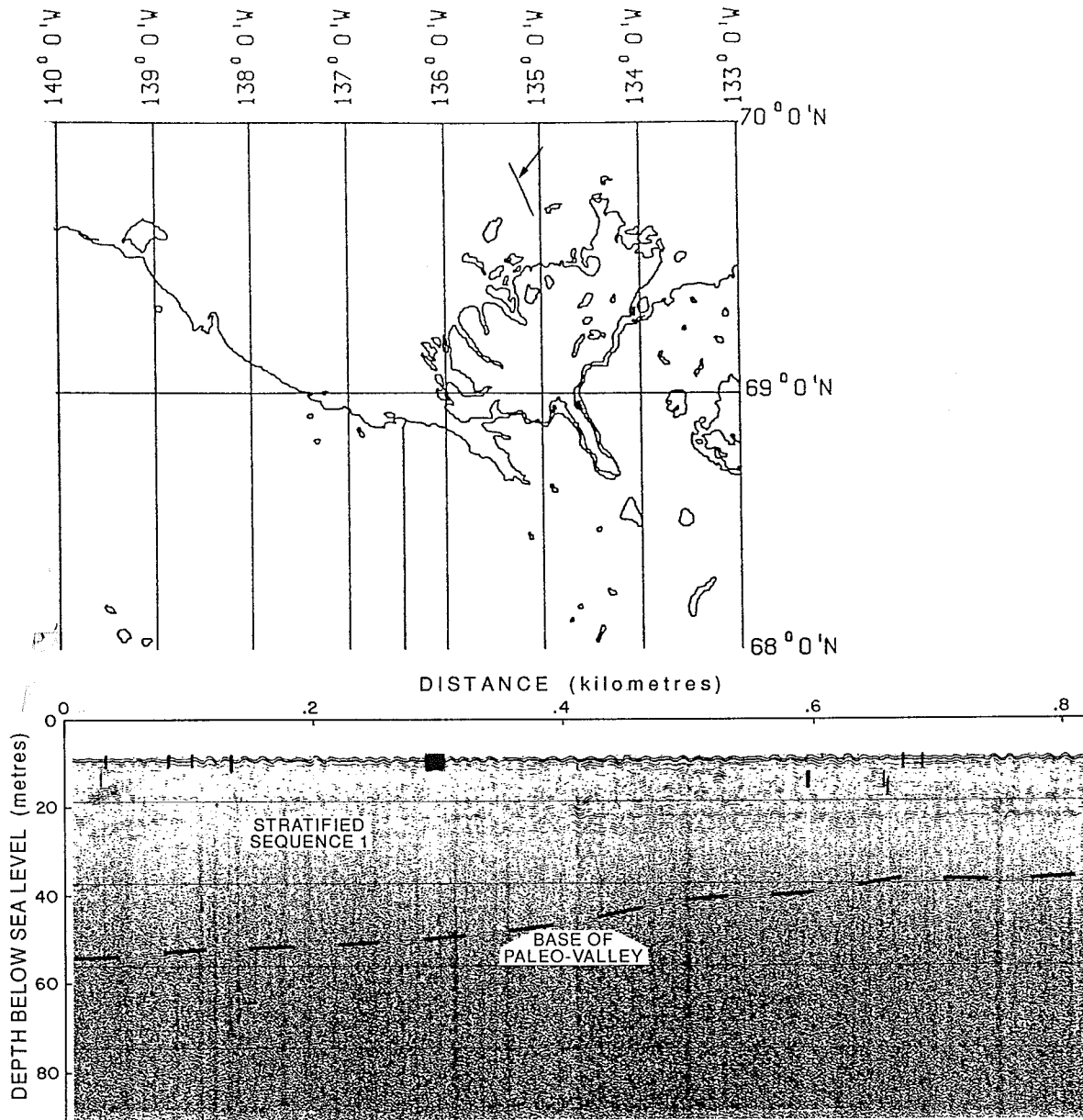
A stratified sequence up to 25 m thick, equivalent to Sequence 1 of Hill et al. (in prep.), overlies this clearly unconformable surface. The unit becomes more poorly stratified upwards and in deeper water. At the edge of the gas-masked zone, a strong gas-charged reflector is apparent within the stratified sequence at approximately 15 m b.s.l. (Fig. 7.14). This reflector is similar to one observed in Mackenzie Trough and occurs at exactly the same depth, implying some relationship between the two reflectors and possible regional significance to the -15 m b.s.l. datum.

#### **7.4.3 *Akpak Bank***

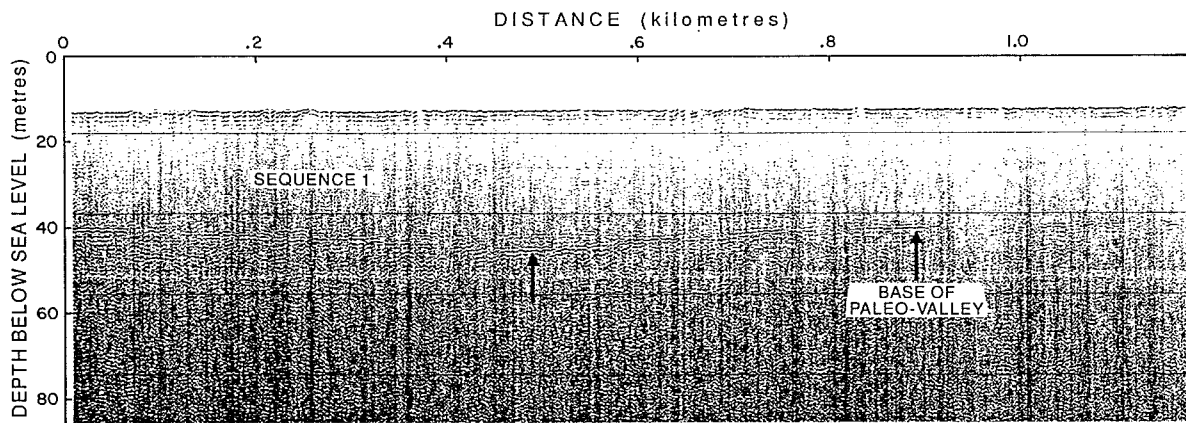
On the middle shelf of Akpak Bank, a relatively simple stratigraphy consisting of a lower complex stratified acoustic sequence overlain by a thin transparent sequence is present. An erosional unconformity separates the two sequences and, in places, thin basin-fill sequences are present at the unconformity. The boundary with Ikit Trough and Kugmallit Trough are clearly



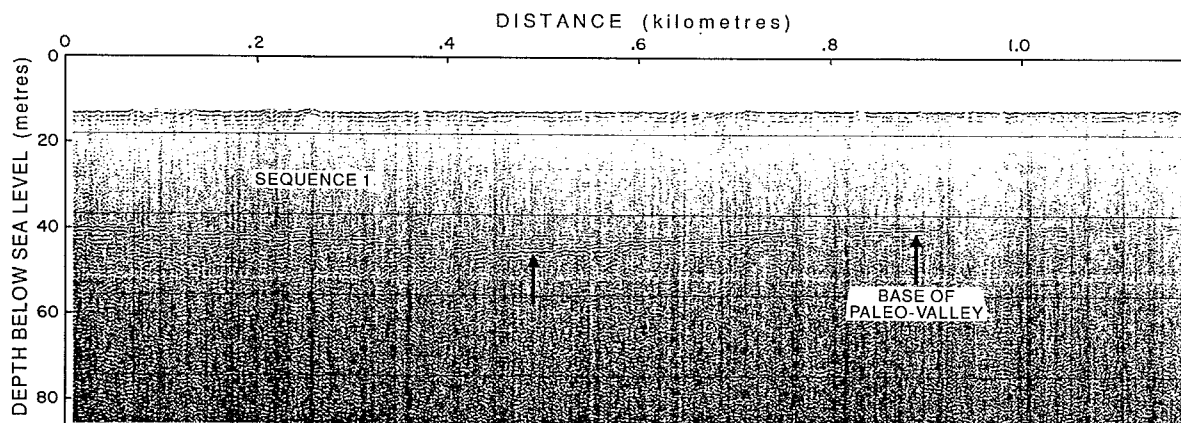
**Figure 7.11** Ikit Trough seismic stratigraphy from Hill et al. (in press).



**Figure 7.12** Seismic profile 86-15, showing erosional base of the Ikit Trough reflector.

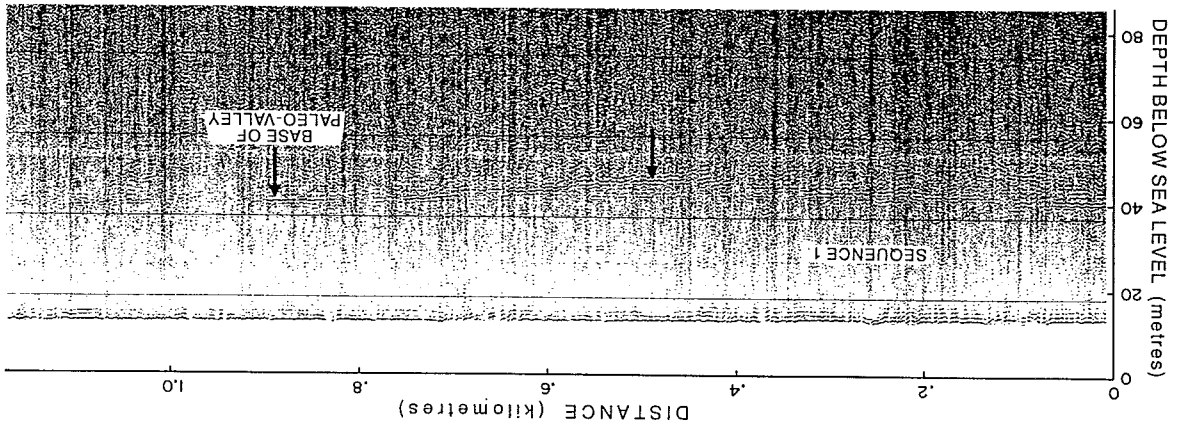


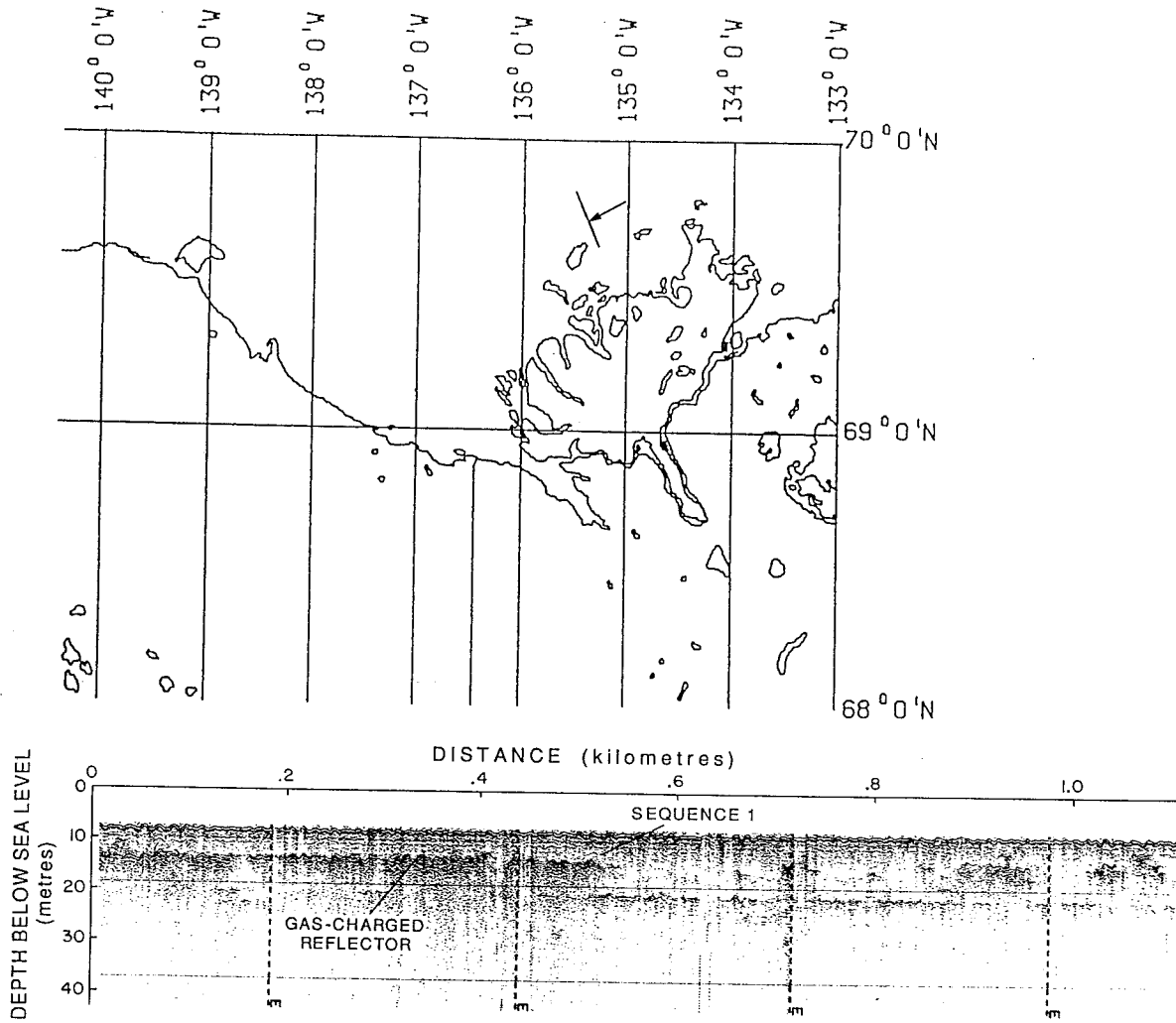
**Figure 7.13** Line drawing of seismic profile 86-20, showing a strong reflector which may represent a deeper part of Ikit Trough. For location, see Figure 7.7.



**Figure 7.13** Line drawing of seismic profile 86-20, showing a strong reflector which mayich may represent a deeper part of Ikit Trough. For location, see Figure 7.7.

Figure 7.13 Line drawing of seismic profile 86-20, showing a strong reflector which mayich may represent a deeper part of Ikit Trough. For location, see Figure 7.7.





**Figure 7.14** Seismic profile 86-16, showing gas enhanced 20 ms reflector.

seen on the middle shelf, and provide the clearest sections for distinguishing seismic sequences.

On the inner shelf, the actual boundary of Ikit Trough is not clearly seen, due to the poor quality of the NAH86 records, but it can be approximately placed just north of North Head. Over most of the bank, a clear unconformity can be distinguished separating an upper transparent to stratified sequence (sequence 1) from an underlying acoustically opaque unit (sequence 3 or 4).

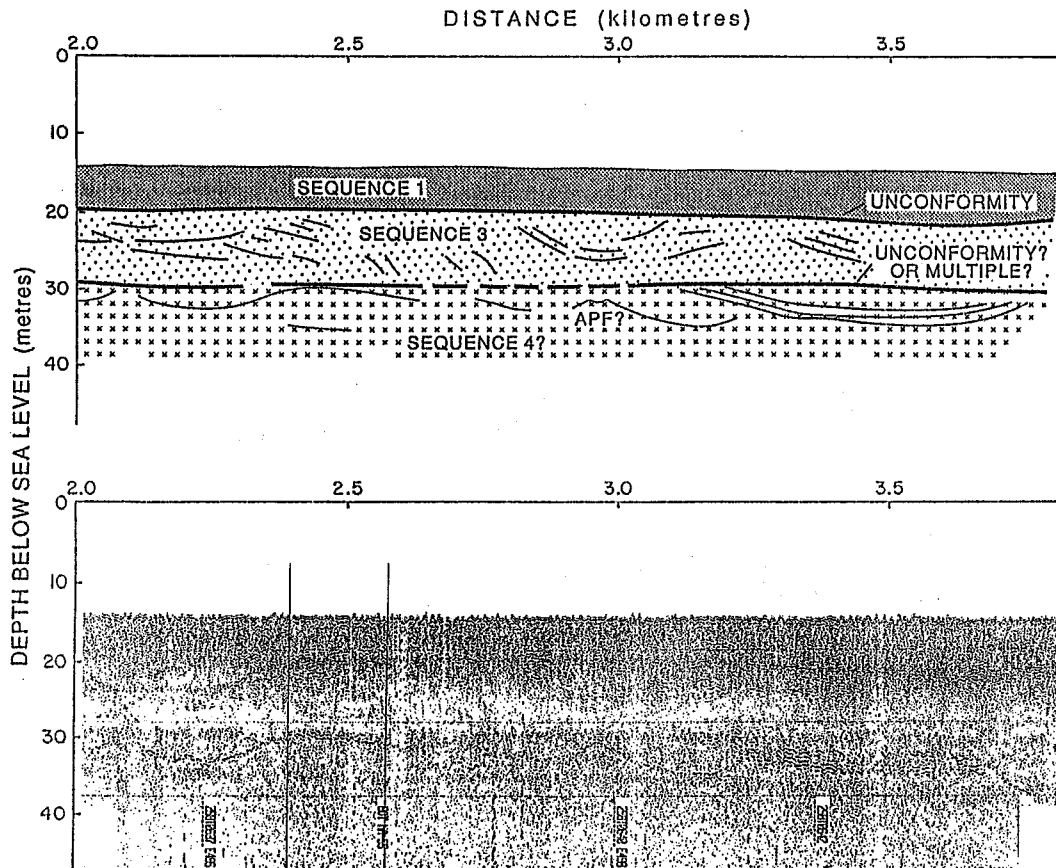
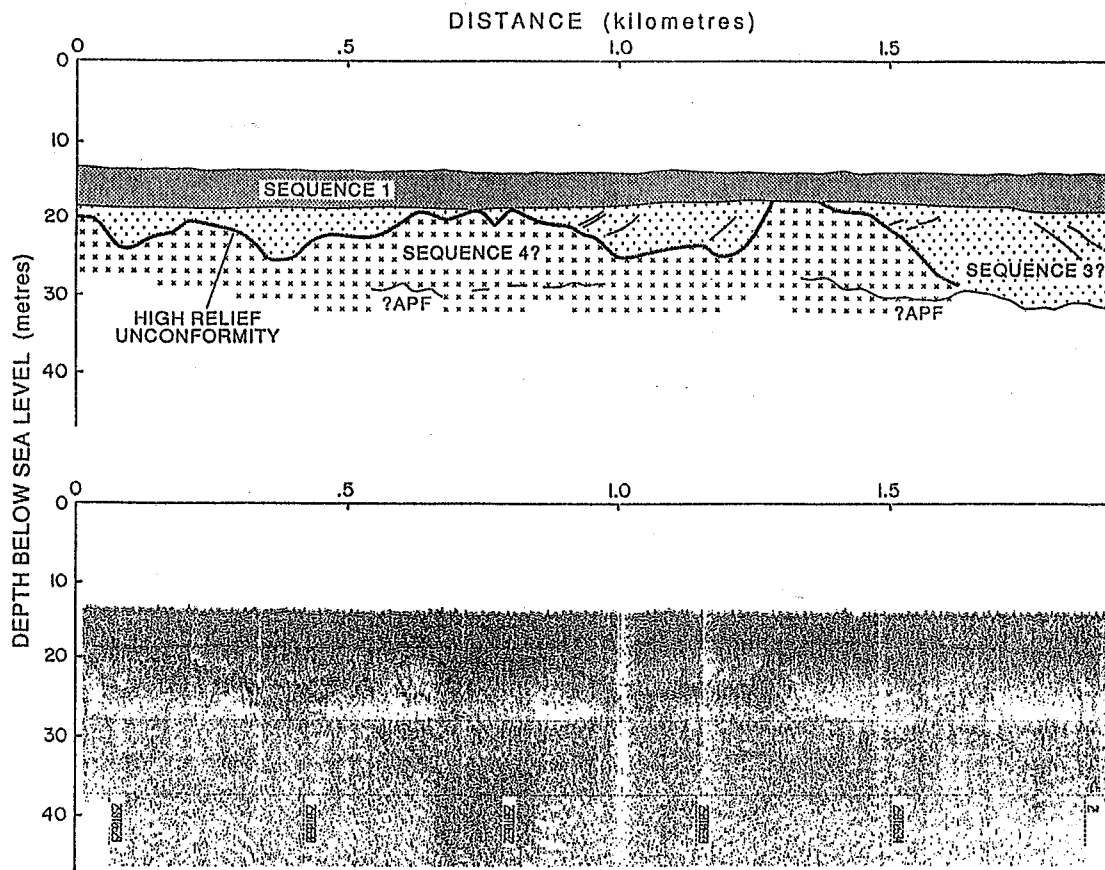
The most striking feature of this area is the relief on the unconformity surface (Fig. 7.15). Over much of the area, the unconformity is a very irregular surface, showing numerous small basins up to 10 m deep and from tens to hundreds of metres in width. These basins characteristically have steep margins and hummocky bases. They are separated by more elevated areas which take two forms. Where the relief is relatively low and the inter-basin areas are less-elevated, they show a hummocky relief which is similar to the basin-bottoms (Fig. 7.15). More elevated areas are flat-topped and are clearly eroded and planed off (Fig. 7.16).

Transparent to stratified sediments of sequence 1, overlying and infilling the irregular unconformity surface, are thinner than in Ikit Trough, reaching 10 m in places, but commonly being less than 5 m. The lower part of the basin infill is commonly well-stratified and onlaps the unconformity. Gas is common in this sequence, but shows a very patchy distribution, not being concentrated for long distances on any one reflector.

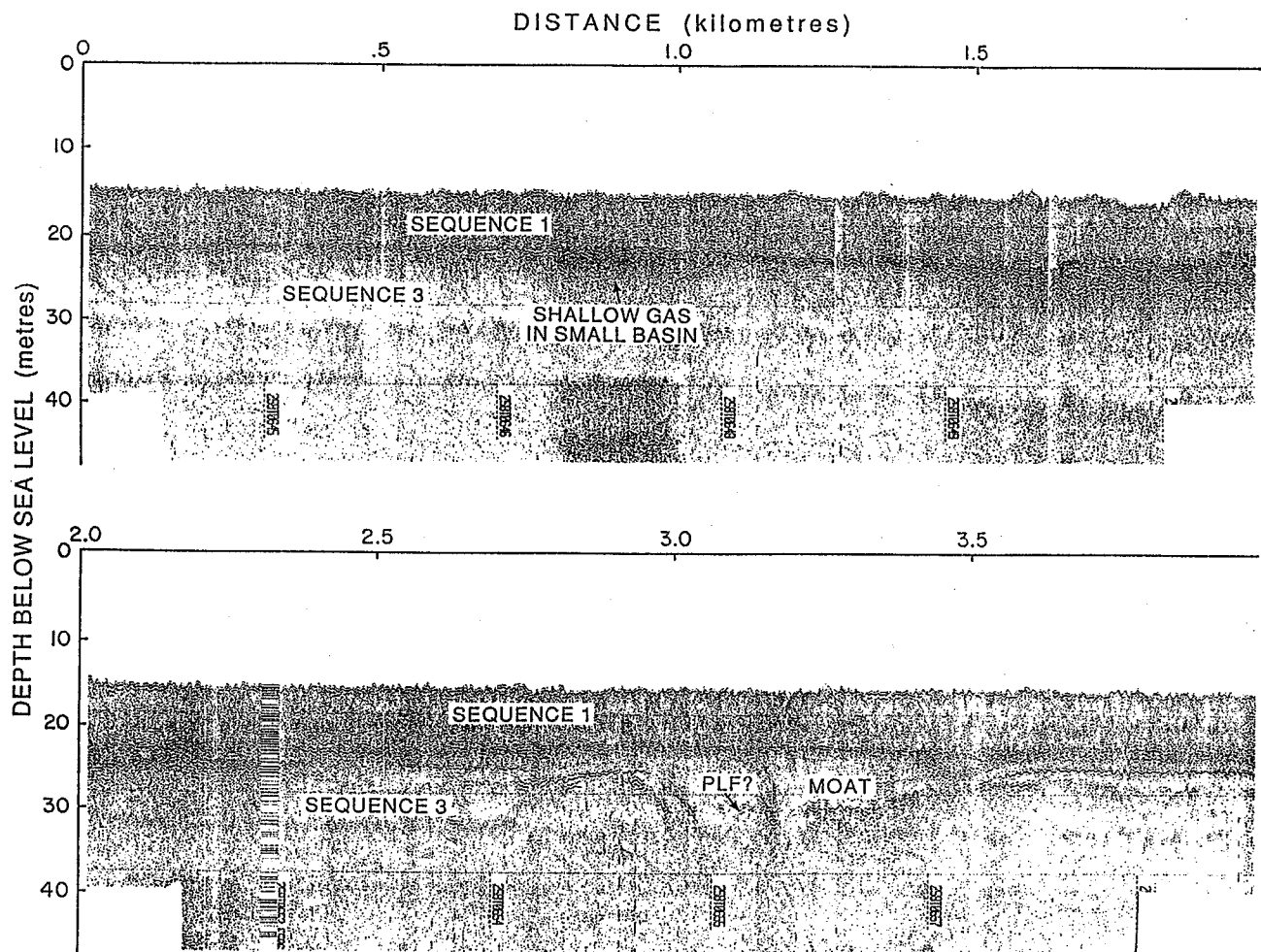
The sequence below the unconformity is generally acoustically opaque, although irregular and often dipping reflectors are common. Hummocky acoustic permafrost (APF; O'Connor, 1982a) is most commonly observed below the flat-topped unconformity highs (Fig. 7.15a). These highs often show complex stratification immediately below the unconformity and in one location a possible lower unconformity may be present where a shallow basin appears to be truncated along a surface below the high (Fig. 7.15b). This suggests that at least two seismic sequences are present below the shallowest unconformity (sequences 3 and 4). In most of the seismic sections, the unconformity between these two sequences is not obvious, but the units may be identified tentatively on the basis of seismic character. Sequence 3 is characterized by progradational reflectors, cut and fill structures and a flat upper surface. Sequence 4, in contrast, shows little internal stratification with the exception of APF reflectors and hyperbolic point reflectors resulting from surface roughness. Sequence 3 commonly infills relief on the surface of sequence 4 (Fig. 7.15a).

A detailed seismic interpretation has been made along a dip line northeast of North Head. Along this line, two major highs in the unconformity pierce the seabed for a length of approximately 3 km (Fig. 7.17). Underlying reflectors dip steeply beneath the highs and strong APF reflectors, also steeply-dipping, are present. Inshore of these features, the unconformity dips down to approximately 9 m below seabed and is overlain by the transparent to stratified sequence. A very shallow gas layer once again masks the underlying sequence in water depths less than 5 m.



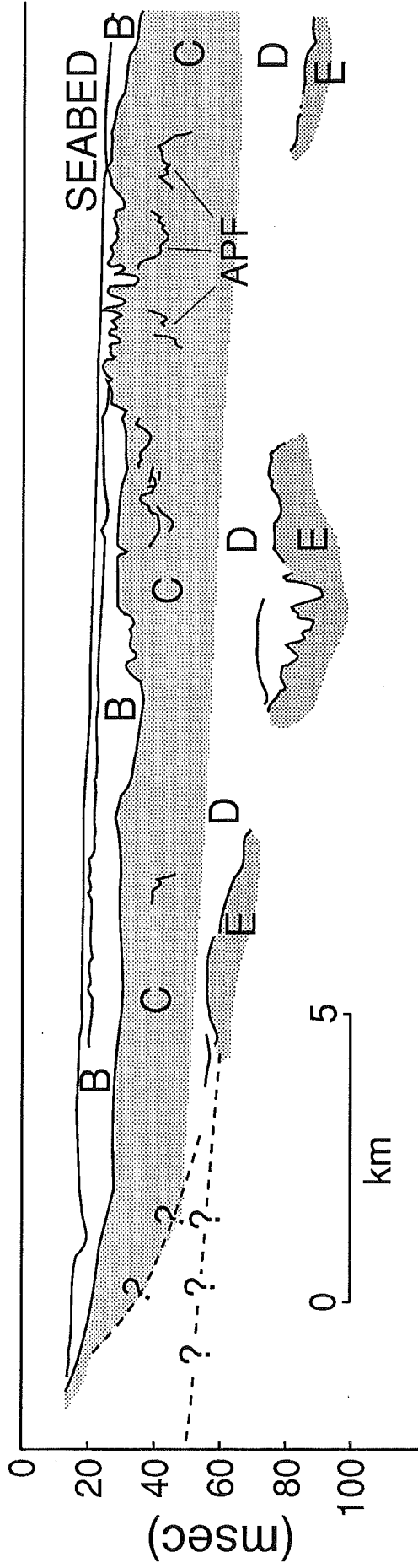


**Figure 7.15** Seismic profile 87-2 showing irregular unconformity surface. Bottom profile is a continuation of the upper profile.



**Figure 7.16** Seismic profile 87-2 showing planed off highs and truncation of underlying reflectors. Bottom profile is a continuation of the upper profile.

# NORTH POINT COASTLINE



**Figure 7.17** Schematic drawing of seismo-stratigraphy off the east side of North Head, showing sub-bottom high and presence of APF (acoustic permafrost). Unit B (Holocene age) and unit D are silty-clay deposits, whereas units C and E are sand deposits. The stratigraphy near shore is unresolved. It depends on which model proves to be accurate: (a) stratigraphic continuity or (b) pinch out (Lewis, 1989; S. Blasco, pers. comm 1990).

#### **7.4.4 Interpretation of Seismic Data**

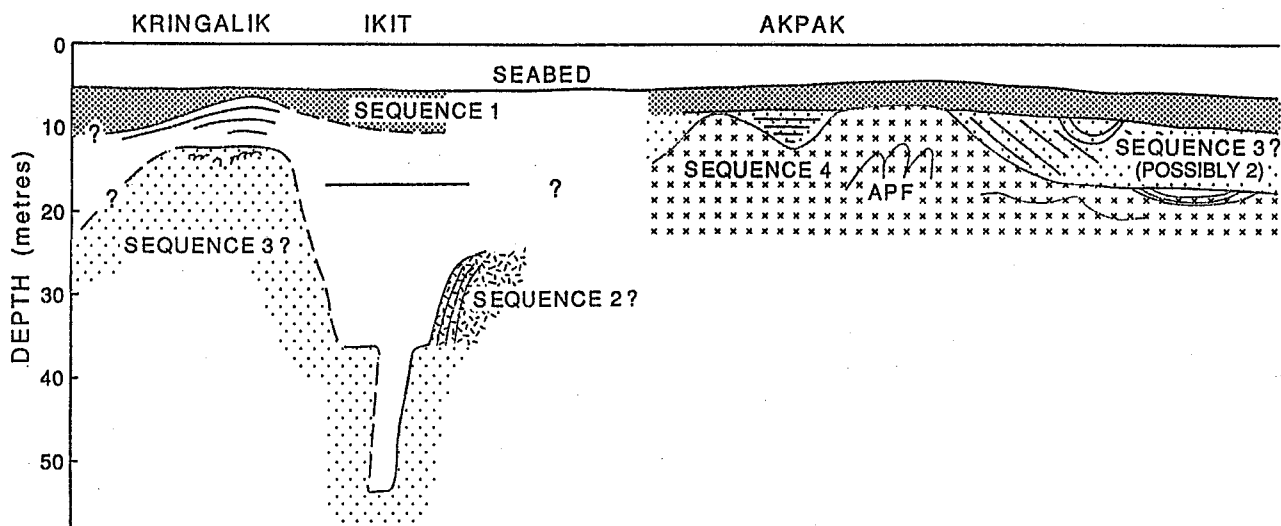
A schematic interpretation of the inner shelf seismic stratigraphy for the whole Garry Island to Summer Island region is shown in Figure 7.18. The relationships between the Kringalik, Ikit and Akpak regions are not known due to a lack of suitable data at the boundaries. Based on the similarities to the middle shelf stratigraphy, it is likely that the Ikit Trough is incised into late Wisconsinan outwash sediments of sequence 3. The marginal infill of the trough by sequence 2 is the only clear occurrence of sequence 2 on the inner shelf. However, it has previously proved difficult to distinguish between sequences 2 and 3 on Kringalik Bank (Hill et al., in prep.). The Ikit Trough was interpreted by Hill et al. to have been incised during the relative sea-level minimum in the late Wisconsinan. The irregular, sometimes contorted and APF-bearing sequence 4 on Akpak Bank must pre-date sequence 3 and is probably related to ice-thrust sediments (pre-Early Wisconsinan) observed in coastal exposures. This sequence may also include deposits related to the last advance of glacial ice into the region. Coarse deposits such as diamicton, gravel and sand may be indistinguishable from dense, ice-thrust sediments.

Sequence 3 appears to infill much of the irregular topography of the underlying sequence, especially on the eastern side of Akpak Bank. To the west, however, the relief on the upper surface of sequence 4 is directly overlain and infilled by stratified fine-grained sediments of sequence 1. The preservation of this relief implies either that the relief formed subaqueously (possibly by an ice margin grounded on the shelf) or that the relief was preserved during Holocene transgression through rapid deposition of fine grained sediment. Preservation of relief during transgression may be facilitated by the rapid infilling of thermokarst lakes subsequent to breaching at the coastline. This process appears to be occurring in the region today due to the high sediment supply from the Mackenzie River.

Sequence 1 contains a complex set of internal stratification geometries. The strong, gassy reflector at 15 m, equivalent to a similar reflector on the inner shelf of the Mackenzie Delta, may represent a maximum advance of the Holocene delta. The delta deposits infilled a substantial part of Ikit Trough before transgression resumed. The bank-like features present within sequence 1, on Kringalik Bank, are interpreted to be inner shelf or coastal mud banks, similar to the accumulations observed today along the western coast of North Point. The origin of these features is not clear as the seismic penetration is poor, but it is likely that they were constructed around former islands (similar to Pelly and Hooper Island). As the islands were eroded away, the mud banks may have become stranded and overlapped by younger sediments.

### **7.5 Lithostratigraphy and Sedimentology**

Two main sources of data are available in the Garry Island to Summer Island region (Fig.



**Figure 7.18** Summary sketch seismic section for the Garry Island to Summer Island region.

7.7): (a) short (< 2m) vibracores; and (b) longer (20-30 m) rotary drill boreholes. Coverage is inconsistent over the three seismically distinct regions discussed in section 7.4. The longer boreholes are concentrated in the Akpak Bank region. However, these regions provide a useful framework for discussion of the lithostratigraphy.

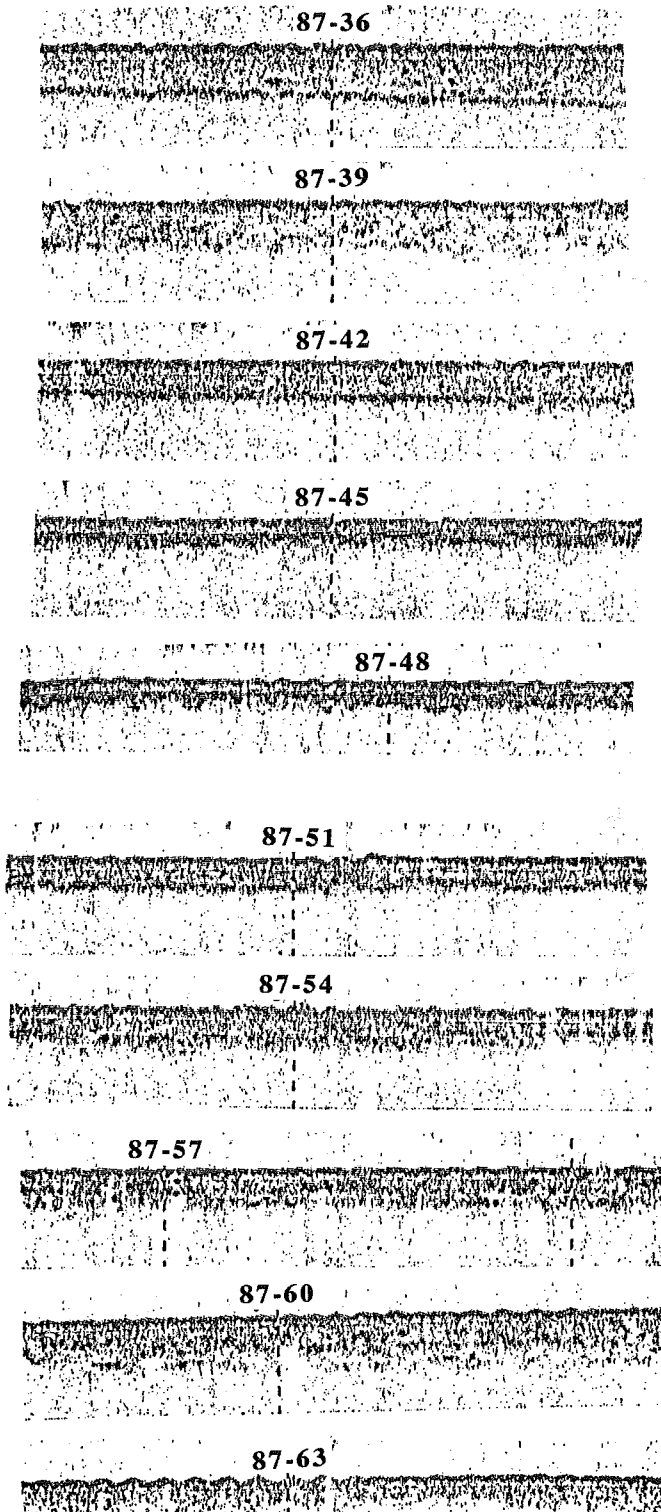
### **7.5.1 *Kringalik Bank***

A set of 10 vibracores were collected in an east-west transect along seismic line 86-20, in approximately 8.5 m of water (Fig. 7.7). The transect is across a buried bank feature within sequence 1 (Fig. 7.9). The bank surface, seen as a strong reflector, comes within 2 m of the seabed in this region. Vibracores were collected at the crest of the bank and on the adjacent flanks with the objective of penetrating the bank surface and determining facies distributions within the bank, and from crest to flank (Fig. 7.19). Although no penetration through the bank surface is achieved by the 7 kHz system, acoustic character above the bank surface changes from crest to trough. In general, reflections are more densely distributed within the condensed sequence near the bank crest than on the flanks, where the acoustic character becomes more transparent.

Lithologic columns for the ten vibracores are shown in Figure 7.20. Radiocarbon dates on shells from cores 39, 48, and 60 confirm that the sequence on the bank crest is condensed with respect to the adjacent flanks. There is also good correspondence between the position of the core with respect to the bank, the acoustic character of the seabed and the sediment facies present in the cores.

On the flanks (cores 36, 39, 42 and 63), where the sequence overlying the bank is relatively thick, and the acoustic character is transparent, the proportion of silt and sand to clay is relatively low. Thick intervals of bioturbated silty clay are interbedded with thin beds of silt, rarely more than 1 cm thick (Fig. 7.21). The thickness and proportion of silt beds decreases up core, giving an overall fining upwards sequence.

On the crest of the bank (cores 45, 48, 51, 54, 57 and 60), silt and sand are more common. Silt occurs in thicker beds, up to 20 cm thick, with relatively thin interbeds of clay. Sand is restricted to cores from the western side of the bank (cores 45, 48 and 51), where the sequence above the bank surface reflector is most condensed. Although the thickness of sediment is difficult to measure accurately from the 7 kHz profiles, the bank surface reflector occurs at approximately 1.8 m and 1.6 m below seabed in cores 45 and 48 respectively. These depths correspond quite closely to a distinctive facies change in both cores. On this basis, the cores can be divided into two sequences, which are interpreted to be related to their positions above and below the bank surface reflector. The sequence below the reflector is referred to as the bank sequence, while the sequence above the reflector is referred to as the onlapping sequence.



**Figure 7.19** Site specific 7 kHz profiles at locations of Cores 87-36 to 87-63, showing reflection character.

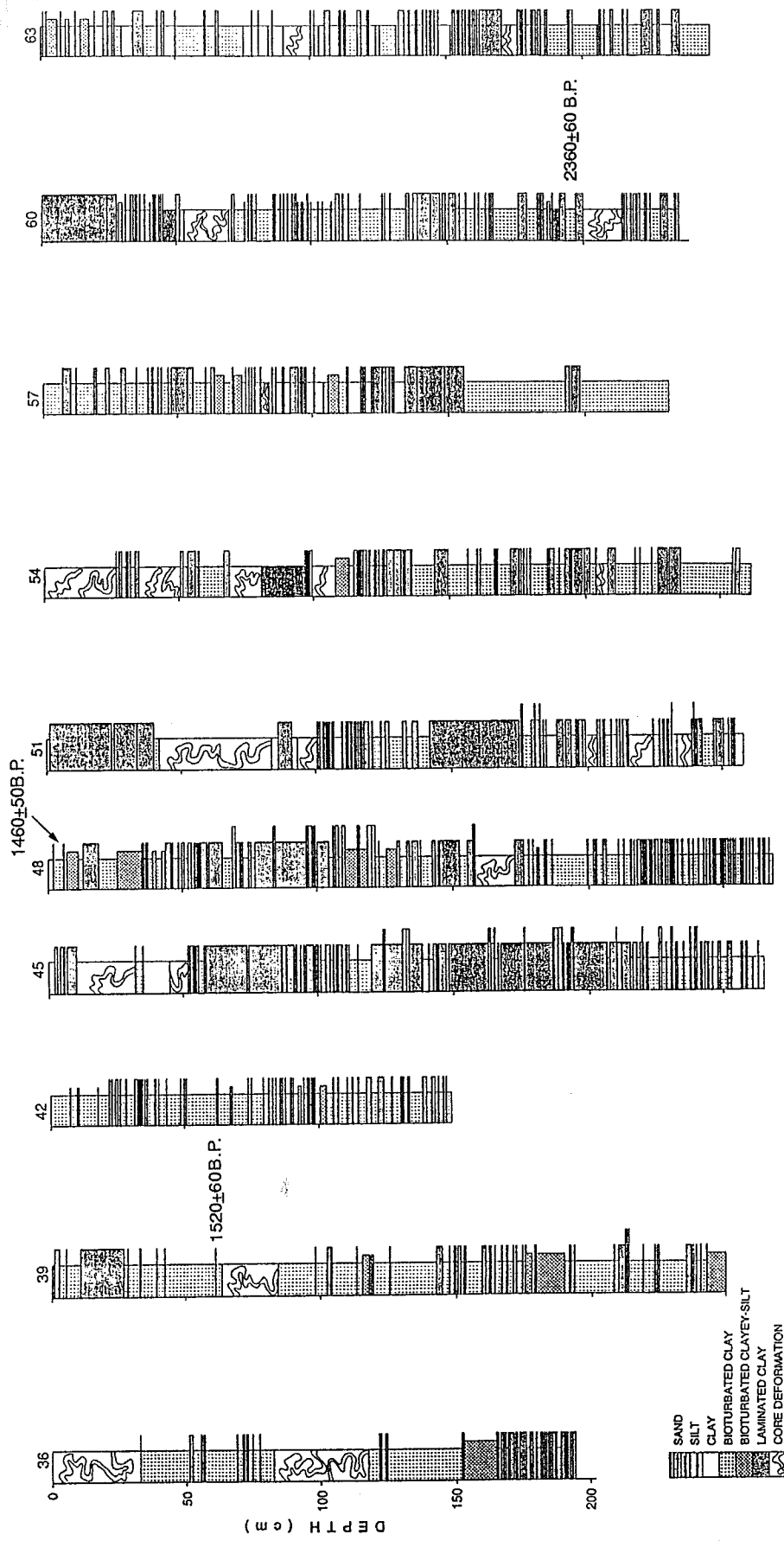
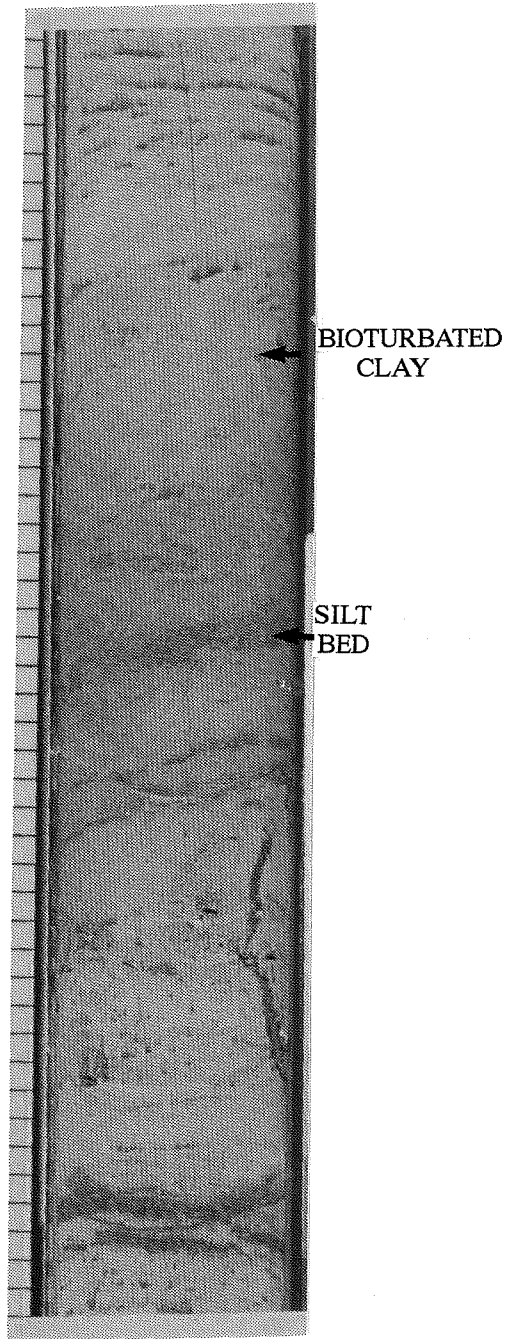


Figure 7.20 Lithologic logs of vibracore transect across buried bank feature within sequence 1 (Fig 7.9).





**Figure 7.21** Typical lithology on the flanks of the bank where the sequence is thickest. Thin graded silt beds in predominantly bioturbated silty clay sequence, Core 87-036, 30-70 cm.

### *Bank Sequence*

Sediments below the bank surface reflector are predominantly thin-bedded alternations of sand, silt and clay (Fig. 7.22). Average bed thickness is in the order of a few millimetres to a few centimetres. Sand is a minor component of the sequence, with silt and clay varying in relative importance. Beds are commonly bioturbated, resulting in sandy and silty patches up to 1 cm across (Fig. 7.22). Sand patches occur even where there are no adjacent sand beds to provide an obvious source of the sand. Some of the coarser beds have ripple cross-lamination and form thin, irregular beds within the finer-grained sequence (Fig. 7.22).

A distinctive poorly sorted bed is present in core 45 (Fig. 7.23a). The bed consists of patches of sand, silt, clay and particulate organic material in a poorly sorted mixture. A small number of fine gravel clasts are also included in the bed. Clay is present as rounded mud clasts at two levels near the top and near the base. The base of the bed is formed by a clay layer, which is highly fissured and almost brecciated. The fissures in the clay layer are filled with silty sediment from the overlying bed. The poorly sorted, patchy character of this bed suggests that it was deposited as a debris flow or slurry. The flow appears to have almost incorporated the underlying clay layer prior to deposition.

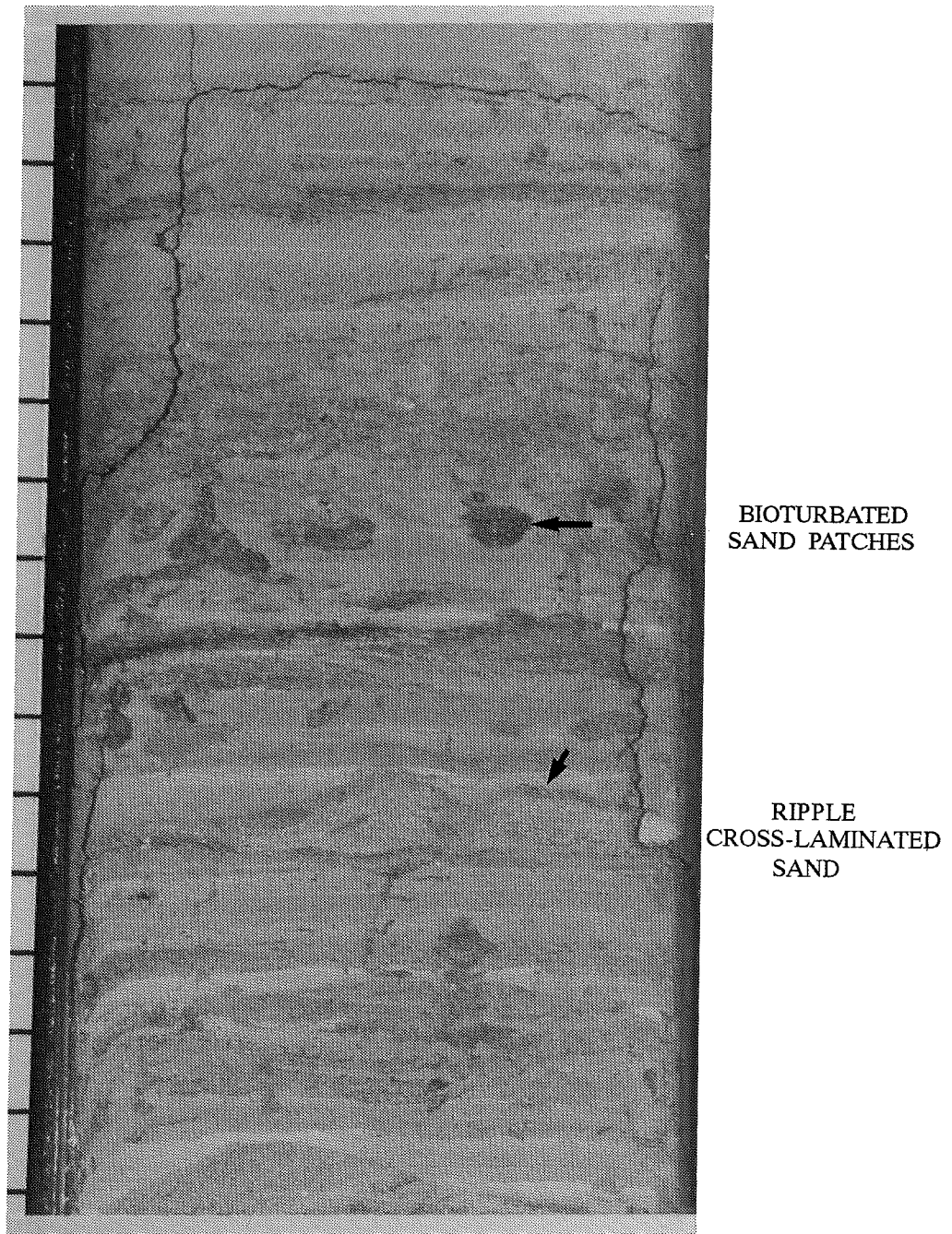
Three post-depositional features are also characteristic of the bank sequence:

(i) Irregular, sub-vertical cracks which occur in arrays that generally taper downwards into single cracks (Fig. 7.23b). Individual cracks are rarely seen to converge, suggesting that their form is filamentous or discontinuous rather than planar. The cracks are not infilled by sediment, but appear to be coated with purple brown, possibly carbonaceous material and commonly have an oxidised rim.

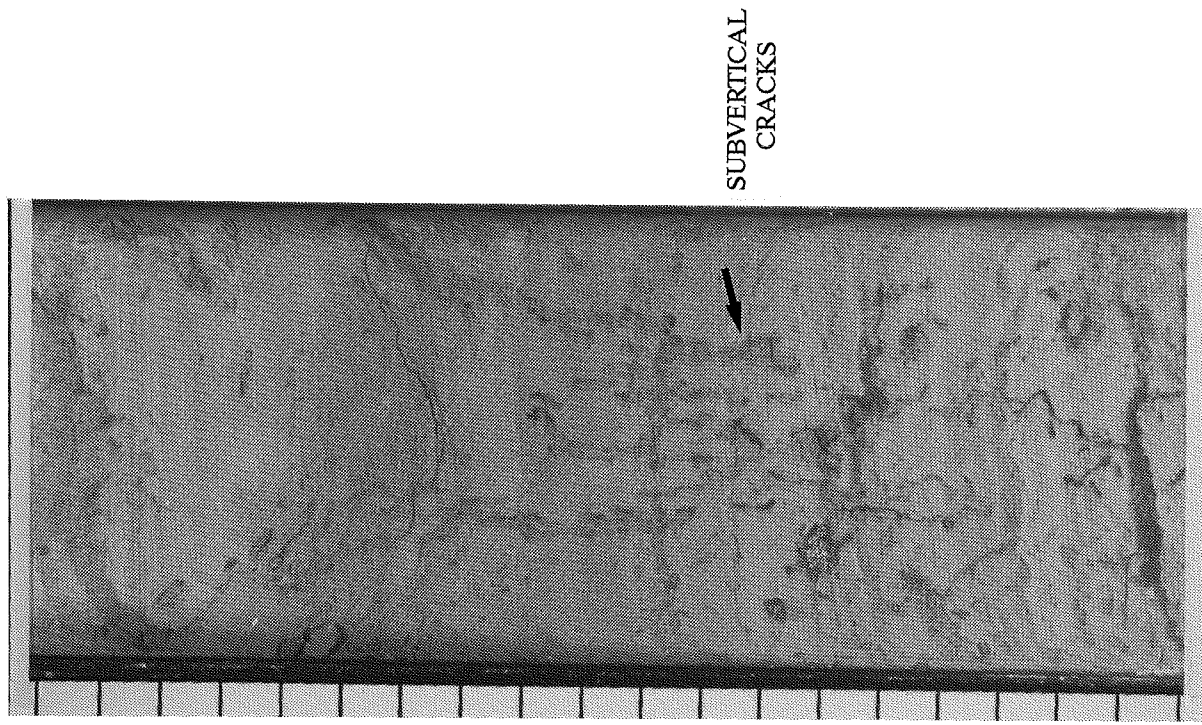
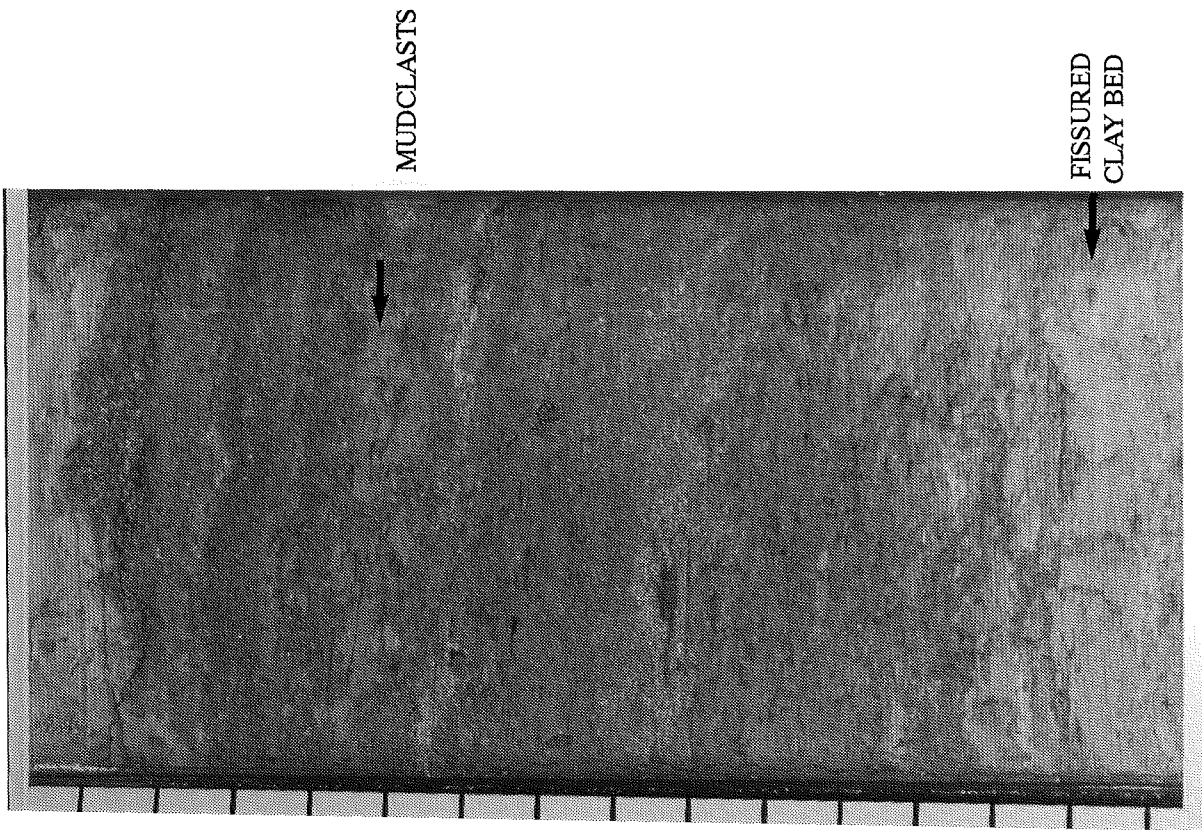
(ii) Many of the sand beds also show oxidisation in the form of a rusty brown coloration. Finer sediments, in places, show a much patchier oxidation, generally associated with the sub-vertical cracks described above, or with iron monosulphide nodules described below.

(iii) Small, 1 to 2 mm sized iron monosulphide nodules occur in association with the oxidised sand beds as well as scattered through the finer sediments. In the split cores, the nodules have a yellowish brown colour on the surface, but when broken open, they are seen to have black interiors. The composition of the nodules was determined by EDAX (P. Stoffyn, personal communication).

The sedimentological characteristics of the bank sequence described above are consistent with the interpretation that the bank was, at times, subaerially exposed. The presence of a bed interpreted to be of debris flow origin also supports the subaerial interpretation. Small slumps have been documented on tidal flats, particularly on the banks of run-off channels (Clifton, 1982). Subaerial debris flows are particularly common along the Beaufort coast where freeze-thaw mechanisms are active.



**Figure 7.22** Bank sequence lithologies: (a) Thin bedded sand, silt and clay, with sand-filled burrows, Core 87-045, 231-246 cm.



**Figure 7.23** (a) Poorly sorted slurry bed; Core 87-045, 186-202 cm; (b) Sub-vertical cracks, Core 87-048, 164-184 cm.

The origin of the post-depositional features cannot be determined unequivocally. Several hypotheses for the origin of the sub-vertical cracks can be proposed:

(a) They could be simply related to coring disturbance. However, this would appear to be too coincidental as the only cores showing this disturbance are cores 45, 48 and 51, all of which can be related to the bank feature.

(b) They could be rootlet structures. This would be compatible with their fibrous, tapering form and the presence of carbonaceous material on the crack surfaces. Clifton (1982) describes similar features to be characteristic of supratidal vegetation from estuarine tidal flats.

(c) They could be incipient ice-wedges. This hypothesis is supported only by their similarity in form and scale to ice wedges observed in cliffs along the Beaufort coast (e.g. Mackay and Matthews, 1983).

(d) They could be expansion cracks related to gas. Seismic records strongly suggest the presence of shallow gas in these sediments. The association with iron monosulphides, whose formation would be favoured by reducing conditions provided by excess methane in the sediments, also supports this hypothesis.

Further research into structures observed in modern intertidal flats along the Beaufort coast is required to better interpret the depositional environment represented by the bank sequence described above. This might also help to verify or rule out some of the hypotheses for the origin of the sub-vertical cracks.

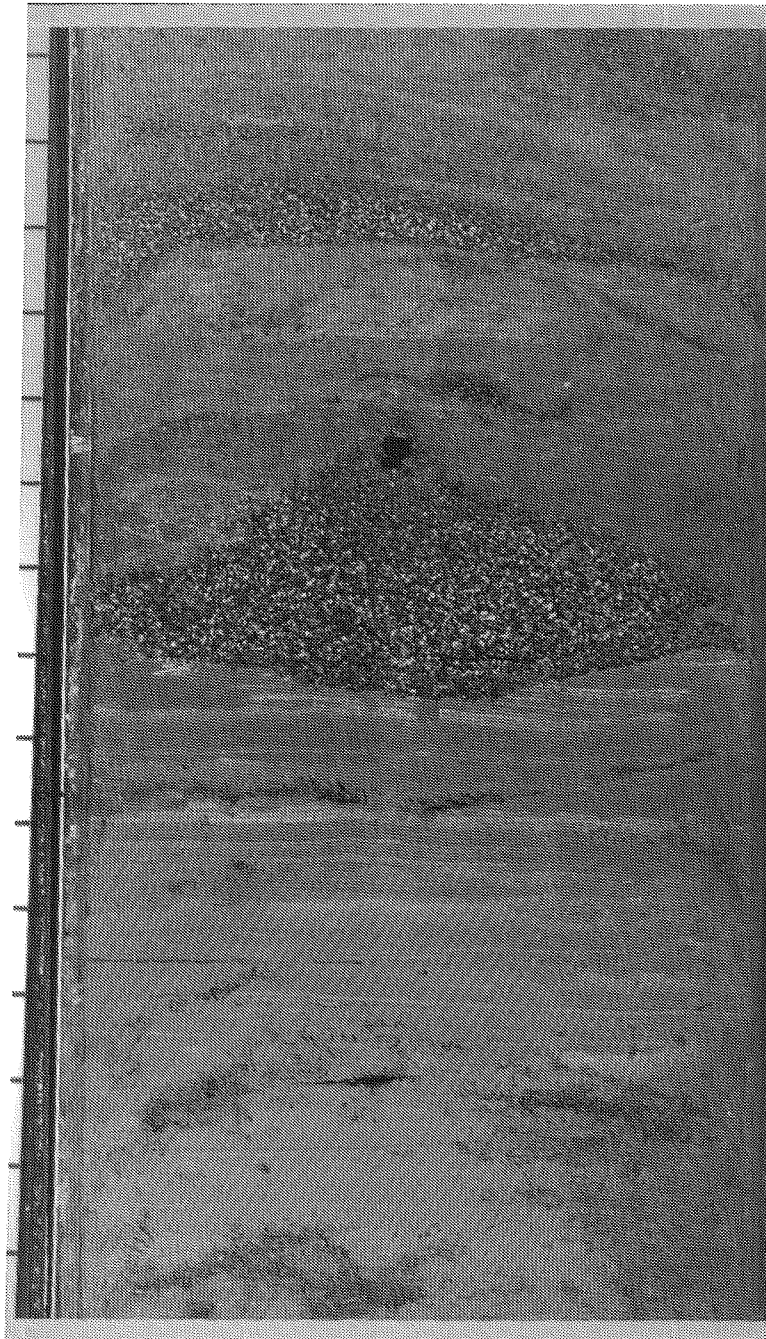
### *Onlapping Sequence*

The onlapping sequence in most cores consists primarily of thick graded silt beds similar to those observed in shallow water off the Mackenzie Delta (see section 6.5). Several facies can be distinguished within the onlapping sequence:

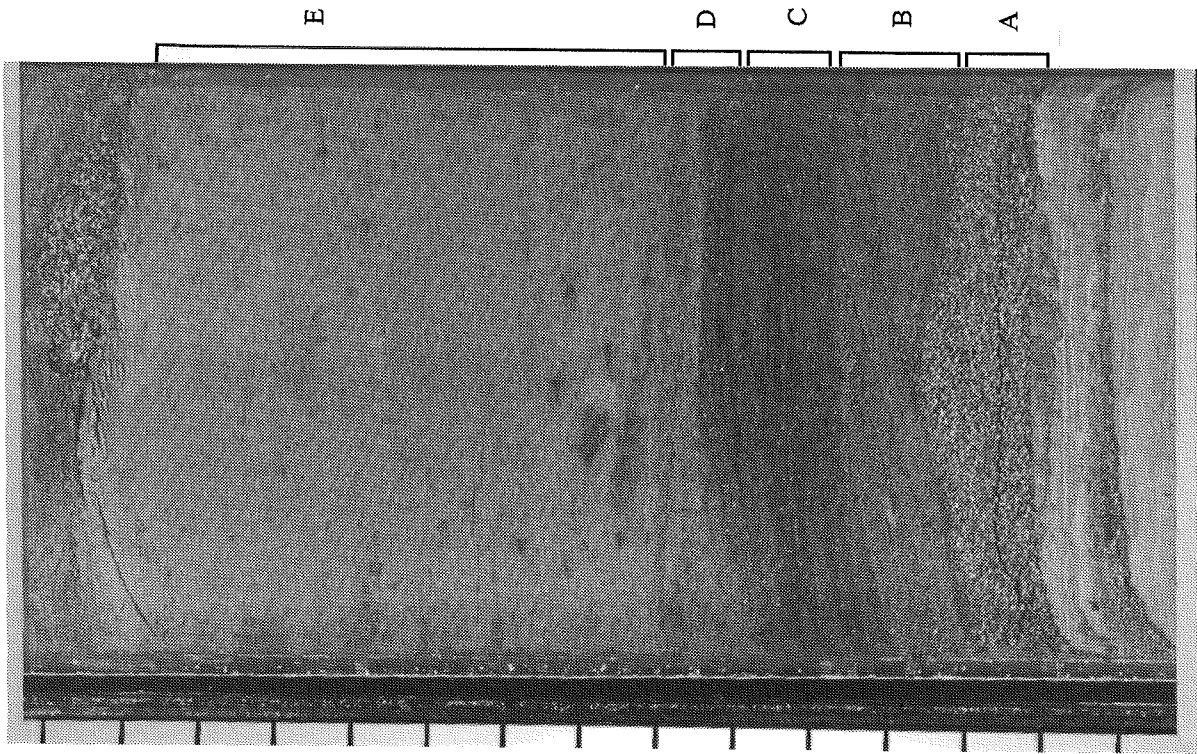
(i) *Starved sand ripple lenses* are found in a distinctive sequence within core 48 (Fig. 7.24) and as part of a deformed unit in core 45. Both these occurrences lie immediately above the bank sequence. The medium-grained sand lenses float in a matrix of fine silty clay. Bioturbation, in the form of sandy patches, and deformed laminae in the surrounding clay are associated with the sand lenses.

(ii) Sharp-based, *graded beds* of sand, silt and clay are common. Several types of graded bed are observed, ranging from complex sequences with several distinct units (Fig. 7.25a), to simple sequences of silt and clay (Fig. 7.25b). The complex bed shown in Figure 7.25a has five distinct units: A. Well-sorted fine to medium sand base, with a rippled top; B. Cross-laminated fine sand and muddy silt; C. Parallel-laminated muddy, organic-rich silt; D. Low angle ripple cross-laminated sand and silt; E. Massive mud. The bed in Figure 7.25b contains a concentration of shells and shell fragments and simply grades from muddy silt to silty clay. Some of the thicker

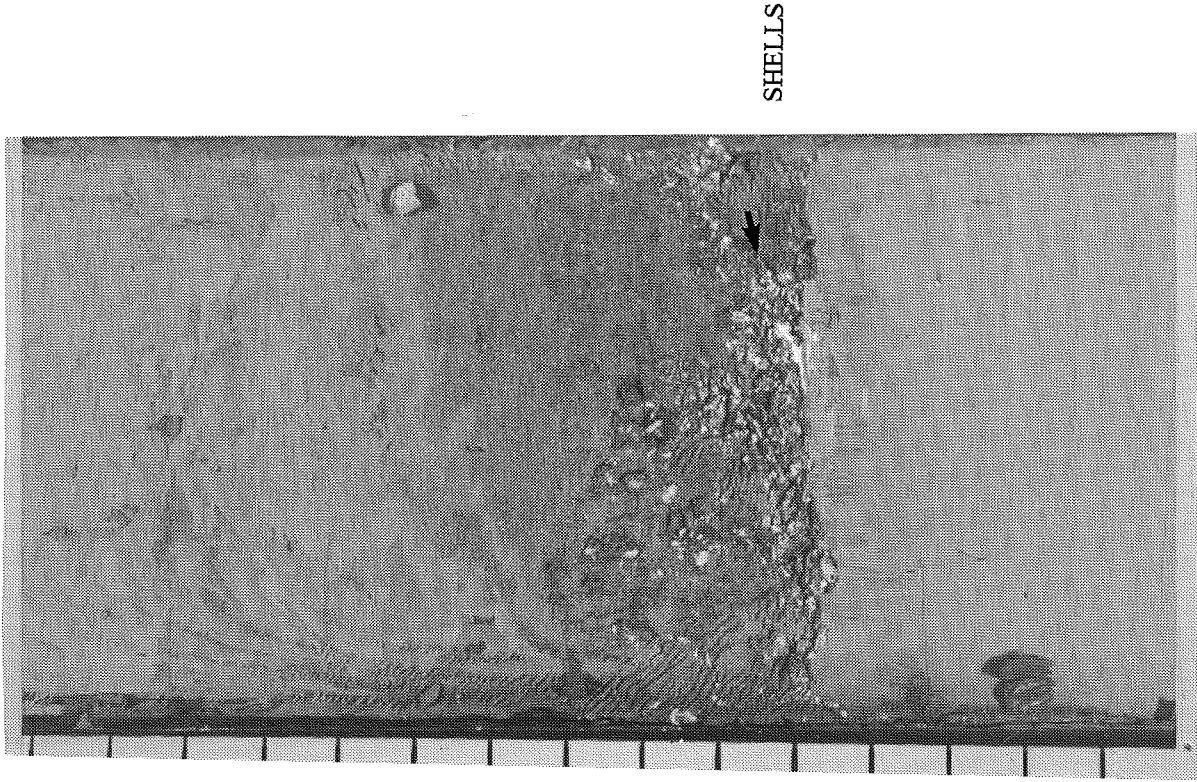




**Figure 7.24** Lenticular sand Core 87-048, 112-128 cm.



(a)



(b)

**Figure 7.25** (a) Complex graded bed with five units, Core 87-048, 83-98 cm; (b) graded bed with shell hash, Core 87-048, 7-22 cm.

graded beds are predominantly silt, and commonly show fine parallel laminations.

(iii) Some beds of muddy silt show *multiple grading*, fining from a sandy base through muddy silt to clay, then coarsening back into muddy silt. The example in Figure 7.26 shows a third interval of reverse and normal grading. The three cycles are interpreted to result from the same depositional event.

Lenticular bedding, as described in (i) above, is characteristic of sub-tidal and inter-tidal environments where periods of strong flow alternate with periods of slack water (Reineck and Wunderlich, 1968). Some of the sand lenses are symmetrical and may have a wave origin. The position of the lenticular bedding, immediately above the bank sequence suggests that it may have been deposited in very shallow water during the early stages of transgression. As such, it may be considered a subtidal bank deposit. The overlying sequence of graded silt beds, with minor sand, is similar to inner shelf sediments observed off the Mackenzie Delta (see section 6.5) and off North Point (Hill and Nadeau, 1989). The graded silts represent storm resuspension under strong wave and current conditions. The fining upwards trend present in most of the onlapping sequence represents a progressive deepening of water during transgression.

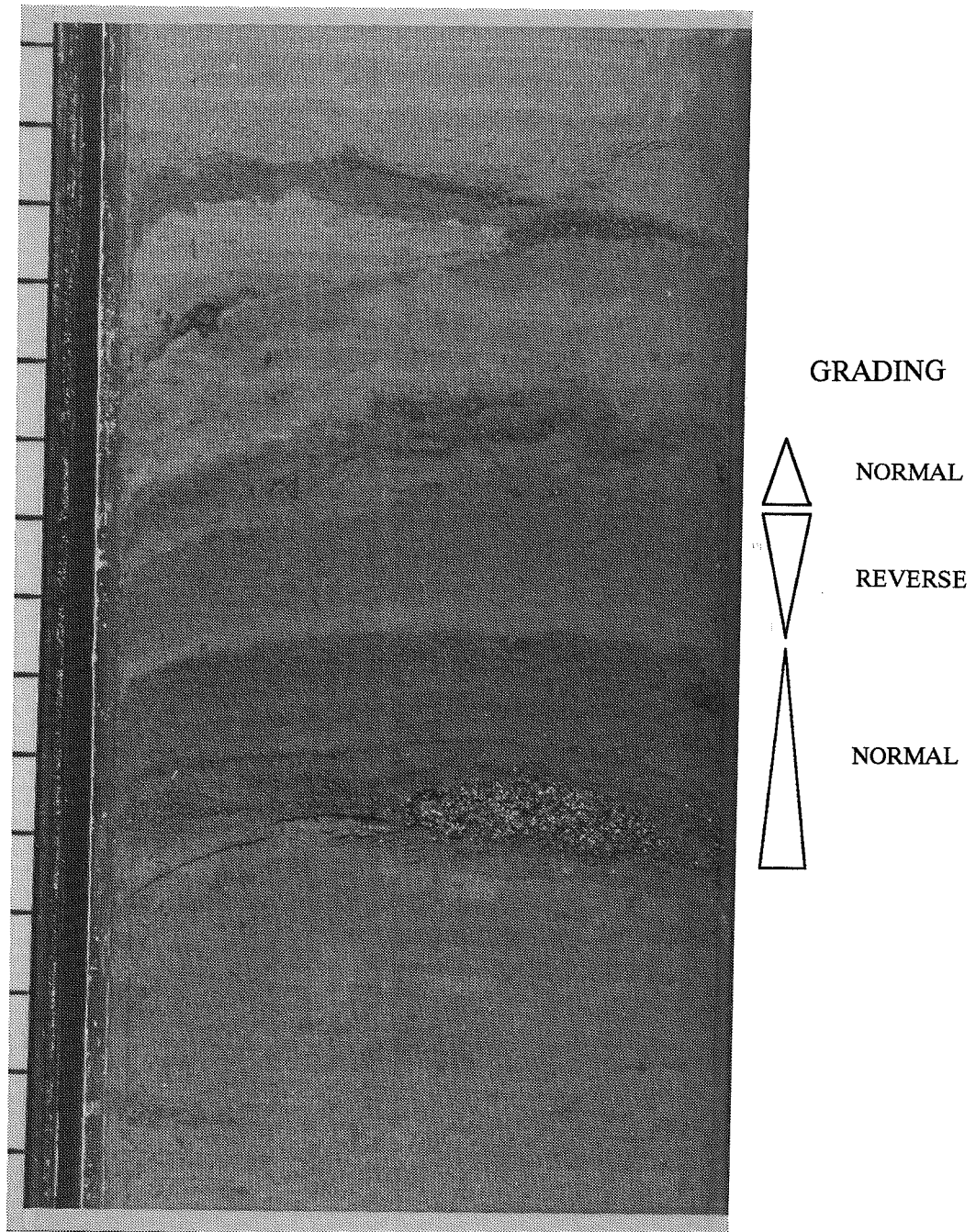
### 7.5.2 *Ikit Trough*

A shore perpendicular transect of vibracores was collected in Ikit Trough, between Hooper and Pelly Islands (Fig. 7.7). The cores range in water depth from approximately 4 to 8m. Figure 7.27 shows the generalised lithology found in these cores. Two accelerator radiocarbon dates, on shell samples from cores 75 and 81, give mean sedimentation rates of 0.71 mm/a and 0.46 mm/a respectively. In common with cores from the Mackenzie delta and Kringalik inner shelf regions, these cores contain mainly thin to medium-bedded graded silt beds with silty clay interbeds. Silt beds are similarly thicker and clay interbeds thinner in shallower water. In deeper water, the silts become thinner and the clay interbeds become thicker.

None of the cores contain the spectacular wave and current structures present in the shallow water cores in the Mackenzie Delta. Rather, bioturbation, of both silt and clay intervals is more pronounced. Where the bioturbation is pervasive through a predominantly silty interval (Fig. 7.28), the lithology is identified in Figure 7.27 as bioturbated silt. This lithology is particularly common in shallower water, where the silt beds are thicker. This characteristic of the sequence presumably indicates a less regularly reworked seabed. The time between resuspension events must be relatively long, when compared with the delta region, to allow bioturbation to have a significant impact.

A set of boreholes were drilled on the eastern side of Ikit Trough during the spring of 1984 (Fig. 7.29, 7.30). The stratigraphy and sedimentology of these boreholes were initially reported by Hill et al., 1986. A more detailed sedimentological analysis of the same cores was carried out

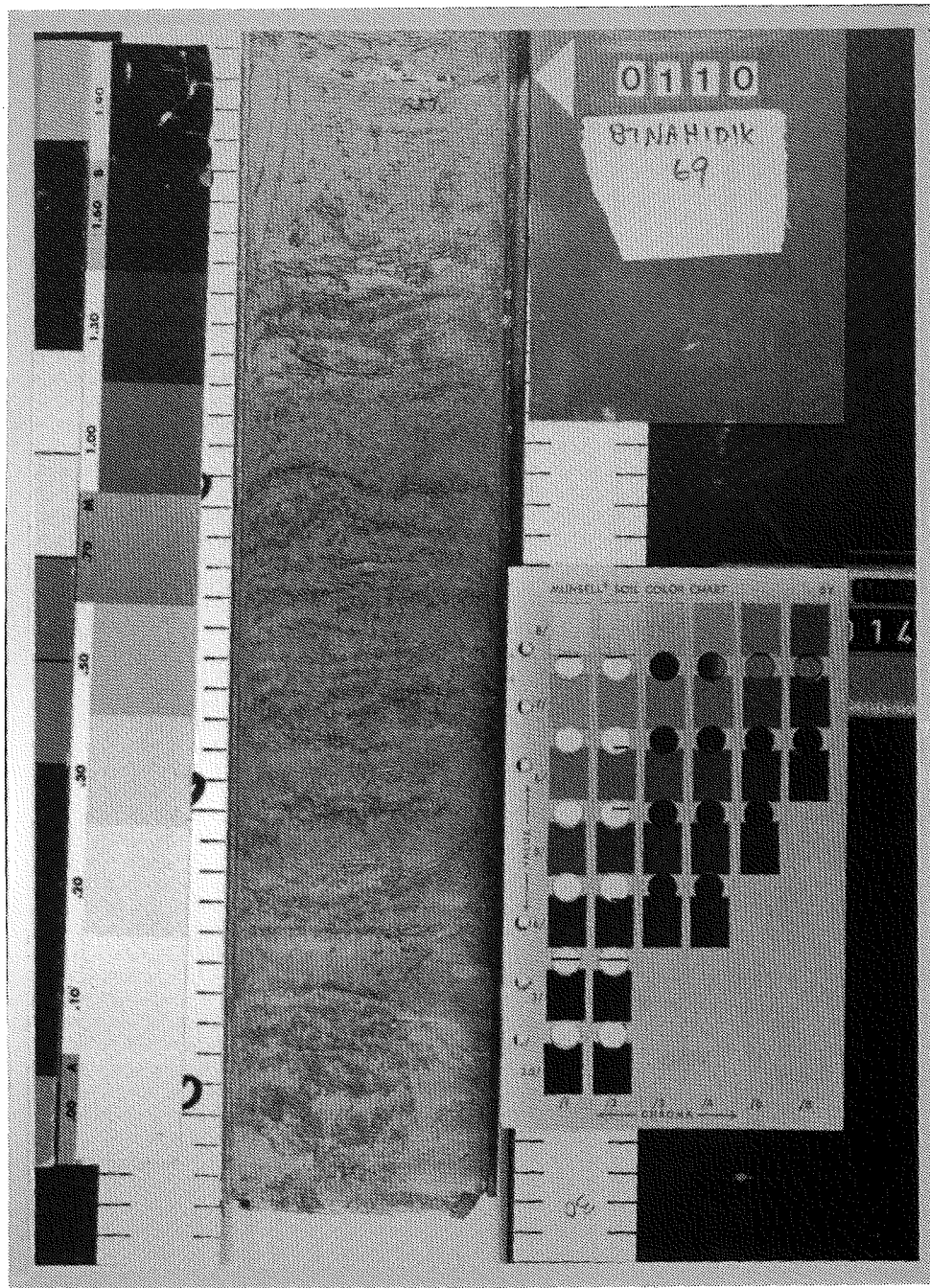




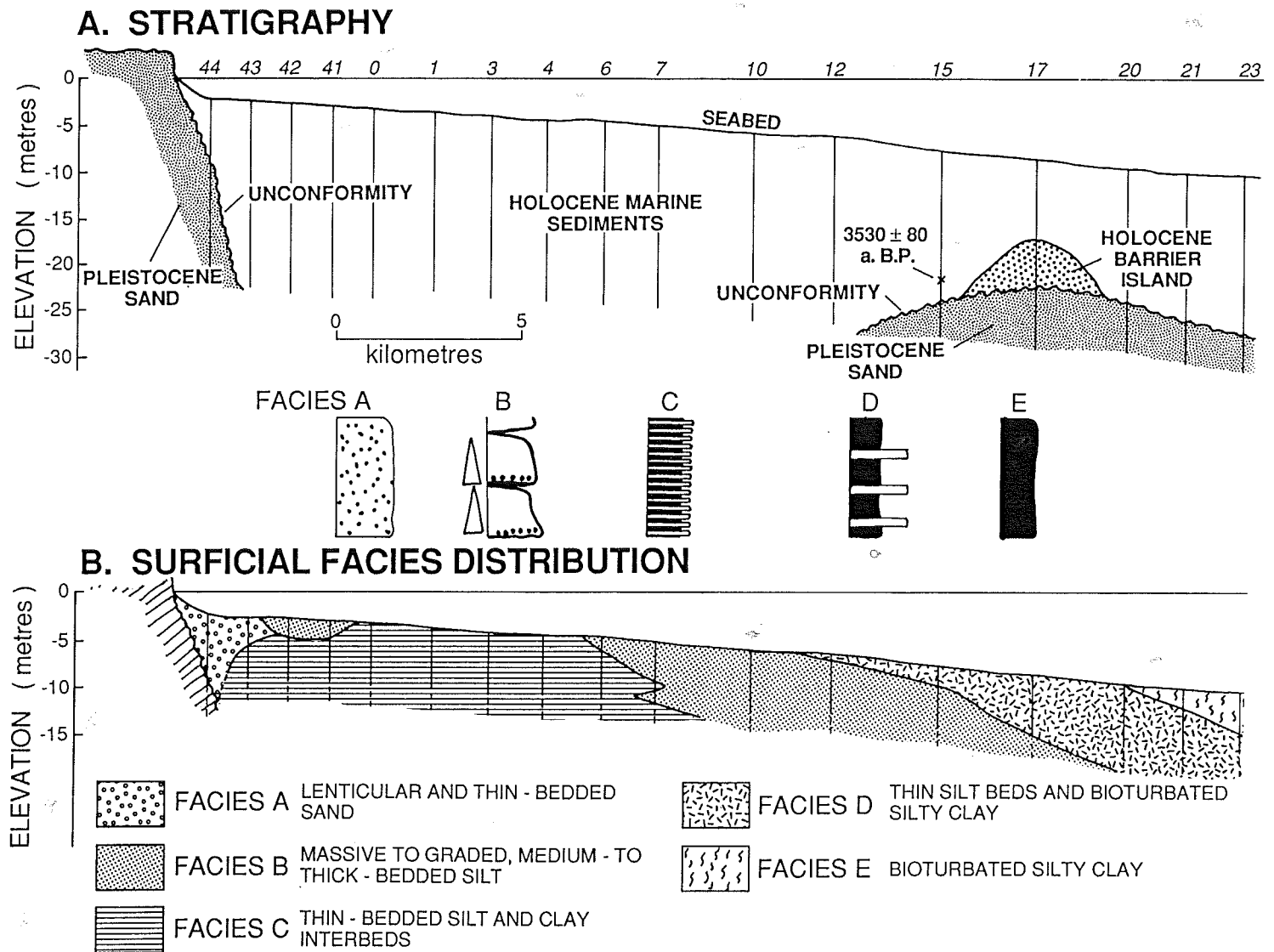
**Figure 7.26** Multiple graded bed, Core 87-048, 75-90 cm.



**Figure 7.27** Transect of Cores 87-66 87-84, in the Ikit Trough region, showing generalized lithology. Note abundance of bioturbated silt beds.



**Figure 7.28** Pervasively bioturbated silt beds Core 87-069, 110-140 cm.



**Figure 7.29** Stratigraphy and surficial facies distribution of the 1984 North Head boreholes (from Hill and Nadeau, 1989).

and reported in Hill and Nadeau (1989). Results of this analysis are summarised in Figure 7.29. The transect of boreholes extends northwestwards into Ikit Trough. The margin of the trough corresponds to the western coastline of North Point. Brown sands, similar in character to sands of the Kittigazuit Formation, occur in the borehole closest to shore (hole 44) and at depth further offshore (holes 15 through 23). The offshore sand forms a low-relief bank, on which is a narrow ridge of sand, interpreted as a barrier island deposit. Holocene silt and clay, with minor sands, infill the trough topography. The silts and clays contain low numbers of foraminifera (*Elphidium spp.*) and are therefore marine in origin. A single radiocarbon date of 3530±80 yrs B.P., on wood from 13.4 m in borehole 15 confirms the Holocene age of the silt and clay sequence.

The organization of near-surface sediment facies has been interpreted by Hill and Nadeau (1989) to reflect sedimentation dominated by resuspension of seabed sediments by storm waves and currents. The thickest silt beds (facies B in Figure 7.29) occur between 4.2 and 5.5 m water depth. This zone is interpreted to be the zone of maximum resuspension during storms. Storm waves are of sufficient height to affect the seabed at these water depths. The frequency of waves capable of reworking the seabed decreases rapidly with distance offshore from this zone, so that the resulting sediment facies consists of thin beds of silt and thick bioturbated intervals of silty clay. Inshore of the maximum suspension zone, bed thickness decreases in the opposite direction, indicating a shoreward loss of wave energy. This trend reverses again only very close to the coast.

Two other notable facies are observed in the 1984 boreholes (Fig. 7.30; Hill et al., 1986). Bioturbated silts are present at depth, landward of the offshore high. These may have been deposited in a relatively sheltered environment behind the high, so that resuspension events were relatively uncommon, allowing bioturbation to destroy primary bedding. Lenticular sands are also present, immediately above the offshore bank and in shallow water close to the coast, where a large mudbank is presently developing. This is similar to its occurrence on Kringalik Bank. The close relationship of this facies to shallow, possibly inter-tidal or supra-tidal banks suggests that lenticular sands are diagnostic of very shallow water conditions close to such a bank.

### **7.5.3 Akpak Bank**

Part of the 1984 borehole program extended onto Akpak Bank (boreholes 32, 34, 36 and 38; Fig. 7.30). The four boreholes show considerable variation within the few kilometres of this short transect. The brown well-sorted sand previously described from the Ikit Trough boreholes is present within about 10 m of the seabed. Two other lithologies are also present. In borehole 38, a hard, gravelly diamicton, at least 8 m thick was recovered. The diamicton is immediately overlain by a organic rich silt and clay. A similar organic-rich deposit is found in borehole 34, together with a peat which directly overlies the brown sand. These deposits contain a distinctive non-marine algal assemblage (Burden, 1986), are interpreted to be lacustrine in origin and probably

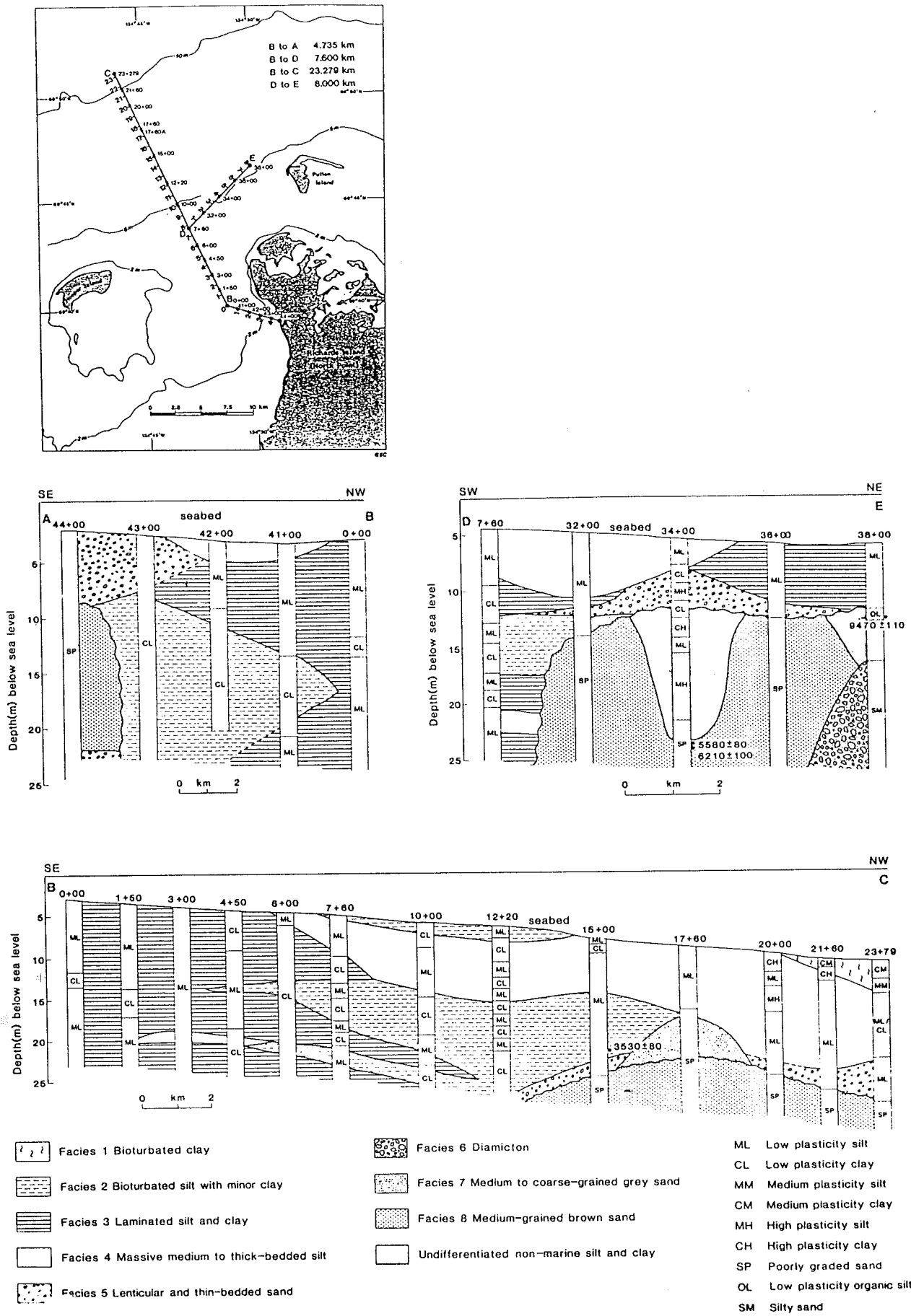


Figure 7.30 Deeper sediment facies from the 1984 North Head boreholes (from Hill et al., 1986).

formed in thermokarst lakes on the pre-transgression land surface. Three dates from the two sequences were obtained. Two dates on peat and organic silt from the base of the lacustrine sequence in borehole 34, gave ages of  $5580 \pm 80$  yrs B.P. and  $6210 \pm 100$  yrs B.P. respectively. An organic silt sample from the top of the lacustrine sequence in borehole 38, was dated at  $9470 \pm 100$  yrs B.P. All these dates are compatible with the development of thermokarst lakes in the region over the last 12,000 years (Rampton, 1988).

## **7.6 Geotechnical Properties**

High quality geotechnical data are available from the borehole transect off North Head (Fig. 7.7). These data can be extrapolated with reasonable confidence to most of the Garry Island to Summer Island region. Hill et al. (1986) demonstrated that different fine-grained sediment facies showed significantly different geotechnical properties. These differences are summarised in Table 7.2. On the plasticity chart of Figure 7.31, it can be seen that the four main sediment facies plot in distinctive areas on the chart. There is a broad continuum in plasticity from the high plasticity bioturbated clay, through laminated silt and clay to the low plasticity bioturbated silt, reflecting for the most part, the changing silt composition. The massive silt crosses almost the entire range in plasticity, although points are more concentrated in the low plasticity range.

In general, the more clay-rich sediments also have higher water contents than the siltier sediments. Shear strength varies greatly with lithology, primarily as a function of the silt content of the sediment. This can be seen in the downhole plots of Figure 7.32. In particular, the laminated silt and clay shows wide fluctuations in strength from less than 10 kPa to over 50 kPa over distances of a few centimetres.

Table 7.3 summarises the properties of the coarser-grained sediments in the North Head boreholes. Of particular note is the diamicton, which consists of gravelly silty sand with 30 to 33% clay. The diamicton was extremely stiff, and dense, being almost impossible to remove from the Shelby tubes.

## **7.7 Sediment Erosion, Transport and Deposition**

There are several important studies concerning the wave, current and sediment transport regime of the inner shelf region of Richards Island (Davidson et al., 1988; Hodgins et al., 1986; Hodgins, 1988). These studies primarily concern the resuspension of sediment by the combined interaction of waves and currents. As the inner shelf of this region has a very low slope and the bottom sediments are predominantly fine-grained, these studies deal with an important part of the coastal sediment transport system. In this section, available data on waves, currents and fine-grained sediment transport processes will be discussed. On the other hand, there have been no studies of sediment transport on the highly active spit-barrier systems of the outer islands or of the

**Table 7.2** Physical properties of fine-grained sediments, North Head borehole transect (from Hill et al. 1986).

<b>Lithology</b>	<b>Shear Strength (kPa)</b>	<b>Water Content (%)</b>	<b>Liquidity Index (%)</b>
Bioturbated clay	5 - 50	35 - 55	0.2 - 1.7
Bioturbated silt	5 - 35	21 - 38	-0.2 - 1.9
Laminated silt and clay	4 - 85	25 - 50	0.0 - 1.8
Massive silt	4 - 75	20 - 49	-1.0 - 1.7

**Table 7.3** Grain size distributions for coarse-grained sediments, North Head borehole transect (from Hill et al. 1986).

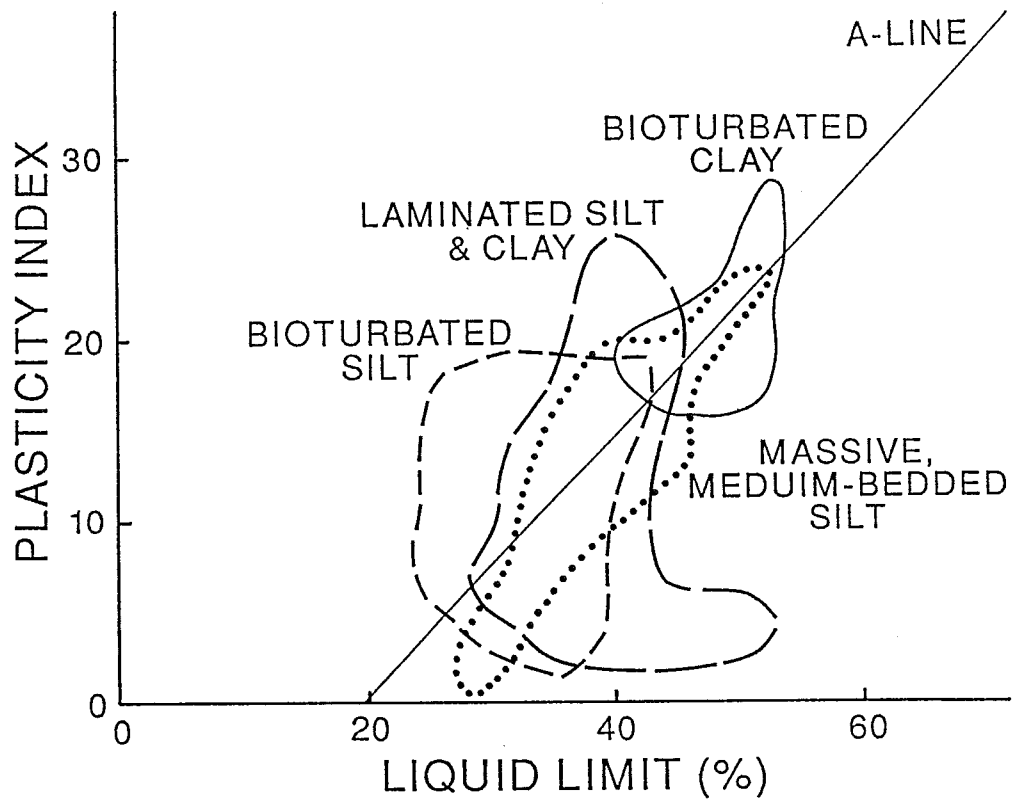
<b>Lithology</b>	<b>Classification</b>	<b>% Sand</b>	<b>% Silt</b>	<b>% Clay</b>
Thin-bedded sand	Low plasticity silt	0 - 10	54 - 59	30 - 45
Diamicton	Silty sand*	48 - 49	18 - 21	30 - 33
Grey sand	Poorly graded sand*	87 - 95	5 - 12	0 - 5
Brown sand	Poorly graded sand	80 - 98	0 - 16	0 - 6

\* Contained up to 1 % gravel.

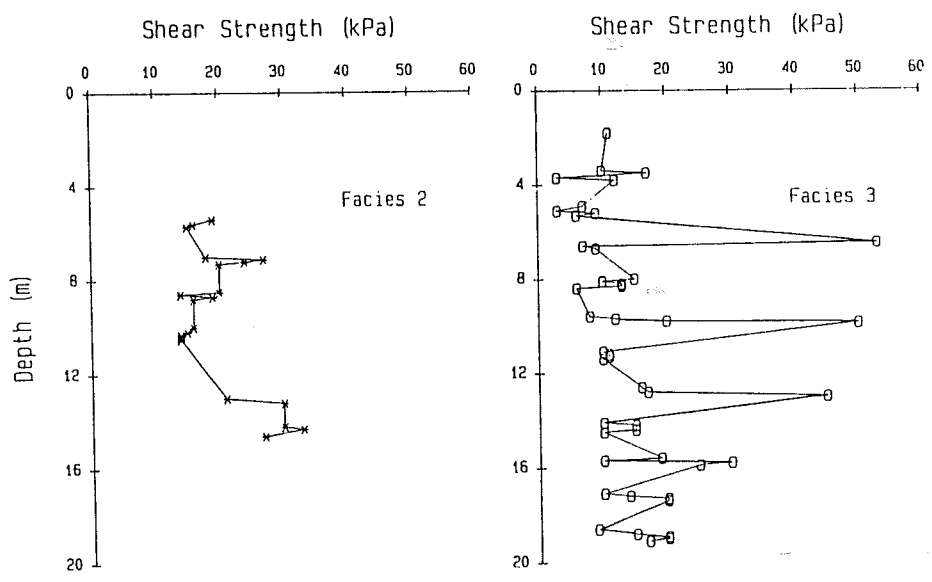
**Table 7.4** Predicted deep water wave heights for various return periods, for North Head, based on a 14 year wave hindcast (from Pinchin et al., 1985).

<b>Return Period (years)</b>	<b>Wave Height (<math>H_s</math>)</b>
1.0	2.9
5.0	5.0
10.0	5.2
20.0	5.4
50.0	5.7
100.0	5.9





**Figure 7.31** Plasticity chart for 1984 North Head borehole sediments.



**Figure 7.32** Downhole shear strength plots for bioturbated silts and laminated silts and clays, North Head boreholes.

mainland coast. Therefore little mention will be made in this section of beach sediment transport. The single exception is in the modelling work of Pinchin et al. (1985), who predicted sediment transport at North Head. However these predictions do not take into account the interaction of waves with a low angle muddy seafloor, where active resuspension is occurring. Studies from other muddy coastlines suggest that significant attenuation of waves can occur as they travel over a muddy bottom (Wells and Coleman, 1981).

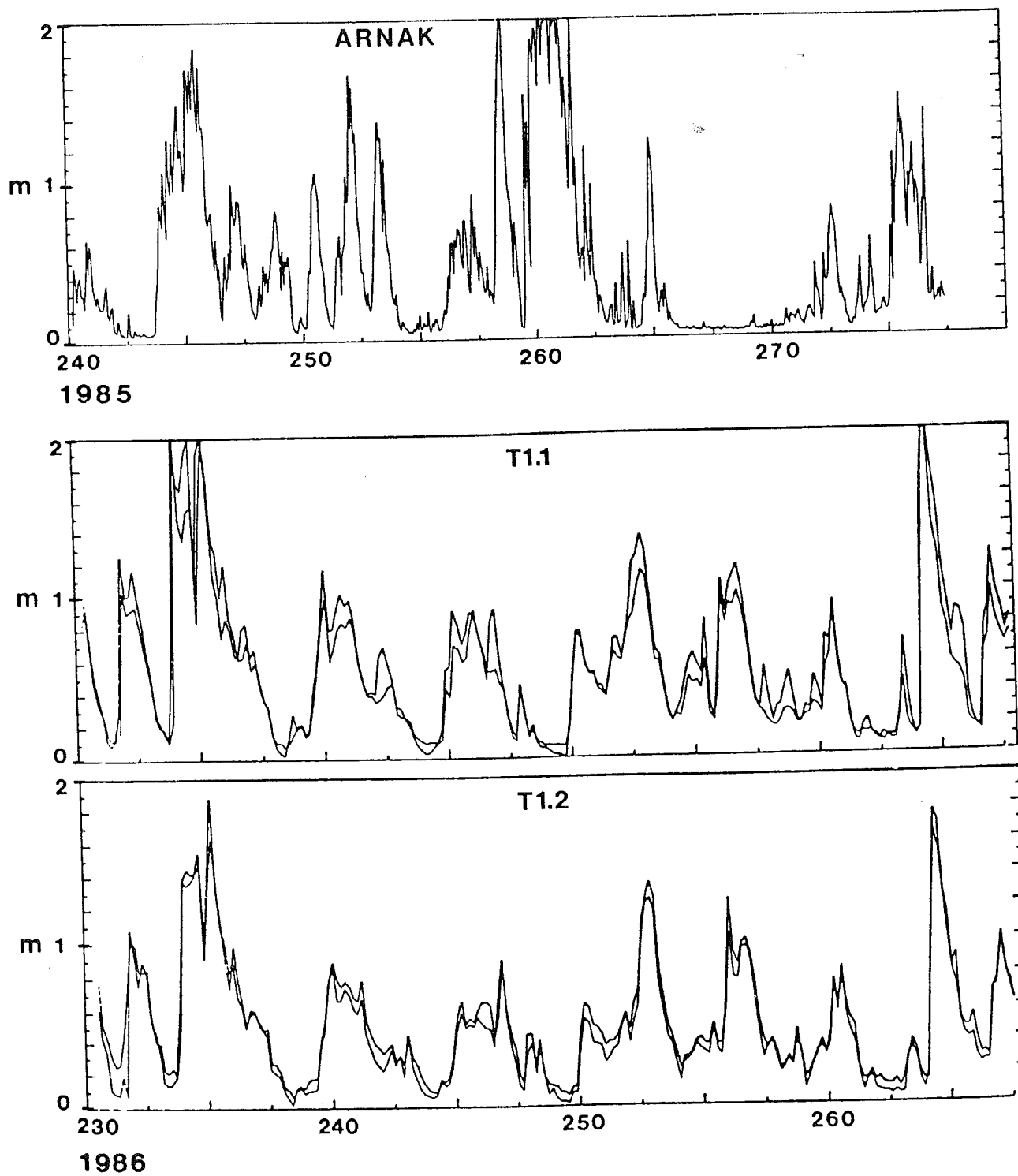
### **7.7.1 Waves**

As discussed in previous sections, winds in this part of the Beaufort Sea blow predominantly from two directions. Northwesterlies generally provide the strongest winds, whereas easterlies tend to be lighter, but significant in duration. Philpott et al. (1985) conducted a hindcast analysis for waves at North Head. The hindcast was more complicated at North Head than at other sites because, as well as the usual deep water hindcast which is refracted inshore, a second hindcast was required to take into account waves generated in the shallow water area of Beluga Bay. The two hindcasts were combined to give a total wave spectrum for use in sediment transport predictions on the North Head coast. Predicted wave heights from the deep water hindcast are shown in Table 7.4.

Measurements of waves in the area have been limited, but relatively long data sets are available from three sites (Davidson et al., 1988; for locations see Fig. 7.7). Wave parameters were derived from burst sample current data collected in 1985 at the Arnak drill site, northeast of North Head in 7.6 m of water. Two data sets are available from an ESRF program in 1986. The two sites, T1.1 and T1.2 were in 10.5 and 5.9 m of water respectively, and were located northwest of North Head. Wave height data from the three sites are shown in Figure 7.33. The strongest storms that occurred during the two deployment periods produced maximum significant wave heights of 2 m. A regression analysis on wind and wave data from 1986 indicates that northerly and westerly winds were the most effective in generating surface waves (Davidson et al., 1988).

### **7.7.2 Currents**

Currents have been measured at several sites on the inner shelf (Fig 7.34) and Davidson et al. (1988) have completed an analysis of these data. Current time series data are shown on this figure as a cluster plot with each point representing one velocity observation and the scatter of the plot indicating the variance of the velocity. Although strong currents reaching more than 75 cm/s have been recorded at these sites, the direction of the current is highly variable, although there is a weak tendency towards flow subparallel to the contours at the deeper sites. As a result of the high variance, the mean velocities are low (between 2 and 10 cm/s, with a standard deviation between 9



**Figure 7.33** Significant wave height time series for three sites on the Garry Island to Summer Island inner shelf.

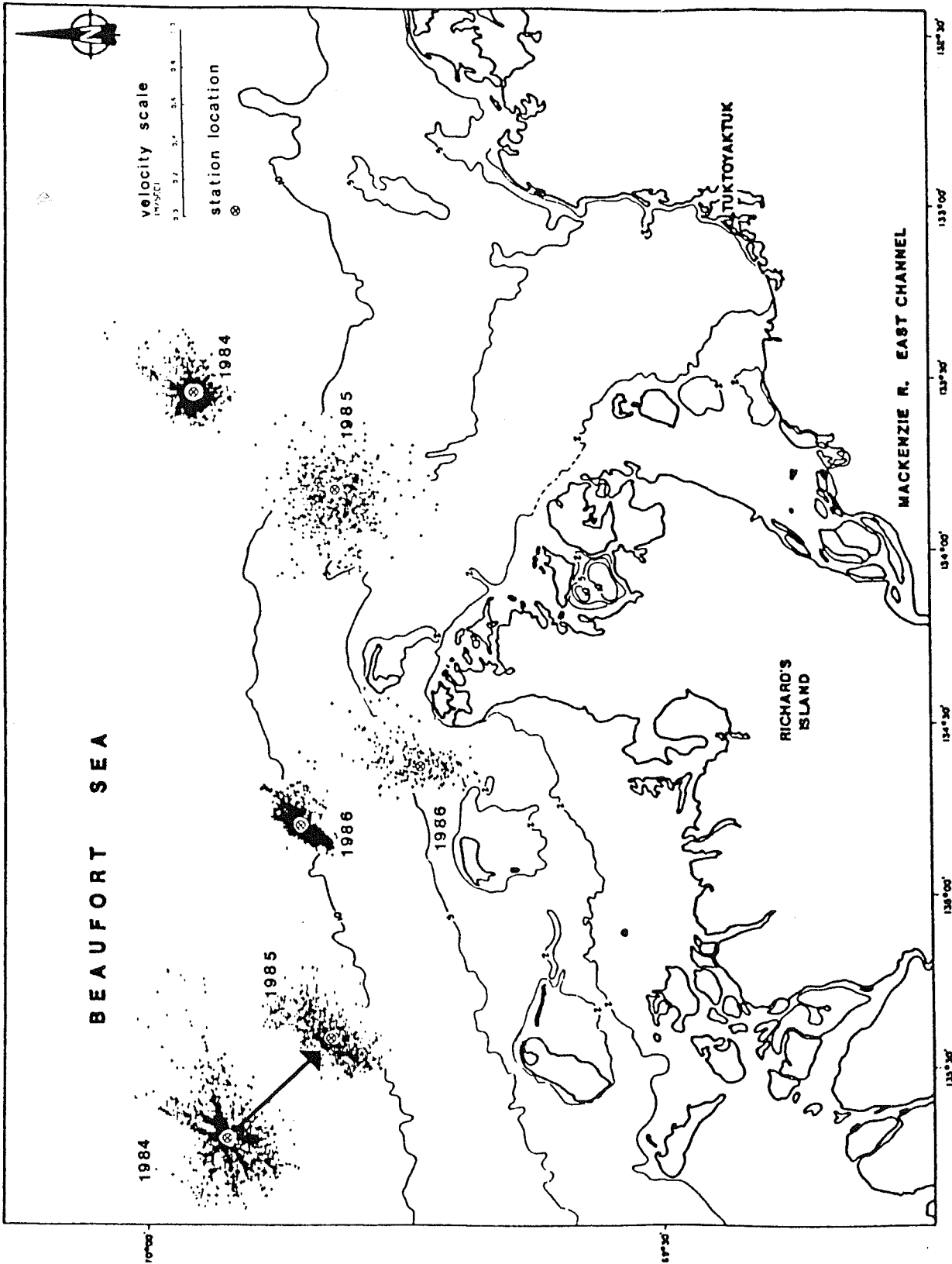


Figure 7.34 Current meter records from the inner shelf north of Richards Island (from Davidson et al., 1988).

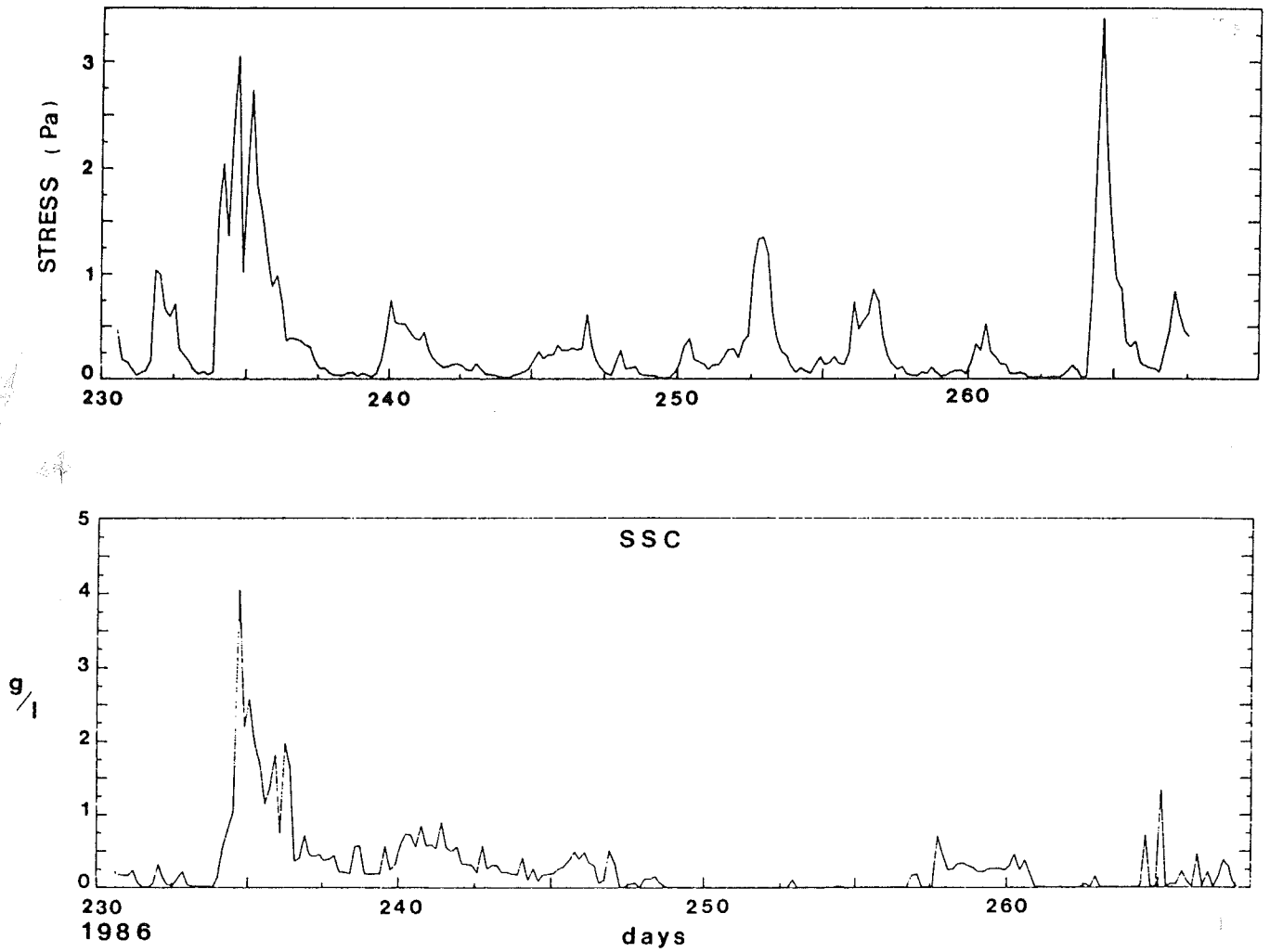
and 26 cm/s). Most of this variance is in the low frequency (periods longer than 24 hours) and is related to direct wind-forcing of the currents, as confirmed by a highly significant correlation between winds and currents. Correlation analysis indicates that the maximum current response always occurs for winds blowing from the west to southwest, roughly parallel to shore. The current response in the cross-shelf direction is much lower.

### 7.7.3 *Sediment Transport*

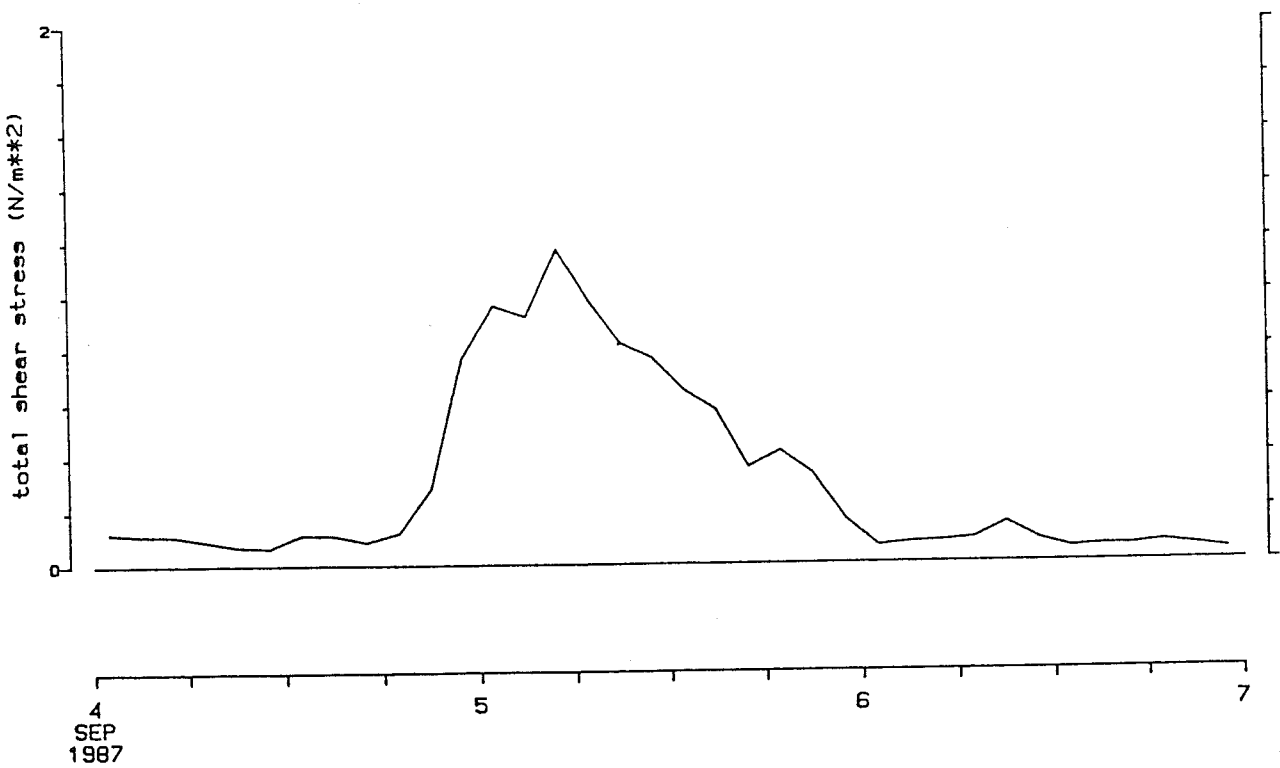
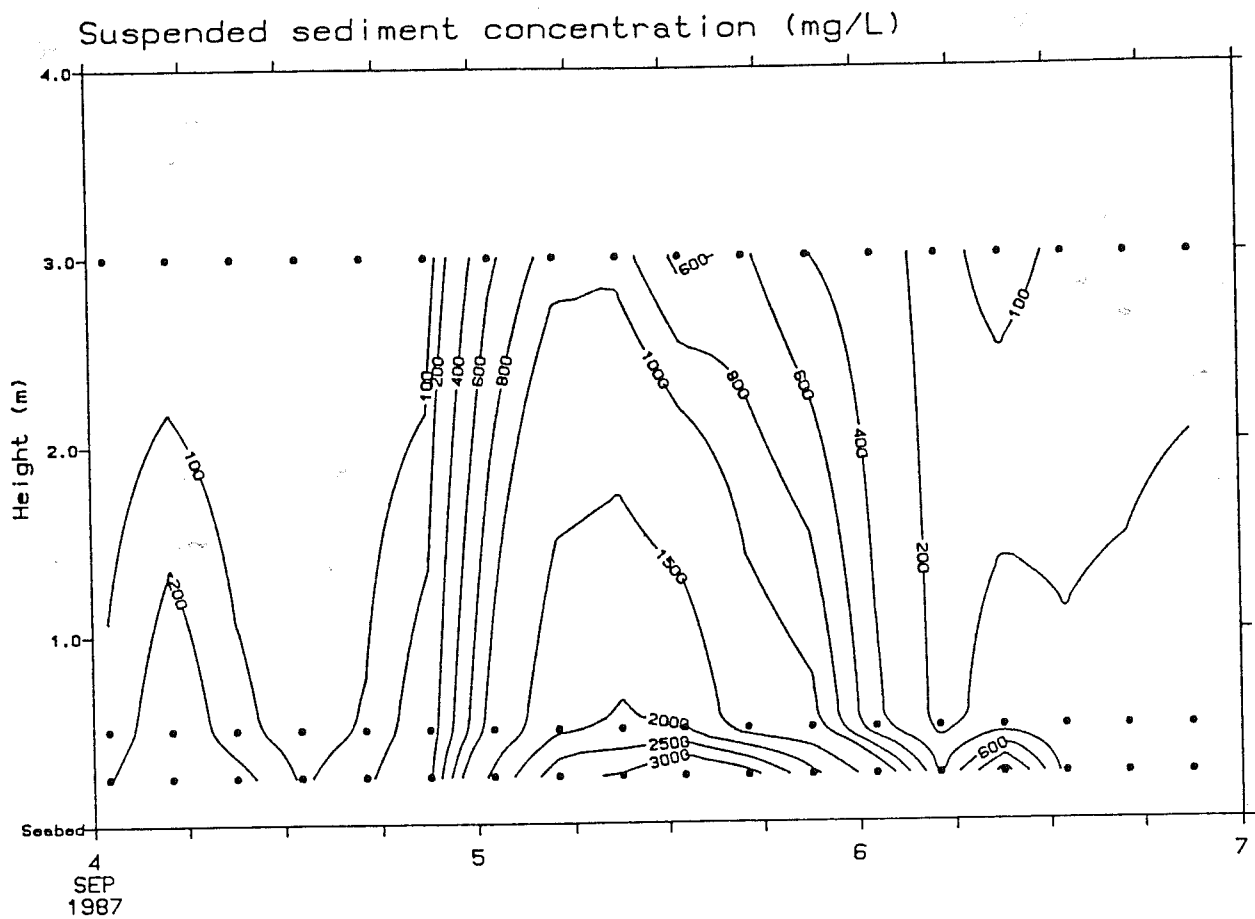
Davidson et al. (1988) used the 1986 wave and current data sets to calculate bottom stresses. The calculations were based on the method of Grant and Madsen (1979) which considers the non-linear interactions between surface waves and a steady current. Davidson et al. calculated the contributions of oscillatory motions and steady currents to the mean bottom stress and showed that the oscillatory component is 3 to 4 times larger than the steady component for all the sites where wave data were available.

A time series of suspended sediment concentration (SSC), from an optical backscatter sensor mounted 1 m above the seabed, was obtained at the T1.2 site in conjunction with wave and current measurements. This site was in 5.9 m of water. A plot of the SSC data and the bottom stress for the same time interval is shown in Figure 7.35. The SSC plots shows that very high concentrations of sediment, up to 4000 mg/l were measured during a storm on days 234-235 (22-23 August). A second major storm on days 264-265 produced only a moderate increase in SSC. This result is puzzling as calculated peak bottom stresses were actually higher during the second storm. A correlation between bottom stress and SSC was highly significant, but the regression only explained 33% of the variance. The remainder of the variance may be explained by advection of sediment from the Mackenzie plume, but the absence of a marked resuspension during the second storm needs to be explained. Possible explanations include (i) an increase in the critical erosion stress of the seabed sediments between the two storms; and (b) that resuspension has a time-dependant response, so that the second storm was not sufficiently long-lived to produce the extreme suspension of the first storm.

Hodgins (1988) made a detailed study of a storm induced suspension from data gathered at a site east of North Point in 1987 (Fig. 7.7). For this study, an array of OBS sensors at heights of 0.25, 0.5 and 3 m above the seabed were successfully obtained, as well as wave and current data. The results of this study (Fig. 7.36) show that sediments close to the bed (>50 cm) are brought into suspension as soon as the bottom stress begins to increase. The maximum measured SSC (>3000 mg/l) close to the bed occurs at a lag of 4 to 8 hours after the time of maximum stress and tends to lag the stress once the latter begins to decrease. Although SSC data equivalent to the 1986 measurements at 1 m above seabed were not successfully obtained, it appears that concentrations at this level would not have exceeded 2000 mg/l.



**Figure 7.35** Time series of (a) bottom stress derived from wave and current measurements at the T1.2 site, and (b) suspended sediment concentrations (SSC) from an optical backscatter sensor, mounted 1 m above the seabed.



**Figure 7.36** Suspended sediment concentrations and bottom stress near the seabed east of North Point from the 1987 program (from Hodgins, 1988).



It is possible that the lag observed in the 1987 data (and in fact in the first storm of the 1986 data) is the cause of the low SSC's measured during the second 1986 storm, which was relatively short-lived. However, the reason for such a lag is not understood. Hodgins (1988) used a model that balances particle settling with upward turbulent diffusion (based on Shi et al., 1985), to further evaluate the resuspension event. However, the model fails to account for the lag of peak SSC on the peak stress discussed above, or for the continuing high concentrations of sediment high in the water column after the peak stress.

## 8. KUGMALLIT BAY

In this section, a discussion of seismic stratigraphy and the sedimentology of gravity cores collected in 1986 from Kugmallit Bay will be discussed. Other aspects of the coastal geology of Kugmallit Bay are discussed in sections 7 and 9.

### 8.1 Seismic Stratigraphy

High resolution seismic data are available in Kugmallit Bay from both NAH86 and NAH87 cruises. Most of the data is from the NAH86 cruise (Fig. 8.1) and is of poor quality. Nevertheless, mapping of the major reflectors was possible. The NAH87 survey lines are restricted to the outer part of the bay, but provide better quality records for interpretation of more subtle features.

Kugmallit Bay is the inner shelf and coastal expression of Kugmallit Trough (O'Connor, 1982). The seismic stratigraphy of Kugmallit Trough is similar to that of Ikit Trough, consisting of an erosional unconformity defining a broad valley, which is infilled by two sequences, a marginal progradational sequence and an overlapping stratified sequence (Hill et al., in prep.).

The large paleo-valley of Kugmallit Trough, defined by a distinct basal unconformity, can be traced into Kugmallit Bay (Fig. 8.2). The deepest part of the valley runs through the centre of Kugmallit Bay and has a flat base at between 20 and 22 m b.s.l. The valley floor is locally interrupted by closed "scour" holes with depths to 25 or 30 m b.s.l. The margins of the valley are relatively steep and bounded by flat terraces becoming narrower as the channel funnels into Kugmallit Bay. A smaller valley seaward of Tuktoyaktuk Harbour joins with the main valley 9 km west of the harbour entrance. A small but deep scour hole is present at the confluence of the two valleys.

Although the base of the valley can be mapped from the poor-quality NAH86 records, details of the sequences above and below the unconformity are commonly obscured. Acoustic penetration in the sequence below the valley base is very poor, except for a few weak dipping reflectors. Two NAH87 lines at the mouth of Kugmallit Bay (Fig. 8.1), however, show that the basal reflector of the Kugmallit valley system is complex. An irregular wedge-shaped unit (KU2a) is present at the eastern margin of the valley, near Toker Point (Fig. 8.3). The wedge is approximately 5 m thick at thick at the eastern margin of the bay and becomes thinner towards the axis of the valley, and finally indistinguishable from the underlying sequence (KU2b). Stratification within the wedge is poorly-defined, but characteristically hummocky or inclined. The unconformity marking the top of the sequence is characterized by numerous hyperbolic reflectors indicating a rough surface.

A stratified sequence fills most of the sub-bottom valley and onlaps both the underlying

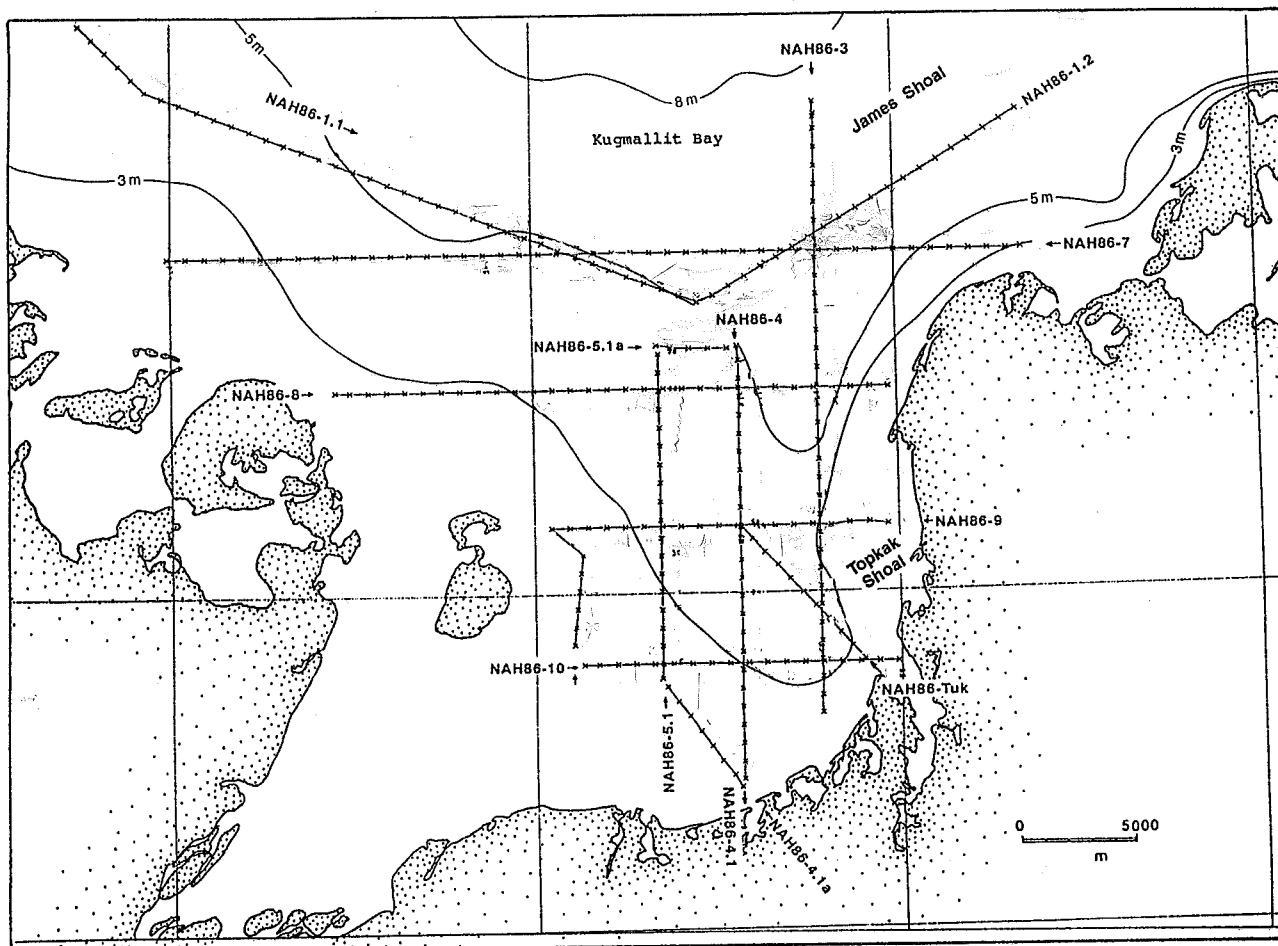
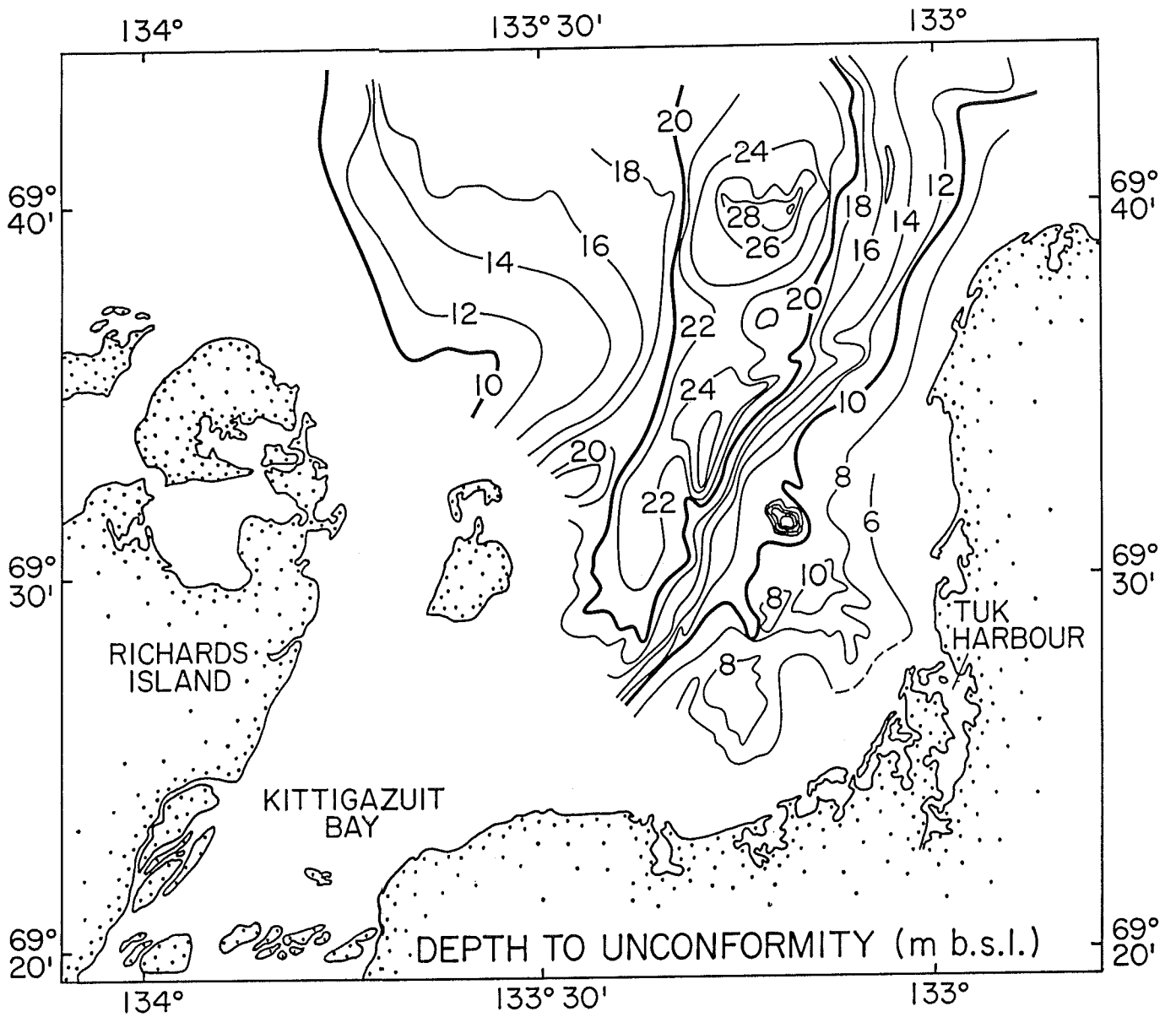
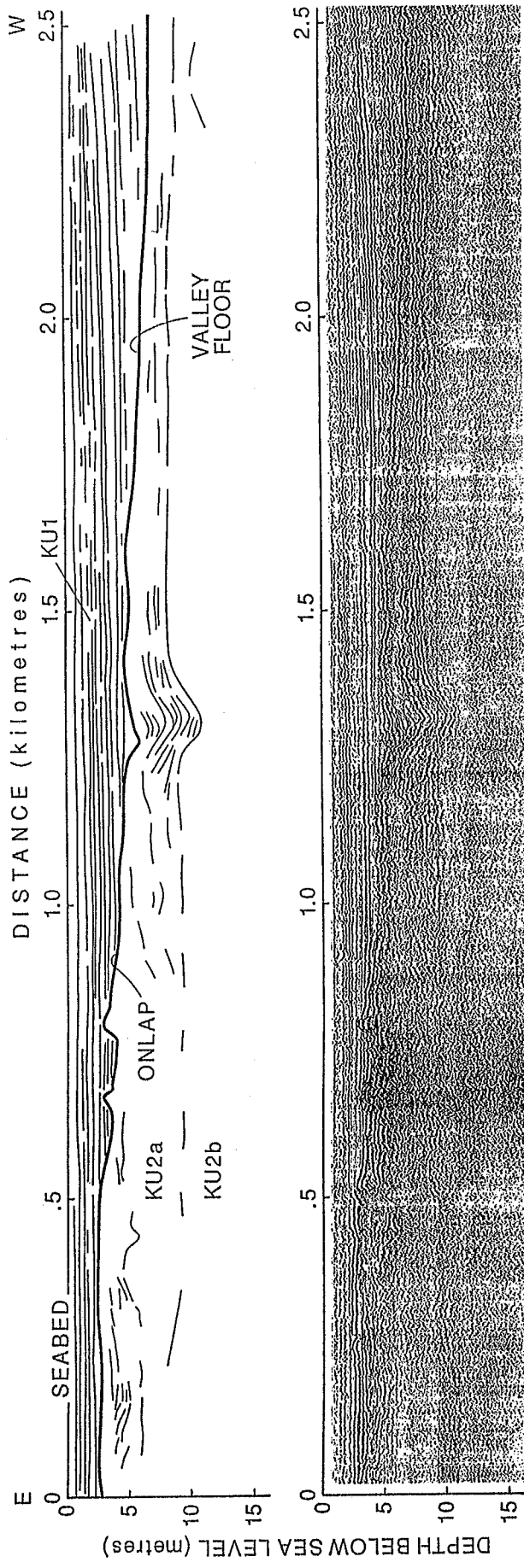


Figure 8.1 NAH86 seismic track plot from Kugmallit Bay.



**Figure 8.2** Depth to unconformity map of Kugmallit Bay, based on NAH86 and NAH87 seismic records (after Jenner, 1987).



**Figure 8.3** Seismic profile NAH87-3 with interpreted line drawing, west of Toker Point. Note section orientation shows west to the right and east to the left.

sequences (Fig. 8.3). Stratification is best-defined in the deeper parts of the valley and lower parts of the sequence, becoming more broken up towards the west and in the upper part of the sequence. In the vicinity of James Shoal, a 3 to 4 m high constructional feature (KU1b) is present within the basal part of the stratified sequence (Fig. 8.4). This causes a divergence of the valley into two separate parts, to the east and west of James Shoal. The upper part of the stratified sequence onlaps the shoal in the western sub-valley, whereas the eastern, smaller sub-valley is infilled by eastward migrating clinoforms which downlap onto underlying reflectors.

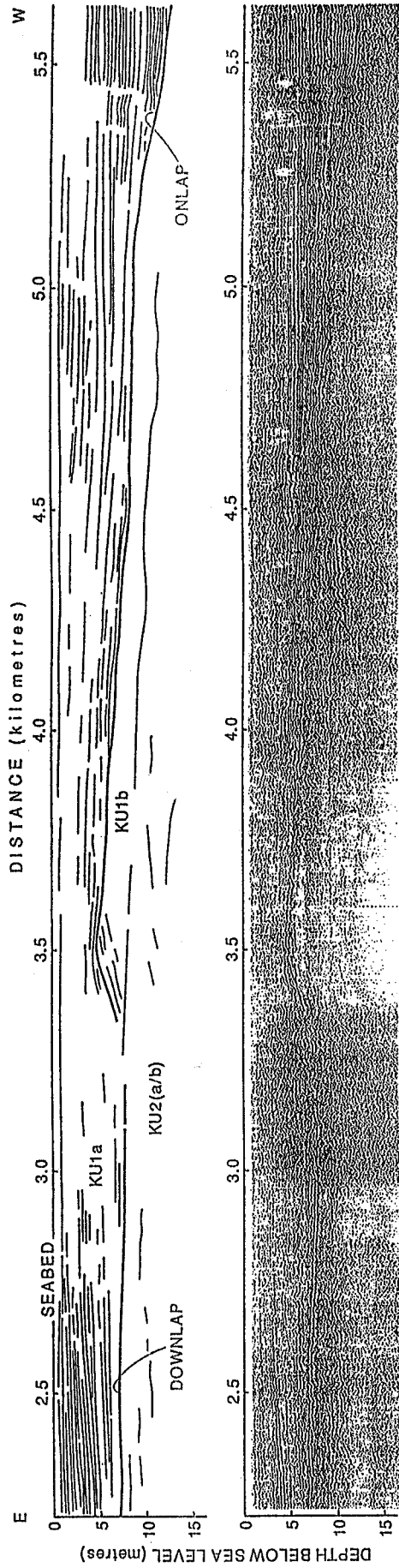
At the head of Kugmallit Bay, close to the mouth of East Channel, the valley bottom can be distinguished as a hummocky reflector which deepens markedly from 7 to 8 m at the margin to more than 18 m towards the axis of the bay (Fig. 8.5). The sequence below this reflector is probably equivalent to unit KU2 (a or b) in Figure 8.3. The base is overlain by a stratified sequence, wedging out from the break in slope and filling the irregular valley floor to a thickness of at least 8 m. The top of the sequence is marked by a relatively strong reflector, which locally has higher amplitude as a result of gas-charging. This unit has a much more stratified character than the wedge-shaped unit KU2a in Figure 8.3, so that it is unclear whether the two units are correlative. An alternative and possibly better correlation is that it is equivalent to KU1b in Figure 8.4. The top-bounding reflector of this unit is onlapped by an upper stratified sequence (demonstrably correlative with KU1a) which fills the remaining relief in the bay.

A second shoal, Topkak Shoal, is present 6 km north of Tuktoyaktuk (Fig. 8.1) and has different characteristics from the sequence at James Shoal. Topkak Shoal occurs on the eastern marginal terrace of the Kugmallit paleo-valley and although seismic data quality across the shoal is poor (and therefore not reproduced here), it appears to be related to a high in the sequence underlying the paleo-valley floor (KU2), rather than to the valley-fill sequence (KU1) as in James Shoal. KU1 wedges out over the shoal and the KU2 sequence appears to outcrop at the seabed.

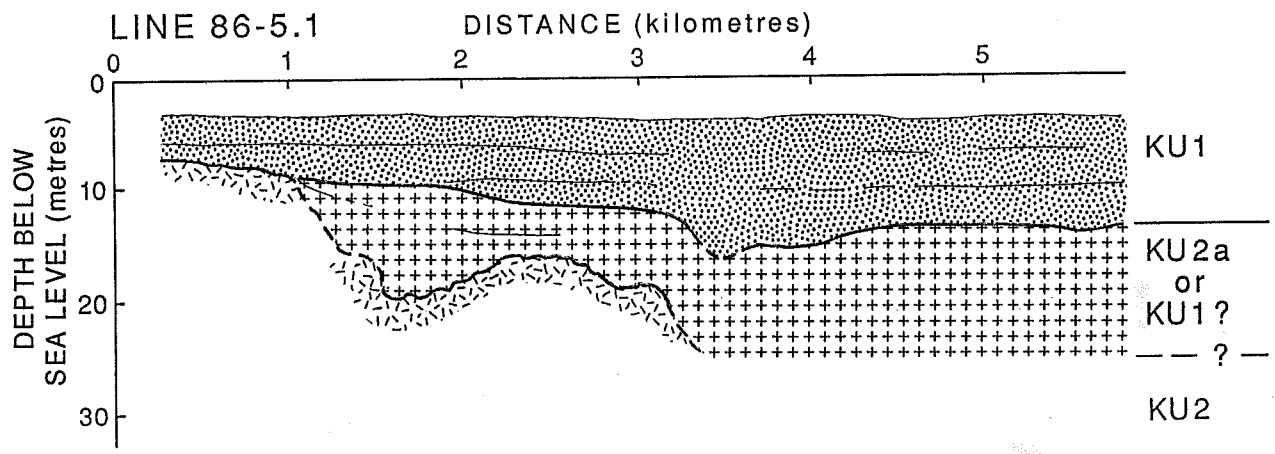
Gas-charged sediments are relatively rare in Kugmallit Bay in comparison to areas to the west. However, short intervals of gas-masking are observed along the margins of the bay and more rarely within the stratified sediments of the bay axis. In one location at the mouth of the bay, the gas can be observed to breach the seabed and produces pockmarks, clearly visible in the sidescan sonar record (Fig. 8.6).

## **8.2 Lithostratigraphy and Sedimentology**

A set of gravity cores were collected from Kugmallit Bay, on the NAH86 cruise. These cores were examined by K. Jenner as part of course requirements at Dalhousie University (Jenner, 1987). The cores were collected along two transects that cross Topkak Shoal (Fig. 8.7), where seismic unit KU2 outcrops at or close to the seabed. Six sediment facies can be distinguished in these cores:

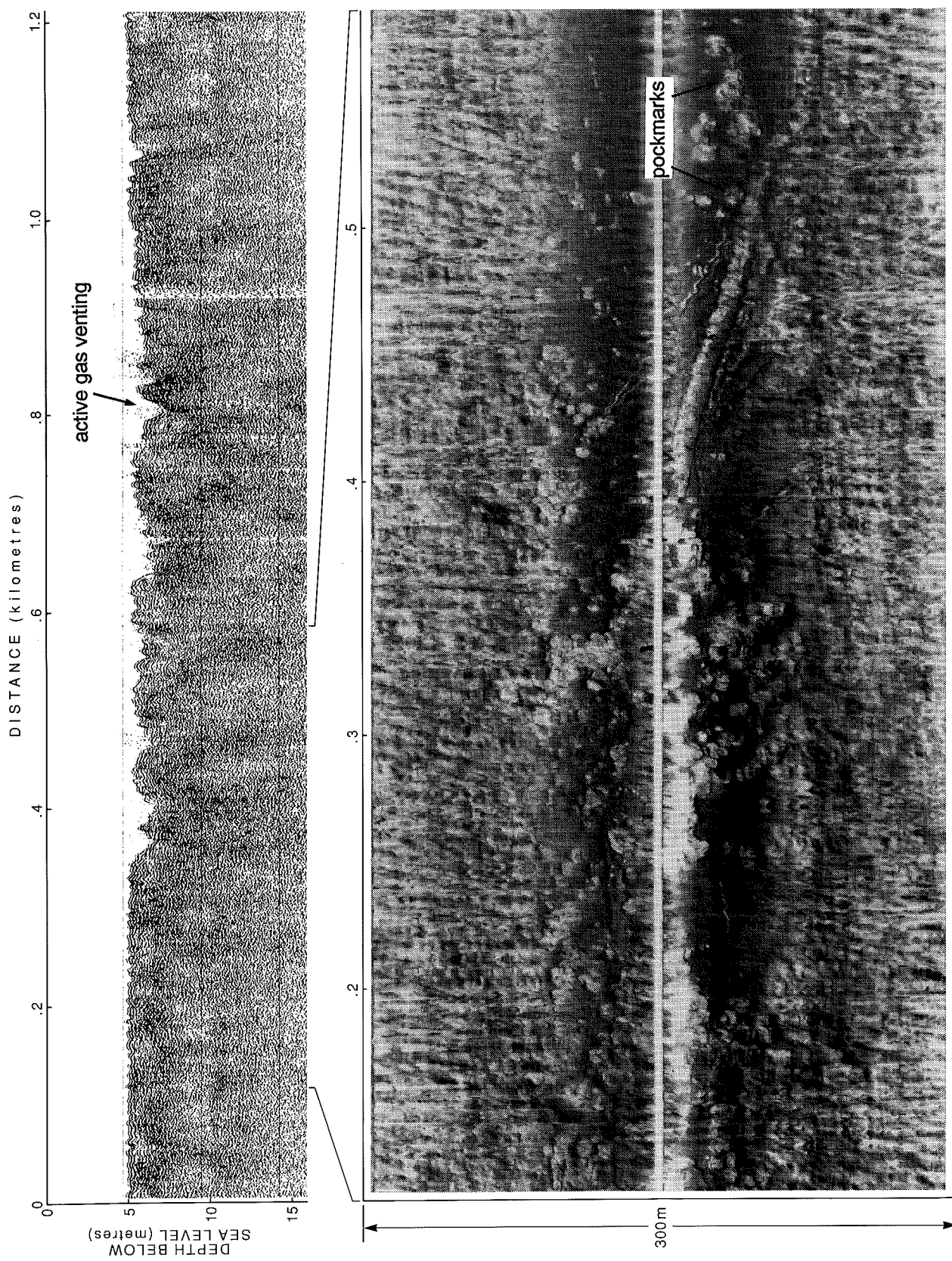


**Figure 8.4** Seismic profile NAH87-3 with interpreted line drawing (continuation of profile in Figure 8.3) just south of James Shoal.



**Figure 8.5** Sketch section of seismic profile NAH86-5.1. Original record is too noisy for reproduction.





**Figure 8.6** Seismic and sidescan sonar records NAH87-3, west of James Shoal, showing pockmarks on seabed and active gas venting.

### **1. *Homogeneous to laminated clay***

Olive grey homogeneous to bioturbated clay with rare silt laminae and shells forms the uppermost portion of the sediment column in water depths less than 5 metres.

### **2. *Laminated to very thin-bedded clay and silt***

Repetitious very thin (< 3 mm) basal silt laminae grade up into thin clay beds up to 2 cm in thickness. Fine-grained sand laminae are rare. The beds commonly dip at a low angle, rarely showing low angle truncations.

### **3. *Bioturbated silt and clay***

This facies predominates within Kugmallit Bay. It consists of cyclic depositional units, from 1 to 5 cm thick, consisting of thin wavy silt bases grading upwards into silty clay and clay intervals. Bioturbation occurs throughout the facies, and is commonly seen at bed boundaries.

### **4. *Graded sand and silt***

Well sorted fine to medium-grained sand laminae up to 3 mm thick grade up into thin beds of silt and clay forming cyclic sequences from 2 to 7 cm thick. The sandy bases are erosional and sharp, but may show partial disruption by bioturbation. Circular, isolated sand burrows and lenses are present within the siltier intervals.

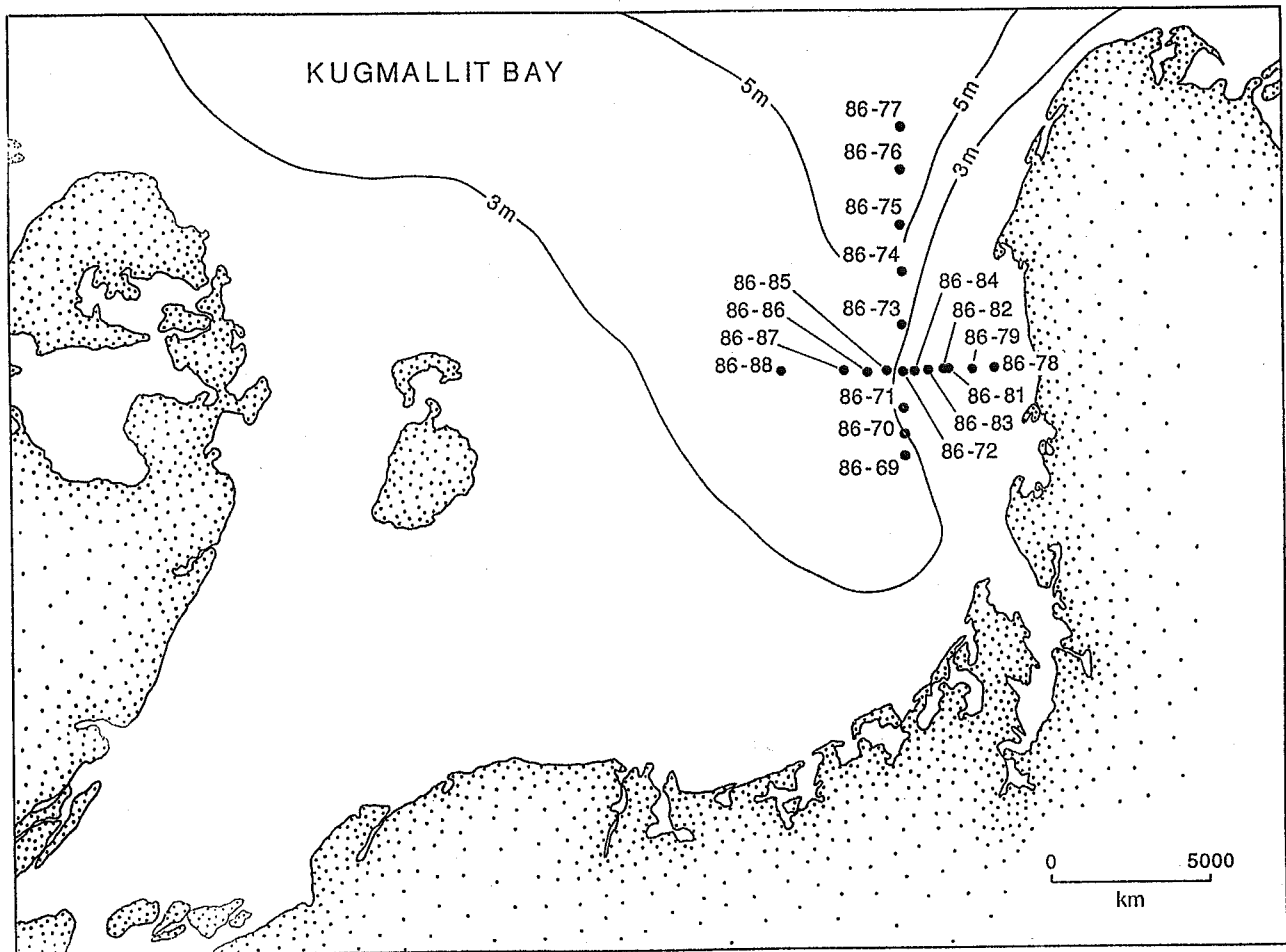
### **5. *Thin-bedded silt***

Thin silt beds up to 5 cm thick separated by thin clay laminae are characteristic of this facies. The silt beds are sharp based and graded. This facies is spatially limited within Kugmallit Bay.

### **6. *Laminated silt and clay***

This distinctive facies consists of alternating sub-horizontal silt laminations with subordinate amounts of clay as interbeds. Individual laminae show sharp bases and are without exception less than 5 mm thick. Low angle truncations are observed amongst multiple sets of laminae.

The distribution of these facies along the two transects is shown in Figures 8.8 and 8.9. The cores typically show a fining- and thinning-upwards sequence from graded sand and silt, through bioturbated silt and clay, and laminated very thin-bedded clay and silt, to homogeneous clay. On Topkak Shoal, in cores 71, 72, and 73, the thin-bedded silt and laminated silt and clay facies occur in the middle of the fining upwards sequence. Other cores on the shoal are short (less



**Figure 8.7** Location map for gravity cores collected in Kugmallit Bay on NAH86 cruise (from Jenner, 1987).

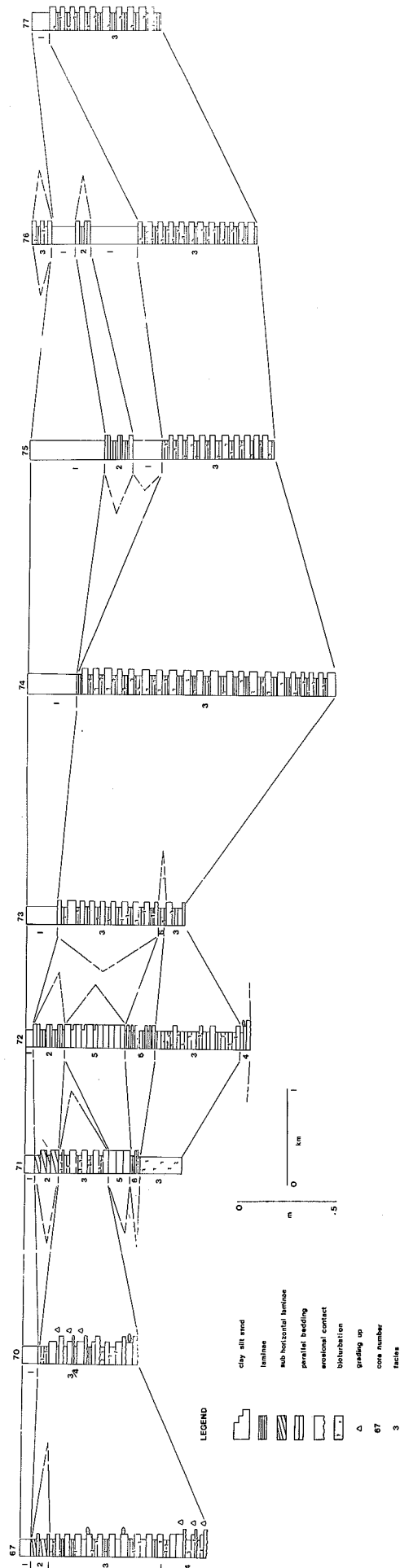
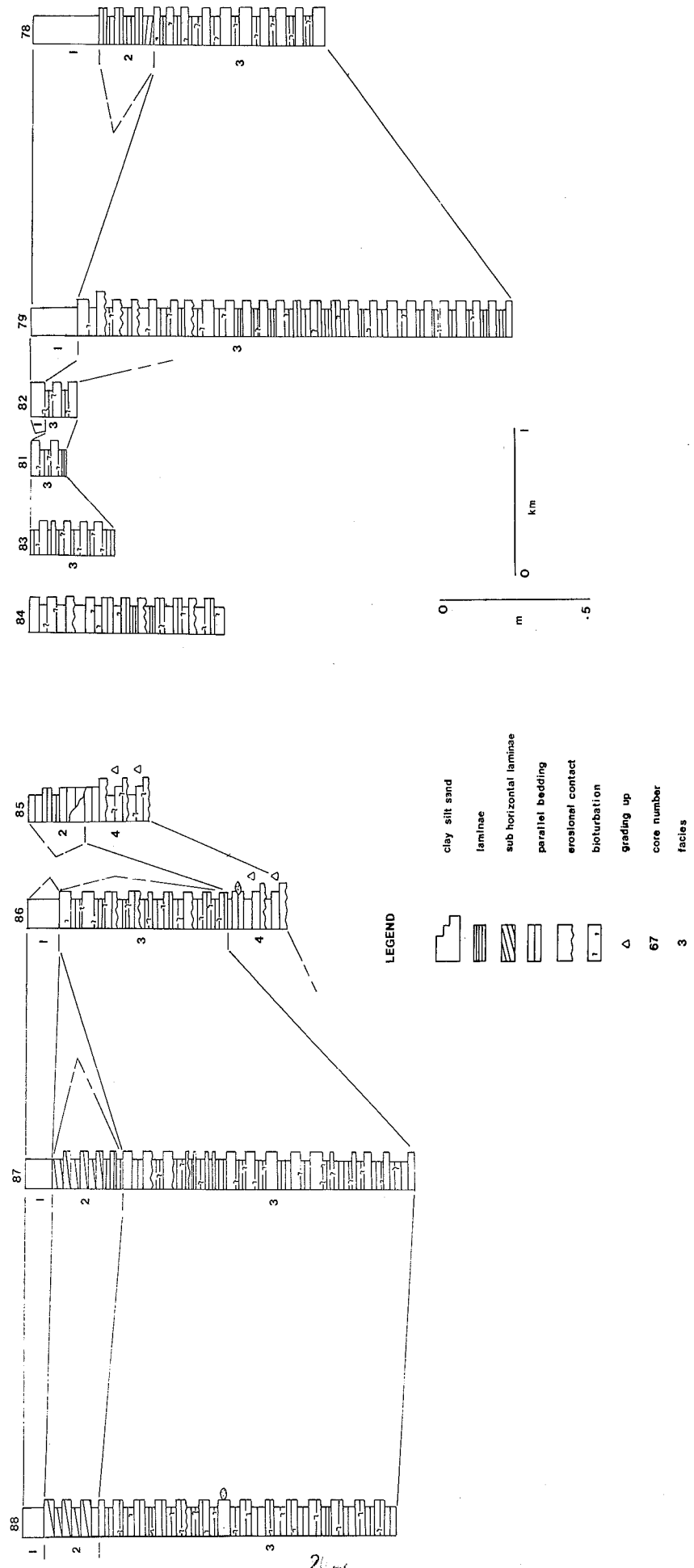


Figure 8.8 North-south core transect in Kugmallit Bay showing distribution of sediment facies (from Jenner, 1987).



**Figure 8.9** East-west core transect in Kugmallit Bay showing distribution of sediment facies (from Jenner, 1987).

than 0.5 m), probably reflecting a hard sub-bottom to the shoal.

Although neither detailed biostratigraphic analysis nor radiocarbon dating of these cores have been carried out, the fine grained sediments recovered are probably Holocene, post-transgression deposits. Bioturbation may be used as an indicator of relative rate of deposition, with the more heavily bioturbated sediment representing low net accumulation rates, and sediment with well-preserved primary structures representing relatively high rates of net accumulation. The various facies represent deposition from suspension under different dynamic conditions, resulting from either primary plume transport within Kugmallit Bay or by resuspension as a result of wave and current action, particularly on shoals such as Topkak Shoal. As Kugmallit Bay is substantially sheltered from strong westerly or northwesterly winds, direct deposition from the plume may be a more important process, compared to the wave dominated area off North Head (Hill and Nadeau, 1989).

The fining- and thinning-upwards sequence, characteristic of most cores in the bay, probably reflects continuing transgression of Kugmallit Bay during Holocene sea-level rise. Seismic profiles and boreholes from offshore in Kugmallit Trough typically show an upward transition from a well-stratified siltier sequence to a transparent clay sequence (Hill et al., in press). The origin of the intervening sequence of graded and laminated silts, above the sub-bottom bank, is not clear. It may represent a period of increased wave and current activity during the late Holocene, or possibly some local change in bank morphology, such as erosion of an island or headland, seaward of the core sites.

## 9. TUKTOYAKTUK PENINSULA

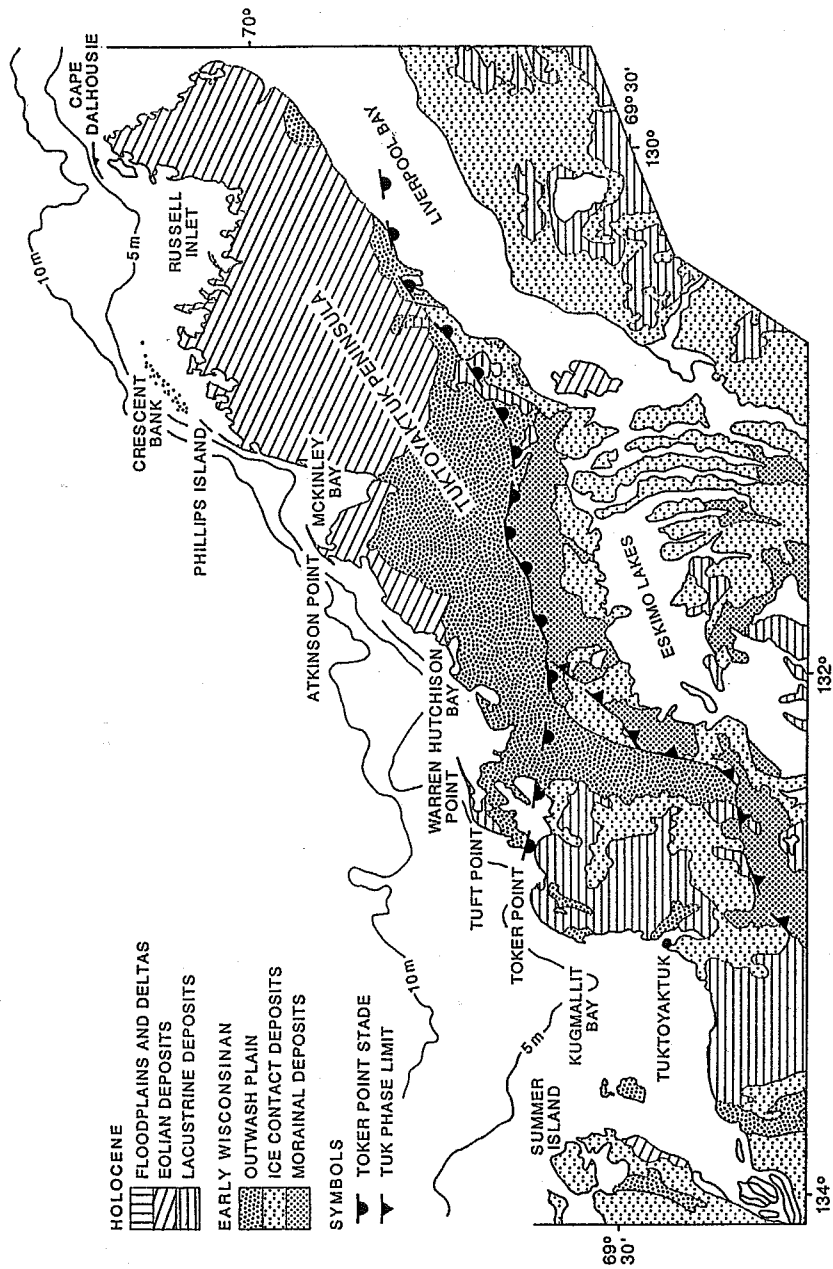
The Tuktoyaktuk Peninsula extends northeastwards from Kugmallit Bay as a low relief plain, separated on its eastern shore from the mainland by Liverpool Bay (Fig. 9.1). In this section, only the northwest-facing coast is discussed. The coastline is very irregular, with several large bays, particularly Hutchison Bay, McKinley Bay and Russell Inlet, separating very irregular, drowned thermokarst lake topography.

### 9.1 Quaternary Geology

Rampton (1988) has identified an ice margin position on the Tuktoyaktuk Peninsula, which he assigned to the Toker Point Stade (Fig. 9.1), and correlated with the Buckland Glaciation on the Yukon Coastal Plain (Rampton, 1982). This limit is the maximum all-time limit of Laurentide ice in the region (Hughes et al., 1981; Dyke and Prest, 1987) and is considered to be of early Wisconsinan age by Rampton (1982, 1988). Some question remains about the age of this event as the Laurentide maximum limit can be traced south to the Bonnet Plume Basin where it has been dated at less than 39,000 years (Hughes et al., 1981). On the other hand, there is clear evidence for a younger ice limit to the south and west of the Tuktoyaktuk Peninsula in the Sitidgi Lake area and the Mackenzie Delta. This limit is marked by the Tutsieta Lake Moraine (Hughes, 1988) and is assigned to the late Wisconsinan Sitidgi Stade by Rampton (1988).

Associated with the Toker Point limit on the Tuktoyaktuk Peninsula is a second ice limit, the Tuk Phase limit (Mackay et al., 1972; Fyles et al., 1972; Rampton, 1988), which coincides with the Toker Point limit east of Hutchison Bay, but splits and is traced parallel to Eskimo Lakes to the southwest (Fig. 9.1). The Tuk Phase limit was initially thought to be late Wisconsinan in age by Mackay et al. (1972) and Fyles et al. (1972), but Rampton (1988) re-interpreted this limit to be associated with early Wisconsinan glaciation. Along the Tuk Phase limit, there are a number of ice margin features and deposits which attest to a complex deglacial history. Subglacial meltwater channels have been identified in the Eskimo Lakes area and a prominent proglacial meltwater channel crosses the Tuktoyaktuk Peninsula and can be traced to the head of McKinley Bay (Rampton, 1988). This channel can be traced offshore in seismic records and can be seen to incise sediments tentatively interpreted as late Wisconsinan age (Hequette and Hill, 1989). This relationship suggests that late Wisconsinan ice may have extended further north than the Tutsieta Lake limit of Hughes (1988) and may have been responsible for the ice contact features of the Tuk Phase limit. Outwash valley trains cross the southeastern portion of the Tuktoyaktuk Peninsula and outwash sands associated with the Toker Point Stade cover much of the peninsula (Rampton, 1988).

There is no formal stratigraphy for the deposits of the Tuktoyaktuk Peninsula. From the



**Figure 9.1** Location map for the Tuktoyaktuk Peninsula, showing geology, ice margins and place names.



regional study of Rampton (1988) and my own observations, the majority of coastal exposures consist of well-sorted brown sand, interpreted by Rampton (1988) to be glaciofluvial sediments related to the Toker Point or Tuk Phase ice margin. Boreholes from the Tuktoyaktuk area show that the sand in that locality is medium- to fine-grained, contains some silt beds and gravel in cross-bedded units and in parts contains excess ice. Sand, in one borehole, extends to at least 60 m below the surface. However, there is no certainty whether the sand comprises one, or several, stratigraphic units. West of Toker Point, inside the Toker Point limit, a thin deposit (generally 1 to 8 m thick) of clayey diamicton (morainic material of Rampton) is present above the sand.

## **9.2 Coastal Morphology**

The coastline of the Tuktoyaktuk Peninsula consists of (i) numerous headlands and narrow peninsulas, formed by the breaching of thermokarst lakes during coastal retreat, and consisting of low sandy bluffs with fringing beaches; (ii) crescentic embayments of various sizes, with fringing beaches and drowned tundra coastlines; (iii) flanking spits prograded from the headlands and progressively enclosing the embayments; (iv) long barrier islands, detached from the mainland coast, but commonly anchored by small islands.

### ***9.2.1 Headland and Peninsula Sea Cliffs***

Harper et al. (1985) classified cliffs along the Tuktoyaktuk Peninsula as predominantly low tundra or ice-poor cliffs. Cliffs constitute 55% of the coastline; they are generally low, sandy bluffs, rarely higher than 4 m and commonly less than 2 m high. Nevertheless local variations occur along this section of the coast. Along the south and east side of Kugmallit Bay, cliffs have low elevations (<2 m) and are formed of glacial diamicton containing gravels and pebbles. From Tuktoyaktuk to Cape Dalhousie, bluffs can reach more than 5 m in height and consist of Pleistocene sand of glacial origin (Rampton, 1988). Ground ice is common in the Quaternary deposits of the Tuktoyaktuk Peninsula (Mackay, 1971), but ice content is difficult to estimate in the cliffs because commonly a large part of the slope is covered by colluvium. Therefore, coastal sections previously classified as ice-poor cliffs may contain a high proportion of ground ice in certain cases. For example, east of Toker Point, severe storm-induced erosion in 1988 resulted in dramatic retreat of the cliff which appeared to be composed of massive ice, up to 4 m thick, overlain by about 1 m of sand capped by peat. Although the sand unit forming the cliffs commonly contains excess ice, retrogressive thaw failures are not common east of Toker Point, probably because of the low elevation of the cliff and frequent reworking of the cliff face by wind and wave action. It is also possible that the sandy material composing the cliffs limits such processes.

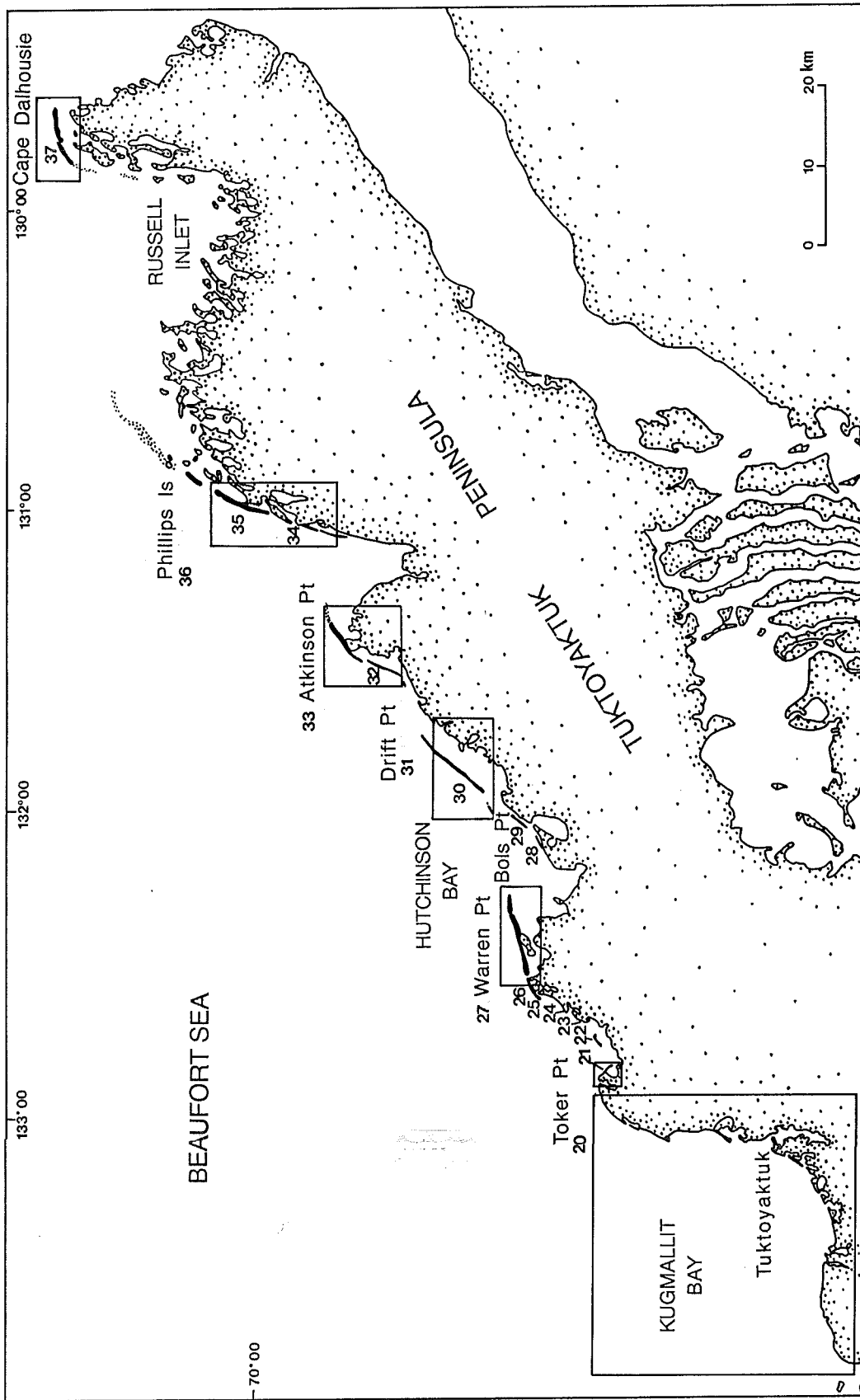
### **9.2.2. Drowned Tundra Coast**

Parts of the Tuktoyaktuk Peninsula consist of very low-lying tundra which is being drowned without the formation of an erosive bluff or beach. These very specific environments are classified in Harper et al. (1985) as submerged tundra extending into nearshore and foreshore areas. The flat bottoms of drained thermokarst lakes that are being transgressed by the sea have also been mapped as drown tundra coast (Harper et al., 1985). The complex thermokarst topography, commonly in the form of frost-heave polygons, is preserved as the transgression takes place, so that these coastlines show irregular, small-scale topography. The spatial occurrence of this type of coastal environment represents about 16% of the Tuktoyaktuk Peninsula coastline and the most extensive drowned tundra coastal section is located between Bols Point and Atkinson Point (Fig. 9.2). This type of environment has been termed "pitted topography" (Ruz et al., in press) because of the occurrence of numerous thermokarst ponds. Inundated tundra are usually found in sheltered environments such as along backbarrier lagoon coasts or in thermokarst embayments. Their foreshore margins commonly consist of silty sand flats with transverse bars, roughly perpendicular to the coastline, as seen south of Atkinson Point. In some cases, the tundra may be overlain by thin coastal marsh deposits.

### **9.2.3 Spits and Barrier Islands**

Along Tuktoyaktuk Peninsula spits and barrier islands are common, representing nearly 30% of the coastline. They show an interesting variety of coastal accumulation landforms. From the south shore of Kugmallit Bay to the tip of Tuktoyaktuk Peninsula, coastal accumulation features vary in shape, length and width (Table 9.1). Southwest of Tuktoyaktuk the coastline is very indented and coastal landforms have developed at the entrance of small embayments. Spits and barrier-spits along this section of the coast are very short (generally in the order of 500 m) and very narrow (< 80 m). They are composed of coarse sands and gravels derived from morainic deposits in eroded bluffs.

From Tuktoyaktuk to Toker Point, sandy features predominate. All the coastal landforms occurring along this section of the coast are spits, attached to an eroding bluff, and prograding in the direction of the local littoral drift. Spits are usually linear features straightening the coastline, but some are more complex, such as Topkak Point and Tibjak Point (Fig.9.3) where the distal sections consist of recurved ridges. Some spits progress from both headland, partially enclosing a thermokarst lake, as in Tininerk Bay and at Toker Point. All the spits along this part of the coastline consist of medium to fine well-sorted sand. They are short (< 2.5 km long), narrow (100 to 150 m wide), and generally low-elevation features. In some cases, such as Topkak Point, the crest elevation can reach more than 3 m due to the presence of coastal dunes. Behind this spit a tidal marsh developed where typical tidal creeks occur.



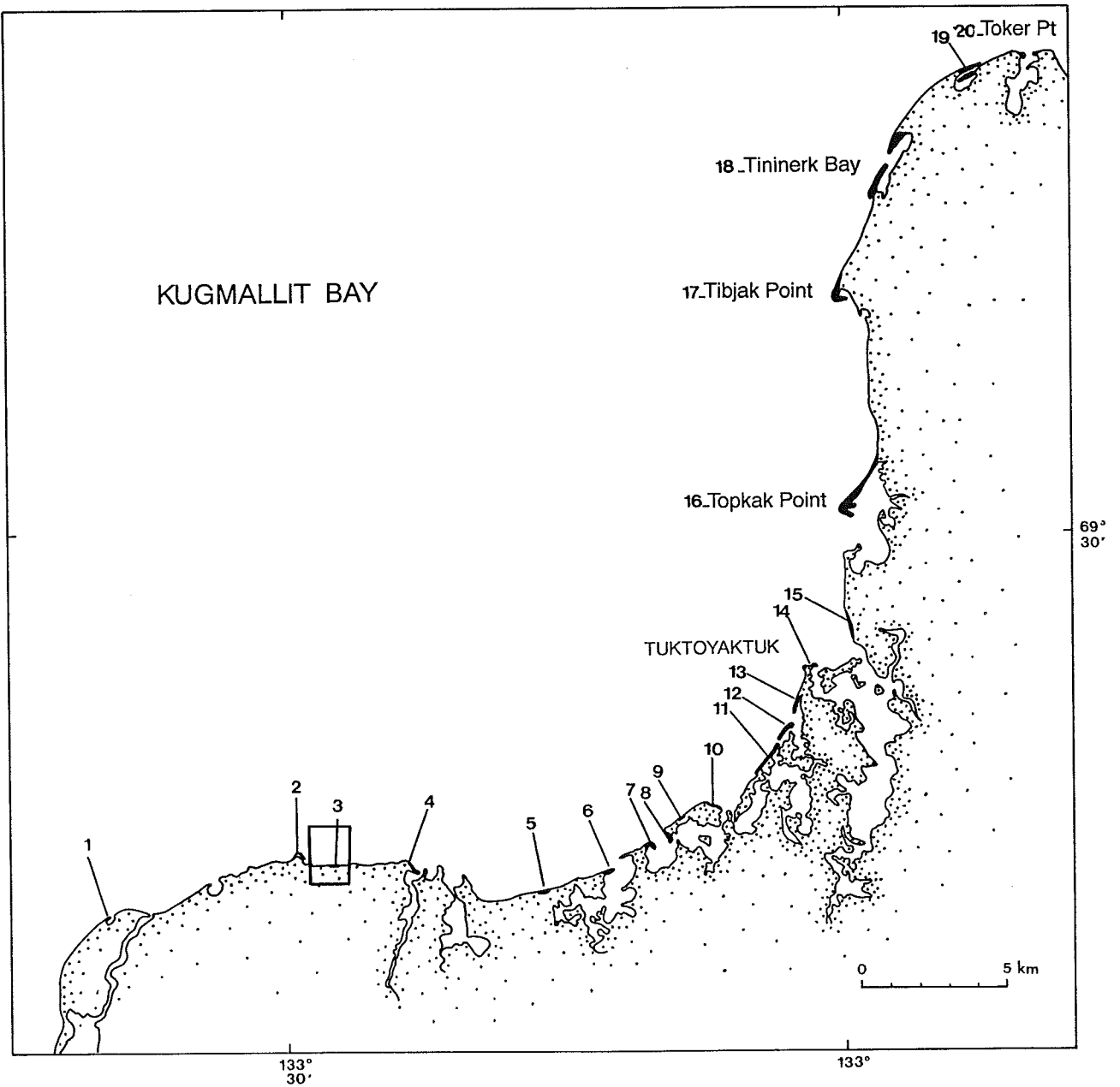
**Figure 9.2** Map of the Tuktoyaktuk Peninsula showing the location of the other figures referenced in the text. Numbers refer to locations in Table 9.1.

Table 9.1 Dimensions and retreat rates of spits and barrier islands along the Tuktoyaktuk Peninsula. See Fig. 9.2 for locations. (S): South end; (N): North end; (W): West end; (E): East end; (M): Middle portion.

N <sup>o</sup> and name (when available) of coastal accumulation features	Length (m)	Width (m)	Height (m)	Mean retreat rate (ma <sup>-1</sup> )
1	350	75		
2	500	50		
3	375	45		
4	900	45		
5	700	50		
6	550	80		-1.6
7	400	70		
8	400	80		
9	760	115		
10	470	85		
11	2 000	60	≈ 1.0	2.2
12	800	60	≈ 1.0	2.4
13	470	25		
14	320	25		
15	1 100	90		
16. Topkak Pt.	2 250	100	1.5-3	-0.9 (S) -1.15 (M) -1.3 (N)
17. Tibjak Pt.	1 565	100	1.0-2	-1.0
18. Tininerle Bay	S 1 540 N 2 280	150 150	1.0-2	
19.	1 670	155		
20. Toker Pt.	W 950 E 620	97 64	<1.0	
21. Mingnuk Pt.	1 650	100		-2.2
22. Kukjuktuk Bay Barrier Island	1 850	148	1.5	-4.25 (E) -2.8
23.	500	120		
24.	650	100		
25. Tuft Pt.	1 150	180	<1.0	-1.9
26.	600	150		
27. Warren Pt.	9 580	500	1.0-1.5	-1.7 (W) -1.8 (M) -1.0 (E)

Table 9.1 continued

N <sup>o</sup> and name (when available) of coastal accumulation features	Length (m)	Width (m)	Height (m)	Mean retreat rate (m a <sup>-1</sup> )
28.	1 550	50	≈ 1.0	
29. Bols Pt. Barrier Island	2 275	160	<1.0	-1.2
30. West Atkinson Barrier Island	10 500	250	<1.0	-3.1 (S) -3.5 (N)
31. Drift Pt.	955	185	<1.0	-1.9
32. Atkinson Barrier Island	4 420	175	0.7-0.8	-1.6 (S) -2.0 (M) -1.65 (N)
33. Atkinson Point				
-South Spit	2 280	140	1.0	-1.65
-North Spit	4 900	350-500	0.8	-1.95
34. East McKinley Bay				
-North Spit	920	150	≈ 1.0	-2.0
-South Spit	3 570	130	<1.0	-2.15
-South Barrier Island	4 000	160	<1.0	-1.85
35. South Phillips Island Spit				
-North Spit	3 900	335	≈ 1	-3.3 (N) -2.35 (S)
-South Spit	3 700	180	1.0-1.5	-1.9
36. Phillips Island	2 200	300		
37. Cape Dalhousie	7 620	250	0.9	-4.53 (W) -2.1 (M) -2.86 (E)



**Figure 9.3** Location map of the spits and barrier islands of the south and east coast of Kugmallit Bay. Numbers refer to locations in Table 9.1. Box shows the location of Figure 9.10.

Eastward of Toker Point, the coastline consists of a series of bays: Hutchison Bay, McKinley Bay, Seal Bay and Russel Inlet (Fig. 9.2 ) that are separated by headlands from where long sandy accumulation features have developed. Spits and barrier islands are generally low (<1 m) and extensively overwashed during storm events. They can measure up to 10 km in length and can be very wide (up to 600 m). In most cases they face the dominant wave approach from the NW.

#### *Warren Point Barrier System*

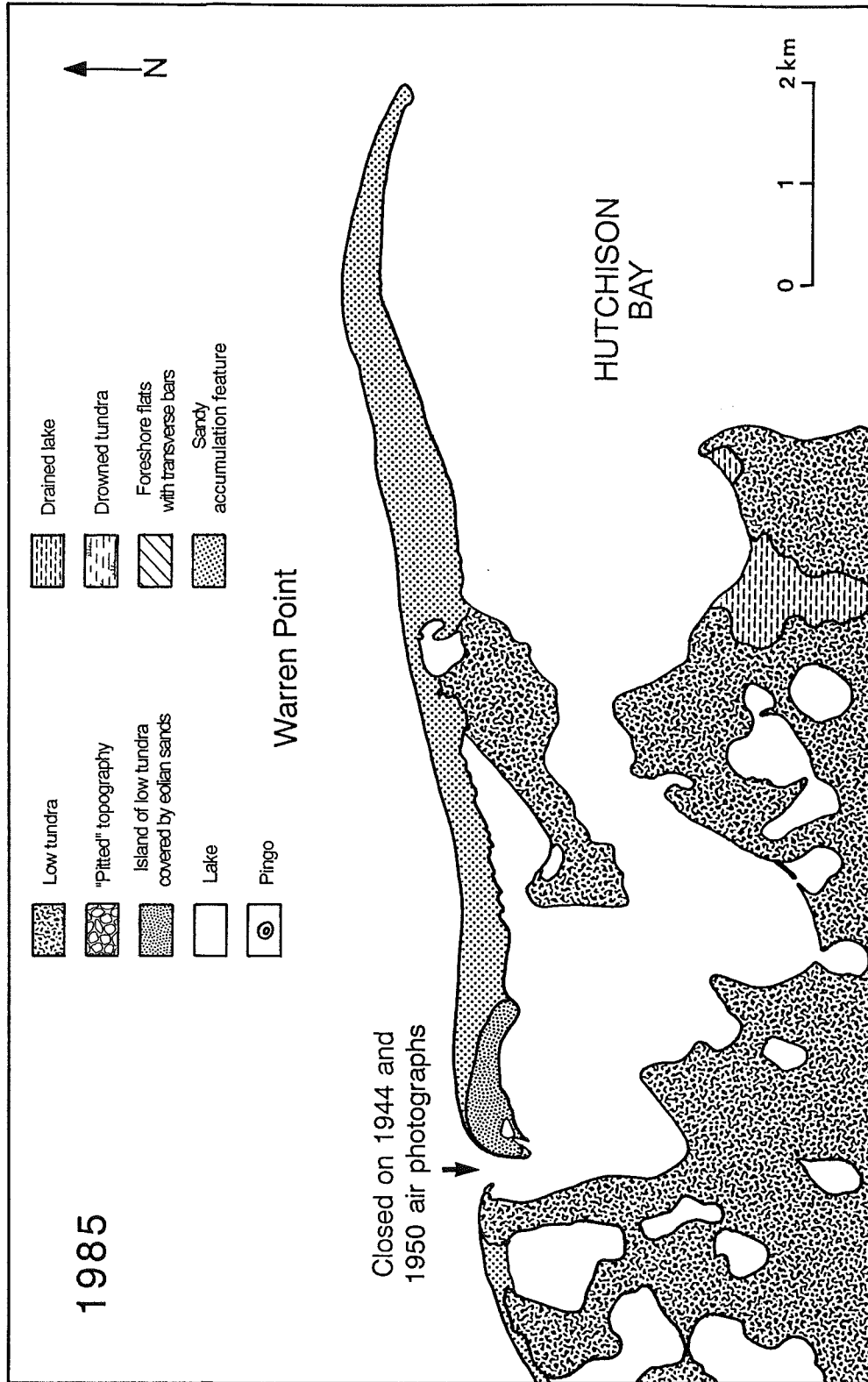
Warren Point, located on the western side of Hutchison Bay, is a 10 km long sandy barrier spit which encloses a large lagoon (Fig. 9.4). In its central part, the barrier is attached to a tundra island that is a remnant of low elevated tundra. From this island, the barrier extends eastward into Hutchison Bay and westward to a second small tundra remnant, forming a low cliff on the seaward side of the barrier, and covered by small aeolian dunes. Aeolian processes are very active along this part of the barrier, reworking the sands underlying the tundra and the beach sands. Less developed dunes also occur on the central anchor point of the barrier. At this location, the beach is very narrow ( $\approx$  120 m) while it widens westward and eastward. To the west, the barrier is 350 m wide and characterised by broad washover flats. The eastern part has very low-elevation (<1 m) and is up to 600 m wide. The distal end consists of a frequently submerged sand flat where a pronounced system of transverse bars occurs.

#### *West Atkinson Barrier*

The West Atkinson Barrier is located northeast of Hutchinson Bay, from Bols Point to Drift Point, forming the longest barrier island of the Tuk Peninsula. This 10.5 km long sandy barrier (Fig. 9.5) is not linked to a headland but separates a wide lagoon from the Beaufort Sea. In 1985 the backshore side of this barrier showed numerous washover flats and the foreshore was characterised by swash bars. The southwestern end of the barrier island was prolonged by a subtidal bar and a small arcuate-shaped barrier island showing seaward convexity. This barrier is located offshore of an area of inundated tundra and lies on a shallow platform.

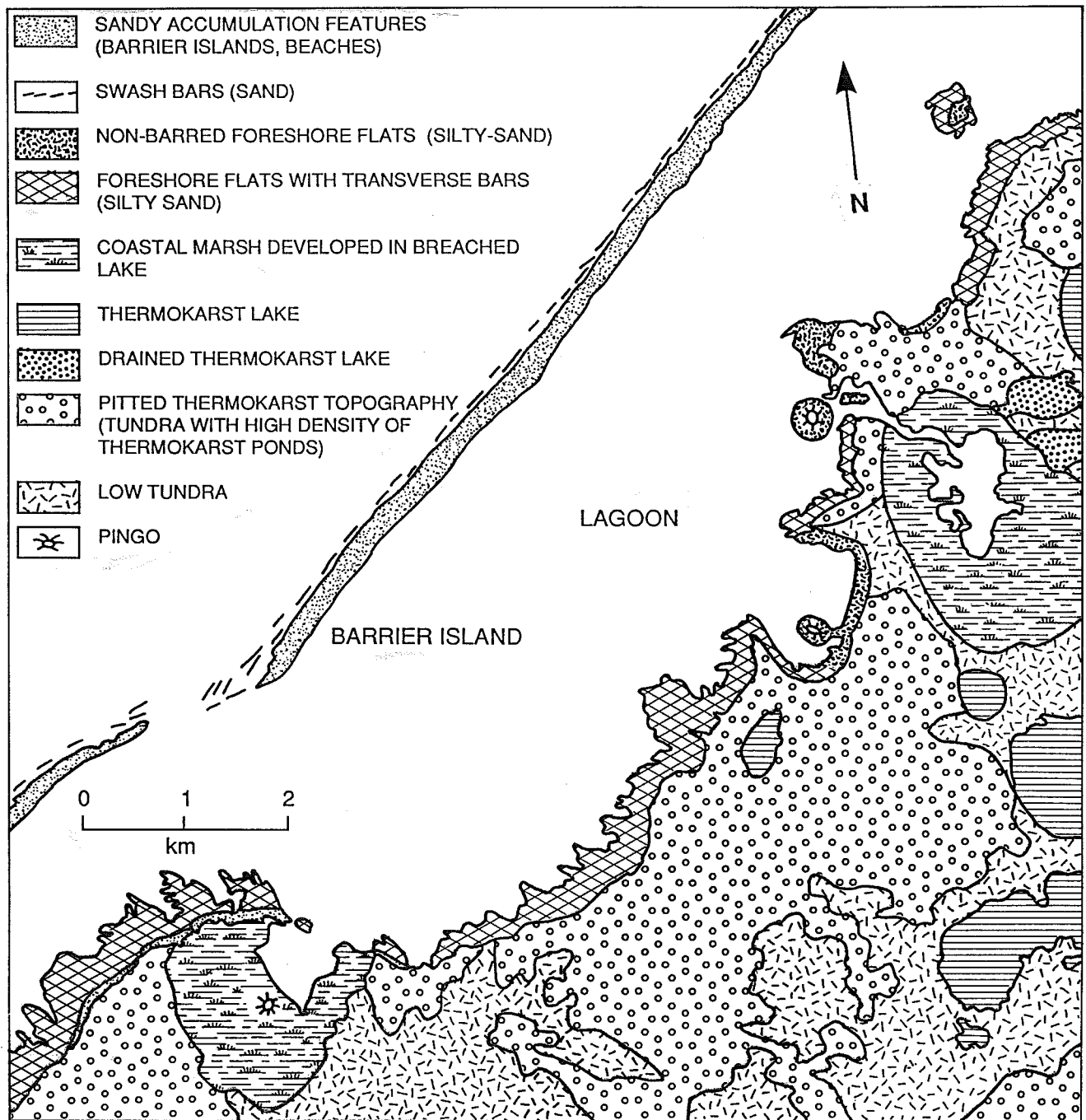
#### *Atkinson Point Spit-Barrier System*

Atkinson Point is a prominent headland located at the end of a peninsula on the west side of McKinley Bay (Fig. 9.6). The headland is cut into a 500 m long sandy cliff up to 2 m in height. To the northeast, a broad sand spit extends 3 km from the headland and is extended by a series of short, narrow bars forming a discontinuous and frequently overwashed distal end. A line of breakers extending several kilometres further into McKinley Bay indicates that a subtidal bar, perhaps previously part of the Atkinson spit system, is present. The wider (350-500 m) proximal barrier is characterised by washover flats, which in 1985, showed a major healed inlet with an

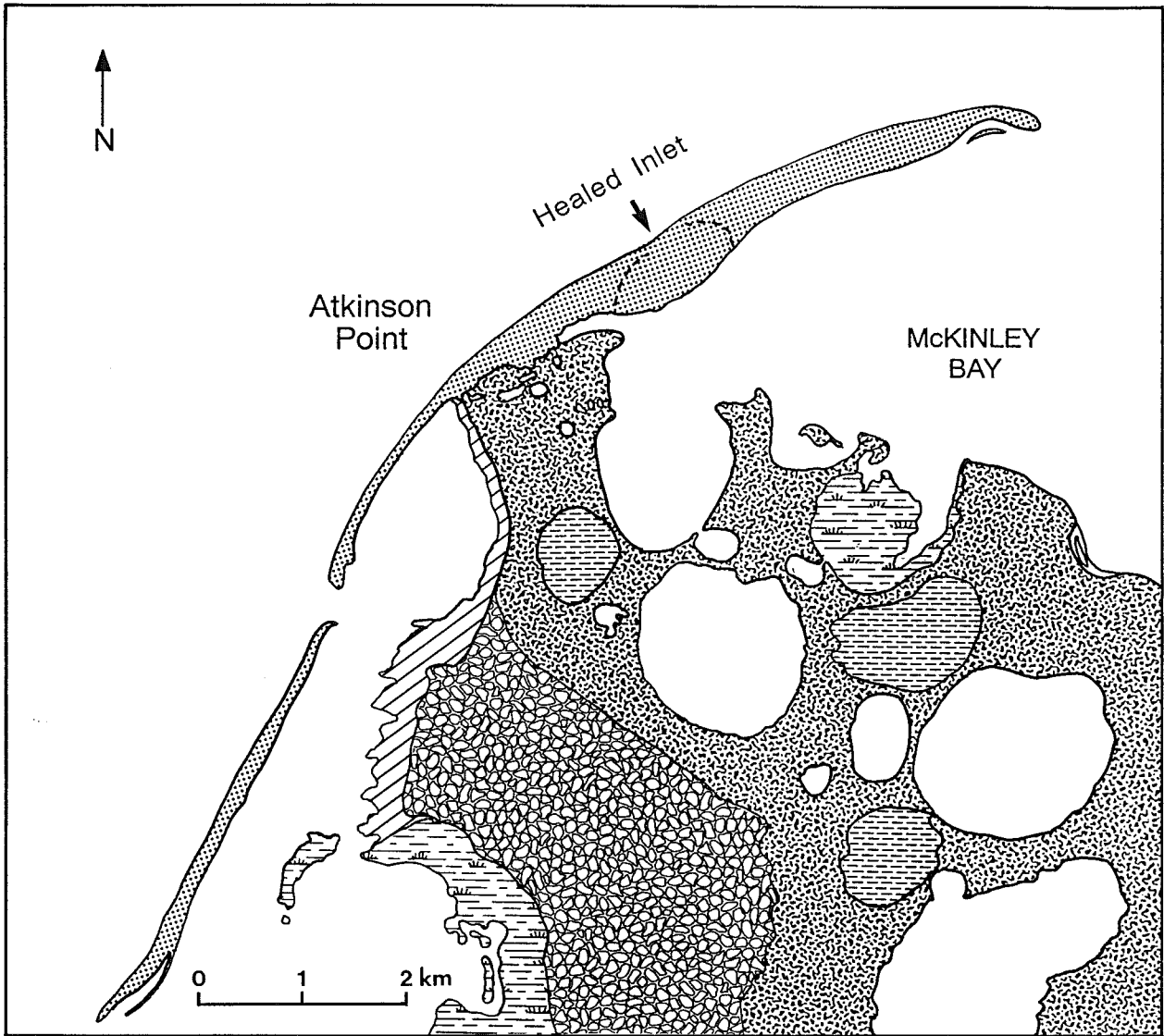


**Figure 9.4** Warren Point barrier-spit system. Legend applies to remaining spit and barrier figures in Chapter 9 unless otherwise included.





**Figure 9.5** Interpretation of sedimentary environments in the area of the Southwest Atkinson barrier island along the Tuktoyaktuk Peninsula (from Ruz et al., in prep.).



**Figure 9.6.** Atkinson Point spit and barrier island system.

abandoned flood delta, and a complex subtidal bar platform in front of the beach. The western part of Atkinson Point is a system of spit and barrier islands extending almost 6 km to the southwest. These are composed of fine sand like the eastern spit but are narrower (150 m). The spit and the barrier island are separated by an inlet with both ebb and flood tidal deltas. In 1985, the end of the spit showed at least two recurved ends testifying to its southward progradation. The southern distal end of the barrier island is more complex and is extended by two small barrier islands separated by tidal inlets. They are the extension of the Drift Point spit and are perhaps the remnants of a continuous barrier linking Atkinson Point and Drift Point.

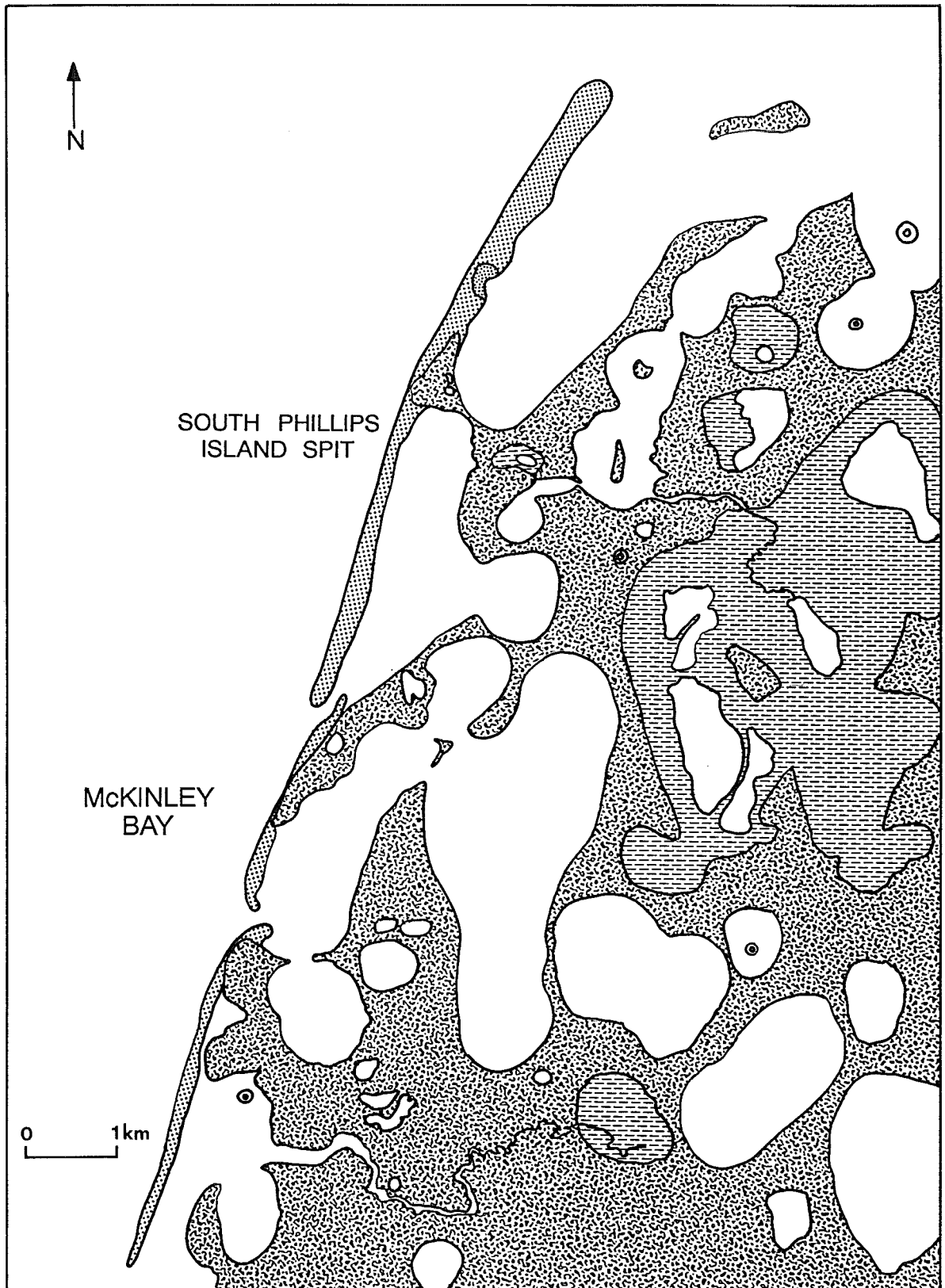
#### *East McKinley Bay and Phillips Island Barrier-Spit Complex*

Along the eastern shore of McKinley Bay sandy eroding bluffs can be more than 5 m high; they alternate with sand spits and barriers. In the bay itself, the sandy coastal accumulations consist of three narrow spits extending southward (Fig. 9.7), anchored by tundra headlands, and enclosing several large thermokarst lagoons. Each lagoon is connected to the ocean by an inlet at its southern end. The southernmost spit is truncated by an inlet and extended by a small barrier island. Northeast of McKinley Bay, a wide (> 300 m) spit attached to a small sandy headland extends northeastwards over more than 3 km. This spit shows a morphology dominated by overwash processes. A wide inlet showing subtidal ebb and flood structures separates this spit from a small barrier island (Phillips Island). Further to the northeast, small tundra remnants are prolonged by Crescent Bank, a wide subtidal feature that extends over more than 10 km. The small tundra islands are almost entirely reworked by wind action into dune fields.

#### *Cape Dalhousie Barrier Island System*

At the northeastern tip of the peninsula, seaward of Cape Dalhousie (Fig. 9.2) a broad sandy barrier links several small tundra islands forming a 7.5 km long system. In 1985, three small tundra remnants anchored the system. The barrier consisted of broad washover flats with transverse bars on the backshore and parallel swash bars on the foreshore.

From the above descriptions, two major conclusions can be drawn concerning depositional landforms. (1) The smaller coastal landforms are located in sheltered areas while long spits or barrier islands (in the order of several kilometres in length), are usually facing the northwest or the north and are more exposed to high energy waves. These major depositional features are all located in coastal areas where there is a high availability of sand. (2) The configuration of the spits along this coastal section show net longshore sediment transport to the east. Even when two spits developed from the same headland, the eastern one is more developed (eg. Warren Point and Atkinson Point spits). Longshore sediment transport estimates (Pinchin et al., 1985) confirm the



**Figure 9.7** The spits of the eastern shore of McKinley Bay.

geomorphological evidence. According to these estimates, based on twelve numerical models, the potential sediment transport rate along Tuktoyaktuk Peninsula is in the order of  $1.0 \times 10^5 \text{ m}^3 \text{ a}^{-1}$  in an eastward direction near McKinley Bay.

#### **9.2.4. Inner Shelf Morphology**

Compared to the areas to the west, the inner shelf of the Tuktoyaktuk Peninsula has a relatively steep slope extending out to 10 m water depth. West of Atkinson Point, the seabed slopes at an average of  $0.05^\circ$ . In this region, two areas of shoals, James Shoal and Beluga Shoal interrupt the regional slope (Fig. 9.1). Beluga Shoal, north of Hutchison Bay, is topped by a small intertidal sand bank. To the east of this region, the shelf slopes seaward at an average of  $0.15^\circ$ , forming a narrower inner shelf zone, shoaling only in areas adjacent to coastal spits and barriers (e.g. Crescent Bank, as described above).

Sidescan and sub-bottom profiler records from the Karluk 1987 cruise revealed that a field of large-scale hydraulic bedforms occur in shallow water (<10 m water depth) near Topkak Point. These bedforms are shoreface connected sand ridges, averaging 2 m in height and 100 m width and aligned roughly parallel to the shoreline. Analyses and mapping of sediment distribution and seabed morphology using the sediment samples and the acoustic data collected on the Karluk '87 cruise should provide new insights in the sediment dynamics of the shoreface/inner shelf zone of the eastern Beaufort Sea (see recommendations in section 10.1.2.iii).

### **9.3 Rates of Coastline Change**

#### **9.3.1 Cliff Retreat**

Retreat rate measurements from aerial photographs are available for the Tuktoyaktuk Peninsula, as far east as the eastern shore of McKinley Bay (Harper et al., 1985). Average values of retreat rate obtained by this method were 2.0 m/a for the coast between Tuktoyaktuk Harbour and Toker Point, and 1.1 m/a for the coast between Toker Point and McKinley Bay. This is broken down by environment, according to the coastal classification used by Harper et al. (1985) in Table 9.2. The results of this analysis indicate that there is great variability within single coastal types. Only the inundated tundra coastlines stand out as retreating significantly faster than other environments, but there are only three measurements from this environment, and the irregular morphology would make consistent measurements very difficult. Surprisingly, there appears to be no systematic difference between retreat of exposed bluffs and lagoon shore lying behind the large barrier systems. No retreat rates were obtained for sections of ice-rich cliffs.

Resurvey measurements of erosion in ice-rich cliffs were conducted at Toker Point and Tibjak Point (Table 9.3). Hequette (1989) resurveyed the profiles set up by Gillie (1986) and

**Table 9.2** Average retreat rates calculated by coastal type (data from Harper et al., 1985).

<b>Coastal Classification</b>	<b>Retreat Rate (m/a)</b>	<b>n</b>
Ice Poor	1.27 ± 0.97	13
Low Tundra	1.56 ± 0.99	11
Inundated Tundra	3.62 ± 1.86	3
Barrier Beach	0.51 ± 0.42	9
Lagoon Shore	1.10 ± 1.28	22
Hutchison Bay (all environments)	0.90 ± 0.99	31
McKinley Bay (all environments)	1.31± 0.95	51

**Table 9.3** Ground survey measurements of coastal retreat along the Tuktoyaktuk Peninsula.

<b>Profile</b>	<b>Gillie 16/7/86 (m)</b>	<b>Hequette 09/8/88 (m)</b>	<b>Erosion (m)</b>	<b>Rate (m)</b>
<b>Toker Point</b>				
TP-11	42.5	34.55	7.95	3.9
TP-8	57.0	44.7	12.3	6.15
TP-7	58.0	52.5	5.5	2.75
TP-6	74.6	51.5	23.1	11.55
<b>Profile</b>	<b>Hequette 9/86 (m)</b>	<b>Hequette 09/8/88 (m)</b>	<b>Erosion (m)</b>	<b>Rate (m)</b>
<b>Tibjak Point</b>				
87-3	27.9	23.3	4.6	4.6

recorded retreat rates between 2.75 m/a and 11.55 m/a over the two year period. At Tibjak Point (north of the beach study site), Héquette also measured a retreat of 4.6 m between September 1987 and August 1988. These relatively high rates of retreat probably do not indicate that ice-rich cliffs are eroding much faster than other cliff-types, but rather probably illustrate the episodic nature of erosion along this coast. In each case surveyed by Héquette, a layer of massive ice was present in the cliff and erosion occurred through block failure of ice wedge polygons.

### **9.3.2. Spit and Barrier Evolution**

#### ***Spit and Barrier Island Migration***

Geomorphological evidence such as active washover fans along the spits and barrier islands, erosion of the seaward side of coastal dunes and the presence of freshwater peat beds on the foreshore strongly suggest that coastal accumulation features along Tuktoyaktuk Peninsula are undergoing landward migration. Several authors have reported retreat of barrier and spits at specific sites (Lewis and Forbes, 1975; Rampton and Bouchard, 1975; Forbes and Frobel, 1985) and recently Héquette and Ruz (in press) and Ruz et al (in prep.) have conducted a detailed analysis of spit and barrier migration and evolution.

The primary data used in the Héquette and Ruz (in press) study of barrier migration are aerial photographs. Measurements of shoreline changes (accretion or retreat) were done by comparing 1950, 1972, and 1985 vertical aerial photographs, at scales varying from approximately 1:40 000 to 1:60 000. The measurements were used to calculate annual retreat or accretion rates of the coastal spits and barrier islands. Results of this study confirm that these coastal features are still experiencing landward migration at various rates (Table 9.1). Between 1950 and 1985, the mean recession rate was 3.1 m a<sup>-1</sup> for the barrier islands and 1.7 m a<sup>-1</sup> for the spits, but individual measurements along the coastline revealed retreat rates ranging from 0.9 to 3.3 m a<sup>-1</sup> for the spits and 1.5 to 4.5 m a<sup>-1</sup> for the barrier islands.

Along the spits, erosion rates are usually higher in the proximal part and lower at the distal part. At Warren Point and Topkak Point for example (Table 9.1), retreat rates decrease towards the tip of the spit, varying from 1.7 to 1.0 m a<sup>-1</sup> and from 1.3 to 0.9 m a<sup>-1</sup> respectively. This can also be seen at Mingnuk spit where air photograph comparison shows that the most significant erosion occurred at the proximal part of the spit while accumulation took place at the extremity, this type of coastal evolution being typical of growing spits. Landward migration rates are higher along barrier islands and are usually quite similar along a single barrier island although higher retreat rates have been measured in the central part of the barrier in certain cases. No significant longshore migration of barrier islands has been measured. Tidal inlet migration has been observed west of Atkinson Point (Fig. 9.6), where the progradation of the spit between 1950 and 1985 caused a 150 m southwestward migration of the tidal inlet with a corresponding erosion of the adjacent barrier

island.

Least squares regression analyses of retreat rate, as a function of exposure to deep-water wave power, and potential longshore sediment supply, have been carried out. The regression analyses showed linear relationships between retreat rates and wave power, but revealed moderate to poor correlation coefficients. Correlation between retreat rates and sediment supply estimates revealed a better relationship (correlation coefficient = 0.77), showing that the availability in sediment supply is a major control on the landward migration of the spits and barrier islands (Fig. 9.8). Because of higher sediment supply from adjacent eroding bluffs, spits are retreating at slower rates compared to barrier islands that have no direct sediment supply and are dominated by overwash processes (Fig. 9.9).

### *Spit and Barrier Island Development and Evolution*

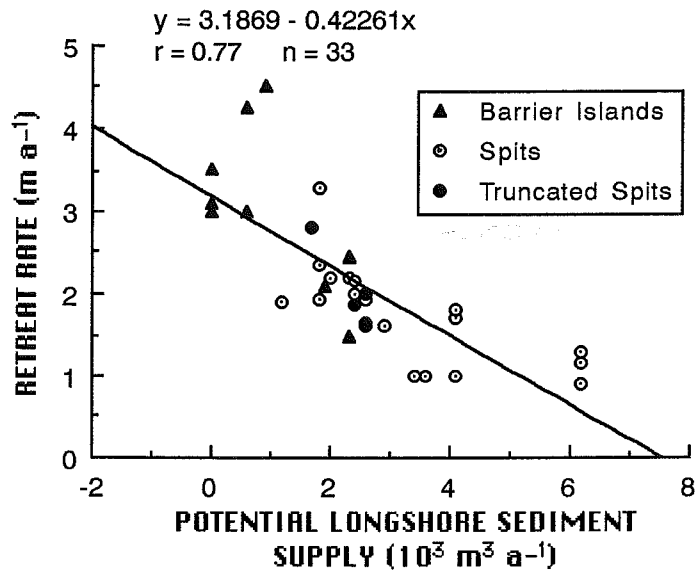
A detailed study on the development and evolution of coastal depositional features has been carried out and a schematic evolutionary model has been proposed (Ruz et al., in prep.). In this study two major stages in coastline evolution have been distinguished: (1) lake breaching and spit development and (2) barrier island development.

#### (i) Lake breaching and barrier-spit development:

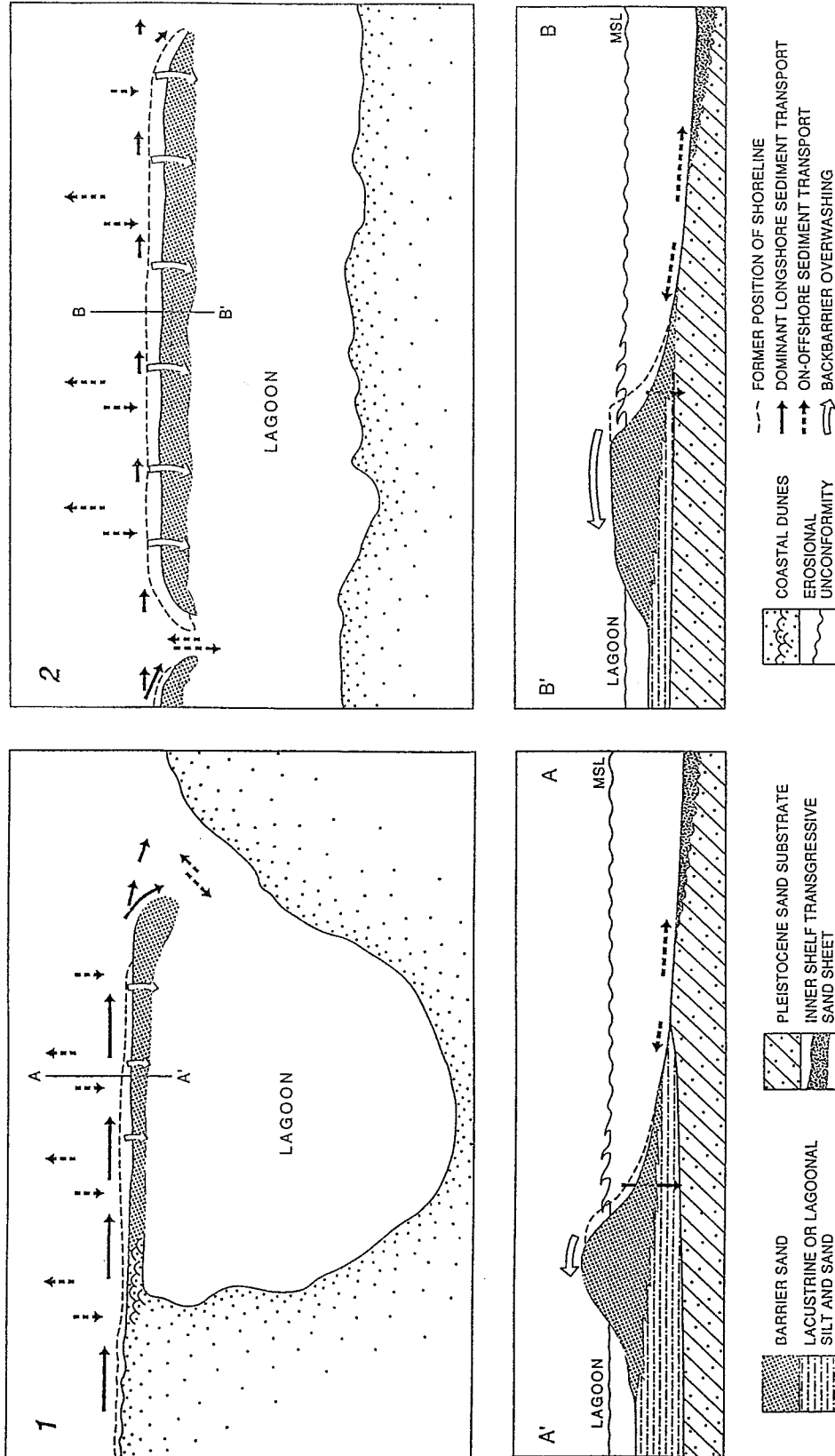
The occurrence and the degree of development of coastal depositional landforms is primarily controlled by sediment supply, energy input to the coastal system, relative sea-level changes, and pre-existing topography. Where the sea is transgressing over a topography of thermokarst lakes, as on the Tuktoyaktuk Peninsula, coastal retreat induces the breaching of the lakes and erosion of the adjacent relief. The subsequent morphological changes of the coast will greatly depend on the initial depth of the breached lake. Several examples along the Canadian Beaufort coast show that a shallow lake (water depth < 3 m) will likely be dried out and the exposed bottom will be successively eroded by the sea. In the case of a deeper lacustrine basin, the breaching of the lake will result in the formation of a coastal embayment. If the lake is too deep, the water depth of the newly formed embayment will be so great that it may limit or completely restrict the development of a spit. This situation occurs in the northeastern part of the Tuktoyaktuk Peninsula where numerous breached lakes are transformed into embayments without any spit development, despite a high availability of sand in the eroding bluffs. If the water depths permits, a barrier-spit will develop across an embayment as the former lake is more and more open to the sea. The dimensions, shape and sediment texture of the accreting spit will depend on the availability of material in the adjacent bluffs, the grain-size of such sediments, and the local inshore wave climate.

This type of coastal evolution is exemplified by air photograph comparisons at a site on the





**Figure 9.8.** Relationship between the rates of landward migration of the spits and barrier islands of the Tuktoyaktuk Peninsula and the rates of potential longshore sediment supply (after Héquette and Ruz, in press).



**Figure 9.9** Conceptual geomorphic model of spit and barrier island migration in the southeastern Canadian Beaufort Sea showing idealized plane view and cross-section with major sediment transport paths. 1: Spit; 2: Barrier island (from Héquette and Ruz, in press.).

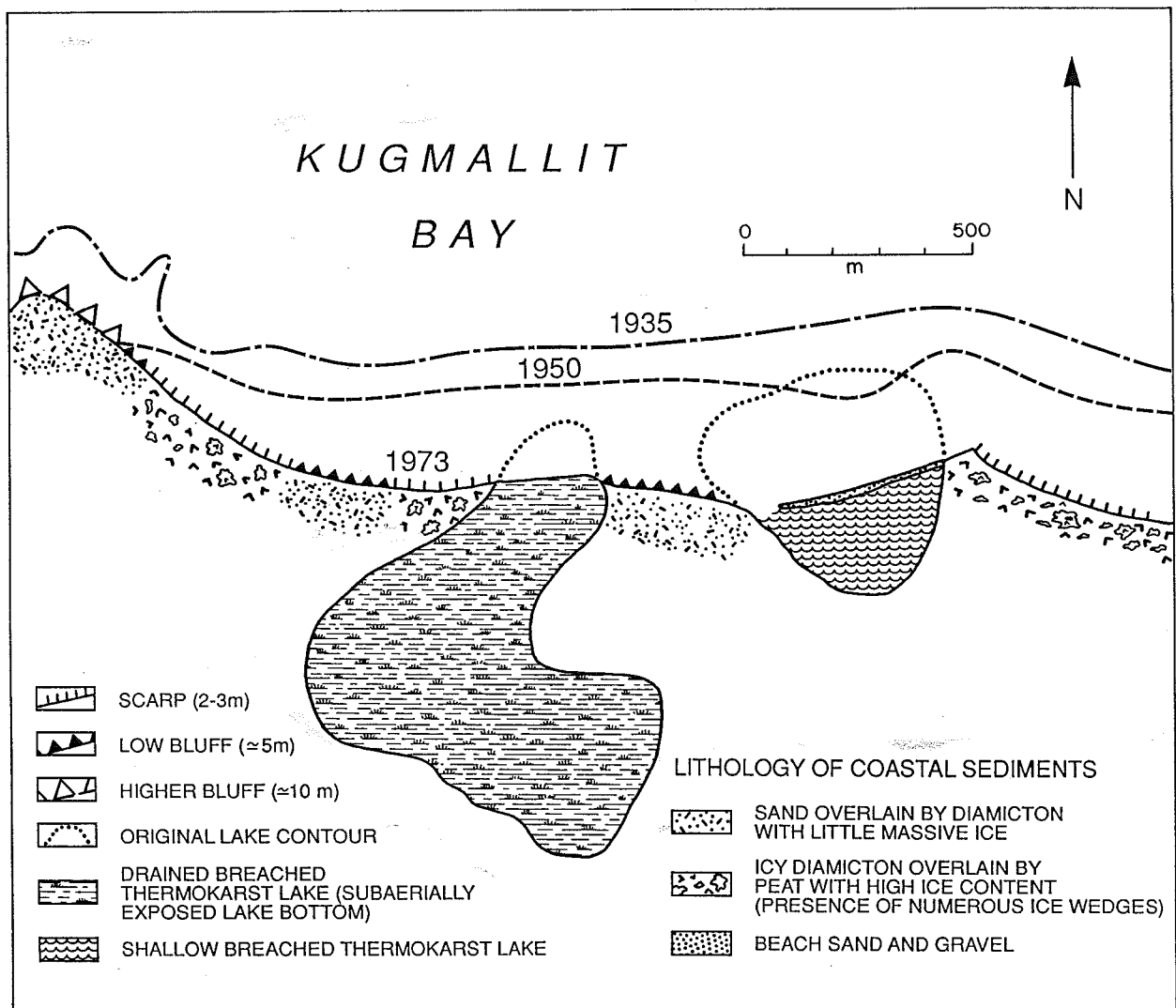
south shore of Kugmallit Bay (Fig. 9.10) where Mackay (1986) previously carried out measurements of coastal erosion. On a 1935 oblique air photograph (No A 5026 - 35R), two lakes of 500 to 1000 m in diameter were visible at distances of about 110 and 170 m from the shoreline respectively. From 1935 to 1950, coastal retreat ranged from about 80 to 160 m depending upon the coastal section considered. By 1950, coastal retreat had induced the breaching of the easternmost lake while the lake to the west had been drained by headward erosion. During the following years, the shoreline continued to retreat very rapidly, the retreat rate being as much as 10 m a<sup>-1</sup> at some locations. By 1973, the drained lake to the west had undergone further erosion but a small barrier-spit, 300 m in length, had formed across the small former lake to the east. The spit was composed of sand and gravel with some cobbles. The relatively coarse character of the clastic material constituting the spit is primarily controlled by the sediment source (mainly the diamicton in this case) rather than the wave energy at the shoreline.

The tendency in such a situation is an evolution towards a complete closure of the lake, as shown by some examples of barrier-spit progradation along the Tuktoyaktuk Peninsula. Immediately west of Toker Point, for example, air photographs show that in 1950 a breached lake was open to the sea through a small inlet separating a complex sandy double spit. In 1985, the development of the two spits has induced the complete closure of the embayment and the formation of a small barrier beach.

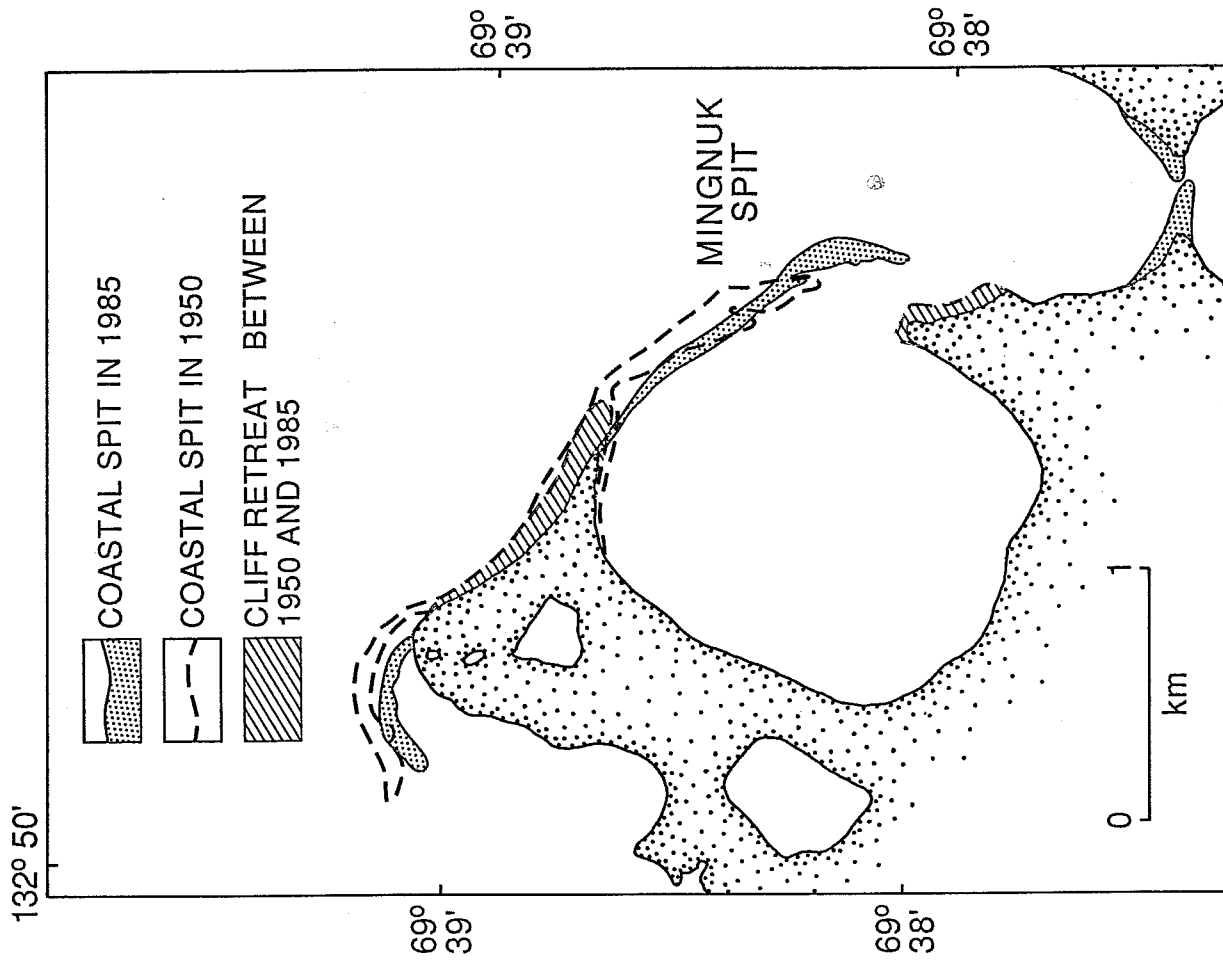
The longshore component of sediment transport strongly controls the evolution of the spits, leading to progradation if sediment supply is sufficient. However, in many cases, barrier-spit development does not result in complete closure of the embayment. East of Toker Point, Mingnuk spit is a small barrier-spit which developed from an eroding headland (Fig. 9.11). Between 1950 and 1985 the spit and its anchor point have migrated landward (about 100 m) and the erosion of the cliff has favored a corresponding elongation of the spit which became thinner, particularly at its proximal end. During the summer of 1988 this spit was truncated and became a small barrier island despite a severe erosion of the adjacent cliff.

(ii) Barrier island development:

The examination of 1950's, 1970's, and 1985 air photographs of the Tuktoyaktuk Peninsula coast revealed several examples of spits becoming detached from the mainland and forming new barrier islands of small dimension (in addition to the example previously described at Mingnuk Point). Although, no examples of large-scale barrier island formation have been observed, the coastal morphology and evolution of barrier-spits and the distribution and location of barrier islands strongly suggest that most of the barrier islands developed from spits. At Atkinson Point (Fig. 9.6), geomorphic evidence suggests that the formation of the barrier island resulted from the truncation of the westernmost spit. The barrier island and the spit have very similar



**Figure 9.10** Evolution of the coastline between 1935 and 1973 at one site on the southern shore of Kugmallit Bay, west of Tuktoyaktuk (site 3 in Fig. 9.5.). Only the largest lakes are shown. (From Ruz et al., in prep.).

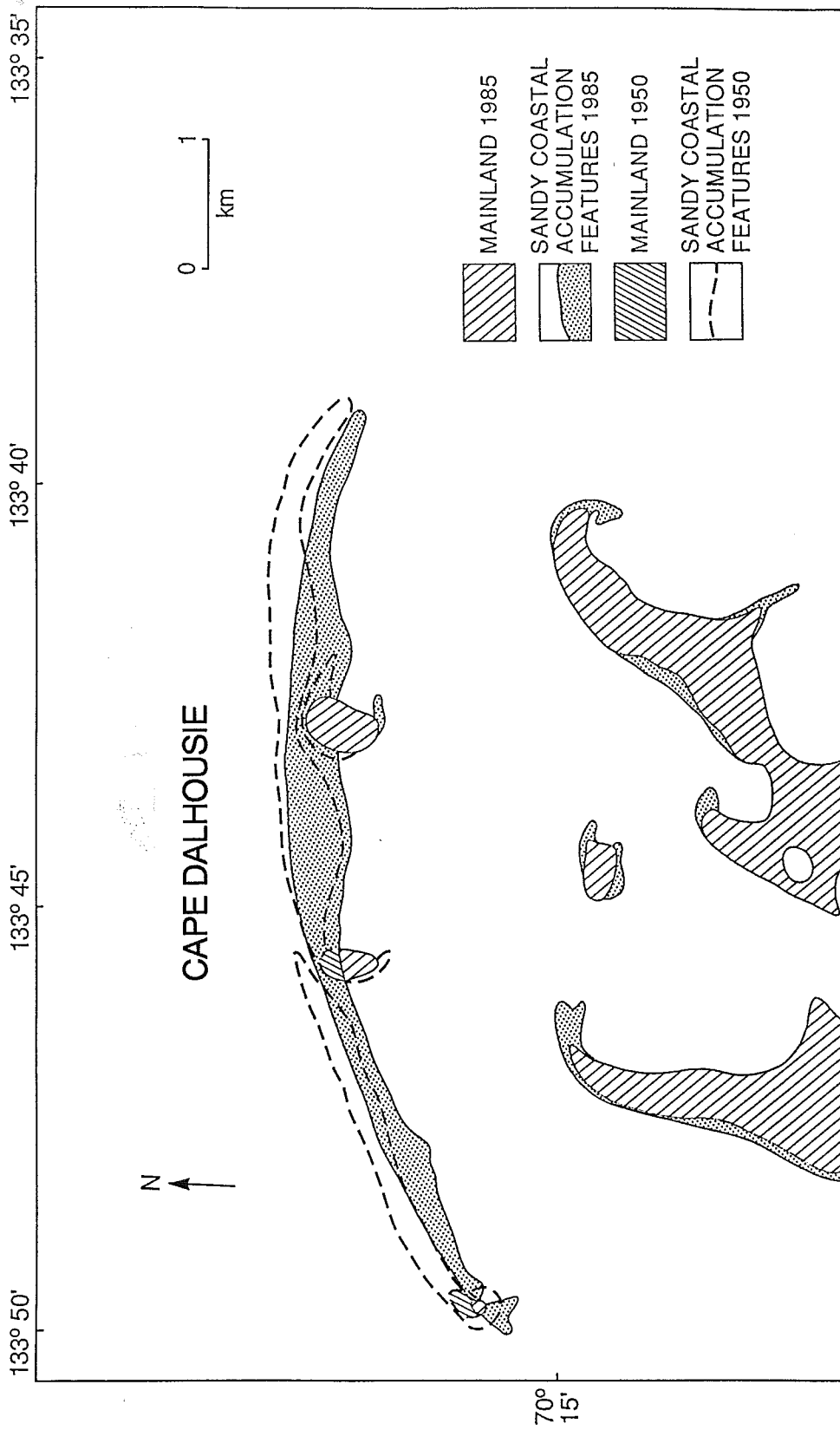


**Figure 9. 11** Comparison of 1950 and 1985 aerial photographs showing the coastwise progradation and the retreat of Mingnuuk spit and the erosion of the adjacent bluffs (from Héquette and Ruz, in press).

morphological characteristics: crest elevation (1 m), width (150 m) and grain-size (fine sand). Furthermore, they are both retreating landward at a rate of about 1.7 m a<sup>-1</sup>, presumably because of similar sediment supply induced by by-passing and the same exposure to incoming waves (Héquette and Ruz, in prep.). This type of evolution also prevails along the eastern side of McKinley Bay where a long and narrow sandy spit is almost truncated and transformed into barrier island, separated only by a small inlet.

At the tip of the Tuktoyaktuk Peninsula, the Cape Dalhousie barrier island system is a major barrier system facing the NNW (Fig. 9.12). In that area, the mainland topography is characterized by large thermokarst lakes oriented NNE-SSW, perpendicular to the easterly winds. The topography of the land between the lakes is very irregular and consists of a succession of higher relief and low tundra areas. The partial submergence of this topography resulted in the formation of many embayments separated by thin bands of land. Rising sea-level also induced the formation of small islands by flooding the low tundra between areas of higher relief. The Cape Dalhousie barrier island developed between some of these small islands. Air photographs reveal that in 1950 the barrier system was formed of spits attached to small remnants of the mainland, forming islands. Between 1950 and 1985, the whole system retreated at a rate up to 4.5 m a<sup>-1</sup>. During that period, the small islands were eroding providing sand to the sandy depositional features. Due to longshore progradation and landward migration, the spits evolved into a continuous barrier island system, integrating the small mainland remnants. Another example of this sort of barrier island can also be found in Kukjuktuk Bay (Fig. 9.2) where a barrier island was formed by the longshore development of spits linked to a remnant of the eroded mainland.

The occurrence of a shallow platform associated with a barrier island is also an important parameter favouring barrier island development. The West Atkinson barrier island (Fig. 9.5) lies on a platform extending seaward from the barrier for a distance of 700 to 900 m where a break in slope occurs at the 2 m isobath. The platform also extends landward in the backbarrier region, in the form of a shallow lagoon. This 10.5 km long sandy barrier is anomalous compared to the other barrier islands in the area as there is no evidence of a former headland from which it could have been developed. Because of the topographic setting of this barrier island, the mainland beach detachment can not be ruled out as an alternate mode of formation. The mainland beach detachment mechanism implies a rising sea level partially submerging a beach ridge and inducing the formation of a lagoon by flooding a flat area behind the ridge. The mainland shore of the West Atkinson backbarrier lagoon is retreating rapidly as a result of the submergence of a low and flat coastal tundra plain. Because the mainland shoreline retreats at a higher rate than the barrier, the lagoon width increased by 100 m from 1950 to 1985, contributing to the development of a shallow platform. The importance of a platform substructure in the development of barrier islands has been emphasized by several authors (Oertel, 1985; Otvos, 1985). In this case, the correspondence of the



**Figure 9.12** Aerial photograph comparison showing the landward migration of Cape Dalhousie barrier island system between 1950 and 1985 (after Héquette and Ruz, in press).

barrier island to the shallow platform suggests that the barrier island formed on the platform or that its landward migration was slowed down on this feature. It is also possible that the formation of this barrier island resulted from a combination of mainland beach detachment and alongshore spit progradation, the littoral drift along this section of the coast leading to the formation of a long continuous barrier.

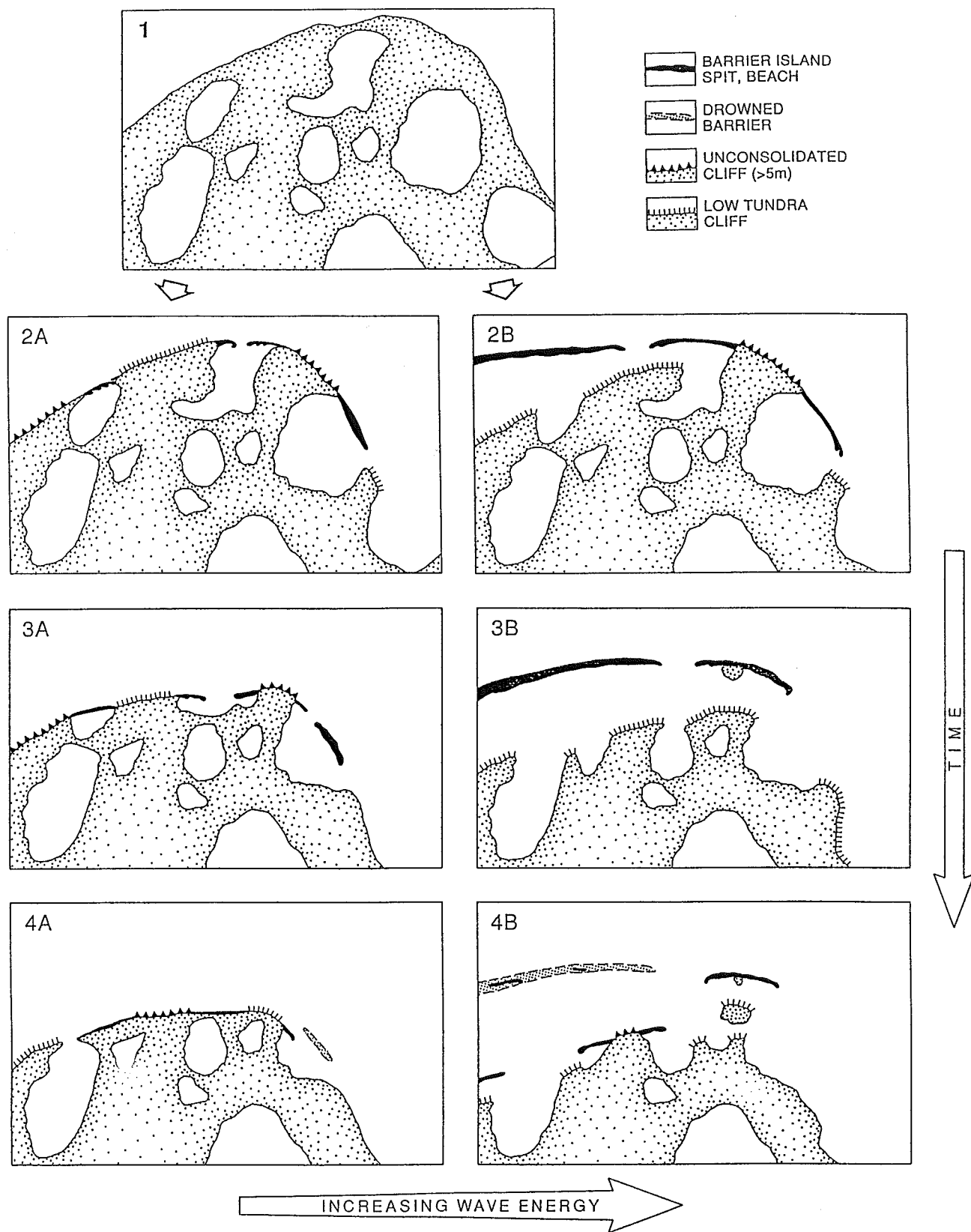
Geomorphic evidence indicates that the principal mode of formation of barrier island along the coast of the Tuktoyaktuk Peninsula results from the truncation of spits connected to the mainland or to small islands. Mainland beach detachment seems probable in certain circumstances but less common.

(iii) Evolutionary model of coastal development:

According to the preceding observations, it appears that in the thermokarst topography of the southern Canadian Beaufort Sea coastal plain, the sea-level rise and concomitant coastal erosion result in the breaching of thermokarst lakes. If a local source of sediment is available in nearby bluffs and if the water depths in the former lake permits, a barrier-spit will develop across the new embayment as the coastline retreats. The magnitude and direction of longshore sediment transport are also of primary importance in this mode of formation as they determine the volume of sediment entering and escaping the system along the coast. Lateral growth of spits results in the complete closure of an embayment if certain conditions are fulfilled: sufficient sediment supply and longshore transport potential, low hydraulic pressure of the backbarrier lagoon, and suitable water depths in the embayment. Where the water depths in the embayment do not allow further spit progradation, despite significant longshore sediment supply, the sediment transported along the spit contributes to the infilling of the lagoon either at the tip or directly over the crest by overwashing (Fig. 9.9). As the spit is slowly retreating, littoral sand probably represents a significant proportion of the lagoon-fill sediment.

Following spit formation, two main types of barrier island development can occur which are both related to the specific thermokarst environment of this region. Because the topography consists of higher relief areas with high or low ice content, separated by lakes or low tundra areas, sand will be supplied in sufficient quantity to a barrier-spit as long as the spit is attached to an eroding sandy headland (Fig. 9.13. 2A). However, as the coastline continues to retreat, a depression, a flat area of low tundra or an ice-rich terrain will be reached by the sea resulting in higher coastal retreat rates and a significant decrease in sediment supply. Consequently, the barrier-spit will experience a sediment deficit leading to increased erosion along the spit and transformation into barrier island by inlet formation (Fig. 9.13. 3A). Possible examples of this mode of formation are found at Mingnuk Spit and Atkinson Point. The second type of barrier island development is the result of accelerated coastal erosion behind a spit resulting in a small





**Figure 9.13** Schematic geomorphic model illustrating the stages of barrier island formation in the southeastern Canadian Beaufort Sea from an hypothetical bluff shoreline (1). The model shows two different types of evolution depending on the exposure of the coast to wave energy (A: sheltered coastal environment; B: wave-exposed coastal environment). In the more exposed areas, the highest rates of coastal erosion result in larger amount of sediment supplied to the littoral zone which make possible the construction of larger coastal accumulation features. (From Ruz et al., in prep.).

tundra island with attached spits becoming stranded offshore (Fig. 9.13. 3B), like in the case of the Cape Dalhousie barrier island system. This type of barrier island development is similar to formation by "backing tundra erosion" as proposed by Short (1979) for some of the barrier islands of the Alaskan Beaufort coast. In all cases, the mainland shore of the lagoon has no beach or only a poorly developed beach as the barrier island protects the mainland from wave action.

Air photo comparisons suggest that the dimensions and thus sediment volume of the barrier islands are fairly stable over short time-scales, presumably because of both longshore and onshore sediment supply. However, at a longer time-scale, all these barriers are ephemeral. Because the mainland shore is in many cases retreating at a higher rate than the barrier island (due to low regional gradient and/or high ice content), the barrier becomes more and more stranded offshore. It seems that longshore sediment transport is more significant than onshore transport as the stranded offshore barrier islands become starved of sediment. Then, with continuing transgression, several possibilities of evolution exist for the barrier depending on the mainland topography and rate of sea-level rise. If sea-level is not rising too rapidly, a barrier island may recycle the backbarrier sands on the foreshore and shoreface, as the barrier retreats by overwash processes. This results in more frequent storm overwashing and in higher rates of landward migration with possible overstepping of the barrier (Héquette and Hill, 1989; Ruz et al., in prep.). When a lagoon with significant water depths occurs behind a spit or a barrier island, the landward migration results in the infilling of the lagoon with complete drowning of the barrier in the depression (Fig. 9.13, 3A to 4A) regardless of the rate of sea-level rise. In all cases, when spits and barrier islands are drowned in depressions or overstepped on a shallow platform, a new spit or beach develops behind it, along the mainland coastline.

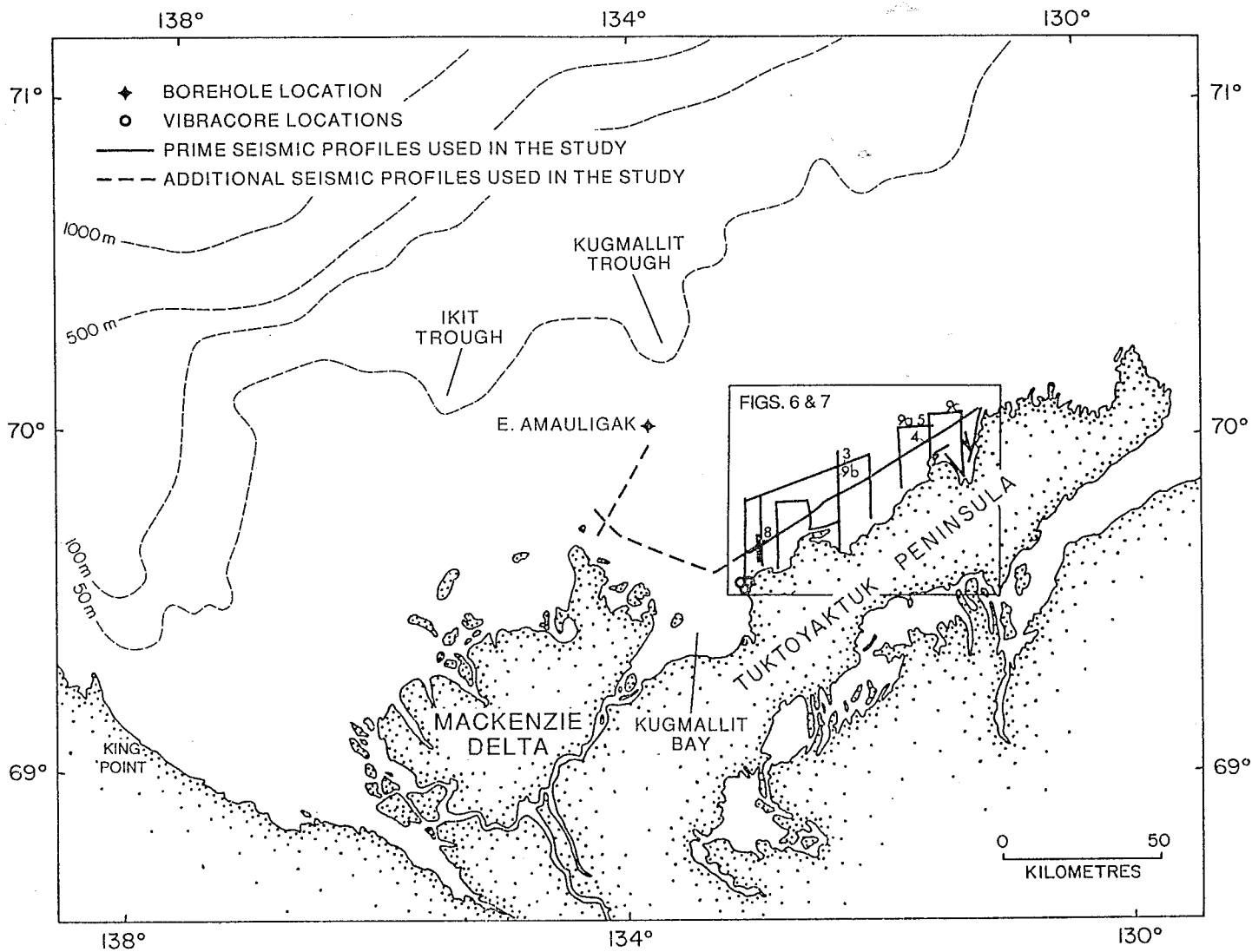
#### **9.4 Seismic Stratigraphy**

A regional survey of the inner shelf between Toker Point and McKinley Bay was completed from the R/V Karluk in August 1987 (Fig. 9.14; Hequette, 1988). The results of the seismic analysis were reported in Hequette and Hill (1989) and are briefly summarised here.

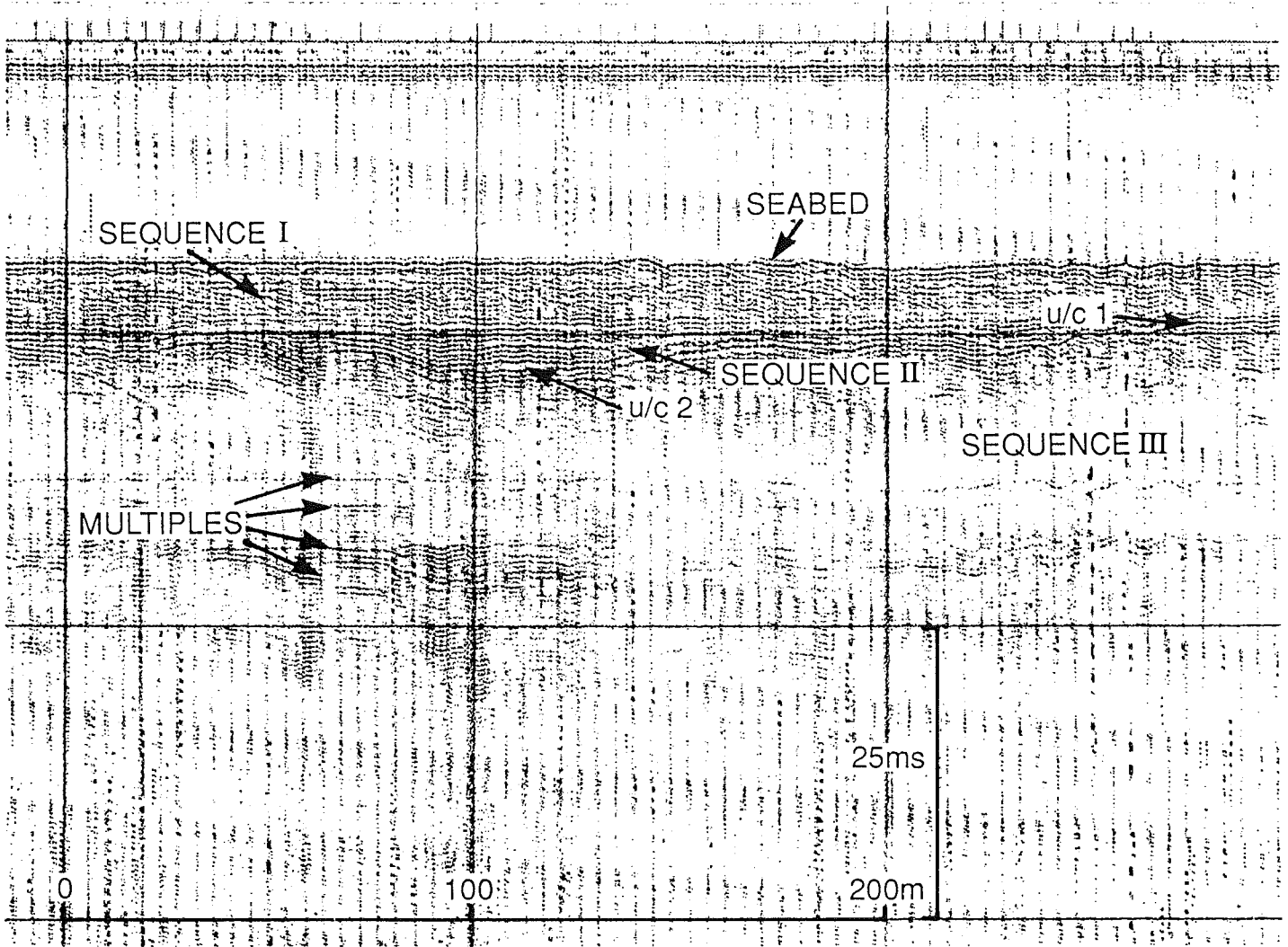
Three seismic sequences were recognised on the high resolution seismic profiles (Figs. 9.15 and 9.16):

**Sequence 1:** stratified parallel and sub-parallel reflectors, varying in thickness from 2 to 8 milliseconds (1.5 to 6 m).

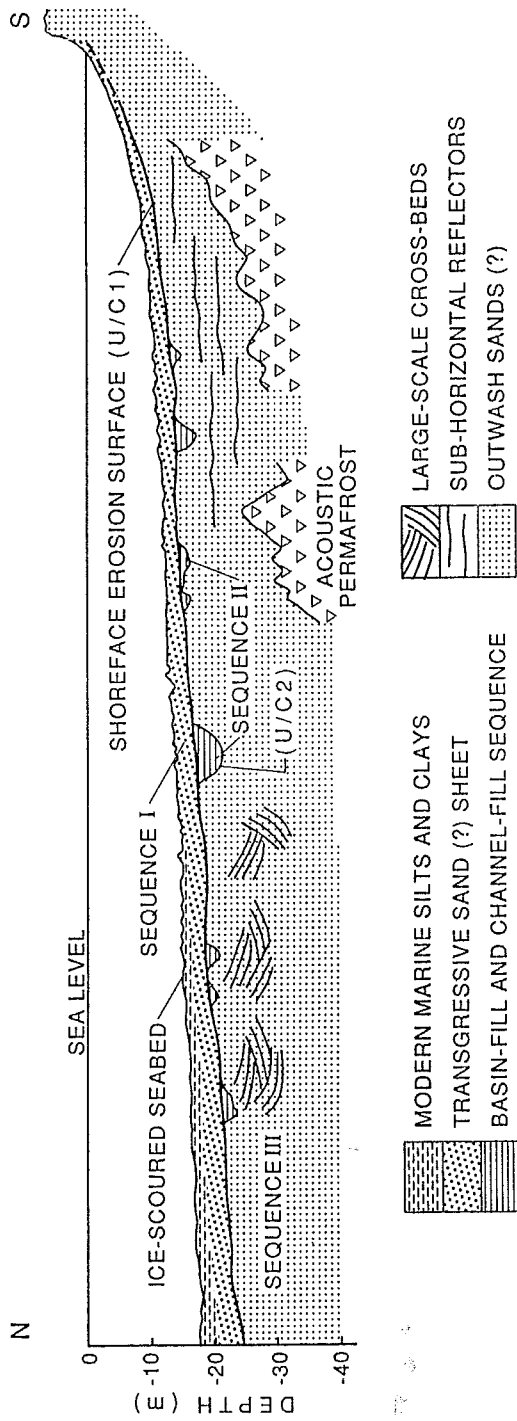
**Sequence 2:** a discontinuous sequence of variable character, including parallel, subparallel, hummocky and chaotic reflectors, as well as reflector-free configurations. This sequence is often



**Figure 9.14** Locations of seismic profiles and vibracores (from Hequette and Hill, 1989).



**Figure 9.15** Typical seismic profile from Tuktoyaktuk Peninsula inner shelf (from Hequette and Hill, 1989).



**Figure 9.16** Summary of seismic units from Tuktoyaktuk Peninsula inner shelf (from Hequette and Hill, 1989).

localised in depressions.

**Sequence 3:** characterised by poor acoustic penetration and sigmoidal progradational or discontinuous reflectors. Cut-and-fill cross stratification is common. This sequence also shows parallel, sub-parallel and chaotic reflectors in places.

Two regional reflectors, interpreted as unconformities (U/C's) separate the units. Sequence 1 is bounded by the seabed and U/C 1, and Sequence 2 by U/C's 1 and 2. U/C 2 forms the upper boundary of sequence 3, but the base is never seen. U/C 1 is interpreted as the shoreface erosion surface produced by shoreface retreat during the Holocene sea level rise. U/C 2 is interpreted as the pre-transgression land surface and is preserved where channels and thermokarst lake basins had sufficient relief to survive the transgression.

Although no deep borehole data are available to provide a chronostratigraphy, sequence 1 and 2 are reasonably interpreted as Holocene in age. Sequence 2 consists of lacustrine and alluvial sediments preserved in channels and lake basins. Sequence 1 consists of shallow water transgressional facies, and includes a possible drowned barrier-lagoon complex near Atkinson Point.

Sequence 3 is more complex and difficult to interpret without borehole control. It is broadly similar in acoustic character to sequence 3 of Hill et al. (in press) on the middle shelf. This unit is equivalent to the Tingmiark Sand, a late Wisconsinan outwash deposit that covers much of the middle shelf (Hill et al., in press). There is no apparent stratigraphic break between the two sequences on the inner and middle parts of the shelf. However, in both cases, sequence 3 contains many possible erosion surfaces, any of which, although interpreted as internal stratification, might be interpreted as a significant stratigraphic break. The importance of this interpretation is that a large channel incised into sequence 3 can be traced into McKinley Bay to link with an outwash channel that crosses the Tuktoyaktuk Peninsula and is related to the Tuk Phase limit of Mackay et al. (1972), Fyles et al. (1972) and Rampton (1988). If this correlation is correct, it implies a late Wisconsinan age for the Tuk Phase limit. Mackay et al. (1972) and Fyles et al. (1972) initially interpreted the Tuk Phase limit to be late Wisconsinan in age, but later interpretations of ice positions during the Wisconsinan have suggested that ice did not reach that far north in the late Wisconsinan (Rampton, 1988; Hughes, 1988).

To better constrain these interpretations, a chronostratigraphy for inner shelf sediments in this region is clearly needed. This would require strategically placed boreholes to penetrate well into sequence 3 to obtain biostratigraphic and age dating material, as well as to enable a comparison between sequence 3 sediments and the sands exposed on land.

## **9.5 Lithostratigraphy**

As mentioned above, there is a major dearth of core or borehole data from this region. Three short vibracores were collected through the upper part of sequence 1, just south of Tibjak Point (Fig. 9.14). The cores (described in more detail in Hequette and Hill, 1989) consist of fine to coarse sand with occasional pebbles and silty intervals. They do not provide any chronological constraint to the seismic stratigraphy. Hequette has also collected short cores from marshes in coastal lagoons along the coast. These cores are presently being interpreted by Hequette. A palynological report by the Bujak-Davies Group on the cores completed under this contract is included under separate cover.

Industry boreholes from the Hutchison Bay area recovered a sequence of fine to medium-grained, well-sorted brown sand, up to 40 m thick, with intervals of silt and rare, rounded gravel clasts, overlain by 0 to 6 m of silty clay. No ice or ice-bonded sediments were encountered in these holes. A similar sequence is found in boreholes on the inner shelf off McKinley Bay.

## **9.6 Geotechnical Properties**

There is no publicly available geotechnical data from the coastal zone of the Tuktoyaktuk Peninsula, beyond the lithological data noted above.

## **9.7 Sediment Erosion, Transport and Deposition**

A study of nearshore wave and current conditions and associated beach profile changes at Tibjak Beach was carried out in August and September 1987. Wave and current data from this study are incorporated into the following regional discussion of sediment transport processes. A further discussion of morphological changes at Tibjak Beach, over the duration of the program, is included at the end of this section.

### ***9.7.1 Influence of Mackenzie Plume***

Analysis of satellite imagery combined, with salinity, temperature and SSC measurements over several years suggests that the Mackenzie River water forms a surface low salinity layer over much of the Beaufort Sea during the summer months (Harper and Penland, 1982; Fissel and Birch, 1984; Fissel et al., 1987). The plume is deflected eastwards by westerly winds and the associated eastward, wind-driven surface currents. The water mass distribution over the shelf, east of Kugmallit Bay, is controlled primarily by changes in wind speed and direction over periods of several days (Fissel et al., 1987).

Harper and Penland (1982) observed a band of high SSC along the Tuktoyaktuk Peninsula coast on satellite images following several different periods of westerly winds. They interpreted this to be an easterly deflection of plume water resulting from the westerly winds. However,

Fissel et al. (1987) found that the high SSC band along the same section of coast, following a storm in 1986, was not associated with low salinities or high temperatures characteristic of Mackenzie plume water. This suggests that the enhanced SSC in the inner shelf was the result of local resuspension processes resulting from increased wave and current energy during the storm. This is significant, because under the Harper and Penland model, the inner shelf was thought to be an important sink for fine sediment. However, the more recent observations of Hequette and Hill (1989) suggest that fine sediment is not common inshore of the 10 m isobath off the Tuktoyaktuk Peninsula.

### **9.7.2 Waves**

A wave hindcast for deep water waves off Atkinson Point was computed by Pinchin et al. (1985) and the results are given in Table 9.4 as return periods for various wave heights. The one year return period wave height of 4.1 m is considerably higher than the equivalent wave on the northeast-facing Yukon coast, but slightly lower than the values computed for North Head. The difference in the latter case is most likely related to fetch limitation by sea-ice in the northern quadrant.

Wind data from Tuktoyaktuk and wave measurements in 3.5 m of water at the Tibjak Beach site are shown in Figures 9.17 and 9.18. Due to the shallow water depth and short duration, these data cannot be compared directly with the wave hindcast results. The data show several significant storm events with significant wave heights reaching 1 m or more. Peak periods of these waves reached 8 to 10 s. All the storms involved winds from the west to northwest directions and positive storm surges, with amplitudes between 0.4 and 0.8 m, occurred during each event. There were no strong easterly winds during the measurement period, but as Tibjak beach faces to the west northwest, easterly winds would not produce any significant wave activity at the site.

### **9.7.3 Currents**

Near-bottom current measurements are available for sites in 8 m of water at the West Atkinson drill site at the mouth of Hutchison Bay (Fig. 9.1) in 1981, and in 3.5 m and 5 m at Tibjak Beach in 1987 (Fig. 9.19). These data indicate that strong coastal currents are present along the Tuktoyaktuk Peninsula. At West Atkinson, the mean current speed, over a 50 day period in August and September, was 16.3 cm/s and the maximum current speed measured was 56.3 cm/s (Fissel and Birch, 1984). At the Tibjak Beach sites (Fig. 9.19), the mean speeds were 7.2 cm/s and 9.6 cm/s for the 3.5 m and 5 m sites respectively (Fissel and Byrne, 1988). Maximum currents reached 35.6 cm/s and 34.2 cm/s. At all sites, the currents were directed predominantly parallel to the shoreline.



**Table 9.4** Predicted deep water wave heights for various return periods for Atkinson Point, based on 14-year hindcast of winds at Tuktoyaktuk.

<b>Return Period (years)</b>	<b>Significant Wave Height (<math>H_s</math>)</b>
1.0	4.1
5.0	4.7
10.0	4.9
20.0	5.1
50.0	5.3
100.0	5.5



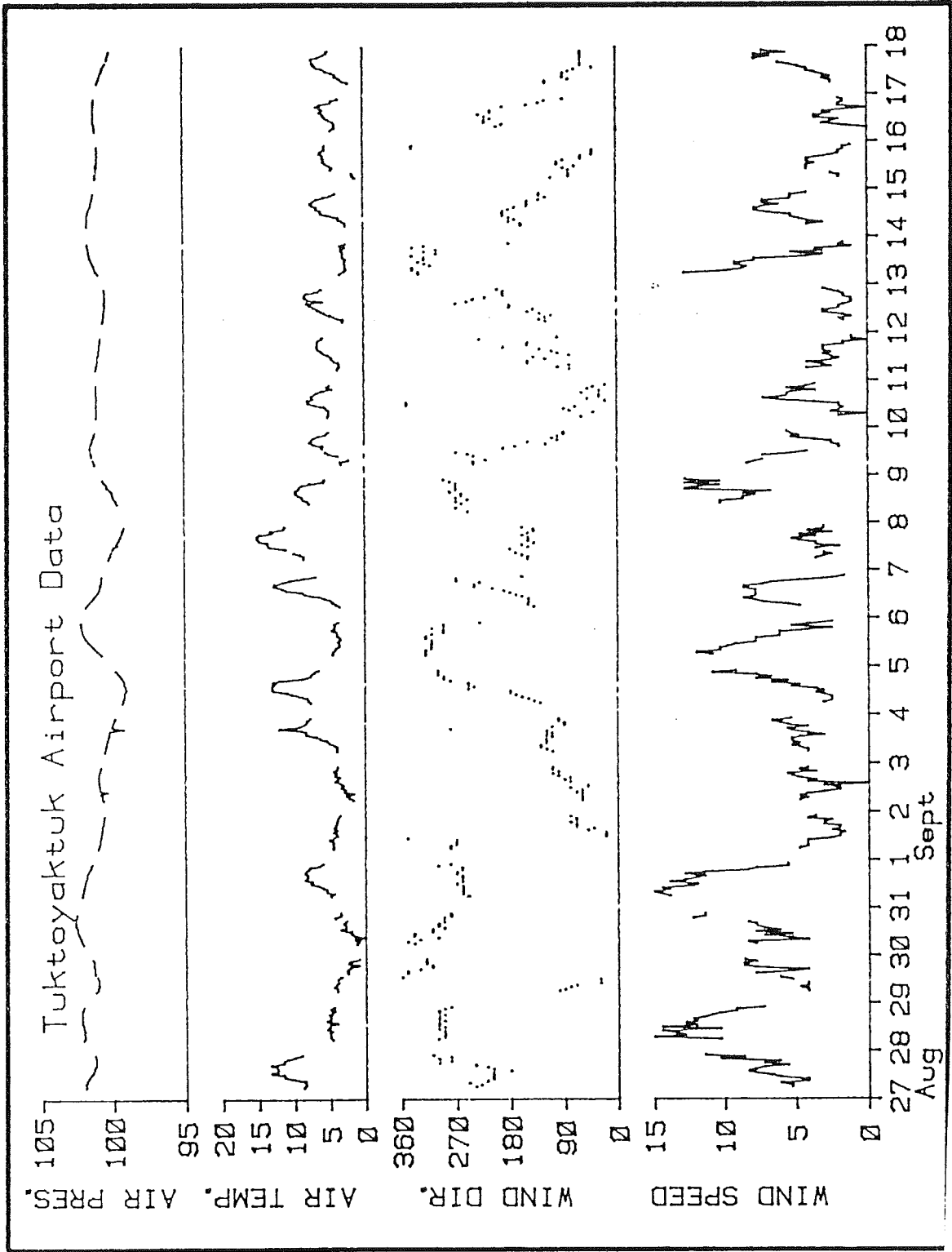


Figure 9.17 Wind speed and direction from Tuktoyaktuk during the Tibjak Beach program, Aug 27 to Sept. 17, 1987 (from Fissel and Byrne, 1988).

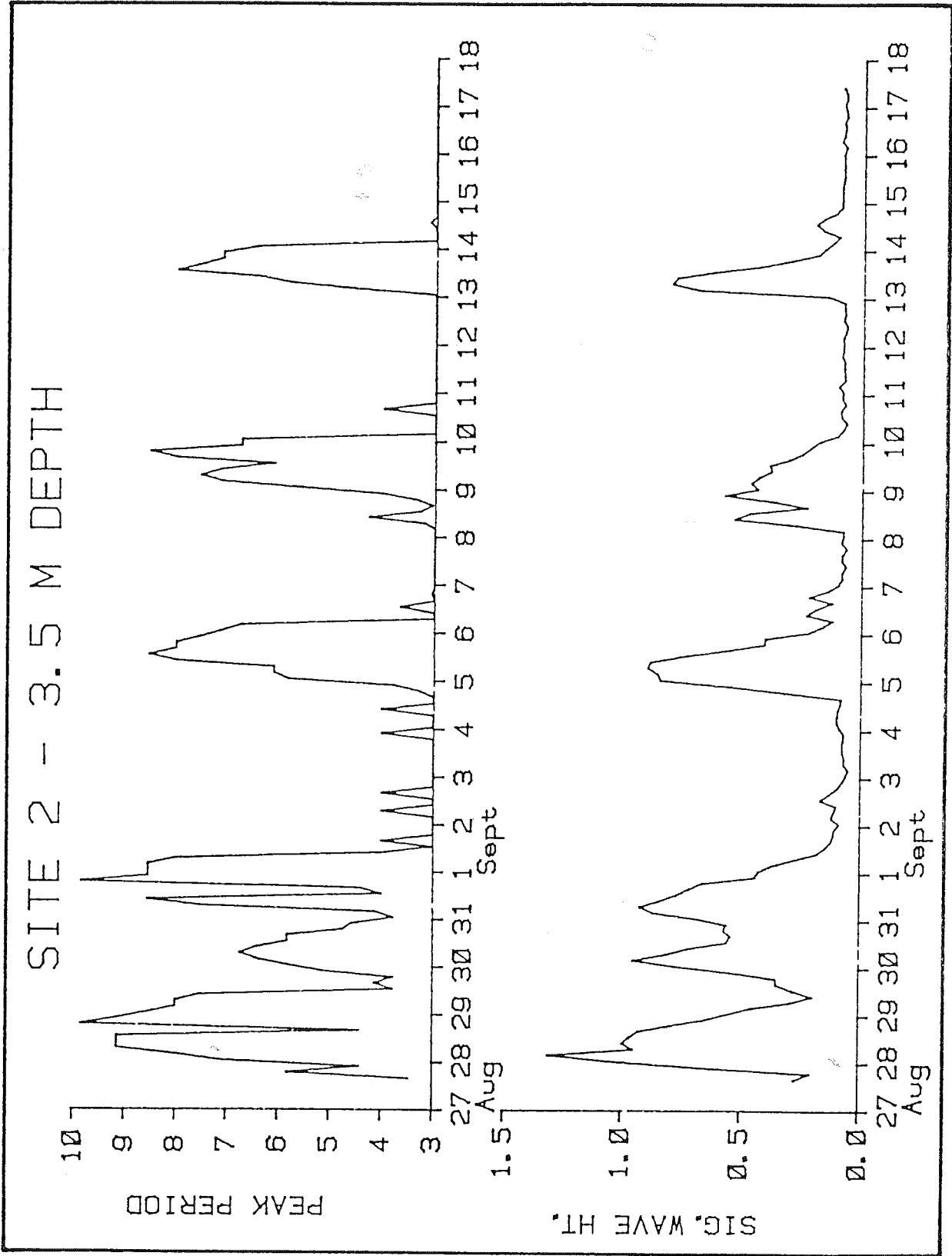
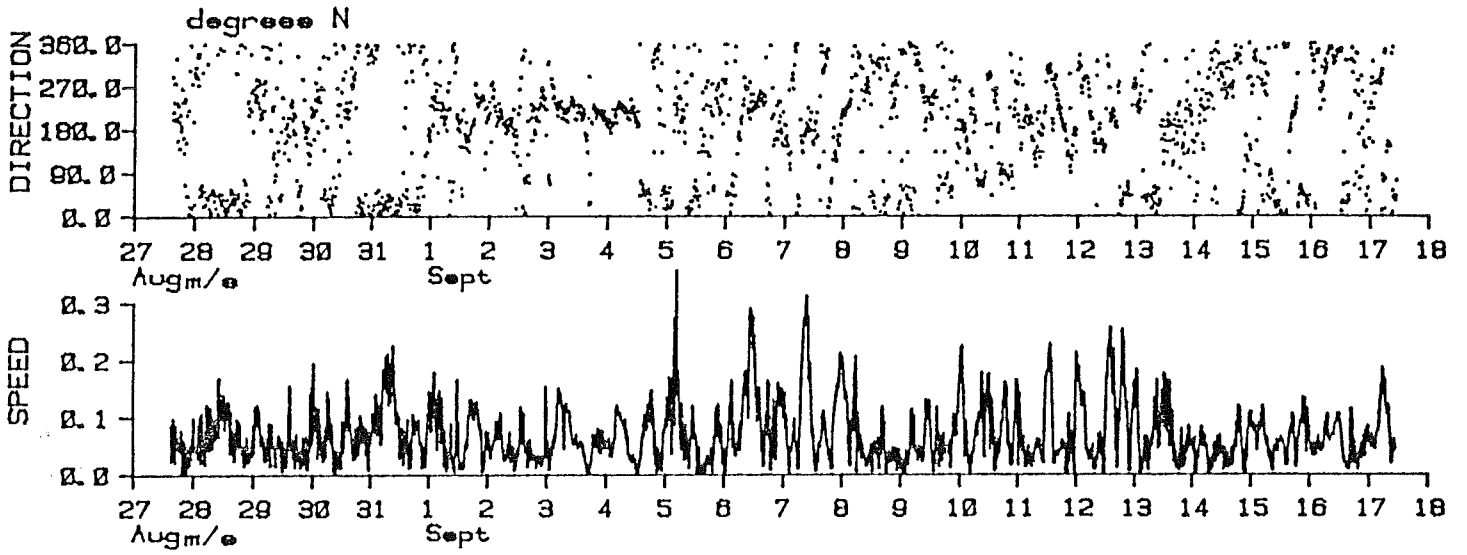


Figure 9.18 Significant wave height and wave period time series for Tibjak Beach, Aug 27 to Sept. 17, 1987 (from Fissel and Byrne, 1988).

### CURRENTS AT SITE 2 Depth: 3.5 M



### CURRENTS AT SITE 3 Depth: 5.0 M

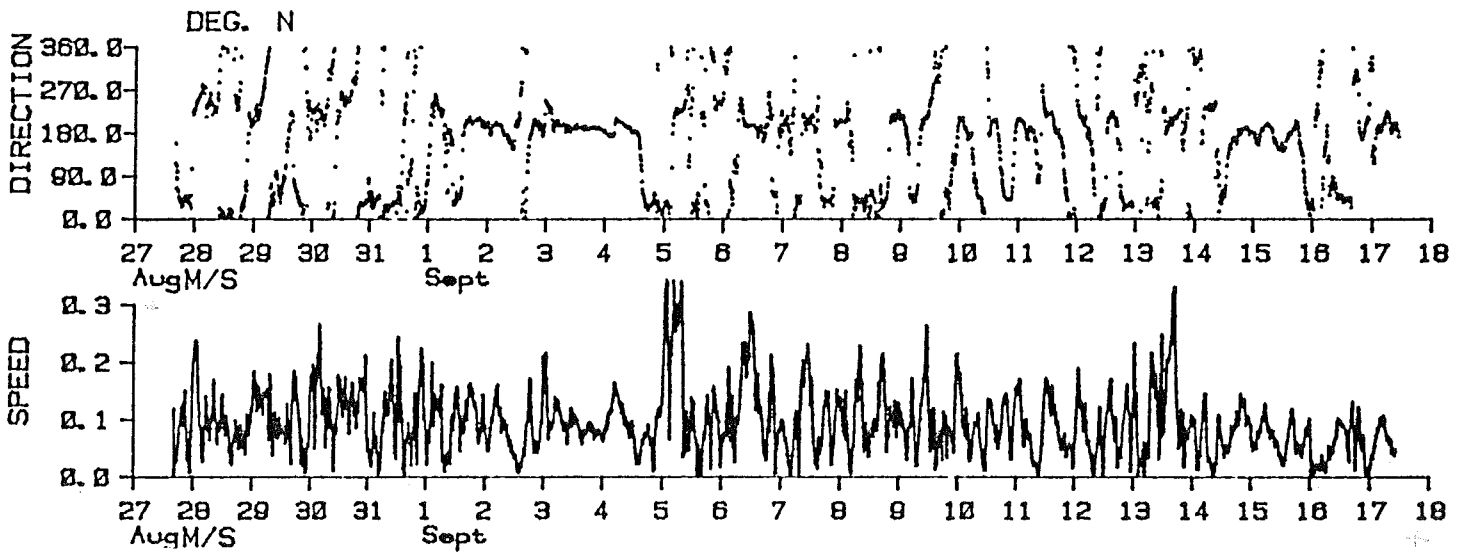


Figure 9.19 Currents at Tibjak Beach, August 27 to September 17, 1987 (from Fissel and Byrne, 1988).

At West Atkinson, the currents were well-coupled to surface winds measured at Tuktoyaktuk (Fissel and Birch, 1984), but at Tibjak Beach, the coupling, although not demonstrated quantitatively, appeared to be weaker and less consistent (Fissel and Byrne, 1988). This is likely to be due to the different aspects of the two locations. On the west-northwest-facing beach at Tibjak, winds from the northwest quadrant are frequently blowing directly onshore, perpendicular to contours, so that there is a less-pronounced set-up in either alongshore direction. At West Atkinson, the more north-facing aspect means that any strong winds from the northwest quadrant will result in strong easterly current flow.

#### ***9.7.4 Sediment Transport***

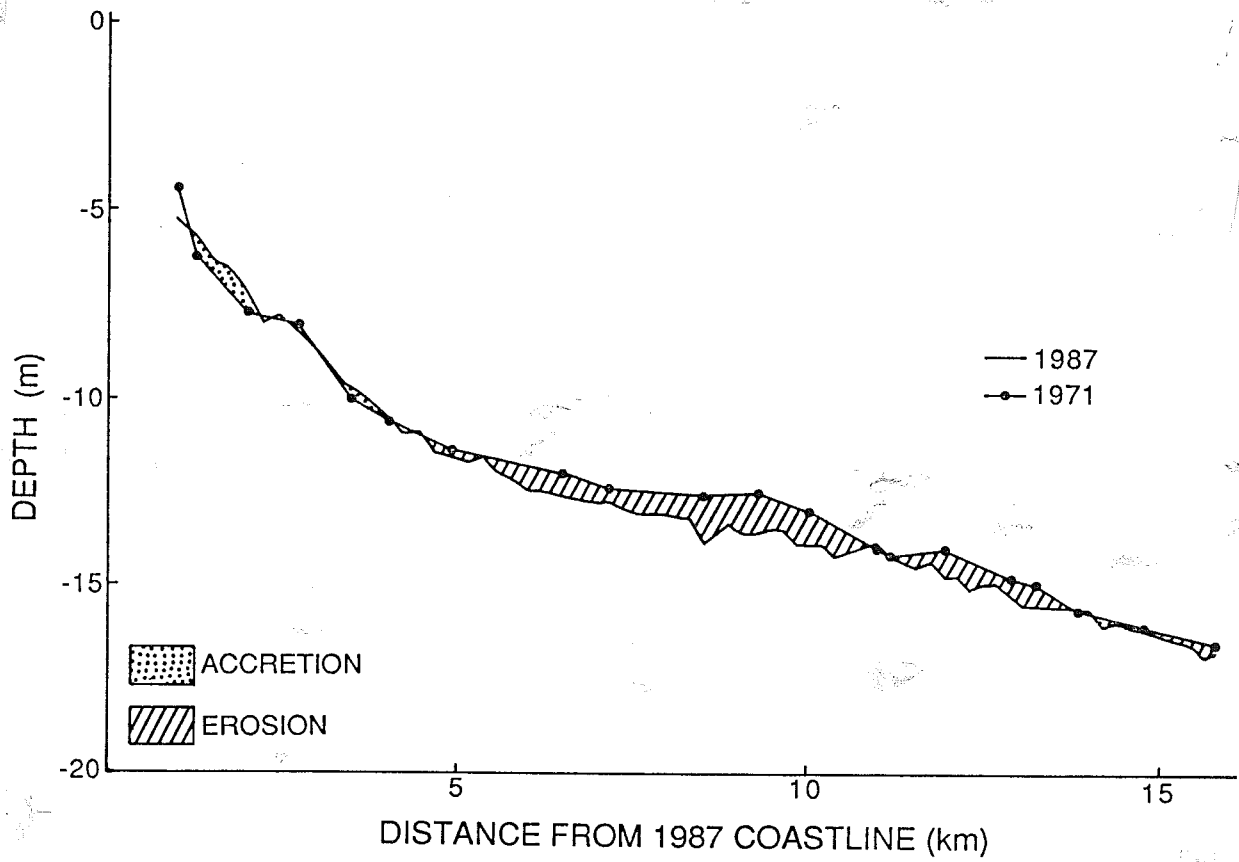
Pinchin et al. (1985) provided estimates of longshore sediment transport at Atkinson Point, based on the wave hindcast results and various published sediment transport equations. The average sediment transport for two locations (nodes) at the site was estimated at 107,000 m<sup>3</sup>/a and 95,000 m<sup>3</sup>/a towards the east. No attempt has been made so far to estimate sediment transport from any other method, so it is not clear how realistic this estimate of sediment transport is. Pinchin et al. (1985) point out that several factors are difficult to take into account in sediment transport calculations, particularly those involving equilibrium profile adjustments when large amounts of sediment are lost to washover. This is likely to be a significant problem on the low barrier systems along the Tuktoyaktuk Peninsula, whose elevations are commonly less than 1 m above mean sea level and where evidence for washover is abundant. An additional consideration is raised by Hequette and Barnes (1990), who suggest that significant erosion of the lower shoreface can occur through ice scour (Fig. 9.20). This has the effect of changing the equilibrium profile and causes landward migration of the shoreface and adjacent bluff.

#### ***9.7.5 The Tibjak Beach Study***

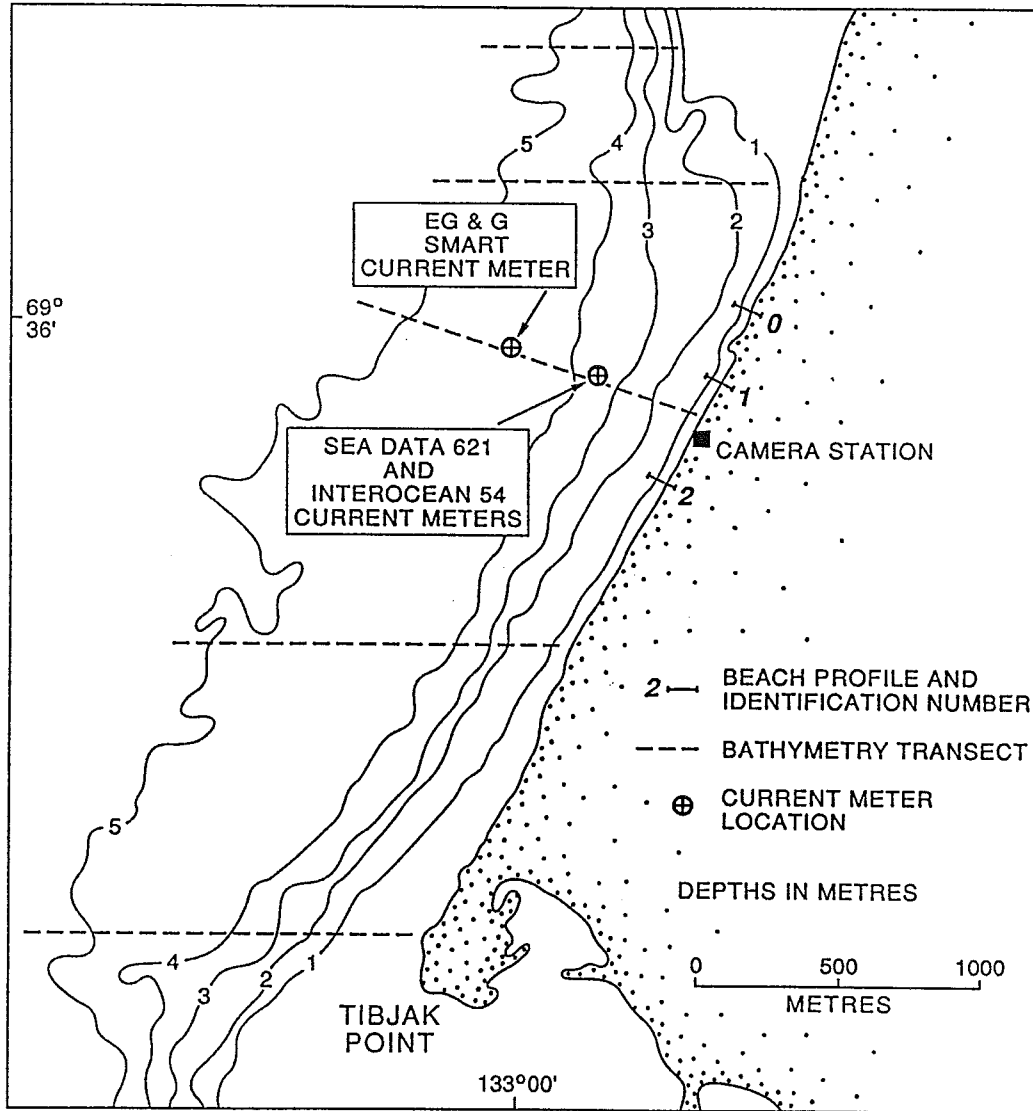
A detailed study of sediment transport at Tibjak Beach was carried out in 1987. This work is described fully in the accompanying report by Hequette, Jenner and Hill. The following is a summary of that report.

##### ***Description of the Study Site***

Between 22 August and 17 September, a program to investigate coastal sediment transport processes and associated beach morphology changes was carried out at Tibjak Beach, 15 km north of Tuktoyaktuk, where wave and current meters were deployed in the nearshore zone (Fig. 9.21). During the same period, beach profiles, sediment samples, bathymetric and sidescan sonar records were collected. In addition, video cameras recorded images of the beach and nearshore zone



**Figure 9.20** Shoreface profile changes due to ice scour (from Hequette and Barnes, 1990).



**Figure 9.21** Map showing the study site and location of current meters, video camera and beach transects.

simultaneously with the current meters.

Tibjak Beach is a 2.5 km long beach of medium-grained ( $M_z$ : 0.4 mm) well-sorted sands ( $S_i$ : 0.36  $\emptyset$ ). The beach is extended southward by Tibjak Point, a small sandy spit about 1.5 km long (Fig. 9.21). To the north, rapidly retreating sandy cliffs up to 5 m high supply sediment to the beach. The coastline faces WNW and is exposed to the dominant wave approach. A slightly oblique nearshore bar, about 40 cm high, extends towards the southwest just below low tide level along the central part of Tibjak Beach. As seen at low tide, this bar may be truncated in places. The subaerial beach at the study site possesses a very steep slope ( $9^\circ$  to  $10^\circ$ ) which immediately flattens to about  $1.5^\circ$  in the subtidal zone. Farther offshore, the bottom slopes decrease to approximately  $0.6^\circ$ . Bottom sediments across the shoreface are essentially sandy (0.2-0.35 mm), and the upper metre typically consists of fine to coarse sand with occasional gravel-size clasts, sometimes interbedded with silty sand or silt laminae (Hequette and Hill, 1989).

### *Methods*

Directional wave and current measurements were obtained using a Sea Data model 621 instrument in 3.5 m water depth. The instrument was programmed to burst sample every three hours during 1024 consecutive seconds (17.07 minutes burst record duration). The Sea Data 621 data have been subject to spectral wave analysis to compute appropriate wave parameters (Fissel and Byrne, 1988). The processed data include maximum amplitude of velocity fluctuations (which essentially corresponds to wave orbital velocity), mean wave direction, significant wave height ( $H_s$ ), and peak wave period ( $T_p$ ). In addition, mean current velocity and direction, and pressure have been computed as the mean of each three-hourly burst data set. An InterOcean S4 and an EG & G Smart current meter were also used to record currents in 3.5 and 4.5 water depths respectively. Technical specifications on the current meters are summarised in section 3.5.2. Directly landward of the current meter sites, two video cameras were operated on the coastline during the period of wave and current measurements to monitor changes in beach and oceanographic conditions. The cameras were activated every 3 hours, simultaneously with the current meters off the beach, for a two minute period.

A wave refraction analysis has been carried out for the significant wave of each recorded burst from the measurement site in 3.5 m water depth to the break point. The wave refraction analysis was performed by using the computer software WAVENRG (May, 1974) which consists of forward tracking of wave orthogonals from a specified depth across a depth-matrix representation of the seabed, given an initial wave height, period, and direction. The final output gives the following wave statistics at break point: wave angle ( $\alpha_b$ ), water depth ( $d_b$ ), wave phase velocity ( $C_b$ ), ratio of wave group velocity to phase velocity ( $n_b$ ), significant wave height ( $H_{sb}$ ),



and the longshore component of wave energy flux ( $P_{1s}$ ). Longshore sediment transport has been estimated using two predictor equations based on wave energy flux to give a range of potential longshore transport estimates. One is the CERC (1977) formula and the other is the Queen's formula (Kamphuis et al., 1986) which includes the effect of sediment size and beach slope on the rate of energy dissipation in the surf zone. Details on the longshore transport calculations can be found in Héquette et al. (1990).

#### *Atmospheric and Oceanographic Conditions*

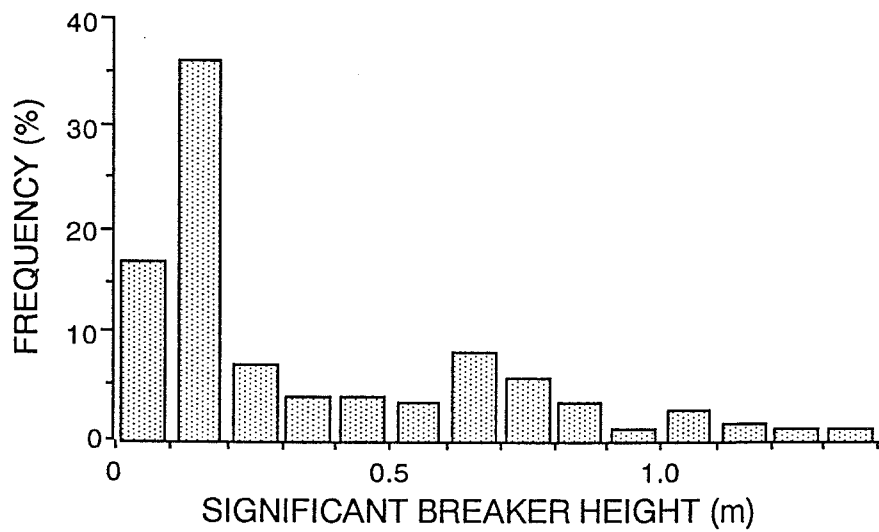
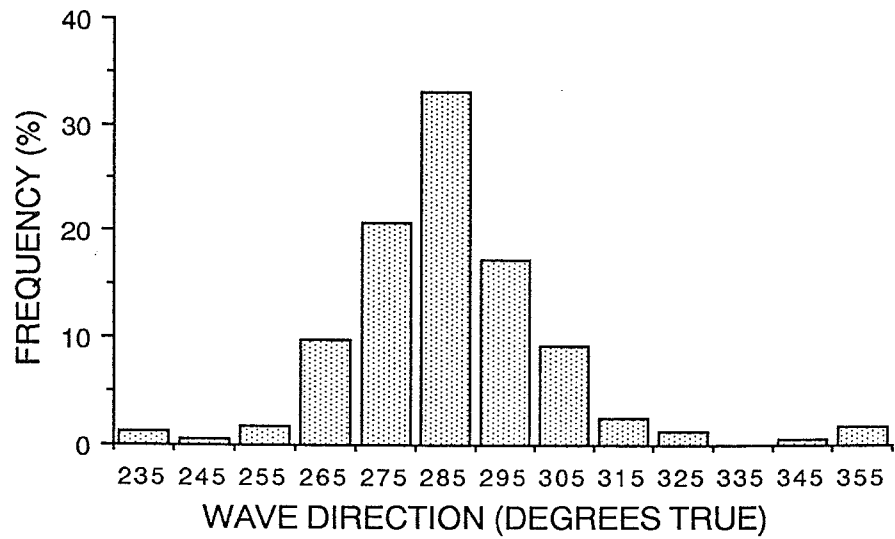
During the period of this study, the wave regime was dominated by waves from the west and northwest directions due to the predominance of west to northwesterly winds (Fig. 9.22). Several strong wind events resulted in significant wave activity in the nearshore zone, and waves with significant breaker heights of more than 1 m (Fig. 9.23) and significant periods up to 8.6 sec occurred on August 28, 30 and 31, and again on September 5. Significant wave events of somewhat reduced magnitude also occurred on September 8-9 and 13. High water levels (storm surges up to 0.85 m above mean sea level) and peak values in mean current velocities corresponded to each of these wave events.

#### *Visual Estimations of Breaking Waves*

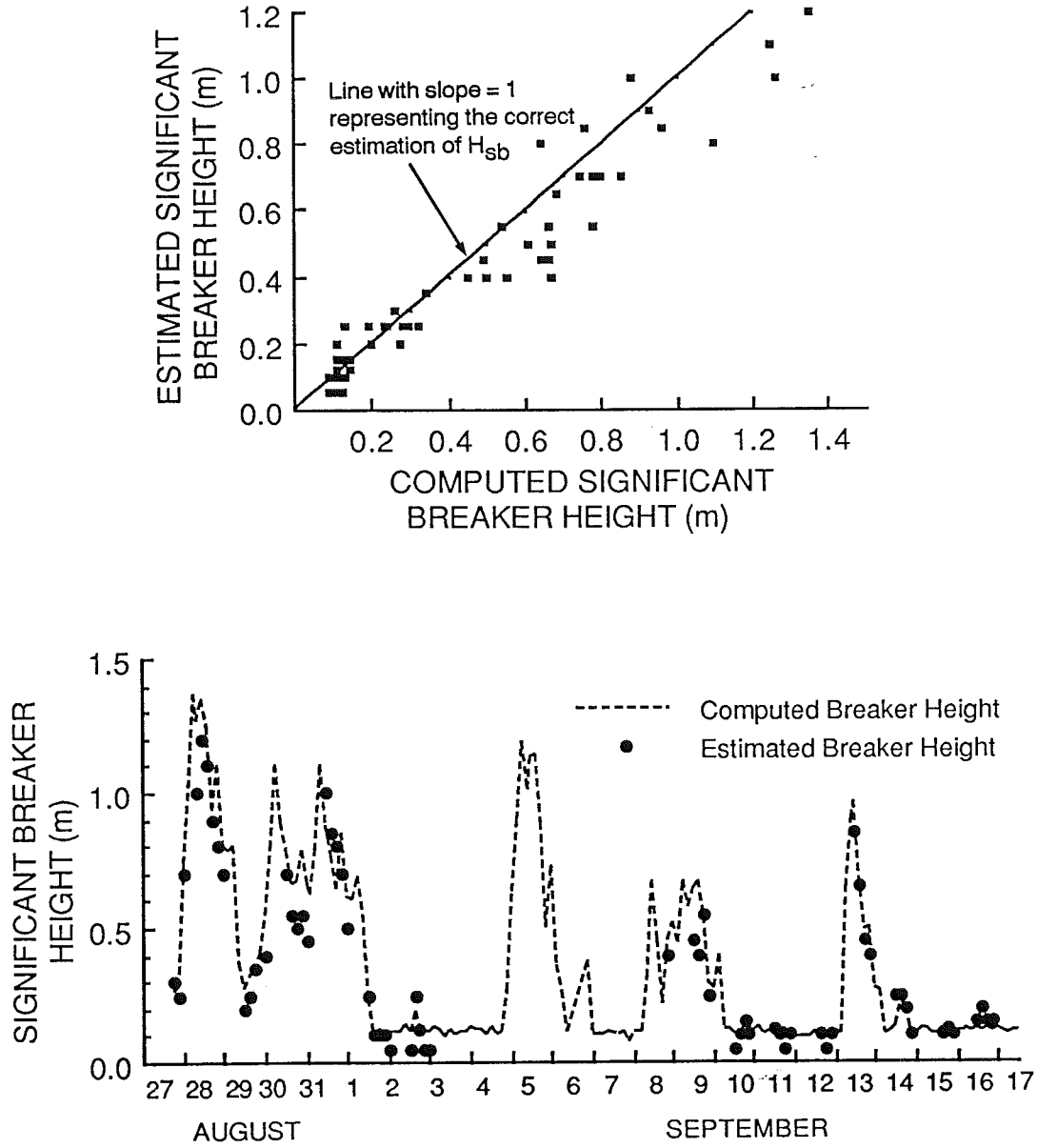
Significant breaker heights have been estimated using the video records. After comparison with computed breaker height, visual estimations of breaker height proved to be accurate within  $\pm 20\%$  for 75% of the observations, although some waves were underestimated, especially for the largest waves (Fig. 9.23). The video records were also used to distinguish the type of breaking waves. Surging, plunging, and spilling breakers and a transitional type of spilling and plunging have been distinguished. The determination of breaker type using the surf-scaling parameter,  $\epsilon$ , (Guza and Inman, 1975), agreed reasonably well with previous breaker type predictions (Fig. 9.24). During the high-magnitude wave events, breakers were mainly of the spilling or plunging type. The type of breaking wave appeared to be strongly controlled by water level fluctuations and incident wave amplitude. Morphodynamic beach states (Wright and Short, 1984) were defined using beach and nearshore topographic and bathymetric data, visual estimations of breaker types, and values of  $\epsilon$  for every three-hourly wave data set. The modal beach state consists of an intermediate state between the "transverse bar" and the "ridge and runnel" types, but the subaerial beach is strongly reflective and the outer surf zone is highly dissipative.

#### *Beach Changes and Longshore Sediment Transport*

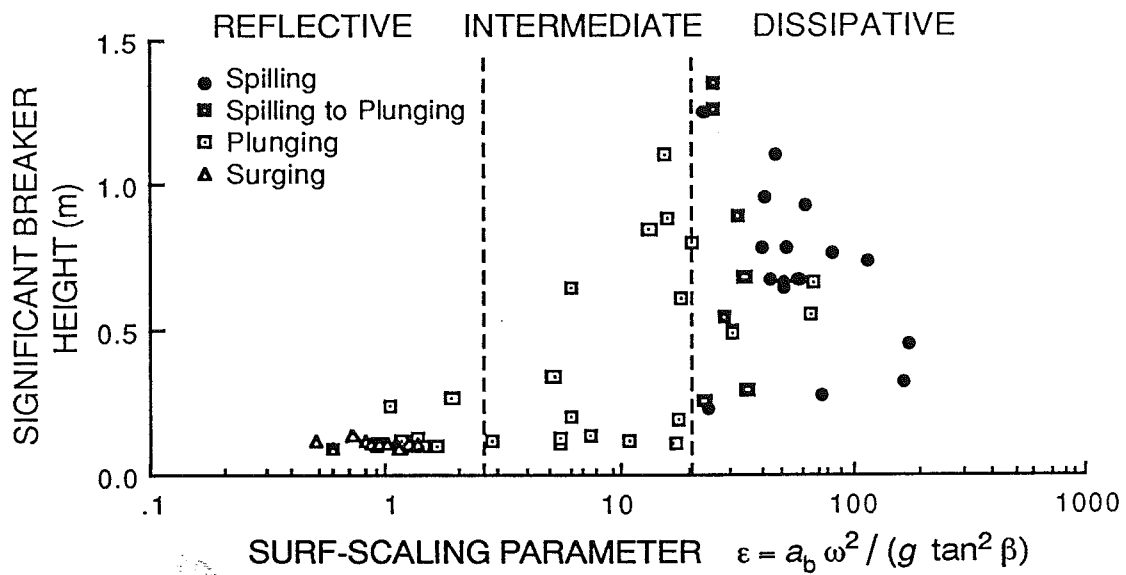
The wave activity which occurred in late August and early September in the nearshore zone



**Figure 9.22** Distribution of wave direction (upper diagram) and of significant wave height at breaking (lower diagram).



**Figure 9.23** Comparison of visual estimates of wave breaker height using video records with computed breaker height after refraction of the waves recorded in 3.5 m water depth.



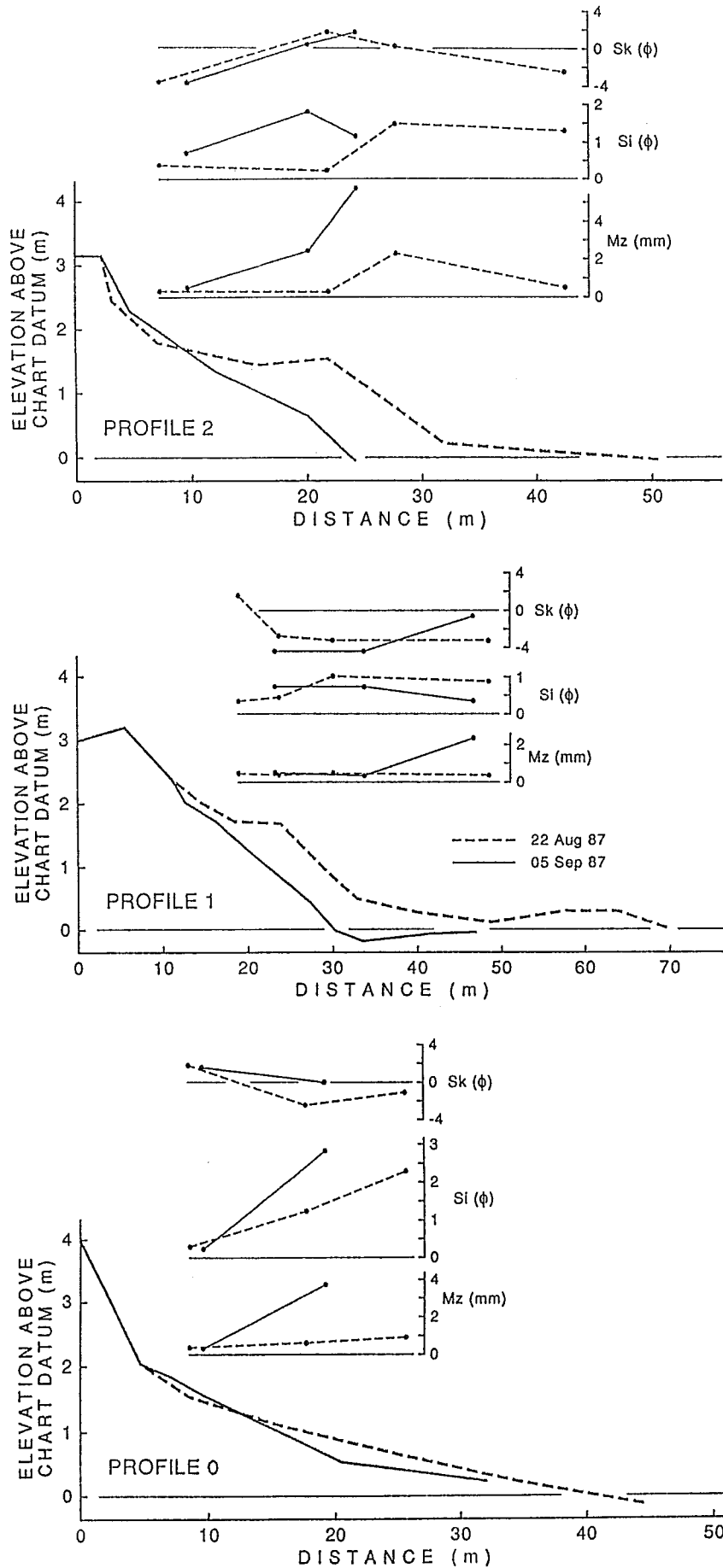
**Figure 9.24** Relationship between breaker height ( $H_b$ ) and the surf-scaling parameter ( $\epsilon$ ). Breaking wave types are visual estimations using video records. The limits between beach morphodynamic domains are values from Wright and Short (1984) and from Carter (1988).

resulted in significant morphological and sedimentological changes on the beach. As shown on the beach profiles surveyed on September 5, the action of erosive waves combined with high water levels resulted in the destruction of the berm visible on 22 August (Fig. 9.25). Beach sediments also showed changes in grain-size from August 22 to September 5. Although the size of the subaerial beach sands was of about 0.4 mm on both days, gravel was observed on the lower foreshore and at the step of the beach on September 5 (Fig. 9.25). It is believed that these sediments represent a lag deposit, exposed in response to the erosive action of storm waves. Changes in beach volume were estimated by calculating the cross-sectional area of eroded sediment on the beach profiles between August 22 and September 5. A volume of  $18.2 \times 10^3 \text{ m}^3$  was estimated to have been eroded along the beach excluding the spit at Tibjak Point, and therefore probably represents a minimum value. Longshore sediment transport was estimated using the CERC (1977) and the Queen's formulae (Kamphuis et al., 1986). Except for one storm on 31 August and 1 September for which the resulting longshore transport was oriented southward, the sediment transport was directed northward during all the other wave events. For the entire period of the study, longshore sediment transport calculations gave a net transport of  $6.9 \times 10^3 \text{ m}^3$  towards the north (CERC) and  $2.6 \times 10^3 \text{ m}^3$  (Queen's). These estimates are consistent with the surveyed profiles which show a decrease in beach erosion from north to south along this part of the beach. The northward transport along Tibjak Beach during westerly storms probably results in the infilling of the small embayment located to the north of the beach which exhibits a very flat and shallow bathymetry (Fig. 9.21). Southward sand transport is probably induced by waves from the northwest, north and northeast quadrants which represent a significant proportion of the total wave occurrence.

From the beginning of the wave measurement period on August 27 to September 5, when the beach profiles were resurveyed, the potential longshore transport ranged from  $1.9 \times 10^3 \text{ m}^3$  to  $4.3 \times 10^3 \text{ m}^3$  to the northeast according to the Queen's and CERC formulae respectively. As relatively calm conditions prevailed before August 27, it is believed that beach changes were negligible prior to the storm of August 28-29. Therefore, it is assumed that the calculation of beach erosion ( $\approx 18.2 \times 10^3 \text{ m}^3$ ) is a suitable estimate for the period August 27 - September 5. Although longshore sediment transport calculations represent some approximation, the potential longshore sediment transport seems low compared to the observed volume of sand removed from the beach. The longshore transport calculated with the Queen's formula is one order of magnitude lower than the observed eroded volume. These results suggest that a proportion of the beach sand was transported seaward.

### *Coastal Currents*

Large wave orbital velocities were measured during each strong wind event from the west



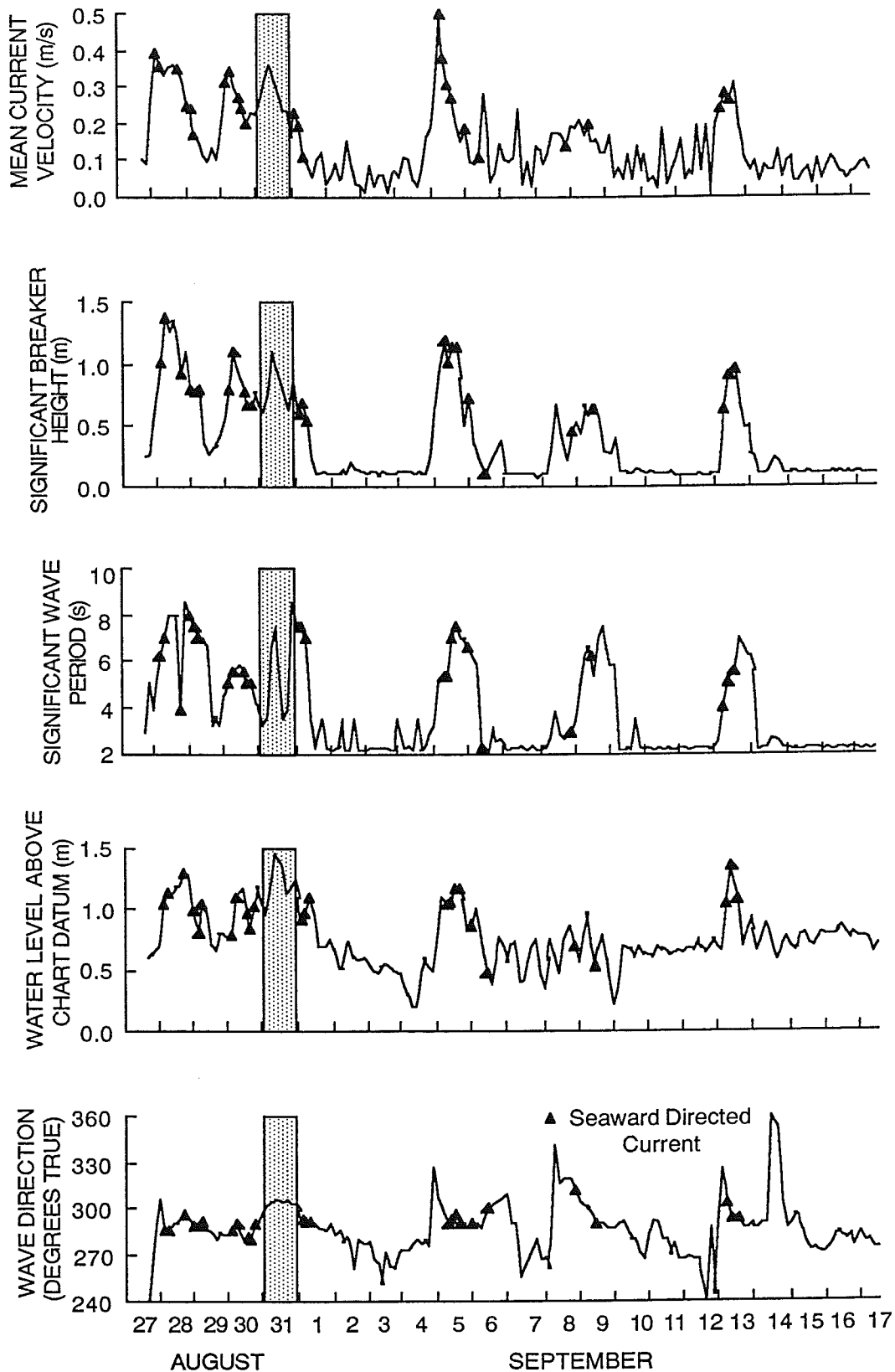
**Figure 9.25** Variations in beach profile and sediment texture at Tibjak Beach (see Fig. 9.12 for beach profile location).

and northwest, with peak values ranging from 0.65 to 1.3 m s<sup>-1</sup> (Fissel and Byrne, 1988), and as expected wave orbital currents were directed onshore. At both measurement sites, in 3.5 and 4.5 m water depths, the distribution of mean current direction was bimodal, setting in the longshore direction either to the NNE (170° to 210°) or SSW (350° to 30°).

Further analyses of the current direction data from the Sea Data instrument revealed a secondary component corresponding to seaward-directed currents. Virtually all the periods of seaward-directed currents correspond to peaks in mean current velocities (Fig. 9.26). The presence or absence of seaward currents is controlled by the direction of wave approach with respect to the shore-normal direction (Fig. 9.26). Seaward-directed currents occurred only when wave approach was from south of shore-normal. Current speeds were typically in the range of 0.25 to 0.35 m s<sup>-1</sup> but a mean current velocity up to 0.5 m s<sup>-1</sup> was recorded during the September 5 storm event. In 4.5 m water, the speed of seaward current was always less than 20 m s<sup>-1</sup>, showing a marked seaward decrease in current velocity.

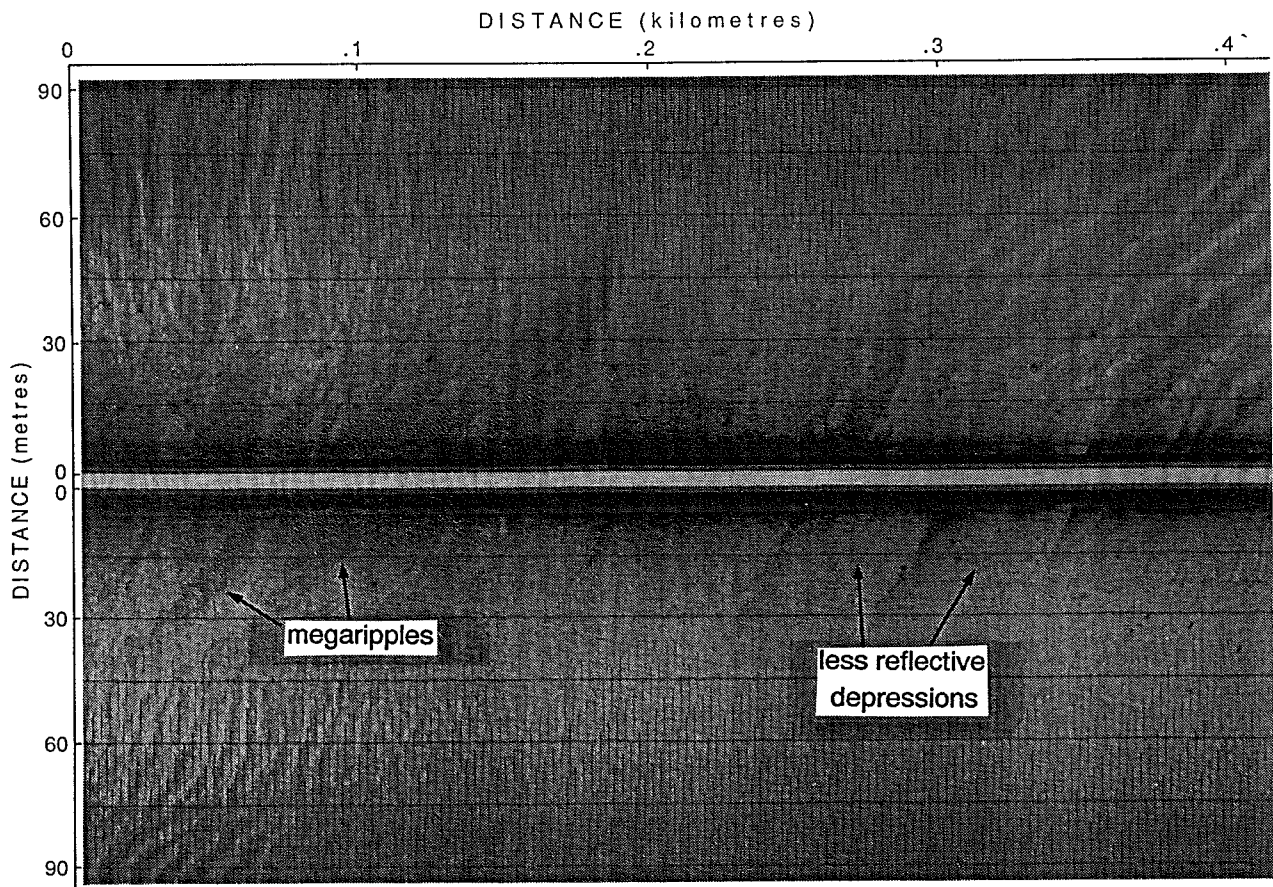
Two types of nearshore flow circulation can explain such seaward-directed currents: (i) rip current cell circulation; or (ii) storm-induced bottom return flow. Lower current velocities recorded at the same water depth by the InterOcean current meter, only a few tens of metres alongshore from the Sea Data 621 instrument, suggest a laterally-restricted flow consistent with rip current circulation. The fact that the nearshore bar is discontinuous in places may also represent evidence for the action of rip currents. Seaward-directed currents may also be generated by near-bottom returning flows induced by storm surges. Time-series measurements of mean current velocities (Fig. 9.26) show that during each storm-event, seaward currents almost always began at the peak of current activity and continue to occur during a decreasing phase. This shows that seaward currents occur after the initial storm-induced increase in mean current velocity. This could represent a residual flow after release of the onshore stress (or coastal set-up) created by a storm surge. Such conditions can also intensify upper shoreface rip current circulation (Swift et al., 1985). Therefore, in the absence of conclusive evidence, seaward-directed currents on the Tibjak Beach shoreface may be a result of either storm-driven circulatory rip current circulations or near-bottom surge return flows or by a combination of the two.

On September 6, the day after the storm that resulted in the strongest offshore-directed currents, side-scan sonar records revealed megaripples oriented almost parallel to the shore, in about 4 m water depth, at the current meter sites and over at least 800 m to the southwest (Fig. 9.27). They form megarippled bands that are oriented nearly perpendicular to the beach. The elongated coast-perpendicular shape of these megaripple fields is caused by the intersection of less reflective areas which probably represent fine sand (Fig. 9.27). These strips of sand correspond to flat, shallow channel-like depressions 15 to 20 cm deep, with sharp boundaries that truncate megaripple crests, and therefore formed after the megaripples. We tentatively explain these less



**Figure 9.26** Time-series plot of mean current velocity, significant breaker height, significant wave period, mean water level, and wave direction obtained from Sea Data model 621 current meter data recorded in 3.5 m water depth offshore of Tibjak Beach (instrument water depth is 2.4 m). Note that the significant breaker height represents computed values from significant wave height as recorded in 3.5 m water depth after refraction using a computer simulation; water depth is variable as it depends on the breaker height. The shaded area represents a storm event during which no offshore-directed currents occurred.





**Figure 9.27** Sidescan sonar record showing bands of megaripples and flat shallow channel-like features perpendicular to the coast, 200 m southwest of the Sea Data 621 current meter, 6 September 1987. Shore side at bottom. Water depth along side-scan trackline is 4.0 m above chart datum.

reflective areas as the product of channelized flows produced by seaward-directed currents. It is believed that the megaripples were formed by incident wave-induced currents, possibly during the increasing phase of the September 5 storm event, and that they were subsequently incised by the seaward-directed currents.

Seaward-directed currents may be responsible for a significant part of the shoreface sediment dispersal pattern. A flow velocity of  $0.5 \text{ m s}^{-1}$  at 1.0 m above seabed, as recorded during the September 5 storm event, represents the threshold for movement of 0.4 mm sand (Miller et al., 1977). As bottom sediment across the upper shoreface consists mainly of medium to fine sand (0.2-0.35 mm), considerable offshore transport is probably associated with the most significant storms. Therefore, seaward-directed storm currents may represent a major mechanism contributing to the production of the transgressive sand sheet that occurs on the inner shelf of the Tuktoyaktuk Peninsula (Hequette and Hill, 1989).



## 10. PRIORITIES FOR FUTURE COASTAL PROGRAMS

The final objective of this report is to make recommendations concerning future research on the Beaufort Sea coast. The approach taken here is to (i) identify items for immediate follow-up; (ii) identify major data and information gaps that the NOGAP D1 project was unable to fill; (iii) summarize the needs of various "client" sectors for AGC research, including local communities, industry, and government departments; (iv) identify priority issues that AGC should address in future programs; and (v) recommend research programs to address the priority issues. A short section recommending methods for improving communications with client groups and colleagues is also included.

### 10.1 Immediate Follow-Up

The interpretations presented in this report represent a first order analysis of the data collected during the NOGAP D.1 project. There are several areas in which further work to maximize use of the data presently available is warranted. These are briefly described below.

#### *10.1.1. Publication of Selected Topics of Scientific Interest*

Despite the large amount of money spent on marine geoscientific research in the Beaufort Sea region, relatively little information has reached the scientific community through journal publication. Although the information in this report will be made available through the GSC Open File system, journal publication still provides the most reliable method of ensuring widespread distribution to the scientific community. GSC Open File reports are available only at a few centres across Canada, and are poorly advertised, whereas reputable scientific journals are available in all major centres of Canada and most of the developed world. Beaufort Sea geoscience research has suffered in the past from a degree of isolation from the international community, due largely to the lack of cross-fertilization that can result from publication in international journals. It would be extremely beneficial to both the scientific community in general, and to the scientists involved in future Beaufort Sea research, to maximise the distribution of knowledge on the Beaufort Sea coastal zone through publication in scientific journals. The refereeing process involved in journal publication also adds considerable authority to the interpretations presented in consulting reports. This is important because future decisions on industrial and municipal development will depend on the output of NOGAP Project D.1. It is much easier to justify the findings of a publication that has been independently reviewed and published, than of a consultant's report that is reviewed in house and not widely distributed.

Of the information included in this report, there are several topics worthy of publication. These are listed in table 10.1, with provisional titles and lead authors. The relevant sections of this

**Table 10.1** List of potential publications resulting from NOGAP Project D.1

1. Late Quaternary stratigraphy and development of the Mackenzie Delta (Hill, Lewis, Blasco).
2. Facies development at the distributary mouth of the Mackenzie Delta (Jenner)
3. Seismic stratigraphy of the inner shelf of the Canadian Beaufort Sea: Mackenzie Delta to Kugmallit Bay (Hill)
4. A Holocene sea-level curve for the Canadian Beaufort Sea region (Hill, Hequette and Ruz)
5. Sedimentation on a storm-dominated muddy shelf: Mackenzie Delta and adjacent regions. (Hill)
6. Geotechnical properties of fine-grained coastal sediments of the Beaufort Sea and their relationships to sediment facies. (Hill, Moran and Christian)
7. A model of coastal evolution in a transgressed thermokarst topography, Canadian Beaufort Sea (Ruz, Hequette and Hill)
8. Spit and barrier island migration, Canadian Beaufort Sea coast (Hequette and Ruz)
9. Sediment transport on Tibjak Beach (Hequette and Hill)
10. Coastal dune development, Canadian Beaufort Sea (Ruz and Hequette)

report can be used as a basis for journal-quality manuscripts (as required for the contract). However, a certain amount of time spent on checking, verifying interpretations, editing and re-writing would be necessary before journal-quality manuscripts could be produced.

### ***10.1.2 New Research on Existing Data***

The following studies would add considerably to knowledge of the coastal zone, without needing further field work.

#### **(i) Grain-Size and Compositional Characterization of Fine-Grained Sediments from the Coastal Zone**

Numerous cores and grab samples have been collected from the Beaufort Sea coastal zone and inner shelf during the NOGAP project and considerable facies variation has been noticed. Furthermore, variation in composition, particularly with regard to particulate organic material, is also characteristic of these sediments. Before predictions of sediment transport and siltation rates can be developed, a detailed knowledge of the regional variation in grain size and composition is desirable. Detailed grain size spectra, using Coulter Counter or Sedigraph should be obtained on samples selected to be representative of both lateral and downcore variations. Particulate organic content can be estimated from smear slides, backed up by an incineration method. Mineralogical analysis by XRD on selected samples would also provide important baseline data.

#### **(ii) Detailed Analysis of Storm Resuspension Events**

An important set of simultaneous wave, current and suspended sediment concentration data is available following the Hodgins et al. (1986) Nearshore Sediment Dynamics Study for ESRF. The data consists of three-hourly burst samples and mean values and was used by Hill and Nadeau (1989) to verify the process of fine sediment resuspension under combined wave and currents. Several storms of varying magnitudes occurred during the deployment period, yet resuspension was not apparent during every storm. In this study, the characteristics of each storm through detailed examination of the burst data would be undertaken in an attempt to determine critical thresholds for erosion and deposition in this environment.

#### **(iii) Analysis of Sidescan Sonar Data from the Tuktoyaktuk Inner Shelf**

A sidescan survey of the nearshore and inner shelf off the Tuktoyaktuk Peninsula between Kugmallit Bay and McKinley Bay was carried out from the Karluk in 1987. A preliminary review of these data, including the single line used in the accompanying report

by Hequette et al. (1990) show that there are a large number of bedforms present along this section of the coast. These data therefore include a large amount of information concerning coastal processes and sedimentation.

**(iv) Analysis of Sidescan Sonar Data from the Mackenzie Delta and Adjacent Regions**

During the NOGAP D.1 project, sidescan sonar records were passed to J. Shearer for analysis of ice-scours, under a PERD contract. Various features in cores from the Mackenzie Delta and offshore islands suggest the possible presence of bedforms, mudbanks, liquefaction features and possible gas escape structures. A preliminary assessment of the importance of these features could be obtained through re-examination of the sidescan records.

**(v) Further Analysis of Seaward-Directed Currents, Tibjak Beach**

In the study of Tibjak Beach sediment transport processes, certain storm events were associated with strong currents, flowing seaward from the beach to offshore (see section 9.7.5). The origin of these currents is not understood. Spectral analysis of current data, using individual burst records may distinguish between rip current and bottom return flows due to storm set up.

**(vi) Comparison of Numerical Model and Field Data for the Tibjak Beach Study**

An original objective of the wave and current measurements at Tibjak Beach was to provide field measurements of shallow water waves and currents that could be used to assess the validity of the numerical model of coastal sediment transport of Pinchin et al. (1985). Unfortunately, simultaneous deep water wave measurements from an industry wave rider buoy near the Amauligak drill site are not available due to technical problems. However, some progress could be made by comparing the shallow water measurements directly with shallow water waves based on a deep water wave hindcast and numerical transformation of the waves into shallow water. This study may then yield useful information regarding the validity of the equations used in the numerical model.

## **10.2 Data and Information Gaps**

Much of the data collection to date has been very regional in nature, and it can be argued that data coverage could be much improved in most areas. However, there are some areas in which basic and important information is almost entirely absent. These areas are identified as

major data gaps and are listed below:

***(i) Regional high resolution seismic and sidescan coverage***

Along the Yukon coast, only one useable seismic line is available in shallow water between Kay Point and Shallow Bay. It is therefore impossible to evaluate the regional extent of units identified in Figure 5.8. Although there is a large suite of boreholes available at King Point, they cannot be placed into a seismostratigraphic context and extrapolation of the sedimentological and geotechnical data to adjacent areas is not therefore possible. West of Herschel Island, there is one single seismic line from the Karluk'85 cruise, which again does not give adequate coverage for coastal studies. From a basic mapping requirement, extending survey coverage to the Yukon inner shelf and coastal zone would therefore be desirable.

Coverage of the coastal waters east of Shallow Bay, while superior to the Yukon coast, is still not adequate for regional correlation or detailed interpretations of depositional environments. Denser coverage is required seaward of the Mackenzie Delta, where cores reveal numerous sedimentary structures indicating migration of bedforms and liquefaction. Sidescan coverage of this area would therefore be important for mapping areas of mobile bedforms and possible liquefaction failures (see item 10.1.2.iv).

***(ii) Borehole data from the Mackenzie Delta inner shelf and coastal zones***

The broad, shallow platform fronting the Mackenzie Delta is very difficult to access by boat and although seismic lines have been run into 3 m of water, there are no deep boreholes with detailed sedimentological descriptions or stratigraphic information available. Between 3 m water depth and the coastline, there is an extensive area where there is no data available at all. This area can only be practically accessed during winter. The Mackenzie Delta is one of the world's largest deltas and exerts a large influence over sedimentation in the Beaufort Sea. A series of deep boreholes through the Holocene and late Pleistocene section would provide an enormous amount of information on the development of the delta, and the history of sedimentation in the Beaufort region as a whole.

***(iii) Current data from Mackenzie Delta/Trough***

The observations summarised in section 6.7.3 suggest that an energetic current regime is present in Mackenzie Trough and may extend to the Mackenzie Delta coast. Current speeds over 1 m/s have been estimated from visual observations, but there are no current measurements available from Mackenzie Trough. Attempts to recover data from 10 m of water in the delta coastal zone failed due to the loss of a mooring (Fissel and Byrne,



1988). The potential for extreme currents and strong scour conditions makes current measurements essential before industry operations could be considered in Mackenzie Trough.

***(iv) Current and sediment data during periods of ice-cover and break-up***

There are very few current data sets available from winter or spring seasons. Baseline information on under-ice currents during the winter is lacking. Perhaps most critically, coastal zone currents during break-up, when the Mackenzie River discharge is at a maximum, are not known. Furthermore, siltation in nearshore environments is likely to be important during the Mackenzie River freshet in late May and early June, when sediment discharge is at a maximum. This would have particular relevance to the maintenance of a pipeline trench during this time of year. A study designed to measure currents and determine sedimentation rates during freshet is therefore important (see section 10.3.3).

***(v) Circulation in Kugmallit Bay***

As probably the most densely used coastal areas for marine activity, there has been surprisingly little effort to determine the circulation patterns within Kugmallit Bay. The bay is close to the major oil discovery at Amauligak and to the planned pipeline route. It would therefore be one of the higher risk areas for a potential oil spill. A knowledge of circulation within Kugmallit Bay during different times of year would be important should an oil spill occur. This research does not fall directly within EMR's mandate, but the information would be required by EMR and Environment Canada, for policy decisions and by the GSC's coastal geologists when evaluating the potential oiling of beaches and clean-up strategies during an emergency. The data would also be directly useful to the GSC for research on sedimentary processes and sedimentation in the region.

***(vi) Borehole data from Tuktoyaktuk Peninsula coastal zone***

There has been a very limited amount of coring carried out in the coastal zone of the Tuktoyaktuk Peninsula. In terms of the NOGAP Project D.1 objectives, there is a major gap in knowledge of the nearshore bottom materials that would be built upon in the course of development. As the sub-bottom is thought to be sandy over most of this region, a borehole program would be more effective than coring. Furthermore, important stratigraphic information could be obtained in a region beyond the Wisconsin ice limit, where the stratigraphy is therefore likely to be more continuous.

### 10.3 AGC'S 'Clients' and Their Needs

The following discussion is based on discussions with numerous individuals from industry, Inuvialuit groups and government departments. A list of those interviewed is given in Table 10.2.

#### 10.3.1 *Industry Plans and Perspectives*

There are three primary operators active in the Beaufort Sea at the time of writing:

**Amoco Canada Petroleum Co. Ltd.**, with interests assumed from Dome Petroleum Ltd, largely in the offshore beyond the coastal zone.

**Esso Resources Canada Ltd.**, with significant onshore gas discoveries at Parson's Lake and Taglu, as well as several prospects in coastal waters of the Mackenzie Delta and Richards Island.

**Gulf Canada Ltd.**, which has a major oil discovery at Amauligak, north of Tuktoyaktuk in approximately 30 m of water, as well as several other prospects in the offshore.

Oil and gas development in the Beaufort Sea is presently at a transition point. With several large discoveries, industry is poised to move into a production stage. Esso and partners presently have an application for a gas export licence before the National Energy Board, based on the production of onshore reserves. The favoured method of transport for the gas to southern markets would be via gas pipeline from the delta to Norman Wells, and south along the Mackenzie Valley. Esso's development scenario involves initial development of onshore fields at Taglu and Parson's Lake, followed within 5 to 10 years by development of shallow water fields in the Mackenzie Delta region. This planning is based on the export of gas to the U.S.

Oil production is likely to be inhibited by low world oil prices, but it can be assumed that, should oil prices rise, the production of Beaufort oil will be triggered, particularly Gulf's Amauligak development. Gulf have already initiated engineering studies related to the routing of an oil pipeline from Amauligak to North Head and are therefore well-placed to commence production planning.

Based on this scenario, three main issues related to production can be envisaged for which geoscience information will play a key role (Fig. 10.1):

- (i) Gas production islands will be constructed in the coastal zone, possibly linked to onshore gas plants by gravel roads.

**Table 10.2** Persons interviewed during the course of this study for the evaluation of AGC's client needs.

Amoco Canada Petroleum Co. Ltd.	Kevin Hewitt Alan Hippman Rocque Goh
Esso Resources Canada Ltd.	Ken Croasdale
Gulf Canada Ltd.	Chris Graham Brian Rogers Dave McGonigal
Inuvialuit Land Administration	Jane Bicknell
Joint Fisheries Management Board	Norm Snow Gary Wagner
NWT Municipal and Community Affairs	Michael O'Rourke
NWT Public Works	Siva Suttendra
Yukon Natural Resources	Steven Fuller
Parks Canada	Gordon Antoniuk Bill Dolan
Fisheries and Oceans Canada	Mike Lawrence Nancy Witherspoon
Indian and Northern Affairs Canada	Bob Gowan Ted Lawrence Vlado Schilder
Public Works Canada	Bill Smith

(ii) A buried oil pipeline will be constructed from Amauligak to pumping stations onshore. The presently favoured plan routes the pipeline to shore east of North Head, although other possible routings (e.g. Toker Point) have not been ruled out.

(iii) Large volumes of aggregates are likely to be required for the armouring of islands and caisson berms, as well as for construction of causeways linking shallow water islands to onshore gas plants.

Industry presently consults AGC regularly for information on regional geology, geotechnical engineering, sediment transport and coastal stability related to the planning of site investigations, geohazards and environmental considerations. It can be anticipated that, with the onset of serious production activity, the demand for information from AGC will increase dramatically. Furthermore, the coastal zone is more complex than the offshore, with respect to sediment properties, permafrost conditions and shallow gas, and is a zone of high energy with respect to wave, currents and sediment transport. The demand for geoscience information in the coastal zone is therefore likely to be very high when production takes off. This increase in demand argues clearly for a strong program of geological research in the Beaufort Sea coastal zone over the next ten years.

### ***10.3.2 Inuvialuit Communities***

In the past, much effort has been placed by the AGC in co-operating with and assisting industry activities in the Beaufort Sea. The coastal zone impacts much more directly on the local communities along the Beaufort Sea coast. Tuktoyaktuk is the only coastal community lying directly in the NOGAP study area. However, a broader area should be considered for future studies, in order to incorporate Paulatuk, Sachs Harbour and Holman, which fall within the Western Arctic (Inuvialuit) Claims Settlement (Fig. 10.2). Consideration should therefore be given to extending regional coastal surveys (such as the video and air photo surveys into Amundsen Gulf).

Under the agreement, the Inuvialuit have established two main administrative bodies: the Inuvialuit Regional Council (IRC), responsible for reviewing all development on Inuvialuit lands through the Inuvialuit Lands Administration Commission (ILAC); and the Inuvialuit Game Council (IGC), responsible for all wildlife management and environmental reviews. At the local level, each community has a Hunters and Trappers Committee which sends a representative to IGC.

There are several joint management committees, involving Inuvialuit, federal and territorial representatives. IGC has set up a screening review process for environmental impact assessment. All activities on Inuvialuit lands are first screened by the Environmental Impact Screening Committee and those requiring more detailed review are reviewed by the Environmental Impact

Review Board often through a public hearing process. Recommendations from this process are not binding, but government must respond to the recommendations within 30 days if they are not accepted.

Within IGC there are also two Wildlife Management Advisory Councils (one each for the Yukon and NWT) and a Fisheries Joint Management Committee, which recommend research projects, carried out for the most part by government agencies, particularly DFO. There is meant to be a Research Advisory Council, but this role is presently and will probably continue to be played by the Science Institute of the Northwest Territories.

AGC must deal with all these agencies where appropriate in the future. Two major issues affecting Inuvialuit communities in the region can be identified:

*(i) Environmental Protection*

Probably the largest concern that communities have in common is the protection of wildlife resources and consequently the natural environment of the region. It is difficult to predict exactly what questions are likely to be raised over the next few years, but they are likely to revolve around the impacts of oil and gas development. The EIRB is likely to be faced with numerous problems related to oil spill and environmental impact. AGC should establish strong contacts with the EIRB and with Game Councils at the local level, to make these organizations aware of the expertise within AGC, and ensure that appropriate advice and information is provided them when required. A communications program aimed at the EIRB and local communities, through their Game Councils, should therefore accompany any future research programs on the Beaufort coast.

One particular issue related to the coastal zone concerns the important fish habitats in coastal embayments, particularly along the Tuktoyaktuk Peninsula. These areas and the adjacent streams provide important wintering grounds for several important fish species used by the local communities. Geological information will be important in assessing the effects of an oil spill in this critical environment. Furthermore, changes in barrier island morphology, particularly as the result of global change or development activity, which may result in different patterns of sea-ice and/or circulation patterns, could have a major impact on this fish habitat.

*(ii) Coastal Erosion and Dredging Problems*

The hamlet of Tuktoyaktuk has a severe erosion problem. The hamlet is situated on a narrow peninsula on the eastern shore of Kugmallit Bay, exposed to strong northwesterly storms. Problems in the past have led to the removal of the schoolhouse, and attempts to provide shore protection have failed. Shore protection is the responsibility of Public Works Canada, who are considering a possible beach nourishment solution, which will cost \$1.5 million in its first year. Officials at Public Works expressed interest in sediment budget and sediment transport studies at

Tuktoyaktuk, to assist with planning of shore protection.

Dredging of the approaches to Tuktoyaktuk Harbour is necessary to allow the access of large vessels. This has been a concern to the petroleum operators rather than to community groups. The Department of Public Works have received complaints from Northern Transportation Co. Ltd. (now part-owned by the Inuvialuit) regarding difficulties their barges have encountered entering Paulatuk and Coppermine harbours, due to siltation and channel instability.

### ***10.3.3 Government Regulatory Requirements***

Jurisdiction over oil and gas regulatory roles is in a state of transition. Previously, the regulatory role for both onshore and offshore exploration has been a federal responsibility, with the onshore being taken by Indian and Northern Affairs and the offshore by the Canada Oil and Gas Lands Administration (COGLA). Responsibility for the onshore has recently passed to the territorial governments.

Government regulators are charged with ensuring safe delivery of oil and gas resources through a licensing procedure. Responsibility for demonstrating any proposed project's safety belongs to the company. Regulators require background information on regional geology, geotechnical conditions and sedimentary processes, particularly as they relate to geohazards, as a basis for decision-making.

The information required by regulators is therefore general in nature rather than site-specific. Project proposers are expected to provide the detailed information on which to base a decision. Regulators need background information to ensure that all potential geohazards have been considered and that the proposer has dealt with the issue in a comprehensive and balanced way.

In terms of guiding future coastal research therefore, there are no specific directions required by government regulators. AGC should aim to develop a regional understanding of coastal zone geology and processes related to geohazards, and to make this expertise available to COGLA, DIAND and the territorial governments upon request.

## **10.4 Recommendations: Priority Issues**

There are four principal issues related to the Beaufort Sea coast that the Atlantic Geoscience Centre should respond to in the next 5 years. The priority of these issues is based on the following general criteria: (i) the benefit to Canadian society; (ii) the benefit to Canadian industrial interests; (iii) the benefit to Canadian contributions on global issues; (iv) the time frame needed for response. The same definition of the coastal zone (i.e. extending from the cliff line to the 10 m isobath) is used here, as for the previous NOGAP program.

## **PRIORITY 1: IDENTIFICATION OF POTENTIAL GEOHAZARDS TO OIL AND GAS DEVELOPMENT**

The federal government has a responsibility to regulate development of oil and gas fields in the Mackenzie Delta - Beaufort Sea region. It is incumbent on the government to identify and acquire a knowledge of the potential geohazards related to the coastal zone, with particular regard to the routing of pipelines, construction of artificial islands and siting of support facilities. Although principal responsibility for regulation and assessment of development projects rests with other agencies, the Atlantic Geoscience Centre is responsible for acquiring the necessary geological information and knowledge of geohazards in the coastal zone, in order to provide advice on these issues when required. In this study, potential geohazards related to gas and gas hydrates, permafrost and thaw settlement, ice push and ice scour, current scour, siltation, and liquefaction have been identified. With industry predicting the development of offshore discoveries in the latter part of this decade, the need for this information is immediate. It would be of benefit to both government regulators and industry to have clear analysis and documentation of potential geohazards in the coastal zone.

**Recommendation 1:** AGC should conduct a specific geohazard assessment of the Beaufort Sea coastal zone that includes: (i) mapping of geohazard distribution; (ii) descriptions of key processes and engineering significance; and (iii) public reporting of assessment results.

## **PRIORITY 2: OIL SPILL PREPAREDNESS**

The low-lying, complex coastline, with its abundant wetland habitats, make the Beaufort Sea coast particularly susceptible to an oil spill, should one occur. Oil clean-up efforts are inevitably focused on the coastline and require an understanding of coastal environments and processes. Geologists usually contribute to these efforts by assessing the potential for oiling of beaches and other coastal environments, the burial of deposited oil and tar by natural sedimentation processes (thus inhibiting clean-up) and the potential for remobilization of oil by natural processes. An oil-spill atlas and emergency response plan for the Beaufort Sea coast have been prepared by Environment Canada and already involves AGC scientists on a stand-by basis. Adequate response to an oil spill will require an understanding of sedimentation processes in the various coastal environments in the region. Taking the Mackenzie Delta as an example, the studies of Jenner (1989) have show that sedimentation in distributary mouth environments is largely controlled by water levels, which are in turn influenced by river flood and storm surge events. The same processes would greatly influence oil dispersion, deposition and clean-up requirements, in the case of an oil spill. Studies of sedimentation patterns and processes in deltas, estuaries, coastal embayments, lagoons, marshes and tidal flats will be particularly important, as these areas are not only highly susceptible to oiling but also are important staging grounds for various bird species,

and access points to spawning and over-wintering grounds for many fish species.

**Recommendation 2:** AGC should acquire knowledge of sedimentation patterns and processes in all key coastal environments susceptible to oil spill. Particular emphasis should be placed on ecologically important environments such as deltas, coastal embayments, lagoons, marshes and tidal flats.

### **PRIORITY 3: RESPONSE TO LAND-USE PLANNING AND COMMUNITY NEEDS**

With the settlement of the Inuvialuit land claim and imminent settlement of native claims along the Yukon coast, land-use planning and management of the coastal zone may become an important issue in the next 5 years. S.L. Ross Environmental Research is presently developing a geographic database for the Mackenzie Delta - Beaufort Sea Land Use Planning Commission. For the most part, planners and communities in the region are not familiar with the work of the GSC or AGC. It is important, particularly in view of the remoteness of AGC from the region, that AGC take the initiative and promote communication with these groups. The results of this study suggest that community organizations will ask for information regarding: (i) the sensitivity of the coastline to oil spill; (ii) coastal erosion at Tuktoyaktuk; and (iii) sensitivity of important fish and wildlife environments at the coast to climate warming.

**Recommendation 3:** AGC should include areas of interest to the communities in its field programs and make efforts to promote communication with land-use planners and community organizations in the Beaufort Sea region.

### **PRIORITY 4: INPUT TO ENGINEERING DESIGN PROBLEMS**

Geological information is commonly used by industry engineers when designing foundation structures for pipelines, artificial islands and shore-based facilities. Several types of study traditionally carried out by AGC can be identified as useful to design engineers: (i) regional mapping and stratigraphic interpretation; (ii) sedimentology, interpretation of depositional environments and prediction of geotechnical properties; (iii) sediment dynamics and seabed processes. An important additional contribution that AGC can make is in the assessment of the impacts of global greenhouse warming on engineering designs. In particular, the stability of the coast over the design-life of coastal structures is important in determining factors such as setback and burial depth.

**Recommendation 4:** AGC should continue to support industry through studies of regional stratigraphy and sedimentation processes in the Beaufort Sea coastal zone, and should develop a new program to assess the impacts of climate change on coastal stability in the region.



## 10.5 Recommended Programs

The following research programs are designed to address the priority issues discussed above. Although four separate programs are outlined in priority order, they do not correspond directly to the four priority issues, but can be clearly related to requirements outlined above. The programs should be considered complementary, meaning that interaction between them would be desirable. For example, a complete geohazard analysis would require both regional mapping and specific process studies. So, if resources are limited, important elements from different programs might be selected to address the specific priority issue. The components of each program are discussed in terms of required field work, data analysis and outputs.

### *10.5.1 Regional Mapping Program: Beaufort Sea Nearshore and Inner Shelf*

This program is aimed at (i) providing a Quaternary stratigraphic framework for the region, including onshore-offshore correlation; and (ii) mapping of geohazards. An understanding of the Quaternary stratigraphic framework is prerequisite to an analysis of geohazards. The program should be regional in scope, including at least the region between Hershel Island and Cape Dalhousie, although greater survey density would be desirable in the area of highest potential for development, between Mackenzie Delta and McKinley Bay.

#### *(i) Field Requirements:*

(a) AGC should continue development of the Seistec line and cone receiver system for improving the quality of high resolution seismic surveys in shallow water. Some experimentation with different sources (e.g. sparker and airgun) would be desirable to obtain deeper penetration.

(b) A systematic program of seismic and sidescan surveying should be carried out. Such a program would be most efficiently carried out from a small vessel such as the Karluk, that can be chartered for several weeks per season. One week of Nahidik time per year is insufficient for obtaining regional coverage over a reasonable time frame. With the Karluk, regional coverage of the Beaufort sea coastal zone could be obtained in 3 to 4 seasons of 6 weeks.

(c) Nahidik should be used for vibracoring and other special work requiring heavy equipment e.g. air guns, Sea Carousel. Sampling programs should be designed for both stratigraphic and specific hazard investigations (e.g. sampling for gas).

(d) A drilling program should be considered to investigate the lithostratigraphy of the Mackenzie Delta and Tuktoyaktuk Peninsula inner shelf and nearshore regions.

(e) Collaborative fieldwork with Quaternary geologists from Terrain Sciences Division should be instigated, to compare land exposures of key units with offshore units.

*(ii) Data Analysis:*

(a) The preliminary seismic stratigraphy presented in this report should be developed and refined, through regional mapping of seismic units, mineralogical, biostratigraphic and geochemical studies on borehole materials.

(b) Collaboration with TSD to correlate between onshore and offshore sequences is essential.

(c) Maps of observed geohazard distribution should be prepared (e.g. maps of acoustic permafrost distribution, shallow gas occurrences, pockmarks, liquefaction features etc.) and interpretations of the geological conditions causing various geohazards should be attempted.

*(iii) Outputs:*

(a) GSC paper on Geohazard Assessment for the Beaufort Sea coastal zone.

(b) Journal papers on the stratigraphy of the Beaufort Sea coastal zone, correlations with the onshore and Quaternary geological history of the region.

### **10.5.2 Dynamics of Muddy Shoreface and Inner Shelf Environments**

The aims of this program are: (i) to develop an understanding of the dynamics of sediment erosion, transport and deposition under ice during the freshet and under combined wave and current action during the open water season; (ii) to assess the scour and siltation geohazard potential in the coastal zone; and (iii) evaluate the effects of sediment entrainment on wave energy dissipation across the muddy inner shelf and shoreface.

*(i) Field Requirements*

(a) A pilot field study to investigate the fate of sediment discharged to the Beaufort Sea during the freshet should be carried out. The study would consist of mapping river discharge channels in the ice, measurements of current flow, suspended sediment concentration, salinity and temperature, and deployment of sediment traps to measure sedimentation rates. The work would be conducted from the ice just prior to and during freshet in late May, continuing to early June when ice conditions become unsafe.

(b) A larger scale study could then be considered if results of the pilot study suggest that significant sedimentation and/or current scour is occurring during the freshet period. This might involve the deployment of low-cost instrument packages through the ice prior to freshet, followed by a second set of bottom-mounted instruments as soon as break-up has occurred.

(c) During the open water season, measurements of critical erosion and deposition stresses under unidirectional currents should be made with Sea Carousel. As sediment properties change significantly inshore of the 10 m isobath, a transect of sites across the coastal zone should be

occupied. Vibracores and grab samples should be taken at each site for physical property measurements.

(d) A field study to test models of sediment erosion and deposition under combined wave and current motions could then be designed, based on analysis of these data and previous studies.

*(ii) Data Analysis*

(a) Analyses of facies, grain size and composition of samples from the coastal zone, collected on Nahidik 86 and 87 should be carried out to determine the appropriate locations for Sea Carousel deployments.

(b) Values of critical erosion stress and critical stress at deposition under unidirectional flow, from Sea Carousel, should then be related to sediment properties, including grain size, composition and geotechnical parameters.

(c) Available data from the Seaconsult studies of 1986 and 1987 should then be analyzed in the light of the measured critical stresses under unidirectional flow, to develop hypotheses concerning combined wave and current dynamics. A field measurement program should be designed to test these hypotheses.

*(iii) Outputs*

(a) Journal paper on freshet processes.

(b) Section on scour and siltation in Geohazard Assessment paper (see outputs of section 10.5.1).

(c) Journal papers on sediment properties distributions, and relationships between sediment properties and critical stresses.

(d) Paper on model for erosion and deposition under combined wave and current action.

### **10.5.3 Coastal Sedimentary Environments Program**

This program involves the sedimentological study of various coastal environments, aimed principally at determining sedimentation patterns and processes for oil spill preparedness. However, the facies models developed in these studies would be of great benefit in the interpretation, geotechnical characterization and prediction of transgressive deposits (Unit B) in the offshore. Several key environments have had little attention in the past and should be studied in more detail, including deltas, coastal embayments, lagoons, marshes and tidal flats.

*(i) Field Requirements:*

(a) Field programs, similar to the study by Jenner (1989) of the Mackenzie Delta distributary mouth, would be appropriate for each particular depositional system. Field work for

each study would be based around a summer field camp, the party being equipped with a small boat or zodiac, and lightweight equipment for coring and sampling. Where possible, the summer field work should be supplemented by some form of observation or monitoring program during spring freshet and break-up, and fall freeze-up.

(b) A morphological map for the depositional system should be prepared during the field program, detailing the principal environments, sediment facies and associated zonations of vegetation, palynomorphs, forams and ostracods.

(c) Measurements of key processes (e.g. waves, currents, water levels, freezing, desiccation) at strategic locations should be carried out over the entire field season.

(d) Coring of the various environments should be attempted to develop a three-dimensional facies model. Lightweight coring systems capable of penetrating permafrost need to be developed.

*(ii) Data Analysis:*

(a) Analysis should be aimed at developing a facies model that incorporates horizontal facies distributions and process observations.

(b) Vertical sequence development should be interpreted in terms of the three-dimensional development of the depositional system through time and the response of the system to sea-level changes.

(c) The biostratigraphic zonation and resulting vertical sequences of palynomorphs, forams and ostracods should be documented.

*(iii) Outputs:*

(a) Journal papers on facies models for the various coastal environments.

(b) Oil-spill response manual for the Beaufort Sea coast, summarizing sedimentation patterns and processes for use by industry, environment officials and communities.

#### **10.5.4 Cliff, Beach and Barrier Monitoring Program**

This program aims to (i) continue acquisition of baseline information on rates of coastline change; and (ii) investigate the relative roles of various controls on coastal stability.

*(i) Field Requirements*

(a) Measurements should be continued on an annual basis at as many of the monumented cliff, beach and barrier sites as feasible, with the objective of building a long-term set of annual retreat measurements for future studies. AGC should consider the involvement of local organizations in the region, such as the Science Institute of the N.W.T., the Arctic College and the Inuvik Scientific Resource Centre. Personnel from these organizations may be able to conduct

surveys at a lower cost than AGC.

(b) A small number of sites should be selected for more detailed monitoring of processes over a period of several years. These might be included in the transect of monitoring sites proposed during the meeting of USGS and GSC scientists in Boulder, Colorado in March 1990 (P.W. Barnes and R.B. Taylor, report in preparation). These sites should be continuously monitored through all seasons of the year. Field studies should be based on single littoral cells and attempts should be made to accurately quantify processes and changes within the selected cells. Detailed repetitive surveys of the cliff and littoral sediment (and ground ice) budget should be combined with measurements of climatic parameters, as well as wave, current, water level and ice scour regimes during the study period.

(c) AGC should continue to seek ways of improving the resolution of the late Holocene sea-level curve. Detailed examination of marsh and lagoon sequences along the coast may provide sequences suitable for radiocarbon dating and sea-level reconstruction. Sampling to establish modern zonations of freshwater, brackish and marine indicators is necessary before accurate reconstructions can be made.

#### *(ii) Data Analysis*

(a) A classification of cliff, beach and barrier types along the Beaufort Sea coast should be developed to assist in the selection of sites and key parameters.

(b) As the stability and process database develops, quantitative relationships between the various parameters should be established.

(c) Detailed palynological and micropaleontological studies of key sea-level sites should be carried out before further radiocarbon dating is attempted for sea-level reconstruction.

#### *(iii) Outputs*

(a) Journal papers on coastal classification and sea-level change.

(b) Database on coastal stability.

### **10.6 Coordination and Communication**

An important priority issue that is not addressed by the research programs described above is the need to communicate the results to potential users of the information. These users include industry, government agencies and community groups in the Beaufort region. To date, this information flow has not been very efficient. AGC has both a responsibility and a need to improve communication with its client groups. Even within the Geological Survey of Canada, there is a lack of communication between different divisions (particularly AGC and TSD). The following

recommendations relate to these communication issues.

### ***10.6.1 Communication with Non-Technical Organizations***

AGC should establish, develop and co-ordinate an information program for Beaufort Sea projects, aimed at Inuvialuit groups (Inuvialuit Lands Administration, Game Councils), and non-technical federal and territorial agencies. This could take the form of (i) a six-monthly newsletter summarizing programs in non-technical language and preferably translated to Inu; (ii) a speaking tour of key arctic communities e.g. Yellowknife, Whitehorse, Inuvik, Tuk, Aklavik, Sachs Harbour, Paulatuk, Old Crow, to explain the program and obtain feedback regarding community concerns.

### ***10.6.2 Communication with Other Technical Agencies and Industry***

Technical agencies with whom information should be shared on a regular basis include Terrain Sciences Division, the United States Geological Survey, the Institute of Ocean Sciences, Indian and Northern Affairs Canada, National Hydraulics Research Institute, Department of Fisheries and Oceans, Amoco, Esso, and Gulf. Communication could be achieved through one or more of the following methods: (i) an annual technical bulletin of results, containing abstracts, preprints and published papers, and summaries of progress; (ii) a schedule of regular seminars in Calgary, Ottawa and Victoria where the new results are presented; (iii) appoint a coordinator for Beaufort Sea coastal studies who is responsible for liaison and communication.



## REFERENCES

- Arctec Newfoundland Ltd., 1987. Effect of Sea Ice on Beaufort Sea Coastal Processes. Geological Survey of Canada Open File Report 1688, 104 p.
- Baird, W.F., and Hall, K.R., 1980. Wave hindcast study, Beaufort Sea: Report by Hydrotechnology Ltd., Ottawa, Ont. for Gulf Canada Resources Inc., Calgary. (Available from Pallister Resource Management Ltd., Calgary, Alberta, as Beaufort EIS Report RWE 28), 81 p.
- Barnes, P.W. 1982. Marine ice-pushed boulder ridge. *Arctic*, **35**, p. 312-316.
- Blasco, S.M., Brigham -Grette, J. and Hill, P.R., 1989. Offshore constraints on the late Pleistocene glacial history at the mouth of the Mackenzie River; In: Carter, L.D., Hamilton, T.D., and Galloway, J.P. (eds.), 1989, Late Cenozoic history of the interior basins of Alaska and the Yukon: U.S. Geological Survey Circular 1026, p. 15-17.
- Blasco, S.M., Fortin, G., Hill, P.R., O'Connor, M.J., and Brigham-Grette, J.K., 1990. The Late Neogene/Quaternary Stratigraphy of the Canadian Beaufort Continental Shelf. In Grantz, A., Johnson, L., and Sweeny, J.F. (eds.), *The Arctic Ocean region: Boulder, Colorado*, Geological Society of America, *The Geology of North America*, v. L, p. 491-502.
- Birch, J.R., 1988. Current meter and wind data collected at CANMAR drillships, 1980-1986. Report prepared for Energy, Mines and Resources, Canada, Indian and Northern Affairs, Canada, Canada Oil and Gas Lands Administration, Ottawa, Ontario, 287 p.
- Bowen, A.J., Chartrand, D.M., Daniel, P.E., Glodowski, C.W., Piper, D.J.W., Readshaw, J.S., Thibault, J., and Willis, D.H., 1986. Canadian Coastal Sediment Study, Final report of the Steering Committee. National Research Council Canada Technical Report No. 26603, 96 p.
- Brigham-Grette, J., Blasco, S.M., Lewis, J.F., Meagher, L., and Hill, P.R. in press. Shallow Pleistocene stratigraphy of the Yukon Shelf, Canadian Beaufort sea, and correlations with the Alaskan Beaufort Sea; Unpublished report to Geological Survey of Canada, Dartmouth, N.S..
- Burden, E., 1986. Mid and late Wisconsinan through Holocene biostratigraphic zonation of Beaufort Sea Shelf sediments from the Yukon Shelf west of Herschel Island to the Mackenzie River Delta. Unpublished report to the Geological Survey of Canada, 58 p.
- Burgess, M., Judge, A., Taylor, A., and Allen, V., 1982. Ground temperature studies of permafrost growth at a drained lake site, Mackenzie Delta. In: French, H.M. (ed.) *Proceedings of Fourth Canadian Permafrost Conference* (Calgary, Alberta), National Research Council of Canada, Associate Committee on Geotechnical Research, p. 3-11.
- Burns, B.M, 1973. *The Climate of the Mackenzie Valley - Beaufort Sea*. Environment Canada, Climatological Studies No. 24, 227 p.
- CERC (Coastal Engineering Research Centre), 1977. *Shore Protection Manual* (3rd ed.), US Army Corps of Engineers, Fort Belvoir, Va.
- Clifton, H.E., 1982. Estuarine deposits. In: Scholle, P.A., and Spearing, D., (eds.) *Sandstone Depositional Environments*. AAPG, Tulsa, Oklahoma, p. 179-189.



Cote, R.P., Lerand, M.M., and Rector, R.J., 1975. Geology of the Lower Cretaceous Parsons Lake Gas Field, Mackenzie Delta, Northwest Territories. In: Yorath, C.J., Parker, E.R., and Glass, D.J. (eds.) *Canada's Continental Margins; Canadian Society of Petroleum Geologists Memoir No. 4*, p. 613-632.

Cwynar, L.C., 1982. A late-Quaternary vegetation history from Hanging Lake, northern Yukon. *Ecological Monographs*, **52**, 1-24.

Dallimore, S.R., and Wolfe, S.A., 1988. Ground ice associated with glaciafluvial sediments, Richards Island, N.W.T., Canada. In: *Proceedings, 5th International Conference on Permafrost, Trondheim, Norway, Aug. 2-5, 1988*, p. 127-131.

Dallimore, S.R., Kurfurst, P.J., and Hunter, J.A.M., 1988. Geotechnical and geothermal conditions of near-shore sediments, southern Beaufort Sea, Northwest Territories, Canada. *Proceedings, 5th International Conference on Permafrost, Trondheim, Norway, Aug. 2-5, 1988*, p. 132-137.

Das, B.M., 1983. *Advanced Soil Mechanics*. New York, McGraw-Hill, 511 p.

Davidson, S., de Margerie, S. and Lank, K., 1988. Sediment transport in the Mackenzie River plume. *Geological Survey of Canada Open File Report 2303*, 123 p.

Davies, K.F., 1975. Mackenzie River input to the Beaufort Sea: Beaufort Sea Project, Technical Report 15, Institute of Ocean Sciences, Sidney, B.C., 72 p.

Department of Public Works, 1971. Investigation of storm, September 13-16, 1970 - Mackenzie Delta region, Beaufort Sea. Unpublished Technical Report, Ottawa, 20 p.

D.F. Dickins Associates Ltd., 1987. Aerial reconnaissance survey of ice break-up processes in the Canadian Beaufort Sea coastal zone. *Geological Survey of Canada Open File Report 1687*, 16 p.

Dietrich, J.R., Dixon, J., and McNeil, D.H., 1985. Sequence analysis and nomenclature of Upper Cretaceous to Holocene strata in the Beaufort-Mackenzie Basin. *In Current Research, part A, Geological Survey of Canada, Paper 85-1A*, p. 613-628.

Dome Petroleum Ltd. and others, 1982. Beaufort Sea Environmental Impact Statement.

Dyke, A.S., and Prest, V.K. 1987. Paleogeography of northern North America, 18 000 - 5 000 years ago. *Geological Survey of Canada, Map 1703A*, scale 1:12,500,000.

Earth and Oceans Research Ltd., 1986. Interpretation of acoustic data from the Yukon Shelf and Mackenzie Trough. Unpublished report to Geological Survey of Canada, 117 p.

Fehr, S., 1986. CSS John P. Tully, operations report for shallow high resolution marine geophysical survey, Yukon Shelf, Canadian Beaufort Sea. Unpublished contract report by McGregor Geosciences Ltd to Geological Survey of Canada, Dartmouth, N.S.

Fissel, D.B., and Birch, J.R., 1984. Sediment Transport in the Canadian Beaufort Sea; *Geological Survey of Canada Open File Report 2069*, 44 p..

- Fissel, D.B., and Byrne, O.J., 1988. Current and directional wave measurements in the Beaufort Sea coastal zone, August-September, 1987. Unpublished report to Geological Survey of Canada, 44 pp.
- Fissel, D.B., Bradstreet, M.S.W., and Moen, J., 1987. Watermass distributions in the Canadian Beaufort Sea. *Proceedings of Oceans* 87, 3, p. 910-916.
- Fissel, D.B., Birch, J.R., and Melling, H., in prep. Interannual variability of oceanographic conditions in the southeastern Beaufort Sea. Contract report for Dept. of Fisheries and Oceans, Sidney, B.C.
- Forbes, D.L., 1980. Late-Quaternary sea levels in the southern Beaufort Sea. Geological Survey of Canada, Current Research, Paper 80-1B, p. 75-87.
- Forbes, D.L., 1981. Babbage river Delta and Lagoon: Hydrology and Sedimentology of an Arctic Estuarine System. Unpublished Ph.D. thesis, University of British Columbia, 554 p.
- Forbes, D.L., 1989. Letter to the Editor. *Arctic*, 42, p. 182.
- Forbes, D.L. and Frobel, D. 1985. Coastal erosion and sedimentation in the Canadian Beaufort Sea. *In* Current Research, Part B, Geological Survey of Canada, Paper 85-1B, p. 69-80.
- Forbes, D.L. and Frobel, D. 1986. Coastal Video Survey: Canadian Beaufort Sea Coast. Geological Survey of Canada, Open File 1256. Available at GSC, Dartmouth Office only.
- Forbes, D.L., Blasco, S.M., and Hill, P.R., 1987. Holocene sedimentation in the lower Babbage River and Herschel Basin, northern Yukon. In program with abstracts, 12th International Congress, Ottawa. International Union for Quaternary Research, 167 p.
- Fortin, G., 1990. Regional geological framework for the late Neogene Quaternary strata beneath the Canadian Beaufort continental shelf. Unpublished report to Geological Survey of Canada, 180 p.
- Fyles, J.G., Heginbottom, J.A. and Rampton, V.N., 1972. Quaternary geology and geomorphology, Mackenzie Bay to Hudson Bay; XXIV International Geological Congress (Montreal, Quebec) Guidebook Excursion A-30.
- Gillie, R.D., 1985. King Point coastal zone sediment transport study (Contractors Report on Field Operations); Geological Survey of Canada Open File Report 1260, 30 p. plus 8 appendices.
- Gillie, R.D., 1986. King Point coastal zone sediment transport study, phase 2: Data reduction and preliminary interpretation (ed., R.B. Taylor); Geological Survey of Canada Open File Report, 25 p. plus appendices.
- Gillie, R.D., 1987. Beaufort Sea coastal morphology study. Geological Survey of Canada Open File Report 1826, 189 p.
- Gornitz, V., Lebedeff, S. and Hansen, J., 1982. Global sea-level trends in the past century. *Science*, 215, p. 1611-1614.

- Grant, W.D. and Madsen, O. S. 1979. Combined wave and current interaction with a rough bottom. *J. Geophys. Res.*, **84**, p. 1797-1808.
- Harper, J.R., and Penland, S., 1982, Beaufort Sea Sediment Dynamics: Unpublished report by Woodward-Clyde Consultants, Victoria, B.C. for Geological Survey of Canada, Dartmouth, N.S., 125 p.
- Harper, J.R., and Penland, S., 1987, Beaufort Sea Sediment Dynamics, 2nd Edition: Unpublished report by Woodward-Clyde Consultants, Victoria, B.C. for Geological Survey of Canada, Dartmouth, N.S., 125 p.
- Harper, J.R., and Swift, S., 1985. Beaufort Sea Geophysical Survey; Scoping Study. Geological Survey of Canada, Open File 1690, 68 p.
- Harper, J.R., Henry, R.F., and Stewart, G.G., 1988. Maximum storm surge elevations in the Tuktoyaktuk region of the Canadian Beaufort Sea. *Arctic*, **41**, p. 48-52.
- Harper, J.R., Reimer, P.D., and Collins, A.D., 1985. Canadian Beaufort Sea: Physical shore-zone analysis. Geological Survey of Canada Open File 1689: 105 p.
- Harry, D.G., 1985. Ground ice slumps, Beaufort Sea coast, Yukon Territory. In 14 th Arctic Workshop, Arctic Land-Sea Interactions, Abstracts; Bedford Institute of Oceanography, Dartmouth, N.S., p. 115-117.
- Henry, R.F., 1975. Storm Surges. Beaufort Sea Project Technical Report No. 19, Department of the Environment, Victoria, B.C., 41 p.
- Henry, 1984. Flood hazard delineation at Tuktoyaktuk. Fisheries and Oceans, Canadian Contractor Report of Hydrography and Ocean Sciences No. 19, Sidney, B.C. Institute of Ocean Sciences, 28 p.
- Henry, R.F. and Heaps, N.S., 1976. Storm surges in the southern Beaufort Sea. *Journal of the Fisheries Research Board of Canada*, **33**, p. 2362-2376.
- Hequette, A., 1988. Field Survey and Cruise Report, U.S.G.S. R/V Karluk, 20 August - 16 September 1987, Tuktoyaktuk Peninsula Coast and Inner Beaufort Shelf. In Hill, P.R. (Ed.) 1988. Report of Field Activities: 1987. G.S.C. Project 830007, Beaufort Sea Coastal Zone Geotechnics. Geological Survey of Canada Open File Report 1902, 153 p.
- Hequette, A. 1989. 1988 Canadian Beaufort Sea Coast Survey. Field Survey Report . Cruise Report No. 88310; Geological Survey of Canada Open File Report 2084, 15 p..
- Hequette, A., and Barnes, P.W., 1990. Coastal retreat and shoreface profile variations in the Canadian Beaufort Sea. In P.R. Hill (ed.), *The Beaufort Sea Coastal Zone, Marine Geology*, **91**, p. 113-132.
- Hequette, A. and Hill, P.R., 1989. Late Quaternary seismic stratigraphy of the inner shelf seaward of the Tuktoyaktuk Peninsula, Canadian Beaufort Sea. *Can. J. Earth Sci.*, **26**, p. 1990-2002.

Hequette, A. and Ruz, M.H., in prep. Spit and barrier island migration in the southeastern Canadian Beaufort Sea. To be submitted to Jour. Coast. Res.

Hequette, A., Jenner, K.A., and Hill, P.R., 1990. Beach morphodynamics and sediment transport at Tibjak Beach, Canadian Beaufort Sea Coast; Geological Survey of Canada Open File Report 2280, 43 p..

Herlingveaux, R.H., and de Lange Boom, B.R., 1975. Physical oceanography of the Southeastern Beaufort Sea. Beaufort Sea Project Technical Report No.18, Environment Canada.

Hill, P.R. (ed.) 1988a. Report of Field Activities: 1987. G.S.C. Project 830007, Beaufort Sea Coastal Zone Geotechnics. Geological Survey of Canada Open File Report 1902, 153 p.

Hill, P.R., 1988b. Effects of Changing Northern Climate on the Beaufort Sea Coast and Related Industrial Development. Proceedings of the 3rd Meeting on Northern Climate, Whitehorse, Yukon, September 7 - 8, 1988, p. 163-180.

Hill, P.R., 1990. Coastal geology of the King Point area, Yukon Territory, Canada. *In* P.R. Hill (ed.), *The Beaufort Sea Coastal Zone, Marine Geology*, **91**, p. 93-111.

Hill, P.R., and Nadeau, O.C., 1989. Storm-dominated sedimentation on the inner shelf of the Canadian Beaufort Sea. *Journal of Sedimentary Petrology*, **59**, p. 455-468.

Hill, P.R., Blasco, S.M. and O'Connor, M.J., in prep. Late Quaternary stratigraphy and sedimentation of the eastern Canadian Beaufort Shelf. Submitted to *Can. J. Earth Sci.*

Hill, P.R., Forbes, D.L., Dallimore, S.R., and Morgan, P., 1986a, Shoreface development in the Canadian Beaufort Sea: *In*: Skafel, M.G. (ed.), *Proceedings, Symposium on Cohesive Shores*, National Research Council of Canada, Publication No. 26134, p. 428-448.

Hill, P., Moran, K., Kurfurst, P., and Pullan, S., 1986b. Geotechnical, geophysical and sedimentological properties of seabottom sediments near Richards Island, southern Beaufort Sea. 3rd Canadian Marine Geotechnical Workshop, St. John's, Nfld., June 1986, p. 301-327.

Hirst, S.M., Miles, M., Blachut, S.P., Goulet, L.A., and Taylor, R.E., 1988. Quantitative synthesis of the Mackenzie Delta ecosystems. Draft report for Inland Waters Directorate, Environment Canada.

Hodgins, D.O., 1983. A review of extreme wave conditions on the Beaufort Sea: Report by Seaconsult Marine Research Ltd., Vancouver, B.C. for Marine Environmental Data Service, Department of Fisheries and Oceans, Ottawa, Ont., 160 p.

Hodgins, D.O., 1988. Sediment-Storm Interaction Study, NOGAP B.6. Unpublished report to Fisheries and Oceans Canada, 94 p.

Hodgins, D.O., and Harry, K.F. 1982. On the occurrence of extreme storm and wind-wave fetches conditions in the southeastern Beaufort Sea. Report prepared for Esso Resources and submitted as EIS Support Document. Available from Pallister Resources Ltd., Calgary.

- Hodgins, D.O., LeBlond, P.H., and Brink-Kjaer, O., 1981. A hindcast study of extreme water levels in the Beaufort Sea: Report by Seaconsult Marine Research Ltd., Vancouver, B.C., for Esso Resources Canada Ltd. (Available from Pallister Resources Management Ltd., Calgary, Alberta as Beaufort EIS Report RWE 36), 231 p.
- Hodgins, D.O., Sayao, O.J., Kinsella, E.D., and Morgan, P.W., 1986. Nearshore sediment dynamics - Beaufort Sea. The 1986 Monitoring program. Environmental Studies Revolving Funds Report 054, Ottawa, 195 p.
- Hopkins, D.M., 1982. Aspects of the paleogeography of Beringia during the late Pleistocene. In: Hopkins, D.M., Matthews, J.V. Jr., Schweger, C. E., and Young, S.B. (eds.) *Paleoecology of Beringia*. New York, Academic Press, p. 3-28.
- Hopky, G.E., Chipczak, D.B., and Lawrence, M.J., 1986. Seasonal salinity, temperature and density data for the Canadian Beaufort Sea shelf, 1984-1985. Canadian Data Report of Fisheries and Aquatic Sciences No. 593, 249 p.
- Hopky, G.E., Chipczak, D.B., and Lawrence, M.J., 1987. Seasonal salinity, temperature and density data for the Canadian Beaufort Sea shelf, 1986. Canadian Data Report of Fisheries and Aquatic Sciences No. 661, 268 p.
- Hopky, G.E., Chipczak, D.B., and Lawrence, M.J., 1988. Seasonal salinity, temperature and density data for the Canadian Beaufort Sea shelf, 1987. Canadian Data Report of Fisheries and Aquatic Sciences No. 685, 162 p.
- Hopky, G.E., Chipczak, D.B., and Lawrence, M.J., 1986. Salinity, temperature and density data for the Canadian Beaufort Sea shelf, March 1988. Canadian Data Report of Fisheries and Aquatic Sciences No. 712, 17 p.
- Huggett, W.S., Woodward, M.J., Stephenson, F., Hermiston, W., and Douglas, A.N., 1975. Near bottom currents and offshore tides. Beaufort Sea Project Technical Report No. 16. Environment Canada, 38 p.
- Hughes, O.L., 1987. Late Wisconsinan Laurentide glacial limits of northwestern Canada: the Tutsieta Lake and Kelly Lake phases. Geological Survey of Canada Paper 85-25, 19 p.
- Hughes, O.L., Harington, C.R., Janssens, J.A., Matthews, J.V., Jr., Morlan, R.E., Rutter, N.W., and Schweger, C.E., 1981. Upper Pleistocene stratigraphy, paleoecology, and archaeology of the northern Yukon interior, eastern Beringia 1. Bonnet Plume Basin. *Arctic*, **34**, p. 329-365.
- Hyvarinen, H and Ritchie, J.C., 1975. Pollen stratigraphy of Mackenzie Pingo sediments, N.W.T., Canada. *Arctic and Alpine Research*, **7**, 261-272.
- Jenner, K.A., 1987a. Seismic stratigraphy of Kugmallit Bay: an interpretation. Unpublished term paper, 23 p.
- Jenner, K.A., 1987b. Nearshore facies - Mackenzie Delta. Unpublished term paper, 18 p.
- Jenner, K.A., 1989. Modern deltaic sedimentation in an arctic setting: Olivier Islands, Mackenzie Delta, Northwest Territories. Unpublished M.Sc. thesis, Dalhousie University, Halifax, N.S., 119 p.

Johnston, G.H., and Brown, R.J.E., 1965. Stratigraphy of the Mackenzie River delta, Northwest Territories, Canada. *Geological Survey of America Bulletin*, **76**, p.103-112.

Judge, A., 1986. Permafrost distribution and the Quaternary history of the Mackenzie - Beaufort region: a geothermal perspective. In: Heginbottom, J.A., and Vincent, J.-S., (eds.) *Correlation of Quaternary Deposits and events around the margin of the Beaufort Sea. Contributions from a Joint Canadian-American Workshop, April 1984. Geological Survey of Canada Open File Report 1237*, p. 41-45.

Kamphuis, J.W., Davies, M.H., Nairn, R.B. and Sayao, O.J., 1986. Calculation of littoral sand transport rate. *Coastal Engineering*, **10**, 1-21.

Konrad, J.-M., 1985. Undrained cyclic behaviour of Beaufort Sea silt. *Proceedings of Arctic '85, ASCE, San Francisco, Ca., March 25-27, 1985*, p. 830-837.

Kovacs, A., 1983. Shore ice ride-up and pile-up features, Part I: Alaska's Beaufort Sea coast. *CRREL Report 83-9, US Army Corps of Engineers, Hanover, New Hampshire*, 59 p.

Kovacs, A., 1984. Shore ice ride-up and pile-up features, Part II: Alaska Beaufort Sea coast - 1983 and 1984. *CRREL Report 84-26, US Army Corps of Engineers, Hanover, New Hampshire*, 29 p.

Kovacs, A. and Mellor, M., 1971. Investigations of ice islands in Babbage Bight. *Technical Note In: Investigations of Effects in the Mackenzie Delta Region; Canada, Department of Public Works, Engineering Programs Branch, November 1971*.

Kozo, T.L. and Robe, R.Q., 1986. Modelling winds and open-water buoy drift along the eastern Beaufort sea coast, including the effects of the Brooks range. *J. Geophys. Res.*, **91**, p. 13011-13032.

Kurfurst, P.J., 1986. Geotechnical investigations of the near-shore zone, North Head, Richards Island, N.W.T. *Geological Survey of Canada Open File 1376*, 82 p.

Kurfurst, P.J., 1988. Geotechnical investigations of northern Richards Island, N.W.T. - Spring 1987. *Geological Survey of Canada Open File Report 1707*, 137 p.

Lewis, C.P., 1988. Mackenzie Delta Sedimentary Environments and Processes. *Contract Report to Water Resources Branch, Environment Canada. Draft version only available*.

Lewis, J.F., 1989. Regional surficial geology:southcentral Beaufort Shelf, Beaufort Sea, Northwest Territories; draft unpublished report prepared for Geological Survey of Canada, Dartmouth, N.S., 107 p.

Lewis, C.P. and Forbes, D.L., 1975. Coastal sedimentary processes and sediments, Southern Beaufort Sea. *Beaufort Sea Project Technical Report No. 24, Environment Canada*.

Lewis, J.F., and Meagher, L., 1987. Upper Tertiary and Quaternary geology and morphology of the western Beaufort (Yukon) continental shelf and slope. *Unpublished report to Geological Survey of Canada*, 136 p.

- Mackay, J.R., 1959. Glacier ice-thrust features of the Yukon coast. *Geographical Bulletin*, No. 13, p. 5-21.
- Mackay, J.R. 1960. Notes on small boat harbours of the Yukon coast. *Geographical Bulletin*, No. 15, p. 19-30.
- Mackay, J. R. 1963 a. Notes on the shoreline recession along the coast of the Yukon Territory. *Arctic*, **16**, p. 195-197.
- Mackay, J.R. 1963 b. The Mackenzie Delta Area, N.W.T. Geological Survey of Canada, Miscellaneous Publication No. 8, 202 p.
- Mackay, J.R., 1966. Segregated epigenetic ice and slumps in permafrost, Mackenzie Delta area, N.W.T. *Geographical Bulletin*, **8**, p. 59-80.
- Mackay, J.R., 1971. The origin of massive icy beds in permafrost, western Arctic coast. *Can. J. Earth Sci.*, **8**, p. 397-422.
- Mackay, J.R., 1974. Ice-wedge cracks, Garry Island, Northwest Territories. *Can. J. Earth Sci.*, **11**, p. 1366-1383.
- Mackay, J.R., 1975. The stability of permafrost and recent climate change in the Mackenzie Valley, N.W.T. In: Report of Activities, Part B, Geological Survey of Canada Paper 75-1B, p. 173-176.
- Mackay, J.R. 1979. Pingos of the Tuktoyaktuk Peninsula area, Northwest Territories. *Geogr. Phys. Quat.*, **33**, p. 3-61.
- Mackay, J.R., 1980. Deformation of ice-wedge polygons, Garry Island, Northwest Territories. In: Current Research, Part A, Geological Survey of Canada, Paper 80-1A, p. 287-291.
- Mackay, J.R. and Matthews, J.V. Jr., 1983. Pleistocene ice and sand wedges, Hooper Island, Northwest Territories. *Canadian Journal of Earth Sciences*, **20**, p. 1087-1097.
- Mackay, J.R., Rampton, V.N., and Fyles, J.G. (1972). Relict Pleistocene permafrost, western Arctic, Canada. *Science*, **176**, p. 1321-1323.
- MacNeill, M.R. and Garrett, J.R., 1975. Open water surface currents. Beaufort Sea Project, Technical Report No. 17, Environment Canada.
- Markham, W.E., 1975. Ice climatology of the Beaufort Sea. Beaufort Sea Project Technical Report No. 26, Environment Canada, 87 p.
- Marko, J.R., Fissel, D.B., Wilson, M.A., and Huston, D. 1983. Background and evaluation of impacts of Liard River hydroelectric development in the southeastern Beaufort Sea. Unpublished report for B.C. Hydro and Power Authority, available at the Arctic Institute, University of Alberta, 81 p.
- Marsh, P. and Bigras, S., 1988. Evaporation from Mackenzie Delta lakes, N.W.T., Canada. *Arctic and Alpine Research*, **20**, p. 220-229.

- Marsh, P. and Hey, M., 1988. The flooding hydrology of Mackenzie Delta lakes. Environment Canada, Inland Waters Directorate, NHRI Contribution No. 88008, Saskatoon, Sask., 25 p.
- Marsh, P. and Ferguson, M., 1988. Sediment regime of lakes in the Mackenzie Delta. Environment Canada, Inland Waters Directorate, NHRI Contribution No. 88016, Saskatoon, Sask., 67 p.
- May, J.P., 1974. WAVENRG: A computer program to determine the distribution of energy dissipation in shoaling water waves with examples from coastal Florida. In: W.F. Tanner (Ed.), *Sediment Transport in the Nearshore Zone*, Florida State University, Tallahassee, Fl., p. 22-80.
- McDonald, B.C. and Lewis, C.P., 1973. Geomorphic and sedimentologic processes of rivers and coast, Yukon coastal plain. Canada, Environmental-Social Committee, Northern Pipelines, Task Force on Northern Oil Development, Report 73-39, 245 p.
- McDonald, R.W., Wong, C.S., and Erickson, P.E., 1987. The distribution of nutrients in the southeastern Beaufort Sea: implications for water circulation and primary production. *J. Geophys. Res.*, **92**, p. 2939-2952.
- McGladrey, K.M., 1984. Multidisciplinary geophysical and hydrographic survey off the Yukon coast. Cansite Surveys, unpublished contract report to Canadian Hydrographic Service.
- McGregor GeoScience Ltd., 1986. Shallow water high resolution seismic survey, Canadian Beaufort Sea. Unpublished report to Geological Survey of Canada, 23 p.
- McLaren, P., 1982. The coastal geomorphology, sedimentology and processes of eastern Melville western Byam Martin Islands, Canadian Arctic archipelago. Geological Survey of Canada, Bulletin No. 333, 39 p.
- McLaren, P., 1986. Sediment transport trends at King Point, Beaufort Sea. Unpublished subcontractor report to Dobrocky Seatech. In: Gillie, 1986, King Point coastal zone sediment transport study, Phase 2: data reduction and preliminary interpretation (ed. R.B.Taylor); Geological Survey of Canada Open File report, 25 p. plus appendices.
- McLaren, P., and Bowles, D., 1985. The effects of sediment transport on grain-size distributions; *Journal of Sedimentary Petrology*, **55**, p. 457-470.
- Melling, H., and Lewis, E.L., 1982. Shelf drainage flows in the Beaufort Sea and their effect on the Arctic Ocean pycnocline. *Deep Sea Research*, **29**, p. 967-985.
- Milne, A.R., and Herlingveaux, R.H., 1977. Crude oil in cold water. Beaufort Sea Project Summary report, Institute of Ocean Sciences, Sidney, B.C., 119 p.
- Mitchum, R.M. Jr., Vail, P.R., and Thompson, S. III, 1977. Seismic stratigraphy and global changes in sea level, part 2: the depositional sequence as a basic unit for stratigraphic analysis. In C.E. Payton (ed.), *Seismic Stratigraphy - Applications to Hydrocarbon Exploration*. American Association of Petroleum Geologists, Memoir 26, p. 53-62.
- Moran, K., Hill, P.R and Blasco, S.M., 1989. Interpretation of piezocone penetrometer profiles in sediment from the Mackenzie Trough, Canadian Beaufort Sea. *Journal of Sedimentary Petrology*, **59**, p. 88-97.



- Morgan, P., 1986. Sediment transport study at King Point, Yukon Territory. In: Current Research, Part B, Geological Survey of Canada, Paper 86-1B, p. 859-863.
- Mysak, L.A., and Manak, D.K., 1989. Arctic sea-ice extent and anomalies, 1953-1984. *Atmosphere-Ocean*, 27, 376-405.
- O' Connor, M.J., 1982 a. Shallow acoustic permafrost in the southern Beaufort Sea. Unpublished report to Geological Survey of Canada by M.J. O'Connor and Associates Ltd., 114 p.
- O'Connor, M.J., 1982b. Regional surficial geology of the southern Beaufort Sea. Unpublished report to Geological Survey of Canada by M.J. O'Connor and Associates Ltd., 188 p.
- O'Connor, M.J., 1985. Surficial Geology of the Mackenzie Trough. Unpublished report to the Geological Survey of Canada, 188 p.
- O'Connor, M.J. and Associates Ltd., 1986. Investigation of subsurface conditions at King Point, Yukon Territory. Unpublished report to Indian and Northern Affairs Canada, 163 p.
- Oertel, G.F., 1985. The barrier island system. *Marine Geology*, 63, p.1-18.
- Otvos, E.G., 1985. Barrier island formation through nearshore aggradation - stratigraphic and field evidence. *Marine Geology*, 43, p. 195-243.
- Pelletier, B.R. 1975. Sediment dispersal in the southern Beaufort Sea. Beaufort Sea Project Technical Report No. 25a. Department of the Environment, Victoria, B.C., 80 p.
- Pilkington and Associates, 1988. A study of the occurrence of strudel scours in the Canadian Beaufort Sea; Geological Survey of Canada Open File Report 2272, 76 p.
- Pinchin, B.M., and Nairn, R.B., 1987. Beaufort Sea Coastal Sediment Study: Evaluation of inshore wave climate and coastal sediment transport prediction techniques at King Point Yukon. Effects of a structure at King Point, Yukon. Geological Survey of Canada Open File Report 1770, 219 p.
- Pinchin, B.M., Nairn, R.B., and Philpott, K.L., 1985, Beaufort Sea Coastal Sediment Study: Numerical estimation of sediment transport and nearshore profile adjustment at coastal sites in the Canadian Beaufort Sea: Geological Survey of Canada, Open File Report 1259, 712 p.
- Poley, D.F., 1981. A detailed study of a submerged pingo-like feature in the Canadian Beaufort Sea, Arctic Canada. Unpublished B.Sc. Hons. thesis, Dalhousie University, Halifax, N.S., 93 p.
- Pollard, W.H., and Dallimore, S.R., 1988. Petrographic characteristics of massive ground ice, Yukon coastal plain, Canada. In: Proceedings, 5th International Conference on Permafrost, Trondheim, Norway, Aug. 2-5, 1988, p. 224-229.
- Prior, D.B. and Coleman J.M., 1980. Sonograph mosaics of submarine slope instabilities, Mississippi River Delta. *Marine Geology*, 36, p. 227-239.

- Prior, D.B., Yang, Z.S., Bornhold, B.D., Keller, G.H., Lu, N.Z., Wiseman, W.J., Jr., Wright, L.D., Zhang, J., 1986. Active slope failure, sediment collapse and silt flows on the modern subaqueous Huanghe (Yellow River) Delta. *Geo-Marine Letters*, **6**, p. 85-95.
- Quinlan, G., and Beaumont, C., 1981. A comparison of observed and theoretical postglacial relative sea level in Atlantic Canada. *Can. J. Earth Sci.*, **18**, p. 1146-1163.
- Rampton, V.N., 1973. The history of thermokarst in the Mackenzie-Beaufort regions, Northwest Territories, Canada. International Union of Quaternary Research, 9th Congress, Christchurch, New Zealand, Abstracts, p. 299.
- Rampton, V.N., 1982. Quaternary geology of the Yukon coastal plain. Geological Survey of Canada Bulletin 317, 49 p.
- Rampton, V.N., 1988. Quaternary geology of the Tuktoyaktuk coastlands, Northwest Territories. Geological Survey of Canada, Memoir 423, 98 p.
- Rampton, V.N. and Bouchard, M., 1975. Surficial geology of Tuktoyaktuk, District of Mackenzie. Geological Survey of Canada, Paper 74-53, 17 p.
- Rampton, V.N., and Mackay, J.R., 1971. Massive ice and icy sediments throughout the Tuktoyaktuk Peninsula, Richards Island and nearby areas, District of Mackenzie. Geological Survey of Canada, Paper 71-21, 16 p.
- Reimnitz, E., and Kempema, E.W., 1982. Dynamic ice-wallow relief of northern Alaska's nearshore. *Journal of Sedimentary Petrology*, **52**, p. 451-461.
- Reimnitz, E., and Kempema, E.W., 1983. High rates of bedload transport measured from infiling rate of large strudel scour craters in the Beaufort Sea, Alaska. *Continental Shelf Research*, **1**, p. 237-251.
- Reimnitz, E., and Kempema, E.W., 1987. Field observations of slush ice generated during freeze-up in arctic coastal waters. *Marine Geology*, **77**, p. 219-231.
- Reimnitz, E. and Maurer, D.F., 1978. Storm surges in the Alaskan Beaufort Sea. U.S. Geological Survey Open File Report, 78-593, 13 p.
- Reimnitz, E. and Maurer, D.F., 1979. Effects of Beaufort Sea surges on the Beaufort Sea coast, Northern Alaska. *Arctic*, **32**, p. 329-344.
- Reimnitz, E., Graves, S.M. and Barnes, P.W., 1985. Beaufort Sea coastal erosion, shoreline evolution, and sediment flux. U.S. Geological Survey Open File Report No. 85-380.
- Reimnitz, E., Roderick, C.A., and Wolf, S.C., 1974. Strudel scour: a unique arctic marine geologic phenomena. *Journal of Sedimentary Petrology*, **44**, p. 408-420.
- Reineck, H.-E. and Singh, I.B., 1980. Depositional sedimentary environments with reference to terrigenous clastics. Second Edition. Springer-Verlag, New York, 549 p.
- Reineck, H.E., and Wunderlich, F., 1968. Classification and origin of flaser and lenticular bedding. *Sedimentology*, **11**, p. 99-104.

Ritchie, J.C. and Hare, F.K., 1971. Late Quaternary vegetation and climate near the Arctic tree line of northwestern North America. *Quaternary Research*, 1, p. 331-342.

Ruz, M.-H., Hequette, A., and Hill, P.R., in prep. A model of coastal evolution in a transgressed thermokarst topography, Canadian Beaufort Sea.

Shearer, J.M., 1971. Preliminary interpretation of shallow seismic reflection profiles from the west side of Mackenzie Bay, Beaufort Sea. In: Report of Activities, Part B, Geological Survey of Canada, Paper 71-1, p. 131-138.

Shearer, J.M., 1972. Geological structure of the Mackenzie Canyon area of the Beaufort Sea. Geological Survey of Canada, Report of Activities, Paper 72-1A, p. 179-180.

Shi, N.C., Lawrence, H.I., and Downing, J.P., 1985. Predicting suspended sediment concentration on continental shelves. *Marine Geology*, 62, p. 255-275.

Simpkin, P.G., 1988. Detailed analysis of high resolution seismic reflection system requirements for shallow water surveys in the Canadian Beaufort Sea. Unpublished report to Geological Survey of Canada.

Taylor, R.B. 1978. The occurrence of grounded ice ridges and shore ice piling along the northern coast of Somerset Island, N.W.T. *Arctic*, 31, p. 133-149.

Thompson, R.B., 1983. Break-up patterns of landfast ice, southern Beaufort Sea, 1975-1982. Scientific Services, Atmospheric Environment Service, Western Region, Edmonton; Report 83-7, 5 p. plus appendix.

Yorath, C.J and Norris, D.K., 1975. The tectonic development of the southern Beaufort Sea and its relationship to the origin of the Arctic Ocean Basin. In: Yorath, C.J., Parker, E.R., and Glass, D.J. (eds.) *Canada's Continental Margins*, Canadian Society of Petroleum Geologists, Memoir No. 4, p. 589-611.

Yorath, C.J., Norris, D.K., and Young, F.G., 1980. Geology, Beaufort-Mackenzie Basin, District of Mackenzie and Yukon Territory. Geological Survey of Canada, Map 1509A.

Young, F.G., Myhr, D.W., and Yorath, C.J., 1976. Geology of the Beaufort-Mackenzie Basin. Geological Survey of Canada, Paper 76-11, 65 p.

Walsh, J.E., and Johnson, C.M., 1979. An analysis of arctic sea ice fluctuations. *Jour. Phys. Oceanog.*, 9, p. 580-591.

Wells, J.T., and Coleman, J.M., 1981. Physical processes and fine-grained sediment dynamics, coast of Surinam, South America. *Journal of Sedimentary Petrology*, 51, p. 1053-1068.

**APPENDIX**

**Summaries of Contracts Carried out under NOGAP Project D.1  
1984-1988**



## CONTRACT STUDY

**Company:** Arctec Newfoundland Ltd

**Title:** Effect of Sea-Ice on Beaufort Sea Coastal Processes

**Geographic Area:** U.S. Border to Cape Dalhousie

**Cost:** \$34,936

**Objectives:** To investigate the significance of sea-ice for Beaufort Sea shoreline processes and to identify critical information gaps to guide planning for the future. The project included two hypothetical case studies (King Point and North Head) to assess the impact of ice-related processes on man-made structures.

### Conclusions:

1. Two types of processes were recognized: (a) modification of marine-related processes; and (b) direct sea-ice/shoreline interaction.
2. Sea-ice modifies marine processes by (a) limiting the annual duration over which marine-related sediment transport processes are active; (b) limiting fetch and therefore wave energy; and (c) modifying wave energy at the shoreline.
3. Research recommended on (a) effects of engineering structures, ice management structures and climatic changes on duration of ice cover; (b) theoretical understanding of wave generation in broken ice cover; (c) occurrence of fetch limitation by sea-ice; (d) process and climatology of wave attenuation by sea-ice and frazil-ice.
4. Sea-ice interacts directly with the shoreline through: (a) ice-scour and ice-push; (b) ice-override; (c) ice-wallow; (d) strudel scour; (e) anchor-ice sediment transport.
5. Research recommended on (a) beach surveys immediately after break-up to determine depth and frequency of seabed disturbance by ice-scour and -push; (b) assembly of historical database on ice override from aerial surveys and available remote imagery; (c) surveys of areas of known ice-override; (d) aerial reconnaissance surveys during freeze-up to identify ice-wallow sites, followed by beach surveys before and after storm events; (e) similar reconnaissance surveys for strudel scours, with sidescan surveys; (f) laboratory and numerical modelling of strudel scour process; (g) field observations and sampling of sediment incorporation into the ice cover.

**Reference:** Arctec Newfoundland Ltd., 1987. Effect of sea ice on Beaufort Sea coastal processes. GSC Open File Report 1688, 104 p.

**Location of Report:** GSC Offices in Dartmouth, Ottawa, Calgary and Vancouver  
Copies available from Precision Microfilming Services Ltd., Halifax.

## CONTRACT STUDY

**Company:** Arctic Sciences Ltd.

**Title:** Current and directional wave measurements in the Beaufort Sea Coastal Zone, August - September 1987.

**Geographic Area:** Mackenzie Delta and Tibjak Beach

**Cost:** \$74,470

**Objectives:** To obtain directional wave and current measurements at three shallow water sites (one off the Mackenzie Delta in 9 m of water, and the other two off Tibjak Beach in 3.5 m and 5.0 m of water), to monitor beach changes through time lapse video cameras and to conduct preliminary data analysis.

### Conclusions:

1. The Seadata instrument moored off the Mackenzie Delta was lost.
2. An extensive set of current and directional wave measurements were collected at Tibjak Beach over a 21 day period. Five significant wind events and comparatively large open water fetch resulted in substantial wave activity within the coastal zone. Wave events had a significant wave height of 0.6 to 1.3 m and peak periods of 6.5 to 9.8 seconds.
3. Large orbital wave velocities were measured during the wind events, with typical amplitudes of 0.2 to 0.4 m/s and peak values up to 1.3 m/s. The wind-driven alongshore currents were generally low amplitude (up to 0.35 m/s) and not correlated to wind and wave activity. Peak current fluctuation amplitudes greatly exceeded the alongshore current by a factor ranging from 3 to 10.

**Reference:** Fissel, D.B., and Byrne, O.J., 1988. Current and directional wave measurements in the Beaufort Sea coastal zone, August-September, 1987; Geological Survey of Canada Open File Report 2069, 44 p.

**Location of Report:** GSC Offices in Dartmouth, Ottawa, Calgary and Vancouver  
Copies available from Precision Microfilming Services Ltd., Halifax.

## CONTRACT STUDY

**Company:** ASA Consulting Ltd.

**Title:** Sediment Transport in the Mackenzie River Plume

**Geographic Area:** Inner shelf, Richards Island region.

**Cost:** Est. \$30,000

**Objectives:** To develop a conceptual model quantifying the relative importance of estuarine circulation, wind-induced currents, and wave-induced oscillatory currents in reworking bottom sediments on the inner shelf. The study used wave and current data collected by industry and ESRF study data.

### Conclusions:

1. The hydrodynamic regime is dominated by storm response inducing both steady currents and waves.
2. Wave-induced orbital velocities are comparable to the steady component of flow but their effect on bottom boundary dynamics greatly increases the total bottom stress affecting sediment reworking. The importance of wave orbital velocities and steady currents increases in shallow water.
3. No evidence of classical two-layer estuarine circulation was found.
4. Observed sediment concentrations are strongly correlated with bottom stress, but this relationship accounts for only 33% of the SSC variance, probably due to advection of sediment from elsewhere or from changes in critical stress for erosion due to depositional and weathering history.
5. Dispersive processes dominate the transport of suspended sediment on the inner shelf. This can be conceived as a diffusion away from the inner shelf.
6. The settling and erosion of sediment is dominated by storm events. The hydrodynamic gradient (shore normal) will favour a net offshore drift of sediment.

**Reference:** Davidson, S., de Margerie, S. and Lank, K., 1988. Sediment transport in the Mackenzie River plume. Geological Survey of Canada Open File Report 2303, 123 p.

**Location of Report:** GSC Offices in Dartmouth, Ottawa, Calgary and Vancouver  
Copies available from Precision Microfilming Services Ltd., Halifax.



## CONTRACT STUDY

**Company:** Challenger Surveys Ltd.

**Title:** Seismic survey positioning CCGS Nahidik and R/V Karluk, Beaufort Sea, 1987.

**Geographic Area:** Mackenzie Delta to Kugmallit Bay

**Cost:** \$92,027

**Objectives:** To provide Syledis positioning for survey vessels.

**Conclusions:** Positioning provided as required.

**Reference:** Challenger Surveys Ltd., 1987. Seismic survey positioning CCGS Nahidik and R/V Karluk, Beaufort Sea, 1987. Geological Survey of Canada Open File Report 2304, 260 p. plus 4 enclosures.

**Location of Report:** Magnetic tape with Atlantic Geoscience Centre (AGC)  
Data Section, Dartmouth N.S..

## CONTRACT STUDY

**Company:** Dalhousie University

**Title:** Sedimentation in a Distributary Mouth Region of the Mackenzie Delta

**Geographic Area:** Mackenzie Delta

**Cost:** \$14,000

**Objectives:** To investigate sediment transport processes and resulting facies distribution in the Olivier Islands distributary mouth environment.

### **Conclusions:**

1. The Olivier Islands represent a localized phase of sedimentation with the overall transgressive framework of the Mackenzie Delta.
2. Sediment transport during the open water season is controlled by river flood events and storm surges. Floods introduce high concentrations of suspended sediment during moderate water levels, whereas storm surges elevate water levels allowing accretion of mudflats and delta islands.
3. Seven facies were recognized.
4. Major controls on delta development are transgression, the Arctic climate and storms.
5. Patterns of delta growth differ from lower latitude deltas in: (i) the confinement of recent progradation to the lobate shape of the present coastline; (ii) the predominance of upstream sedimentation; (iii) the absence of a distinct prodelta; (iv) the presence of channel-fill deposits below subaqueous bar sediments and (v) thin, poorly developed levees.
6. The Olivier Islands depositional model appears to be unique to high-latitude deltas and may be used as a model for localized arctic sedimentation within a very shallow, transgressive framework.

**Reference:** Jenner, K.A., 1989. Modern deltaic sedimentation in an arctic setting: Olivier Islands, Mackenzie Delta, Northwest Territories. Unpublished M.Sc. thesis, Dalhousie University, Halifax, N.S., 119 p.

**Location of Report:** Dalhousie University, Science Library ; Don Forbes, S. Blasco and P. Mudie (AGC) have copies; Kim Jenner has master copy.

## CONTRACT STUDY

**Company:** D.F. Dickins Associates Ltd.

**Title:** Aerial reconnaissance survey of ice break-up processes in the Canadian Beaufort Sea coastal zone.

**Geographic Area:** U.S border to Cape Dalhousie

**Cost:** \$24,718

**Objectives:** To study the nearshore ice break-up along the Beaufort Sea coast, for assessment of how different ice processes affect coastal sediment transport in the Beaufort Sea.

### Conclusions:

1. The study produced a comprehensive slide set and video coverage of the coastline between May 31 and June 21, 1987.
2. Pile-up features up to 12.5 m high were surveyed in 4 and 10 m of water off Atkinson Point and Nuneluk Spit respectively.
3. Strudel scour features were documented off the Babbage River delta. The maximum depth of strudel scour pit was 2 m.
4. Areas of ice overflow were mapped in the vicinity of Garry and Ellice Islands and off the deltas of the Blow, Babbage, Running and Firth Rivers.
5. The landfast ice was unusually smooth in 1987 compared to other years. There was no evidence for ice-shoreline interaction at any sites of interest for future developments, but these observations may not be typical. Additional surveys at these sites is recommended.
6. NOAA satellite images provide a valuable record of the extent of overflowing and are recommended if information on specific past years is required.

**Reference:** D.F. Dickins Associates Ltd., 1987. Aerial reconnaissance survey of ice break-up processes in the Canadian Beaufort Sea coastal zone. Geological Survey of Canada Open File No. 1687, 16 p.plus appendices

**Location of Report:** GSC Offices in Dartmouth, Ottawa, Calgary and Vancouver  
Copies available from Precision Microfilming Services Ltd., Halifax.  
Slide collection located at AGC Data Section  
Video tapes located at AGC's video lab (contact D. Frobél).

## CONTRACT STUDY

**Company:** Dobrocky Seatech Ltd.

**Title:** Canadian Beaufort Sea Physical Shorezone Analysis.

**Geographic Area:** U.S. Border to Baillie Islands

**Cost:** (Est.) \$75,000

**Objectives:** To provide: (i) an inventory of shorezone character; (ii) an assessment of coastal stability; (iii) an assessment and review of oceanographic, terrestrial and other environmental factors that affect the character of the coastal zone; (iv) a coastal information database for computer manipulation; (v) graphic presentation of selected resource information on 1:50,000 scale maps; (vi) a synthesis of the coastal information for resource managers; (vii) a presentation of results to resource managers in Whitehorse, Yellowknife and Ottawa.

### Conclusions:

1. Six coastal types were defined from the database.
2. Erosional landforms predominate over accretional landforms.
3. Most sections of the coast are retreating at rates greater than 1 m/yr.
4. The presence of significant quantities of ground ice is one of the primary causes of retreat.
5. It is hypothesized that the Canadian Beaufort Sea is undergoing relative sea-level rise which is contributing to rapid retreat.
6. Barrier islands on the Yukon coast appear to be more stable, and ice push is thought to be the major process there.

**Reference:** Harper, J.R., Reimer, P.D., and Collins, A.D., 1985. Canadian Beaufort Sea: Physical shore-zone analysis. Geological Survey of Canada Open File 1689: 105 p.

**Location of Report:** GSC Offices in Dartmouth, Ottawa, Calgary and Vancouver  
INAC offices in Hull, Whitehorse and Yellowknife.  
Copies available from Precision Microfilming Services Ltd., Halifax.

## CONTRACT STUDY

**Company:** Dobrocky Seatech Ltd.

**Title:** Operations Report, King Point Sediment Transport Study

**Geographic Area:** King Point, Yukon Territory

**Cost:** \$25,978

**Objectives:** To conduct field measurements of directional waves and currents in the coastal zone off King Point, in conjunction with a detailed site survey, for calibration of the numerical hindcast model of Pinchin et al. (1985).

### Conclusions:

1. The program extended from 24 August to 16 September 1985.
2. Two Seadata directional wave and current meters were deployed in 2.5 m and 6 m of water and apparently obtained data. Five Aanderaa current meters were deployed between 5 and 15 m of water. Two were lost and data was apparently obtained with the remaining three.
3. An Aanderaa weather station recorded wind speed, direction and barometric pressure at the beach.
4. A detailed survey of the nearshore, beach and lagoon at King point was obtained at 200 m spacing or better.
5. Sediment samples were collected from the beach and nearshore. Suspended sediment samples from the surf zone were also obtained through a pumping system.
6. Wave heights up to 1.5 m were observed at the beach. A NW storm event occurred on September 15, with winds gusting to 40 km/hr and a storm surge of approx. 8 m. Stronger wind events (estimated up to 80 km/hr) from the south caused no significant wave attack on the beach.

**Reference:** Gillie, R.D., 1985. King Point coastal zone sediment transport study (Contractors Report on Field Operations); Geological Survey of Canada Open File Report 1260, 30 p. plus 8 appendices.

**Location of Report:** GSC Offices in Dartmouth, Ottawa, Calgary and Vancouver  
Copies available from Precision Microfilming Services Ltd., Halifax.

## CONTRACT STUDY

**Company:** Dobrocky Seatech Ltd.

**Title:** Beaufort Sea Geophysical Scoping Study.

**Geographic Area:** Coastal Waters, Beaufort Sea.

**Cost:** \$4,498

**Objectives:** To recommend a strategy for conducting nearshore geophysical surveys in the Canadian Beaufort Sea, including (i) evaluation of suitable geophysical equipment for operating in nearshore areas; (ii) evaluation and identification of suitable vessels; (iii) evaluation of equipment deployment strategies.

### **Conclusions:**

1. A single-screw shallow draft displacement type vessel is most suitable for remote operations in the Beaufort Sea. Vessel size of 12 to 23 m appears optimum. The vessel should be capable of self-contained support for 2-3 weeks and of riding out storms. Vessels of this nature are very limited in the region.
2. It is possible to run echo sounder, side scan sonar, sub-bottom profiler and high resolution seismic systems from this kind of vessel. Two separate auxiliary generators are required to power this equipment and approximately 5 m of bench space is required for the recording systems.
3. It is unlikely that a vessel of this size could support an air gun or water gun system because of compressor and pump sizes. Boomers or small sparkers are more appropriate.

**Reference:** Harper, J.R., Swift, S., and Simpkin, P. 1985. Beaufort Sea Geophysical Scoping Study. Geological Survey of Canada, Open File Report 1690, 68 p. plus 5 appendices.

**Location of Report:** GSC Offices in Dartmouth, Ottawa, Calgary and Vancouver  
Copies available from Precision Microfilming Services Ltd., Halifax.

## CONTRACT STUDY

**Company:** Dobrocky Seatech Ltd  
(later R.D. Gillie, following closure of Dobrocky)

**Title:** Beaufort Sea Coastal Morphology Study

**Geographic Area:** Komakuk Beach to Cape Dalhousie

**Cost:** \$13,096

**Objectives:** 1. To collect beach profile and sediment data at representative sites to supplement existing data. 2. To resurvey monumented cliff sections to determine erosion rates. 3. To make observations and sample coastal sections which have received little attention to date.

### **Conclusions:**

1. Forty beach profiles at ten sites and 137 measurements of cliff position at 12 sites were measured between July 13 and 27, 1986.
2. Plotted and tabulated data are presented.
3. Comparison of cliff positions with previous measurements indicate erosion rates between 0.6 and 2.7 m/yr.

**Reference:** Gillie, R.D., 1987. Beaufort Sea coastal morphology study. Geological Survey of Canada Open File No. 1826, 189 p.

**Location of Report:** GSC Offices in Dartmouth, Ottawa, Calgary and Vancouver  
Copies available from Precision Microfilming Services Ltd., Halifax.

## CONTRACT STUDY

**Company:** Dobrocky Seatech Ltd  
(later R.D. Gillie, following closure of Dobrocky)

**Title:** Continuation of King Point coastal zone sediment transport study, reduction and preliminary interpretation.

**Geographic Area:** King Point

**Cost:** (Est.) \$20,000

**Objectives:** To prepare plots and figures of wind, wave, current and profile data from the King Point sediment transport study.

### **Conclusions:**

This report was not completed due to the closure of Dobrocky. R. D. Gillie produced basic data sets and a rough draft of a report. The data includes plots and tables of wave and current data, nearshore, beach and lagoon profiles, sediment grain size analysis and miscellaneous observations. A report by Geosea Consulting on the Interpretation Grain Size Trends is also included.

**Warning:** The wave data included in this report is suspect. A discussion of the possible problems with the data is included in Pinchin and Nairn (1988).

**Reference:** Gillie, R.D., 1986. King Point coastal zone sediment transport study, phase 2: data reduction and preliminary interpretation (ed. R.B. Taylor); Geological Survey of Canada Open File Report , 25 p. plus appendices.

**Location of Report:** GSC Offices in Dartmouth, Ottawa, Calgary and Vancouver  
Copies available from Precision Microfilming Services Ltd., Halifax.



## CONTRACT STUDY

**Company:** Earth and Oceans Research Ltd.

**Title:** Geophysical Operations Report, CCGS Nahidik, September 1987, Beaufort Sea

**Geographic Area:** King Point to Tuktoyaktuk

**Cost:** \$22,110

**Objectives:** Conduct high resolution seismic and sidescan sonar survey of coastal zone, including a test of the prototype IKB Seistec line and cone receiver system, on the Nahidik '87 cruise.

### **Conclusions:**

1. The prototype IKB Seistec line and cone receiver system proved to have good signal to noise characteristics and was relatively immune to deterioration (compared to streamer records) until weather conditions seriously deteriorated. A suggested improvement would be to incorporate the source into the same towed body and heave compensate the whole system.
2. By comparison, poor records were obtained with the Datasonics Bubble Pulser also used on the cruise, due to the low frequency and low signal to noise ratio.

**Reference:** Earth and Oceans Research Ltd., 1987. Geophysical operations Report, CCGS Nahidik, September 1987, Beaufort Sea. Unpublished contractors report to the Geological Survey of Canada, 16 pp + Appendices.

**Location of Report:** AGC Data Section.

## CONTRACT STUDY

**Company:** I.K.B. Technologies Ltd.

**Title:** Detailed analysis of high resolution seismic reflection system requirements for shallow water surveys in the Canadian Beaufort Sea (and development of a line and cone receiver array).

**Geographic Area:** General, but based on sediment property information from inner shelf off North Head.

**Cost:** \$11,000

**Objectives:** (i) Through acoustic modelling to determine design specifications for a high resolution seismic system for use in shallow coastal water of the Canadian Beaufort Sea; (ii) to design a prototype line and cone receiver array.

### **Conclusions:**

1. The most significant problem causing low signal to noise ratios in Beaufort sea coastal sediments is the effect of volume scattering between thinly spaced silt, sand and clay layers in the Holocene sequence.
2. This is combined with the effects of wide angle reflection and refraction included in returns to horizontal hydrophone arrays in conventional streamers in water depths less than 10 m.
3. The proposed design solution is to construct a directional hydrophone array that receives only vertical reflections and maximises the signal to noise ratio.
4. Acoustic modelling of a hypothetical sediment column allowed specifications for a prototype line and cone hydrophone system to be developed.
5. A prototype system was constructed.

**Reference:** IKB Technologies Ltd., 1988. Detailed analysis of high resolution seismic system requirements for shallow water surveys in the Canadian Beaufort Sea. Unpublished contract report to the Geological Survey of Canada.

**Location of Report:** S. Blasco (AGC) has a single copy.

## CONTRACT STUDY

**Company:** McGregor Geoscience Ltd.

**Title:** CCGS Nahidik Operations Report for Shallow, High Resolution, Marine Geophysical Survey, Mackenzie Bay/Kugmallit Bay, Canadian Beaufort Sea, September 1986.

**Geographic Area:** Mackenzie Bay to Kugmallit Bay

**Cost:** \$29,476

**Objectives:** Conduct high resolution seismic and sidescan sonar survey of coastal zone, on the Nahidik '86 cruise.

**Conclusions:**

Approximately 650 line km of data were collected using surface towed boomer source, ministreamer, single hydrophone, sidescan sonar and 3.5/7.0 kHz profiler. Data quality varied according to water depth and sea conditions. Problems were related to transducer ringing, ship noise, multiples and sea conditions.

**Reference:** McGregor Geoscience Ltd., 1986. CCGS Nahidik Operations Report for Shallow, High Resolution, Marine Geophysical Survey, Mackenzie Bay/Kugmallit Bay, Canadian Beaufort Sea, September 1986. Unpublished report to Geological Survey of Canada, 23 pp.

**Location of Report:** AGC Data Section

## CONTRACT STUDY

**Company:** M-C Surveys Ltd.

**Title:** Survey Positioning on CCGS Nahidik, Beaufort Sea, 1986

**Geographic Area:** Shallow Bay to Kugmallit Bay

**Cost:** \$58,280

**Objectives:** To provide positioning for the Nahidik'86 cruise

**Conclusions:**

1. An integrated Syledis and Hyperfix system was used and the overall quality of navigation was good, indicating proper calibration.
2. Paper plots are included in the report. A nine-track tape was supplied to AGC.

**Reference:** MC Surveys Joint Venture, 1986. Bedford Institute of Oceanography Navigation and Positioning of CCGS Nahidik in the Beaufort Sea, 1986. Unpublished report to Geological Survey of Canada, 19 p. + Appendices.

**Location of Report:** AGC Data Section

## CONTRACT STUDY

**Company:** M.J. O'Connor and Associates Ltd.

**Title:** Investigation of Subsurface Conditions at King Point, Yukon Territory  
(2 volumes, Vol. 1 Report; Vol. 2 Appendices).

**Geographic Area:** Yukon coast

**Cost:** \$465,000. Contributors: Indian and Northern Affairs Canada, and Energy Mines and Resources (G.S.C.) through PERD and NOGAP programs.

**Objectives:** To investigate the geotechnical conditions, onshore, at the coast and offshore of the King Point barrier beach, as baseline information related to the possible development of an onshore aggregate source and related marine terminal.

**Conclusions:** (Coastal related conclusions only)

1. A series of boreholes were drilled on land, on the barrier beach and in the nearshore to offshore.
2. Gravel, sand, silt and clay lithologies were encountered in the nearshore zone. All sediments appear to be stiff to hard in consistency and may represent older sediments that have been exposed to subaerial exposure prior to the recent marine transgression.
3. Although no massive ice was encountered in either barrier or nearshore boreholes, some of the shallow nearshore sediments and sediments underlying the barrier were ice-bonded and contained visible ice. Thus, whereas existing foundation conditions are generally believed to be excellent for marine structures, engineering design must consider the thermal interaction of the structure with the permafrost affected sediments which presently exist at or near the seabed.
4. Lagoon sediments are unfrozen and compressible. Infilling of the lagoon may result in consolidation of the sediment and settlement of the fill.
5. A sub-contract study by J.R. Harper included in the report summarized existing information e.g. retreat rates of adjacent cliffs at an average of approx. 0.6 m/a and convergent longshore transport. It was anticipated that proposed harbour developments would cause substantial accumulation of sediment in harbour basins and channels. More data on sediment transport should be obtained.

**Reference:** M.J. O'Connor and Associates Ltd. 1986. Investigation of Subsurface Conditions at King Point, Yukon Territory , Vol. 1: Report 160 p. , Vol. 2: Appendices.

**Location of Report:** Indian and Northern Affairs, Canada Library, Ottawa, Ont.  
Atlantic Geoscience Science Data section, Dartmouth, N.S.

## CONTRACT STUDY

**Company:** Keith Philpott Consulting Ltd.

**Title:** Beaufort Sea Coastal Sediment Study: Numerical Estimation of Sediment Transport and Nearshore Profile Adjustment at Coastal Sites in the Canadian Beaufort Sea.

**Geographic Area:** Herschel Island to Atkinson Point

**Cost:** (Est.) \$120,000

**Objectives:** To develop a numerical model for estimation of inshore wave climates, influence of storm surges on coastal processes, alongshore sediment transport rates, nearshore profile adjustments and the impacts of structures on coastal processes.

### Conclusions:

1. The study shows that there is a shortage of suitable wind, water level, wave, geomorphologic and sediment data for quantitative coastal process studies.
2. For accurate wave hindcasts, it is necessary to redefine the ice limits on a weekly basis and to interpolate daily fetch values. It is also necessary to devise a method of changing from deep water to shallow water hindcast models as the ice edge moves in.
3. Conventional refraction analysis with forward tracking of unidirectional monochromatic waves can produce misleadingly inaccurate results.
4. Surges have little effect on mean alongshore sediment transport rates, but do have an impact on nearshore profiles.
5. The twelve alongshore sediment transport predictors produce a wide range of results. The Nielsen et al. (1978) breaking wave model was judged to be best overall among detailed predictors. Bulk models gave more stable results.
6. The coastal profile adjustment model SEGAR was difficult to calibrate against the small amount of available data.
7. A beach plan model was successfully used to predict shoreline changes at King Point.

**Reference:** Pinchin, B.M., Nairn, R.B., and Philpott, K.L., 1985, Beaufort Sea Coastal Sediment Study: Numerical estimation of sediment transport and nearshore profile adjustment at coastal sites in the Canadian Beaufort Sea: Geological Survey of Canada, Open File 1259, 712 p.

**Location of Report:** GSC Offices in Dartmouth, Ottawa, Calgary and Vancouver  
Copies available from Precision Microfilming Services Ltd., Halifax.

## CONTRACT STUDY

**Company:** Keith Philpott Consulting Ltd.

**Title:** Evaluation of Inshore Wave Climate and Coastal Sediment Transport Prediction techniques at King Point, Yukon and Effects of a Structure at King Point, Yukon.

**Geographic Area:** King Point

**Cost:** \$28,840

**Objectives:** (i) A critical evaluation of the estimation techniques used in the previous study; and (ii) assessment of the impact on coastal processes of a structure at a different location than in the previous study.

### **Conclusions:**

1. The field program did not provide the data required to perform a comprehensive evaluation of the sediment transport estimation techniques.
2. From the hindcasts, it was determined that the winds generating waves at offshore locations were from a different direction than the winds generating the waves at King Point. It follows that previous hindcasts based on winds measured at Tuktoyaktuk may not be accurate. However the extended data set at Tuk provides the best option for estimating waves at coastal site, in the absence of better measurements.
3. Improved sediment transport predictions did not result from the data collected at King Point.

**Reference:** Pinchin, B.M., and Nairn, R.B., 1987. Beaufort Sea Coastal Sediment Study: Evaluation of inshore wave climate and coastal sediment transport prediction techniques at King Point Yukon. Effects of a structure at King Point, Yukon. Geological Survey of Canada Open File Report 1770, 219 p.

**Location of Report:** GSC Offices in Dartmouth, Ottawa, Calgary and Vancouver  
Copies available from Precision Microfilming Services Ltd., Halifax.

## CONTRACT STUDY

**Company:** Pilkington and Associates (now Canatec Consultants Ltd.)

**Title:** A Study of the Occurrence of Strudel Scours in the Canadian Beaufort Sea

**Geographic Area:** Herschel Island to Baillie Islands

**Cost:** Est. \$5000 NOGAP contribution, Funded by DSS Unsolicited Proposal Fund.  
Total (est.) \$15,000

**Objectives:** To document the timing of break-up and find evidence for strudel scour activity from archival remote sensing data.

### Conclusions:

1. Flooding of the sea ice surface at the mouths of the Mackenzie River channels occurs in early May in the form of shore normal tongues of water.
2. By mid-May, flooding extends 15-20 km from shore adjacent to the main channels particularly around Middle Channel, the Olivier Islands, in Shallow Bay and Harry Channel. The flooding appears to be limited by small shear ridges that develop along tidal cracks.
3. By late May, the ice has melted lagoons out to the 1.5 to 2 m water depth, allowing river water direct access to the ocean under the ice.
4. During the last week in May, or early June, the flood waters drain off the ice and by mid-June, there is open water along the entire coast of Richards Island.
5. Flooding occurs at the mouths of the Anderson and Mason rivers in Liverpool Bay in mid to late May, and in Phillips Bay in early June.
6. The majority of flooding off Richards Island is over grounded or near-grounded ice in water depths less than 2 m. Strudels are unlikely to occur in water depths less than 1.4 m of water.
7. Strudel scours are most likely to occur in deeper water north of the Reindeer Channel - Olivier Islands area, but no evidence was found in SLAR data to support this (however, the SLAR resolution is marginal for seeing features of this scale).

**Reference:** Pilkington and Associates, 1988. A study of the occurrence of strudel scours in the Canadian Beaufort Sea; Geological Survey of Canada Open File Report 2272, 76 p.

**Location of Report:** GSC Offices in Dartmouth, Ottawa, Calgary and Vancouver  
Copies available from Precision Microfilming Services Ltd., Halifax.



